

DEMOCRATIC AND POPULAR REPUBLIC OF ALGERIA  
MINISTRY OF HIGHER EDUCATION AND SCIENTIFIC RESEARCH

UNIVERSITY OF BROTHERS MENTOURI-CONSTANTINE  
FACULTY OF EXACT SCIENCES  
DEPARTMENT OF CHEMISTRY

Number Order :.....

Serie :.....

## THESIS

Presented for the obtaining of the degree of Doctor of Science  
Specialty: Organic Chemistry  
Option: Phytochemistry

By  
Farida LARIT

Entitled

**Phytochemical and Biological Studies of Two Algerian Medicinal  
Plants: *Cytisus villosus* Pourr. (Fabaceae) and *Hypericum afrum* Lam.  
(Hypericaceae)**

### Members of Jury:

Pr. Salah AKKAL	University of Brothers Mentouri, Constantine	Chairman
Dr. Samira BENYAHIA	Higher School of Industrial Technologies, (ESTI)-Annaba	Supervisor
Pr. Stephen J. CUTLER.	University of South Carolina, USA	Examiner
Pr. Souad AMEDDAH	University of Brothers Mentouri, Constantine	Examiner
Pr. Nouredine GHERRAF	University of Mohamed Larbi Ben M'Hidi, Oum EL Bouaghi	Examiner
Pr. Abbas BOUKHARI	University of Badji Mokhtar, Annaba	Examiner

**\*July 2<sup>nd</sup> 2017\***

## *DEDICATION*

*All praise and glory to the Almighty ALLAH who gave me courage and patience to carry out this work,  
May ALLAH will give me strength I need to carry on...*



*A ALLAH le tout puissant, pour m'avoir donné la patience, la volonté et le courage nécessaire pour  
mener à bien ce travail.*



## ACKNOWLEDGMENTS

First of all, I would like to express my deepest gratitude to all **Heads of the Department of Chemistry and the Faculty of Exact Sciences, University of Brothers Mentouri, Constantine**, I am also very grateful to the **Algerian Ministry of Higher Education and Scientific Research** for a Scholarship (PNE 2014/2015), and the **University of Mississippi, USA**, without their support I would not have been able to achieve what I have achieved.

I would like to thank my advisor, **Dr. Samira Benyahia**, Lecturer, Higher School of Industrial Technologies, (ESTI), Annaba, for giving me the opportunity to work on this project and for her continuous encouragement. In addition, I would like to thank **Dr. Stephen J. Cutler**, Major Professor, Professor of Medicinal Chemistry, University of South Carolina, USA, I am so grateful that he has given me the opportunity to pursue my research in his laboratory and he has always been there for advice and assistance and providing me with a compatible and supportive atmosphere for the research. Additionally, his magnetic personality has inspired me and will have a significant positive impact on my career and life.

I am deeply thankful to **Pr. Salah AKKAL**, University of Constantine for encouragement during this work, for also serving as Chairman of my thesis committee. I am also thankful to **Pr. Souad AMEDDAH**, University of Brothers, Constantine, **Pr. Nouredine GHERRAF**, University Larbi Ben M' Hidi and **Pr. Abbes BOUKHARI** for serving as member of my thesis, for giving his valuable time to discuss and guide my dissertation work.

I am deeply grateful to **Pr. Samir Benayache** for giving me the opportunity to pursue my doctoral research in his laboratory and for his encouragement. Thanks are also due to **Pr. Fadila Benayache** for her continuous encouragement and kindness.

I am profoundly grateful to **Dr. Juan Francisco Leon** for his help, guidance and assistance of my research work, also for his friendship and kindness.

I am deeply thankful to **Dr. Khaled M. Elokely** and **Dr. Manal Nael** for their friendship, kind and generous help and for their invaluable contribution in this work especially for molecular modeling work and CD calculation.

I would also like to thank **Dr. Mohamed M. Radwan**, who has provided me with excellent knowledge in spectroscopy, for his invaluable advice, helpful suggestions and assistance especially in structural elucidation. Special thanks to **Dr. Mohammed Zaki** for his friendship and his great assistance in data management. and his willingness to help with any problems I faced and who even after leaving Ole Miss still offered help and suggestions.

I am also thankful to **Dr. Amer Tarawneh** for his friendship, assistance and help.

I want to give special thanks to **Dr. Samir A. Ross**, for his continuous encouragement during my stay in the University of Mississippi.

I want to give my sincere thanks to **Dr. Robert Doerksen** for great course of Drug Action and Design I, for sharing his knowledge and helping me to understand the principles of computational chemistry, also for his kindness and encouragement. I would like also to acknowledge **Drs. Daneel Ferreira, Jordan Zjawiony** for courses of Organic chemistry and Natural Products Chemistry.

Thanks are also due to **Drs. Narayan D. Chaurasiya, Melissa Jacob, Shabana I. Khan, David S. Pasco and Babu Tekwani**, for MAO testing, antimicrobial, antimalarial, cytotoxicity, Transfection and Luciferase.

I would like also to thank **Dr. Yan-Hong Wang** for his generous assistance in the HPLC analysis work. I

## Acknowledgment

am also thankful to **Dr. Baharhi Avula** for HR-ESI-MS.

Hearty thanks to my friends **Dr. Shaymaa Makram Mostafa**, **Dr. Nesma Mohamed**, **Dr. Enas Ebrahim**, **Dr. Munia Swailleh** and to the Egyptian community in Oxford, Mississippi, for their friendship, and continuous help and assistance. Many thanks to all my friends in the University of Mississippi, especially **Dr. Yelkaira Vasquez**, **Dr. Cristina Avonto**, **Dr. Marco Mottinilli**, **Dr. Sebastiano Intagliata**, **Dr. Walid Alsharif**, **Dr. John Alexander Lobur** and **Mrs. Tracy Case Koslowski** and her family, for the nice multicultural time I spent with them, for their friendship, help and assistance.

I would like to express my appreciation to all the people around me during my stay at the University of Mississippi. Sincere thanks to those who gave freely their time and facilitated my research work. Also, many thanks to all the faculty, staffs and graduate students in the Department of Medicinal Chemistry.

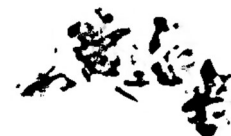
I would like to extend my thanks to **Dr. Piotr P. Wiczorek**, Prof. Dr. Hab. Inz., Faculty of Chemistry, Opole University, for giving me the opportunity to pursue a part of my research in his laboratory. Thanks are also due to **Dr. Izabela Jasika-Misiak**, Lecturer, Faculty of Chemistry, Opole University, and **Mrs. Alicja M. Nadzikiewicz-Szpon**, st. tech. Faculty of Chemistry, Opole University, for their friendship and help. I greatly appreciate all the help, friendship, technique support and love from the members of his Team during my stay in Opole.

No words can express my gratitude to **Pr. Farida Hobar**, Rector of the University of Mohamed Larbi Ben M'Hidi, Oum EL Bouaghi, for her help, continuous assistance, her kindness and friendship, her great personality has inspired me forever.

Finally, I would like to thank all my colleagues and friends in the Department of Chemistry, University of Constantine, especially **Mouna Hamlaoui**, **Nabila Zaabat**, **Hanane Belbache** and **Nesrine Benarous** for their friendship, encouragement and assistance.

Last but not least, I am deeply thankful to my parents, my sisters and brothers and to everyone who has been part of my life 's journey.

Farida Larit



## LIST OF ABBREVIATIONS

°C	Degrees Celsius.
<i>br.s.</i>	broad singlet.
BuOH	<i>n</i> -Butanol;
CB1	Cannabinoid1
CB2	Cannabinoid2
CC	Columnchromatography
CDCl <sub>3</sub>	deuterated chloroform.
CD <sub>3</sub> OD	deuterated methanol.
CD	Circulardichroism
CH <sub>2</sub> CL <sub>2</sub>	Dichloromethane;
CHCl <sub>3</sub>	Chloroform;
CNS	Central Nervous System.
1D	Onedimensional
2D	Twodimensional
DCM	Dichloromethane
<i>d</i>	doublet.
<i>dd</i>	doublet of doublet.
DA	Dopamine.
DCM	Dichloromethane.
DEPT	Distortionless Enhancement by Polarization Transfer.
DFMO	DiFluoroMethylOrnithine.
DMSO- <i>d</i> <sub>6</sub>	Deuterated Dimethyl Sulfoxide.
DMEM	Dulbecco's Modified Eagle's Medium.
DEPT	Distortionlessenhancementbypolarizationtransfer
ECD	Electronic circular dichroism.
EtOAc	Ethyl acetate.
Ext	Extract.
FAD	Flavin adenine dinucleotide.
FBS	Fetal Bovine Serum.
FID	Flame ionization detector.
Fig.	Figure.
Fr.	Fraction.
GPCRs	Gprotein-coupledreceptors.
GC/MS	Gas Chromatography/ Mass Spectrometry.
GLC	Gas Liquid Chromatography.
Galac.	$\beta$ -D-galactopyranoside.
Glu.	$\beta$ -D-glucopyranoside.
1H-	1H COSY Homo-nuclear Correlation Spectroscopy.
HepG2	Human hepatoma cells.
HMBC	Heteronuclear Multiple Bond Connectivity.
HMQC	Heteronuclear Multiple Quantum Coherence.
HR-ESI-MS	High resolution Electro Spray Ionization Mass.
Hz	Hertz.
ID	Internal Diameter.

## List of Abbreviations

inh.	inhibition.
<i>J</i>	coupling constant.
L	Length.
<i>J</i>	coupling constant.
L	Length.
μ	micron.
M+	Molecular ion peak.
m	multiplet.
MAO	Monoamine oxidase;
MAO-A	Recombinant human inhibitor;
MAO-B	Recombinant human inhibitor.
Me	Methyl.
MeCN	Acetonitrile HPLC grade
mg	milligrams.
min.	minutes.
mL	milli Liters.
NCNPR	National Center of Natural Products Research.
NMR	Nuclear Magnetic Resonance.
No.	Number.
NOESY	Nuclear Over-hauser Enhancement Spectroscopy.
PCM	Polarizable Continuum Model.
ppm	part per million.
Ref.	References.
<i>R<sub>f</sub></i>	Retardation factor.
rha.	$\alpha$ -L-rhamnopyranoside.
rut.	$\beta$ -D-rutinoside.
ROESY	Rotating-frame Enhancement Spectroscopy.
RP	Reversed Phase.
s	singlet.
S.D.	Standard Deviation.
SPE	Solid-phase extraction cartridge.
TF	Total flavonoid
TLC	Thin Layer Chromatography.
TMS	Tetra Methyl Silane.
TOCSY	Total correlation spectroscopy
TPC	Total phenolic content
UV/Vis	Ultra-Violet/Visible.

## TABLE OF CONTENTS

<b><u>DEDICATION</u></b> .....	<b>II</b>
<b><u>ACKNOWLEDGMENTS</u></b> .....	<b>III</b>
<b><u>LIST OF ABBREVIATIONS</u></b> .....	<b>V</b>
<b><u>TABLE OF CONTENTS</u></b> .....	<b>VII</b>
<b><u>LIST OF TABLES</u></b> .....	<b>XIII</b>
<b><u>LIST OF FIGURES</u></b> .....	<b>XVIII</b>
<b><u>PREFACE</u></b> .....	<b>1</b>
<b><u>PART I: General Introduction</u></b> .....	<b>4</b>
<b>CHAPTER 1: Background</b> .....	<b>5</b>
<b>I.1. Background</b> .....	<b>6</b>
<b>I.1.1. Literature review of the genus Cytisus</b>	<b>13</b>
<b>I.1.1.1. Phytochemical review of Cytisus</b>	<b>14</b>
<b>I.1.1.2. Biological Review of Cytisus</b>	<b>22</b>
<b>I.1.2. Classification of Fabaceae and the Genus Cytisus L</b>	<b>22</b>
<b>I.1.3. Use of Cytisus genus in traditional medicine</b>	<b>24</b>
<b>I.1.4. Economic Importance of the family of Fabaceae and Cytisus genus</b>	<b>24</b>
<b>I.1.5. Taxonomical identification of Cytisus villosus (Pourr.) in the plant kingdom</b>	<b>25</b>
<b>I.1.6. Description of the plant under investigation</b>	<b>25</b>
<b>I.1.7. Geographic distribution of Cytisus villosus</b>	<b>26</b>
<b>I.1.8. Literature review on the genus Hypericum</b>	<b>27</b>
<b>I.1.8.1. Phytochemical review of Hypericum</b>	<b>28</b>
<b>I.1.8.2 Biological review of Hypericum</b>	<b>40</b>
<b>I.1.9. Classification of Clusiaceae and Hypericum L. genus</b>	<b>41</b>
<b>I.1.10 Use of Hypericum in traditional medicine...</b>	<b>42</b>
<b>I.1.11.Economic Importance of Clusiaceae and Hypericum.....</b>	<b>43</b>
<b>I.1.12. Taxonomical identification of Hypericum afrum in the plant kingdom...</b>	<b>44</b>
<b>I.1.13. Description of the plant under investigation...</b>	<b>44</b>
<b>I.1.14. Geographic distribution of Hypericum afrum...</b>	<b>45</b>
<b>CHAPTER 2: Material, Apparatus and Methods</b> .....	<b>46</b>

I.2. Material, Apparatus and Methods ..	47
I.2.1. . Material	47
I.2.1.1.Plants Material	47
I.2.1.2.Materials for chemical study	47
I.2.1.3.Material for UPLC-UV/MS analysis	49
I.2.1.4.Materials for biological study	49
<b>I.2.2. Apparatus</b>	<b>50</b>
I.2.2.1.Apparatus for chemical study	50
I.2.2.2 Apparatus for analytical study	52
I.2.2.3.Apparatus and chromatographic conditions for UPLC-UV/MS analysis	52
I.2.2.4.Apparatus for biological study...	52
<b>I.2.3 Methods</b>	<b>53</b>
I.2.3.1.Analytical StudyA.1. Hydrolysis of flavonoids glycosides	53
I.2.3.2. Conformational analysis and geometry optimization...	55
I.2.3.3.Biological Study...	56
I.2.3.4.Molecular modeling study...	65
<b>I.3. References</b>	<b>67</b>
<b><u>PART II: Phytochemical study of <i>Cytisus villosus</i> and <i>Hypericum afrum</i></u></b>	<b>80</b>
<b>CHAPTER 1: Phytochemical screening, extraction, fractionation and isolation of constituents of <i>Cytisus villosus</i>...</b>	<b>81</b>
II.1. Phytochemical screening, extraction, fractionation and isolation of constituents of <i>Cytisus villosus</i>	82
II.1.1. Preliminary phytochemical screening	82
II.1.2. Quantitative evaluation of Total phenol and flavonoids content	82
II.1.3. Extraction and initial fractionation	84
II.1.3.1. Hydroalcoholic extraction	84
II.1.3.1.1. Isolation of the constituents of the chloroform fraction	84
II.1.3.1.2. Isolation of the constituents of the Ethyl acetate	85
II.1.3.1.3. Isolation of the constituents of the <i>n</i> -butanol fraction	87
II.1.3.2. Alkaloids Extraction	88
II.1.3.2.1. Isolation of the constituents of the Alkaloids fraction	89



<b>II.1.4.</b>	Identification and structural elucidation of the compounds isolated from <i>Cytisus villosus</i>	90
<b>II.1.4.1</b>	<b>Alkaloids</b>	<b>90</b>
<b>II.1.4.1.1.</b>	Compound CVK1	90
<b>II.1.4.2.</b>	<b>Terpenoids</b>	<b>98</b>
<b>II.1.4.2.1.</b>	Compound CVT1	98
<b>II.1.4.3.</b>	<b>Isoflavonoids</b>	<b>110</b>
<b>II.1.4.3.1.</b>	Compound CVS1	<b>110</b>
<b>II.1.4.3.2.</b>	Compound CVS2	122
<b>II.1.4.4.</b>	<b>Flavonoids</b>	<b>128</b>
<b>II.1.4.4.1.</b>	Compound CVF1	<b>128</b>
<b>II.1.4.4.2.</b>	Compound CVF2	<b>134</b>
<b>II.1.4.4.3.</b>	Compound CVF3	141
<b>II.1.5.</b>	<b>References</b>	<b>150</b>
<b>CHAPTER 2: Phytochemical screening, extraction, fractionation and isolation of constituents of <i>Hypericum afrum</i></b>		<b>153</b>
<b>II.2.</b>	Phytochemical screening, extraction, fractionation and isolation of constituents of <i>Hypericum afrum</i>	154
<b>II.2.1</b>	Preliminary phytochemical screening	154
<b>II.2.2.</b>	Determination of Total phenolic and Total flavonoid contents	154
<b>II.2.3.</b>	Extraction and initial fractionation	155
<b>II.2.3.1.</b>	Hydroalcoholic extraction	155
<b>II.2.3.2.</b>	Isolation of the active constituents of the chloroformic fraction	156
<b>II.2.3.3.</b>	Isolation of the active constituents of the ethyl acetate fraction	157
<b>II.2.3.4.</b>	Isolation of the active constituents of the butanolic fraction	158
<b>II.2.4.</b>	Identification and structure elucidation of the compounds isolated from <i>Hypericum afrum</i>	159
<b>II.2.4.1</b>	<b>Sterols</b>	159
<b>II.2.4.1.1</b>	Compound HAT1	159
<b>II.2.4.2.</b>	<b>Phloroglucinols</b>	164
<b>II.2.4.2.1.</b>	Compound HAP1	164
<b>II.2.4.3.</b>	<b>Naphthodianthrones</b>	175

<b>II.2.4.3.1.</b>	Compound <b>HAN1</b>	<b>175</b>
<b>II.2.4.3.2.</b>	Compound <b>HAN2</b>	<b>178</b>
<b>II.2.4.4.</b>	<b>Flavonoids</b>	<b>181</b>
<b>II.2.4.4.1.</b>	Compound <b>HAF1</b>	<b>181</b>
<b>II.2.4.4.2.</b>	Compound <b>HAF2</b>	<b>186</b>
<b>II.2.4.4.3.</b>	Compound <b>HAF3</b>	<b>191</b>
<b>II.2.4.4.4.</b>	Compound <b>HAF4</b>	<b>198</b>
<b>II.2.4.4.5.</b>	Compound <b>HAF5</b>	<b>205</b>
<b>II.2.4.4.6.</b>	Compound <b>HAF6</b>	<b>212</b>
<b>II.2.4.5.</b>	<b>Biflavonoids</b>	<b>218</b>
<b>II.2.4.5.1.</b>	Compound <b>HAB1</b>	<b>218</b>
<b>II.2.4.6.</b>	<b>Cinnamic acid derivatives</b>	<b>225</b>
<b>II.2.4.6.1.</b>	Compound <b>HAC1</b>	<b>225</b>
<b>II.2.4.6.2</b>	Compound <b>HAC2</b>	<b>234</b>
<b>II.2.5.</b>	<b>References</b>	<b>242</b>
	<b><u>Part III. Biological Study</u></b>	<b>246</b>
<b>III.1.</b>	Opioid &cannabinoid receptor binding affinity	247
<b>III.2.</b>	Antimalarial assay	248
<b>III.3.</b>	Antimicrobial activity	250
<b>III.4.</b>	Antiprotozoal assay	252
<b>III.5.</b>	Cytotoxicity	259
<b>III.6.</b>	Transfection and luciferase assays	261
<b>III.7.</b>	Antioxidant activity	261
<b>III.7.1.</b>	2,2-Diphenyl-1-picrylhydrazyl (DPPH) Assay	262
<b>III.7.2.</b>	Assay for the Inhibition of Cellular Oxidative Stress and anti-inflammatory activity	266
<b>III.8.</b>	Monoamine oxidase inhibition (MAOI) assay	270
<b>III.9.</b>	<b>References</b>	<b>277</b>
	<b><u>PART IV: Molecular Modeling and MD Simulation Studies</u></b>	<b>279</b>
<b>IV.</b>	Molecular Modeling and MD Simulation Studies	280
<b>IV.1</b>	Introduction	280
<b>IV.2.</b>	Medicinal Chemistry and Drug discovery	<b>281</b>

<b>IV.3</b>	Docking Methodologies: Background	281
<b>IV.4.</b>	Molecular Mechanics	282
<b>IV.4.1.</b>	Background	<b>282</b>
<b>IV.4.2.</b>	Molecular mechanics principles	<b>282</b>
<b>IV.4.3.</b>	Quantum mechanics (QM) compared to Molecular mechanics (MM)	<b>283</b>
<b>IV.4.4.</b>	Applicability of Molecular Mechanics	<b>284</b>
<b>IV.4.5.</b>	Types of terms in molecular mechanics	<b>284</b>
<b>IV.4.5.1.</b>	Bonded Interactions	284
<b>IV.4.5.2.</b>	Anharmonicity and cross-terms	<b>285</b>
<b>IV.4.5.3.</b>	Non-bonded interactions	<b>285</b>
<b>IV.4.6.</b>	Molecular Mechanics Energy	286
<b>IV.5 .</b>	Force-field definition	<b>288</b>
<b>IV.5.1.</b>	AMBER force field	<b>289</b>
<b>IV.5.2.</b>	AMBER force field details	<b>289</b>
<b>IV.5.3.</b>	CHARMm/CHARMM force field	289
<b>IV.5.4.</b>	CVFF force field	<b>290</b>
<b>IV.5.5.</b>	OPLS force field	<b>290</b>
<b>IV.6</b>	Molecular Dynamics (MD) and related methods	290
<b>IV.6.1.</b>	Background	<b>290</b>
<b>IV.6.2.</b>	Molecular Dynamics: aspects	291
<b>IV.6.3.</b>	Molecular Dynamics Simulation: Applicability	291
<b>IV.7.</b>	Monoamine Oxidases Properties	292
<b>IV.7.1.</b>	Crystallographic and Structural Properties of MAO Isoenzymes	292
<b>IV.7.2.</b>	Biosynthesis and Biodegradation of Neurotransmitters	293
<b>IV.7.3.</b>	Classifications of Monoamine Oxidase Inhibitors	296
<b>IV.8.</b>	Aim of the Molecular Modeling study	296
<b>IV.9.</b>	Results and discussion	297
<b>IV.9.1.</b>	Docking	297
<b>IV.9.2.</b>	MD Simulation	302
<b>IV.9.3.</b>	Conclusion	309
<b>IV.10.</b>	References	<b>310</b>
<b><u>General summary, Conclusion &amp; perspectives</u></b>		<b>315</b>

<b><u>RÉSUMÉ : Étude Phytochimique et Biologique de deux Plantes Médicinales Algériennes</u></b> <b><u><i>Cytisus villosus</i> Pourr. (Fabaceae) et <i>Hypericum afrum</i> Lam. (Hypericaceae)</u></b>	329
<b><u>ملخص</u></b>	350
<b><u>Abstract</u></b>	351
<b><u>RESUME</u></b>	352

## LIST OF TABLES

### PART I: CHAPTER 1&2

<b>Table I 1.</b> Reported isolated flavonoids from different Cytisus species.....	14
<b>Table I 2.</b> Reported isolated Alkaloids from different Cytisus species .....	16
<b>Table I 3.</b> Reported isolated Alkenols from different Cytisus species .....	17
<b>Table I 4.</b> Reported isolated Alkanone from different Cytisus species .....	18
<b>Table I 5.</b> Reported isolated Alicyclic from different Cytisus species .....	18
<b>Table I 6.</b> Reported isolated Benzenoid from different Cytisus species.....	18
<b>Table I 7.</b> Reported isolated carotenoids from different Cytisus species .....	19
<b>Table I 8.</b> Reported isolated coumarins from different Cytisus species .....	19
<b>Table I 9.</b> Reported isolated steroids from different Cytisus species .....	20
<b>Table I 10.</b> Reported isolated Lipids from different Cytisus species .....	20
<b>Table I 11.</b> Reported isolated Monoterpenes from different Cytisus species.....	21
<b>Table I 12.</b> Reported isolated Phenyl propanoids from different species of Cytisus .....	21
<b>Table I 13.</b> A list of biological activities reported from certain species of Cytisus .....	22
<b>Table I 14.</b> Reported isolated Essential oil components of different Hypericum species .....	28
<b>Table I 15.</b> Reported isolated triterpenoids and derived sterols of different Hypericum species	30
<b>Table I 16.</b> Reported isolated Benzoic and Cinnamic acid derivatives .....	32
<b>Table I 17.</b> Reported isolated flavonol glycoside and biflavones different Hypericum species .	33
<b>Table I 18.</b> Reported isolated tannins and proanthocyanidines of different Hypericum species	35
<b>Table I 19.</b> Reported isolated xanthones of different Hypericum species.....	36
<b>Table I 20.</b> Reported isolated anthraquinones and derives of different Hypericum species .....	37
<b>Table I 21.</b> Reported isolated phloroglucinols of different Hypericum species.....	38
<b>Table I 22.</b> A list of biological activities reported from different Hypericum species.....	40
<b>Table I 23.</b> A list of the used chromatographic solvent systems: .....	48
<b>Table I 24.</b> Assay conditions for cannabinoid binding assay	63
<b>Table I 25.</b> Assay conditions for opioid binding assay	64

**PART II: CHAPTER 1**

<b>Table II.1. 1.</b> Results of the preliminary phytochemical screening of <i>Cytisus villosus</i> aerial parts	82
<b>Table II.1. 2.</b> Total phenolic and flavonoid contents of crud extract fractions from <i>C. villosus</i>	83
<b>Table II.1. 3.</b> $^1\text{H}$ -, $^{13}\text{C}$ -NMR and HMBC spectral data of compound <b>CVK1</b>	90
<b>Table II.1. 4.</b> $^1\text{H}$ -, $^{13}\text{C}$ -NMR and HMBC spectral data of compound <b>CVT1</b>	99
<b>Table II.1. 5.</b> $^1\text{H}$ NMR and $^{13}\text{C}$ NMR spectroscopic data of compound <b>CVS1</b> (400 MHz, 100 MHz, DMSO- $d_6$ , J in Hz, $\delta$ in ppm)	111
<b>Table II.1. 6.</b> $^1\text{H}$ -, $^{13}\text{C}$ -NMR and HMBC spectral data of compound <b>CVS2</b>	122
<b>Table II.1. 7.</b> $^{13}\text{C}$ -NMR and HMBC spectral data of compound <b>CVF1</b> (400 MHz, 100 MHz, DMSO- $d_6$ )	128
<b>Table II.1. 8.</b> $^1\text{H}$ -, $^{13}\text{C}$ -NMR and HMBC spectral data of compound <b>CVF2</b> (400 MHz, 100 MHz, DMSO- $d_6$ )	134
<b>Table II.1. 9.</b> $^1\text{H}$ -, and $^{13}\text{C}$ -NMR spectral data of compound <b>CVF3</b>	141

**PART II: CHAPTER 2**

<b>Table II.2. 1.</b> Results of the preliminary phytochemical screening of <i>H. afrum</i> aerial parts .....	154
<b>Table II.2. 2.</b> Total phenolic and flavonoid contents of <i>H. afrum</i> fractions .....	155
<b>Table II.2. 3.</b> <sup>1</sup> H-, <sup>13</sup> C-NMR and HMBC spectral data of compound <b>HAT1</b> (600 MHz, 175 MHz, CDCl <sub>3</sub> ) .....	159
<b>Table II.2. 4.</b> <sup>1</sup> H-, <sup>13</sup> C-NMR and HMBC spectral data of compound <b>HAP1</b> .....	165
<b>Table II.2. 5.</b> <sup>1</sup> H-NMR spectral data of compound <b>HAN1</b> (500 MHz, DMSO-d <sub>6</sub> ) ..	175
<b>Table II.2. 6.</b> <sup>1</sup> H-NMR spectral data of compound <b>HAN2</b> (500 MHz, DMSO-d <sub>6</sub> ) ..	178
<b>Table II.2. 7.</b> <sup>1</sup> H-, <sup>13</sup> C-NMR and HMBC spectral data of compound <b>HAF1</b> (400 MHz, 100MHz, DMSO-d <sub>6</sub> ) .....	181
<b>Table II.2. 8.</b> <sup>1</sup> H-, <sup>13</sup> C-NMR and HMBC spectral data of compound <b>HAF2</b> (400 MHz, 100MHz, DMSO-d <sub>6</sub> ) .....	186
<b>Table II.2. 9.</b> <sup>1</sup> H-, <sup>13</sup> C-NMR and HMBC spectral data of compound <b>HAF3</b> (400 MHz, 100MHz, DMSO-d <sub>6</sub> ) .....	191
<b>Table II.2. 10.</b> <sup>1</sup> H-, <sup>13</sup> C-NMR and HMBC spectral data of compound <b>HAF4</b> (400 MHz, 100MHz, Methanol-d <sub>4</sub> , DMSO-d <sub>6</sub> ) .....	198
<b>Table II.2. 11.</b> <sup>1</sup> H-, <sup>13</sup> C-NMR and HMBC spectral data of compound <b>HAF5</b> (400 MHz, 100MHz Methanol-d <sub>4</sub> ) .....	205
<b>Table II.2. 12.</b> <sup>1</sup> H-, <sup>13</sup> C-NMR and HMBC spectral data of compound <b>HAF6</b> (400 MHz, 100MHz, Methanol-d <sub>4</sub> ) .....	212
<b>Table II.2. 13.</b> <sup>1</sup> H-, <sup>13</sup> C-NMR and HMBC spectral data of compound <b>HAB1</b> (400 MHz, 100MHz, DMSO-d <sub>6</sub> ) .....	218
<b>Table II.2. 14.</b> <sup>1</sup> H-, <sup>13</sup> C-NMR and HMBC spectral data of compound <b>HAC1</b> (400 MHz, 100MHz, DMSO-d <sub>6</sub> ) .....	225
<b>Table II.2. 15.</b> <sup>1</sup> H-, <sup>13</sup> C-NMR and HMBC spectral data of compound <b>HAC2</b> (400 MHz, 100MHz Methanol-d <sub>4</sub> ) .....	234

**PART III:**

**Table III. 3.** Results for cannabinoid and opioid receptor binding assay (percent of inhibition): 248

**Table III. 4.** Antimalarial screen results of extracts ..... 249

**Table III. 5.** Antimalarial screen results of some isolated compounds ..... 249

**Table III. 6.** Antibacterial and antifungal results of plant extracts..... 251

**Table III. 7.** Antibacterial and antifungal results of pure compounds isolated ..... 251

**Table III. 8.** Antiprotozoal activities of the plants extracts ..... 256

**Table III. 9.** Results of secondary antiprotozoal screening of plants fractions ..... 256

**Table III. 10.** Results of secondary antiprotozoal screening of pure compounds isolated from *H. afrum* and *C. villosus* ..... 257

**Table III. 11.** Cytotoxic activity of Fractions and certain pure compounds from *C. villosus* and *H. afrum*..... 260

**Table III. 12.** Activity of New Compound **HAP1** (IC<sub>50</sub> values in μM) against Cancer-Related Signaling Pathways in HeLa Cells ..... 261

**Table III. 13.** Antioxidant properties of fractions from *C. villosus* and *H. afrum* as determined by 2,2-diphenyl 1-picrylhydrazyl (DPPH) radical scavenging..... 263

**Table III. 14.** Potential antioxidant activity of fractions and certain isolated pure compounds.... 267

**Table III. 15.** Potential Anti-inflammatory Activity of fractions and certain pure compounds.... 268

**Table III. 16.** Potential Anti-inflammatory Activity of fractions and certain pure compounds..... 269

**Table III. 17.** Inhibition of recombinant human Monoamine Amine Oxidase-A and B by *Hypericum afrum* and *Cytisus villosus* fractions and pure constituents..... 274

**Table III. 18.** Inhibition of recombinant human Monoamine Amine Oxidase-A and B by *Hypericum afrum* and *Cytisus villosus* pure constituents..... 275



**GENERAL SUMMARY**

**Table 1.** A list of the isolated compounds from *Cytisus villosus* aerial parts ..... 318

**Table 2.** A list of the isolated compounds from *Hypericum afrom* aerial parts ..... 321

**Tableau 1.** La teneur totale en composés phénoliques et flavonoïdes de l'espèce *C. villosus* .. 332

**Tableau 2.** Liste des molécules séparées à partir de l'espèce *Cytisus villosus* ..... 332

**Tableau 3.** La teneur totale en composés phénoliques et flavonoïdes des fractions de l'espèce *H. afrom* ..... 335

**Tableau 4.** Liste des molécules isolées à partir de l'espèce *Hypericum afrom* ..... 335

## LIST OF FIGURES

### PART I: CHAPTER 1&2

<b>Figure I 1.</b> Some famous compounds derived from natural source.....	2
<b>Figure I 2.</b> Biosynthetic pathways of secondary metabolites in plants .....	7
<b>Figure I 3.</b> Terpenoids biosynthesis.....	8
<b>Figure I 4.</b> Biosynthesis of universal intermediates, skeleton structures, and some Lys-derived alkaloids found in plants.....	9
<b>Figure I 5.</b> Simplified pathway of the synthesis of phenolic compounds. ....	11
<b>Figure I 6.</b> Classification of phenolic compounds.....	11
<b>Figure I 7.</b> Scheme of the flavonoid biosynthetic pathway in plant cells.....	12
<b>Figure I 8.</b> Photos of some Cytisus species ( <b>A.</b> CytisusScoparius, <b>B.</b> Cytisus multiflorus, <b>C.</b> Cytisus purpureus Scop, <b>D.</b> Cytisus striatus) .....	23
<b>Figure I 9.</b> Photo of Cytisus villosus shrub and its leaves & flowers.....	26
<b>Figure I 10.</b> Geographic distribution map for Cytisus genus .....	26
<b>Figure I 11.</b> Photo of some Hypericum species. A; Hypericum olympicum, B; Hypericum Perfoliatum flowers, C; Hypericum aegypticum, D; Hypericum calycinum. ....	42
<b>Figure I 12.</b> Photo of Hypericum afrum Lam specimen .....	44
<b>Figure I 13.</b> Geographic distribution map for species of Hypericum L. genus .....	45
<b>Figure I. 20.</b> Typical TLC photography of certain extracts and fractions of the two species C.villosus and H. afrum colorized with 0.05% DPPH. ....	59

**PART II: CHAPTER 1**

<b>Figure II.1. 1.</b> Standard curve of Quercetin for the determination of TF .....	83
<b>Figure II.1. 2.</b> Standard curve of Gallic acid for determination of TPC .....	83
<b>Figure II.1. 3.</b> Evaluation of total phenolic and flavonoids in the plant extracts .....	83
<b>Figure II.1. 4.</b> Extraction and fractionation of the powdered aerial parts of <i>Cytisus villosus</i> .....	84
<b>Figure II.1. 5.</b> Fractionation of the chloroform fraction of <i>C. villosus</i> and isolation of its compounds .....	86
<b>Figure II.1. 6.</b> Fractionation of the ethyl acetate fraction of <i>C. villosus</i> and isolation of its compounds .....	86
<b>Figure II.1. 7.</b> Fractionation of the butanolic fraction of <i>C. villosus</i> isolation of its compounds ....	87
<b>Figure II.1. 8.</b> Acid-base extraction of alkaloids of <i>Cytisus villosus</i> .....	88
<b>Figure II.1. 9.</b> Fractionation of the Alkaloid fraction from <i>C. villosus</i> and isolation of its compounds .....	89
<b>Figure II.1. 10.</b> Profiles of silica gel TLC of compound <b>CVK1</b> .....	90
<b>Figure II.1. 11.</b> Important HMBC (H→C) COSY ( ) of compound <b>CVK1</b> .....	93
<b>Figure II.1. 12.</b> Conformation of (-)- Sparteine ( <b>CVK1</b> ) A),C-chair conformer (B), C-boat conformer(C) .....	93
<b>Figure II.1. 13.</b> Positive HR-ESI-MS of compound <b>CVK1</b> .....	93
<b>Figure II.1. 14.</b> <sup>1</sup> H-NMR Spectrum of Compound <b>CVK1</b> (CDCl <sub>3</sub> , 400 MHz).....	94
<b>Figure II.1. 15.</b> <sup>13</sup> C-NMR Spectrum of Compound <b>CVK1</b> (CDCl <sub>3</sub> , 100 MHz) .....	94
<b>Figure II.1. 16.</b> DEPT 135 Spectrum of Compound <b>CVK1</b> .....	95
<b>Figure II.1. 17.</b> Comparison of <sup>13</sup> C-NMR and DEPT-135 Spectrum of Compound <b>CVK1</b> .....	95
<b>Figure II.1. 18.</b> <sup>1</sup> H- <sup>1</sup> H COSY Spectrum of Compound <b>CVK1</b> .....	96
<b>Figure II.1. 19.</b> HSQC Spectrum of Compound <b>CVK1</b> .....	96
<b>Figure II.1. 20.</b> HMBC Spectrum of Compound <b>CVK1</b> .....	97
<b>Figure II.1. 21.</b> Profiles of silica gel TLC of compound <b>CVT1</b> : .....	98
<b>Figure II.1. 22.</b> Important HMBC (H→C) and <sup>1</sup> H- <sup>1</sup> H COSY (—) correlation of compound <b>CVT1</b> .....	101
<b>Figure II.1. 23.</b> The conformers of compound <b>CVT1</b> .....	103
<b>Figure II.1. 24.</b> The experimental and calculated ECD spectra of compound <b>CVT1</b> .....	103
<b>Figure II.1. 25.</b> Mass spectra of compound <b>CVT1</b> .....	104
<b>Figure II.1. 26.</b> <sup>1</sup> H-NMR Spectrum of Compound <b>CVT1</b> .....	105
<b>Figure II.1. 27.</b> <sup>13</sup> C- NMR Spectrum of Compound <b>CVT1</b> .....	105
<b>Figure II.1. 28.</b> DEPT-135 Spectrum of Compound <b>CVT1</b> .....	106
<b>Figure II.1. 29.</b> Comparison of <sup>13</sup> C-NMR and DEPT-135 Spectra of Compound <b>CVT1</b> .....	106
<b>Figure II.1. 30.</b> HSQC Spectrum of Compound <b>CVT1</b> .....	107
<b>Figure II.1. 31.</b> HSQC-TOCSY Spectrum of compound <b>CVT1</b> .....	107
<b>Figure II.1. 32.</b> <sup>1</sup> H- <sup>1</sup> H COSY Spectrum of Compound <b>CVT1</b> .....	108
<b>Figure II.1. 33.</b> TOCSY Spectrum of compound <b>CVT1</b> .....	108
<b>Figure II.1. 34.</b> HMBC Spectrum of Compound <b>CVT1</b> .....	109
<b>Figure II.1. 35.</b> Profiles of silica gel TLC of compound <b>CVS1</b> .....	110
<b>Figure II.1. 36.</b> Important HMBC (H→C) and TOCSY ( ) correlations of the compound <b>CVS1</b> .....	113
<b>Figure II.1. 37.</b> The most abundant conformers of the (S,S) isomer of compound <b>CVS1</b> .....	114
<b>Figure II.1. 38.</b> The calculated and experimental ECD of compound <b>CVS1</b> .....	115
<b>Figure II.1. 39.</b> Negative HR-ESI-MS-TOF of compound <b>CVS1</b> .....	115

<b>Figure II.1. 40.</b> <sup>1</sup> H-NMR Spectrum of Compound <b>CVS1</b> .....	116
<b>Figure II.1. 41.</b> Expanded <sup>1</sup> H-NMR Spectrum of Compound <b>CVS1</b> .....	117
<b>Figure II.1. 42.</b> <sup>13</sup> C-NMR Spectrum of Compound <b>CVS1</b> (DMSO-d <sub>6</sub> , 125 MHz).....	117
<b>Figure II.1. 43.</b> DEPT-135 Spectrum of Compound <b>CVS1</b> .....	118
<b>Figure II.1. 44.</b> Comparison of <sup>13</sup> C-NMR and DEPT-135 Spectrum of compound <b>CVS1</b> .....	118
<b>Figure II.1. 45.</b> HSQC Spectrum of Compound <b>CVS1</b> .....	119
<b>Figure II.1. 46.</b> TOCSY Spectrum of Compound <b>CVS1</b> .....	119
<b>Figure II.1. 47.</b> HSQC-TOCSY Spectrum of Compound <b>CVS1</b> .....	120
<b>Figure II.1. 48.</b> HMBC Spectrum of Compound <b>CVS1</b> .....	120
<b>Figure II.1. 49.</b> Expanded HMBC Spectrum of Compound <b>CVS1</b> .....	121
<b>Figure II.1. 50.</b> Important HMBC (H→C) correlations of the compound <b>CVS2</b> .....	124
<b>Figure II.1. 51.</b> Negative HR-ESI-MS of compound <b>CVS2</b> .....	124
<b>Figure II.1. 52.</b> <sup>1</sup> H-NMR Spectrum of Compound <b>CVS2</b> (Methanol-d <sub>4</sub> , 400 MHz).....	125
<b>Figure II.1. 53.</b> <sup>13</sup> C-NMR Spectrum of Compound <b>CVS2</b> .....	125
<b>Figure II.1. 54.</b> DEPT-135 Spectrum of Compound <b>CVS2</b> .....	126
<b>Figure II.1. 55.</b> HMQC Spectrum of Compound <b>CVS2</b> .....	126
<b>Figure II.1. 56.</b> HMBC Spectrum of Compound <b>CVS2</b> .....	127
<b>Figure II.1. 57.</b> Important HMBC (H→C) correlations of the compound <b>CVF1</b> .....	129
<b>Figure II.1. 58.</b> Mass spectra of compound <b>CVF1</b> .....	130
<b>Figure II.1. 59.</b> <sup>1</sup> H-NMR Spectrum of Compound <b>CVF1</b> .....	131
<b>Figure II.1. 60.</b> <sup>13</sup> C-NMR Spectrum of Compound <b>CVF1</b> .....	131
<b>Figure II.1. 61.</b> DEPT-135 Spectrum of Compound <b>CVF1</b> .....	132
<b>Figure II.1. 62.</b> HMQC Spectrum of Compound <b>CVF1</b> .....	132
<b>Figure II.1. 63.</b> HMBC Spectrum of Compound <b>CVF1</b> .....	133
<b>Figure II.1. 64.</b> Expanded HMBC Spectrum of Compound <b>CVF1</b> .....	133
<b>Figure II.1. 65.</b> Important HMBC (H→C) and <sup>1</sup> H- <sup>1</sup> H COSY ( ) correlations of compound <b>CVF2</b> .....	136
<b>Figure II.1. 66.</b> Positive HR-ESI-MS of compound <b>CVF2</b> .....	137
<b>Figure II.1. 67.</b> <sup>1</sup> H-NMR Spectrum of Compound <b>CVF2</b> .....	137
<b>Figure II.1. 68.</b> <sup>13</sup> C-NMR Spectrum of Compound <b>CVF2</b> (101 MHz, DMSO-d <sub>6</sub> ).....	138
<b>Figure II.1. 69.</b> DEPT 135 Spectrum of Compound <b>CVF2</b> .....	138
<b>Figure II.1. 70.</b> Comparison of <sup>13</sup> C- and DEPT NMR spectra of Compound <b>CVF2</b> .....	139
<b>Figure II.1. 71.</b> HSQC Spectrum of Compound <b>CVF2</b> .....	139
<b>Figure II.1. 72.</b> HMBC Spectrum of Compound <b>CVF2</b> .....	140
<b>Figure II.1. 73.</b> Important HMBC correlation (H→C) of compound <b>CVF3</b> .....	144
<b>Figure II.1. 74.</b> Mass spectra of compound <b>CVF3</b> .....	145
<b>Figure II.1. 75.</b> <sup>1</sup> H-NMR Spectrum of Compound <b>CVF3</b> .....	146
<b>Figure II.1. 76.</b> Expanded <sup>1</sup> H-NMR Spectrum of Compound <b>CVF3</b> .....	146
<b>Figure II.1. 77.</b> <sup>13</sup> C-NMR Spectrum of Compound <b>CVF3</b> .....	147
<b>Figure II.1. 78.</b> DEPT-135 Spectrum of Compound <b>CVF3</b> .....	147
<b>Figure II.1. 79.</b> Comparison of <sup>13</sup> C-NMR and DEPT-135 Spectrum of Compound <b>CVF3</b> .....	148
<b>Figure II.1. 80.</b> HSQC spectrum of Compound <b>CVF3</b> .....	148
<b>Figure II.1. 81.</b> HMBC spectrum of Compound <b>CVF3</b> .....	149
<b>Figure II.1. 82.</b> <sup>1</sup> H- <sup>1</sup> H COSY spectrum of Compound <b>CVF3</b> .....	149

**PART II: CHAPTER 2**

**FigureII.2. 1** Evaluation of total phenolic and flavonoids in the H. afrum fractions 155

**FigureII.2. 2.** Extraction and fractionation of the powdered aerial parts of Hypericum afrum..... 155

**FigureII.2. 3.** Fractionation of the Chloroform fraction and isolation of its compounds ..... 156

**FigureII.2. 4.** Fractionation of the Ethyl acetate fraction and isolation of its compounds ..... 157

**FigureII.2. 5.** Fractionation of the butanolic fraction and isolation of its compounds ..... 158

**FigureII.2. 6.** <sup>1</sup>H-NMR Spectrum of Compound **HAT1** (CDCl<sub>3</sub>, 600 MHz)..... 161

**FigureII.2. 7.** <sup>13</sup>C-NMR Spectrum of Compound **HAT1**(CDCl<sub>3</sub>, 175 MHz) ..... 162

**FigureII.2. 8.** DEPT135 Spectrum of Compound**HAT1**..... 162

**FigureII.2. 9.** Comparison of <sup>13</sup>C-NMR and DEPT135 Spectrum of Compound**HAT1** ..... 163

**FigureII.2. 10.** HSQC Spectrum of Compound **HAT1** ..... 163

**FigureII.2. 11.** Profiles of silica gel TLC of compound **HAP1**..... 164

**FigureII.2. 12.**Important COSY ( ) and HMBC (H→C) correlation of compound **HAP1**..... 167

**FigureII.2. 13.** The experimental and calculated ECD spectra of compound **HAP1**168

**FigureII.2. 14.** The most abundant conformers of isomer (R, R ) of compound **HAP1** ..... 168

**FigureII.2. 15.** Negative HRESIMS of compound **HAP1** ..... 169

**FigureII.2. 16.** The IR spectrum of compound **HAP1** ..... 169

**FigureII.2. 17.**<sup>1</sup>H-NMR Spectrum of Compound**HAP1**(CDCl<sub>3</sub>, 500 MHz)..... 170

**FigureII.2. 18.**<sup>13</sup>C-NMR Spectrum of Compound **HAP1** (CDCl<sub>3</sub>, 125 MHz)..... 171

**FigureII.2. 19.**DEPT135 Spectrum of Compound **HAP1** ..... 172

**FigureII.2. 20.** Comparison of <sup>13</sup>C-NMR and DEPT135 Spectra of Compound **HAP1** ..... 172

**FigureII.2. 21.** HSQC Spectrum of Compound **HAP1** ..... 173

**FigureII.2. 22.** <sup>1</sup>H-<sup>1</sup>H COSY Spectrum of Compound **HAP1** ..... 173

**FigureII.2. 23.** HMBC Spectrum of Compound **HAP1** ..... 174

**FigureII.2. 24.** Negative HR-ESI-MS of Compound **HAN1**..... 177

**FigureII.2. 25.** <sup>1</sup>H-NMR Spectrum of Compound **HAN1**(DMSO-d<sub>6</sub>, 500 MHz) .... 177

**FigureII.2. 26.** Negative HR-ESI-MS of Compound **HAN2**..... 180

**FigureII.2. 27.** <sup>1</sup>H-NMR Spectrum of Compound **HAN2** (DMSO-d<sub>6</sub>, 500 MHz) ... 180

**FigureII.2. 28.** Positive HR-ESI-MS of Compound **HAF1** ..... 183

**FigureII.2. 29.**<sup>1</sup>H-NMR Spectrum of Compound **HAF1**(DMSO-d<sub>6</sub>, 400 MHz) ..... 183

**FigureII.2. 30.** <sup>13</sup>C-NMR Spectrum of Compound **HAF1**(DMSO-d<sub>6</sub>, 100 MHz).... 184

**FigureII.2. 31.** DEPT-135 Spectrum of Compound **HAF1**..... 184

**FigureII.2. 32.** HSQC Spectrum of Compound **HAF1** ..... 185

**FigureII.2. 33.** HMBC Spectrum of Compound **HAF1** ..... 185

**FigureII.2. 34.** Positive HR-ESI-MS of Compound **HAF2** ..... 188

**FigureII.2. 35.**<sup>1</sup>H-NMR Spectrum of Compound **HAF2**(DMSO-d<sub>6</sub>, 400 MHz) ..... 188

**FigureII.2. 36.** <sup>13</sup>C-NMR Spectrum of Compound **HAF2** (DMSO-d<sub>6</sub>, 100 MHz)... 189

**FigureII.2. 37.** DEPT-135 Spectrum of Compound **HAF2**..... 189

**FigureII.2. 38.** HSQC Spectrum of Compound **HAF2** ..... 190

**FigureII.2. 39.** HMBC Spectrum of Compound **HAF2** ..... 190

FigureII.2. 40..Important HMBC (H→C) and COSY (H—H) correlations of compound HAF3 .....	193
FigureII.2. 41. Negative HR-ESI-MS of compound HAF3.....	193
FigureII.2. 42.... <sup>1</sup> H-NMR Spectrum of CompoundHAF3(DMSO-d <sub>6</sub> , 400 MHz)....	194
FigureII.2. 43. <sup>13</sup> C-NMR Spectrum of CompoundHAF3(DMSO-d <sub>6</sub> , 100 MHz) ...	194
FigureII.2. 44. DEPT135 Spectrum of Compound HAF3.....	195
FigureII.2. 45. . Comparison of <sup>13</sup> C-NMR and DEPT135 Spectrum of Compound HAF3.....	195
FigureII.2. 46. <sup>1</sup> H- <sup>1</sup> H COSY Spectrum of Compound HAF3.....	196
FigureII.2. 47. HSQC Spectrum of Compound HAF3 .....	196
FigureII.2. 48. HMBC Spectrum of Compound HAF3 .....	197
FigureII.2. 49. Important HMBC (H→C) and COSY (—) correlation of compound HAF4.....	200
FigureII.2. 50. Negative HR-ESI-MS spectrum of compound HAF4.....	201
FigureII.2. 51. <sup>1</sup> H-NMR Spectrum of Compound HAF4(Methanol-d <sub>4</sub> , 400 MHz) .	201
FigureII.2. 52. <sup>13</sup> C-NMR Spectrum of Compound HAF4 (Methanol-d <sub>4</sub> , 100 MHz) .....	202
FigureII.2. 53. DEPT135 Spectrum of Compound HAF4.....	202
FigureII.2. 54. HSQC Spectrum of Compound HAF4 .....	203
FigureII.2. 55. COSY spectrum of compound HAF4.....	203
FigureII.2. 56. HMBC Spectrum of Compound HAF4 .....	204
FigureII.2. 57 Important HMBC (H→C) correlation of compound HAF5. ....	207
FigureII.2. 58. Negative HR-ESI-MS of compound HAF5.....	207
FigureII.2. 59. <sup>1</sup> H-NMR Spectrum of Compound HAF5(Methanol-d <sub>4</sub> , 400 MHz) .	208
FigureII.2. 60. <sup>13</sup> C-NMR Spectrum of CompoundHAF5 (Methanol-d <sub>4</sub> , 100 MHz) .	209
FigureII.2. 61. DEPT135 Spectrum of Compound HAF5).....	209
FigureII.2. 62. Comparison of <sup>13</sup> C-NMR and DEPT 135 spectra of compound HAF5 .....	210
FigureII.2. 63. HSQC Spectrum of Compound HAF5 .....	210
FigureII.2. 64. HMBC Spectrum of Compound HAF5.....	211
FigureII.2. 65. Important HMBC (H→C) correlation of compound HAF6.....	214
FigureII.2. 66. Negative HR-ESI-MS of compound HAF6.....	215
FigureII.2. 67. <sup>1</sup> H-NMR Spectrum of Compound HAF6(Methanol-d <sub>4</sub> , 400 MHz) .	215
FigureII.2. 68. <sup>13</sup> C-NMR Spectrum of Compound HAF6(Methanol-d <sub>4</sub> , 100 MHz) .	216
FigureII.2. 69. DEPT135 Spectrum of Compound HAF6.....	216
FigureII.2. 70. HSQC Spectrum of Compound HAF6 .....	217
FigureII.2. 71. HMBC Spectrum of Compound HAF6.....	217
FigureII.2. 72. . Important HMBC (H→C) correlation of compound HAB1 .....	221
FigureII.2. 73 Positive HR-ESI-MS of Compound HAB1 .....	221
FigureII.2. 74. <sup>1</sup> H-NMR Spectrum of CompoundHAB1(DMSO-d <sub>6</sub> , 400 MHz) .....	222
FigureII.2. 75. <sup>13</sup> C-NMR Spectrum of Compound HAB1 (DMSO-d <sub>6</sub> , 100 MHz) ...	222
FigureII.2. 76. DEPT-135 Spectrum of Compound HAB1 .....	223
FigureII.2. 77. Comparison of <sup>13</sup> C-NMR and DEPT 135 of compound HAB1.....	223
FigureII.2. 78. HMBC Spectrum of Compound HAB1.....	224
FigureII.2. 79. Expanded HMBC Spectrum of Compound HAB1 .....	224
FigureII.2. 80. Key HMBC (H→C) and <sup>1</sup> H- <sup>1</sup> H COSY (—) correlations of compound HAC1 .....	227
FigureII.2. 81. Mass spectra of compound HAC1. .A. Negative HR-ESI-MS B. Positive HR-ESI-MS .....	228
FigureII.2. 82. <sup>1</sup> H-NMR Spectrum of CompoundHAC1(DMSO-d <sub>6</sub> , 400 MHz).....	229

**FigureII.2. 83.**  $^{13}\text{C}$ -NMR Spectrum of Compound **HAC1**(DMSO- $d_6$ , 100MHz).....230  
**FigureII.2. 84.** DEPT135 Spectrum of Compound **HAC1**.....230  
**FigureII.2. 85.** Comparison of DEPT135and  $^{13}\text{C}$ -NMR spectra of Compound **HAC1**  
.....231  
**FigureII.2. 86.** HSQC Spectrum of Compound **HAC1**.....231  
**FigureII.2. 87.** HMBC Spectrum of Compound **HAC1**.....232  
**FigureII.2. 88.**  $^1\text{H}$ - $^1\text{H}$  COSY Spectrum of Compound **HAC1** .....232  
**FigureII.2. 89.** NOESY spectrum of compound **HAC1**.....233  
**FigureII.2. 90.** Key HMBC (H→C) and  $^1\text{H}$ - $^1\text{H}$  COSY (—) correlations of compound  
**HAC2** .....236  
**FigureII.2. 91.** Mass spectra of compound **HAC2**. A. Positive HR-ESI-MS B. Negative  
HR-ESI-MS .....237  
**FigureII.2. 92.**  $^1\text{H}$ -NMR Spectrum of Compound **HAC2** (400 MHz).....238  
**FigureII.2. 93.**  $^{13}\text{C}$ -NMR Spectrum of Compound **HAC2**(100 MHz).....238  
**FigureII.2. 94.** DEPT-135 Spectrum of Compound **HAC2** .....239  
**FigureII.2. 95.** Comparison of  $^{13}\text{C}$ -NMR and DEPT-135 Spectra of Compound **HAC2**  
.....239  
**FigureII.2. 96.**  $^1\text{H}$ - $^1\text{H}$  COSY Spectrum of Compound **HAC2** .....240  
**FigureII.2. 97.** HSQC Spectrum of Compound **HAC2**.....240  
**FigureII.2. 98.** HMBC Spectrum of Compound **HAC2**.....241

**PART III**

**Figure III. 1.**Leishmania parasite ..... 252

**Figure III. 2.** Parasite, *Trypanosoma brucei* surrounded by red blood cells in a smear of infected blood. .... 253

**Figure III. 3.**Life Cycle of Leishmania (Centers for Disease Control and Prevention)..... 254

**Figure III. 4.**Life cycle of African trypanosomiasis (Centers for Disease Control and Prevention) ..... 255

**Figure III. 5.** In vitro primary screening of *C. villosus* (C.V) and *H. afrum* (H.A) aerial parts fractions for antitrypanosomal activity against *Trypanosoma brucei brucei*. .... 258

**Figure III. 6.** In vitro screen of compounds isolated from *C.villosus* and *H.afrum* aerial parts against *Trypanosoma brucei brucei*. .... 258

**Figure III. 7.** Radical scavenging effect of *Cytisus villosus* fractions on DPPH radical. .... 263

**Figure III. 8.** Radical scavenging effect of *Hypericum afrum* fractions on DPPH radical. .... 264

**Figure III. 9.**Comparison between total phenolic and flavonoid contents (TPC, TF) and DPPH (IC<sub>50</sub>) data in different fractions of plants under investigation. .... 265

**Figure III. 10.**Relationship between total phenolic content and antioxidant activity of *C. villosus* and *H. afrum*. fractions by DPPH assay. .... 265

**Figure III. 11.**Relationship between total flavonoid content and antioxidant activity of *C. villosus* and *H. afrum* fractions by cellular antioxidant assay. .... 265

**Figure III. 12.**Antioxidant activity of *Hypericum afrum* fractions at different concentrations by cellular antioxidant assay(CAA); data represent mean ± SD; n=3 level of significance: \*P < 0.05. .... 267

**Figure III. 13.** Antioxidant activity of *Cytisus villosus* fractions at different by cellular antioxidant assay(CAA). .... 268

**Figure III. 14.** The mechanism of potentiation of cardiovascular effects of tyramine: the 'cheese reaction' (Youdim et al., 2006) ..... 271

**Figure III. 15.**Sites of action of Parkinson's Disease Drugs role of Monoamine Oxidase in Dopamine Metabolism (Youdim et al., 2006)..... 272



**PART IV**

**Figure IV. 1.** Chemical Structures of compounds 1 (CVS2), 2 (CVF1), 3 (HAF1) and 4 (HAF2) ..... 281

**Figure IV. 2.** Molecular Mechanic ..... 285

**Figure IV. 3.** Molecular Mechanics Energy ..... 286

**Figure IV. 4.** Bending Energy ..... 287

**Figure IV. 5.** Torsional energy ..... 287

**Figure IV. 6.** Non-bonded energy..... 288

**Figure IV. 7.** Biliverdin reductase with NADPH cofactor, in water (Fu et al., 2012) ..... 291

**Figure IV. 8.** MAO-A structure is shown in illustration. The FAD-binding domain illustrated with blue, the substrate-binding domain red, and the C-terminal membrane region green..... 293

**Figure IV. 9.** MAO-B structure is shown in illustration. The FAD-binding domain illustrated with blue, the substrate-binding domain red, and the C-terminal membrane region green..... 293

**Figure IV. 10.** Chemical structures of some amines which are related with MAO isoenzymes (VARNALI, 2012)..... 294

**Figure IV. 11.** Biosynthesis of neurotransmitters Serotonin and Dopamine (Hare and Loer, 2004). ..... 295

**Figure IV. 12.** Biodegradation of catecholamines via COMT and MAO enzymes (Klabunde, 2009). ..... 295

**Figure IV. 13.** The binding mode of genistein in MAO A. Genistein is shown as pink balls and sticks. The interacting amino acids are shown as grey sticks. Protein is shown as cartoon with yellow helices, pink strands and green loops. All possible hydrogen bonds in the range of 3.5 Å are shown as yellow dots. .... 298

**Figure IV. 14.** The binding mode of chrysin in MAO A. Chrysin is shown as pink balls and sticks. The ..... 299

**Figure IV. 15.** The binding mode of genistein in MAO B. Genistein is shown as pink balls and sticks. The interacting amino acids are shown as grey sticks. Protein is shown as cartoon with yellow helices, pink strands and green loops. All possible hydrogen bonds in the range of 3.5 Å are shown as yellow dots..... 299

**Figure IV. 16.** The binding mode of chrysin in MAO B. Chrysin is shown as pink balls and sticks. The interacting amino acids are shown as grey sticks. Protein is shown as cartoon with yellow helices, pink strands and green loops All possible hydrogen bonds in the range of 3.5 Å are shown as yellow dots..... 300

**Figure IV. 17.** The binding mode of quercetin in MAO A. Quercetin is shown as pink balls and sticks. The interacting amino acids are shown as grey sticks. Protein is shown as cartoon with yellow helices, pink strands and green loops. All possible hydrogen bonds in the range of 3.5 Å are shown as yellow dots. .... 301

**Figure IV. 18.** The binding mode of myricetin in MAO A. Myricetin is shown as pink balls and sticks. The interacting amino acids are shown as grey sticks. Protein is shown as cartoon with yellow helices, pink strands and green loops. All possible hydrogen bonds in the range of 3.5 Å are shown as yellow dots. .... 301

**Figure IV. 19.** Ligand RMSF (HAF1)..... 302

**Figure IV. 20.** Protein-ligand contacts of compound HAF1. Four types protein-ligand interactions were monitored throughout the simulation: hydrogen bond, hydrophobic, ionic and water bridges. .... 303

<b>Figure IV. 21.</b> 2D interaction diagram of the detailed ligand atom interactions of compound <b>HAF1</b> with the surrounding amino acid residues of MAO-A. ....	305
<b>Figure IV. 22.</b> Ligand Torsion Profile ( <b>HAF1</b> ).....	305
<b>Figure IV. 23.</b> Ligand RMSF ( <b>HAF2</b> ). ....	306
<b>Figure IV. 24.</b> Protein-ligand contacts of compound <b>HAF2</b> . Hydrogen bonds, hydrophobic, ionic and water bridges were monitored throughout the simulation. ....	307
<b>Figure IV. 25.</b> 2D interaction diagram of compound <b>HAF2</b> with the amino acid residues of binding site of MAO-A.....	307
<b>Figure IV. 26.</b> Ligand Torsion Profile ( <b>HAF2</b> ).....	308

## PREFACE

**M**edicinal plants, especially those with ethnobotanical evidence of use for medicinal purposes, have become the sources of new drug candidates. The World Health Organization (WHO) estimates that 80% of the world's population depends on traditional medicine for treating their everyday health problems. A survey of plant-derived pure compounds used as drugs in countries hosting WHO-Traditional Medicine Centers indicated that, of 122 compounds identified, 80% were used for the same or related ethnomedical purposes and were derived from only 94 plant species (Cragg and Newman, 2013). Thus, it can be reasonably argued that medicinal plants have contributed a lot to the modern drug discovery (Jachak and Saklani, 2007; Raskin et al., 2002). Historically, the majority of new drugs were natural products or were inspired by natural compounds (secondary metabolites), over 120 of the most important medicines, including penicillin (1) and cyclosporine (2), are obtained from fungal extracts (Borel and Kis, 1991; Chain, 1979)

Some relevant examples are galegine (3), from *Galega officinalis* L., which was the model for the synthesis of metformin and other bisguanidine-type antidiabetic drugs (Graham et al., 2011). papaverine (4) from *Papaver somniferum* which formed the basis for verapamil used in the treatment of hypertension (Rates et al., 2015) One of the best example of ethnomedicine's role in guiding drug discovery and development is that of the antimalarial drugs, particularly quinine (5) and artemisinin (6) (Buss et al., 1995).

Plants have a long history of use in the treatment of cancer (Cragg and Newman, 2013). It is estimated that 60% of cancer therapeutics have been derived from nature whether directly through isolation or indirectly through semi-synthesis (Ibrahim et al., 2008). Various examples have been reported such as the Pacific yew tree (*Taxus brevifolia*) to treat breast cancer (Abal et al., 2003; Wani et al., 1971) and Diospyrin (7) from *Diospyros* species as a potential lead molecule to new drug against cancer as well as several other diseases like leishmaniasis, trypanosomiasis, malaria and tuberculosis (Hazra et al., 1987).

Research regarding natural psychoactive compounds has given a wealth of information to the disciplines of neuroscience. Some of them have been shown to exert beneficial effects for Parkinson's disease and depression. Prescribed as mild antidepressant therapeutic, commercially available products of *H. perforatum* are among the bestselling, most successful and effective herbs

in the world. Janssen's Alzheimer's drug, Galantamine (also called galanthamine, marketed by Janssen as Reminyl) was originally isolated from several plants, including daffodil bulbs, but is now synthesized (Loy and Schneider, 2006) is another example of pharmacognostic evaluation of medicinal plants Throughout time, many plants have been used for the treatment of mental problems. The acetylcholine receptor system was uncovered through the alkaloids nicotine from *Nicotiana* spp. and muscarine from *Amanita muscaria*, and was further probed using the belladonna alkaloids atropine and scopolamine, as well as (+)-tubocurarine from the tropical plant *Chondrodendron tomentosum*) Amphetamine, a derivative of ephedrine and cathinone from *Catha edulis*, continues to aid in unraveling the complexities of the dopamine receptor system (White and Kalivas, 1998). A good number of those are alkaloid-containing plants, as alkaloids are known to interact strongly with receptors in the central nervous system, but in recent years it has become clear that flavonoids may also play a role in enzyme- and receptor systems of the brain, exerting various effects on the central nervous system, including prevention of the neurodegeneration associated with Alzheimer's and Parkinson's diseases (Jäger and Saaby, 2011). It has been reported that Inhibitors of the monoamine oxidases have been used clinically for the treatment of depression, as well as Parkinson's, Alzheimer's and other neurodegenerative diseases (Gaweska and Fitzpatrick, 2011).

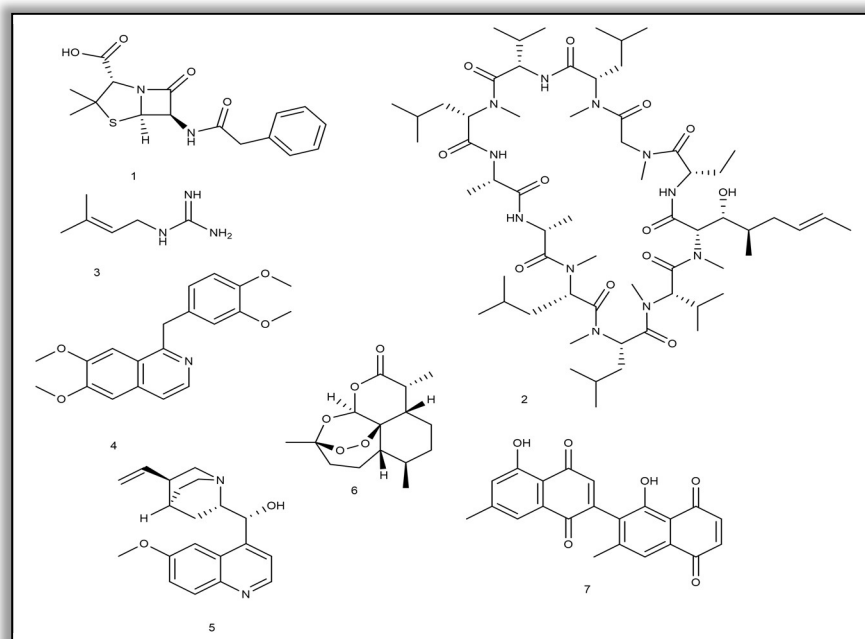


**Figure I 1.** Some famous compounds derived from natural source

During early 20th century, most of the drug discovery efforts were focused on extraction of the traditionally important medicinal plants and isolation of bioactive constituents. The advent of modern science, availability of advanced *in vitro* screening methods and sophisticated separation techniques were helpful in speeding up the drug discovery process from medicinal plants. With the adaptability of *in vitro* bioassays to screen hundreds of samples in a single run, it became possible for scientists to pursue a high volume of leads from ethnobotanical literature for screening against a particular disease target. After the preliminary screening, positive lead extracts would be subjected to chromatographic separations, followed by secondary screening procedures to obtain the pharmacologically relevant molecule(s) as the drug candidate. More natural product research is needed due to: unmet medical needs; remarkable diversity of structures and activities and utility as biochemical probes.

The aim of this study is to investigate the *in vitro* biological activity and to isolate lead active secondary metabolites of two plants namely, *Cytisus villosus* Pourr. and *Hypericum afrum* Lam. These plants have been selected for this study especially the endemic species *Hypericum afrum* has not previously been subjected to either chemical or biological investigations, and very few studies for *Cytisus villosus* Pourr.

The present study was planned to include the following parts:

**PART I:** General Introduction

- Chapter 1: Background
- Chapter 2: Material, Apparatus and Methods

**PART II:** Phytochemical study of Plants under investigation

- Chapter 1: Phytochemical study of *Cytisus villosus*
- Chapter 2: Phytochemical study of *Hypericum afrum*.

**PART III:** Biological studies on the plants under investigation.

**PART IV:** Molecular modeling and MD simulation studies



*PART I:*  
*GENERAL INTRODUCTION*



*“Until man duplicates a blade of grass, nature can laugh at his so-called scientific knowledge. Remedies from chemicals will never stand in favorable comparison with the products of nature, the living cell of the plant, the final result of the rays of the sun, the mother of all life...”*

*- Thomas A. Edison, Inventor*

## *CHAPTER 1: BACKGROUND*

### I.1. Background

Medicinal plants contain bioactive phytochemicals, defined as secondary metabolites that are produced to protect the plants. Since plants are stationary autotrophs, they need to develop survival strategies against a number of challenges, including engineering their own pollination and seed dispersal, nutrient deprivation, solar radiation and the coexistence of herbivores and pathogens in their immediate environment (Kennedy and Wightman, 2011). Therefore, plants have evolved biochemical pathways for the production of secondary metabolites in vegetative (e.g. leaf, stem and root) and reproductive (e.g. flower, fruit and seed) regions in response to specific environmental stresses. They also serve as an attractant (e.g. color, pheromones) for pollinating insects or fruit-dispersing animals (Kennedy and Wightman, 2011). These secondary metabolites are unique to specific plant species or genera and are not involved in the plants' primary metabolic requirements (Harborne, 1993).

Plant secondary metabolites are classified into three main groups based on their biosynthetic origin:

- i) terpenes
- ii) nitrogen-containing alkaloids
- iii) phenolic compounds

These secondary metabolites are synthesised from important building blocks (shikimic acid, acetyl coenzyme A, mevalonic acid and 1-deoxyxylulose-5-phosphate) via different pathways, such as shikimate, acetate, mevalonate and deoxyxylulose (Mahmoud and Croteau, 2002) (Figure I.2).

Terpenes is the largest group of secondary metabolites, which consists of more than 30,000 lipid-soluble compounds, derived biosynthetically from units of isoprene (Kennedy and Wightman, 2011). They possess at least one 5-carbon isoprene units. The number of attached isoprene units determine the classification of terpenes:

1 = hemiterpenes, 2 = monoterpenes, 3 = sesquiterpenes, 4 = diterpenes, 5 = sesterpenes, 6 = triterpenes and 8 = tetraterpenes (Kennedy and Wightman, 2011).

In the late nineties after the discovery of a novel non-mevalonate (non-MVA) pathway, the whole concept of terpenoid biosynthesis has changed. In higher plants, the conventional acetate-mevalonate (Ac-MVA) pathway operates mainly in the cytoplasm and mitochondria and



synthesizes sterols, sesquiterpenes and ubiquinones predominantly. The plastidic non-MVA pathway however synthesizes hemi-, mono-, sesqui- and di-terpenes, along with carotenoids and phytol chain of chlorophyll. In this paper, recent developments on terpenoids biosynthesis are reviewed with respect to the non-MVA pathway (Dubey et al., 2003) (Figure I.3).

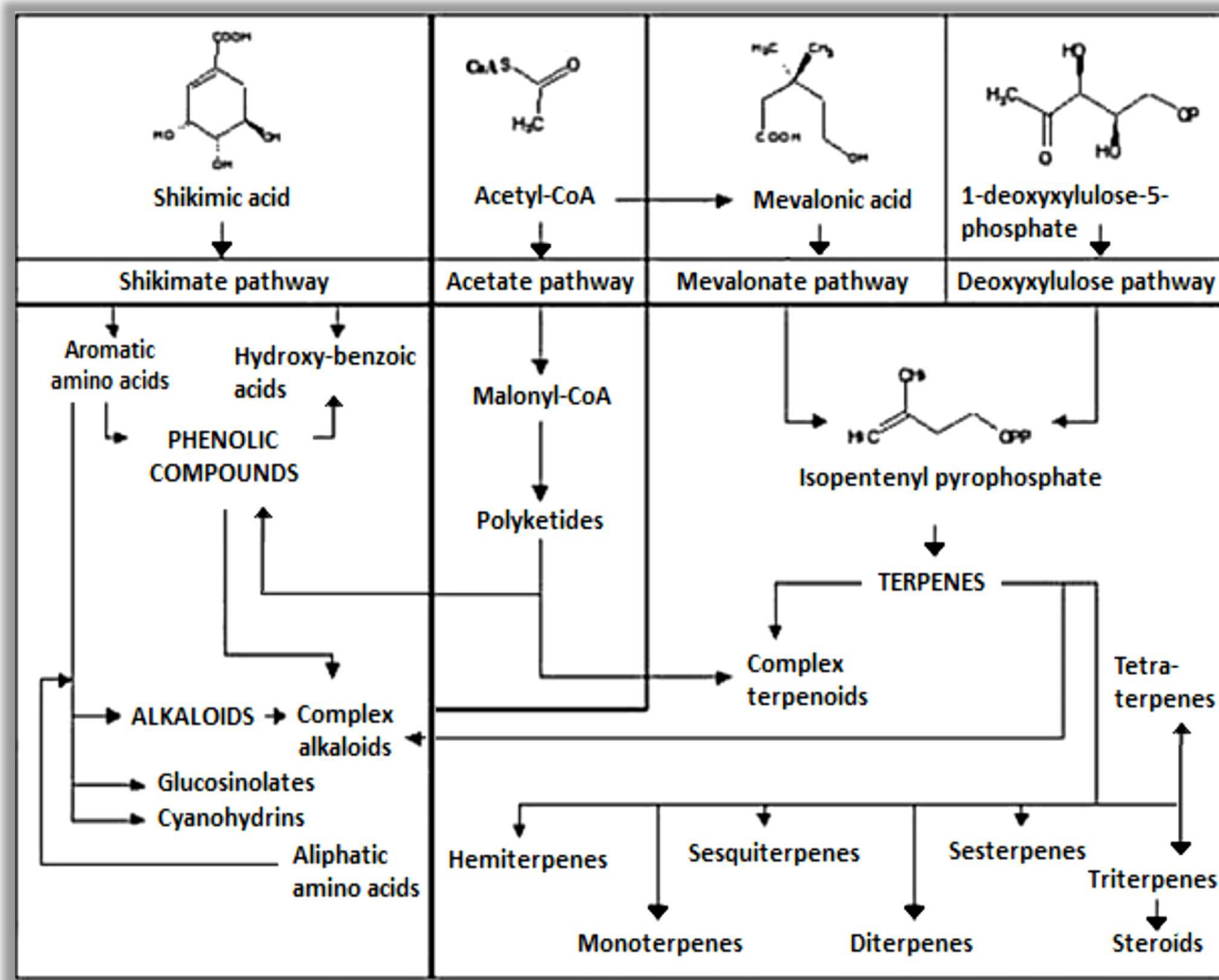
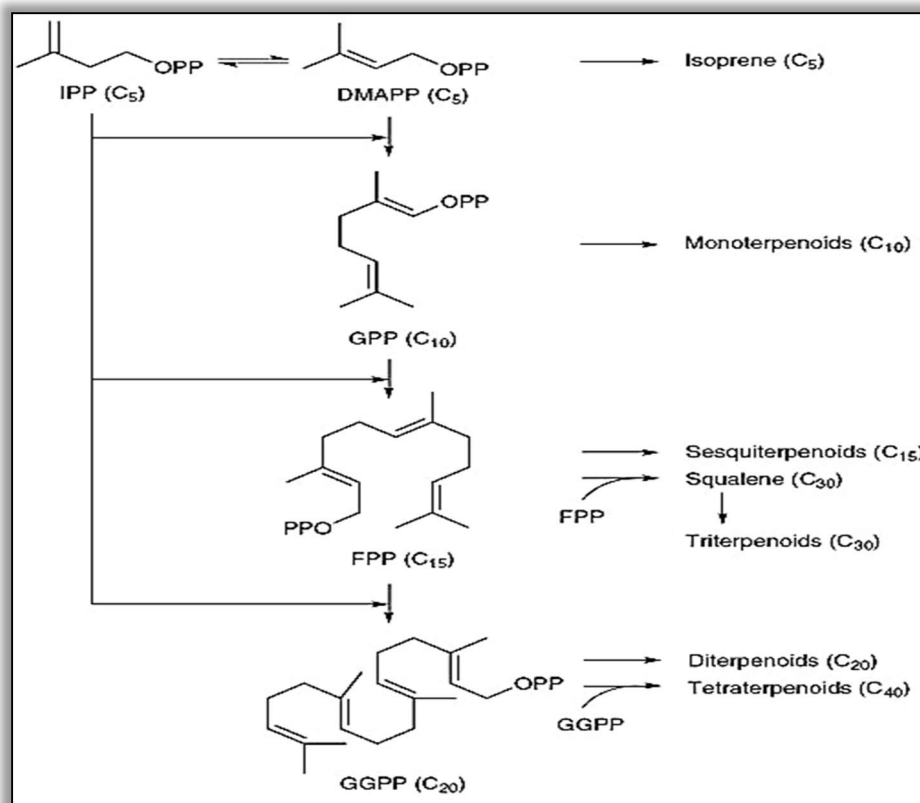


Figure I 2. Biosynthetic pathways of secondary metabolites in plants (Ribera and Zuñiga, 2012).



**Figure I 3.** Terpenoids biosynthesis.

The second largest secondary metabolite group is the alkaloids which constitute nitrogen-containing natural product bases that occur mainly in plants. About 20% of the flowering plant species are known to produce alkaloids (Kutchan, 2005). To date, over 12,000 plant-derived alkaloids have been reported, and they are grouped into various classes based on their origin and the nature of the nitrogen-containing moiety. Alkaloids commonly originate from the amino acids, L-ornithine, lysine, nicotinic acid, tyrosine, phenylalanine, tryptophan, anthranilic acid, and histidine, and thus contain pyrrolidine, pyrrolizidine, piperidine, quinolizidine, indolizidine, pyridine, quinoline, isoquinoline, indole, and imidazole ring systems (Figure I.4).

Alkaloids are also known to originate from mixed biosynthetic pathways, the most important of which include terpenoid and steroidal alkaloids. A limited number of alkaloids that contain a purine ring (e.g., caffeine) also occur in plants.

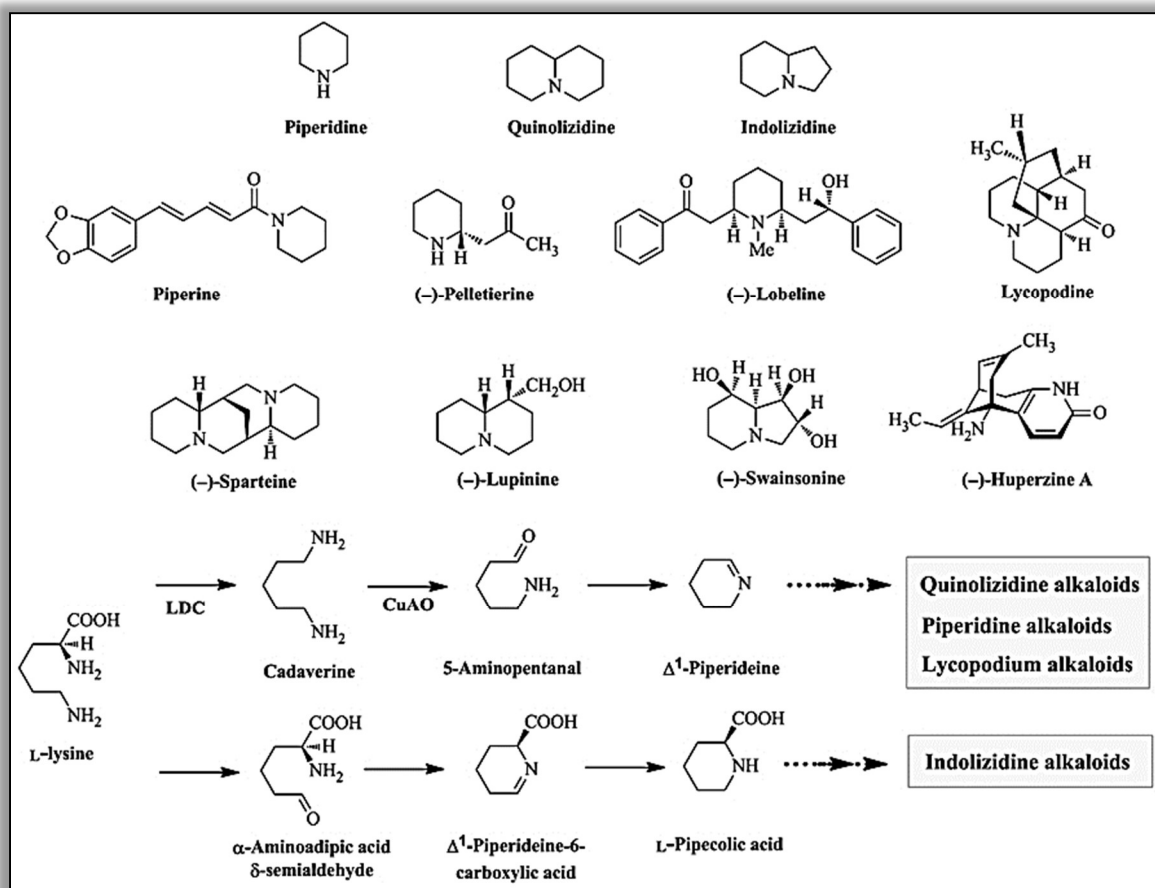


**Figure I 4.** Biosynthesis of universal intermediates, skeleton structures, and some Lys-derived alkaloids found in plants (Bunsupa et al., 2012).

The third largest group is the phenolic compounds, which are synthesised via the phenylalanine precursor in the shikimate pathway (Figure I.5). Phenolic compounds are characterised by having at least one aromatic ring bearing one or more hydroxyl groups, which can undergo esterification, methylation, etherification or glycosylation reactions (Fresco-Taboada et al., 2013). As a result, ~ 10, 000 structural variants, ranging from a simple molecule to a complex high-molecular polymer have been identified thus far (Kennedy and Wightman, 2011). These compounds are generally categorised into different classes such as phenolic acids, flavonoids, stilbenes, coumarins, quinones, lignans, curcuminoids and tannins (Figure I.6).

The categorization is based on:

- i) the nature and complexity of the basic carbonaceous skeleton;
- ii) the degree of skeletal modification (e.g. oxidation, hydroxylation, methylation, etc.)
- iii) the link between the base unit and other molecules, including primary and secondary metabolites (Ewané et al., 2012).

Of these phenolic compounds, flavonoids represent the largest and most diverse group, with ~ 6,000 identified compounds (Kennedy and Wightman, 2011). All flavonoids have the basic skeleton of a phenylbenzopyrone structure (C6-C3-C6) consisting of two aromatic (benzene) rings linked by a heterocyclic pyrane ring (Figure I.6).

These compounds are further subdivided into flavones, flavonols, flavanones, flavanonols, isoflavones, flavan-3-ols, glycosylflavonoids, chalcones, aurones and anthocyanins, according to modifications of the basic skeleton (Bowsher et al., 2008)(Figure I.7).

Flavonoids are one of the common components in the human diet. they have been known for a long time to exert diverse biological effects and in particular to act as antioxidants and anti-inflammatory, antiviral, and especially as preventive agents against cancer.

The most recognized drugs used in pharmaceuticals are terpenoids, including the anticancer drug, taxol, isolated from the bark of *Taxus brevifolia* (Taxaceae) and the antimalarial drug, artemisinin isolated from the leaves of *Artemisia annua* (Asteraceae) (Mbaveng et al., 2014).

Bioactive alkaloids isolated from plants include the, vinblastine and vincristine, isolated from the leaves of *Catharanthus roseus* (Apocynaceae) (Noble, 1990), and antipsychotic and antihypertensive drugs, reserpine, isolated from the roots of *Rauwolfia serpentina* (Apocynaceae) (Bhatara et al., 1997).

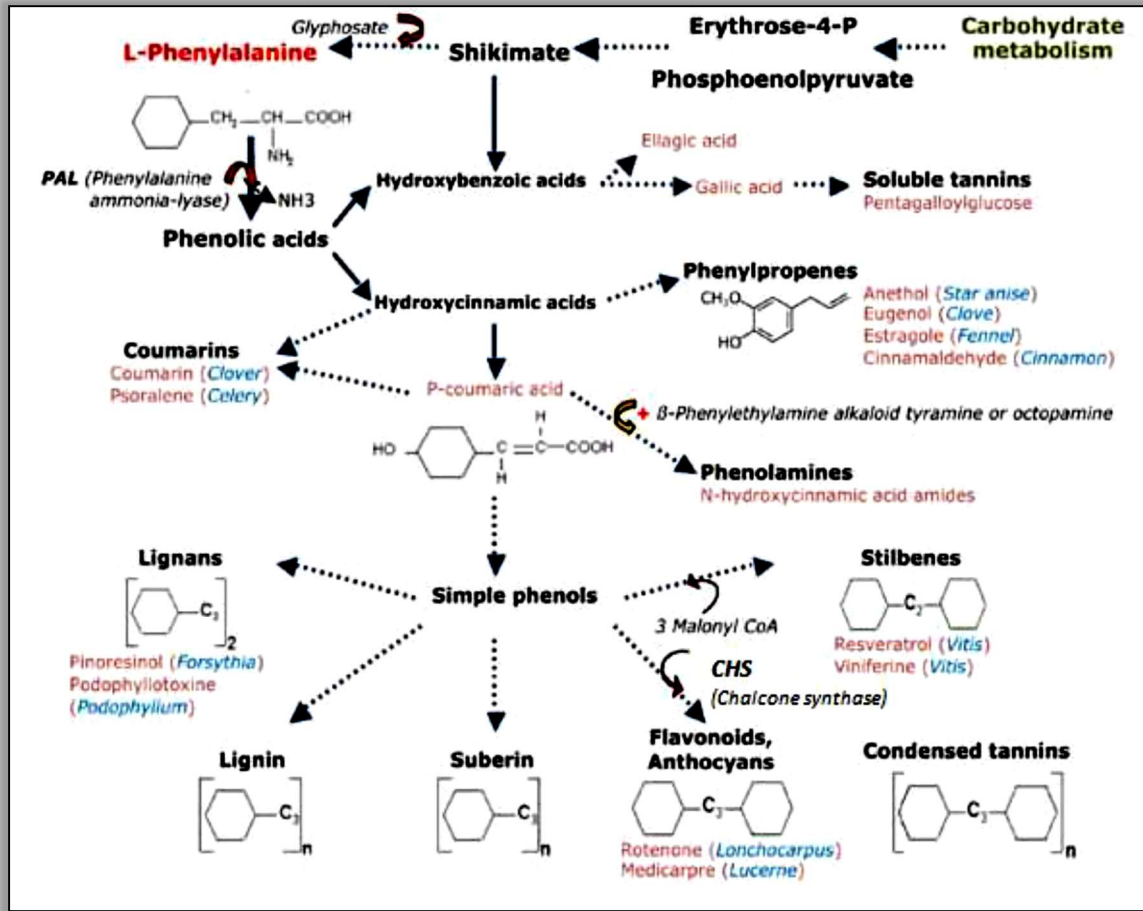


Figure I 5. Simplified pathway of the synthesis of phenolic compounds (Ewané et al., 2012).

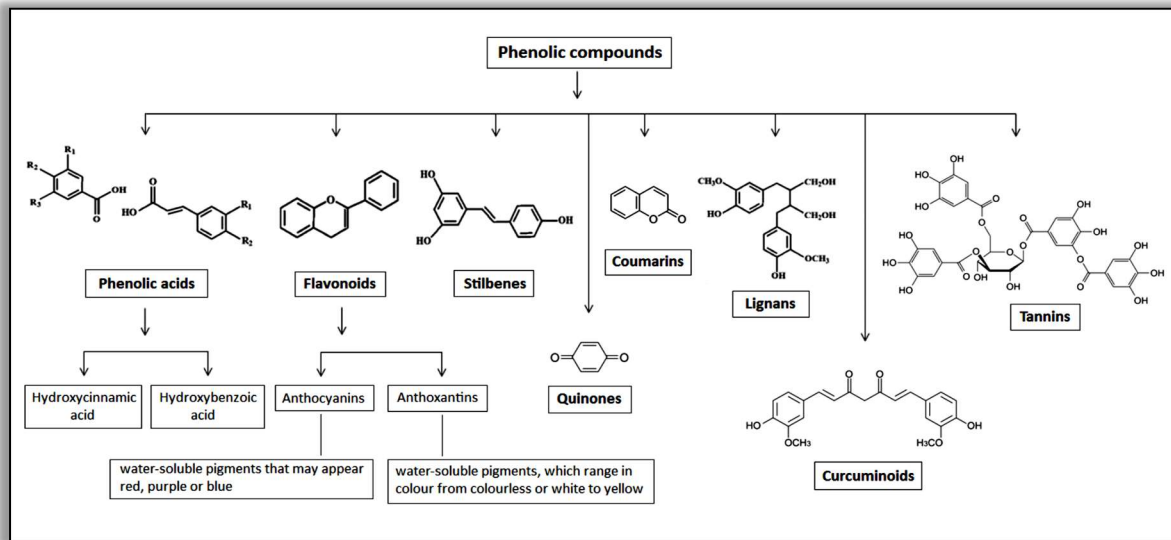


Figure I 6. Classification of phenolic compounds.

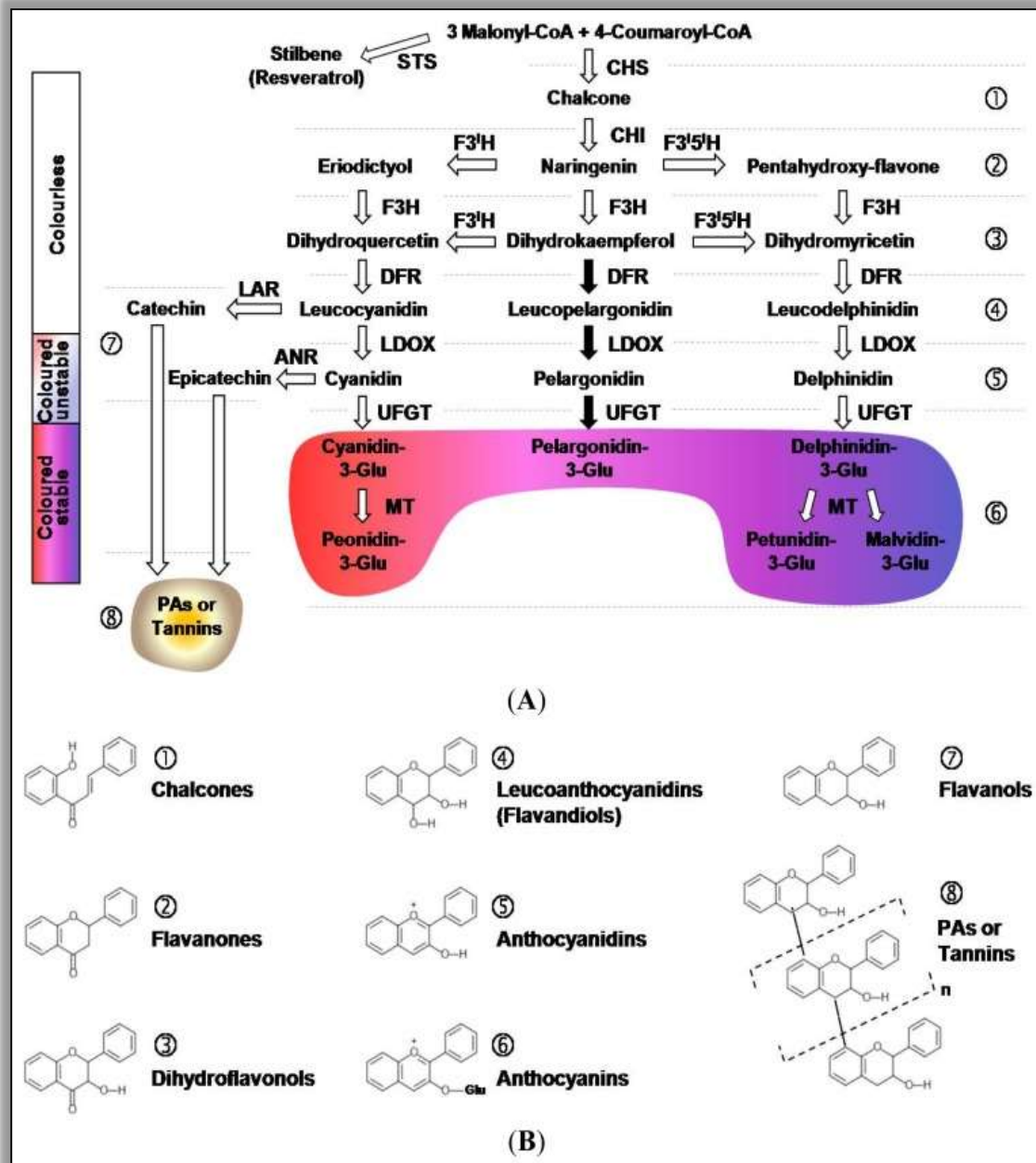


Figure I 7. Scheme of the flavonoid biosynthetic pathway in plant cells (Petrucca et al., 2013).

**I.1.1. Literature review of the genus *Cytisus***

The genus *Cytisus* has been reported to contain quinolizidine alkaloids, flavonoids, phenylethylamines, lectins, and monoterpenes. The major compounds isolated from this genus include the alkaloids sparteine, lupanine, isosparteine, ammoderien, and related derivatives (Iwu, 2014). tyramine, epinine, salsolidine, and related phenylethylamine, genisteine, quercetin, and their glycosides, and caffeic acid P-Coumaric acids. The seeds contain lectins and the volatile oil yields eugenol, phenol, cresol, isovaleric acid, benzoic acid, and benzylalcohol, as well as cis-3-hexen-1-ol and 1-octen-3-ol. The flavone 6"-O-acetyl-scoparin, the flavonols kaempferol, rutin, quercetin, quercitrin and isorhamnetin, and the isoflavones genistein and sarothamnoside has been found in the species *Cytisus scoparius* (Sundararajan and Koduru, 2014), while the species *Cytisus nigrians* and *Cytisus albus* were shown to contain the isoflavones ononin and genistein (Hanganu et al., 2010a; Hanganu et al., 2010b).

*Cytisus* has been reported to show, anti-diabetic, hypnotic, sedative, antioxidant, hepatoprotective, antispasmodic, hypotensive and estrogenic effects (Jalili et al., 2013; Nirmal et al., 2008; Pereira et al., 2012a). The therapeutic properties and, in particular, the antioxidant activity of the different *Cytisus* species is related to their high concentration of phenolic compounds (Luís et al., 2009).

The pharmacological activity of the known *Cytisus scoparius* (Sundararajan and Koduru, 2014) was attributed due to its several constituents like 6"-O-acetyl scoparin (Brum-Bousquet et al., 1977), flavonals like rutin, quercetin, isorhamnetin, quercitrin and kaempferol (Sundararajan et al., 2006) and isoflavones namely genistein and sarothamnoside. Alkaloids like spartein, sarothamine and lupamine were also reported to be present in *Cytisus scoparius* (González et al., 2013). Cytisine, an alkaloid with high affinity for the  $\alpha 4\beta 2$  nicotinic acetylcholine receptor subtype, was being used in eastern and central Europe to help people quit smoking before any smoking cessation aids, this compound extracted for first time from the seeds of *Cytisus laburnum* (Dale and Laidlaw, 1912), can exert an antidepressant-like effects (Mineur et al., 2007). Namely *C. multiflorus* species has been used as an ethnopharmacological agent for centuries mainly due to its diuretic, anti-inflammatory, anti-hypertensor and antidiabetic properties (Gião et al., 2007) . However, this genus has been far less studied than other of the same tribe.

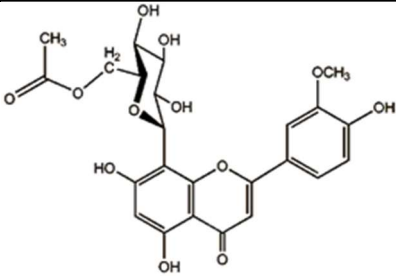
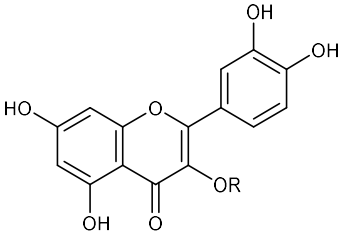
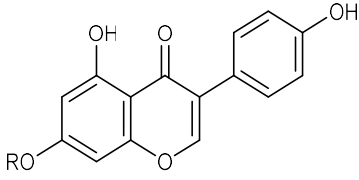
Our studies were concentrated on *Cytisus villosus* Pourr., focused on its pharmacological and chemical properties. So far, the tables below resume the most frequently reported compounds from

*Cytisus* genus as well as the biological activity.

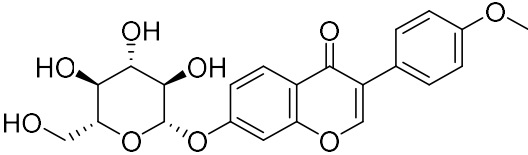
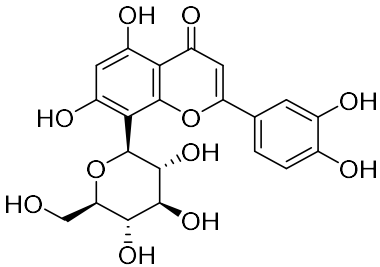
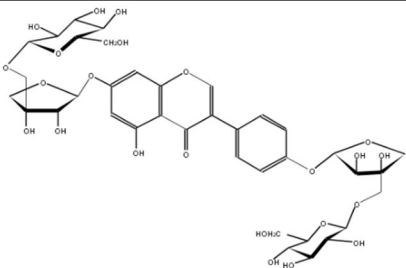
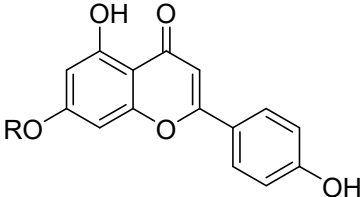
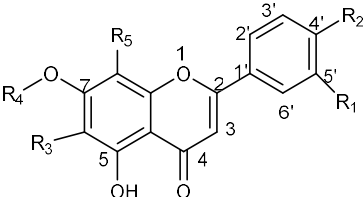
### I.1.1.1. Phytochemical review of *Cytisus*

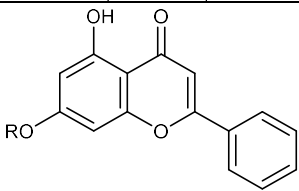
#### A. Flavonoids

**Table I 1.** Reported isolated flavonoids from different *Cytisus* species

No.	Name	Structure			Plant source	Ref.
1	6''-O acetyl scoparin				<i>Cytisus scoparius</i>	(Brum-Bousquet et al., 1977)
						
		R1	R2	R3		
2	Quercetin	H	OH	H	<i>Cytisus scoparius</i>	(Lores et al., 2015)
					<i>Cytisus multiflorus</i>	(Pereira et al., 2012b)
3	Rutin	$\beta$ -Rut	O H	H	<i>Cytisus multiflorus</i>	(Pereira et al., 2012b)
4	Quercitrin	Rha	O H	H	<i>Cytisus multiflorus</i>	(Pereira et al., 2012b)
5	Kaempferol	H	H	H	<i>Cytisus scoparius</i>	(Lores et al., 2015)
6	isorhamnetin	H	OH	CH <sub>3</sub>	<i>Cytisus scoparius</i>	(Barros et al., 2012)
						
R						

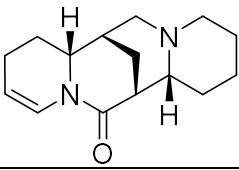
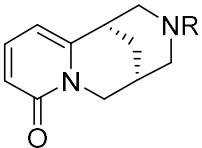


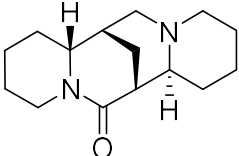
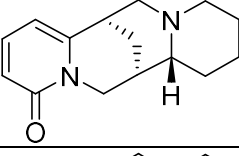
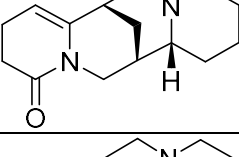
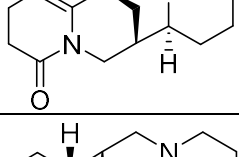
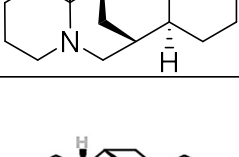
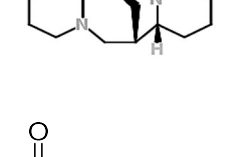
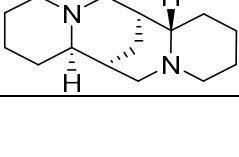
7	genistein	H	<i>Cytisus scoparius</i>	(Viscardi et al., 1984)				
8	Genistin	Glc	<i>Cytisus albus</i>	(Hanganu et al., 2010a)				
9	ononin		<i>Cytisus nigrians</i>	(Hanganu et al., 2010a)				
10	Orientin		<i>Cytisus multiflorus</i>	(Pereira et al., 2012b)				
11	sarothamnocide		<i>Cytisus scoparius</i>	(Viscardi et al., 1984)				
								
R								
12	Apigenin	H	<i>Cytisus multiflorus</i>	(Pereira et al., 2013)				
13	Apigenin-7-O-glucoside	Glc	<i>Cytisus multiflorus</i>	(Pereira et al., 2013)				
								
		R1	R2	R3	R4	R5		
14	2''-O-pentosyl- 6-C-hexosyl-luteolin	OH	OH	Hex-Pent	H	H	<i>Cytisus multiflorus</i>	(Pereira et al., 2012a)

15	2''-O-pentosyl-8-C-hexosyl-luteolin	OH	OH	H	H	Hex-Pent	<i>Cytisus multiflorus</i>	(Pereira et al., 2012a)
16	2''-O-pentosyl-6-C-hexosyl-apigenin	H	OH	Hex-Pent	H	H	<i>Cytisus multiflorus</i>	(Pereira et al., 2012a)
17	2''-O-pentosyl-8-C-hexosyl-apigenin	H	OH	H	H	Hex-Pent	<i>Cytisus multiflorus</i>	(Pereira et al., 2012a)
18	6''-O-(3-hydroxy-3-methylglutaryl)-2''-O-pentosyl-8-C-hexosyl-luteolin	OH	OH	H	H	Hex-Pent-HMG	<i>Cytisus multiflorus</i>	(Pereira et al., 2012a)
19	6''-O-(3-hydroxy-3-methylglutaryl)-2''-O-pentosyl-8-C-hexosyl-apigenin	H	OH	H	H	Hex-Pent-HMG	<i>Cytisus multiflorus</i>	(Pereira et al., 2012a)
								
R								
20	Chrysin	H					<i>Cytisus multiflorus</i>	(Pereira et al., 2012a)
21	Chrysin-7-O-β-D-glucopyranoside	Glc					<i>Cytisus multiflorus</i>	(Pereira et al., 2012a)
Hex-Hexose, Pent-Pentose, Glc-Glucoses, HMG-3-hydroxy-3-methylglutaryl								

## B. Alkaloids

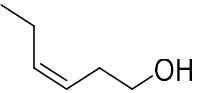
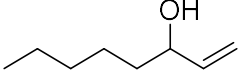
**Table I 2.** Reported isolated Alkaloids from different *Cytisus* species

No.	Name	Structure	Plant source	Ref.
1	(+)-2,3-dehydro-10-oxo-α-isosparteine		<i>Cytisus monspessulanus</i>	(Nihei et al., 2002)
				
R				
2	N-methylcytisine	CH <sub>3</sub>	<i>Cytisus laburnum</i>	(Freer et al., 1987; Wink, 1984)
3	Cytisine	H	<i>Cytisus laburnum</i>	(Dale and Laidlaw, 1912; Freer et al., 1987; Prochaska et al., 2013)

4	Aphylline		<i>Cytisus scoparius</i>	(Gresser et al., 1996)
5	Anagryne		<i>Cytisus scoparius</i>	(Gresser et al., 1996)
6	Monspessulanine		<i>Cytisus monspessulanus</i>	(White, 1964)
7	Aphyllidine		<i>Cytisus monspessulanus</i>	(Nihei et al., 2002)
8	Sparteine		<i>Cytisus scoparius</i>	(Gresser et al., 1996)
9	$\alpha$ -Isosparteine		<i>Cytisus scoparius</i>	(Index, 1989)
10	Lupanine (2-Oxosparteine)		<i>Cytisus scoparius</i>	(Kar, 2003)
11	$\alpha$ -Isolupanin		<i>Cytisus ruthenicus</i>	(Радиковна and Зуфарович, 2015)

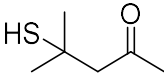
### C. Alkenol

**Table I 3.** Reported isolated Alkenols from different *Cytisus* species

Name	Structure	Plant source	Ref.
cis,Hex-3-en, 1-ol		<i>Cytisus scoparius</i>	(Kurihara and Kikuchi, 1980)
Oct-1-en-3-ol		<i>Cytisus scoparius</i>	

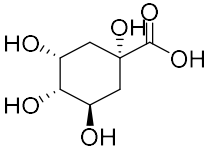
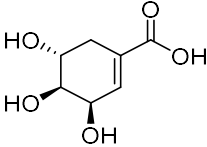
## D. Alkanone

Table I 4. Reported isolated Alkanone from different *Cytisus* species

Name	Structure	Plant source	Ref.
4-Mercapto, 4-methyl, 2-pentanone		<i>Cytisus scoparius</i>	(Tominaga and Dubourdieu, 1997)

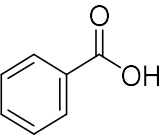
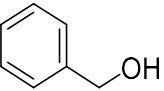
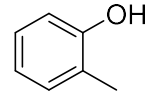
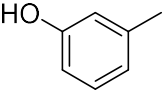
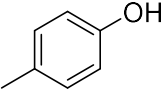
## E. Alicyclic

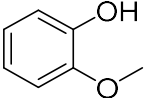
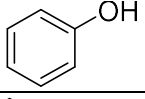
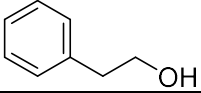
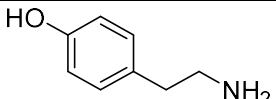
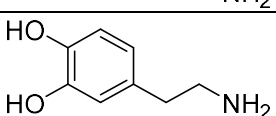
Table I 5. Reported isolated Alicyclic from different *Cytisus* species

Name	Structure	Plant source	Ref.
Quinic acid		<i>Cytisus multiflorus</i>	(Barros et al., 2012)
Shikimic acid		<i>Cytisus scoparius</i>	(Wink et al., 1981)

## F. Benzenoids

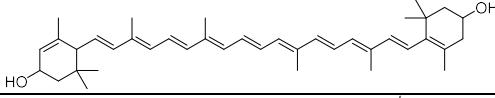
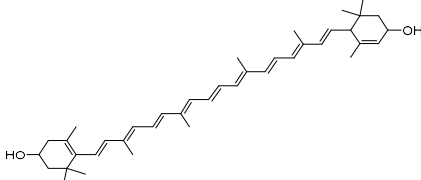
Table I 6. Reported isolated Benzenoid from different *Cytisus* species

Name	Structure	Plant source	Ref.
Benzoic acid		<i>Cytisus scoparius</i>	(Kurihara and Kikuchi, 1980)
Benzyl alcohol			
o-Cresol			
m-Cresol			
p-Cresol			

Guaiacol			
Phenol			
Phenyl ethanol			
Tyramine		<i>Cytisus scoparius</i>	(Murakoshi et al., 1986; Schmalfluss and Heider, 1931)
3-Hydroxy tyramine			

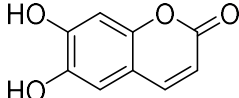
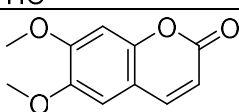
### G. Carotenoids

**Table I 7.** Reported isolated carotenoids from different *Cytisus* species

Name	Structure	Plant source	Ref.
Lutein		<i>Cytisus scoparius</i>	(Egger, 1968)
Xanthophyll			

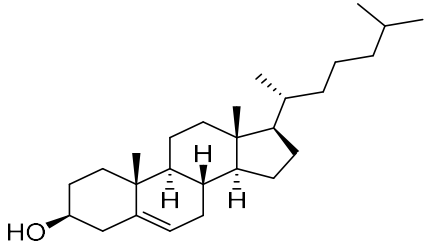
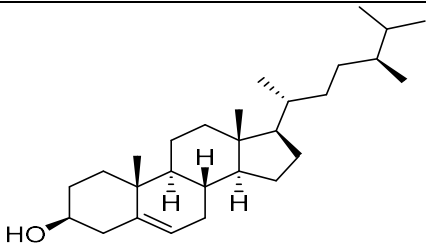
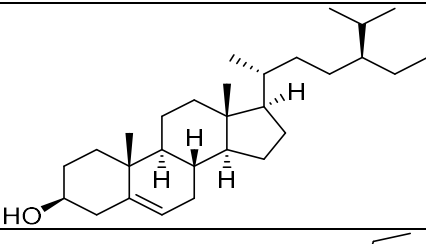
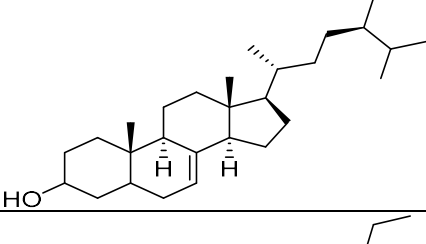
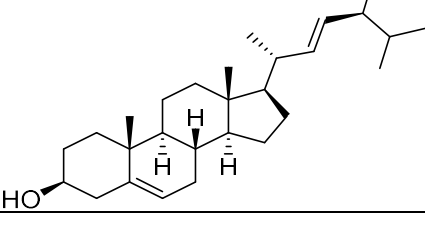
### H. Coumarins

**Table I 8.** Reported isolated coumarins from different *Cytisus* species

Name	Structure	Plant source	Ref.
Aesculetin		<i>Cytisus scoparius</i>	(BRUM and Paris, 1974; Kurihara and Kikuchi, 1980)
Scoparone			

## I. Steroids

Table I 9. Reported isolated steroids from different *Cytisus* species

Name	Structure	Plant source	Ref.
Cholesterol		<i>Cytisus scoparius</i>	(Sundararajan and Koduru, 2014)
Campesterol		<i>Cytisus scoparius</i>	(Sundararajan and Koduru, 2014)
$\beta$ -Sitosterol		<i>Cytisus scoparius</i>	(Sundararajan and Koduru, 2014)
Stigmast 7-en, 3 $\beta$ -		<i>Cytisus scoparius</i>	(Sundararajan and Koduru, 2014)
Stigmasterol		<i>Cytisus scoparius</i>	(Sundararajan and Koduru, 2014)

## J. Lipids

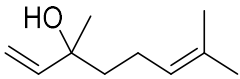
Table I 10. Reported isolated Lipids from different *Cytisus* species

Name	Structure	Plant source	Ref.
Arachidic acid		<i>Cytisus scoparius</i>	

Capric acid			(Kurihara and Kikuchi, 1980)
Caproic acid			
Lauric acid			
Myristic acid			
Enanthic acid			
Palmitic acid			
Pelargonic acid			

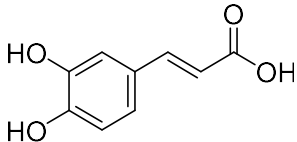
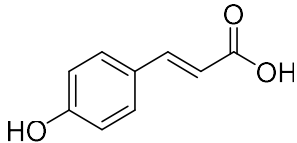
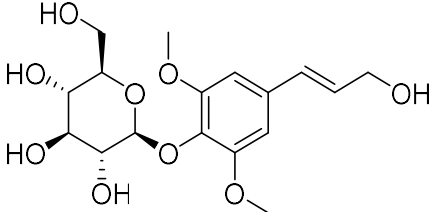
### K. Monoterpenes

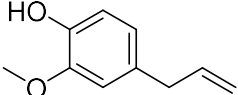
Table I 11. Reported isolated Monoterpenes from different *Cytisus* species

Name	Structure	Plant source	Ref.
Linalool		<i>Cytisus scoparius</i>	(Kurihara and Kikuchi, 1980)

### L. Phenyl propanoids

Table I 12. Reported isolated Phenyl propanoids from different species of *Cytisus*

Name	Structure	Plant source	Ref.
Caffeic acid		<i>Cytisus scoparius</i>	(Kurihara and Kikuchi, 1980)
para- Coumaric acid			
Syringin		<i>Cytisus scoparius</i>	(Sundararajan and Koduru, 2014)

Eugenol			
---------	---	--	--

### I.1.1.2. Biological Review of *Cytisus*

The following biological activities were encountered with some species of *Cytisus*.

**Table I 13.** A list of biological activities reported from certain species of *Cytisus*

No.	Activity	Plant Source	Reference
1	Antioxidant	<i>Cytisus scoparius</i> Link.	(Sundararajan et al., 2006),(Nirmal et al., 2008)
		<i>Cytisus striatus</i>	(Pinela et al., 2011)
		<i>Cytisus multiflorus</i>	(Barros et al., 2011)
	Antidepressant	<i>Cytisus laburnum</i>	(Mineur et al., 2009)
2	Diuretic	<i>Cytisus scoparius</i> Link	(Nirmal et al., 2008)
3	Hypnotic	<i>Cytisus scoparius</i> Link	(Siegel, 1976)
4	Anxiolytic	<i>Cytisus scoparius</i> Link	(Siegel, 1976)
5	Antiparasitic	<i>Cytisus syriacus</i>	(Di Giorgio et al., 2008)
6	Antidiabetic	<i>Cytisus scoparius</i> Link	(e Castro, 1998),(Osório e Castro, 2001)
7	anti-hypertensor	<i>Cytisus scoparius</i> Link	(Gião et al., 2007)
9	Anti-spasmodic	<i>Cytisus scoparius</i> Link	(Gião et al., 2007)

### I.1.2. Classification of Fabaceae and the Genus *Cytisus* L.

Fabaceae is a family of cosmopolitan distribution, with approximately 730 genera and 19,400 species, lying in third place after Asteraceae and Orchidaceae with respect to species richness at a global level (Judd et al., 1999). This high species richness is reflected in great morphological and chemical diversity, from which multiple uses are derived (Waterman et al., 1994). Fabaceae are herbs, shrubs, trees, lianas or vines usually bearing alternate, pinnately compound, pulvinate, stipulate leaves. N-fixing bacteria are common in two subfamilies: Mimosoideae and Papilionoideae. The androperianth is 5-merous with 10 to numerous stamens (Mimosoideae). The gynoecium consists of a single carpel with 2 to many ovules. Fruits are usually legumes, splitting



along two sutures but sometimes indehiscent. The cosmopolitan family contains an estimated 18,000 species in 630 genera. Twenty genera account for nearly half of the species in the family and 16 contain more than 200 species each: Astragalus (2,000), Acacia (1,000), Indigofera (700), Crotalaria (600), Mimosa (500), Desmodium (400), Tephrosia (400), Trifolium (300), Chamaecrista (260), Bauhinia (250), Senna (250), Inga (250), Dalbergia (200), Lupinus (200), Phaseolus (200), and Pithecellobium (200) (Bennett, 2010).

*Cytisus*. (*Leguminosae*) is a large and diversified genus of dicotyledonous plants including approximately 50 species of flowering plants in the family Fabaceae, which are particularly abundant around the Mediterranean Sea, although they are found in distinct geographic regions such as the north and south of Africa, the western and central Europe, the Black Sea and Turkey to the East (Cristofolini and Conte, 2002). *Cytisus* is one of several genera in the tribe Genisteeae which are commonly called brooms. Brooms are 4 to 5 feet tall erect shrubs with alternate leaves. The flowers are arranged in heads and are generally yellow or white.

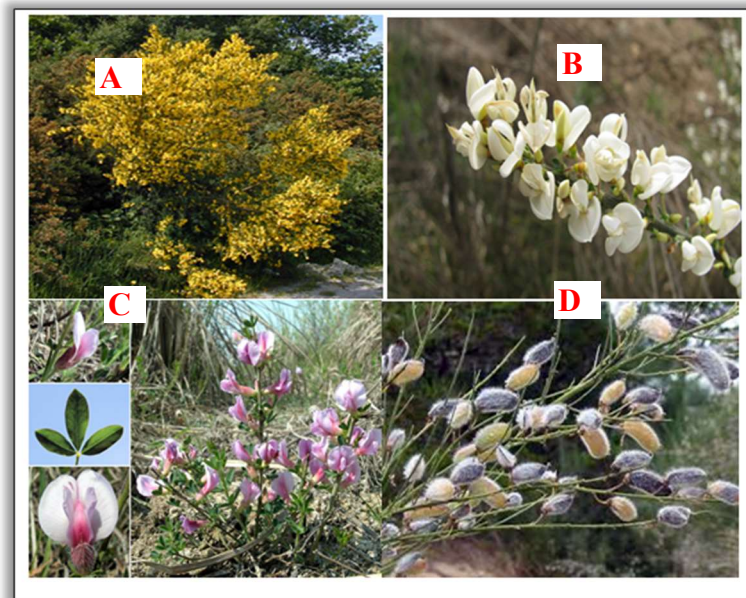


**Figure I 8.**Photos of some *Cytisus* species (A. *Cytisus Scoparius*, B. *Cytisus multiflorus*, C. *Cytisus purpureus* Scop, D. *Cytisus striatus*)

### **I.1.3. Use of *Cytisus* genus in traditional medicine**

*Cytisus* genus is reported to be employed as a diuretic and in the treatment of mild hypertension. A decoction of its leaves is used with lime for chest complaints (Iwu, 2014). Several species of the *Cytisus* genus have been used in traditional medicine mainly due to their antioxidant, cytoprotective, diuretic, hypnotic, anxiolytic, antiparasitic and antidiabetic potentials (Barros et al., 2012) (Sundararajan et al., 2006) (González et al., 2013) (Pereira et al., 2013) (Nirmal et al., 2008) (Di Giorgio et al., 2008). The most known *Cytisus scoparius*, a widely used traditional Chinese herb, is taken to nourish Yin and invigorate the heart & liver in traditional Chinese medicine (TCM) and has a very high medicinal value (Sundararajan and Koduru, 2014). It is well known as a stimulating cardiac tonic and diuretic, useful for treating heart failure and cardiac edema, but with the potential of causing hypertension. Broom tied around the neck was believed to prevent nosebleeds (Hatfield, 2004). *Cytisus multiflorus* (Spanish broom) was used in folk medicine and it is reported to have various health benefits, including anti-inflammatory properties (Nedelcheva et al., 2007).

- *Cytisus villosus* (plant under investigation) has been used by the rural populations as an effective remedy for wounds.

### **I.1.4. Economic Importance of the family of Fabaceae and *Cytisus* genus**

One of the largest angiosperm families, the pea family (fabaceae) features a number of economically significant plants, ranging from important food crops such as fenugreek (*Trigonella foenum-graecum*), green bean (*Phaseolus vulgaris*), lentil (*Lens culinaris*) and peanut (*Arachis hypogaea*) to costly invasive species, *Acacia* species, *Mimosa* species, *Abrus precatorius* and *Cytisus* species. Several tropical members of the Fabaceae have been utilized commercially as sources of timber; example, almendro (*Dipteryx oleifera*), golden chain (genus *Laburnum*), rosary pea (*Abrus precatorius*) and dyes such as senna (*Senna* species), indigo (*Indigofera* species) and logwood (*Haematoxylum campechianum*) (Duke, 2012; Wiersema and Leon, 2016). In socioeconomic terms, their importance for health and human alimentation is highlighted, although they also provide wood resources and dyes, resins, insecticides, fibres, fodder, and so forth (Andriamparany et al., 2014; Bennett, 2010). The nutritional value of Fabaceae is to a great extent due to their ability to fix atmospheric nitrogen for protein synthesis (Dias, 2012). This advantage has led to protein concentrations in leaves and seeds (Allen and Allen, 1981). With regard to medicinal uses, it has been pointed out that they are found amongst the five botanical families

richest in therapeutic properties (Molares and Ladio, 2011). Different *Cytisus* species are vastly used as ornamental plants, as well as for animal nutrition. Other applications of this plant include the collection of their pollen for apiculture purposes and land fertilising in agriculture (García Ciudad et al., 2004; Rodríguez-Riaño et al., 2004; Rodríguez-Riaño et al., 2006; Rodríguez-Riaño et al., 1999).

**I.1.5.** Taxonomical identification of *Cytisus villosus* Pourr. in the plant kingdom (Auvray and Malécot, 2013)

<i>Cytisus villosus</i> (Pourr.)	
<b>Kingdom:</b>	Plantae
<b>Division:</b>	Magnoliophyta
<b>Class:</b>	Magnoliopsida
<b>Order:</b>	Fabales
<b>Family:</b>	Fabaceae (Papilionaceae)
<b>Subfamily</b>	Faboideae
<b>Tribe</b>	Genisteae
<b>Genus:</b>	<i>Cytisus</i>
<b>Species:</b>	<i>Cytisus villosus</i> Pourr. (Syn. <i>Cytisus triflorus</i> L'Hérit.)
<b>Common Name</b>	Broom, Cytise à trois fleurs

**I.1.6. Description of the plant under investigation:**

*Cytisus villosus* is a Shrub 1-2 m erect stem, and spread to many twigs and elongated. Young twigs are angular and covered with long white hairs; the general appearance is grayish. The leaves are deciduous, they all stalked and composed by three oval leaflets rounded, densely hispid, silky on both sides, with a median twice as large (1.5 to 3cm), blackening on drying. The Flowering takes place in April-May. The flowers are large, yellow streaked with papilionaceous corolla, stalked are solitary or 2 or 3 in the axils of upper leaves. Calyx hairy, banner, stained brown, shorter than the hull. The Fruits: The pods (3-3,5cm) are brown, hairy and contain 6-8 brown seeds (Quezel, 1963).



Figure I 9. Photo of *Cytisus villosus* shrub and its leaves & flowers

### I.1.7. Geographic distribution of *Cytisus villosus*

*Cytisus villosus* frequently grows in Algeria, France, Italy, Spain, Portugal, and Tunisia. In Algeria, it is common in the region of the Tell Algéro-constantinois (Quezel, 1963).

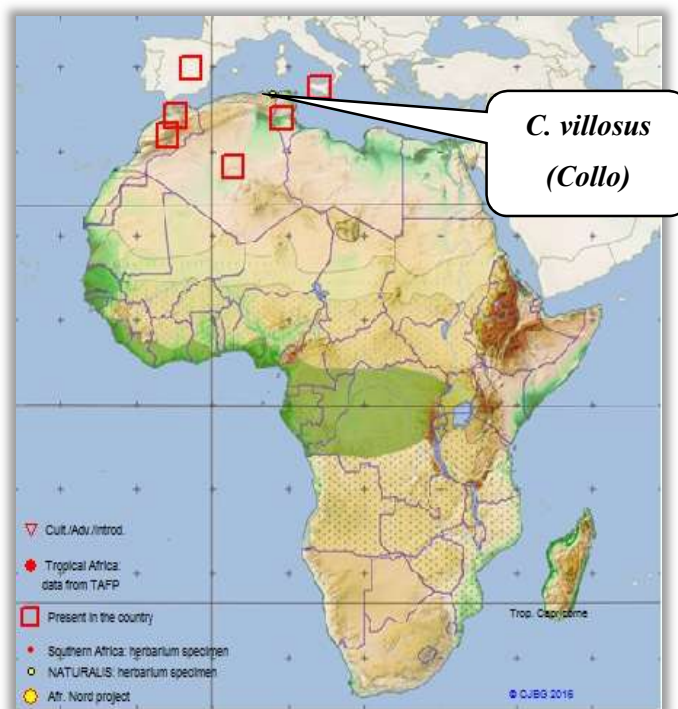


Figure I 10. Geographic distribution map for *Cytisus* genus (Brum-Bousquet et al., 1977).

**I.1.8. Literature review on the genus *Hypericum***

On surveying the literature, Flavonoids and flavonol glycosides make up the largest category of compounds reported from species of *Hypericum* (Table I.18). In addition, flavonoid sulphates with quercetin as the aglycone have been detected in some species (Seabra and Alves, 1989; Seabra et al., 1991; Seabra and Alves, 1988, 1991): Several other phenylpropanoid constituents including coumarins, pyrones and lignans have been reported from species of *Hypericum*, published data is available for the isolation and identification of catechin, epicatechin, procyanidins, cinnamtannin and gallic acid. Xanthenes are found sporadically throughout the plant family, but have been identified in the highest numbers from representatives of four families: Clusiaceae, Gentianaceae, Polygalaceae and Moraceae. Hypericin and pseudohypericin (Table I.21) are the compounds of greatest pharmacological interest in this group, from the perspective of potential antidepressant activity of extracts and potential toxicity due to photosensitization (Barnes et al., 2001; Mathis and Ourisson, 1963b; Rocha et al., 1994). Phloroglucinol derivatives are widely reported to be isolated from several *Hypericum* species.

The genus *Hypericum* has been largely tested in a variety of assays, including in vitro antibacterial, antifungal, antiviral and antioxidant assays and in vivo anti-inflammatory, antinociceptive and antidepressant assays. Pure substances belonging to several classes of bioactive natural products isolated from *H. perforatum*, which have been shown to interact with Gprotein-coupled receptors, transporters and ion channels that are targets of known CNS psychoactive agents, may contribute to the antidepressant effect.

- ***Hypericum afrum* Lam.** (Plant under study) has not previously been subjected to either chemical or biological investigation which motivates us to explore the secondary metabolite pattern of the plant.

In the following, a review of the reported phytochemical and biological studies of different species of *Hypericum*.

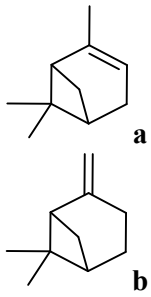
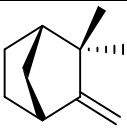
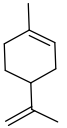
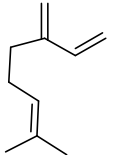
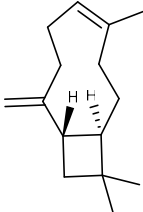
I.1.8.1. Phytochemical review of *Hypericum*

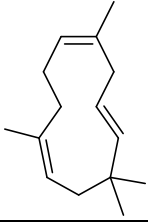
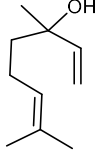
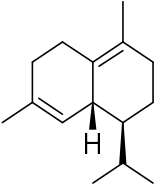
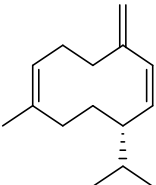
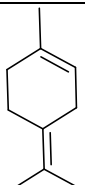
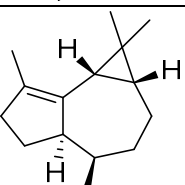
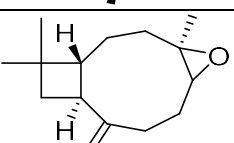
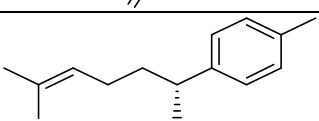
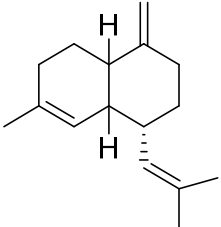
## A. Products of the mevalonate and deoxyxylulose phosphate pathways

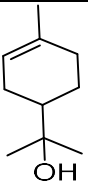
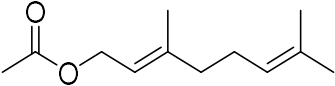
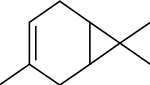
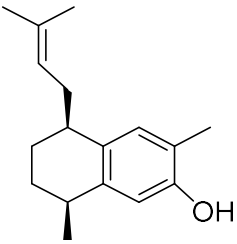
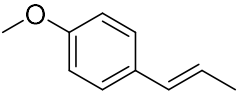
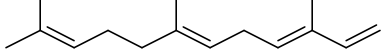
## ➤ Essential oil components

Characteristic oil reservoirs and canals are found in most parts of the *Hypericum* plants, with highest concentrations often seen in the leaves, sepals, petals and along raised glandular lines on the stems (Robson, 1981).

**Table I 14.** Reported isolated Essential oil components of different *Hypericum* species

Name	Structure	Plant	Ref.
$\alpha$ -Pinene (a), $\beta$ -Pinene(b)		<i>H. hyssopifolium</i>	(Cakir et al., 2004)
		<i>H. heterophyllum</i>	(Cakir et al., 2004)
		<i>H. linarioides</i>	(Cakir et al., 2005)
		<i>H. perforiatum</i>	(Pavlović et al., 2006)
		<i>H. rumeliacum</i>	(Pavlović et al., 2006)
		<i>H. richeri</i>	(Ferretti et al., 2005)
		<i>H. rumeliacum</i>	(Couladis et al., 2003)
		<i>H. triquetrifolium</i>	(Bertoli et al., 2003)
<i>H. calycinum</i>	(Erken et al., 2001)		
Camphene		<i>H. dogonbadanicum</i>	(Sajjadi et al., 2001)
Limonene		<i>H. barbatum</i>	(Saroglou et al., 2007)
Myrcene		<i>H. hircinum</i>	(Bertoli et al., 2000)
$\beta$ -Caryophyllene		<i>H. hyssopifolium</i> <i>H. heterophyllum</i>	(Cakir et al., 2004)

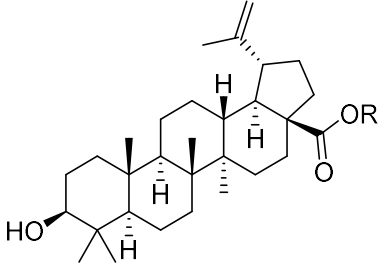
$\alpha$ -Humulene			
Linalool		<i>H. tomentosum</i> <i>H. perforatum</i>	(Hosni et al., 2008)
$\delta$ -Cadinene			
Germacrene-D		<i>H. perforatum</i>	(Mockute et al., 2008)
Terpinolene		<i>H. foliosum</i>	(Santos et al., 1999)
$\alpha$ -Gurjunene		<i>H. balearicum</i> <i>H. delphicum</i> <i>H. aegypticum</i> <i>H. aegypticum</i> <i>H. roeperanum</i>	(Crockett et al., 2007)
Caryophyllene oxide			
$\alpha$ -Curcumene			
$\gamma$ -Muuroolene			

$\alpha$ -Terpineol			
Geranyl acetate			
3-Carene			
7-Hydroxy-calamenene			
(E)-Anethole			
$\beta$ -Famesene (			

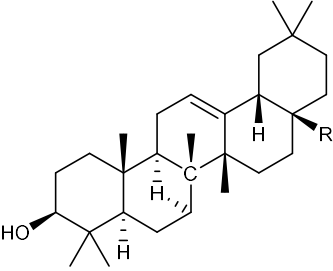
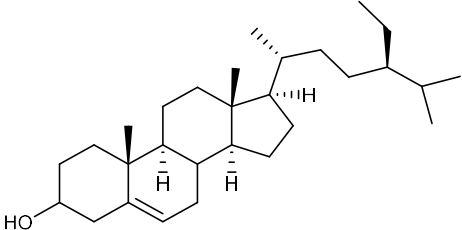
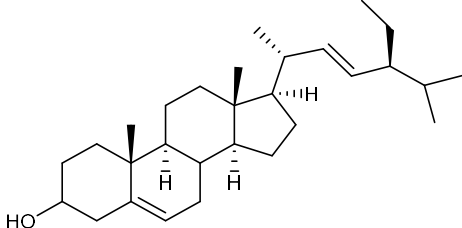
### C. Triterpenoids (including steroids)

Published papers detailing the isolation of triterpenoids and modified triterpenoids such as steroids and phytosterol from *Hypericum* have been relatively few, including reports from *H. elatum* and *H. androsaemum* (Hargreaves et al., 1968).

**Table I 15.** Reported isolated triterpenoids and derived sterols of different *Hypericum* species

Name	Structure	Plant source	Ref.
			
	R		
Betulinic acid	H	<i>H. laricifolium</i> Juss	(Ramírez-González et al., 2013)
Methyl betulinate	CH <sub>3</sub>	<i>H. geminiflorum</i>	(Li and WU, 1997)



			
	<b>R</b>		
Oleanolic acid	COOH	<i>H. geminiflorum</i>	(Li and WU, 1997)
$\beta$ -Amyrin	CH <sub>3</sub>	<i>H. calycinum</i>	(Seger et al., 2004)
			
	<b>R</b>		
$\beta$ -Sitosterol	CH <sub>2</sub> CH <sub>3</sub>	<i>H. riparium</i>	(Tanemossu et al., 2014)
Campesterol	CH <sub>3</sub>		
Stigmasterol			

#### D. Products of the shikimate pathway

##### ➤ *Benzoic and cinnamic acid derivatives*

The most frequently observed compounds in the genus of *Hypericum* species are caffeic acids (Crockett, 2003), Ferulic acid, para- and ortho-coumaric acid, vanillic acid, Shikimic acid, Neochlorogenic acid (5-caffeoylquinic acid) and chlorogenic acid (3-caffeoylquinic acid) have been frequently reported from this genus (see table I.16).

Table I 16. Reported isolated Benzoic and Cinnamic acid derivatives

Name	Structure	Plant source	Ref.
	<b>R</b>		
Caffeic acid	H	<i>H. perforatum</i> , <i>H. androsaemum</i> , <i>H. caprifolium</i> <i>H. hirsutum</i> <i>H. maculatum</i> , <i>H. subalatum</i>	(Ayuga and Rebuelta, 1986; Chen et al., 1989; Kitanov, 1988; Kolodziejski and Gill, 1960; Nahrstedt and Butterweck, 1997)
Ferulic acid	Me	<i>H. caprifolium</i> <i>H. japonicum</i>	(Ayuga and Rebuelta, 1986; Wu et al., 1998b)
	<b>R1</b>	<b>R2</b>	
p-Coumaric acid	R = H	R <sub>1</sub> = OH	
o-Coumaric acid	R = OH	R <sub>2</sub> = H	
<i>Vanillic acid</i>		<i>H. caprifolium</i> <i>H. japonicum</i>	(Ayuga and Rebuelta, 1986; Wu et al., 1998b)
<i>Shikimic acid</i>		<i>H. monogyrrum</i> <i>H. androsaemum</i>	(Hargreaves, 1965; Wang et al., 2002)

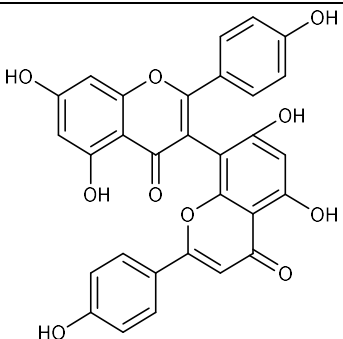
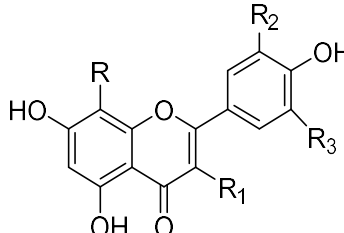
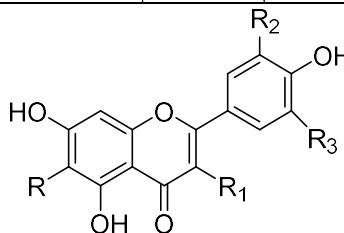
5-O-Caffeoylquinic acid		<i>H. androsaemum</i> ,	(Dias et al., 1999; Zhang et al., 2011)
3-O-Caffeoylquinic acid Chlorogenic acid			

➤ **Flavonoids and biflavones**

Flavonoids and flavonol glycosides make up the largest category of compounds reported from species of *Hypericum*. A summary of the occurrence of the most common flavonols, flavonol glycosides and biflavones is given in table I.17.

**Table I 17.** Reported isolated flavonol glycoside and biflavones different *Hypericum* species

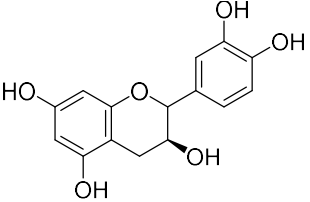
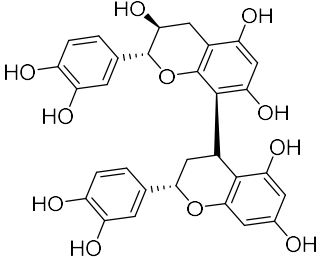
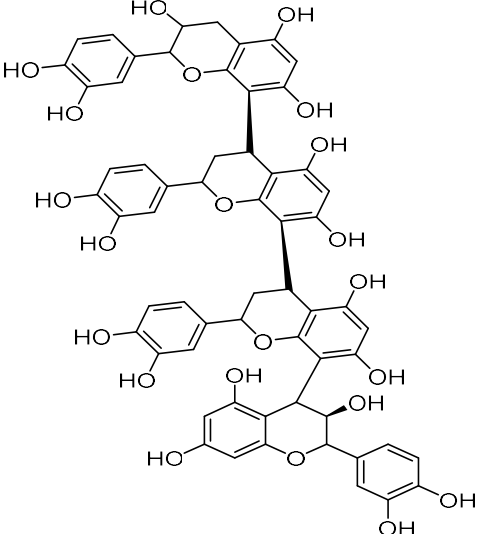
Name	Structure				Plant source	Ref.
	R <sub>1</sub>	R	R <sub>3</sub>	R <sub>4</sub>		
Quercetin	H	OH	-	-	<i>H. japonicum</i> <i>H. perforatum</i> <i>H. nagasawai</i>	(Brolis et al., 1998; Chen et al., 1988; Zhang et al., 2007)
Rutin	β-Rut	O H	-	-		
Hyperoside	β-Gal	OH	-	-		
Quercitrin	α-Glc	O H	-	-		
Isoquercitrin	0-Glc	OH	-	-		
Kaempferol	H	H	-	-		
Amentoflavone					<i>H. perforatum</i>	(Berghöfer and Hölzl, 1989)

13, II8-biapigenin					<i>H. perforatum</i>	(Berghöfer and Hölzl, 1987; Brolis et al., 1998)
						
	R	R1	R2	R3		
Orientin	Glc	H	OH	H	<i>H. nagasawai</i> <i>H. perforatum</i>	(Chen et al., 1988; Greeson et al., 2001)
Myricetin	H	OH	OH	OH		
						
	R	R1	R2	R3		
Miquelianin	H	O-Glc	H	OH	<i>H. hirsutum</i>	(Andrade et al., 1998; Kitanov, 1988; Kitanov et al., 1979)
Lutonaretin	Glc	H	H	OH		

### ➤ Tannins and Proanthocyanidins

Tannin and proanthocyanidins (condensed tannins) constitute a class of oligomeric and polymeric polyphenols with flavan-3-ols as monomeric building blocks (Hellenbrand et al., 2015). Despite the high impact of proanthocyanidins, most papers describing the isolation of these polyphenols from *Hypericum* or other plants discuss only the quantitative aspects.

**Table I 18.** Reported isolated tannins and proanthocyanidines of different *Hypericum* species

Name	Structure	Plant source	Ref.		
Catechin		<i>H. erectum</i>			
Procyanidin B1					
Cinnamtannin A2					(Yazaki and Okuda, 1990; Yazaki et al., 1991)

### ➤ Xanthones

Xanthones have been identified in the highest numbers from the plant family. more 100 xanthones have been isolated and identified from species of *Hypericum* (Crockett and Robson, 2011), many of which differ according to patterns of hydroxy, methoxy, prenyl, butenyl and glycoside substitutions on the base structure. Certain reported isolated compounds of this family are shown in the table I.19.

Table I 19. Reported isolated xanthenes of different *Hypericum* species

Name	Structure	Plant	Ref.
Kielcorin		<i>H. subalatum</i>	(CHEN, 1988)
Euxanthone		<i>H. perforatum</i>	(Yin et al., 2004)
	R		
Garcinone B	i-Pr	<i>H. erectum</i> <i>H. balearicum</i>	(An et al., 2002; Wollenweber et al., 1994)
Toxyloxanthone	H		
Patuloside A		<i>H. p. atulum</i>	(Ishiguro et al., 1999)
Gemixanthone A		<i>H. g. eminiflorum</i>	(Chung et al., 1999)

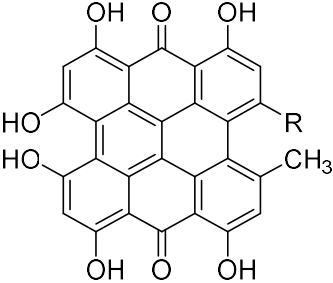
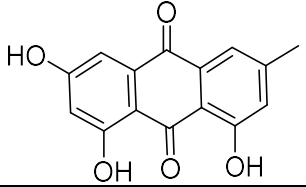
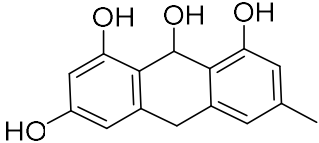
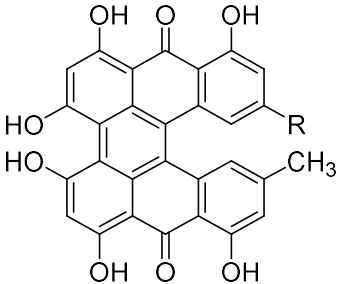
### E. Products of the acetate pathway

#### ➤ *Naphodianthrones and other anthraquinone derivatives.*

Hypericin and pseudohypericin are the two major dianthrones of St John's wort (*Hypericum*

*perforatum*), Their presence in the plant is revealed by the presence of blackish or reddish glands, which are clusters of cells containing lipophilic substances and either one or both of the compounds. Hypericin and pseudohypericin are of greatest pharmacological interest reported to have antidepressant and antiviral effects.

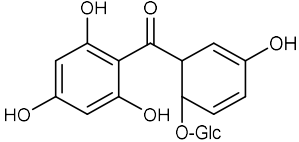
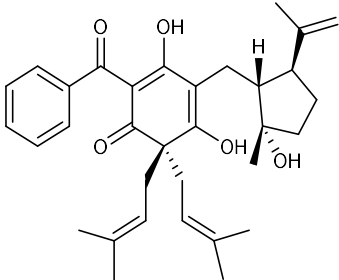
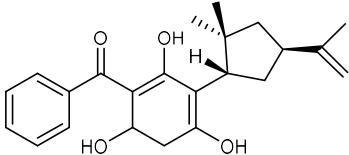
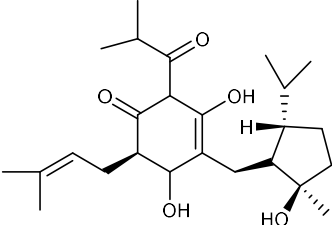
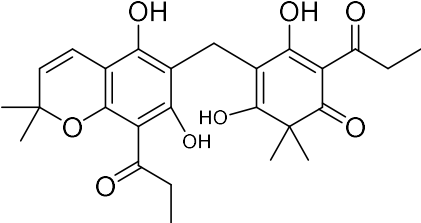
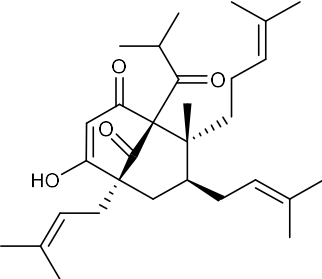
**Table I 20.** Reported isolated anthraquinones and derives of different *Hypericum* species

Name	Structure	Plant source	Ref.
			
	R		
Hypericin	Me	<i>H. perforatum</i>	(Čellárová et al., 1994; Fourneron et al., 1999; Kirakosyan et al., 2000)
Pseudohypericin	CH <sub>2</sub> OH		
Emodin		<i>H. amschaticum</i> <i>H. erectum</i>	(Makovetska, 1999; Mathis and Ourisson, 1963a)
Emodinanthranol			
			
	R		
Protohypericin	Me		
Protopseudohypericin	CH <sub>2</sub> OH		

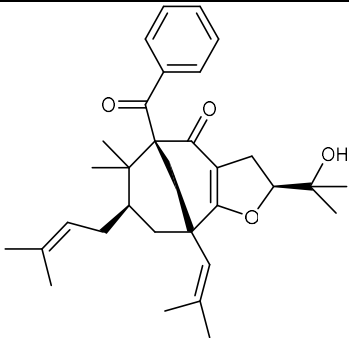
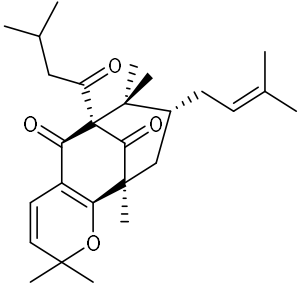
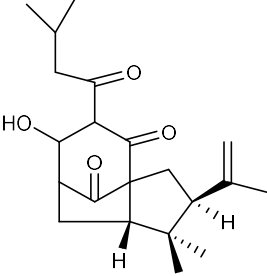
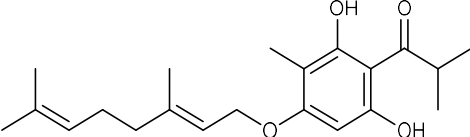
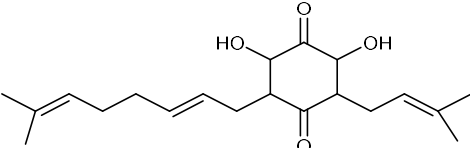
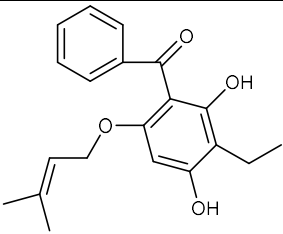
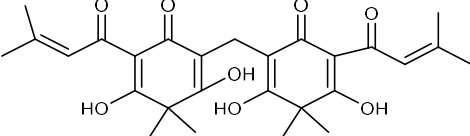
➤ *Phloroglucinol-derivatives*

Phloroglucinol derivatives have been isolated from several plants of *Hypericum* genus. Some examples of structurally unique phloroglucinol derivatives, and the species they have been isolated from, are given in table I.21.

**Table I 21.** Reported isolated phloroglucinols of different *Hypericum* species

Name	Structure	Plant source	Ref.
Hypericophenonoside		<i>H. anulatum</i>	(Kitanov and Nedialkov, 2001)
Hypercalin B		<i>H. revolutum</i>	(Decosterd et al., 1989)
Chinensin		<i>H. monogynum</i>	(Nagai and Tada, 1987)
Paglucinol		<i>H. patulum</i>	(Ishiguro et al., 1998)
Drummondin A		<i>H. Drummondii</i>	(Jayasuriya, 1988)
Hyperevolutin		<i>H. revolutum</i>	(Decosterd et al., 1989)



Hyperibone A		<i>H. scabrum</i>	(Matsuhisa et al., 2002)
Papuaforin A		<i>H. papuanum</i>	(Winkelmann et al., 2000, 2001a, b)
Ialibinone A			
Otogirin		<i>H. erectum</i>	(Tada et al., 1991)
Erectquione A			
Sarothralin		<i>H. japonicum</i>	(Wu et al., 1998a)
Japonicin A			

### I.1.8.2. Biological review of *Hypericum*

Extracts of *Hypericum* other than the known *H. perforatum* have been tested in a variety of assays, including *in vitro* antibacterial, antifungal, antiviral and antioxidant assays and *in vivo* anti-inflammatory, antinociceptive and antidepressant assays. The *in vivo* assays have traditionally used mice or rats as test subjects. It has been reported that the extracts or isolated pure compounds from *Hypericum* genus have been submitted for testing in molecular antidepressant target assays, such as *in vitro* receptor binding (e.g. GABA<sub>A</sub> and GABA<sub>B</sub>, benzodiazepine, serotonin) and enzyme inhibition (e.g. MAO type A and B) assays. Results of previous studies are summarized in the following table:

**Table I 22.** A list of biological activities reported from different *Hypericum* species

No.	Activity	Plant Source	Reference		
1	Antibacterial	<i>H. brasiliense</i>	(Rocha et al., 1995)		
		<i>H. perforatum</i>	(Saddiqe et al., 2010)		
		<i>H. hookerianum</i>	(Mukherjee et al., 2001)		
2	Antifungal	<i>H. hyssopifolium</i>	(Cakir et al., 2004)		
		<i>H. heterophyllum</i>			
		<i>H. caprifoliatum</i> , <i>H. carinatum</i> , <i>H. connatum</i> , <i>H. ternum</i> , <i>H. myrianthum</i> <i>H. iriai</i> <i>H. polyanthemum</i>	(Fenner et al., 2005)		
		3	Antiviral	<i>H. perforatum</i>	(Miskovsky, 2002)
		4	Antioxidant	<i>H. perforatum</i>	(Zou et al., 2004)
<i>H. hyssopifolium</i> L	(Cakir et al., 2003)				
<i>H. androsaemum</i>	(Valentão et al., 2002)				
5	Antimicrobial activity	<i>H. rumeliacum</i>	(Couladis et al., 2003)		
		<i>H. maculatum</i> Crantz	(Gudžić et al., 2002)		
6	Antiplasmodial activity	<i>H. erectum</i>	(Moon, 2010)		
7	Antiprotozoal activity	<i>H. andinum</i> , <i>H. brevistylum</i> , <i>H. caprifoliatum</i> , <i>H. carinatum</i> , <i>H. linoides</i> , <i>H. myrianthum</i> , <i>H. polyanthemum</i>	(Dagnino et al., 2015)		
8	Antimalarial activity	<i>H. lanceolatum</i>	(Zofou et al., 2011)		
9	Antidepressant activity	<i>H. perforatum</i>	(Butterweck et al., 2000; Tian et al., 2014; Wentworth et al., 2000)		
10	anti-inflammatory	<i>H. perforatum</i>	(Sosa et al., 2007)		

		<i>H. canariense</i> L., <i>H. glandulosum</i>	(Rabanal et al., 2005)
11	Antinociceptive	<i>H. caprifoliatum</i> , <i>H. polyanthemum</i>	(Viana et al., 2003)
		<i>H. perforatum</i>	(Galeotti et al., 2010)

### I.1.9. Classification of Clusiaceae and *Hypericum* L. genus

The genus *Hypericum* has been treated as a natural unit by most taxonomists, although the discussion whether to treat this genus and its nearest relatives as a separate family (i.e. Hypericaceae) or as part of subfamily Hypericoideae within Guttiferae has been contentious (Robson, 1981; Stevens, 2007a, b).

The family Clusiaceae (Guttiferae), distributed primarily in tropical and subtropical regions worldwide, has traditionally been defined as having about 50 genera and 1200 species (Cronquist, 1981; Gustafsson et al., 2002). Most temperate species are members of the genus *Hypericum* (450), while the largest tropical genera are *Garcinia* L. (200) and *Clusia* L. (145) (Mabberley, 1997). Representatives of this family generally have opposite simple exstipulate leaves, a superior ovary, and an androecium of few to numerous stamens. The characters of secretory canals and cavities filled with clear, green, or resinous sap in most of the tissues specifically distinguishes this family from other close relatives (Cronquist, 1981). Most species of *Hypericum* possess typical opposite exstipulate leaves with translucent, black, or red glandular punctations, flowers with 5 yellow to orange-tinged petals, stamens grouped into 3-5 fascicles (clusters), ovaries with 3-5 styles, and capsular fruits containing numerous seeds (Crockett and Robson, 2011). While *Hypericum* and its closest generic relatives, as determined by morphology, have at times been treated as a separate family (Hypericaceae), current taxonomic treatments recognize these taxa as belonging to subfamily Hypericoideae within Clusiaceae. Subfamily Hypericoideae includes the tribes Vismieae (e.g. *Vismia* Vand.), Cratoxyleae (e.g. *Cratoxylum* Blume) and Hypericeae (e.g. *Hypericum*), and is defined by the following combination of characters: perfect flowers, usually free styles, glandular punctate leaves and seeds lacking an aril (Cronquist, 1981). Robson (Robson, 1981) recognized five genera within tribe Hypericeae, but noted that they fall into two distinct groups. *Hypericum* and *Santomasia* N.

- ***Hypericum* L. (Clusiaceae)** is a genus of flowering plants, represented by nearly 450 species distributed throughout temperate and tropical mountain regions of the world (Robson, 2003). Morphological characters shared by *Hypericum* species include resin-filled glands, stamens

in bundles (fascicles) and free styles. *Hypericum* and its closest relatives are grouped as a subfamily of Clusiaceae, although some earlier taxonomic classifications have treated it as a separate family (Hypericaceae). Thirty-six taxonomic sections within *Hypericum* are recognized, as defined by floral and vegetative morphology. One of the most widespread members of the genus is common St. John's Wort *Hypericum perforatum* L.), which is considered native to Eurasia and parts of Africa, but has been introduced into many other parts of the world (Crockett and Robson, 2011).

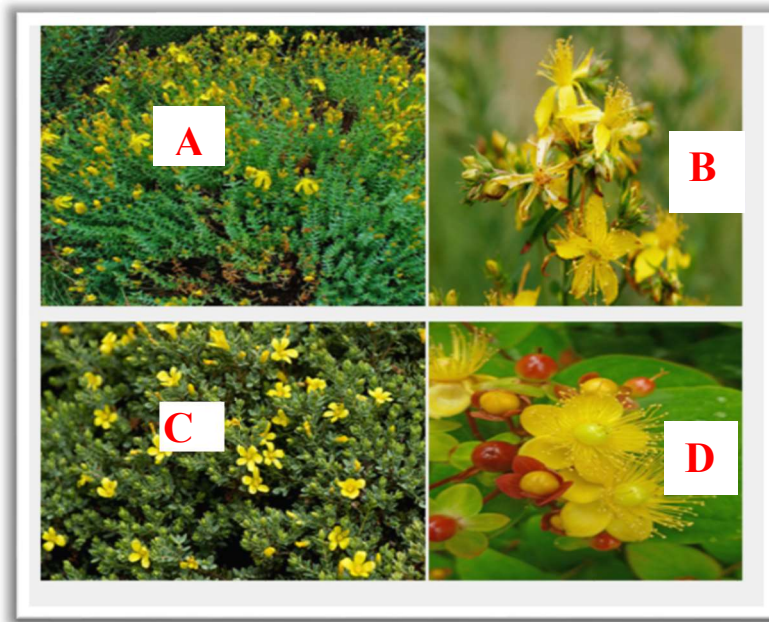


**Figure I 11.** Photo of some *Hypericum* species. A; *Hypericum olympicum*, B; *Hypericum Perfoliatum* flowers, C; *Hypericum aegypticum*, D; *Hypericum calycinum*.

#### **I.1.10. Use of *Hypericum* in folk medicine**

The popular interest in *Hypericum* species have been based on their pharmacological properties and their use in traditional medicines around the world. In fact, *H. perforatum*, commonly known as St. John's wort, is used as poultice, decoction or infusion for sedative and tonic functions and more commonly to treat mild to moderate depression (Crupi et al., 2013). This plant has been used as an herbal remedy for its anti-inflammatory and healing properties since the Middle Ages. It was noted for its wound-healing and diuretic properties as well as for the treatment of back pain ref. St. John's wort has been considered as targets in the research during the past decade, it could be used clinically as antidepressants and anxiolytics. A wide range of studies

support *Hypericum's* place in the treatment of depression (Kessler et al., 2001; Linde et al., 1996). Other areas of therapeutic research for St. John's wort include smoking cessation, premenstrual symptoms, physical symptoms due to mental disorders, and attention deficit hyperactivity disorder, as well as its possible role in treating cancer and HIV (Esposito et al., 2013; Tanaka et al., 2005; Xavier et al., 2012). Not much is known about *Hypericum afrum* and its use in folk medicine.

### **I.1.11. Economic Importance of Clusiaceae and *Hypericum***

Several tropical members of the Clusiaceae have been utilized commercially as sources of timber, drugs, dyes, resins and oils (Wood Jr and Adams, 1976). In addition, representatives from many genera including *Hypericum*, *Garcinia*, *Cratoxylum*, *Calophyllum*L. and *Clusia*, are being investigated for their medicinal potential (Crockett, 2003). Specifically, the genus *Hypericum* has economic importance due to use in traditional medicine and horticulture.

The most widely recognized and economically important species, however, is the common St. John's Wort, *Hypericum perforatum* L. The extracts of *H. perforatum* are available as dietary supplements in the United States and as a botanical medicine in Europe. It is one of the top best-selling botanicals for more than a decade in the US, with \$ 5.6 million in 2013 sales (Lindstrom et al., 2014) and € 70 million in 2004 sales in Germany (Crockett and Robson, 2011). Pharmacological use of the *H. perforatum* and its economic impact prompted the phytochemical study of different plants belonging to the same genus.

**I.1.12. Taxonomical identification of *Hypericum afrum* in the plant kingdom (Brum-Bousquet et al., 1977; Stevens, 2007a)**

<i>Hypericum afrum</i> (Lam.)	
<b>Kingdom</b>	Plantae
<b>Division</b>	Magnoliophyta
<b>Class</b>	Magnoliopsida
<b>Order</b>	Malpighiales
<b>Family</b>	Hypericaceae (Guttiferae)
<b>Genre</b>	<i>Hypericum</i>
<b>Species</b>	<i>Hypericum afrum</i> Lam. (1797)
<b>Common Name</b>	Millepertuis de Numidie

**I.1.13. Description of the plant under investigation:**

*H. afrum* grows in different forms existing as a shrub or herbaceous plant depending on its biological adaptation to the dampness of the environment, is reaching about 1.6 m high, The Leaves are sessile, amplexicaul more or less wavy margins, their dimensions are 10-15 X 3-5 mm. The flowers are from 12 to 15 mm with oval petals, obtuse triangular reaching at most  $\frac{1}{4}$  of the petals length. Stamens very welded in 3-5 groups<sup>13</sup>. The Flowering takes place during the month of June to July permitting the collection of samples in both two forms at different stations in the region of El Taref (Quezel, 1963).

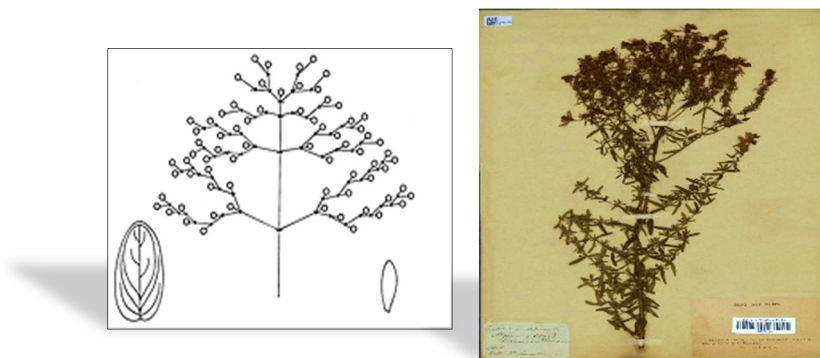


**Figure I 12.** Photo of *Hypericum afrum* Lam specimen (Brum-Bousquet et al., 1977)

**I.1.14. Geographic distribution of *Hypericum afrum***

*Hypericum afrum* is only known from a few sites in Algeria and Tunisia and the area of occupancy is smaller than 500 km<sup>2</sup>, but it occurs at more than 10 locations. The quality of its habitat is declining, but there are no extreme fluctuations. It is therefore considered as Near Threatened. This species is mainly present in wetlands, peat soils and near the springs or the edges of streams, including in forests (Brum-Bousquet et al., 1977).

This species, endemic to Numidia region, is common in the regions of Bejaia, Jijel and Skikda to the Algerian-Tunisian borders. In the region of El-Tarf, this species grows in Cape Rosa Bog where it takes the form of a shrub and in the alder of Ain Khiair where it takes the form of herbaceous.

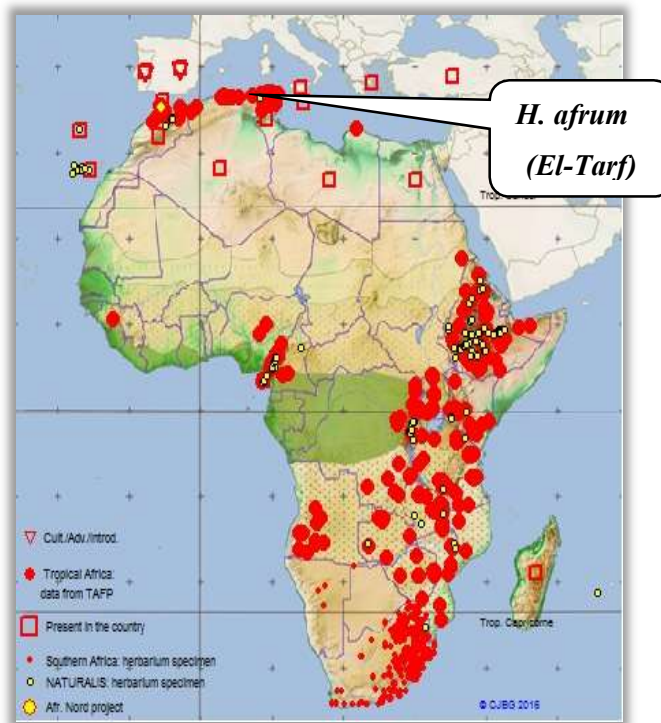


**Figure I 13.** Geographic distribution map for species of *Hypericum* L. genus (Brum-Bousquet et al., 1977)

*CHAPTER 2:  
MATERIAL, APPARATUS AND METHODS*



## I.2. Material, Apparatus and Methods

### I.2.1. . Material

#### I.2.1.1. Plants Material

##### ➤ *Cytisus villosus* Pourr.

The aerial parts of *Cytisus villosus* (Pourr.) were collected from the region of Collo, in the Northeastern Algeria, in April 2010. Plant was identified by Dr. Djamila belouahem-Abed from the National Institute of Forest Research (INRF). A voucher specimen (UM-10232015) has been deposited in the culture collection of the Department of BioMolecular Sciences, University of Mississippi.

##### ➤ *Hypericum afrum* Lam.

The aerial parts of *Hypericum afrum* (Lam.) were collected from El Kala region, El Tarf, in the Northeastern Algeria, in late July 2011. The plant was identified by Dr. Djamila belouahem-Abed from the National Institute of Forest Research (INRF). A voucher specimen (UM-10012014) has been deposited in the culture collection of the Department of BioMolecular Sciences, University of Mississippi.

#### I.2.1.2. Materials for chemical study

##### A. Adsorbents

**A.1. Standard silica gel** (particle size, 40-63 µm, 230×400 mesh), Sorbent Technologies for CC and precoated silica gel plates G60F254 (Aluminum sheets, 200 µm thickness), Sorbent Technologies, United States.

**A.2. Reversed phase (C18) silica gel SPE** CC and precoated C18-W silica TLC plates, aluminium backed, 150 µm, Sorbent Technologies.

**A.3. MN-polyamide-SC-6**, a classical adsorbent with great importance in natural product chemistry. Due to its unique, medium polar properties, polyamides are a useful complement to conventional adsorbents, like silica gels. polyamide powder is a good adsorbent for (CC) for phenols and organic acids, such as formic acid, acetic acid or propionic acid (Carelli et al., 1955). The reason is the ability to form strong hydrogen bonds between its amide and the phenolic hydroxy groups. Due to crosslinking by hydrogen bonds polyamides show sufficiently low solubility in hydrophilic solvents like methanol, ethanol, acetone and dimethyl formamide. The partition coefficient of phenol between polyamide 6 and water is constant up to relatively high phenol concentrations providing an ideal prerequisite for chromatographic separation.

A.4. *Diaion-HP-20-5*, ion exchange resin styrenic adsorbent, particle size > 250 µm, Sorbent Technologies.

A.5. *Sephadex LH-20*, Sigma-Aldrich.

**B. . Solvents:**

**B.1. For extraction**

The solvents used in this work include: n-hexane, chloroform, dichloromethane, ethyl acetate, ethanol, methanol, *n*-butanol, acetonitrile (HPLC grade, Micron filtered), Water (HPLC grade, Micron filtered), Fisher Scientific and formic acid, Acros.

**B.2. For column and TLC**

**Table I 23.** A list of the used chromatographic solvent systems

Solvents combination	Ratios	Code
EtOAc-HCOOH-H <sub>2</sub> O	10:2:3	I
EtOAc-MeOH-NH <sub>4</sub> OH	9:1:1	II
CHCl <sub>3</sub> - EtOAc - HCOOH	5:4:1	III
DCM- EtOAc	9:1	IV
DCM-MeOH	98:2	V
	95:5	VI
	90:10	VII
	85:15	VIII
	80:20	IX
	70:30	X
	60:40	XI
	50:50	XII
CHCl <sub>3</sub> -MeOH	98:2	XIII
	95:5	XIV
	90:10	XV
	85:15	XVI
	80:20	XVII
	70:30	XVIII
	60:40	XIX
H <sub>2</sub> O-MeOH	98:2	XX
	95:5	XXI
	90:10	XXII
	85:15	XXIII
	80:20	XXIV
	70:30	XXV
	60:40	XXVI
n-hexane-ethyl acetate-formic acid	31:14:5	XXVII
n-.hexane-ethyl acetate	9 :1	XXVIII

### **B.3. NMR solvents:**

DMSO-*d*<sub>6</sub>, CD<sub>3</sub>OD, and CDCl<sub>3</sub> were used in the NMR spectral.

### **C. Spraying reagents:**

C.1. Vanillin/H<sub>2</sub>SO<sub>4</sub> for general detection (10% v/v conc. sulphuric acid in ethanol (Godin, 1954).

C.2. Ammonium hydroxide vapour (Chalmers and Mikeš, 1966).

C.3. Dragendorff's reagent, Fluka.

### **D. The standard compounds**

The standard compounds used for the analytical study were isolated at National Center for Natural Products Research (NCNPR) USA. The identity and purity were confirmed by chromatographic (TLC, HPLC), and spectroscopic methods (IR, 1D- and 2D-NMR, HRESIMS).

#### **I.2.1.3. Material for UPLC-UV/MS analysis**

Monosaccharide standards including; D-glucose, D-galactose and L-rhamnose as well as flavonoid glycoside rutin were purchased from Sigma Aldrich, United States. The purity of monosaccharide standards was labeled in the range 97–99%.

#### **I.2.1.4. Materials for biological study**

- The fungal strains (*Candida albicans*, *C. glabrata*, *C. krusei*, *Aspergillus fumigatus* and *Cryptococcus neoformans*) were obtained from NCNPR, Mississippi University, United States.
- . The bacterial strains (*Staphylococcus aureus*, MRS, *Escherichia coli*, *Pseudomonas aeruginosa* and *Mycobacterium intercellulare*) were obtained from NCNPR, Mississippi University, United States.
- . The test organisms, *Plasmodium falciparum* D6, *P. falciparum* W2 and VERO cells for antiplasmodial assay, NCNPR, Mississippi University, United States.
- . The test protozoans, *Leishmania donovani* Promastigote, *L. donovani* Amastigote, *L. donovani* Amastigote/THP, *Trypanosoma brucei* and THP1 used in antiprotozoal assay, NCNPR, Mississippi University, United States.
- . The drug controls (amphotericin B and difluoromethylornithine) are used as positive controls, Ilex Oncology (San Antonio, TX) while DMSO (25%) was used as a negative

control in antiprotozoal assay.

- . The antimalarial drug control chloroquine, Sigma-Aldrich (St. Louis, MO, USA).
- . The antifungal drug control amphotericin B and the antibacterial drug control ciprofloxacin, Sigma-Aldrich (St. Louis, MO, USA).
- . Recombinant human MAO-A and MAO-B, BD Biosciences (Bedford, MA)
- **Cytotoxic activity**

*In vitro* cytotoxic activity was determined against six human cancer cell lines; human leukemia cells (HL-60), skin melanoma (SK-MEL), epidermal carcinoma (KB), breast carcinoma (BT-549), ovarian carcinoma (SKOV-3) cervical carcinoma (HeLa) and two non-cancerous kidney cell lines (LLC-PK<sub>11</sub> and Vero). All cell lines were obtained from the American Type Culture Collection (ATCC, Rockville, MD, USA).

- **Antioxidant assay**

The quercetin and gallic acid standards for total flavonoids and phenol contents, Folin–Ciocalteu reagent, Na<sub>2</sub>CO<sub>3</sub>, Ascorbic acid, 1,1-diphenyl-2-picrylhydrazyl (DPPH) were purchased from, Sigma-Aldrich (Poznan, Poland).

Cellular antioxidant activity was measured in human hepatoma cells (HepG2) as described by Wolfe and Rui (Wolfe and Liu, 2007). HepG2 cells (acquired from American type culture collection, ATCC, Rockville, MD) were grown in DMEM supplemented with 10% FBS and antibiotics (50 unit/mL penicillin and 50 µg/mL streptomycin). For the assay, cells were seeded in the wells of a 96-well plate at a density of 60,000 cells/well and incubated for 24 hrs. Quercetin was used as positive control.

## **I.2.2. Apparatus**

### **I.2.2.1. Apparatus for chemical study**

- Rotatory evaporator (Buchi Rotavapor R-260 connected with Buchi Heating Bath B-490), Germany.
- High speed Vacuum Evaporator (SPD 2010 Speedvac System (Thermo Electron Corp., USA)
- UV irradiation was carried out with a Spectroline UV lamp ENF 240C (Spectromics Corporation, NY, USA) in a sealed chamber.

- Chromatographic glass column (0.5-5cm in diameter) for column chromatography.
- Optical rotation was recorded at ambient temperature using a Rudolph Research Analytical Autopol IV automatic polarimeter, USA.
- IR spectra were recorded on a Bruker Tensor 27 spectrophotometer, Germany.
- HPLC Delta Prep 4000 (Waters Corporation, Milford, Massachusetts, USA) equipped with a dual wavelength detector Model 2487 adjusted at 210 and 254 nm.
- Preparative HPLC columns [Silica gel and C18 (100 A 250 x 15.00, 5 $\mu$ )] were from Phenomenx Luna, USA.
- NMR spectra were acquired on a Varian Mercury 400 MHz spectrometer at 400 (1H) and 100 (13C) MHz in CDCl<sub>3</sub>, using the residual solvent as a ninternal standard. Multiplicity determinations (DEPT) and 2D-NMR spectra (HMQC, HMBC, NOESY) were obtained using standard Bruker pulse programs.
- HRESIMS were obtained by direct injection using a Bruker Bioapex-FTMS with electrospray ionization (ESI), USA.
- **LC-MS Analysis**

The chromatographic experiments were performed using the UPLC system which consisted of Dionex Ultimate 3000 series including a binary pump, a diode-array detector, an autosampler and a column compartment (Thermo Scientific, San Jose, CA, USA). Methanolic extracts of *P. semilanceata* and *Ph. cyanopus* were separated on a Phenomenex Gemini C18 column (3  $\mu$ L, 150  $\times$  3.0 mm I.D.; Phenomenex, Torrance, CA, USA) maintained at 35°C. The mobile phase consisted of a mixture 0.2% formic acid (POCH S.A., Gliwice, Poland) in water and a mixture 0.2% formic acid in acetonitrile (Sigma-Aldrich, Poznań, Poland). A constant flow of 0.2 mL/min was applied. The acetonitrile percentages were: 0–1.5 min, 5%; 1.5–12 min, linearly from 5% to 95%; 12–20 min, 95%; 20–25 min, linearly from 95% to 5%; 25–30 min, (equilibration step), 5%. The effluent from the chromatographic column was injected into microOTOFQ-II time of flight mass spectrometer (Bruker Daltonics, Bremen, Germany) equipped with an electrospray ionization (ESI) interface in the negative mode. Mass data were collected in the product ion scan mode. All solvents were of LC-MS grade.

### **I.2.2.2. Apparatus for analytical study**

- UHPLC/APCI-MS was performed using an Agilent 1290 UHPLC system coupled with an Agilent 6120 single quadrupole mass spectrometer.

### **I.2.2.3. Apparatus and chromatographic conditions for UPLC-UV/MS analysis**

All analyses were performed on a Waters Acquity UPLC™ system (Waters Corp.) that included a binary solvent manager, sample manager, heated column compartment, photodiode array (PDA) detector, and a single quadrupole detector (SQD). The instrument was controlled by Waters Empower 2 software. An Acquity UPLC™ BEH C18 column (100 mm × 2.1 mm I.D., 1.7 μm) also from Waters, was used. The column and sample temperatures were maintained at 35 °C and 25 °C, respectively. The eluent consisted of water with 0.05% formic acid (A) and acetonitrile/methanol/isopropanol (50:25:25, v/v) with 0.05% formic acid (B). Analysis was performed using the following gradient elution at a flow rate of 0.30 mL/min: 14% B to 16.5% B in 22 min, and increasing B to 100% B in next 0.5 min. The composition of mobile phase was changed linearly. The analysis was followed by a 2.5-min washing procedure with 100% B and re-equilibration period of 3.5 min. All solutions were filtered through 0.20-μm membrane filters, and the injection volume was 2 μL. The total run time for analysis was 23 minutes. The PDA detection wavelength was 254 nm.

The ESI source was used in the positive mode. Mass spectrometer conditions were optimized to obtain maximal sensitivity. The source and desolvation gas temperatures were maintained at 150 and 350 °C, respectively. The probe voltage (capillary voltage), cone voltage, and extractor voltage were fixed at 3.0 kV, 45 V, and 3.0 V, respectively. Nitrogen was used as the desolvation gas (650 L/h) and drying gas (25 L/h). Analyte identity was confirmed in selected ion recording (SIR) mode. Mass spectra were obtained at a dwell time of 0.1 s in SIR and 500 Da/sec of the scan rate.

### **I.2.2.4. Apparatus for biological study**

#### **➤ Apparatus for Transfection and Luciferase assay**

The light output was detected in a Glomax® Multi+ detection system with Instinct™ Software (Promega Corporation, Madison, WI, USA).

#### **➤ Apparatus for antimicrobial assay:**

- Bechman/Coulter Z1 (Fullerton, CA, USA) particle counter.
- Hemocytometer counts Olympus IX 70 (Olympus Industrial America, Inc., Melville, New York, USA) Inverted microscope with an Olympus DP12 digital camera.

- Microplate photometer (Packard Spectra Count, Packard Instrument, Downers Grove, IL).
- Microtiter plates (Nunc MicroWell (untreated), Roskilde, Denmark).

### **I.2.3 Methods**

#### **I.2.3.1. Analytical Study**

- i. MS analysis: The drying gas flow was 10 L/min and the nebulizer pressure was 30 psi. The drying gas temperature and vaporizer temperature were set to 250°C and 200°C, respectively. The capillary voltage was 3000 V and the corona current was 4.0 Ma.
- ii. Acidic hydrolysis: by a reported UPLC-UV/MS method (Wang et al., 2012).

**A.1. Hydrolysis of flavonoids glycosides:** About 1 mg of glycoside sample, such as cauloside G or ciwujianoside A1 was dissolved in 200 µL of 2 M HCl and heated at 90°C for 2 hrs. After hydrolysis, the reaction mixture was neutralized with 200 µL of 9 M NH<sub>4</sub>OH, and dried with high purity N<sub>2</sub> gas.

**A.2. Derivatization of the samples:** About 1 mg of each monosaccharide or sample was dissolved in 120 µL of a solution of L-cysteine methyl ester (0.3 mmol/mL) and pyridine. After mixing thoroughly, the reaction mixture was incubated at 90°C for 1 hr. 160 µL of reagent consisting of phenyl isothiocyanate (0.69 mmol/mL) and pyridine was added, and the solution was heated for another hour. The final solution was further diluted 20–200 times before UPLC-MS analysis.

#### **iii. Total phenolic content (TPC)**

The total phenolic was measured spectrophotometry with a modified Folin-ciocalteu method (Tuberoso et al., 2010). Each crud extract fraction (1mg) was dissolved in (70% methanol) (1ml). 20 µl of the extract solution diluted with distilled water (1,58ml) was mixed with 100 µl of Folin-ciocalteu reagent. After 5 min, 300 µl of NaCO<sub>3</sub> (7g/100ml distilled water) solution were added. After 2h of incubation at room temperature, the absorbance was read against a blank (70% methanol) at 760 nm in a 10 mm quartz cuvette. The same procedure was applied to the standard solutions of gallic acid. Total phenol content, expressed as milligrams of gallic acid equivalent (GAE) per gram of extract (GAE mg /g), was calculated on the basis of a standard calibration curve of Gallic acid ( $Y = 0.1157x + 0.087$ ,  $R^2 = 0.9749$ ) All measurements were carried out in triplicate.

**iv. Total flavonoid content**

Total flavonoid content of the plants fractions crud extracts was determined by colorimetric method (Chang et al., 2002; Marinova et al., 2005). Each 0,25ml of the 1mg/ (1ml 70% methanol) crud extract fraction was diluted with 1, 25 ml of distilled water. Then 75 µl of 5% Sodium nitrate (NaNO<sub>2</sub>) solution was added to the mixture. After 6min in darkness at room temperature 150 µl of 10% AlCl<sub>3</sub>.6H<sub>2</sub>O solution was added. The mixture was allowed to stand for 5 min in the dark to complete reaction. Finally, 0,5 ml of 4% NaOH was added with 0,275 ml of distilled water to get a total volume of 2,5ml in the test tubes. After mixing, the absorbance was measured immediately against a blank (70% methanol) at a fixed wavelength 510 nm using spectrometer. Quercetin standard was used the calibration curve. The concentration of total flavonoid content in the test samples was calculated from the calibration plot ( $Y = 1.2308x + 0.0151$ ,  $R^2 = 0.9775$ ) and expressed as mg quercetin equivalent (QE)/g of dried plant material. All the determinations were carried out in triplicate.

**v. Test methods for screening the plants for major classes of phytochemicals**

**A. Test alkaloids**

➤ **Methanol extract preparation**

Two grams of plant material, dried and ground are added to 100 ml of 50% methanol. After sonication for 15 min and stirring overnight, the extracts were filtered and evaporated to dryness using a rotary evaporator. Residues are shown in a few ml of pure methanol. These extracts are subject to the following test.

➤ **Dragendorff test**

A thin layer chromatography we call TLC (silica gel plate 20 x 20 cm,) is performed for a few µl of methanol extract. The migration solvent is EtAc / MeOH / NH<sub>4</sub>OH 50% (9:1:1). After migration, the fluorescent spots at 365 nm are sprayed with Dragendorff reagent (potassium tetraiodobismuthate). The appearance in visible light orange spots indicates the presence of alkaloids.

**B. Terpenoids**

2 g of powdered plant material were added 10 to 20 ml hexane. The mixture is sonicated for 15 min, stirring for 30 min and filtration. A TLC is performed, using benzene as eluent (98-99% pure). After migration, the plate is sprayed with antimony chloride and placed in an oven at 110 ° C for 10 min. Any fluorescence at 365 nm indicates the presence of terpenoids.



### **C. Coumarins**

2 g of powdered plant material was mixed with 10 ml of  $\text{CHCl}_3$ . After heating for a few minutes and filtration, the chloroform extracts are subjected to TLC, wherein the solvent is toluene / EtOAc (93:10). The visualization, after migration, is at 365 nm in the absence and in the presence of  $\text{NH}_3$ .

### **D. Flavonoids**

#### **➤ Qualitative Research:**

The different extracts and fractions of the two plants were subjected to TLC using different solvent elution. The revelation is at 365 nm after spraying with Neu's reagent (2-aminoethyl diphenylboric) 1% in pure MeOH.

### **E. Tannins**

1.5 g dry plant material is placed in 10 ml of 80% MeOH. After 15 minutes of stirring, the extracts were filtered and placed in tubes. The addition of 1%  $\text{FeCl}_3$  can detect the presence or absence of tannins. The color changes to dark blue in the presence of gallic tannins and greenish brown in the presence of catechin tannins.

#### **I.2.3.2. Conformational analysis and geometry optimization**

Circular dichroism, CD, is the difference between the absorption of left and right circularly polarized lights: it is strictly allied to chirality, because it is a manifestation of diastereomer discrimination, the two mirror image objects being the two light beams. CD may be regarded as one of the most powerful techniques for stereochemical analysis: it is sensitive to the absolute configuration as well as to conformational features, which are often completely obscured in the ordinary absorption spectrum. OMEGA 2.5.1.4 was used for conformational sampling (Hawkins and Nicholls, 2012; Hawkins et al., 2010). The 3D structural construction and initial geometry refinement were performed using OMEGA's MMFF94s force field variant with no electrostatic term for Coulomb interactions. In conformational sampling, we used a maximum of 10 kcal/mol an energy window. A root mean square (RMS) Cartesian distance of less than 0.5 was used to remove redundant and duplicate conformers. For the abinitio optimization, we used B3LYP hybrid density functional theory (DFT) and 6-31G\*\* basis set (B3LYP/6-31G\*\*) in Gaussian 09 (Frisch et al., 2009). The geometry in the vacuum and in polarizable continuum DMSO solvent model was optimized.

#### **➤ . ECD calculation**

Time-dependent density functional theory (TDDFT) was used to calculate the ECD spectra.

Electronic excitation energies, oscillator and rotational strengths were calculated using B3LYP/6-31G\*\* at excited states of 40 (Frisch et al., 2009). The PCM methanol solvent model was used in all calculations. The compounds were sketched and energy minimized in Maestro 10.2.010 (Schrödinger Release 2015b). The mixed torsional/low-mode sampling method of MacroModel with OPLS3 force field was used for the conformational search step(Schrödinger Release 2015a). All generated conformers were Boltzmann weighted and geometry optimized using density functional theory (DFT) at 31-6G\*\* level in Gaussian 09 (Frisch et al., 2009). The ECD spectra were then calculated using the time-dependent DFT (TDDFT) at 31-6G\*\* level. The calculated and experimental spectra were compared using SpecDis 1.64 (T. Bruhn, 2013, 2015.).

### **I.2.3.3. Biological Study**

#### **A. Antimicrobial assay**

For all organisms except *Mycobacterium intracellulare* and *Aspergillus fumigatus*, susceptibility testing was performed using a modified version of the CLSI (formerly NCCLS) methods (Rahman et al., 2011; Samoylenko et al., 2009) and optical density was used to monitor growth. Media supplemented with 5% Alamar Blue (Biosource International, Camarillo, CA) was utilized for growth detection of *M. intracellulare* (Franzblau et al., 1998; Samoylenko et al., 2009) and *A. fumigatus* (NCCLS, 1998). Samples were serially diluted in 20% DMSO/saline and transferred in duplicate to 96-well flat bottom microplates. Microbial inocula were prepared by correcting the OD<sub>630</sub> of cell/spore suspension in incubation broth RPMI at pH 4.5 for *Candida albicans*.

Sabouraud dextrose for *Cryptococcus neoformans*, cation-adjusted Muller-Hinton at pH 7.3 for MRSA and 5% Alamar Blue (Biosource International, Camarillo, CA) in Middlebrook 7H9 broth with OADC enrichment, pH = 7.3 for *M. intracellulare* and 5% Alamar Blue in RPMI at pH = 7.3 for *A. fumigatus* to afford final target inocula (1x10<sup>4</sup>, 1x10<sup>5</sup>, 5x10<sup>5</sup>, 2x10<sup>6</sup>, and 3x10<sup>4</sup> cfu/mL, respectively). Drug controls [ciprofloxacin (ICN Biomedicals, OH) for bacteria and amphotericin B (ICN Biomedicals, OH) for fungi] were included in each assay. All organisms were read at either 630 nm using the Biotek Powerwave XS plate reader (Bio-Tek Instruments, VT) or 544ex/590nm (*M. intracellulare*, *A. fumigatus*) using a Polarstar Galaxy plate reader (BMG Lab Technologies, Germany) prior to and after incubation. Minimum fungicidal or bactericidal concentrations were determined by removing 5 µL from each clear well, transferring to agar, and incubating until growth was seen. The MFC/MBC is defined as the lowest test concentration that kills the organism (allows no growth on agar).

In the secondary antimicrobial assay, isolated compounds were dissolved to 20 mg/mL to 2 mg/mL, and were tested at 20, 4, 0.8  $\mu\text{g/mL}$  and  $\text{IC}_{50}$  values vs. all 10 microbial strains using modified Alamar blue assay as previously reported (Bharate et al., 2007). Pure compounds that have an  $\text{IC}_{50}$  of  $\leq 7 \mu\text{g/mL}$  in the secondary assay proceed to the tertiary assay.

In the tertiary Assay, pure compounds are tested vs. all 10 microbes at 20, 10, 5.0, ... 0.02  $\mu\text{g/mL}$  and  $\text{IC}_{50}$  values are calculated. In addition to the  $\text{IC}_{50}$ , the MIC (minimum inhibitory concentration) and either the MFC or MBC (minimum fungicidal or bactericidal concentration, respectively) are reported. The MIC is the lowest test concentration (in  $\mu\text{g/mL}$ ) that inhibits the organism 100%. The MFC or MBC is the lowest test concentration (in  $\mu\text{g/mL}$ ) that kills the organism. While a pure compound may have an MIC, the cells may still be alive, just not growing. The MFC and MBC is a way to monitor the “cidality” or killing ability of the test sample. All  $\text{IC}_{50}$  values are calculated using the XLFit fit curve fitting software.

### **B. . Cytotoxicity**

Each assay was performed in 96-well tissue culture-treated microplates. Cells were seeded at a density of 25,000 cells /well and incubated for 24 h (except HL-60 cells, which were incubated for 3 h). Samples at different concentrations were added and cells were again incubated for 48 h. At the end of incubation, the cell viability was determined using Neutral Red dye (Borenfreund et al., 1990; Samoylenko et al., 2009). In the case of HL-60 cells, viability was determined by a XTT method, as described earlier (Choi et al., 2006; Reddy et al., 2007).  $\text{IC}_{50}$  values were determined from dose-response curves of percent growth inhibition against test concentrations. Doxorubicin was used as a positive control, while DMSO was used as the negative (vehicle) control.

#### **➤ Transfection and Luciferase assay**

HeLa cells (ATCC, Bethesda, MD, USA), Dulbecco's modified Eagle's Medium (Gibco Life Technologies, Grand Island, NY, USA), Fetal bovine serum (Atlanta Biologicals Inc., Atlanta, GA, USA), 0.05% trypsin-EDTA (Gibco Life Technologies, Grand Island, NY, USA), X-treme GENE HP transfection reagent (Roche Applied Science, Indianapolis, IN, USA), (IL-6 and TGF-beta were from R&D Systems, Inc. Minneapolis, MN, USA; m-wnt3a from Peprotech Corporation, Rocky Hill, NJ, USA phorbol 12-myristate 13-acetate (PMA) from Sigma Chemical Company, St. Louis, MO, USA and One-glo-luciferase assay system (Promega corporation, Madison, WI, USA).

### C. Determination of Antioxidant activity

The extracts were dissolved in dimethyl sulfoxide (DMSO) to make a stock solution of 20 mg/mL. The antioxidant activity of the extracts was measured at a concentration of 500 µg/mL by following two methods.

#### C.1: 2,2-Diphenyl-1-picrylhydrazyl (DPPH) Assay

The antioxidant activity of the plant extracts was determined by applying the 2,2 diphenyl 1-picrylhydrazyl (DPPH) radical scavenging method (Brand-Williams et al., 1995). For measurement of samples scavenging activity, in test tubes, 1,8 ml of DPPH stock solution (4,14mg was dissolved in 50 ml of MeOH) was added to aliquots of 0,18 ml of methanolic solutions (1 mg/ml and 10 mg /ml respectively) of the extracts and ascorbic acid at different dilutions (1/2, 1/4, 1/8, 1/16, 1/32). After mixing, the samples were left at room temperature for 30 min in dark. The control was prepared by using 0,18 ml of MeOH instead of the antioxidant extract solution, with DPPH. While a blank contained only methanol was used. The ascorbic acid was used as reference compound. Absorbance at 515 nm was measured using UV/vis spectrophotometer. Triplicate measurements were carried out.

Percent DPPH radical scavenging activity was calculated as follows (Chandra et al., 2014):

$$\text{Percent Radical Scavenging Activity (\%)} = 1 - \left\{ \frac{\text{Abs Sample} - \text{Abs Blank}}{\text{Abs Control} - \text{Abs Blank}} \right\} \times 100.$$

Ascorbic acid showed 95% radical scavenging activity at 20 µM.

IC<sub>50</sub> values were determined from the plotted graph of scavenging activity against the concentrations of samples, which is defined as the antioxidant concentration necessary to decrease the initial DPPH radical by 50% and it's expressed in amount of antioxidant/mmol of DPPH.

The antiradical power (ARP) was calculated as follow:

$$\text{ARP} = 1/\text{IC}_{50}.$$

The total antioxidant capacity was also expressed in mg of Ascorbic acid (mg AAE/g of extract), and was calculated as follow:

Ascorbic acid equivalents:

$$\text{AAE} = \text{ARP extract}/\text{ARP Ascorbic acid}.$$

- TLC coupled with 2,2-diphenyl-1-picrylhydrazyl staining was used for preliminary analysis of certain extracts and fractions of *C. villosus* and *H. afrum* species (Figure I.20)

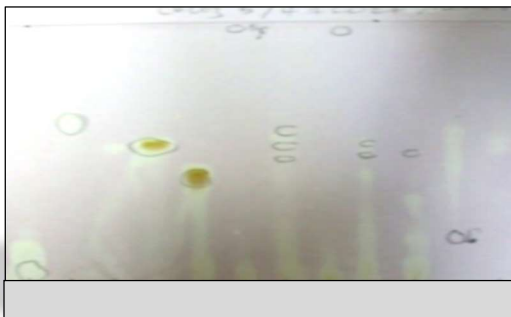


**Figure I. 14.** Typical TLC photography of certain extracts and fractions of the two species *C. villosus* and *H. afrum* colorized with 0.05% DPPH.

### C.2. Cellular Antioxidant Activity Assay (CAA Assay)

The cellular antioxidant activity was measured in HepG2 cells as described by Wolfe and Rui. The method measures the ability of phytochemicals in the plant extracts to prevent intracellular generation of peroxy radicals in response to ABAP (used as a generator of peroxy radicals). The CAA assay is a more biologically relevant method than a chemical assay because it represents the complexity of biological system and accounts for cellular uptake, bioavailability, and metabolism of the antioxidant agent. HepG2 cells (acquired from American type culture collection, ATTC, Rockville, MD) were grown in DMEM supplemented with 10% FBS and antibiotics (50 unit/mL penicillin and 50  $\mu\text{g}/\text{mL}$  streptomycin). For the assay, cells were seeded in the wells of a 96-well plate at a density of 60,000 cells/well and incubated for 24 hrs. The medium was removed and cells were washed with PBS before treating with the test sample (500  $\mu\text{g}/\text{mL}$ ) diluted in the medium containing 25  $\mu\text{M}$  DCFH-DA for 1 hr. After removing the medium, the cells were treated with 600  $\mu\text{M}$  ABAP and the plate was immediately placed on a SpectraMax plate reader for kinetic measurement every 5min for 1 hr (37°C, emission at 538 and excitation at 485 nm). Quercetin was used as the positive control. The antioxidant activity was expressed in terms of CAA units. The area under the curve (AUC) of fluorescence versus time plot was used to calculate CAA units as described by Wolfe and Rui (Chandra et al., 2014; Wolfe and Liu, 2007).

$$\text{CAA unit} = 100 - [(\text{AUC sample} / \text{AUC control}) \times 100]$$

Quercetin showed CAA unit of 77 at 25 $\mu$ M. This indicates that quercetin (at 25  $\mu$ M) caused 77% inhibition of cellular generation of peroxy radicals in HepG2 cells.

➤ **Statistical Analysis**

All the experiments for determination of total phenolics, total flavonoids, and antioxidant properties using DPPH and cellular antioxidant assay (CAA) were conducted in triplicates. The values are expressed as the mean  $\pm$  standard deviation (SD). Analysis of variance and significance of difference among means were tested by one-way ANOVA and least significant difference (LSD) on mean values. Correlation coefficients ( $r$ ) and coefficients of determination ( $r^2$ ) were calculated using Microsoft Excel 2007.

**D. Assay for inhibition of iNOS**

Inhibition of intracellular NO production as a result of iNOS activity was assayed in mouse macrophages (RAW 264.7 cells) as described (Zaki et al., 2013). Cells were seeded at a density of 50,000 cells /well in 96-well plates and grown for 24 hrs. Test samples were added to the cells and after incubating with samples for 30 minutes, LPS (5 $\mu$ g/mL) was added and cells were further incubated for 24 hrs. The activity of iNOS was determined by measuring the level of nitrite in the cell culture supernatant with Griess reagent. The degree of inhibition of nitrite production was calculated in comparison to the vehicle control. IC<sub>50</sub> values were obtained from dose response curves. Cytotoxicity of test samples to macrophages was also determined in parallel to check if the inhibition of iNOS is due to cytotoxic effects.

**E. Reporter Gene Assay for the Inhibition of NF- $\kappa$ B Activity**

Human chondrosarcoma (SW1353) cells were cultured as indicated in the above paragraph. The assay was performed as described earlier (Ma et al., 2007). In brief, cells transfected with NF- $\kappa$ B luciferase plasmid construct were plated in 96-well plates at a density of  $1.25 \times 10^5$  cells/well. After 24 h, cells were treated with the test compounds, and after incubating for 30 min, phorbol 12-myristate 13-acetate (PMA, Sigma-Aldrich) (70 ng/mL) was added and further incubated for 6–8 h. Luciferase activity was measured as described above. Percent decrease in luciferase activity was calculated relative to the vehicle control. Parthenolide (Sigma-Aldrich) was used as a positive control.

#### **F. Antimalarial activity Assay**

Antimalarial was determined in vitro against chloroquine sensitive (D6, Sierra Leone) and resistant (W2, Indo China) strains of *P. falciparum* by measuring plasmodial LDH activity, as described earlier (Makler and Hinrichs, 1993). Compounds are initially tested against the D6 *P. falciparum* strain in a primary screen at 15867 ng/mL in duplicate, and percent inhibitions (% inhibition.) are calculated relative to negative and positive controls. Compounds showing  $\geq 50\%$  inhibition proceed to the secondary assay. In the secondary AP assay, samples were dissolved to 2 mg/mL (pure compounds) and tested at 4760, 1587, and 529 ng/mL and  $IC_{50}$  values vs. both the D6 and W2 strains were reported. In addition to the *P. falciparum* strains, samples are tested in the VERO mammalian cell line as an indicator of general cytotoxicity. The selectivity indices (SI), ratio of VERO  $IC_{50}$  to D6 or W2  $IC_{50}$ , are calculated. All  $IC_{50}$  values are calculated using the XLfit curve fitting software.

#### **G. The antileishmanial assay**

The in vitro antileishmanial and antitrypanosomal assays were done on cell cultures of *L. donovani* promastigotes, axenic amastigotes, THP1-amastigotes, and *Trypanosoma brucei* trypomastigotes by Alamar Blue assays as described earlier (Manda et al., 2014). The assays have been adapted to 384 well micro-plate format. In a 384 well micro-plate, the samples with appropriate dilution were added to the *L. donovani* promastigotes or *L. donovani* axenic amastigotes or *T. brucei* trypomastigotes cultures ( $2 \times 10^6$  cell/mL). The compounds were tested at three concentrations ranging from 40-1.6  $\mu\text{g/mL}$  or 10-0.25  $\mu\text{g/mL}$ . The plates were incubated at 26°C for 72 h (37°C for axenic amastigotes and *T. brucei* trypomastigotes and growth of the parasites in cultures were determined by Alamar Blue assay (Manda et al., 2014). The compounds were also tested against *L. donovani* intracellular amastigotes in THP1 cells employing a parasite-rescue and transformation assay (Jain et al., 2012). The compounds were simultaneously tested for cytotoxicity against THP1 cell cultures. The conditions for seeding the THP1 cells, exposure to the test compounds and evaluation of cytotoxicity were the same as described in parasite-rescue and transformation assay (Jain et al., 2012).  $IC_{50}$  and  $IC_{90}$  values were computed from the dose response curves using XLfit software. DFMO (difluoromethylornithine) was used as positive control.

#### **H. Opioid and cannabinoid receptor binding assay**

10  $\mu\text{M}$  of a positive control [CP-55,940 for cannabinoid receptor binding screen] and [DPDPE

(Delta), nor-Binaltorphiminedihydrochloride(Kappa) and DAMGO (Mu) for opioid receptor binding screen] were used to ascertain non-specific binding (NSB) and 1% ethanol or DMSO in Tris-EDTA buffer was used to ascertain total binding. To eliminate the possibility of contamination in the test compounds or controls, wells with 1% ethanol or DMSO with no membrane were tested. Each test well contained 100  $\mu$ L of the control, 10  $\mu$ L of test compound, or vehicle and 100  $\mu$ L cell membrane. Data was analyzed by a non-linear curve fit model using Graph Pad Prism 5.04 software (GraphPad, La Jolla, CA) and IC<sub>50</sub> values were calculated. The reaction was terminated via rapid filtration with cold Tris-HClbuffer through a UniFilter GF/B 96-well plate pre-soaked with 0.3% BSA. When the filters were dry, 25  $\mu$ L MicroScint was applied to each filter and the plates were read on a Top Count NXT HTS Microplate Scintillation Counter where the counts per minute (CPM) were recorded. Non-specific binding was subtracted from the total binding to find specific binding. Purified compounds exhibiting 50% or greater displacement of radioligand were screened for IC<sub>50</sub> values which were calculated by a non-linear curve fit model using Graph Pad Prizm 5.0 software. Naloxone HCl was used as a positive control.



**Table 1. 24.** Assay conditions for cannabinoid binding assay

	<b>Cannabinoid Binding Assay</b>	
	<b>CB1</b>	<b>CB2</b>
<b>Assay Buffer:</b>	*Tris-EDTA Buffer	*Tris-EDTA Buffer
<b>Radioligand:</b>	CP-55,940,[Side chain-2,3,4(N)-3H]	CP-55,940,[Side chain-2,3,4(N)-3H]
<b>Radioligand Manufacture/Cat#:</b>	Perkin Elmer, Cat# NET1051	Perkin Elmer, Cat# NET1051
<b>Radioligand Concentration (Kd):</b>	1.2195	1.203
<b>Receptor Membrane:</b>	HEK CB1 10/27/14	HEK CB2 6/3/14
<b>Membrane Concentration:</b>	5 ug/well	1 ug/well
<b>Total Binding Control:</b>	0.1% DMSO	0.1% DMSO
<b>Nonspecific Binding Control (NBS):</b>	CP-55,940 (Tocris Bioscience, Cat# 0949)	CP-55,940 (Tocris Bioscience, Cat# 0949)
<b>NSB Concentration:</b>	10uM	10uM
<b>Assay Control 1:</b>	AM 251 (Tocris Bioscience, Cat# 1117)	AM 251 (Tocris Bioscience, Cat# 1117)
<b>Assay Control 2:</b>	AM 630 (Tocris Bioscience, Cat# 1120)	AM 630 (Tocris Bioscience, Cat# 1120)
<b>Assay Incubation:</b>	90 min @ 37°C, gentle agitation	90 min @ 37°C, gentle agitation
<b>Filter Plate:</b>	UniFilter-96 GF/C, pre-treated w/0.5% PEI	UniFilter-96 GF/C, pre-treated w/0.5% PEI
<b>Radioligand % Binding:</b>	87.83	97.58
<b>% Inhibition Control 1:</b>	51.20	10.84
<b>% Inhibition Control 2:</b>	-	46.90
Tris-EDTA Buffer: 50mM Tris-HCl, 20mM EDTA, 154mM NaCl and 0.2% fatty-acid BSA, pH 7.4		

Table I. 25. Assay conditions for opioid binding assay

Opioid Binding Assay			
	Delta	Kappa	Mu
<b>Assay Buffer:</b>	**Tris-HCl Buffer	**Tris-HCl Buffer	**Tris-HCl Buffer
<b>Radioligand:</b>	Enkephalin(DPDPE),[Tyrosyl-3,5-3H(N)]	U-69,593,[Phenyl-3,4-3H]	DAMGO, [Tyrosyl-3,5-3H(N)]
<b>Radioligand Manufacture/Cat#:</b>	Perkin Elmer, Cat# NET922	Perkin Elmer, Cat# NET952	Perkin Elmer, Cat# NET902
<b>Radioligand Concentration (Kd):</b>	1.0325 nM	0.2847 nM	0.95035 nM
<b>Receptor Membrane:</b>	HEKhDOR P10 2/27/16	HEKhKOR P15 10/2/15	HEKhMOR P12 10/19/15
<b>Membrane Concentration:</b>	25 ug/well	15 ug/well	20 ug/well
<b>Total Binding Control:</b>	0.1% DMSO	0.1% DMSO	0.1% DMSO
<b>Nonspecific Binding Control (NBS):</b>	DPDPE (Tocris Bioscience, Cat# 1431)	U-69,593	DAMGO (Tocris Bioscience, Cat# 1171)
<b>NSB Concentration:</b>	10uM	10uM	10uM
<b>Assay Control:</b>	Naloxone hydrochloride (Tocris Bioscience, Cat# 0599)	Naloxone hydrochloride (Tocris Bioscience, Cat# 0599)	Naloxone hydrochloride (Tocris Bioscience, Cat# 0599)
<b>Assay Incubation:</b>	60 min @ RT	60 min @ RT	60 min @ RT
<b>Filter Plate:</b>	UniFilter-96 GF/B, pre-treated w/0.3% BSA	UniFilter-96 GF/B, pre-treated w/0.3% BSA	UniFilter-96 GF/B, pre-treated w/0.3% BSA
<b>Radioligand % Binding:</b>	99.6%	100.4%	99.8%
<b>% Inhibition Control (10 uM Naloxone):</b>	99.1%	99.9%	99.7%
<b>% Inhibition Control (10 nM Naloxone):</b>	28.5%	66.0%	63.3%
**Tris-HCl Buffer:50nM Tris-HCl, pH 7.4			

## **I. MAO inhibition assays**

Fixed substrate concentration and varying inhibitor concentrations were used to determine the IC<sub>50</sub> value. The reactions were carried out in 0.1 M potassium phosphate buffer at pH 7.4. Incubations mixtures contained of MAO-A (5 µg/mL) or of MAO-B (10 µg/mL) in 200 µL reaction mixture. The extracts and test compounds were dissolved in DMSO or in buffer. The reaction mixtures were pre-incubated for 10 minutes at 37 °C followed by the addition of MAO-A/MAO-B to initiate the reactions. The formation of 4-hydroxyquinoline was determined fluorometrically by SpectraMax M5 fluorescence plate reader (Molecular Devices, Sunnyvale, CA) with an excitation and emission wavelength of 320 nm and 380 nm, respectively, using the SoftMax Pro program. IC<sub>50</sub> values were determined by dose-response analysis using ExcelFit.

### **I.2.3.4. Molecular modeling study**

#### **A. Ligand Preparation**

The three dimensional (3D) structures of all ligands were created using LigPrep32 with OPLS2005 force field and charges. All possible ionization, tautomerization and protonation states were generated with Epik33-35 at target pH of 7.4. Stereochemical information were retained during ligand preparation because all stereogenic centers of the ligands are assigned. One low energy ring conformation was allowed per ligand. We kept the lowest energy conformer for each ligand.

#### **B. Protein Preparation**

Protein structural files of the human MAO-A were acquired from the Protein Data Bank (PDB codes: 2BXR36, 2BXS36, 2Z5X37, 2Z5Y37). The protein was prepared for docking operating the Protein Preparation Wizard38, 39 (PrepWizard) of Schrödinger suite. The protein structures were fixed by assigning bond orders, adding all missing hydrogen atoms, and filling in missing side chains and loops using Prime40-42. We retained only those water molecules that are located within 5 Å from the native ligand and are forming at least two hydrogen bonds with non-waters. The hydrogen bonding network was assigned and optimized by considering possible water orientations, minimizing the hydrogens of altered species and by sampling the flips for Asn, Gln, and His. Then, the protein-ligand complexes were relaxed with Impref39 using OPLS2005 force field.

#### **C. Receptor grid preparation**

The receptor grids were generated using Glide version 6.943, 44. The binding pocket was defined by the centroid of the cognate ligand. Ligand protein covalent bonds in crystal structures (PDB ID: 2BXR and 2BXS) were broken during protein preparation to allow for consistent receptor grid

preparation.

#### **D. Docking simulations**

The ligands were docked into the generated receptor grids employing Glide with standard precision (SP) scoring option. Ensemble docking approach was applied utilizing four receptor grids. The docking poses were optimized and the best scoring pose was reserved.

#### **E. Molecular dynamics simulations**

DESMOND<sup>45-47</sup> software was used for the molecular dynamics (MD) simulations. The best scoring poses of compounds 1 and 4 in complex with MAO-A (PDB code: 2Z5Y) were selected and solvated with a TIP4P water solvent model. We used an orthorhombic simulation box with dimensions of 90 Å x 90 Å x 90 Å. The appropriate numbers of solvent molecules were calculated as 19860 and 19861 for 1 and 4; respectively. Sodium ions were added based on the total charge. The solvated complexes were energy-minimized with the DESMOND minimization algorithm for 5000 iterations considering convergence threshold of 1.0 kcal/mol/Å. Short MD simulations were performed before the production step to acquire further structural relaxation. The production step was executed for 40 ns using NPT ensemble, Nosé–Hoover chain thermostat, and Martyna–Tobias–Klein barostat<sup>47</sup>. A time step of 1 fs was used for the RESPA integrator. The short range Coulombic interactions cutoff was set to 9 Å and the Particle Mesh Ewald (PME) method<sup>48</sup> was used to treat the long-range electrostatics. The M\_SHAKE algorithm was used to constrain the hydrogen bonds. The snapshots (frames) were saved at intervals of 4.8.

## REFERENCES

- Abal, M., Andreu, J., Barasoain, I., 2003. Taxanes: microtubule and centrosome targets, and cell cycle dependent mechanisms of action. *Current cancer drug targets* 3, 193-203.
- Allen, O.N., Allen, E.K., 1981. The Leguminosae. A source book of characteristics, uses and nodulation. *The Leguminosae. A source book of characteristics, uses and nodulation.*
- An, T.Y., Hu, L.H., Chen, Z.L., 2002. A new xanthone derivative from *Hypericum erectum*. *Chinese Chemical Letters* 13, 623-624.
- Andrade, P., Seabra, R., Valentao, P., Areias, F., 1998. Simultaneous determination of flavonoids, phenolic acids, and coumarins in seven medicinal species by HPLC/diode-array detector. *Journal of liquid chromatography & related technologies* 21, 2813-2820.
- Andriamparany, J.N., Brinkmann, K., Jeannoda, V., Buerkert, A., 2014. Effects of socio-economic household characteristics on traditional knowledge and usage of wild yams and medicinal plants in the Mahafaly region of south-western Madagascar. *Journal of ethnobiology and ethnomedicine* 10, 1.
- Auvray, G., Malécot, V., 2013. A REVISION OF CYTISUS SECTIONS ALBURNOIDES, SPARTOPSIS AND VERZINUM (GENISTEAE, FABACEAE). *Edinburgh Journal of Botany* 70, 61-120.
- Ayuga, C., Rebuelta, M., 1986. Comparative study of phenolic acids of *Hypericum caprifolium* Boiss. and *Hypericum perforatum* L. *An. R. Acad. Farm* 52, 723-727.
- Barnes, J., Anderson, L.A., Phillipson, J.D., 2001. St John's wort (*Hypericum perforatum* L.): a review of its chemistry, pharmacology and clinical properties. *Journal of pharmacy and pharmacology* 53, 583-600.
- Barros, L., Cabrita, L., Boas, M.V., Carvalho, A.M., Ferreira, I.C., 2011. Chemical, biochemical and electrochemical assays to evaluate phytochemicals and antioxidant activity of wild plants. *Food Chemistry* 127, 1600-1608.
- Barros, L., Dueñas, M., Carvalho, A.M., Ferreira, I.C., Santos-Buelga, C., 2012. Characterization of phenolic compounds in flowers of wild medicinal plants from Northeastern Portugal. *Food and Chemical Toxicology* 50, 1576-1582.
- Bennett, B., 2010. Twenty-Five Economically Important Plant Families. *Encyclopedia of Life Support Systems (EOLSS), UNESCO.*
- Berghöfer, R., Hölzl, J., 1987. Biflavonoids in *Hypericum perforatum* L.; Part 1. Isolation of I3, II8-Biapigenin. *Planta medica* 53, 216-217.
- Berghöfer, R., Hölzl, J., 1989. Isolation of I 3', II 8-Biapigenin (Amentoflavone) from *Hypericum perforatum*. *Planta medica* 55, 91-91.
- Bertoli, A., Menichini, F., Mazzetti, M., Spinelli, G., Morelli, I., 2003. Volatile constituents of the leaves and flowers of *Hypericum triquetrifolium* Turra. *Flavour and Fragrance Journal* 18, 91-94.
- Bertoli, A., Pistelli, L., Morelli, I., Spinelli, G., Menichini, F., 2000. Constituents of *Hypericum hircinum* oils. *Journal of Essential Oil Research* 12, 617-620.
- Bharate, S.B., Khan, S.I., Yunus, N.A., Chauthi, S.K., Jacob, M.R., Tekwani, B.L., Khan, I.A., Singh, I.P., 2007. Antiprotozoal and antimicrobial activities of O-alkylated and formylated acylphloroglucinols. *Bioorganic & medicinal chemistry* 15, 87-96.
- Bhatara, V.S., Sharma, J., Gupta, S., Gupta, Y., 1997. The first herbal antipsychotic. *The American journal of psychiatry* 154, 894.
- Borel, J., Kis, Z., 1991. The discovery and development of cyclosporine (Sandimmune), *Transplantation proceedings*, p. 1867.

- Borenfreund, E., Babich, H., Martin-Alguacil, N., 1990. Rapid chemosensitivity assay with human normal and tumor cells in vitro. *In vitro cellular & developmental biology* 26, 1030-1034.
- Bowsher, C., Steer, M., Tobin, A., 2008. *Plant biochemistry*. Garland Science.
- Brand-Williams, W., Cuvelier, M.-E., Berset, C., 1995. Use of a free radical method to evaluate antioxidant activity. *LWT-Food science and Technology* 28, 25-30.
- Brolis, M., Gabetta, B., Fuzzati, N., Pace, R., Panzeri, F., Peterlongo, F., 1998. Identification by high-performance liquid chromatography–diode array detection–mass spectrometry and quantification by high-performance liquid chromatography–UV absorbance detection of active constituents of *Hypericum perforatum*. *Journal of Chromatography A* 825, 9-16.
- Brum-Bousquet, M., Tillequin, F., Paris, R., 1977. From the twigs of *Sarothamnus scoparius koch* has been isolated a new C-Glycosyl fla-vone: The 6"-O acetyl scoparin. *Lloyd* 40, 591.
- BRUM, B.M., Paris, R., 1974. Flavonoids of common broom (*Sarothamnus scoparius*).
- Bunsupa, S., Yamazaki, M., Saito, K., 2012. Quinolizidine alkaloid biosynthesis: recent advances and future prospects. *Frontiers in plant science* 3.
- Buss, A., Cox, B., Waigh, R., 1995. Natural products as leads for new pharmaceuticals. *Burger's Medicinal Chemistry and Drug Discovery*.
- Butterweck, V., Jürgenliemk, G., Nahrstedt, A., Winterhoff, H., 2000. Flavonoids from *Hypericum perforatum* show antidepressant activity in the forced swimming test. *Planta medica* 66, 3-6.
- Cakir, A., Kordali, S., Kilic, H., Kaya, E., 2005. Antifungal properties of essential oil and crude extracts of *Hypericum linarioides* Bosse. *Biochemical Systematics and Ecology* 33, 245-256.
- Cakir, A., Kordali, S., Zengin, H., Izumi, S., Hirata, T., 2004. Composition and antifungal activity of essential oils isolated from *Hypericum hyssopifolium* and *Hypericum heterophyllum*. *Flavour and Fragrance Journal* 19, 62-68.
- Cakir, A., Mavi, A., Yıldırım, A., Duru, M.E., Harmandar, M., Kazaz, C., 2003. Isolation and characterization of antioxidant phenolic compounds from the aerial parts of *Hypericum hyssopifolium* L. by activity-guided fractionation. *Journal of Ethnopharmacology* 87, 73-83.
- Carelli, V., Liquori, A., Mele, A., 1955. Sorption chromatography of polar substances on polyamides. *Nature* 176, 70-71.
- Čellárová, E., Kimáková, K., Halušková, J., Daxnerová, Z., 1994. The variability of the hypericin content in the regenerants of *Hypericum perforatum*. *Acta biotechnologica* 14, 267-274.
- Chain, E., 1979. The early years of the penicillin discovery. *Trends in Pharmacological Sciences* 1, 6-11.
- Chalmers, R.A., Mikeš, O., 1966. *Laboratory handbook of chromatographic methods*. Van Nostrand.
- Chandra, S., Khan, S., Avula, B., Lata, H., Yang, M.H., ElSohly, M.A., Khan, I.A., 2014. Assessment of total phenolic and flavonoid content, antioxidant properties, and yield of aeroponically and conventionally grown leafy vegetables and fruit crops: A comparative study. *Evidence-Based Complementary and Alternative Medicine* 2014.
- Chang, C.-C., Yang, M.-H., Wen, H.-M., Chern, J.-C., 2002. Estimation of total flavonoid content in propolis by two complementary colorimetric methods. *Journal of food and drug analysis* 10.
- CHEN, M.-T., 1988. Xanthonolignoids from *Hypericum sublatum*. *Heterocycles* 27, 2589-2594.
- Chen, M.T., Kuoh, Y.P., Wang, C.H., Chen, C.M., Kuoh, C.S., 1989. Additional constituents of *Hypericum sublatum*. *Journal of the Chinese Chemical Society* 36, 165-168.
- Chen, M.T., Wan, C.H., Chen, C.M., Kuoh, C.S., 1988. Flavonoids from *Hypericum Nagasawai* Hayata. *Journal of the Chinese Chemical Society* 35, 167-171.

- Choi, Y.-W., Takamatsu, S., Khan, S.I., Srinivas, P.V., Ferreira, D., Zhao, J., Khan, I.A., 2006. Schisandrene, a Dibenzocyclooctadiene Lignan from *Schisandra chinensis*: Structure-Antioxidant Activity Relationships of Dibenzocyclooctadiene Lignans. *Journal of natural products* 69, 356-359.
- Chung, M.-I., Weng, J.-R., Lai, M.-H., Yen, M.-H., Lin, C.-N., 1999. A New Chalcone, Xanthenes, and a Xanthonolignoid from *Hypericum geminiflorum*. *Journal of natural products* 62, 1033-1035.
- Couladis, M., Chinou, I., Tzakou, O., Petrakis, P., 2003. Composition and antimicrobial activity of the essential oil of *Hypericum rumeliacum* subsp. *apollinis* (Boiss. & Heldr.). *Phytotherapy Research* 17, 152-154.
- Cragg, G.M., Newman, D.J., 2013. Natural products: a continuing source of novel drug leads. *Biochimica et Biophysica Acta (BBA)-General Subjects* 1830, 3670-3695.
- Cristofolini, G., Conte, L., 2002. Phylogenetic patterns and endemism genesis in *Cytisus* Desf. *Legumi nosae-Cytiseae*, 37-50.
- Crockett, S.L., 2003. PHYTOCHEMICAL AND BIOSYSTEMATIC INVESTIGATIONS OF NEW AND OLD WORLD HYPERICUM SPECIES (CLUSIACEAE). The University of Mississippi.
- Crockett, S.L., Demirci, B., Başer, K.H.C., Khan, I.A., 2007. Analysis of the volatile constituents of five African and Mediterranean *Hypericum* L.(Clusiaceae, Hypericoideae) species. *Journal of Essential Oil Research* 19, 302-306.
- Crockett, S.L., Robson, N.K., 2011. Taxonomy and chemotaxonomy of the genus *Hypericum*. *Medicinal and aromatic plant science and biotechnology* 5, 1.
- Cronquist, A., 1981. An integrated system of classification of flowering plants. Columbia University Press.
- Crupi, R., Abusamra, Y.A., Spina, E., Calapai, G., 2013. Preclinical data supporting/refuting the use of *Hypericum perforatum* in the treatment of depression. *CNS & Neurological Disorders-Drug Targets (Formerly Current Drug Targets-CNS & Neurological Disorders)* 12, 474-486.
- Dagnino, A.P., de Barros, F.M.C., Ccana-Ccapatinta, G.V., Prophiro, J.S., von Poser, G.L., Romao, P.R., 2015. Leishmanicidal activity of lipophilic extracts of some *Hypericum* species. *Phytomedicine* 22, 71-76.
- Dale, H.H., Laidlaw, P.P., 1912. The physiological action of cytisine, the active alkaloid of laburnum (*Cytisus laburnum*). *Journal of Pharmacology and Experimental Therapeutics* 3, 205-221.
- Decosterd, L.A., Stoeckli-Evans, H., Chapuis, J.C., Msonthi, J.D., Sordat, B., Hostettmann, K., 1989. New Hyperforin Derivatives from *Hypericum revolutum* VAHL with Growth-Inhibitory Activity against a Human Colon Carcinoma Cell Line. *Helvetica Chimica Acta* 72, 464-471.
- Di Giorgio, C., Delmas, F., Tueni, M., Cheble, E., Khalil, T., Balansard, G., 2008. Alternative and complementary antileishmanial treatments: assessment of the antileishmanial activity of 27 Lebanese plants, including 11 endemic species. *The Journal of Alternative and Complementary Medicine* 14, 157-162.
- Dias, A., Seabra, R., Andrade, P., Fernandes-Ferreira, M., 1999. The development and evaluation of an HPLC-DAD method for the analysis of the phenolic fractions from in vivo and in vitro biomass of *Hypericum* species. *Journal of liquid chromatography & related technologies* 22, 215-227.
- Dias, J.S., 2012. Nutritional quality and health benefits of vegetables: a review. *Food and Nutrition Sciences* 3, 1354.

- Dubey, V.S., Bhalla, R., Luthra, R., 2003. An overview of the non-mevalonate pathway for terpenoid biosynthesis in plants. *Journal of biosciences* 28, 637-646.
- Duke, J., 2012. *Handbook of legumes of world economic importance*. Springer Science & Business Media.
- e Castro, V.R.O., 1998. Chromium in a series of Portuguese plants used in the herbal treatment of diabetes. *Biological trace element research* 62, 101-106.
- Egger, K., 1968. Zur identität von Taraxanthin und luteinopoxid. *Planta* 80, 65-76.
- Erken, S., Malyer, H., Demirci, F., Demirci, B., Baser, K., 2001. Chemical investigations on some *Hypericum* species growing in Turkey-I. *Chemistry of Natural Compounds* 37, 434-438.
- Esposito, F., Sanna, C., Del Vecchio, C., Cannas, V., Venditti, A., Corona, A., Bianco, A., Serrilli, A.M., Guarcini, L., Parolin, C., 2013. *Hypericum hircinum* L. components as new single-molecule inhibitors of both HIV-1 reverse transcriptase-associated DNA polymerase and ribonuclease H activities. *Pathogens and disease* 68, 116-124.
- Ewané, C.A., Lepoivre, P., de Bellaire, L.d.L., Lassois, L., 2012. Involvement of phenolic compounds in the susceptibility of bananas to crown rot. A review. *Biotechnologie, Agronomie, Société et Environnement* 16, 393.
- Fenner, R., Sortino, M., Rates, S.K., Dall'Agnol, R., Ferraz, A., Bernardi, A., Albring, D., Nör, C., Von Poser, G., Schapoval, E., 2005. Antifungal activity of some Brazilian *Hypericum* species. *Phytomedicine* 12, 236-240.
- Ferretti, G., Maggi, F., Tirillini, B., 2005. Essential oil composition of *Hypericum richeri* Vill. from Italy. *Flavour and fragrance journal* 20, 295-298.
- Fourneron, J.-D., Herbette, G., Caloprisco, E., 1999. Pseudohypericin and hypericin in St. John's wort extracts. Breakdown of pseudohypericin. *Comptes Rendus de l'Académie des Sciences-Series IIC-Chemistry* 2, 127-131.
- Franzblau, S.G., Witzig, R.S., McLaughlin, J.C., Torres, P., Madico, G., Hernandez, A., Degnan, M.T., Cook, M.B., Quenzer, V.K., Ferguson, R.M., 1998. Rapid, low-technology MIC determination with clinical *Mycobacterium tuberculosis* isolates by using the microplate Alamar Blue assay. *Journal of clinical microbiology* 36, 362-366.
- Freer, A., Robins, D., Sheldrake, G., 1987. Structures of (-)-cytisine and (-)-N-methylcytisine: tricyclic quinolizidine alkaloids. *Acta Crystallographica Section C: Crystal Structure Communications* 43, 1119-1122.
- Fresco-Taboada, A., de la Mata, I., Arroyo, M., Fernández-Lucas, J., 2013. New insights on nucleoside 2'-deoxyribosyltransferases: a versatile biocatalyst for one-pot one-step synthesis of nucleoside analogs. *Applied microbiology and biotechnology* 97, 3773-3785.
- Frisch, M., Trucks, G., Schlegel, H.B., Scuseria, G., Robb, M., Cheeseman, J., Scalmani, G., Barone, V., Mennucci, B., Petersson, G., 2009. Gaussian 09, Revision A. 02, Gaussian. Inc., Wallingford, CT 200.
- Galeotti, N., Vivoli, E., Bilia, A.R., Bergonzi, M.C., Bartolini, A., Ghelardini, C., 2010. A prolonged protein kinase C-mediated, opioid-related antinociceptive effect of St John's Wort in mice. *The Journal of Pain* 11, 149-159.
- García Ciudad, A., Santos, B.F., de Aldana, B.V., Zabalgoceazcoa, I., Gutierrez, M., Criado, B.G., 2004. Use of near infrared reflectance spectroscopy to assess forage quality of a Mediterranean shrub. *Communications in soil science and plant analysis* 35, 665-678.
- Gaweska, H., Fitzpatrick, P.F., 2011. Structures and mechanism of the monoamine oxidase family. *Biomolecular concepts* 2, 365-377.



- Gião, M.S., González-Sanjosé, M.L., Rivero-Pérez, M.D., Pereira, C.I., Pintado, M.E., Malcata, F.X., 2007. Infusions of Portuguese medicinal plants: Dependence of final antioxidant capacity and phenol content on extraction features. *Journal of the Science of Food and Agriculture* 87, 2638-2647.
- González, N., Ribeiro, D., Fernandes, E., Nogueira, D.R., Conde, E., Moure, A., Vinardell, M.P., Mitjans, M., Domínguez, H., 2013. Potential use of *Cytisus scoparius* extracts in topical applications for skin protection against oxidative damage. *Journal of Photochemistry and Photobiology B: Biology* 125, 83-89.
- Graham, G.G., Punt, J., Arora, M., Day, R.O., Doogue, M.P., Duong, J., Furlong, T.J., Greenfield, J.R., Greenup, L.C., Kirkpatrick, C.M., 2011. Clinical pharmacokinetics of metformin. *Clinical pharmacokinetics* 50, 81-98.
- Greeson, J.M., Sanford, B., Monti, D.A., 2001. St. John's wort (*Hypericum perforatum*): a review of the current pharmacological, toxicological, and clinical literature. *Psychopharmacology* 153, 402-414.
- Gresser, G., Witte, L., Dedkov, V.P., Czygan, F.-C., 1996. A survey of quinolizidine alkaloids and phenylethylamine tyramine in *Cytisus scoparius* (Leguminosae) from different origins. *Zeitschrift für Naturforschung C* 51, 791-801.
- Gudžić, B., Djokovic, D., Vajs, V., Palić, R., Stojanovic, G., 2002. Composition and antimicrobial activity of the essential oil of *Hypericum maculatum* Crantz. *Flavour and fragrance journal* 17, 392-394.
- Gustafsson, M.H., Bittrich, V., Stevens, P.F., 2002. Phylogeny of Clusiaceae based on rbcL sequences. *International Journal of Plant Sciences* 163, 1045-1054.
- Hanganu, D., Vlase, L., Neli, O., 2010a. Phytochemical analysis of isoflavons from some Fabaceae species extracts. *Notulae Botanicae Horti Agrobotanici Cluj-Napoca* 38, 57.
- Hanganu, D., Vlase, L., Olah, N., 2010b. LC/MS analysis of isoflavones from Fabaceae species extracts. *Farmacia* 58, 177-183.
- Harborne, J., 1993. Advances in chemical ecology. *Natural Product Reports* 10, 327-348.
- Hargreaves, K., 1965. Shikimic Acid, a Constituent of Tutsan Berries.
- Hargreaves, K., Carnduff, J., Nechvatal, A., 1968. Root-bark constituents of *Hypericum elatum* and *H. androsaemum*. *Phytochemistry* 7, 331.
- Hatfield, G., 2004. *Encyclopedia of folk medicine: old world and new world traditions*. ABC-CLIO.
- Hawkins, P.C., Nicholls, A., 2012. Conformer generation with OMEGA: learning from the data set and the analysis of failures. *Journal of chemical information and modeling* 52, 2919-2936.
- Hawkins, P.C., Skillman, A.G., Warren, G.L., Ellingson, B.A., Stahl, M.T., 2010. Conformer generation with OMEGA: algorithm and validation using high quality structures from the Protein Databank and Cambridge Structural Database. *Journal of chemical information and modeling* 50, 572-584.
- Hazra, B., Saha, A.K., Ray, R., Roy, D.K., Sur, P., Banerjee, A., 1987. Antiprotozoal activity of diospyrin towards *Leishmania donovani* promastigotes in vitro. *Transactions of the Royal Society of Tropical Medicine and Hygiene* 81, 738-741.
- Hellenbrand, N., Lechtenberg, M., Peterleit, F., Sendker, J., Hensel, A., 2015. Isolation and Quantification of Oligomeric and Polymeric Procyanidins in the Aerial Parts of St. John's Wort (*Hypericum perforatum*). *Planta medica* 81, 1175-1181.

- Hosni, K., Msaâda, K., Taârit, M.B., Ouchikh, O., Kallel, M., Marzouk, B., 2008. Essential oil composition of *Hypericum perforatum* L. and *Hypericum tomentosum* L. growing wild in Tunisia. *Industrial crops and products* 27, 308-314.
- Ibrahim, M.A., Shilabin, A.G., Prasanna, S., Jacob, M., Khan, S.I., Doerksen, R.J., Hamann, M.T., 2008. 2-N-Methyl modifications and SAR studies of manzamine A. *Bioorganic & medicinal chemistry* 16, 6702-6706.
- Index, M., 1989. Merck & Co. Rahway, NJ, USA, 1427.
- Ishiguro, K., Nagareya, N., Fukumoto, H., 1998. A phloroglucinol derivative from cell suspension cultures of *Hypericum patulum*. *Phytochemistry* 47, 1041-1043.
- Ishiguro, K., Yamamoto, R., Oku, H., 1999. Patulosides A and B, Novel Xanthone Glycosides from Cell Suspension Cultures of *Hypericum patulum*. *Journal of natural products* 62, 906-908.
- Iwu, M.M., 2014. Handbook of African medicinal plants. CRC press.
- Jachak, S.M., Saklani, A., 2007. Challenges and opportunities in drug discovery from plants. *CURRENT SCIENCE-BANGALORE*- 92, 1251.
- Jäger, A.K., Saaby, L., 2011. Flavonoids and the CNS. *Molecules* 16, 1471-1485.
- Jain, S.K., Sahu, R., Walker, L.A., Tekwani, B.L., 2012. A parasite rescue and transformation assay for antileishmanial screening against intracellular *Leishmania donovani* amastigotes in THP1 human acute monocytic leukemia cell line. *JoVE (Journal of Visualized Experiments)*, e4054-e4054.
- Jalili, J., Askeroglu, U., Alleyne, B., Guyuron, B., 2013. Herbal products that may contribute to hypertension. *Plastic and reconstructive surgery* 131, 168-173.
- Jayasuriya, H., 1988. Biological and Chemical Investigation of Native Mississippi Plants: *Hypericum Drummondii* (Grev. & Hook.) T. & G.
- Judd, W.S., Campbell, C.S., Kellogg, E.A., Stevens, P.F., Donoghue, M.J., 1999. Plant systematics: a phylogenetic approach. *ecologia mediterranea* 25, 215.
- Kar, A., 2003. Pharmacognosy and pharmacobiotechnology. New Age International.
- Kennedy, D.O., Wightman, E.L., 2011. Herbal extracts and phytochemicals: plant secondary metabolites and the enhancement of human brain function. *Advances in Nutrition: An International Review Journal* 2, 32-50.
- Kessler, R.C., Soukup, J., Davis, R.B., Foster, D.F., Wilkey, S.A., Van Rompay, M.I., Eisenberg, D.M., 2001. The use of complementary and alternative therapies to treat anxiety and depression in the United States. *American Journal of Psychiatry* 158, 289-294.
- Kirakosyan, A., Vardapetyan, R., Charchoglyan, A., 2000. The content of hypericin and pseudohypericin in cell cultures of *Hypericum perforatum*. *Russian Journal of Plant Physiology* 47, 270-273.
- Kitanov, G., 1988. Miquelianin and other polyphenols from *Hypericum hirsutum*. *Chemistry of Natural Compounds* 24, 119-120.
- Kitanov, G., Blinova, K., Akhtardzhiev, K., 1979. C-glycoflavonoids from *Hypericum hirsutum*. *Chemistry of Natural Compounds* 15, 199-200.
- Kitanov, G.M., Nedialkov, P.T., 2001. Benzophenone O-glucoside, a biogenic precursor of 1, 3, 7-trioxygenated xanthenes in *Hypericum annulatum*. *Phytochemistry* 57, 1237-1243.
- Kolodziejewski, J., Gill, S., 1960. Flavonoids species of the genus *Hypericum* I. Chromatographic analysis of flavones *Dissertationes Pharmaceuticae* 12, 311-323.
- Kurihara, T., Kikuchi, M., 1980. Studies on the constituents of flowers. XIII. The flower components of *Cytisus scoparius*. *Yakugaku Zasshi* 100, 1054-1057.

- Kutchan, T.M., 2005. A role for intra-and intercellular translocation in natural product biosynthesis. *Current opinion in plant biology* 8, 292-300.
- Li, W.-S., WU, S.-L., 1997. Xanthenes and triterpenoids from *Hypericum geminiflorum*. *Zhonghuá yáoxué zázhi* 49, 145-156.
- Linde, K., Ramirez, G., Mulrow, C.D., Pauls, A., Weidenhammer, W., Melchart, D., 1996. St John's wort for depression—an overview and meta-analysis of randomised clinical trials. *Bmj* 313, 253-258.
- Lindstrom, A., Ooyen, C., Lynch, M.E., Blumenthal, M., Kawa, K., 2014. Sales of herbal dietary supplements increase by 7.9% in 2013, marking a decade of rising sales: turmeric supplements climb to top ranking in natural channel. *HerbalGram* 103, 52-56.
- Lores, M., Pájaro, M., Álvarez-Casas, M., Domínguez, J., García-Jares, C., 2015. Use of ethyl lactate to extract bioactive compounds from *Cytisus scoparius*: Comparison of pressurized liquid extraction and medium scale ambient temperature systems. *Talanta* 140, 134-142.
- Loy, C., Schneider, L., 2006. Galantamine for Alzheimer's disease and mild cognitive impairment. The Cochrane Library.
- Luís, A., Domingues, F., Gil, C., Duarte, A., 2009. Antioxidant activity of extracts of Portuguese shrubs. *Pterospartum tridentatum*, *Cytisus scoparius*.
- Ma, G., Khan, S.I., Benavides, G., Schühly, W., Fischer, N.H., Khan, I.A., Pasco, D.S., 2007. Inhibition of NF- $\kappa$ B-mediated transcription and induction of apoptosis by melampolides and repandolides. *Cancer chemotherapy and pharmacology* 60, 35-43.
- Mabberley, D.J., 1997. The plant-book: a portable dictionary of the vascular plants. Cambridge university press.
- Mahmoud, S.S., Croteau, R.B., 2002. Strategies for transgenic manipulation of monoterpene biosynthesis in plants. *Trends in plant science* 7, 366-373.
- Makler, M.T., Hinrichs, D.J., 1993. Measurement of the lactate dehydrogenase activity of *Plasmodium falciparum* as an assessment of parasitemia. *The American journal of tropical medicine and hygiene* 48, 205-210.
- Makovetska, O., 1999. Biologically active substances of *Hypericum* L. species. Part IV. Sections *Inodora* Stef., *Roscyna* (Spach) R. Keller and *Bupleuroides* Stef. *Farmatsevtichnii Zhurnal* (Kiev) 3, 39-44.
- Manda, S., Khan, S.I., Jain, S.K., Mohammed, S., Tekwani, B.L., Khan, I.A., Vishwakarma, R.A., Bharate, S.B., 2014. Synthesis, antileishmanial and antitrypanosomal activities of N-substituted tetrahydro- $\beta$ -carboline. *Bioorganic & medicinal chemistry letters* 24, 3247-3250.
- Marinova, D., Ribarova, F., Atanassova, M., 2005. Total phenolics and total flavonoids in Bulgarian fruits and vegetables. *Journal of the university of chemical technology and metallurgy* 40, 255-260.
- Mathis, C., Ourisson, G., 1963a. Chemotaxonomic study of the genus *Hypericum*. I. Distribution of hypericin. *Phytochemistry* 2, 157-171.
- Mathis, C., Ourisson, G., 1963b. Étude chimio-taxonomique du genre *Hypericum* I. Répartition de l'hypericine. *Phytochemistry* 2, 157-171.
- Matsuhisa, M., Shikishima, Y., Takaishi, Y., Honda, G., Ito, M., Takeda, Y., Shibata, H., Higuti, T., Kodzhimatov, O.K., Ashurmetov, O., 2002. Benzoylphloroglucinol Derivatives from *Hypericum scabrum*. *Journal of natural products* 65, 290-294.
- Mbaveng, A.T., Hamm, R., Kuete, V., 2014. 19-Harmful and protective effects of terpenoids from African medicinal plants. *Toxicological Survey of African Medicinal Plants*. Oxford: Elsevier, 557-576.

- Mineur, Y.S., Eibl, C., Young, G., Kochevar, C., Papke, R.L., Gündisch, D., Picciotto, M.R., 2009. Cytisine-based nicotinic partial agonists as novel antidepressant compounds. *Journal of Pharmacology and Experimental Therapeutics* 329, 377-386.
- Mineur, Y.S., Somenzi, O., Picciotto, M.R., 2007. Cytisine, a partial agonist of high-affinity nicotinic acetylcholine receptors, has antidepressant-like properties in male C57BL/6J mice. *Neuropharmacology* 52, 1256-1262.
- Miskovsky, P., 2002. Hypericin-a new antiviral and antitumor photosensitizer: mechanism of action and interaction with biological macromolecules. *Current Drug Targets* 3, 55-84.
- Mockute, D., Bernotiene, G., Judzentiene, A., 2008. The essential oils with dominant germacrene D of *Hypericum perforatum* L. growing wild in Lithuania. *Journal of Essential Oil Research* 20, 128-131.
- Molares, S., Ladio, A., 2011. The usefulness of edible and medicinal Fabaceae in Argentine and Chilean Patagonia: environmental availability and other sources of supply. *Evidence-Based Complementary and Alternative Medicine* 2012.
- Moon, H.I., 2010. Antiplasmodial and cytotoxic activity of Phloroglucinol derivatives from *Hypericum erectum* Thunb. *Phytotherapy Research* 24, 941-944.
- Mukherjee, P.K., Saritha, G., Suresh, B., 2001. Antibacterial spectrum of *Hypericum hookerianum*. *Fitoterapia* 72, 558-560.
- Murakoshi, I., Yamashita, Y., Ohmiya, S., Otomasu, H., 1986. (-)-3 $\beta$ -13 $\alpha$ -dihydroxylupanine from *Cytisus scoparius*. *Phytochemistry* 25, 521-524.
- Nagai, M., Tada, M., 1987. Antimicrobial Compounds, Chinesin I and II from Flowers of *Hypericum chinense* L. *Chemistry Letters* 16, 1337-1340.
- Nährstedt, A., Butterweck, V., 1997. Biologically active and other chemical constituents of the herb of *Hypericum perforatum* L. *Pharmacopsychiatry* 30, 129-134.
- Nedelcheva, A.M., Dogan, Y., Guarrera, P.M., 2007. Plants traditionally used to make brooms in several European countries. *Journal of Ethnobiology and Ethnomedicine* 3, 1.
- Nihei, K.-i., Shibata, K., Kubo, I., 2002. (+)-2, 3-Dehydro-10-oxo- $\alpha$ -isosparteine in *Uresiphita reversalis* larvae fed on *Cytisus monspessulanus* leaves. *Phytochemistry* 61, 987-990.
- Nirmal, J., Babu, C.S., Harisudhan, T., Ramanathan, M., 2008. Evaluation of behavioural and antioxidant activity of *Cytisus scoparius* Link in rats exposed to chronic unpredictable mild stress. *BMC complementary and alternative medicine* 8, 1.
- Noble, R.L., 1990. The discovery of the vinca alkaloids-chemotherapeutic agents against cancer. *Biochemistry and Cell Biology* 68, 1344-1351.
- Osório e Castro, V., 2001. Chromium and zinc in a series of plants used in Portugal in the herbal treatment of non-insulinized diabetes. *Acta Alimentaria* 30, 333-342.
- Pavlović, M., Tzakou, O., Petrakis, P., Couladis, M., 2006. The essential oil of *Hypericum perforatum* L., *Hypericum tetrapterum* Fries and *Hypericum olympicum* L. growing in Greece. *Flavour and fragrance journal* 21, 84-87.
- Pereira, O.R., Macias, R.I., Perez, M.J., Marin, J.J., Cardoso, S.M., 2013. Protective effects of phenolic constituents from *Cytisus multiflorus*, *Lamium album* L. and *Thymus citriodorus* on liver cells. *Journal of Functional Foods* 5, 1170-1179.
- Pereira, O.R., Perez, M.J., Macias, R.I., Domingues, M.R., Silva, A., Marín, J.J., Cardoso, S.M., 2012a. *Cytisus multiflorus*: source of antioxidant polyphenols. 11<sup>o</sup> Encontro Química dos Alimentos.
- Pereira, O.R., Silva, A.M., Domingues, M.R., Cardoso, S.M., 2012b. Identification of phenolic constituents of *Cytisus multiflorus*. *Food Chemistry* 131, 652-659.

- Petrussa, E., Braidot, E., Zancani, M., Peresson, C., Bertolini, A., Patui, S., Vianello, A., 2013. Plant flavonoids—biosynthesis, transport and involvement in stress responses. *International journal of molecular sciences* 14, 14950-14973.
- Pinela, J., Barros, L., Carvalho, A.M., Ferreira, I.C., 2011. Influence of the drying method in the antioxidant potential and chemical composition of four shrubby flowering plants from the tribe Genisteae (Fabaceae). *Food and chemical toxicology* 49, 2983-2989.
- Prochaska, J.J., Das, S., Benowitz, N.L., 2013. Cytisine, the world's oldest smoking cessation aid. *Bmj* 347, f5198.
- Quezel, P.S., 1963. Nouvelle flore de l'Algérie et des régions désertiques méridionales.
- Rabanal, R., Bonkanka, C., Hernández-Pérez, M., Sánchez-Mateo, C., 2005. Analgesic and topical anti-inflammatory activity of *Hypericum canariense* L. and *Hypericum glandulosum* Ait. *Journal of ethnopharmacology* 96, 591-596.
- Rahman, A.A., Samoylenko, V., Jain, S.K., Tekwani, B.L., Khan, S.I., Jacob, M.R., Midiwo, J.O., Hester, J.P., Walker, L.A., Muhammad, I., 2011. Antiparasitic and antimicrobial isoflavanquinones from *Abrus schimperi*. *Natural product communications* 6, 1645.
- Ramírez-González, I., Amaro-Luis, J., Bahsas, A., 2013. Xanthonés from aerial parts of *Hypericum laricifolium* Juss. *Natural product communications* 8, 1731-1732.
- Raskin, I., Ribnicky, D.M., Komarnytsky, S., Ilic, N., Poulev, A., Borisjuk, N., Brinker, A., Moreno, D.A., Ripoll, C., Yakoby, N., 2002. Plants and human health in the twenty-first century. *TRENDS in Biotechnology* 20, 522-531.
- Rates, S.M.K., Betti, A.H., Müller, L.G., de Matos Nunes, J., 2015. Plant Toxins as Sources of Drugs, *Plant Toxins*. Springer, pp. 1-21.
- Reddy, M.K., Gupta, S.K., Jacob, M.R., Khan, S.I., Ferreira, D., 2007. Antioxidant, antimalarial and antimicrobial activities of tannin-rich fractions, ellagitannins and phenolic acids from *Punica granatum* L. *Planta medica* 53, 461-467.
- Ribera, A., Zuñiga, G., 2012. Induced plant secondary metabolites for phytopathogenic fungi control: a review. *Journal of soil science and plant nutrition* 12, 893-911.
- Robson, N., 2003. *Hypericum botany*. *Hypericum: the genus Hypericum*. (Medicinal and aromatic plants, industrial profiles 31, 1-22.
- Robson, N.K., 1981. *Studies in the genus Hypericum L.* (Guttiferae).
- Rocha, L., Marston, A., Auxiliadora, M., Kaplan, C., Stoeckli-Evans, H., Thull, U., Testa, B., Hostettmann, K., 1994. An antifungal  $\gamma$ -pyrone and xanthonés with monoamine oxidase inhibitory activity from *Hypericum brasiliense*. *Phytochemistry* 36, 1381-1385.
- Rocha, L., Marston, A., Potterat, O., Kaplan, M.A.C., Stoeckli-Evans, H., Hostettmann, K., 1995. Antibacterial phloroglucinols and flavonoids from *Hypericum brasiliense*. *Phytochemistry* 40, 1447-1452.
- Rodríguez-Riaño, T., Ortega-Olivencia, A., Devesa, J.A., 2004. Reproductive biology in *Cytisus multiflorus* (Fabaceae), *Annales Botanici Fennici*. JSTOR, pp. 179-188.
- Rodríguez-Riaño, T., VALTUEÑA, F.J., Ortega-Olivencia, A., 2006. Megasporogenesis, megagametogenesis and ontogeny of the aril in *Cytisus striatus* and *C. multiflorus* (Leguminosae: Papilionoideae). *Annals of botany* 98, 777-791.
- Rodríguez-Riaño, T., Ortega-Olivencia, A., Devesa, J.A., 1999. Reproductive phenology in three Genisteae (Fabaceae) shrub species of the W Mediterranean Region. *Nordic Journal of Botany* 19, 345-354.
- Saddiqe, Z., Naeem, I., Maimoona, A., 2010. A review of the antibacterial activity of *Hypericum perforatum* L. *Journal of ethnopharmacology* 131, 511-521.

- Sajjadi, S.E., Rahiminezhad, M.R., Mehregan, I., Poorassar, A., 2001. Constituents of essential oil of *Hypericum dogonbadanicum* Assadi. *Journal of Essential Oil Research* 13, 43-44.
- Samoylenko, V., Jacob, M.R., Khan, S.I., Zhao, J., Tekwani, B.L., Midiwo, J.O., Walker, L.A., Muhammad, I., 2009. Antimicrobial, antiparasitic and cytotoxic spermine alkaloids from *Albizia schimperiana*. *Natural product communications* 4, 791.
- Santos, P.A., Figueiredo, A.C., Barroso, J.G., Pedro, L.G., Scheffer, J.J., 1999. Composition of the essential oil of *Hypericum foliosum* Aiton from five Azorean islands. *Flavour and fragrance journal* 14, 283-286.
- Saroglou, V., Marin, P.D., Rancic, A., Veljic, M., Skaltsa, H., 2007. Composition and antimicrobial activity of the essential oil of six *Hypericum* species from Serbia. *Biochemical Systematics and Ecology* 35, 146-152.
- Schmalfuss, H., Heider, A., 1931. Tyramine, hydroxy tyramine, the blood-pressure-raising substances of the pod of the common broom *Sarothamnus scoparius* Wimm.
- Schrödinger Release 2015a. *MacroModel*, Schrödinger, LLC, 2015-2 ed, New York, NY.
- Schrödinger Release 2015b. *MS Jaguar*, Schrödinger, LLC, 2015-2 ed, New York, NY, .
- Seabra, R., Alves, A.C., 1989. Identification of quercetin 3-sulfate in *Hypericum androsaemum*. *Revista Portuguesa de Farmacia*. 1989a 39, 16-18.
- Seabra, R., Vasconcelos, M., Alves, A., 1991. Flavonoids sulphates from *Hypericum undulatum*. *Revista Portuguesa de Farmacologia* 36, 16-18.
- Seabra, R.M., Alves, A.C., 1988. Quercetin 3-glucuronide-3'-sulphate from *Hypericum elodes*. *Phytochemistry* 27, 3019-3020.
- Seabra, R.M., Alves, A.C., 1991. Quercetin 3'-Sulphate from *Hypericum elodes*. *Phytochemistry* 30, 1344-1345.
- Seger, C., Römpf, H., Sturm, S., Haslinger, E., Schmidt, P.C., Hadacek, F., 2004. Characterization of supercritical fluid extracts of St. John's Wort (*Hypericum perforatum* L.) by HPLC-MS and GC-MS. *European journal of pharmaceutical sciences* 21, 453-463.
- Siegel, R.K., 1976. Herbal intoxication: Psychoactive effects from herbal cigarettes, tea, and capsules. *JAMA* 236, 473-476.
- Sosa, S., Pace, R., Bornanciny, A., Morazzoni, P., Riva, A., Tubaro, A., Loggia, R.D., 2007. Topical anti-inflammatory activity of extracts and compounds from *Hypericum perforatum* L. *Journal of Pharmacy and Pharmacology* 59, 703-709.
- Stevens, P., 2007a. *Clusiaceae-Guttiferae, Flowering Plants: Eudicots*. Springer, pp. 48-66.
- Stevens, P., 2007b. *Hypericaceae, Flowering Plants: Eudicots*. Springer, pp. 194-201.
- Sundararajan, R., Haja, N.A., Venkatesan, K., Mukherjee, K., Saha, B.P., Bandyopadhyay, A., Mukherjee, P.K., 2006. *Cytisus scoparius* link-A natural antioxidant. *BMC Complementary and Alternative Medicine* 6, 1.
- Sundararajan, R., Koduru, R., 2014. *Cytisus scoparius*: A review of ethnomedical, phytochemical and pharmacological information. *Indo American Journal of Pharmaceutical Research* 4, 2151-2169.
- T. Bruhn, A.S., Y. Hemberger, 2015. *SpecDis* University of Wuerzburg, , Germany.
- T. Bruhn, A.S., Y. Hemberger, G. Bringmann,, 2013. *Chirality* 243-249.
- Tada, M., Chiba, K., Yamada, H., Maruyama, H., 1991. Phloroglucinol derivatives as competitive inhibitors against thromboxane A<sub>2</sub> and leukotriene D<sub>4</sub> from *Hypericum erectum*. *Phytochemistry* 30, 2559-2562.

- Tanaka, N., Okasaka, M., Ishimaru, Y., Takaishi, Y., Sato, M., Okamoto, M., Oshikawa, T., Ahmed, S.U., Consentino, L.M., Lee, K.-H., 2005. Biyouyanagin A, an Anti-HIV Agent from *Hypericum chinense* L. var. *salicifolium*. *Organic letters* 7, 2997-2999.
- Tanemossu, S.A.F., Franke, K., Arnold, N., Schmidt, J., Wabo, H.K., Tane, P., Wessjohann, L.A., 2014. Rare biscoumarin derivatives and flavonoids from *Hypericum riparium*. *Phytochemistry* 105, 171-177.
- Tian, J., Zhang, F., Cheng, J., Guo, S., Liu, P., Wang, H., 2014. Antidepressant-like activity of adhyperforin, a novel constituent of *Hypericum perforatum* L. *Scientific reports* 4.
- Tominaga, T., Dubourdieu, D., 1997. Identification of 4-mercapto-4-methylpentan-2-one from the box tree (*Buxus sempervirens* L.) and broom (*Sarothamnus scoparius* (L.) Koch). *Flavour and fragrance journal* 12, 373-376.
- Tuberoso, C.I.G., Rosa, A., Bifulco, E., Melis, M.P., Atzeri, A., Pirisi, F.M., Dessì, M.A., 2010. Chemical composition and antioxidant activities of *Myrtus communis* L. berries extracts. *Food Chemistry* 123, 1242-1251.
- Valentão, P., Fernandes, E., Carvalho, F., Andrade, P.B., Seabra, R.M., Bastos, M.d.L., 2002. Antioxidant activity of *Hypericum androsaemum* infusion: scavenging activity against superoxide radical, hydroxyl radical and hypochlorous acid. *Biological and Pharmaceutical Bulletin* 25, 1320-1323.
- Viana, A.F., Heckler, A., Fenner, R., Rates, S.M.K., 2003. Antinociceptive activity of *Hypericum caprifoliatum* and *Hypericum polyanthemum* (Guttiferae). *Brazilian Journal of Medical and Biological Research* 36, 631-634.
- Viscardi, P., Reynaud, J., Raynaud, J., 1984. A new isoflavone glycoside from the flowers of *Cytisus scoparius* Link. (Leguminosae).
- Wang, J., Peng, S.-L., Wang, M.-K., Chen, N.-Y., Ding, L.-S., 2002. [Chemical constituents of *Hypericum monogynum*]. *Zhongguo Zhong yao za zhi= Zhongguo zhongyao zazhi= China journal of Chinese materia medica* 27, 120-122.
- Wang, Y.-H., Avula, B., Fu, X., Wang, M., Khan, I.A., 2012. Simultaneous determination of the absolute configuration of twelve monosaccharide enantiomers from natural products in a single injection by a UPLC-UV/MS method. *Planta medica* 78, 834-837.
- Wani, M.C., Taylor, H.L., Wall, M.E., Coggon, P., McPhail, A.T., 1971. Plant antitumor agents. VI. Isolation and structure of taxol, a novel antileukemic and antitumor agent from *Taxus brevifolia*. *Journal of the American Chemical Society* 93, 2325-2327.
- Waterman, P.G., Sprent, J., McKey, D., 1994. Costs and benefits of secondary metabolites to the Leguminosae. *Advances in Legume Systematics* 5, 129-149.
- Wentworth, J., Agostini, M., Love, J., Schwabe, J., Chatterjee, V., 2000. St John's wort, a herbal antidepressant, activates the steroid X receptor. *Journal of Endocrinology* 166, R11-R16.
- White, E., 1964. 879. Alkaloids of the leguminosae. Part XXVII. The structure of monspessulanine. *Journal of the Chemical Society (Resumed)*, 4613-4614.
- White, F.J., Kalivas, P.W., 1998. Neuroadaptations involved in amphetamine and cocaine addiction. *Drug and alcohol dependence* 51, 141-153.
- Wiersema, J.H., Leon, B., 2016. *World economic plants: a standard reference*. CRC press.
- Wink, M., 1984. N-Methylation of quinolizidine alkaloids: an S-adenosyl-L-methionine: cytosine N-methyltransferase from *Laburnum anagyroides* plants and cell cultures of *L. alpinum* and *Cytisus canariensis*. *Planta* 161, 339-344.

- Wink, M., Witte, L., Hartmann, T., 1981. Quinolizidine alkaloid composition of plants and of photomixotrophic cell suspension cultures of *Sarothamnus scoparius* and *Orobancha rapumgenistae*. *Planta medica* 43, 342-352.
- Winkelmann, K., Heilmann, J., Zerbe, O., Rali, T., Sticher, O., 2000. New phloroglucinol derivatives from *Hypericum papuanum*. *Journal of natural products* 63, 104-108.
- Winkelmann, K., Heilmann, J., Zerbe, O., Rali, T., Sticher, O., 2001a. Further Prenylated Bi-and Tricyclic Phloroglucinol Derivatives from *Hypericum papuanum*. *Helvetica chimica acta* 84, 3380-3392.
- Winkelmann, K., Heilmann, J., Zerbe, O., Rali, T., Sticher, O., 2001b. New Prenylated Bi-and Tricyclic Phloroglucinol Derivatives from *Hypericum p apuanum*. *Journal of natural products* 64, 701-706.
- Wolfe, K.L., Liu, R.H., 2007. Cellular antioxidant activity (CAA) assay for assessing antioxidants, foods, and dietary supplements. *Journal of agricultural and food chemistry* 55, 8896-8907.
- Wollenweber, E., Dörr, M., Roitman, J.N., Arriaga-Giner, F.J., 1994. Triterpenes and a novel natural xanthone as lipophilic glandular products in *Hypericum balearicum*. *Zeitschrift für Naturforschung C* 49, 393-394.
- Wood Jr, C.E., Adams, P., 1976. The genera of Guttiferae (Clusiaceae) in the southeastern United States. *Journal of the Arnold Arboretum (USA)*.
- Wu, Q., Wang, S., Wang, L., Yang, J., Xiao, P., 1998a. New phloroglucinol glycosides from *Hypericum japonicum*. *Chinese Chemical Letters* 9, 469-470.
- Wu, Q.L., Wang, S.P., Du, L.J., Wang, L.W., Yang, J.S., Xiao, P.G., 1998b. Constituents of *Hypericum japonicum*. *Phytotherapy Research* 12, S164-S168.
- Xavier, C.P., Lima, C.F., Fernandes-Ferreira, M., Pereira-Wilson, C., 2012. *Hypericum androsaemum* water extract inhibits proliferation in human colorectal cancer cells through effects on MAP kinases and PI3K/Akt pathway. *Food & function* 3, 844-852.
- Yazaki, K., Okuda, T., 1990. Procyanidins in Callus and Multiple Shoot Cultures of *Hypericum erectum*l. *Planta medica* 56, 490-491.
- Yazaki, K., Yoshida, T., Okuda, T., 1991. Tannin production in cell suspension cultures of *Geranium thunbergii*. *Phytochemistry* 30, 501-503.
- Yin, Z.-Q., Wang, Y., Ye, W.-C., Zhao, S.-X., 2004. Chemical constituents of *Hypericum perforatum* (St. John's wort) growing in China. *Biochemical systematics and ecology* 32, 521-523.
- Zaki, M.A., Balachandran, P., Khan, S., Wang, M., Mohammed, R., Hetta, M.H., Pasco, D.S., Muhammad, I., 2013. Cytotoxicity and modulation of cancer-related signaling by (Z)-and (E)-3, 4, 3', 5'-tetramethoxystilbene isolated from *Eugenia rigida*. *Journal of natural products* 76, 679-684.
- Zhang, L., Jin, Y., Tian, J., 2007. Studies on chemical constituents of *Hypericum japonicum*.
- Zhang, Y., Liu, C., Yu, M., Zhang, Z., Qi, Y., Wang, J., Wu, G., Li, S., Yu, J., Hu, Y., 2011. Application of accelerated solvent extraction coupled with high-performance counter-current chromatography to extraction and online isolation of chemical constituents from *Hypericum perforatum* L. *Journal of Chromatography A* 1218, 2827-2834.
- Zofou, D., Kowa, T.K., Wabo, H.K., Ngemenya, M.N., Tane, P., Titanji, V.P., 2011. *Hypericum lanceolatum* (Hypericaceae) as a potential source of new anti-malarial agents: a bioassay-guided fractionation of the stem bark. *Malaria journal* 10, 1.
- Zou, Y., Lu, Y., Wei, D., 2004. Antioxidant activity of a flavonoid-rich extract of *Hypericum perforatum* L. *in vitro*. *Journal of Agricultural and Food Chemistry* 52, 5032-5039.



Радиковна, П.Р., Зуфарович, Ф.Ф., 2015. СОСТАВ И СЕЗОННАЯ ДИНАМИКА СОДЕРЖАНИЯ АЛКАЛОИДОВ В НАДЗЕМНОЙ ЧАСТИ РАСТЕНИЙ *СНАМАЕСУТИСУС RUTHENICUS* В ГОРНО-ЛЕСНОЙ ЗОНЕ ЮЖНОГО УРАЛА. Химия растительного сырья, 65-69.

*PART II*  
*PHYTOCHEMICAL STUDY OF CYTISUS VILLOSUS AND*  
*HYPERICUM AFRUM*

*CHAPTER 1*

*PHYTOCHEMICAL SCREENING, EXTRACTION,  
FRACTIONATION AND ISOLATION OF  
CONSTITUENTS OF CYTISUS VILLOSUS*

## II.1. Phytochemical screening, extraction, fractionation and isolation of constituents of *Cytisus villosus*

### II.1.1. Preliminary phytochemical screening:

Air-dried powdered aerial parts were subjected to preliminary phytochemical screening for their constituents following the methods described in pages (55-57). The results are summarized in the following table:

**Table II.1.** 1.Results of the preliminary phytochemical screening of *Cytisus villosus* aerial parts

No.	Test	Method/Reagent	Results
1	Alcaloïdes	Dragendorff (Robinson, 1980; Shellard, 1957)	+
2	Tanins	Ferric chloride Formaldehyde (Robinson, 1980; Shellard, 1957)	+
3	Flavonoïdes	Neu's reagent TLC test Sodium hydroxide Ferric chloride (Geissman, 1962)	+
4	Coumarins	UV test (365 nm) (Kamel et al., 2016)	+
5	Terpenes and Steroids	Antimony trichloride test (Hardman and Sofowora, 1972) Lieberman – Buchard's , Salkowski's (Carter, 1947; Cook, 1961)	+
6	Saponins	Froth formation Test (Wall et al., 1954)	-
7	Anthraquinones	Borntrager reaction (Bornträger, 1880)	-
+ = present - = absent			

### II.1.2. Quantitative evaluation of Total phenol and flavonoids content

Polyphenols are a major class of bioactive constituents in the land-plant, many studies have focused on the biological activities of phenolics which are potent antioxidants and free radical scavengers. The antioxidant activity of phenolics is mainly due to their redox properties, which allows them to act as reducing agents, hydrogen donors, and singlet oxygen quenchers. Phenolic compounds are also known to play an important role in stabilizing lipids against peroxidation and inhibiting various types of oxidizing enzymes (Chandra et al., 2014).

Total phenolic and Flavonoid contents were measured for the chloroform, Ethyl acetate and *n*-butanol fractions of *Cytisus villosus* species as described in pages (54-55).

The butanol fraction showed the highest phenolic content with a value of 363.00mg GAE/g dried extract, followed by ethyl acetate fraction with a value of 208.00 mg GAE/g dried extract, and chloroform fraction with a value of 56.00 mg GAE/g dried extract.

The results of Flavonoid content were expressed as mg of Quercetin per g dried extract. The value

of TFC of *C. villosus* fractions ranged between 7.70 and 21.16 mg Quercetin/ g dried extract. The results are shown in table II.1.2.

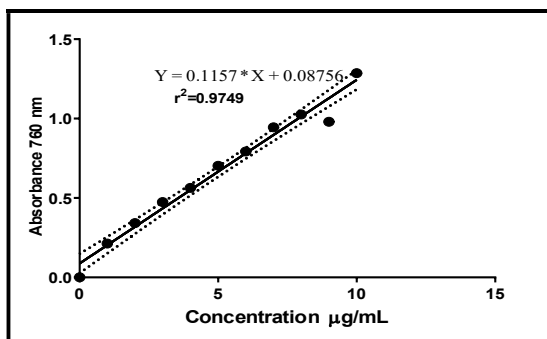


**Figure II.1. 2.**Standard curve of gallic acid for determination of TPC

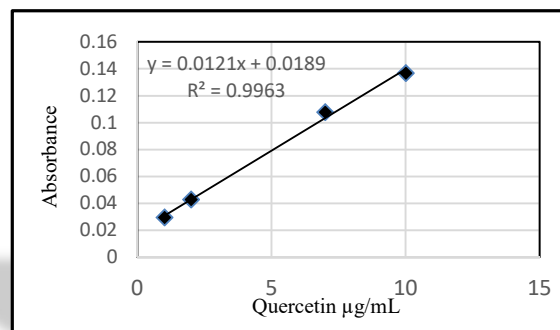


**Figure II.1. 1.**Standard curve of quercetin for the determination of TF

**Table II.1. 2.**Total phenolic and flavonoid contents of crud extract fractions of *C. villosus*

Values expressed are means ±SD of three parallel measurements

Fractions	Total phenolic content (mg GA/g extract)	Total flavonoid content (mg QE/g extract)
Chloroform (CHCl <sub>3</sub> )	56.0±2.50	7.70±0.547
Ethyl acetate (EtOAc)	208.0±8.49	13.95±1.058
<i>n</i> -butanol ( <i>n</i> -but)	363.0±8.32	21.16±1.022

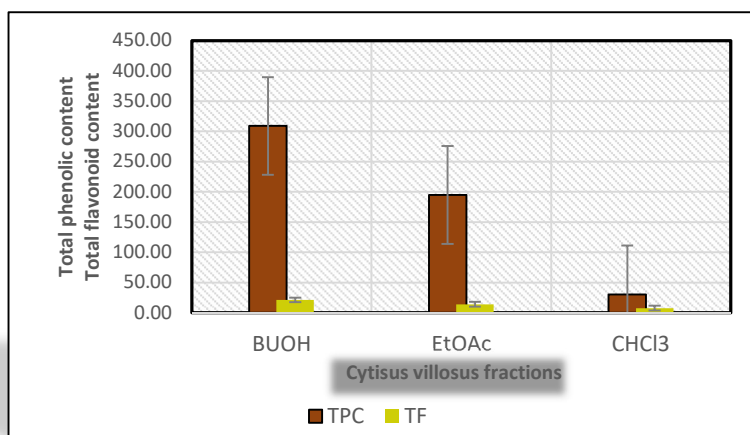


**Figure II.1. 3.**Evaluation of total phenolic and flavonoids in the plant extracts

### II.1.3. Extraction and initial fractionation

#### II.1.3.1. Hydroalcoholic extraction

Dried powdered aerial parts (1000 g) of *Cytisus villosus* Pourr. were macerated at room temperature with EtOH–H<sub>2</sub>O (80:20, v/v) for 24 h, three times. The filtered solvents were combined and evaporated under vacuum at a temperature of 40 °C to give a residue (25 g). The obtained extract was suspended in water (800 mL) and successively partitioned with CHCl<sub>3</sub>, EtOAc and *n*-butanol, yielding 400 mg (CHCl<sub>3</sub>), 5 g (EtOAc) and 10 g (*n*-but) soluble fractions.

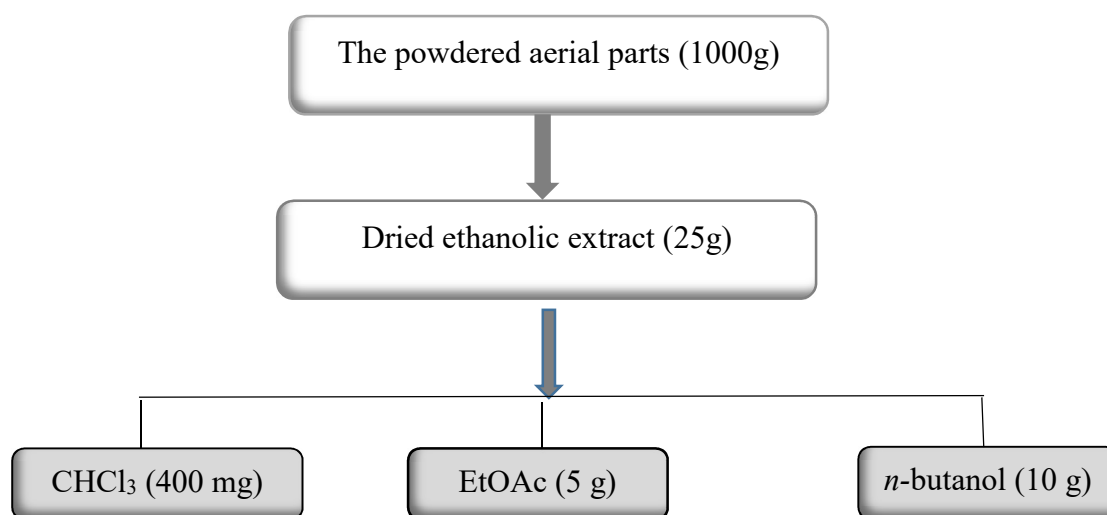


**Figure II.1. 4.** Extraction and fractionation of the powdered aerial parts of *Cytisus villosus*

#### II.1.3.1.1. Isolation of the constituents of the chloroform soluble fraction

The chloroform fraction (400mg) was subjected to silica gel column chromatography (230–400 mesh) using a step-gradient elution with a nonpolar solvent (*n*-hexane) and increasing the gradient with polar solvents (EtOAc and MeOH). The eluate was collected in fractions (20 ml each). Each fraction was monitored by silica gel TLC using systems DCM-EtOAc (9:1), *n*-Hexane-AcOEt (7:3) as developers. Similar fractions were combined together and concentrated under reduced pressure to afford subfractions CCF-(1-6).

- Fraction CCF-2 (*n*-hexane-acetate; 8:2) (75mg) was subjected to Sorbadex 20-LH column chromatography using CH<sub>2</sub>Cl<sub>2</sub>-MeOH (1:1) elution. The eluate was collected in subfractions (3 ml

each). Each fraction was monitored by TLC on silica gel using system DCM-EtOAc (9:1) as developer. Similar subfractions were combined to give subfraction A, B and C. Collected

- subfraction A (10mg) was further purified by analytical TLC using system DCM-EtOAc (9:1) as developer to yield compound **CVS1** (2mg) as a white amorphous solid.
- Fraction CCF-3 (hexane-acetate (7:3) (50mg) was subjected to Sorbadex 20-LH column chromatography using CH<sub>2</sub>Cl<sub>2</sub>-MeOH (1:1) elution and further purified by analytical TLC using system DCM-EtOAc (9:1) to yield compound **CVT1** (2mg) as a white yellowish amorphous solid.

#### **II.1.3.1.2. Isolation of the constituents of the Ethyl acetate soluble fraction**

The ethyl acetate fraction (5 g) was slurried with an equal amount of celite, dried, powdered and subjected to silica gel (180 g) [3 (ID)× 100 (L) cm] CC which was eluted initially with DCM-MeOH (95:5) then gradient elution with DCM-MeOH (90:10), (85:15), (80:20), (50:50), (20:80), and finally with 100% MeOH. Each fraction was monitored by TLC on silica gel using system CHCl<sub>3</sub>-EtOAc-HCOOH (5:4:1) and DCM-MeOH (1:1) as developers. Similar fractions were combined together and concentrated under reduced pressure to give four main subfractions from **CEF-1 to -7**.

- Subfraction CEF-2 (170 mg) was subjected to Sephadex LH-20 using MeOH as an eluent (20 g) [1 (ID)× 50 (L) cm] CC to afford compound **CVS2** (genistein, 5mg) as a light yellow needles.
- Subfraction CEF-3 (161 mg) was subjected to Sephadex LH-20 using MeOH as an eluent (20 g) [1 (ID)× 50 (L) cm] CC to afford compound **CVF1** (chrysin 4 mg) as yellow amorphous solid.
- Subfraction CEF-5, (250mg) was subjected to Sephadex LH-20 using MeOH/DCM (1:1) as an eluent to afford compound **CVF2** (Chrysin-7-*O*-β-D-glucopyranoside).

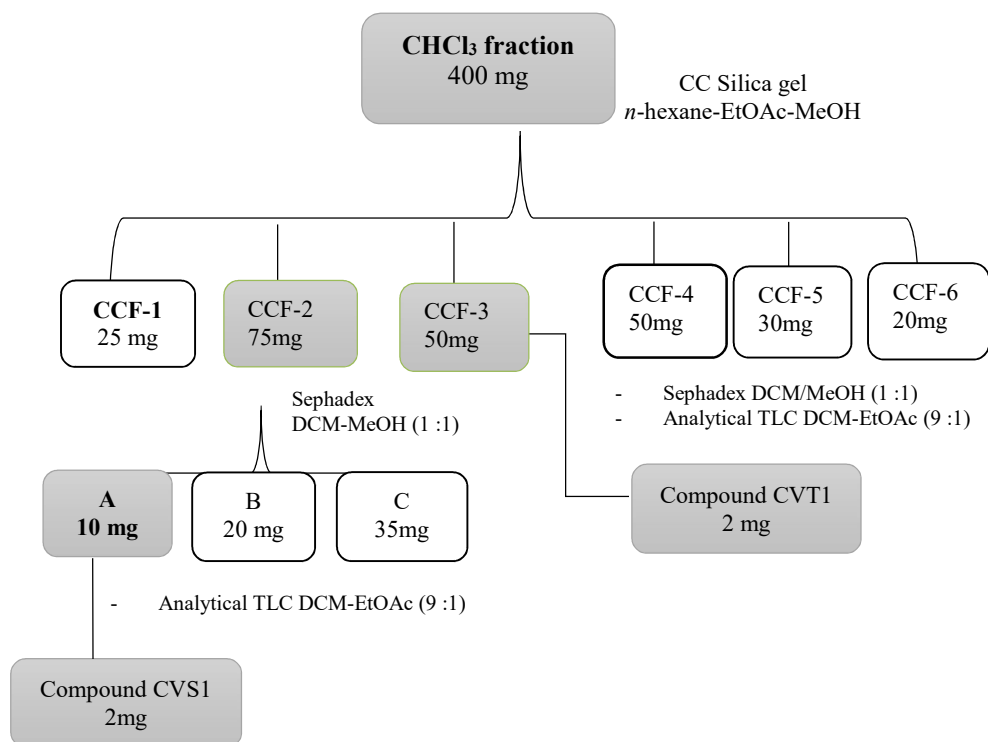


**Figure II.1. 5.** Fractionation of the chloroform fraction of *C. villosus* and isolation of its compounds

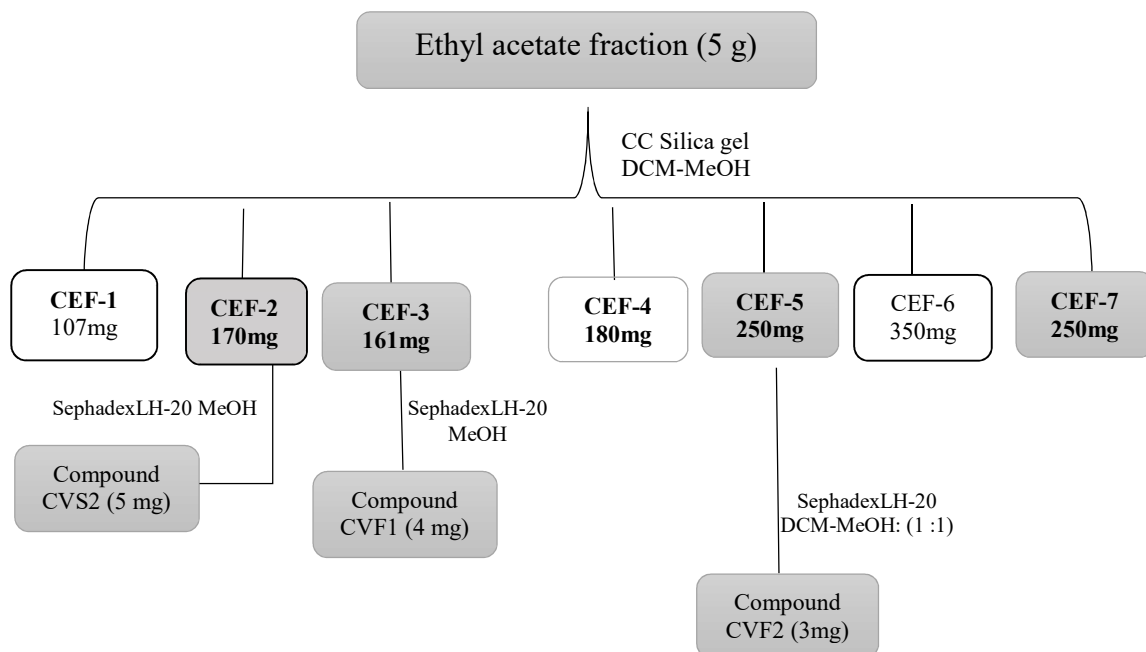


**Figure II.1. 6.** Fractionation of the ethyl acetate fraction of *C. villosus* and isolation of its compounds



### II.1.3.1.3. Isolation of the constituents of the *n*-butanol soluble fraction

- The butanolic fraction (10g) was subjected to Diaion-HP20 column and eluted with distilled water then methanol to give two main subfractions, The aqueous (6g) and the methanolic fraction (4 g).
- The methanolic fraction (4 g) was subjected MN-polyamide-SC-6 (250 g) CC which Was eluted with water then gradient decreased polarities with water-methanol systems (90:10), (80:20), (70:30) and (60:40) (50:50) (30:70) and 100% MeOH. The eluate was collected in subfractions (200 mL each) to give 8 subfractions (CBF-1to-8).
- CBF-3 (250 mg) was dissolved in a small amount of methanol and subjected to Sephadex LH-20 (25 g) CC [1(ID)× 40(L) cm] slurried in MeOH using MeOH-DCM (1:1) as an eluent. The eluate was collected in subfractions (3 ml each). Each fraction was monitored by TLC on silica gel using systemAcOEt/MeOH (8:2) Similar subfractions were combined to give subfraction A, B, C and D. Collected subfraction D was dried to give compound **CVF3** (6 mg).

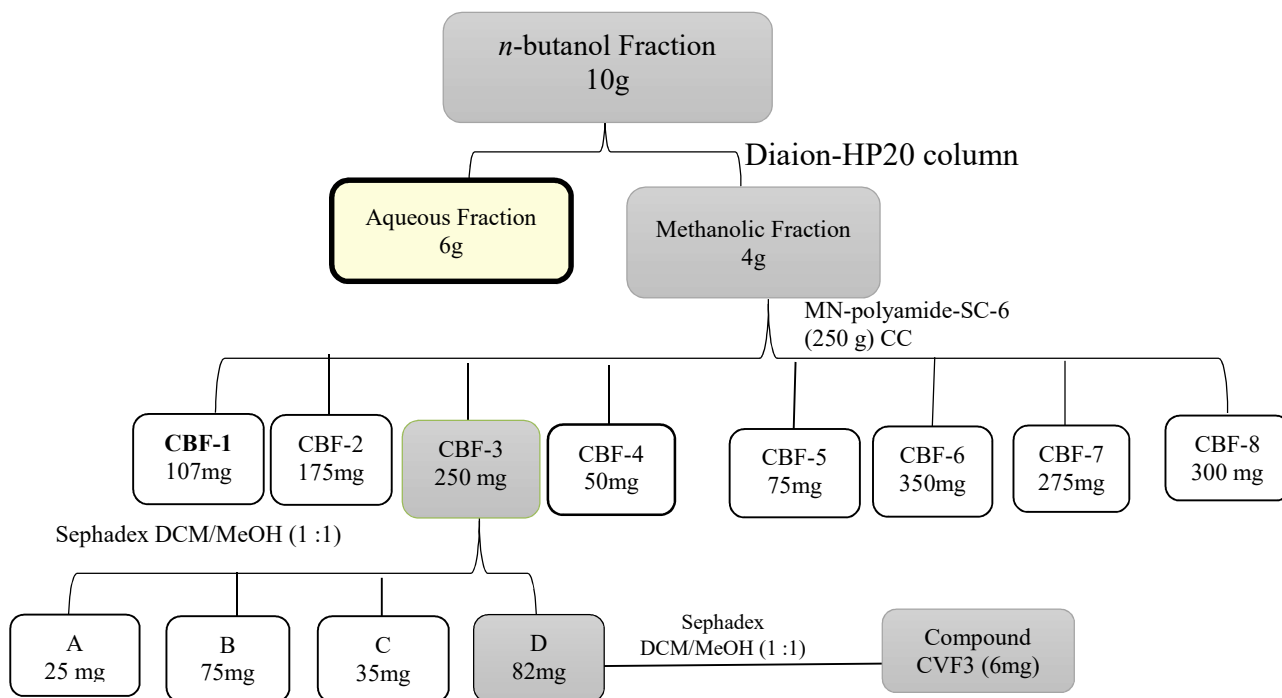


**Figure II.1. 7.** Fractionation of the *n*-butanol fraction of *C. villosus* and isolation of its compounds

### II.1.3.2. Alkaloids Extraction

Dried powdered aerial parts of plant (250 g) were extracted with EtOH–H<sub>2</sub>O (80:20, v/v) for 24 h, three times at room temperature. The combined extracts were concentrated, acidified with hydrochloric acid (0.1 M) and then, extracted with chloroform three times. The aqueous layer was made alkaline with 28% ammonium hydroxide to pH (10-12) and extracted with chloroform three times. The chloroform extracts were combined and dried over anhydrous sodium sulfate and evaporated to dryness in vacuum to give crude alkaloid mixture.

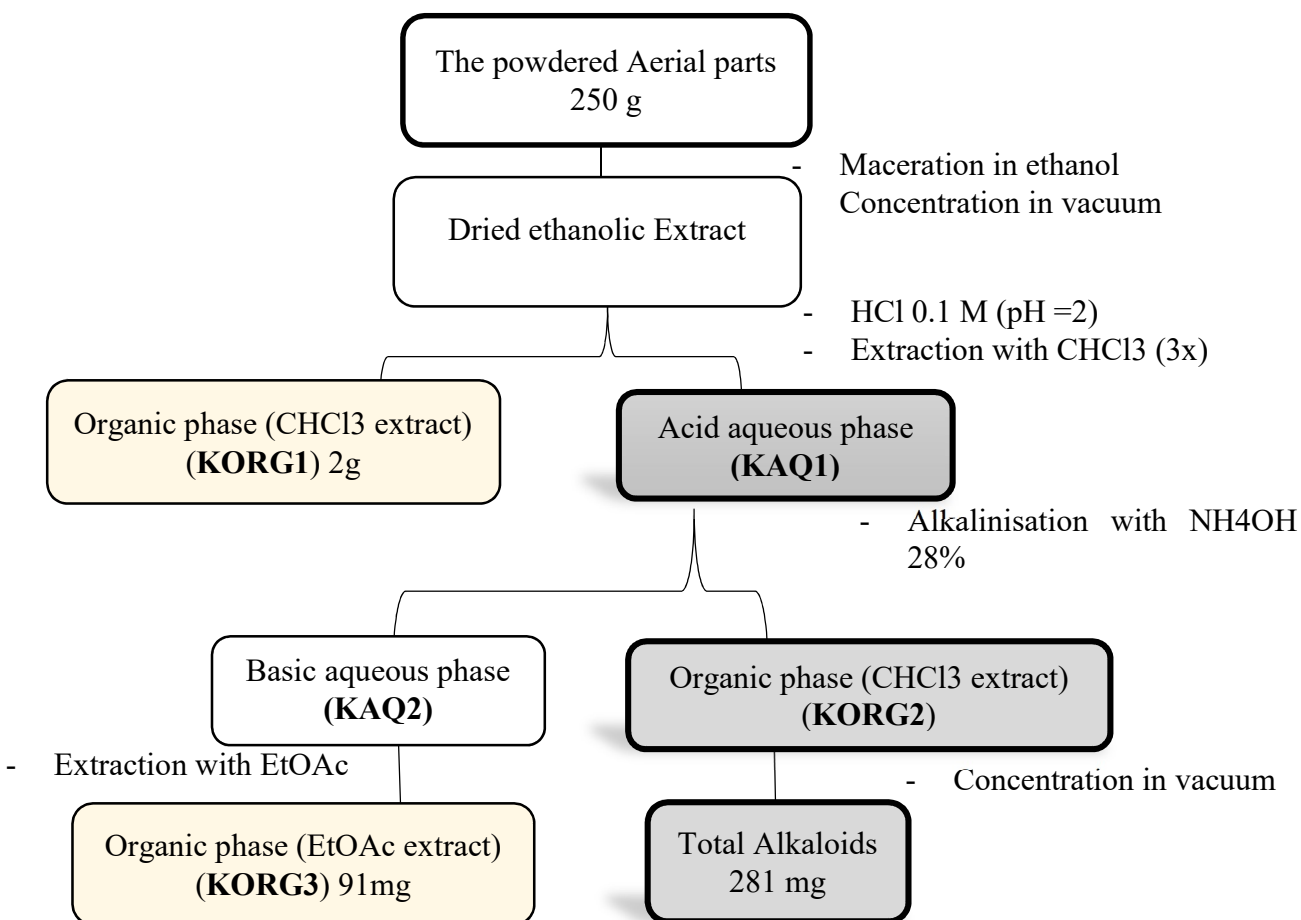
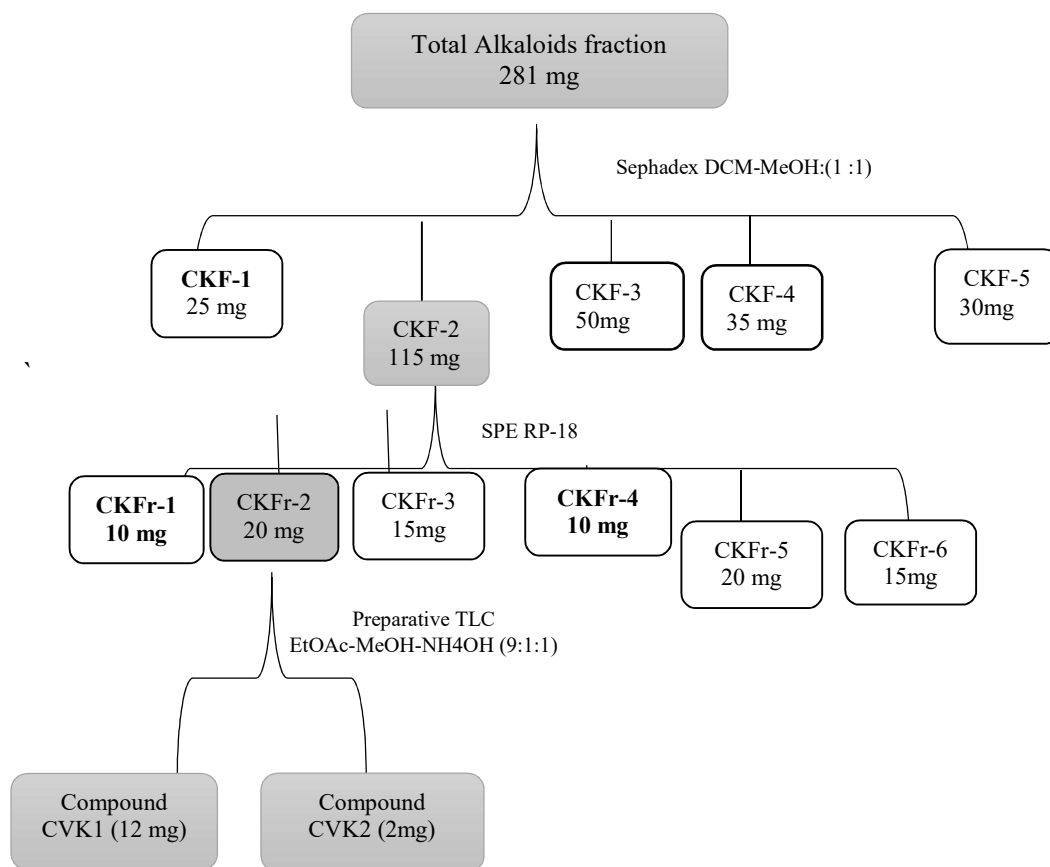


Figure II.1. 8. Acid-base extraction of alkaloids of *Cytisus villosus*

### II.1.3.2.1. Isolation of the constituents of the Alkaloids fraction

The alkaloid fraction was applied to the top of glass column packed with Sephadex LH-20 (30 g). All fractions obtained by Sephadex column were monitored by analytical TLC using system EtOAc-MeOH-NH<sub>4</sub>OH (9:1:1) The eluate was collected in subfractions (5 mL each) to give 5 subfractions (CKF.1-5). Fraction CKF-2 was rechromatographed on SPE RP-18 column chromatography, using MeOH/H<sub>2</sub>O elution to give six subfractions CKFr-1 to CKFr-6. Each fraction was monitored by TLC on silica gel using system EtOAc-MeOH-NH<sub>4</sub>OH (9:1:1). The subfraction Fr-2 (40 mg) was subjected to preparative TLC. using system EtOAc-MeOH-NH<sub>4</sub>OH (9:1:1) for elution to afford sparteine (CVK1) and (CVK2).



**Figure II.1. 9.** Fractionation of the Alkaloid fraction from *C. villosus* and isolation of its compounds

## Identification of the compounds isolated from *Cytisus villosus*

### II.1.4.1. Alkaloids Compounds

#### Compound CVK1

##### i. Physical properties

Compound CVK1 (12 mg) was obtained as a yellow viscous oil. It soluble in chloroform or ether.

##### ii. Chromatographic characters

Compound CVK1. showed  $R_f$  value of 0.16 in system II (Page 48). After spraying with Dragendroff, it appeared as orange red spot (Figure II.1.10).

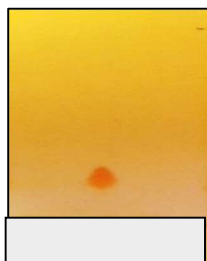


Figure II.1. 10. Profiles of silica gel TLC of compound CVK1

##### iii. Spectroscopic studies

A. UV (MeOH)  $\lambda_{\max}$  nm (log  $\epsilon$ ): 201.0 (3.99).

B. HREIMS: Positive-ion mode  $m/z$  235.211  $[M+H]^+$  (calcd. 235.219), for formula  $C_{15}H_{26}N_2$ .

##### C. $^1H$ -, $^{13}C$ -NMR and HMBC spectral analysis:

The  $^1H$ -,  $^{13}C$ -NMR and HMBC spectral data of compound CVK1 are listed in table II.1.3 and illustrated in figures thereafter.

Table II.1. 3. $^1H$ -,  $^{13}C$ -NMR and HMBC spectral data of compound CVK1 (400 MHz, 100MHz,  $CDCl_3$ )

Position	$\delta_H$ (ppm), multiplicity and $J$ in Hz	$\delta_C$	HMBC (H $\rightarrow$ C)
2	2 $\alpha$ eq, 2.65, m, 1H 2 $\beta$ ax 1.88, m, 1H	56.2	C-4
3	3 $\beta$ eq, 1.52, m, 1H 3 $\alpha$ ax ,1.55 ,m, 1H	25.8	C-4
4	4 $\alpha$ eq 1.64, m, 1H 4 $\beta$ ax 1.30, m, 1H	24.7	C-4
5	5 $\beta$ eq 1.26, m, 1H 5 $\alpha$ ax , 1.40,m, 1H	29.3	C-6
6	1.64, d, $J= 8.9$ Hz, 1H	66.5	C-2,17
7	1.80, d, $J=4.0$ Hz, 1H	33.0	C-7

8	8 $\beta$ ax, 1.02, d, $J=12.2$ Hz, 1H 8 $\alpha$ eq 2.03, m, 1H	27.6	C-7,9,11,17
9	1.45, m, 1H	36.0	C-2
10	10 $\alpha$ eq, 2.49, d, $J=10.9$ Hz, 1H 10 $\beta$ ax, 1.96, m, 1H	61.9	C-6,8 C-2, 9
11	1.92, d, $J=10.8$ Hz, 1H	64.4	C-11
12	12 $\alpha$ eq, 1.36, m, 1H 12 $\beta$ ax, 1.49, m, 1H	34.5	C-11,13
13	13 $\beta$ eq 1.67, m, 1H 13 $\alpha$ ax, 1.25, m, 1H	24.8	C-12
14	14 $\alpha$ eq, 1.56, m, 1H 14 $\beta$ ax, 1.67, m, 1H	25.8	C-15
15	15 $\alpha$ ax 2.00, m, 1H 15 $\beta$ eq 2.77, d, $J=11.6$ Hz, 1H	55.3	C-13
17	17 $\alpha$ ax, 2.32, dd, $J=11.5, 4.0$ Hz 1H 17 $\beta$ eq, 2.70, d, $J=11.5$ Hz, 1H	53.5	C-7,11

#### iv. Discussion and conclusion:

Compound **CVK1** was obtained from the alkaloid extract and purified as yellow oily compound.

The molecular formula of **CVK1** was established as  $C_{15}H_{26}N_2$  by HRESIMS ( $m/z$  235.211[M+H]<sup>+</sup> (calcd. 235.219) (Figure II.1.13).

The structure of **CVK1** was elucidated by interpretation of its NMR spectra, including <sup>1</sup>H, <sup>13</sup>C-NMR, HSQC, <sup>1</sup>H-<sup>1</sup>H COSY and HMBC.

Its <sup>1</sup>H-NMR spectrum (Figure II.1.14) showed the presence of aliphatic signals between 1.0 and 3.0 ppm, the absence of olefinic/aromatic signals and methyl groups suggested a ring system/s. Thus, the presence of four rings was deduced based on its molecular formula and its four degree of unsaturation.

<sup>13</sup>C-NMR (Figure II.1.15) spectrum yielded fourteen separate signals, with high similarity with lupine alkaloids.

**DEPT 135** spectrum (Figure II.1.16) showed four CH and apparently ten CH<sub>2</sub>, comparison between the carbon and **DEPT** experiments, the low field shift signals at  $\delta_C$  66.47 and  $\delta_C$  64.37 ppm are indicative of CH directly bond with a nitrogen atom, signals at  $\delta_C$  61.92,  $\delta_C$  56.20,  $\delta_C$  55.34 and  $\delta_C$  53.48 ppm revealed the CH<sub>2</sub> that surround the nitrogen atoms (Figure II.1.17).

These data conclude that our compound has a structure of the sparteine (Gołębiewski, 1986). Sparteine is a quinolizidine alkaloid isolated from several plants of Fabaceae family. It is the major

alkaloid in scotch broom (*Cytisus scoparius*) (Dewick, 2002). Both enantiomeric forms of spartein are found in nature, (-)-sparteine is much more abundant than (+)-sparteine.

The spectral assignments of protons were straightforward starting from H-15 $\beta$ (eq) at  $\delta_H=2.77$ ppm (Table II.1.3). The deshielding of the proton H-15 $\beta$ (eq) is the result of the electronegativity of the adjacent nitrogen atom, **N-16**, and the magnetic anisotropy of the lone electron pair on N-16 in the *syn* configuration. This effect is most pronounced for H-15 $\beta$ (eq) because of the greater exposure of the electron pair on N-16 compared with that on N-1, as a result of the predominant boat conformation of ring C (Gołębiewski, 1986) (Figure II.12).

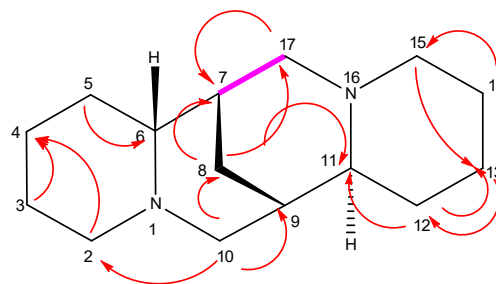
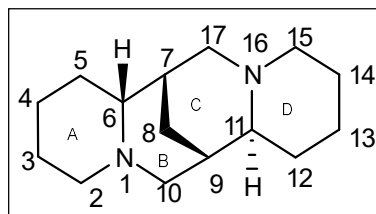
Experiment  $^1\text{H}$ - $^1\text{H}$  homonuclear COSY shows the correlations between the protons 2 $\alpha$  eq( $\delta_H$ 2.65) and 2 $\beta$  ax( $\delta_H$  1.88ppm), 15 $\alpha$ (ax) ( $\delta_H$  2.00ppm) and 15 $\beta$ (eq) ( $\delta_H$  2.77ppm), 8 $\alpha$ (eq)( $\delta_H$  1.00ppm) and 8  $\beta$  ax ( $\delta_H$  2.03ppm) and between 17  $\alpha$  ax ( $\delta_H$  2.32ppm) and 17  $\beta$  eq ( $\delta_H$  2.70ppm) (Figure II.1.18).

The HSQC experiment (Figures II.1.19) revealed one overlapped  $^{13}\text{C}$  signal confirming eleven CH<sub>2</sub> in the molecule and the molecular formula.

The low-field C-17(eq) proton shows geminal ( $J=11.5$ Hz) coupling. The high-field C-17(ax) proton exhibits geminal interaction ( $J=11.5$ Hz), but a much smaller vicinal coupling ( $J=4.0$ Hz). These values are compatible only with a boat conformation for ring C(Gołębiewski, 1986). The large vicinal coupling constants for H-6 ( $J=8.9$ Hz) prove its axial conformation.

The above NMR values are in agreement with those reported for the molecule of (-)-sparteine (Brukwicki and Wysocka, 2003; Duddeck et al., 1995). It has Previously reported on *Cytisus* species (Kolodziejewski et al., 1964; Saito et al., 1994). It has been used as an anti-arrhythmia agent(Bub and Raschack, 1974). It is also used as a chiral base in organic chemistry, and as a ligand in organic chemical synthesis. However, this compound is not FDA approved for human use as an antiarrhythmic agent, and it is not included in the Vaughn Williams classification of antiarrhythmic drugs (Pereira et al., 2012).

The skeleton of sparteine is very flexible, its derivative can assume a conformation with ring C either a boat or a chair (Brukwicki and Wysocka, 2008) in which predominates the conformer possessing boat C ring (Wiewiorowski et al., 1967) (Figure II.1.12).



Structure of Compound CVK1 :  
(-)-sparteine

Figure II.1. 11. Important HMBC (H → C) COSY  
(→) of compound CVK1

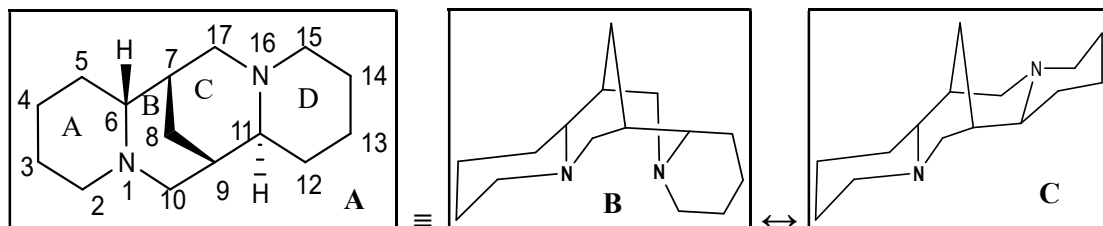


Figure II.1. 12. Conformation of (-)-Sparteine (CVK1) A), C-  
chair conformer (B), C-boat conformer(C)

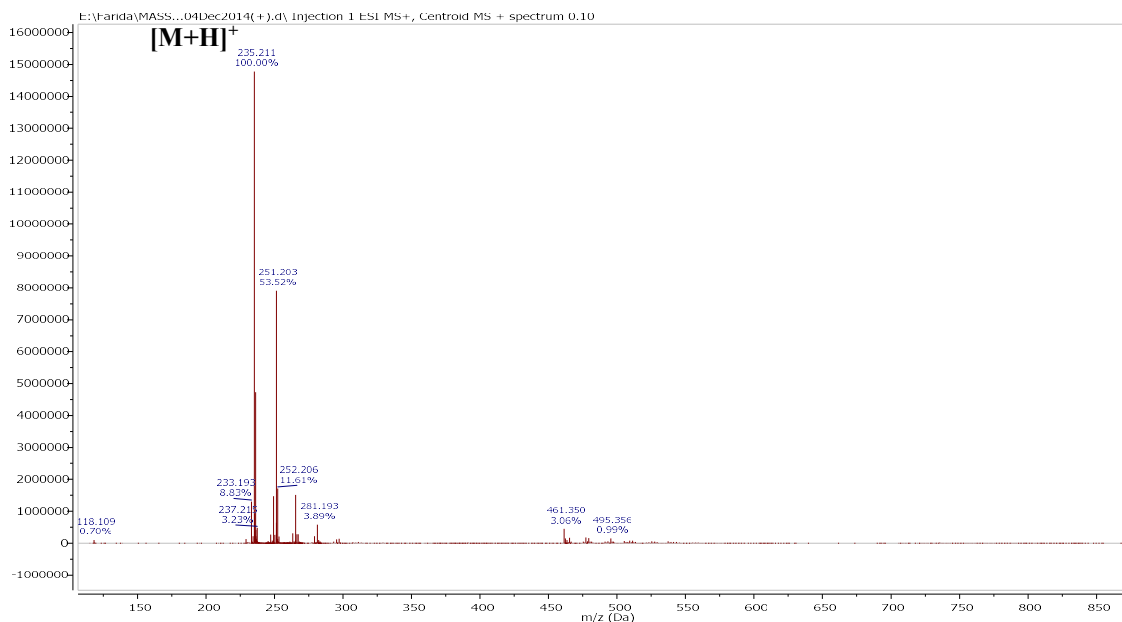


Figure II.1. 13.. Positive HR-ESI-MS of compound CVK1

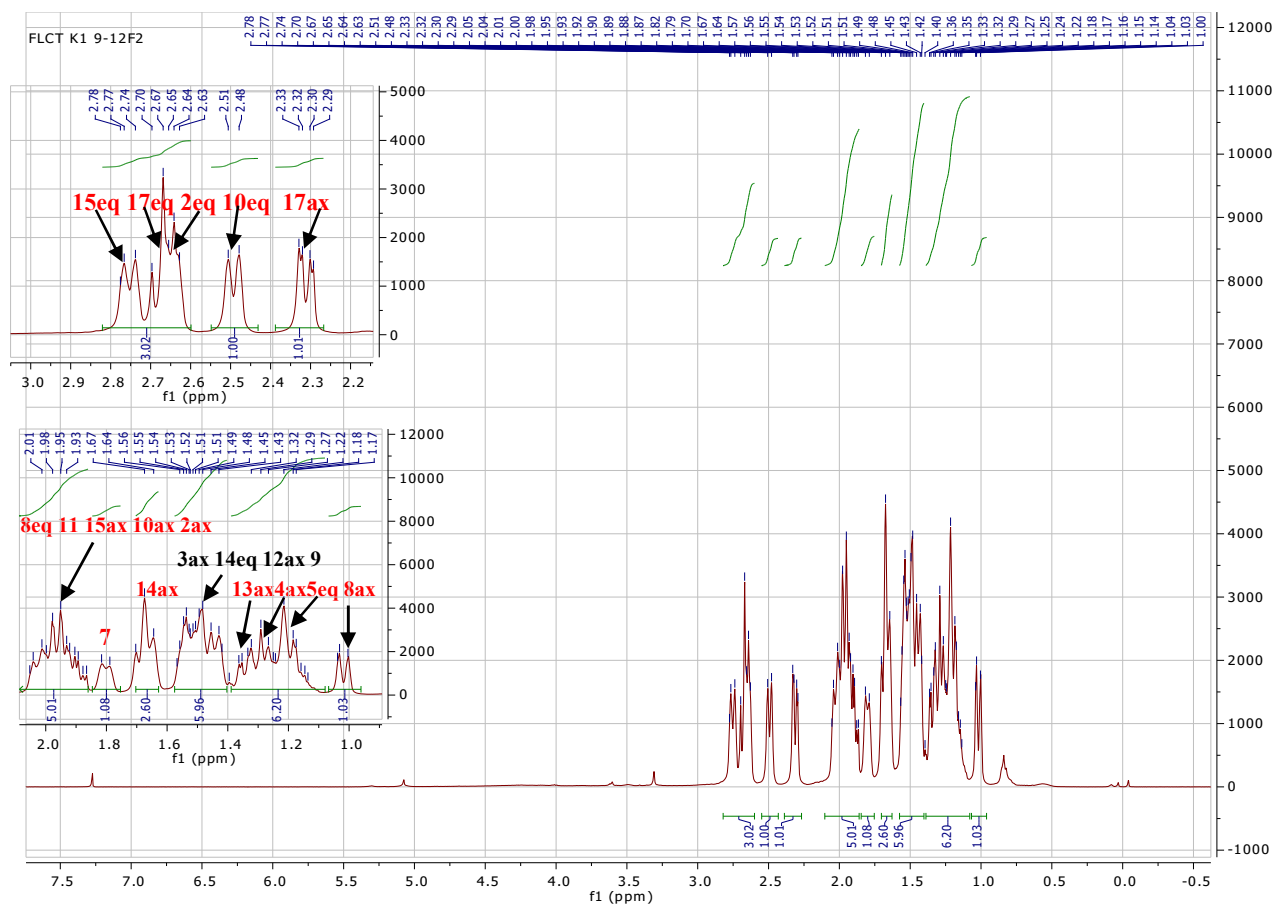


Figure II.1. 14. <sup>1</sup>H-NMR Spectrum of compound CVK1 (CDCl<sub>3</sub>, 400 MHz)

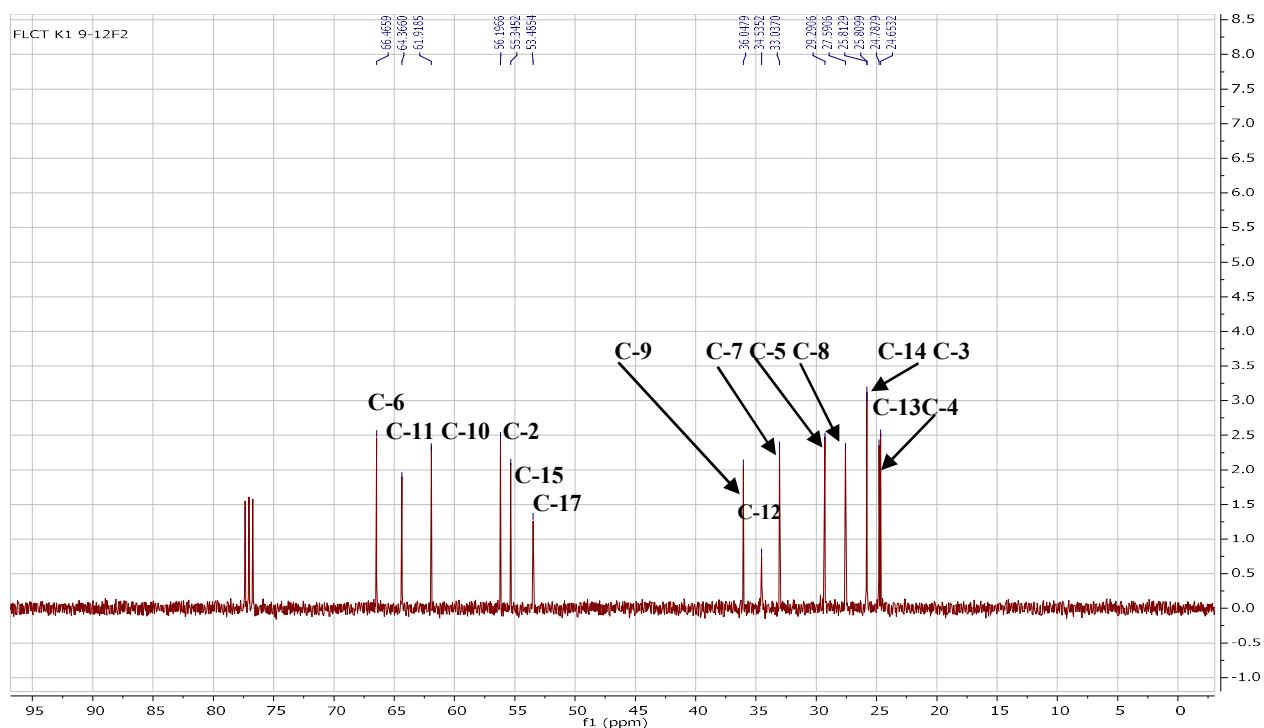


Figure II.1. 15. <sup>13</sup>C-NMR Spectrum of compound CVK1 (CDCl<sub>3</sub>, 100 MHz)



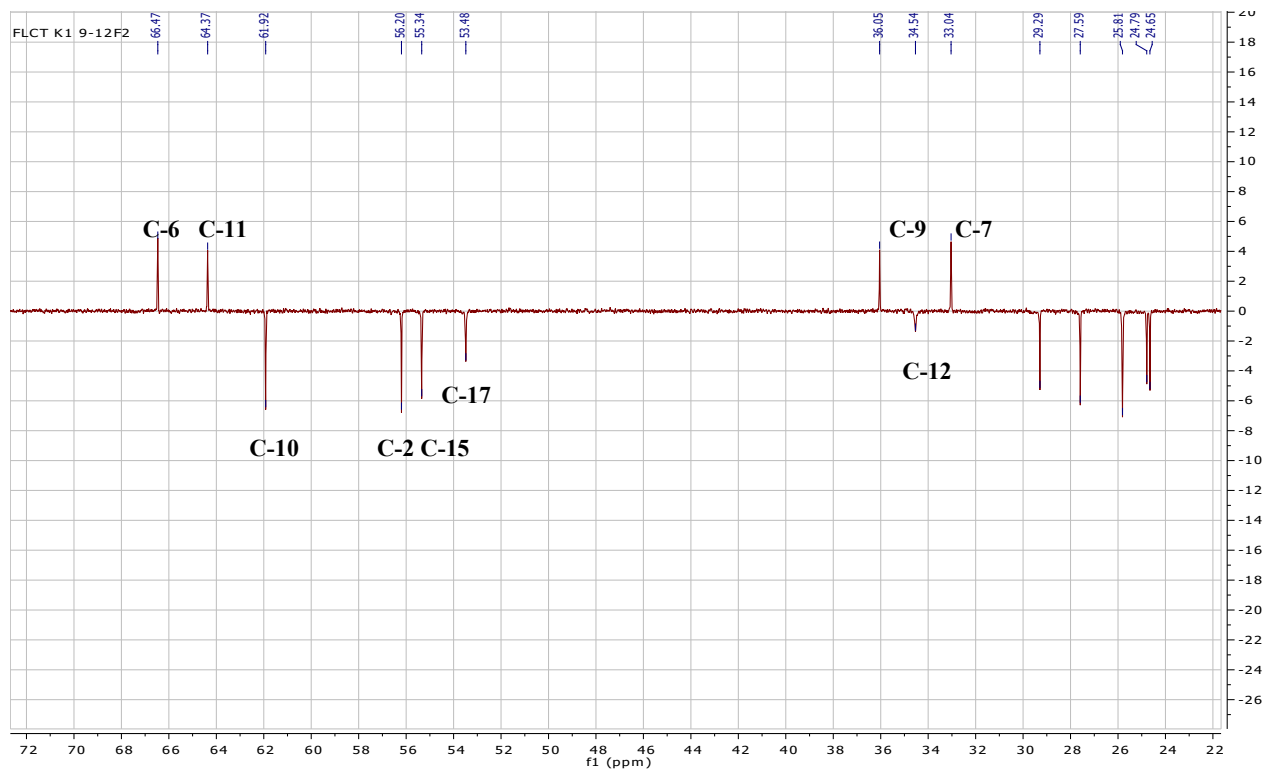


Figure II.1. 16..DEPT 135 Spectrum of compound CVK1

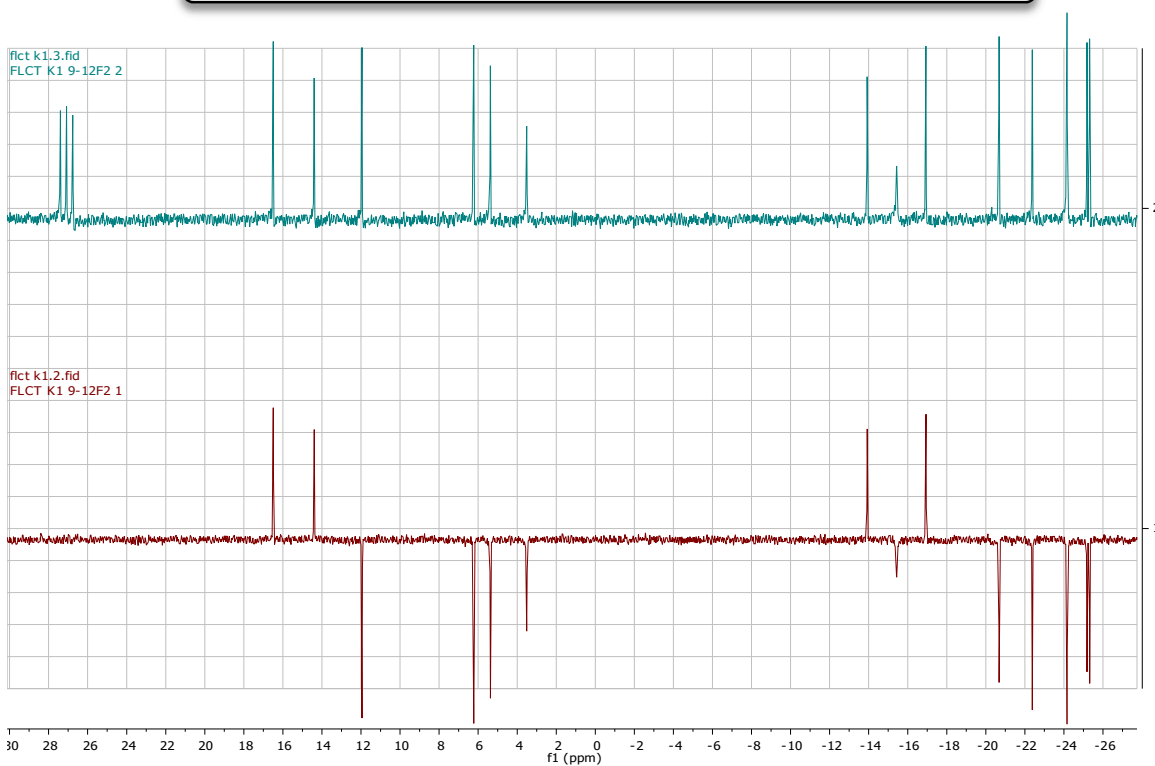


Figure II.1. 17. Comparison of <sup>13</sup>C-NMR and DEPT-135 Spectra of compound CVK1

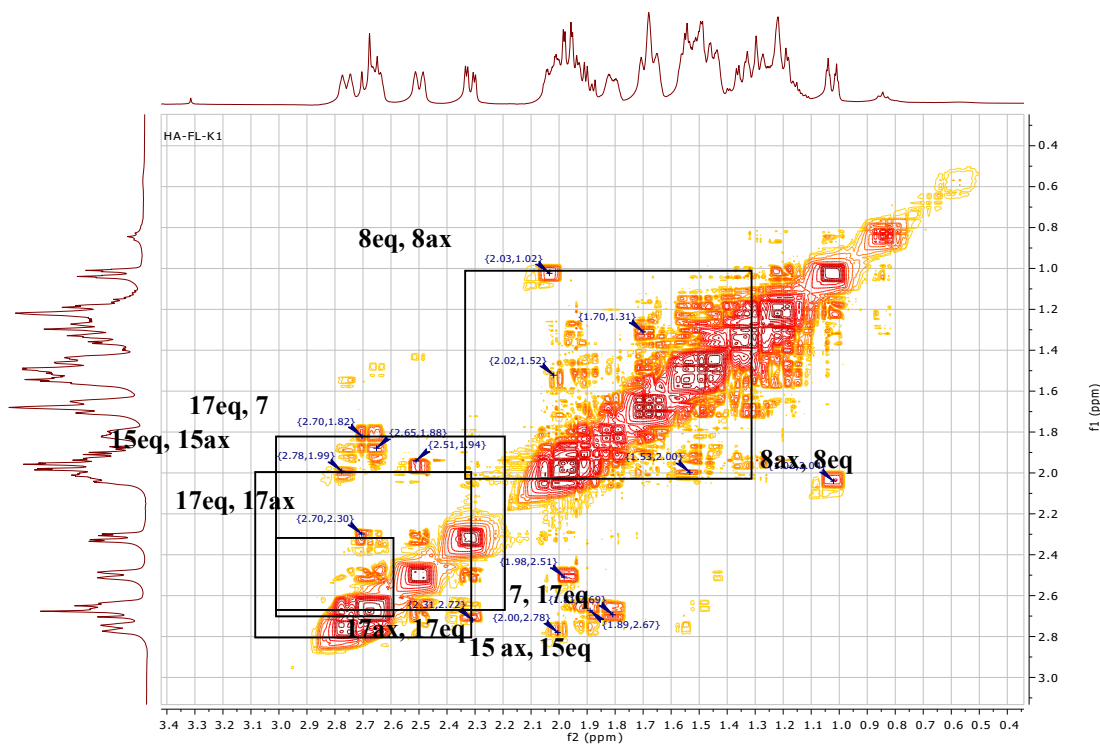


Figure II.1. 18.  $^1\text{H}$ - $^1\text{H}$  COSY Spectrum of compound CVK1

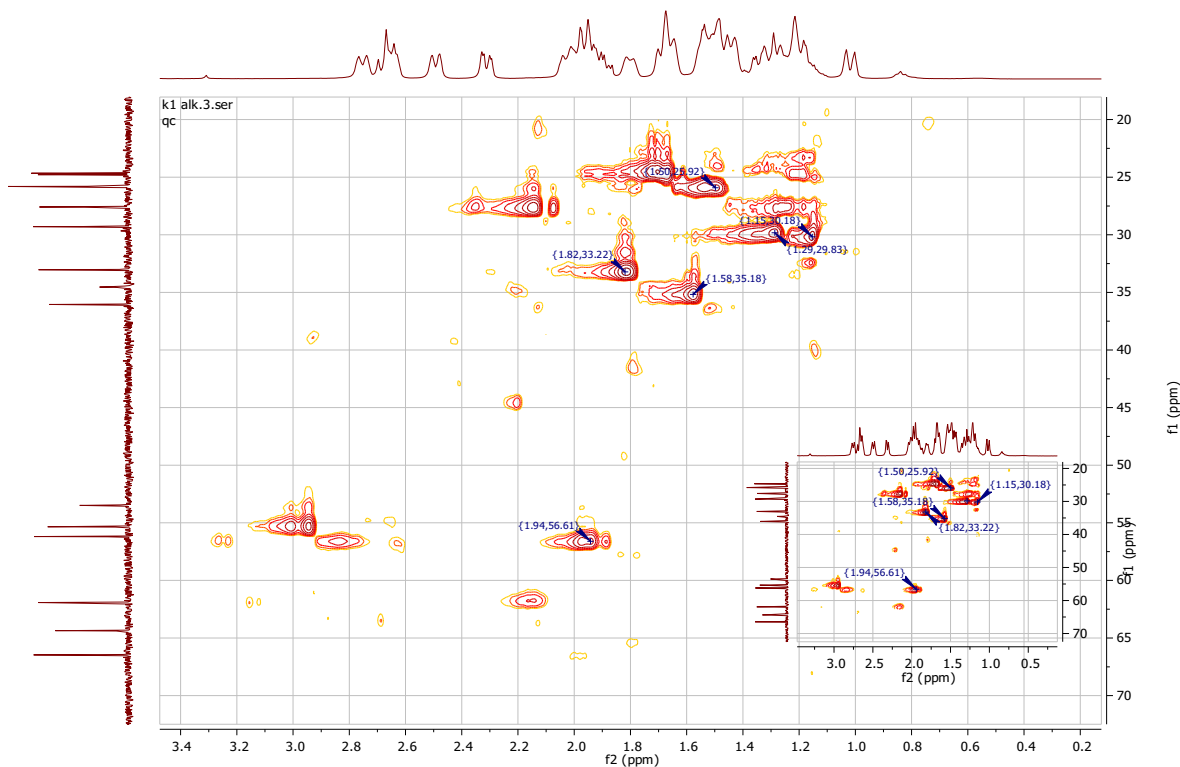


Figure II.1. 19. HSQC Spectrum of compound CVK1

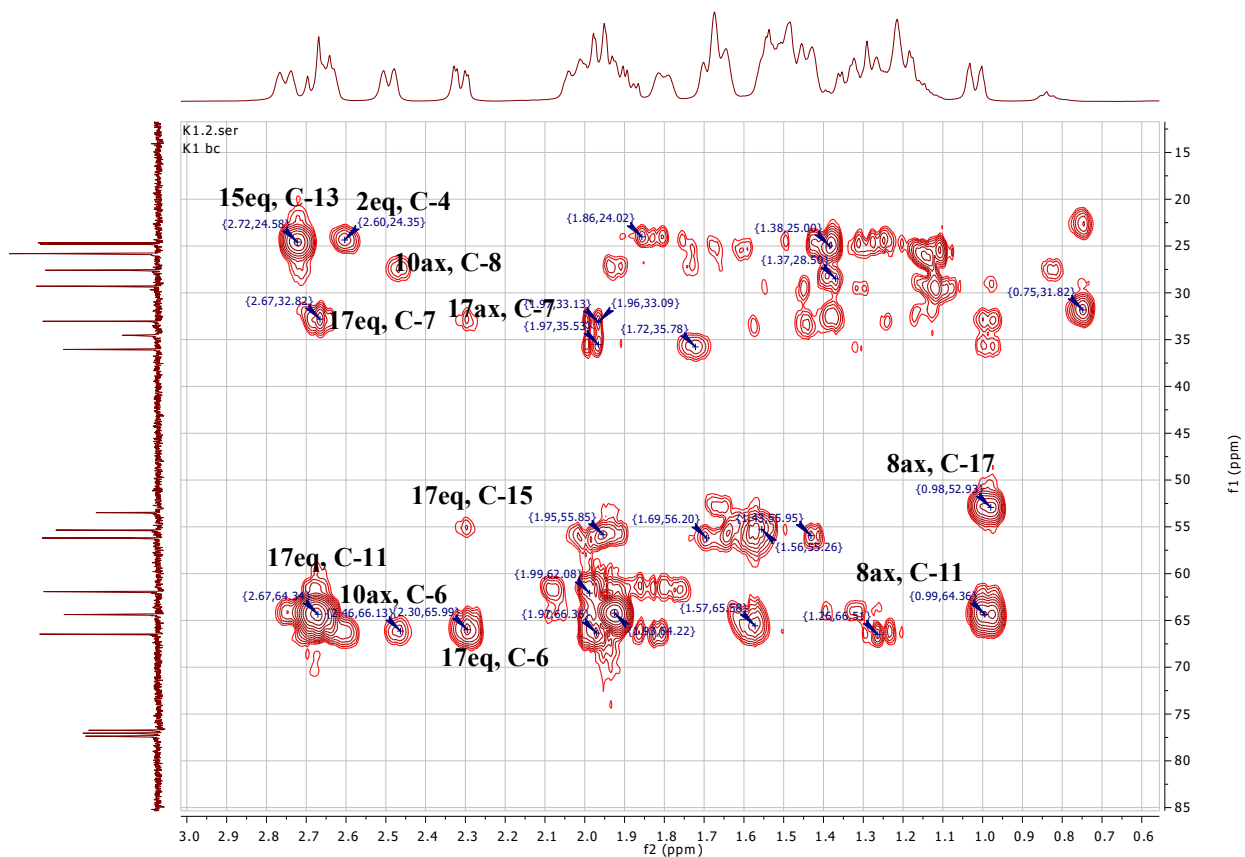


Figure II.1. 20. HMBC Spectrum of compound CVK1

## II.1.4.2. Terpenoids

### II.1.4.2.1. Compound CVT1

#### i. Physical properties

Compound CVT1 (2 mg) was obtained as a yellowish white amorphous powder,  $[\alpha]_D^{20}$ -88.0 ( $c = 0.05$ , MeOH).

#### ii. Chromatographic characters

Compound CVT1 appeared as a light blue florescent zone under UV  $\lambda_{\max}$  366 (Figure II.1.21). It showed  $R_f$  value of 0.50 in system IV (Page 48)

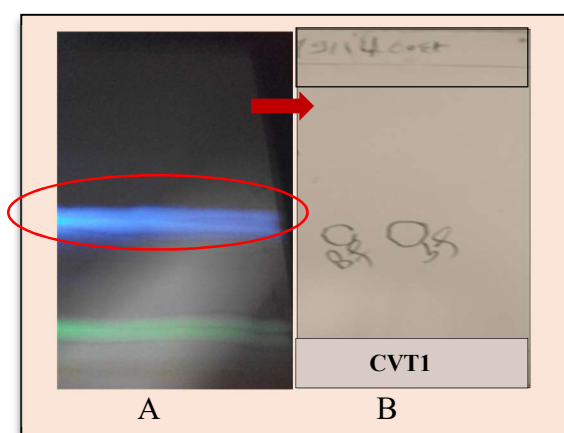


**Figure II.1. 21.** Profiles of silica gel TLC of compound CVT1:  
A. before purification, B. After purification

#### iii. Spectroscopic studies:

**A. UV (MeOH)  $\lambda_{\max}$  nm (log  $\epsilon$ ):** 208 (4.97), 260 (3.79).

**B. HR-ESI-MS:**  $m/z$  197.122  $[M+H]^+$ (calcd 197.120),  $m/z$  219.104  $[M+Na]^+$ (calcd. 219.100) for formula  $C_{11}H_{16}O_3$ .

#### C. $^1H$ -, $^{13}C$ -NMR and HMBC spectral analysis:

The  $^1H$ -,  $^{13}C$ -NMR and HMBC spectral data of compound CVT1 are listed in table II.1.4 and illustrated in figures thereafter.

**Table II.1. 4.**  $^1\text{H}$ -,  $^{13}\text{C}$ -NMR and HMBC spectral data of compound **CVT1** (400 MHz, 100 MHz, DMSO- $d_6$ ,  $J$  in Hz,  $\delta$  in ppm)

Position	$\delta_H$ (ppm), multiplicity, $J$ (Hz)	$\delta_C$ (ppm)	HMBC(H $\rightarrow$ C)	HSQC-TOCSY	$^1\text{H}$ - $^1\text{H}$ -COSY
1	-	171.5	-	-	-
2	-	36.1	-	-	-
3	H-3a, 1.42, dd, 14.2, 3.7, 1H H-3b, 1.87, dt, 14.1, 2.5, 1H	47.0	C-1,2, 4, 7	C-3, 4	H-3b, 4 H-3b, H-4, H-5b
4	4.08, dq, 6.3, 3.4, 1H	65.3	C-2, 6	C-4, 5	H-3a, H-3b, H-5a, H-5b, OH
OH-C-4	5.00, d, 3.2 Hz, 1H.	65.3	C-4,5	C-4, 5	H-4
5	H-5a, 1.63, dd, 13.4, 4.0, 1H H-5b, 2.29, dt, 13.2, 2.5, 1H	45.7	C-3,4,6,7, 12	C-5, 4	H-5b, 4 H-3b,4, H-5a
6	-	86.9	-	-	-
7	-	183.5	-	-	-
8	5.79, s, 1H	112.5	C-1,2, 6,7	C-8	H-12
10	1.38, s, 3H	26.6	C-2, 3,7,11	C-10, 11	-
11	1.19, s, 3H	30.9	C-2, 3,7,10	C-11	-
12	1.67, s, 3H	27.3	C-5, 6,7	C-12	H-8

**iv. Discussion and conclusion:**

Compound **CVT1**, obtained as a yellowish white amorphous powder. The molecular formula of **CVT1** was revealed as  $\text{C}_{11}\text{H}_{16}\text{O}_3$  with four degree of unsaturation, by the positive HR-EIS-MS by a molecular ion peak at  $m/z$  197.122  $[\text{M}+\text{H}]^+$  (calcd. For 197.120) and at  $m/z$  219.104  $[\text{M}+\text{Na}]^+$  (calcd. 219.100) and confirmed by the negative EIS-MS/MS by a molecular ion peak at  $m/z$  391.2151  $[2\text{M}-\text{H}]^-$  (calcd. 391.2098) and at  $m/z$  195.1041  $[\text{M}-\text{H}]^-$  (calcd. 195.0999) (FigureII.1.25).

The  $^1\text{H}$ -NMR spectrum (FigureII.1.26) showed three methyl singlets at  $\delta_H=1.19$  (3H), 1.38 (3H), and 1.67 (3H), which indicated the presence of three methyl groups.

The  $^{13}\text{C}$ -NMR spectrum (FigureII.1.27) showed 11 carbon signals, identified by a DEPT experiment (FigureII.1.28) as one carbonyl group at  $\delta_C$  183.5, one trisubstituted C=C bond ( $\delta_C$ 171.5), one vinyl proton H-C=C ( $\delta_C$  112.5), one oxygenated quaternary C-atom ( $\delta_C$ 86.9), one oxygenated CH ( $\delta_C$  65.3), one regular quaternary C-atom ( $\delta_C$  36.1), two  $\text{CH}_2$  ( $\delta_C$  45.7, 47.0), and three Methyl groups

( $\delta_C$  27.3, 26.6, 30.9). These observations, in combination with the molecular formula, indicated one OH group and two rings.

Extensive 2D-NMR ( $^1\text{H}$ ,  $^1\text{H}$ -COSY, TOCSY, HSQC, HSQC-TOCSY and HMBC) experiments allowed us to define the molecular connectivity.

$^1\text{H}$ - $^1\text{H}$ -COSY (Figure II.1.32) showed cross peak correlations of  $\text{CH}_2(3)$  with H-4 and of H-4 with  $\text{CH}_2(3)$ , of H-4 with  $\text{CH}_2(5)$  and of  $\text{CH}_2(5)$  with H-4.

The  $^1\text{H}$ - $^1\text{H}$  COSY and TOCSY (Figure II.1.32) together with HSQC and HSQC-TOCSY analysis (Figures II.1.30-31) revealed a  $-\text{CH}_2-\text{CH}-\text{CH}_2-$  unit (**CVT1-a**), with the OH group being located at C-H(4) atom deduced from HSQC-TOCSY correlation of the proton of hydroxyl at C-4 with C-4 and C-5 (Figure II.1.31) and the  $^1\text{H}$ - $^1\text{H}$  COSY cross-peak correlation of the proton of the hydroxyl group at C-4 and H-4 (Figure II.1.32).

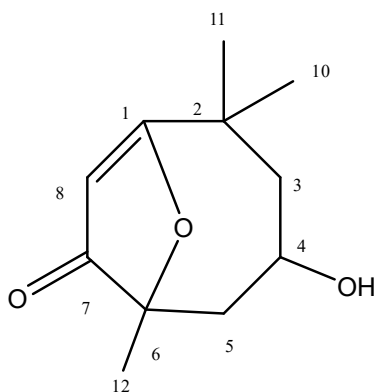
The HMBC cross-peaks from both  $\text{H}_3-10$  ( $\delta_H$  1.38 (s)) and  $\text{H}_3-11$  ( $\delta_H$  1.19) to C-3 ( $\delta_C$  47.0), H-8 ( $\delta_H$  5.79) to C-6 ( $\delta_C$  86.9), C-1 ( $\delta_C$  171.5) and C-2 ( $\delta_C$  38.1), respectively, led to suggest a partial structure **CVT1-b**.

The HMBC (Figure II.1.34) correlations of  $\text{H}_2-\text{C}-5$  ( $\delta_H$  1.63, 2.29) with both C-6 and C-7, of H-4 ( $\delta_H$  4.08) with both C-2 ( $\delta_C$  36.1) and C-6 ( $\delta_C$  86.9), and of  $\text{H}_2-\text{C}-3$  ( $\delta_H$  1.42, 1.87) with both C-2 and  $\text{CH}_3-10$  ( $\delta_C$  26.6) required direct connections of C-3 to C-2, and of C-6 to C-5, respectively, so that **CVT1-a** and **CVT1-b** which were linked via C-6, C-1, C-2, C-6 and C-7 could be joined to the planar structure of **CVT1** to form a planar ring molecule.

The remaining one degree of unsaturation, required the presence of an additional ring. Therefore, the additional O-atom had to form an oxy bridge.

The relatively downfield shifted of the  $^{13}\text{C}$ -NMR data of C-1 ( $\delta_C$  171.5) and the oxygenated quaternary carbon at C-6 ( $\delta_C$  86.9), suggesting the presence of an ether bridge between C-6 and C-1 (Li et al., 2013) resulting in the formation of an oxygen ring.

Therefore, compound **CVT1** was identified as the New compound **4-hydroxy-2,2,6-trimethyl-9-oxabicyclo[4.2.1]non-1(8)-en-7-one**.



Structure of compound CVT1

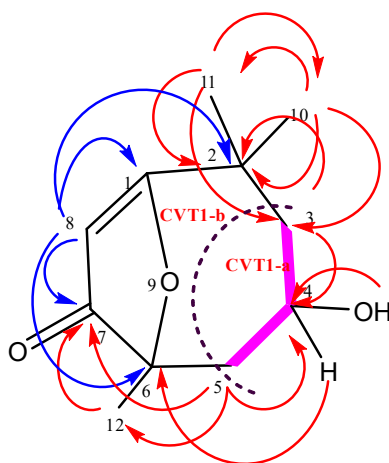


Figure II.1. 22. Important HMBC (H→C) and 1H-1H COSY (—) correlation of compound CVT1

**- Determination of the absolute configuration using ECD method**

Electronic circular dichroism (ECD) has been demonstrated to be a powerful chiroptical tool for the absolute configuration assignment of natural products with various chromophores since the 1960s (Ferris et al., 1971; Slade et al., 2005). CD is the phenomena of a chiral molecule that adsorbs left and right circularly polarized light beams to a different extent. The difference of the absorptions is the measure of the magnitude of CD, which is expressed by the differential molar extinction coefficients as  $\Delta\epsilon = \epsilon_l - \epsilon_r$  (L.mol<sup>-1</sup>·cm<sup>-1</sup>) (Li et al., 2010).

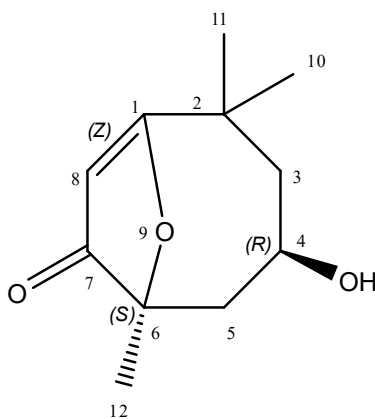
Contrary to the phenomena of optical rotary dispersion (ORD) that any chiral molecule will show absorptions in the UV/vis wavelength range, appropriate chromophores such as carbonyl, diene, aromatic, or a conjugated system should be present in the molecule in order to exhibit measurable

ECD absorptions or Cotton effects. In principle, chiral compounds with the same or similar chromophore(s) and stereochemical environment (including configuration and conformation) exhibit similar ECD spectra, which is the basis for the assignment of the AC of a new chiral molecule compared to those whose AC has been independently established by other methods, such as X-ray crystallography or chemical synthesis.

The calculated electronic transitions and molecular orbitals have allowed chemists to understand ECD at the molecular level. While on one hand the calculations can validate the previously deduced empirical rules, the most exciting aspect is that this approach seems to be able to determine the AC of any chiral molecule that produces a distinct experimental ECD spectrum. The principle is simply based on the comparison of the calculated and experimental ECD spectra: the more closely they match, the more reliable conclusion for the AC assignment can be drawn.

The new compound **CVT1** possess two stereogenic centers (C-4, C-6) and was optically active ( $[\alpha]^{25}_D = -88$ ). Circular dichroism spectra were taken to determine the absolute configuration at carbons C-4 and C-6 in the molecule.

The calculated and experimental ECD spectra were compared for all possible stereoisomers). Compound **CVT1** contains two stereogenic centers. It is highly rigid structure. It showed three conformers (Figure II.1.23) for the (*R*, *S*) and (*S*, *R*) isomers, and one conformer for the (*R*, *R*) and (*S*, *S*) isomers. The calculated ECD spectra of all possible isomers were compared with the experimental one. The (***R*, *S***) isomer matched well the experimental results (Figure II.1.24). The ECD exhibited a negative cotton effect at 200 nm. Thus, the gross structure of **CVT1** established as (***4R,6S***)-4-hydroxy-2,2,6-trimethyl-9-oxabicyclo [4.2.1] non-1(8)-en-7-one.



**Stereochemistry of compound CVT1 :**  
**(*4R,6S*)-4-hydroxy-2,2,6-trimethyl-9-oxabicyclo[4.2.1]non-1(8)-en-7-one**



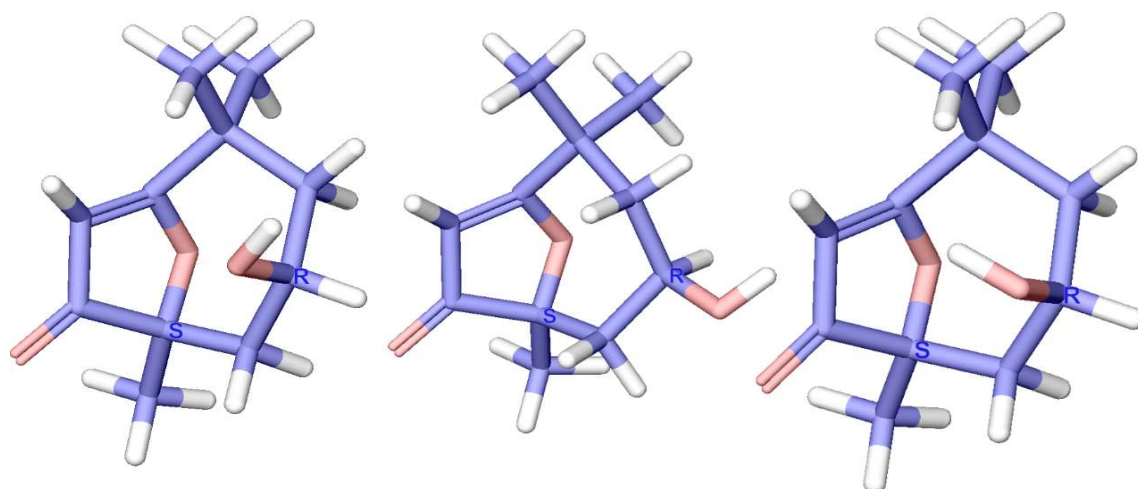


Figure II.1. 23. The conformers of compound CVT1

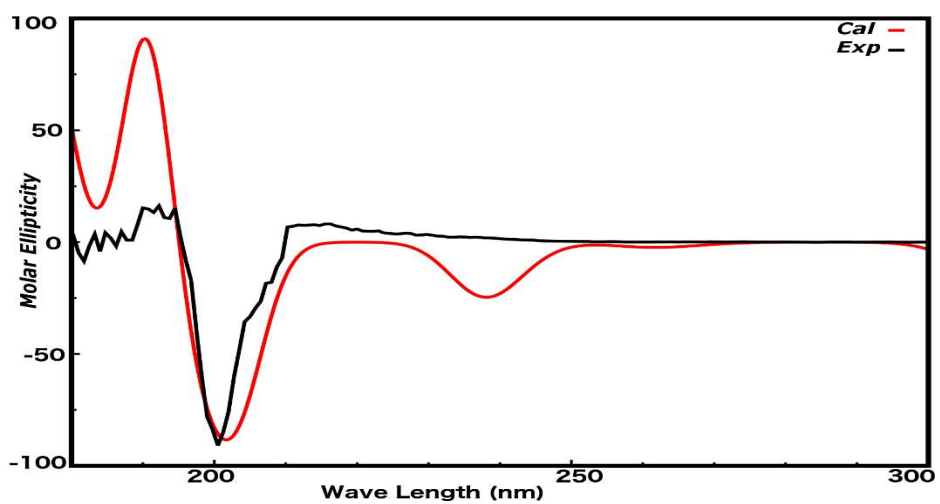
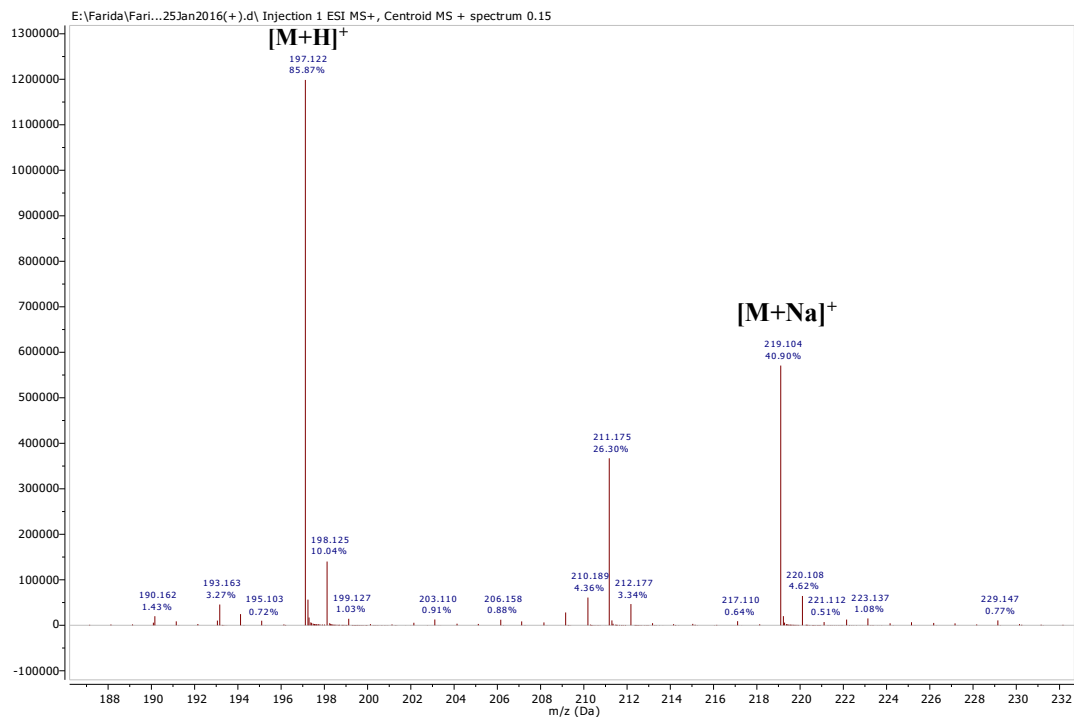
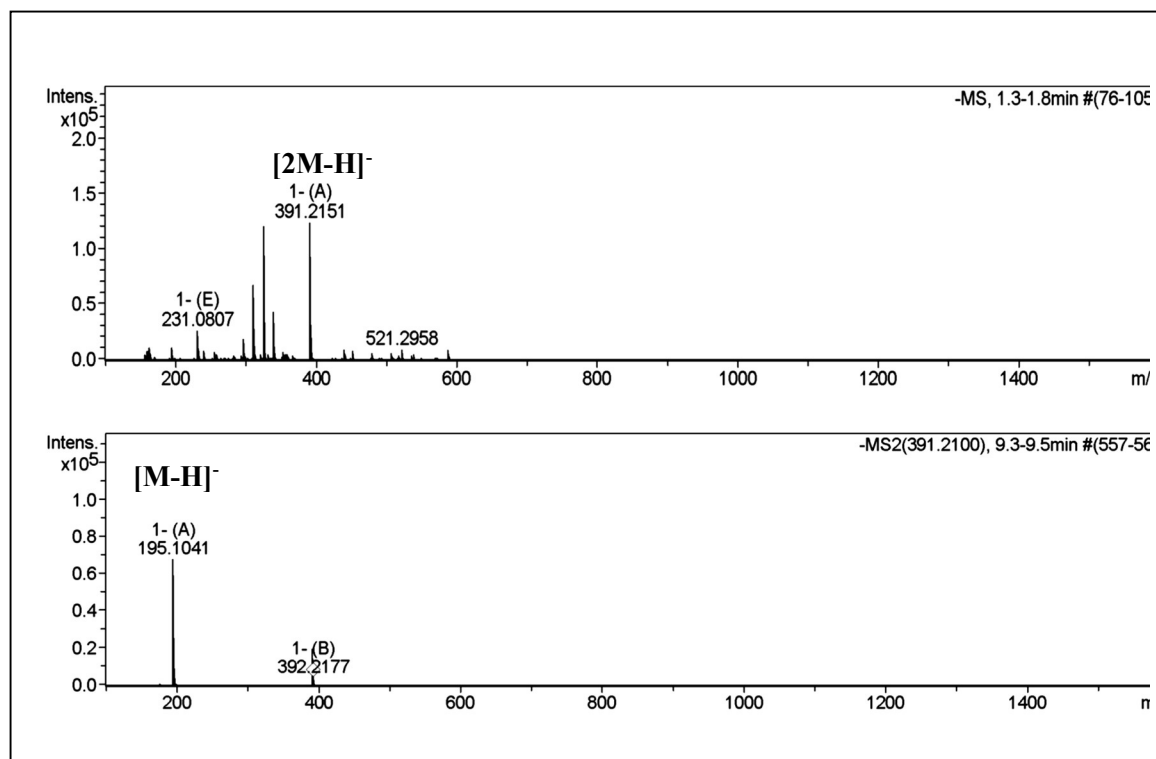


Figure II.1. 24. The experimental and calculated ECD spectra of compound CVT1  
Both spectra showed a negative cotton effect at 200nm



A.



B.

**Figure II.1.** Mass spectra of compound CVT1  
A. Positive HR-ESI-MS, B. Negative ESI-MS/MS

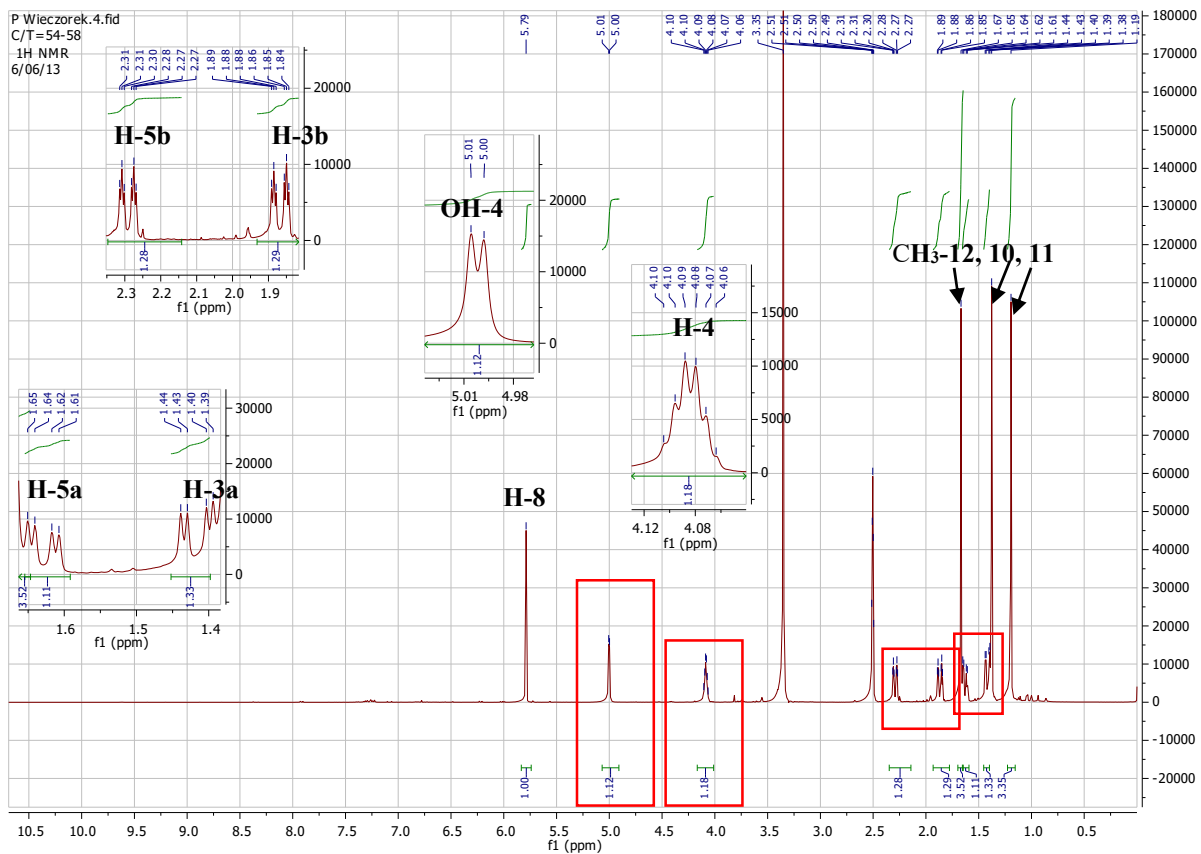


Figure II.1. 26. <sup>1</sup>H-NMR Spectrum of compound CVT1 (DMSO-d<sub>6</sub>, 400 MHz)

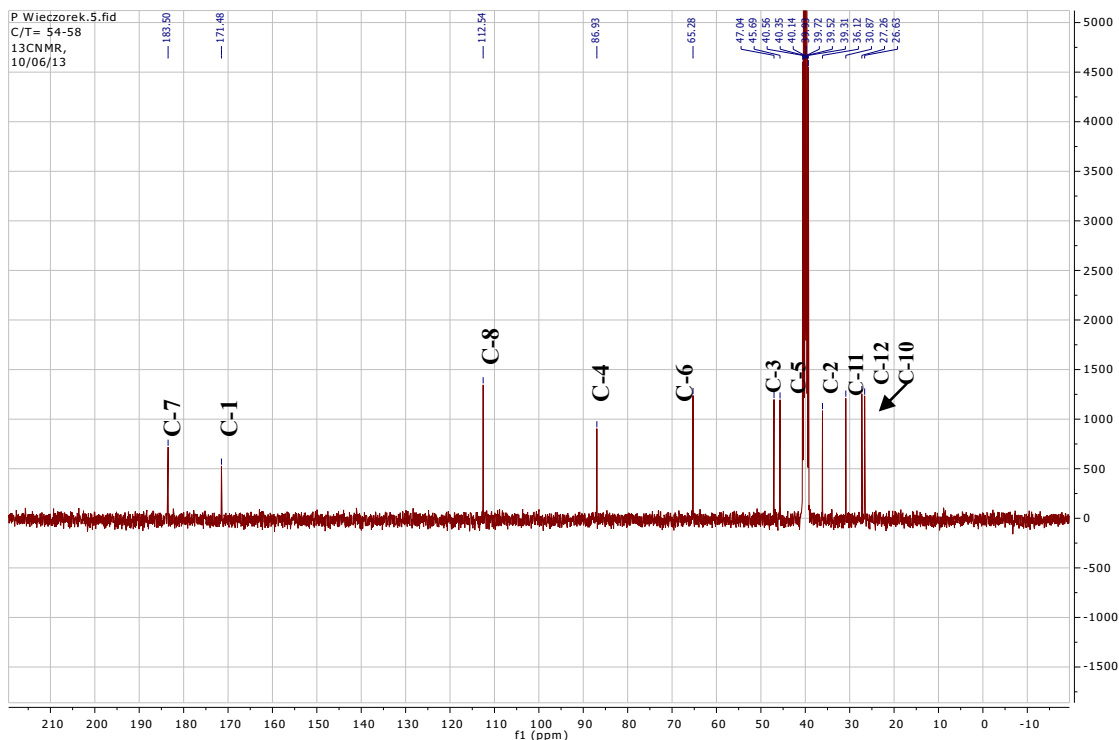
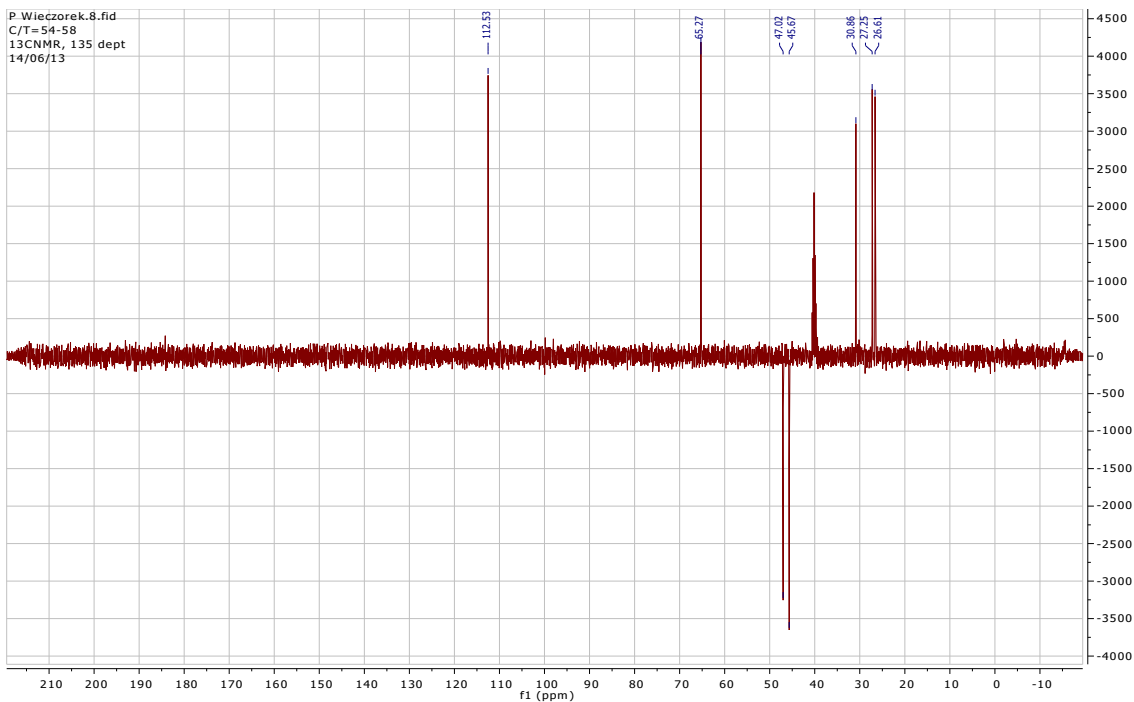
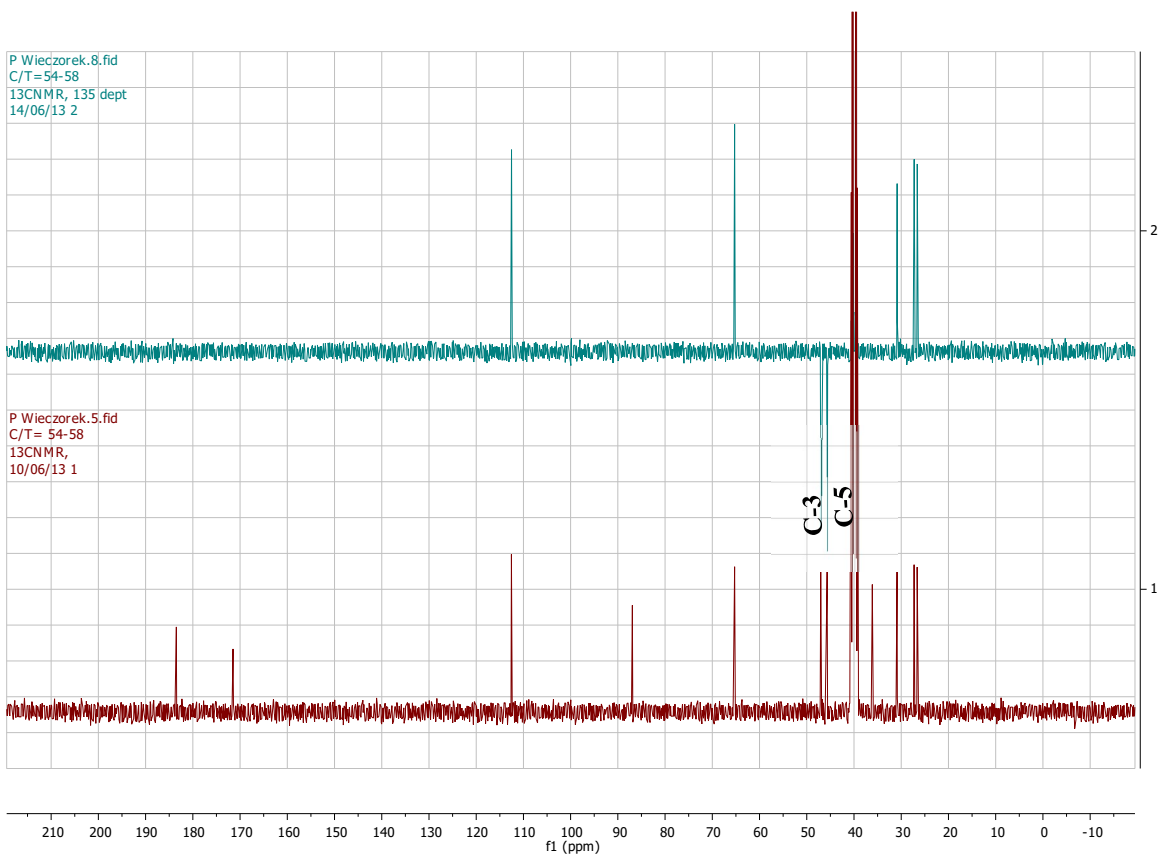


Figure II.1. 27. <sup>13</sup>C- NMR Spectrum of compound CVT1(DMSO-d<sub>6</sub>, 100 MHz)



**Figure II.1. 28..DEPT-135 Spectrum of compound CVT1**



**Figure II.1. 29. Comparison of <sup>13</sup>C-NMR and DEPT-135 Spectra of compound CVT1**

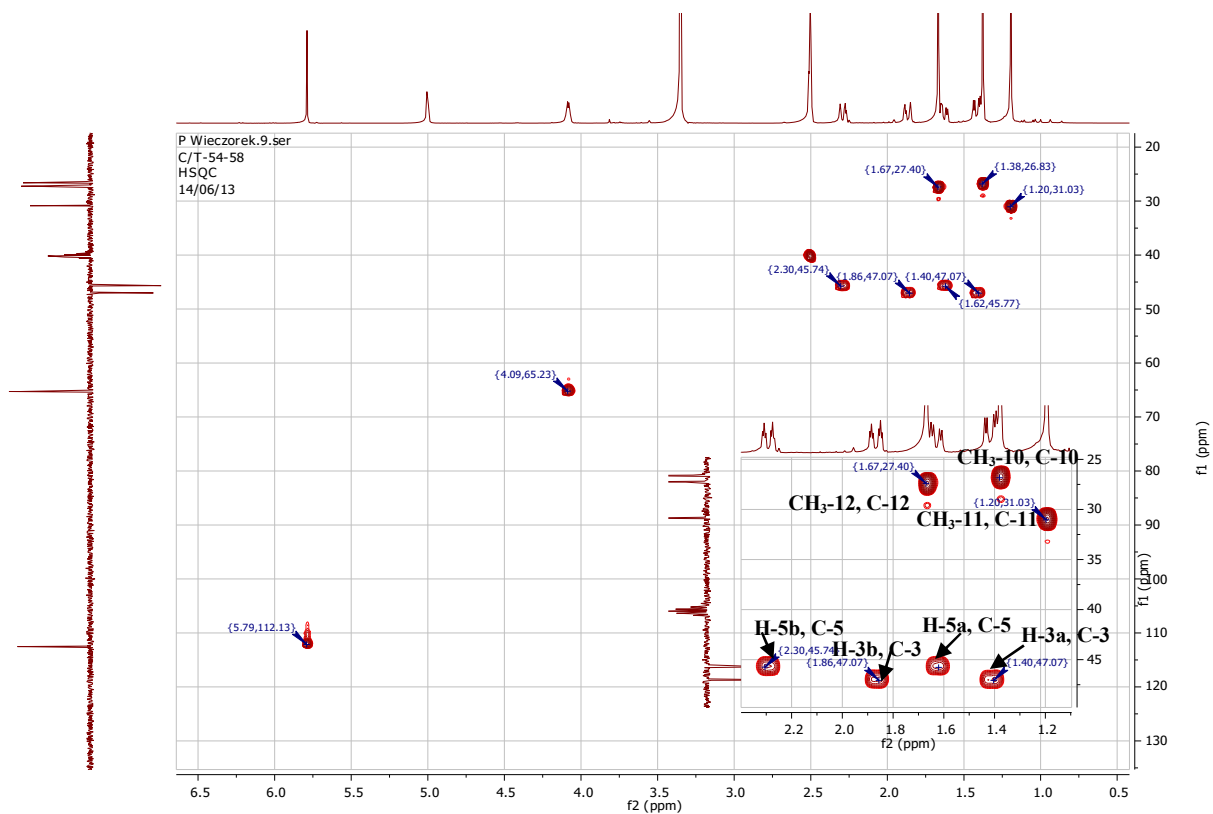


Figure II.1. 30 .HSQC Spectrum of compound CVT1

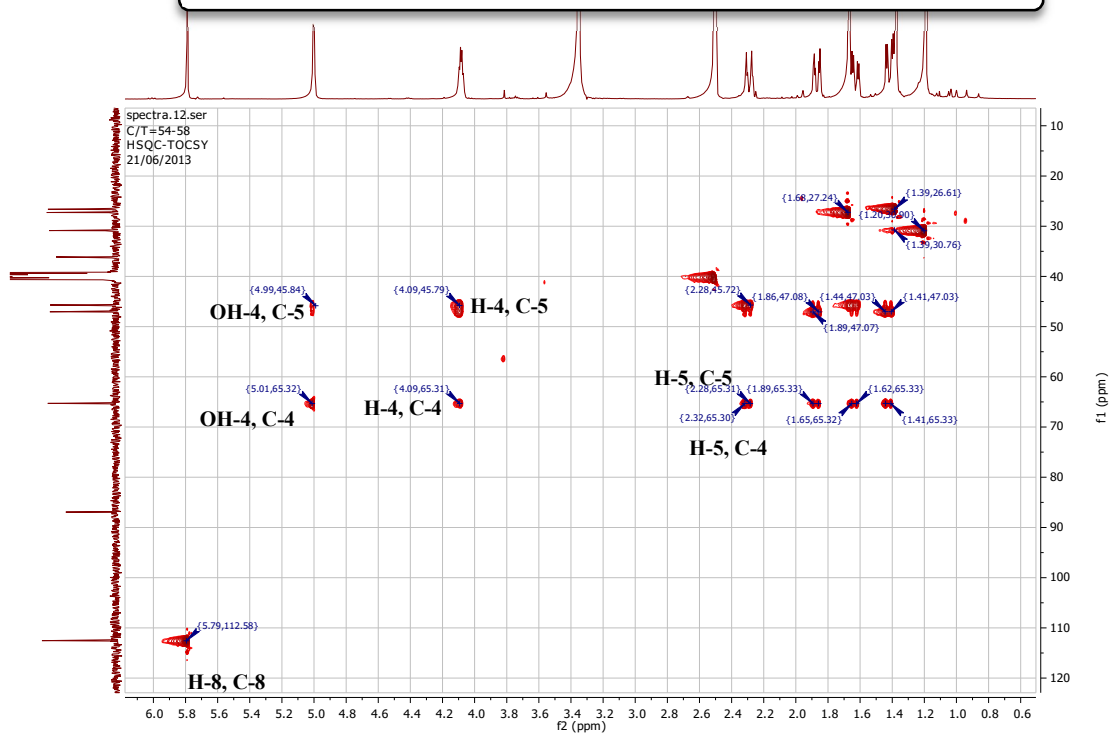


Figure II.1. 31. HSQC-TOCSY Spectrum of compound CVT1

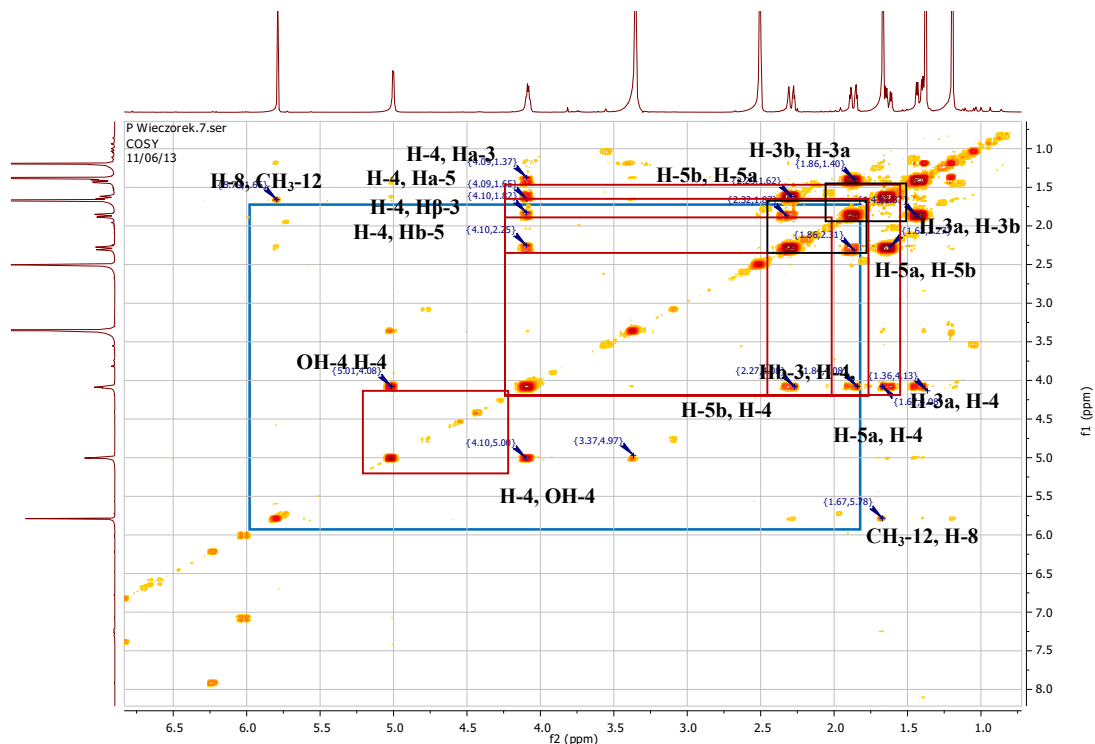


Figure II.1. 32.  $^1\text{H}$ - $^1\text{H}$  COSY Spectrum of compound CVT1

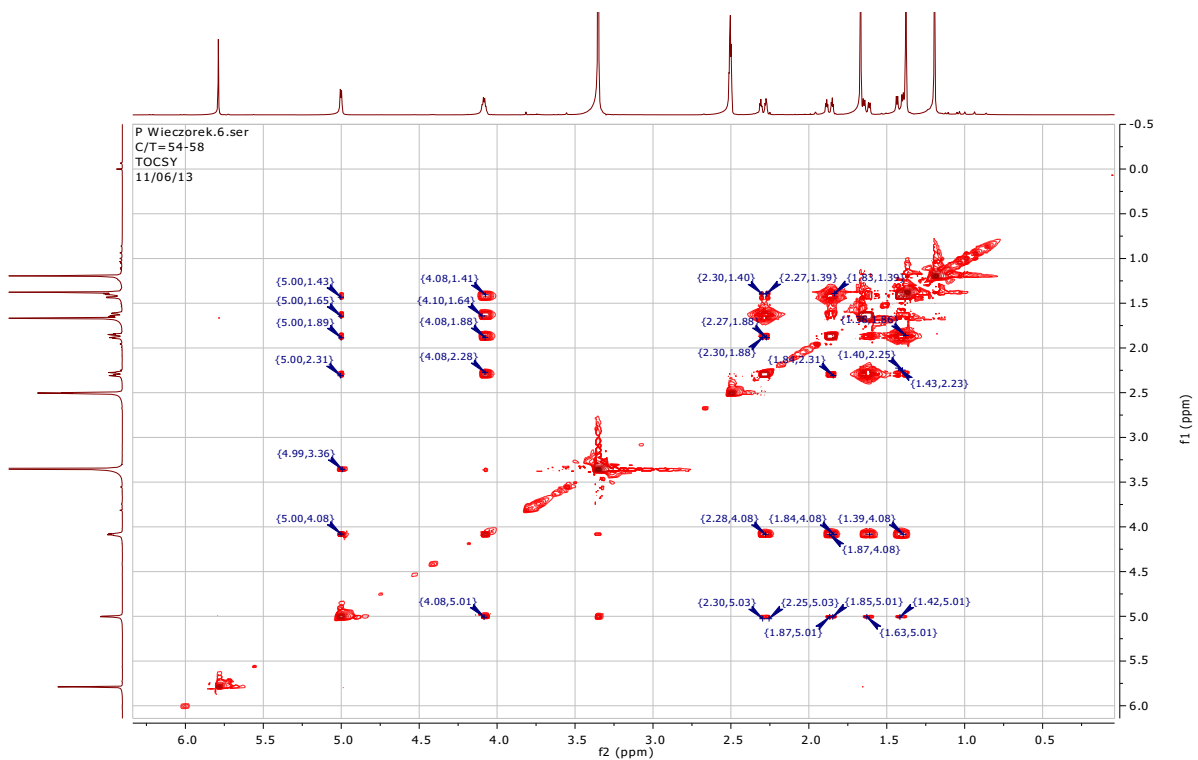
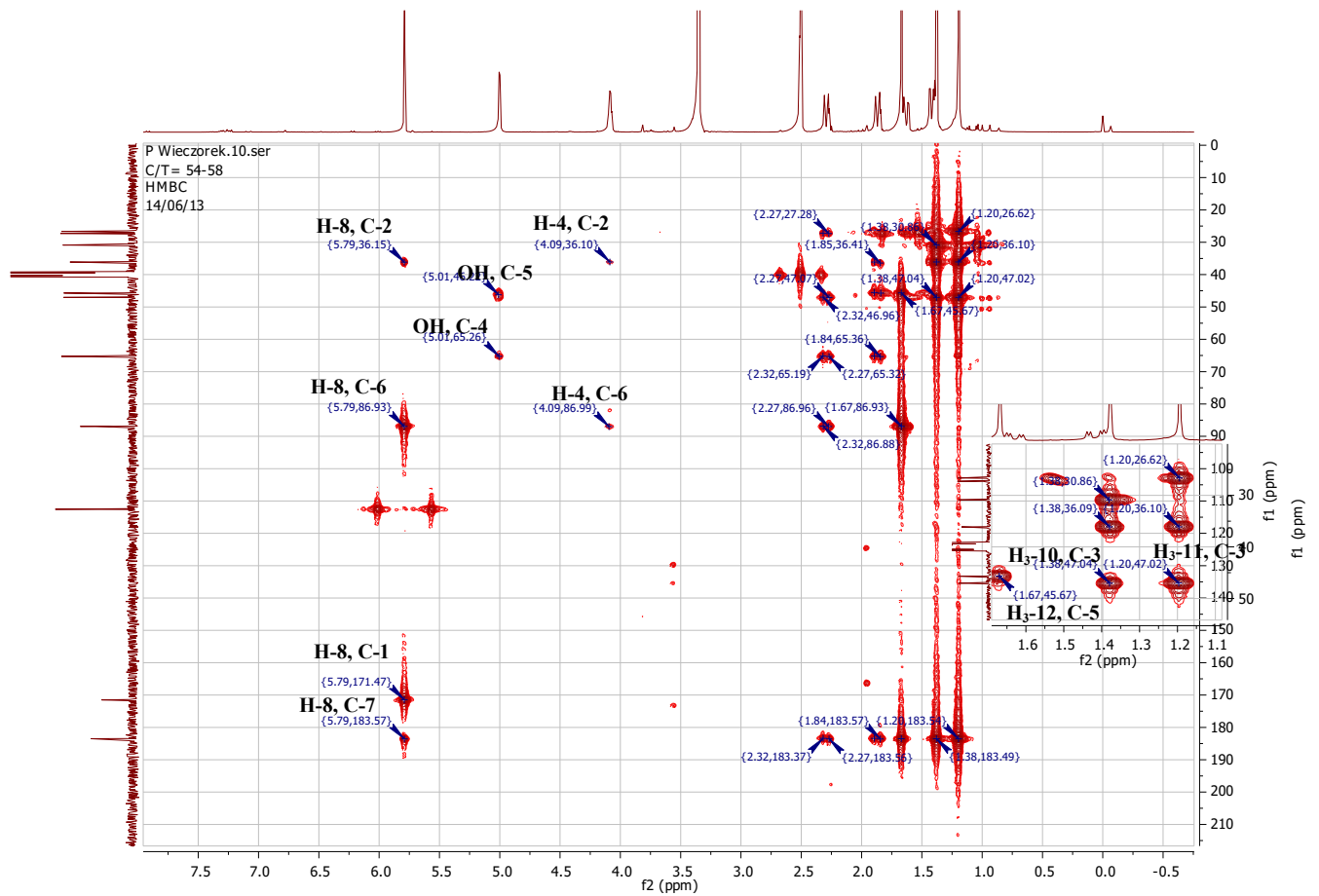


Figure II.1. 33. TOCSY Spectrum of compound CVT1



### II.1.4.3. ISOFLAVONOIDS

#### II.1.4.3.1. Compound CVS1

##### i. Physical properties:

Compound CVS1 (2 mg) was obtained as a yellow amorphous powder,  $[\alpha]_D^{20} -24$  (c 0.05, MeOH).

##### ii. Chromatographic characters

Compound CVS1 appeared as a dark purple spot under UV  $\lambda_{\max}$  254 which attained a pinkish color after spraying with 10% v/v vanillin/H<sub>2</sub>SO<sub>4</sub> and heating at 110 °C (Figure II.1.35). It showed  $R_f$  value of 0.68 in system IV (Page 48).

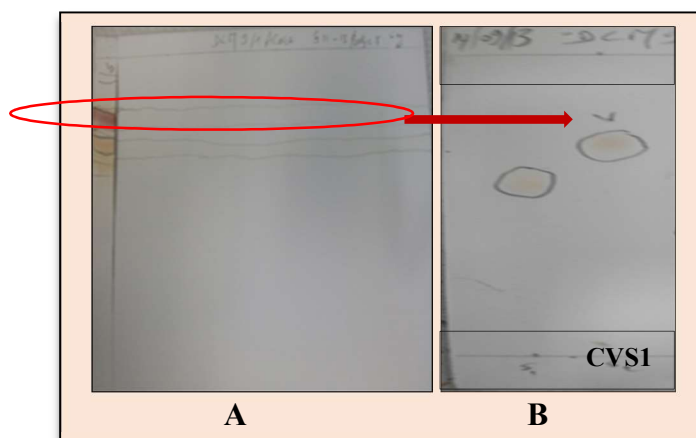


**Figure II.1. 35.**Profiles of silica gel TLC of compound CVS1:

A. before purification, B. After purification

##### iii. Spectroscopic data

**A. UV (MeOH)  $\lambda_{\max}$  nm (log  $\epsilon$ ):** 201.0 (4.29), 310.0 (3.17).

**B. HR-ESI-MS:** m/z 313.0734[M-H<sub>2</sub>O-H]<sup>-</sup> (calcd. 313.0712) for formula C<sub>17</sub>H<sub>16</sub>O<sub>7</sub>

##### **C. <sup>1</sup>H-, <sup>13</sup>C-NMR and HMBC spectral analysis**

The <sup>1</sup>H-, <sup>13</sup>C-NMR and HMBC spectral data of compound CVS1 are listed in table II.1.5 and illustrated in figures thereafter.



**Table II.1. 5.** <sup>1</sup>H NMR and <sup>13</sup>C NMR spectroscopic data of compound **CVS1** (400 MHz, 100 MHz, DMSO-*d*<sub>6</sub>, *J* in Hz,  $\delta$  in ppm)

Position	$\delta_H$ (ppm), multiplicity, <i>J</i> (Hz)	$\delta_C$ (ppm)	HMBC(H→C)	TOCSY	HSQC-TOCSY
2	H-2a, 3.59, d, 3.1, 1H, H-2b, 4.30, m, 1H	66.4	C-3, 4 C-4, C-2'	H <sub>b</sub> -2, H-4 H <sub>a</sub> -2, H-4	C-2, 3, 4 C-2, 3, 4
3	350, m, 1H	40.0	C-2, C-10, C-2'	H <sub>b</sub> -2, H-4	C-2, 3, 4
4	5.52, d, 6.8, 1H	78.5	C-2, C-1', C-2', C-6'	H <sub>a</sub> -2, H <sub>b</sub> -2	C-2, 3, 4
5	6.98, s, 1H	105.8	C-4, C-6, C-7, C-9	-	C-8
6	-	141.5	-	-	-
7	-	147.9	-	-	-
8	6.52, s, 1H	93.6	C-6, C-7, C-9, C-10	-	C-5
9	-	154.1	-	-	-
10	-	118.8	-	-	-
1'	-	113.0	-	-	-
2'	-	149.9	-	-	-
3'	-	136.0	-	-	-
4'	-	151.4	-	-	-
5'	6.55, d, 8.0, 1H	110.3	C-1', 2', 4'	H-6'	C-5', C-6'
6'	7.00, d, 8.0, 1H	126.0	C-4, C-2', C-4'	H-5'	C-6', C-5'
3'-OCH <sub>3</sub>	3.65, s, 3H	60.6	C-3'	-	-O-CH <sub>3</sub>
-O-CH <sub>2</sub> -O-	5.93, d, 8.0, 2H	101.5	C-6, C-7	-	-OCH <sub>2</sub> O-
OH-4'	9.36, br s, 1H	151.4	3', 4', 5'	-	-

#### iv. Discussion and conclusion:

Compound **CVS1** was isolated as a white amorphous solid which gave a HRESIMS mass molecular ion peak at *m/z* 313.0734[M-H<sub>2</sub>O-H]<sup>-</sup> (Calcd. for 313.0712) suggesting the molecular formula of C<sub>17</sub>H<sub>16</sub>O<sub>7</sub> (FigureII.1.39).

The UV spectrum of **CVS1** showed absorption maxima at 208.0 nm (Band II) and 310.0 nm suggesting flavonoid skeleton (Mabry et al., 1970b) (Band I).

The <sup>13</sup>C-NMR (FigureII.1.42) showed 17 carbon signals, identified by DEPT

(Figure II.1.43) as a methylene carbon at  $\delta_C = 66.4$ , one methylenedioxy group at  $\delta_C = 101.5$  ppm, two methine carbon atoms at  $\delta_C = 40.0$  and  $78.5$  ppm, one methoxy group at  $\delta_C = 60.6$  ppm, and four aromatic methine carbons at  $\delta_C = 93.6$ ,  $105.8$ ,  $110.3$  and  $126.0$  ppm (Figure II.44).

The  $^1\text{H-NMR}$  spectrum (Figures II.1.40-41) showed a pair of one-proton, a multiplet at  $\delta_H = 4.32$  ppm and a doublet at  $\delta_H = 3.59$  ppm ( $J = 3.1$  Hz), a multiplet at  $\delta_H = 3.56$  ppm and a doublet at  $\delta_H = 5.52$  ppm ( $J = 6.8$  Hz). These signals were assignable to two H-2 protons, H-3 and H-4 protons, respectively of a 4-hydroxyisoflavan skeleton (Bojase et al., 2001).

The  $^1\text{H}$  and  $^{13}\text{C-NMR}$  spectra of compound **CVS1** showed the presence of a singlet at  $\delta_H = 3.65$  ppm corresponded to  $\delta_C = 60.6$  ppm in **HSQC** (Figure II.45), its correlated with C-3' in **HMBC** suggested methoxy substitution at this position.

The **TOCSY** spectrum (Figure II.1.46) indicated the presence of a cross peak between H-2a and H-2b and H-4 and between H-3 and H-2 and H-4. The corresponding carbons were identified by **HSQC** as, a methylene carbon at  $\delta_C = 66.4$  ppm and two methine carbon atoms at  $\delta_C = 40.0$  and  $78.5$  ppm respectively.

In the  $^1\text{H-NMR}$  further signals were observed which showed the presence of ortho-coupled aromatic doublets at ( $\delta_H$  6.55 and 7.00, each  $J=8.0$  Hz), and a set of one proton aromatic singlets at  $\delta_H = 6.52$  and  $6.98$  ppm. A two protons signal was observed at ( $\delta_H$  5.93, 2H,  $d$ ,  $J=8.0$  Hz) are assigned as one methylenedioxy group Its corresponding carbon was identified by **HSQC** which resonates at  $\delta_C = 101.6$  ppm.

The H-5 proton ( $\delta_H$  6.98) showed **HMBC** correlations with C-6 ( $\delta_C$  141.5), C-7 ( $\delta_C$  147.9), C-9 ( $\delta_C$  154.1) and C-4 ( $\delta_C$  78.5) (Figures II.1.48-49).

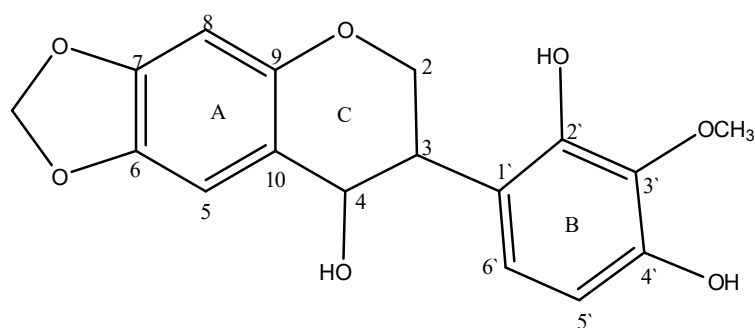
The H-8 proton ( $\delta_H$  6.52) showed **HMBC** correlations with C-6 ( $\delta_C$  141.5), C-7 ( $\delta_C$  147.9), C-9 ( $\delta_C$  154.1) and C-10 ( $\delta_C$  118.8).

The methylene-dioxy protons ( $\delta_H$  5.93) showed **HMBC** correlations with C-6 ( $\delta_C$  141.5) and C-7 ( $\delta_C$  147.9). Hence, the A-ring was shown to have a 6,7 methylene-dioxy substitution.

The H-4 proton ( $\delta_H$  5.52) displayed key **HMBC** correlations which showed connectivity with C-2 ( $\delta_C$  66.4) [correlation with C-ring], C-1' ( $\delta_C$  113), and C-6' ( $\delta_C$  126) [correlations with B-ring], while H-5 proton ( $\delta_H$  6.98) showed **HMBC** correlation with C-4 ( $\delta_C$  78.5) [correlations with A-ring].

Moreover, H-2 protons ( $\delta_H$  3.59 and 4.30) showed HMBC correlations with C-2', C-3 and C-4 while H-3 proton ( $\delta_H$  3.56) showed HMBC correlation with C-10, and H-5 proton ( $\delta_H$  6.98) showed HMBC correlation with C-4, which further confirming linkage of the three rings A, B and C.

The methyl group at  $\delta_H = 3.65$  ppm showed HMBC correlations with C-3' ( $\delta_C$  136.0) (Figure II.1.48). Thus the substitution in the B-ring was determined to be 2',4'-dihydroxy, 3'-methoxy. Consequently, structure **CVS1** was determined to be **2',4'-dihydroxy-3'-methoxy-6,7-methylenedioxyisoflavan-4-ol**.



Structure of compound CVS1

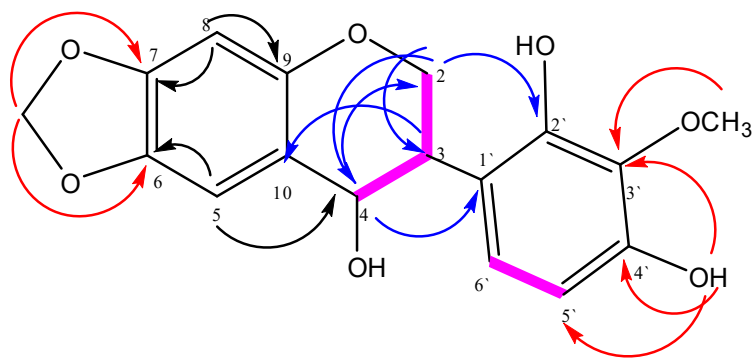


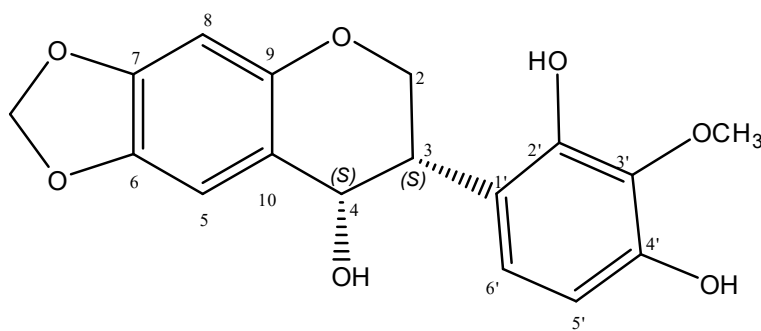
**Figure II.1. 36.** Important HMBC (H→C) and TOCSY ( ) correlations of the compound CVS1

#### - Determination of the absolute configuration

The new compound **CVS1** possess two stereogenic centers (C-3, C-4) and was optically active ( $[\alpha]_{D}^{25} = -24$ ). Circular dichroism spectra were taken to determine the absolute

configuration at carbons C-3 and C-4 in the molecule.

The calculated and experimental ECD spectra were compared for all possible stereoisomers. The (*S, S*) isomer showed perfect fit with a negative cotton effect at ~200 nm (Figure II.1.38). Only 34 conformers were obtained for the (*S, S*) and 12 of them contributed more than 90% in the Boltzmann distribution. The intraligand hydrogen bonds play significant role in ligand stabilization (Figure II.1.37).



**Stereochemistry of compound CVS1:**

**(3*S*, 4*S*)-2',4'-dihydroxy-3'-methoxy-6,7-methylenedioxyisoflavan-4-ol**

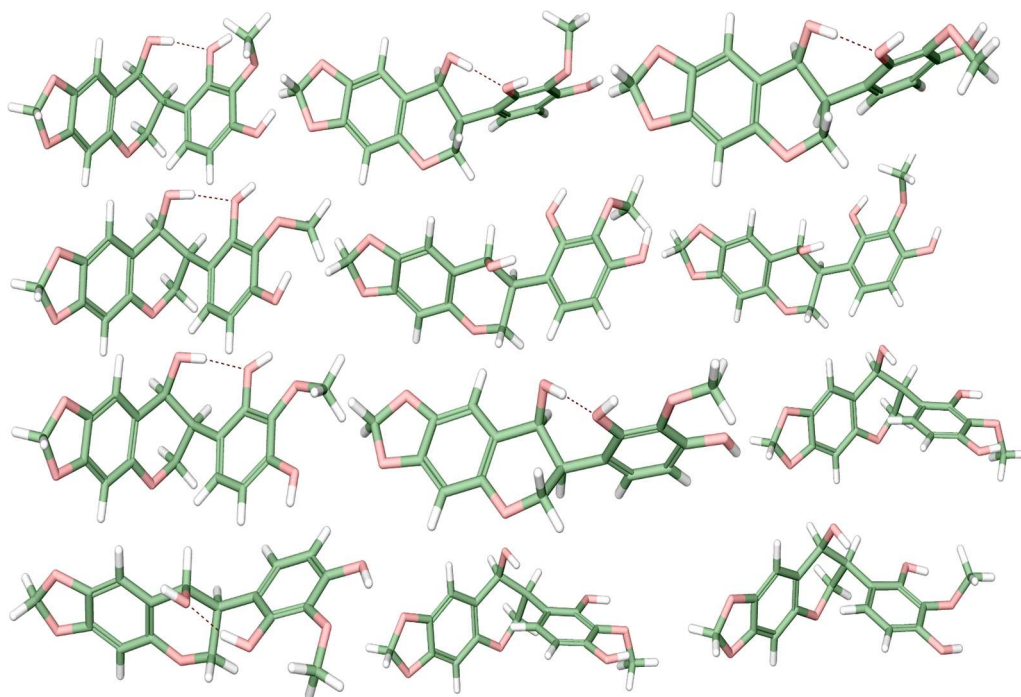


**Figure II.1. 37.** The most abundant conformers of the (*S, S*) isomer of compound CVS1. Hydrogen bonds are shown as dotted lines.

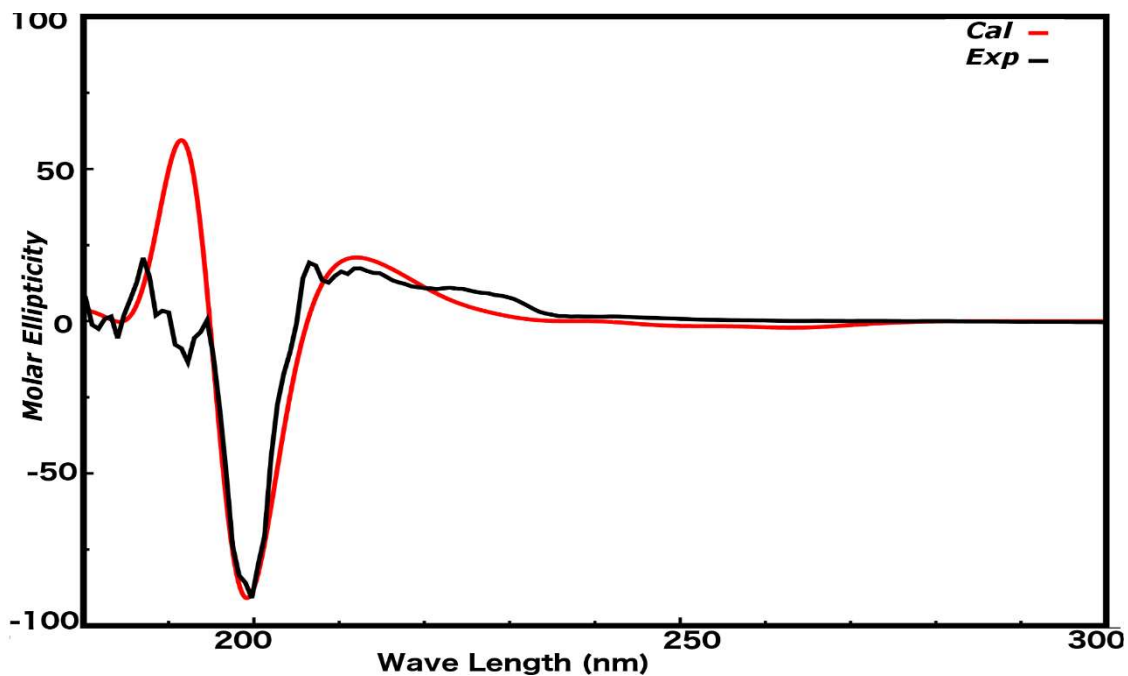


Figure II.1. 38. The calculated and experimental ECD of compound CVS1

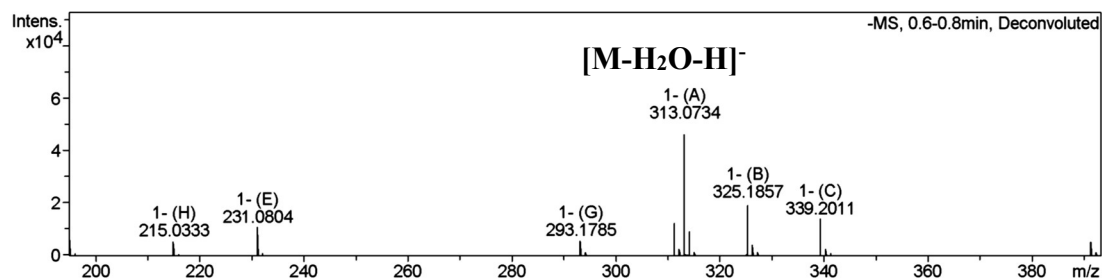


Figure II.1. 39. Negative HR-ESI-MS-TOF of compound CVS1

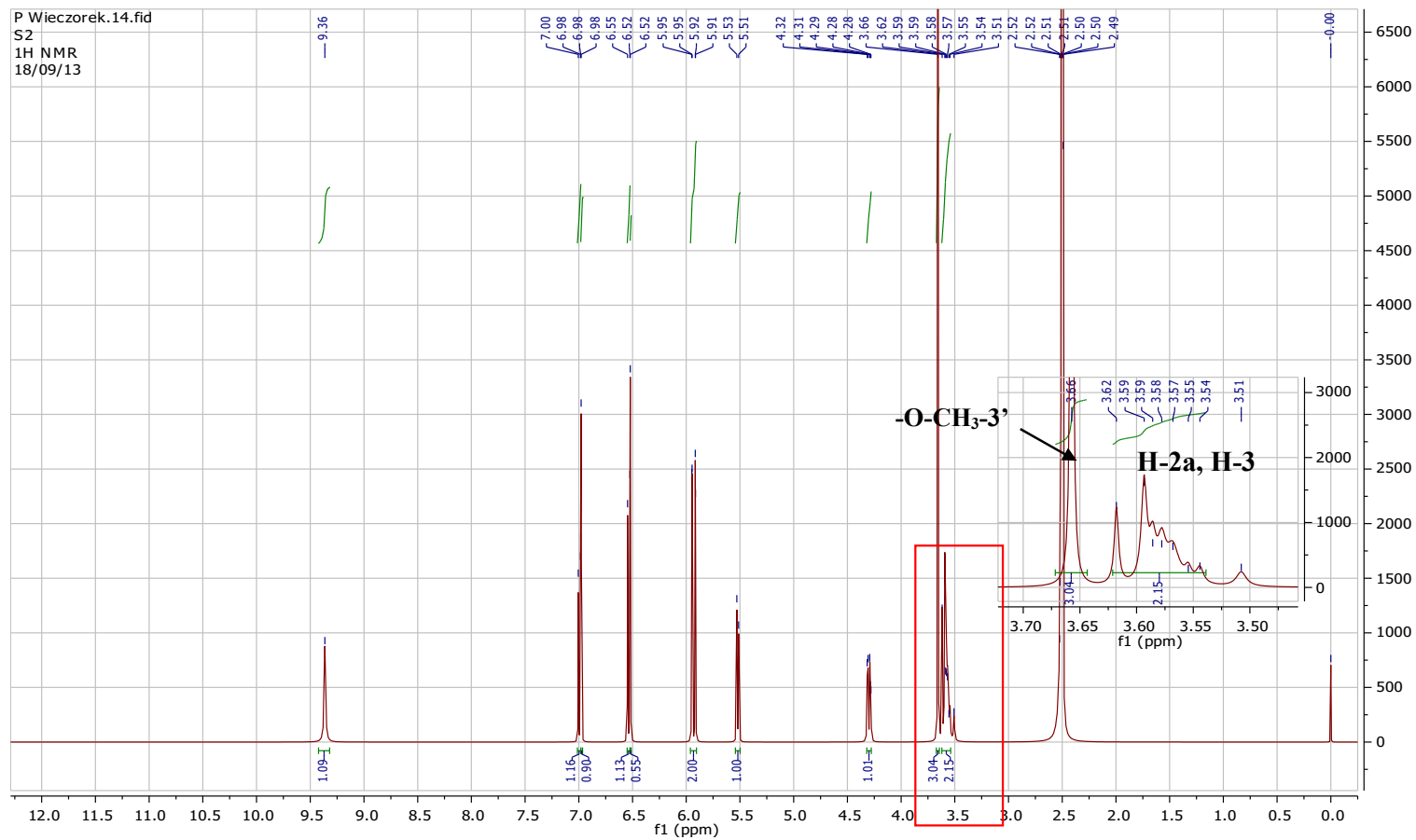
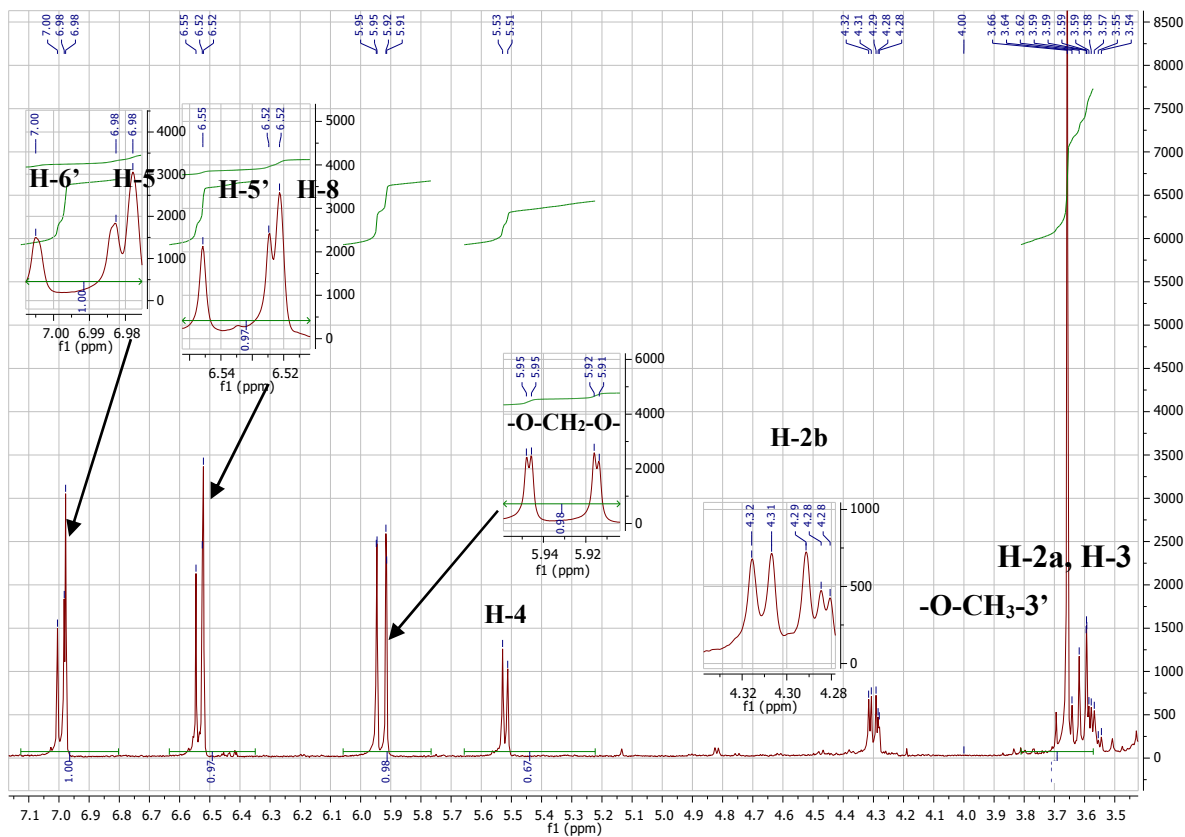
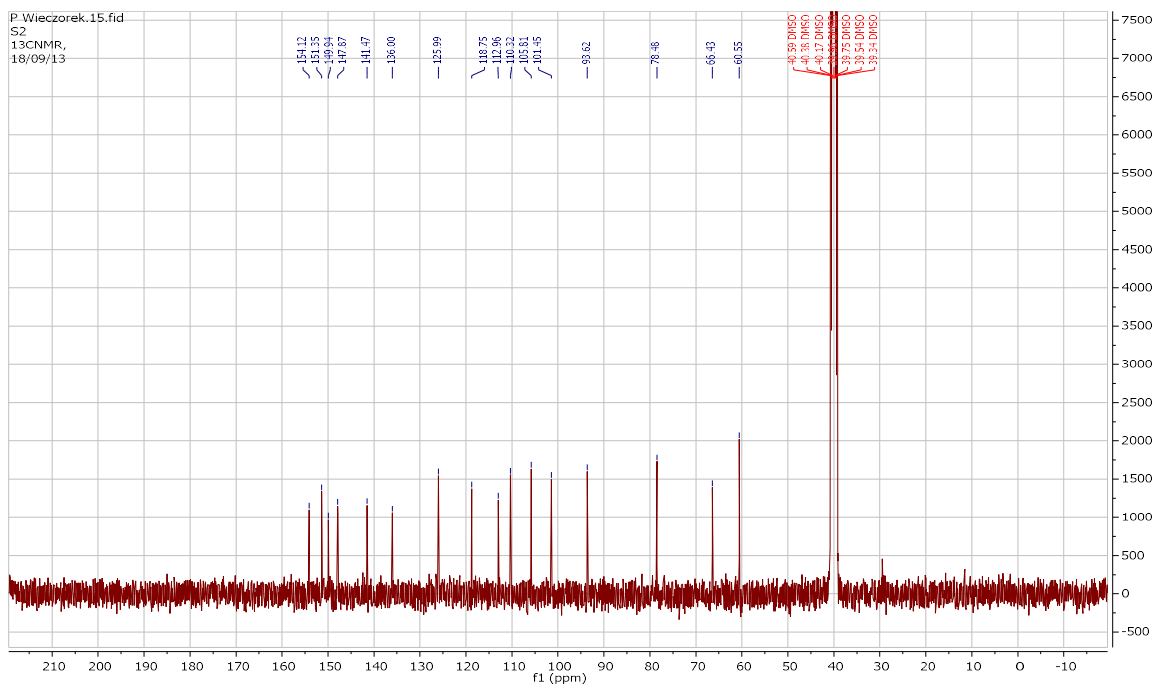


Figure II.1. 40. <sup>1</sup>H-NMR Spectrum of compound CVS1  
(DMSO-*d*<sub>6</sub>, 400 MHz)



**Figure II.1. 41.** Expanded  $^1\text{H-NMR}$  Spectrum of compound CVS1 (DMSO- $d_6$ , 400 MHz)



**Figure II.1. 42.**  $^{13}\text{C-NMR}$  Spectrum of compound CVS1 (DMSO- $d_6$ , 100 MHz)

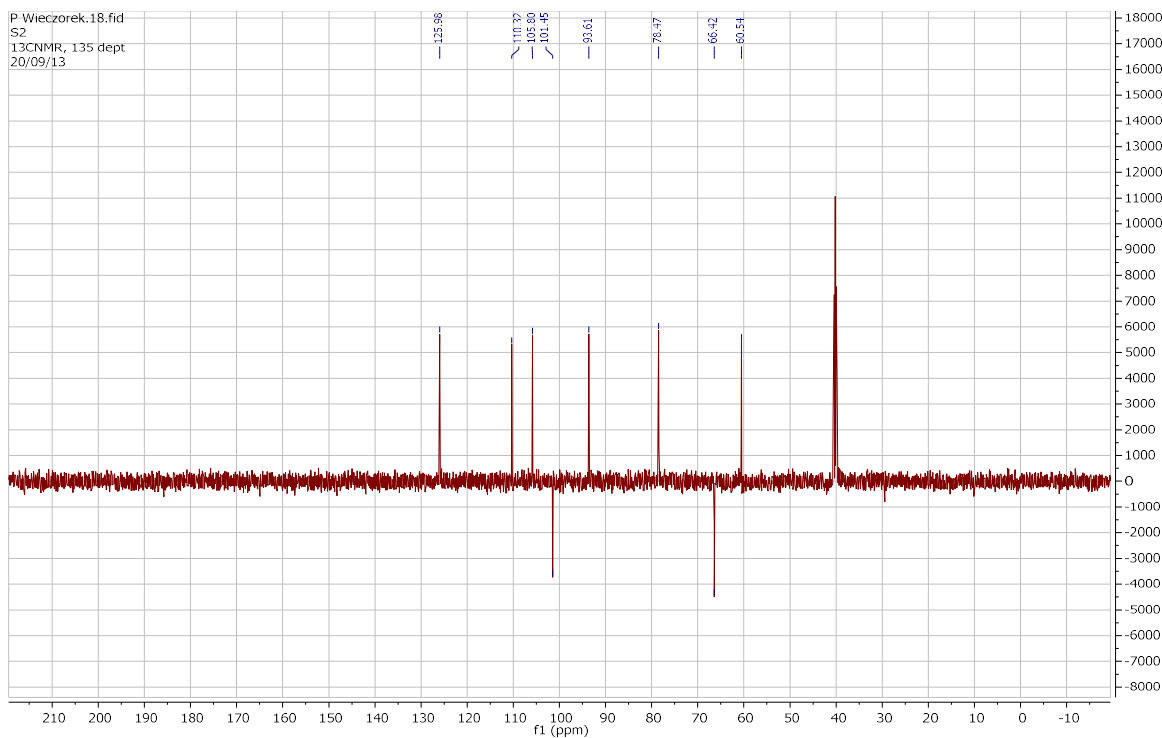


Figure II.1. 43. DEPT-135 Spectrum of compound CVS1

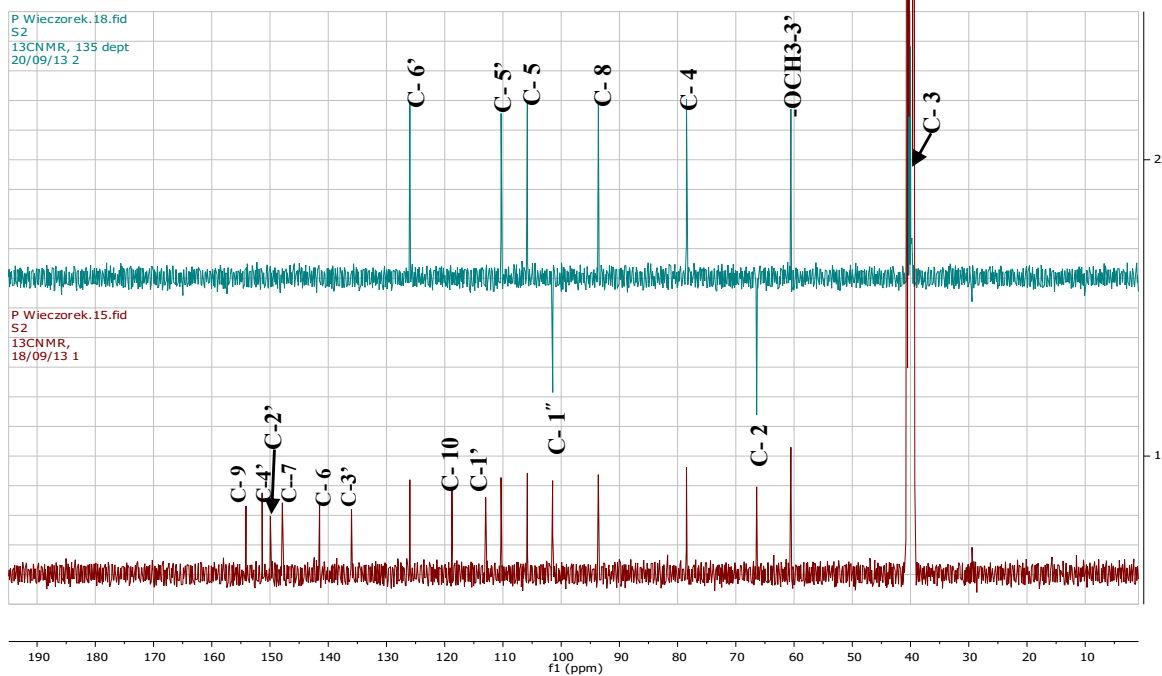


Figure II.1. 44. Comparison of  $^{13}\text{C}$ -NMR and DEPT-135 Spectra of compound CVS1



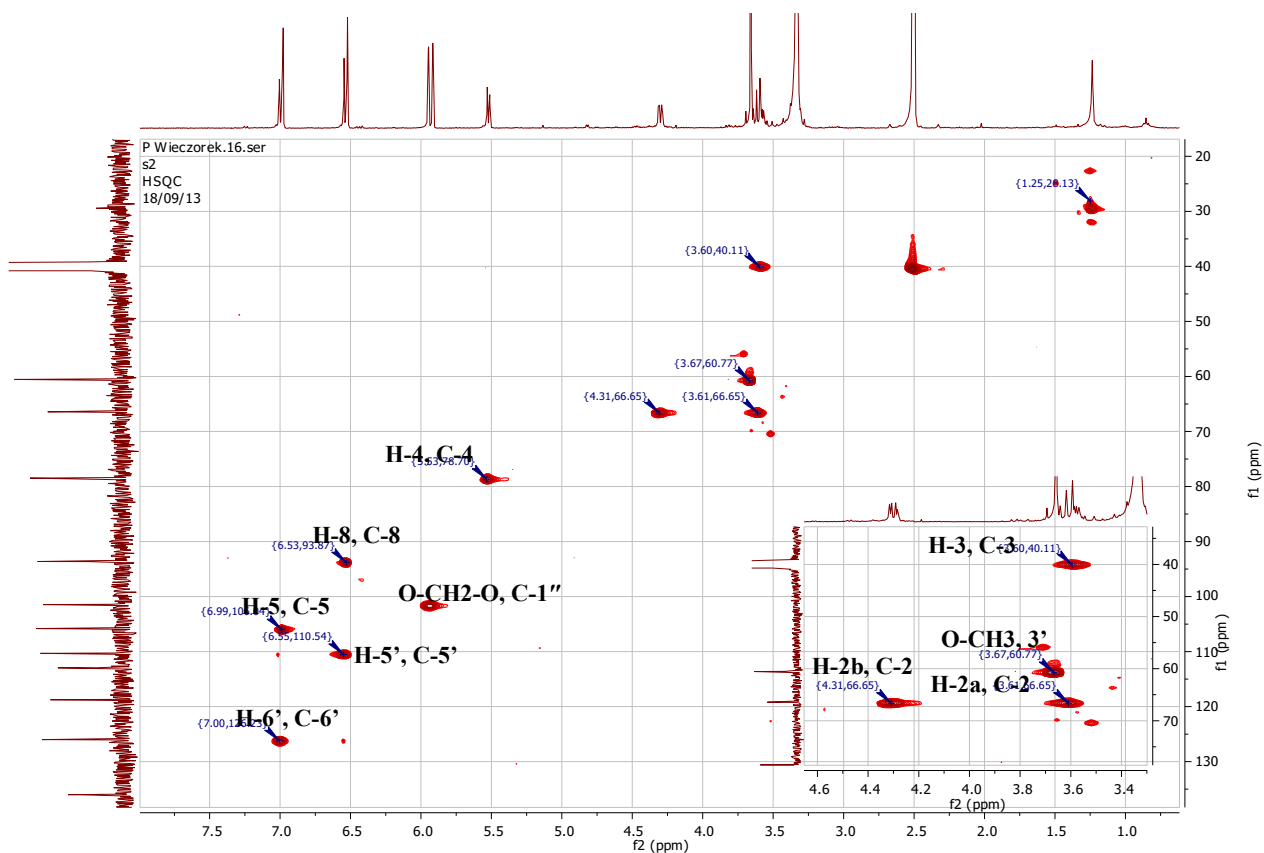


Figure II.1. 45. HSQC Spectrum of compound CVS1

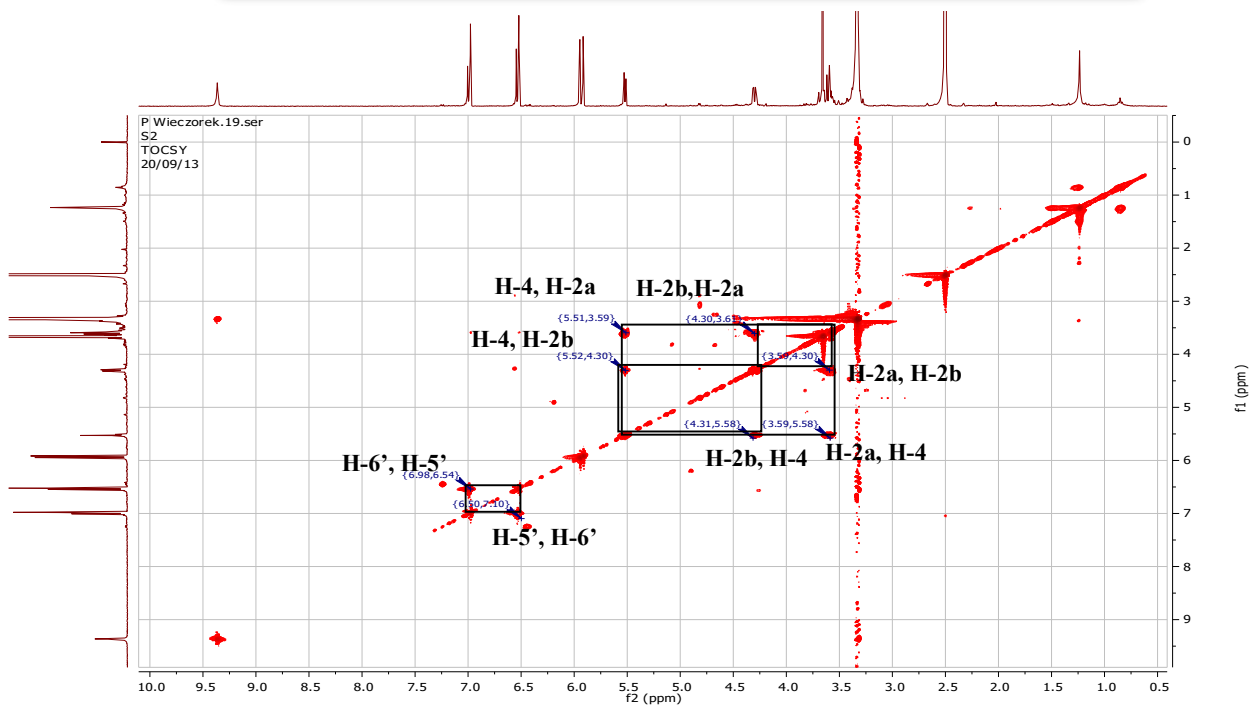
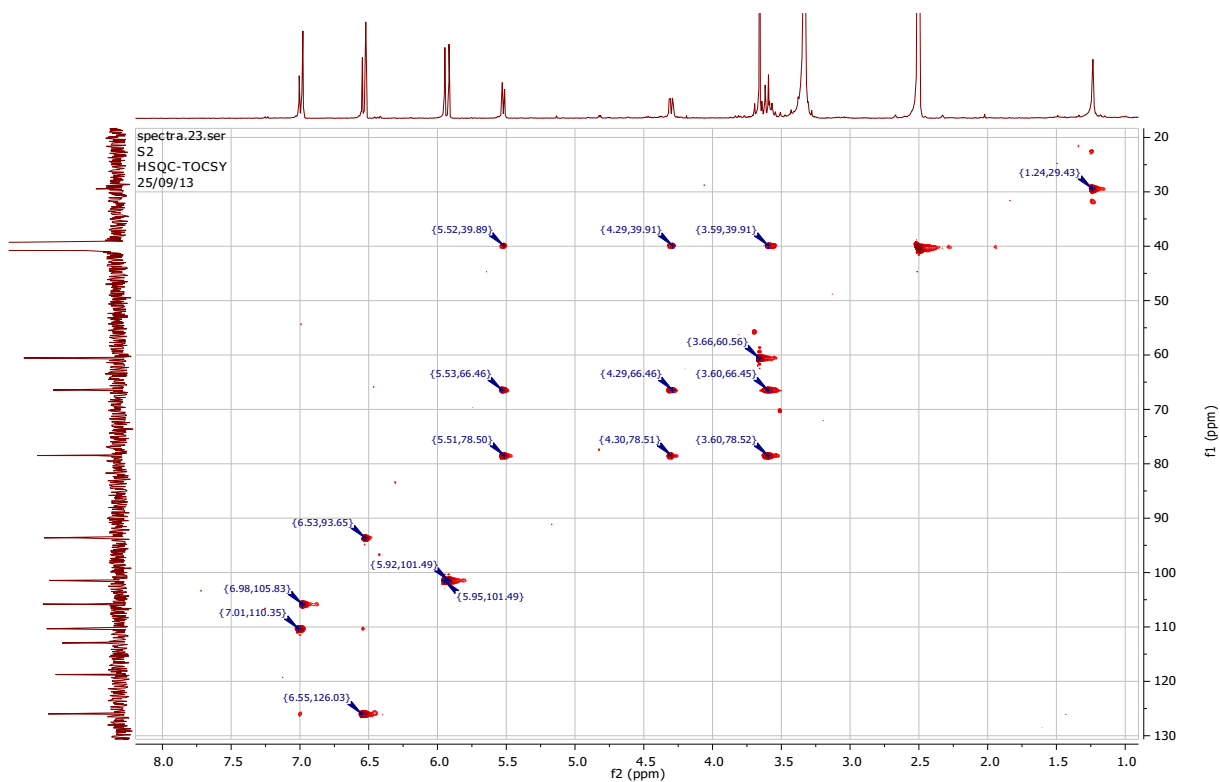
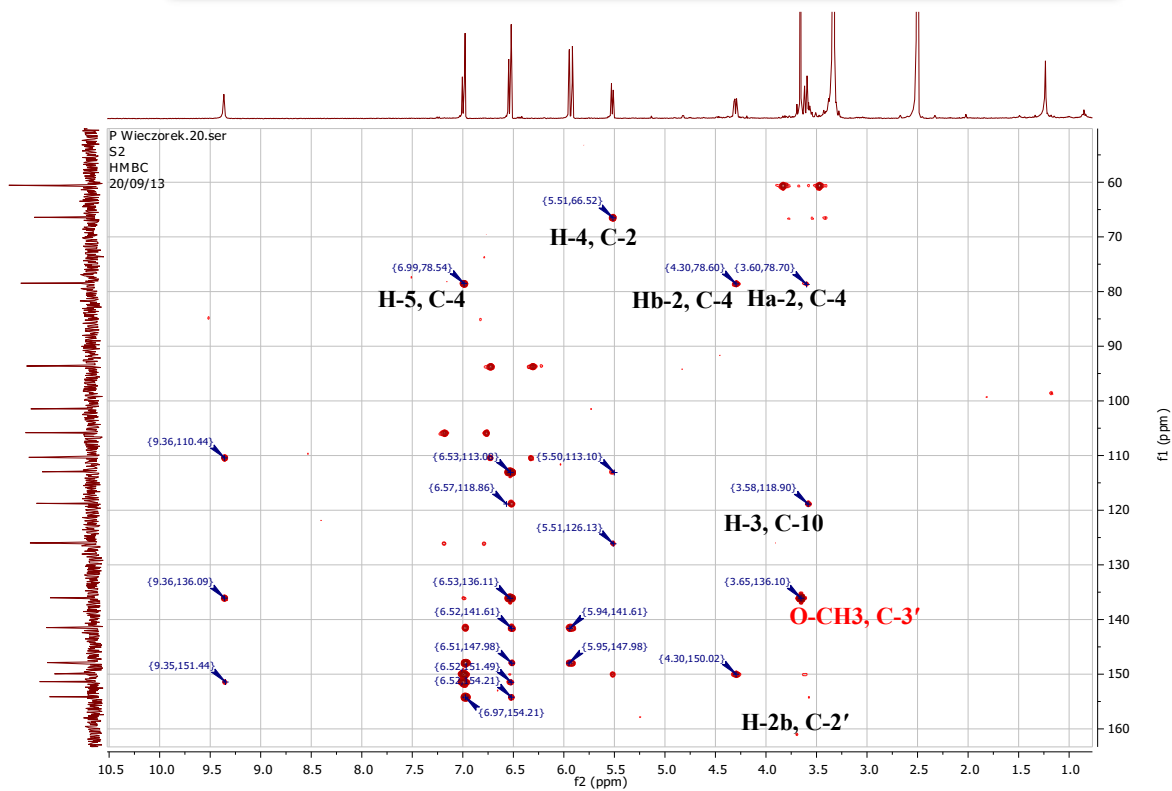


Figure II.1. 46. TOCSY Spectrum of compound CVS1



**Figure II.1. 47. HSQC-TOCSY Spectrum of compound CVS1**



**Figure II.1. 48. HMBC Spectrum of compound CVS1**

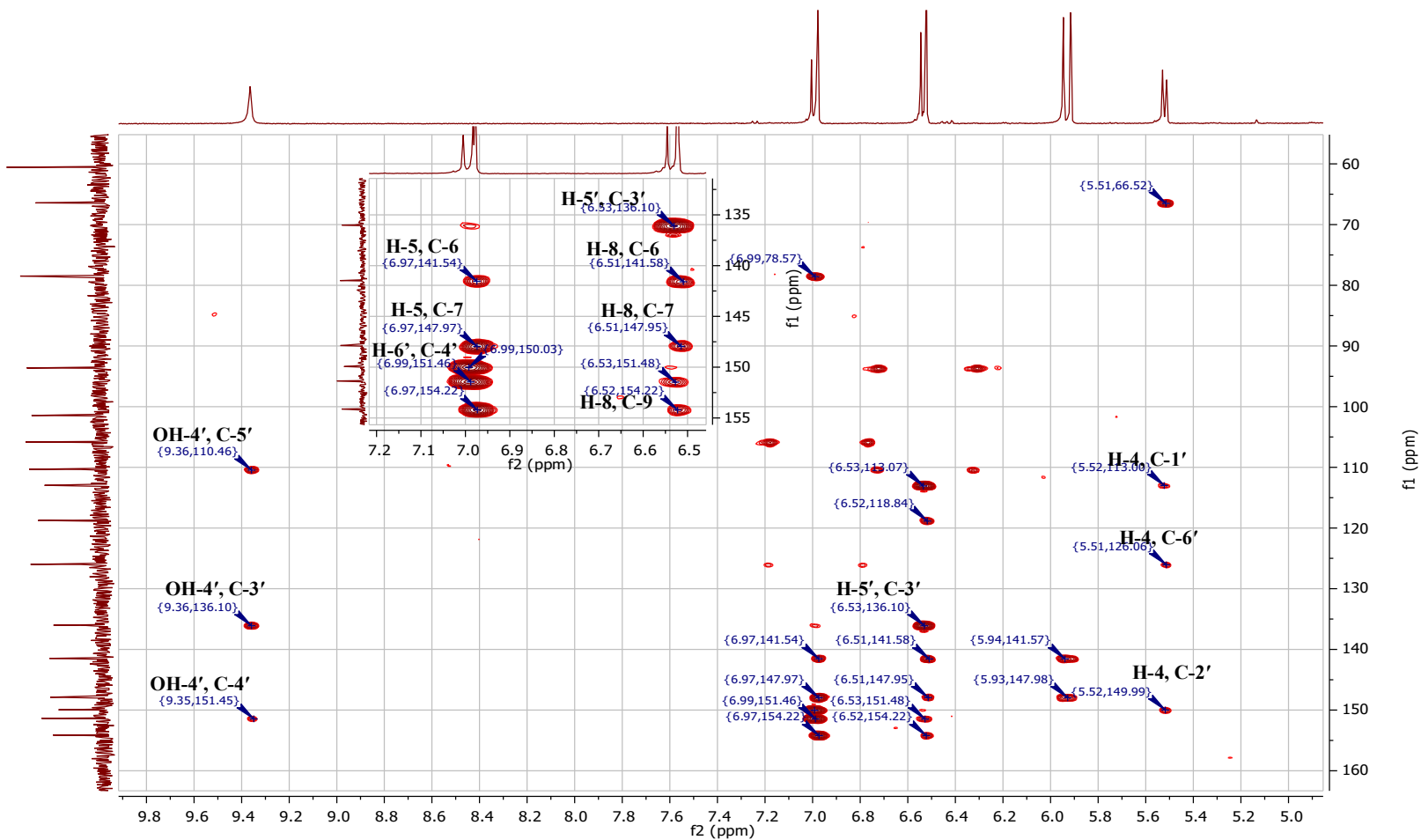


Figure II.1. 49. Expanded HMBC Spectrum of Compound CVS1

### II.1.4.3.2. Compound CVS2

#### i. Physical properties

Compound CVS2 (5 mg) was obtained as colorless needle crystals.

#### ii. Chromatographic characters

Compound CVS2 appeared as a dark spot under UV  $\lambda_{\max}$  254 which attained a yellowish color after spraying with 10% v/v vanillin/H<sub>2</sub>SO<sub>4</sub> and heating at 110 °C. It showed  $R_f$  value of 0.62 in system IIV(Page48).

#### iii. Spectroscopic data

A. UV (MeOH) :  $\lambda_{\max}$  (log  $\epsilon$ ) : 260.1(4.074)

B. ESI-MS,  $m/z$  269.036 [M-H]<sup>-</sup> (calcd. 269.042) for formula C<sub>15</sub>H<sub>10</sub>O<sub>5</sub>

#### C. <sup>1</sup>H-NMR and HMBC spectral analysis

<sup>1</sup>H-, <sup>13</sup>C-NMR and HMBC spectral data of compound CVS2 are listed in table II.1.6 and illustrated in figures thereafter.

**Table II.1. 6.** <sup>1</sup>H-, <sup>13</sup>C-NMR and HMBC spectral data of compound CVS2 (400 MHz, 100MHz, Methanol-*d*<sub>4</sub>).

Position	$\delta_H$ (ppm), multiplicity, J (Hz)	$\delta_C$ (ppm)	HMBC (H→C)
2	8.06, s, 1H	153.4	C-3,4, 1'
3	-	123.3	-
4	-	179.4	
5	-	162.4	
6	6.23, d, J = 2.1 Hz, 1H	98.7	C-5, 8, 10
7	-	164.7	-
8	6.34, d, J = 2.1 Hz, 1H	93.4	C-10, C-7, C-6
9	-	156.7	-
10	-	104.5	-
1'		121.9	
2',6'	7.38, d, J = 8.2 Hz, 2H	130.0	C-3, 1', 3', 4', 5'
3',5'	6.85, d, J = 8.2 Hz, 2H	114,8	1', 4'
4'	-	158.3	-

#### iv. Discussion and Conclusion

Compound **CVS2** (5 mg) was obtained as colorless needle crystals and its molecular formula was established as  $C_{15}H_{10}O_5$  from its Negative HRESIMS spectral data (Figure II.1.51) which showed ion peak at  $m/z$  269.036  $[M-H]^-$  (calcd.269.042).

The UV spectrum of **CVS2** also showed absorption maxima at 260.1 nm (Band II) suggested an isoflavonoid structure (Chaturvedula and Prakash, 2013) .

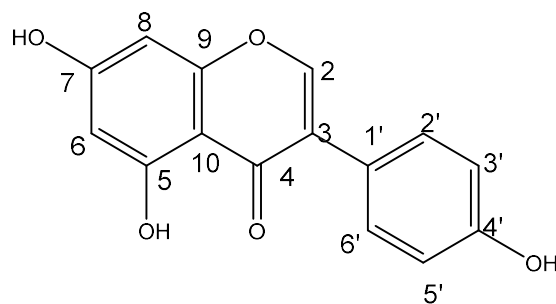
$^1H$ -NMR spectrum of **CVS2** (Figure II.1.52) showed the presence of two meta coupled aromatic protons at 6.23 and 6.34 corresponds to H-6 and H-8 protons. Two doublet at 6.85 and 7.38 for H- 3'/H-5' and H-2'/H-6' protons of ring B (Figure); characteristic for the 4', 5,7-trisubstituted isoflavone.

$^{13}C$ -NMR and DEPT spectra (FiguresII.1.53-54) confirm precedent analysis. The  $^{13}C$ -NMR spectrum shows presence of signals at  $\delta_C = 164,7$  ppm (C-7),  $\delta_C = 123,3$  ppm (C-3),  $\delta_C = 130.0$  ppm (C-2'; C-6'),  $\delta_C = 114,8$  ppm (C-3'; C-5') and  $\delta_C = 98,7$  ppm (C-6).

The  $^1H$ - and  $^{13}C$ -NMR values for all the carbons were assigned on the basis of HSQC and HMBC correlations (FiguresII.1.55-56).

A search in the literature suggested the assigned proton and carbon values were consistent with 4',5,7,-trihydroxyisoflavone, also known as genistein (Akiyama et al., 1987; Coward et al., 1993; Divi et al., 1997), previously reported in the genus of *Cytisus* (Hanganu et al., 2010) .

Genistein, an isoflavone isolated from soybean (Walter, 1941), found to be present in several used medicinal plants. Gensitein is largely studied because of its pharmacological activities. It have been reported to play an important role in breast cancer prevention (Lamartiniere et al., 1998).



**Structure of compound CVS2  
Genistein**

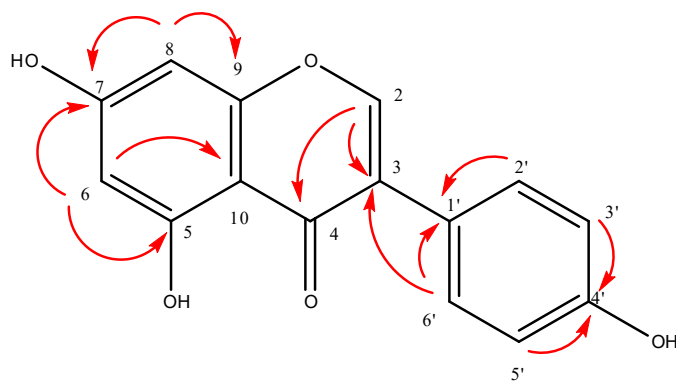


Figure II.1. 50. Important HMBC (H $\rightarrow$ C) correlations of the compound CVS2.

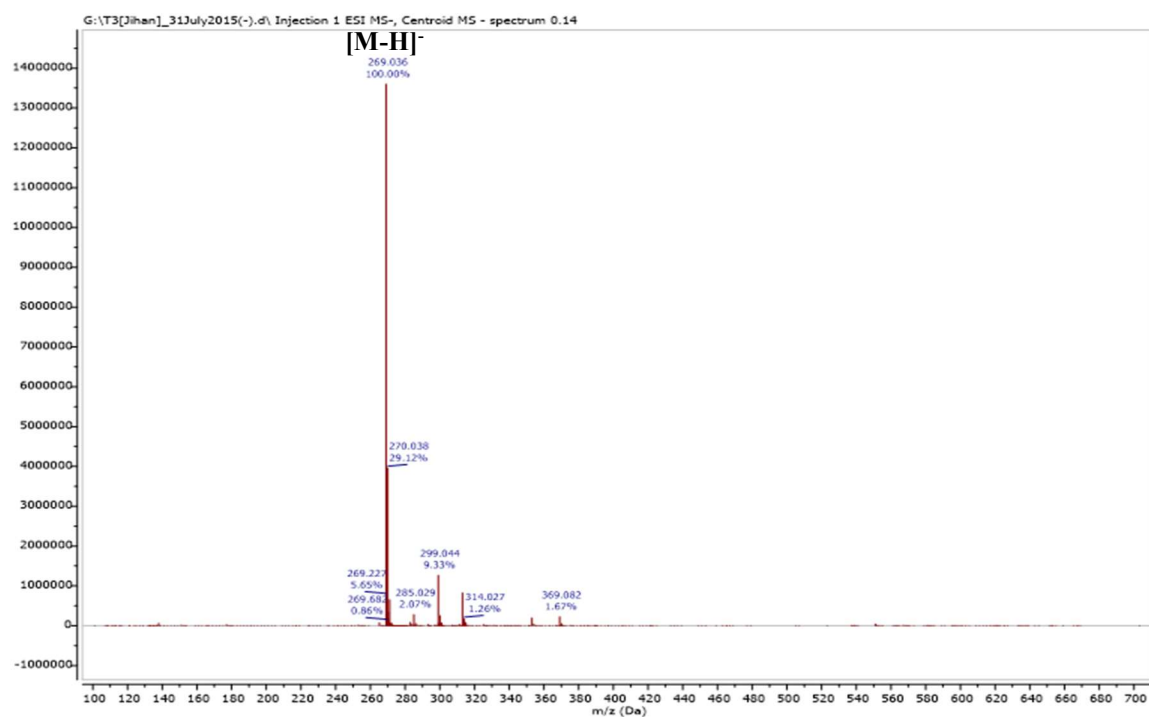


Figure II.1. 51. Negative HR-ESI-MS of compound CVS2.

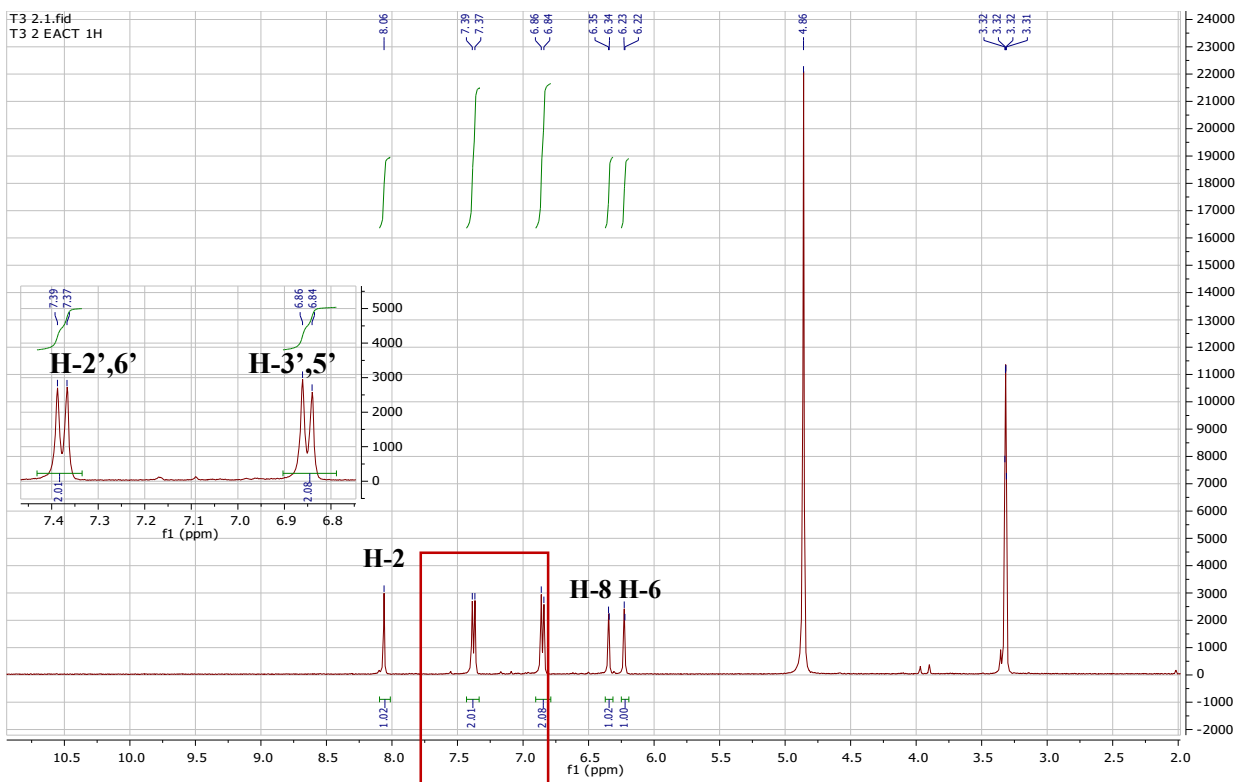


Figure II.1. 52. <sup>1</sup>H-NMR Spectrum of Compound CVS2 (Methanol-*d*<sub>4</sub>, 400 MHz)

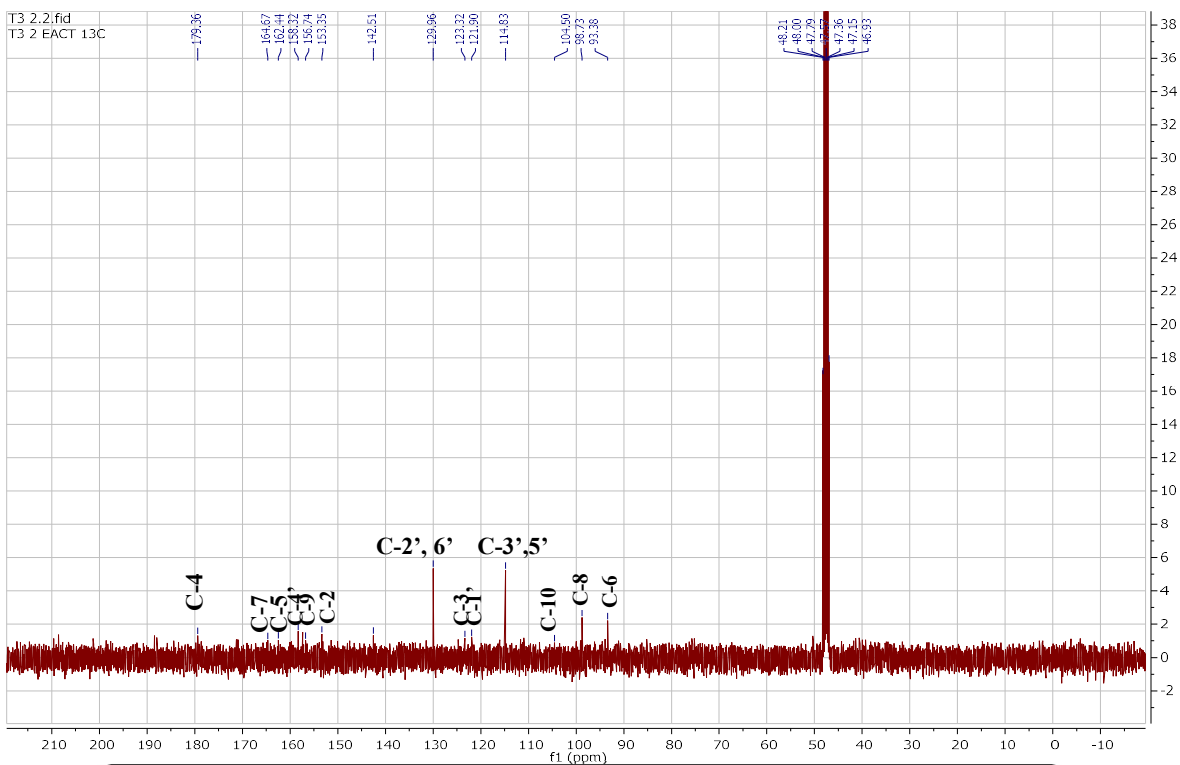


Figure II.1. 53. <sup>13</sup>C-NMR Spectrum of Compound CVS2 (Methanol-*d*<sub>4</sub>, 100 MHz)

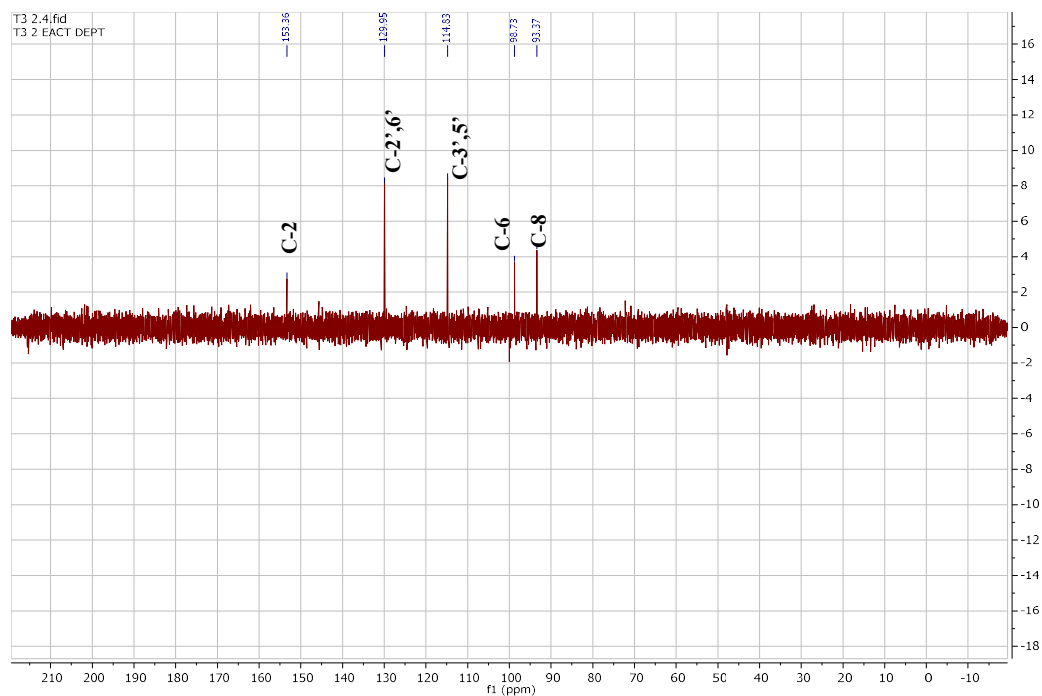


Figure II.1. 54. DEPT-135 Spectrum of Compound CVS2

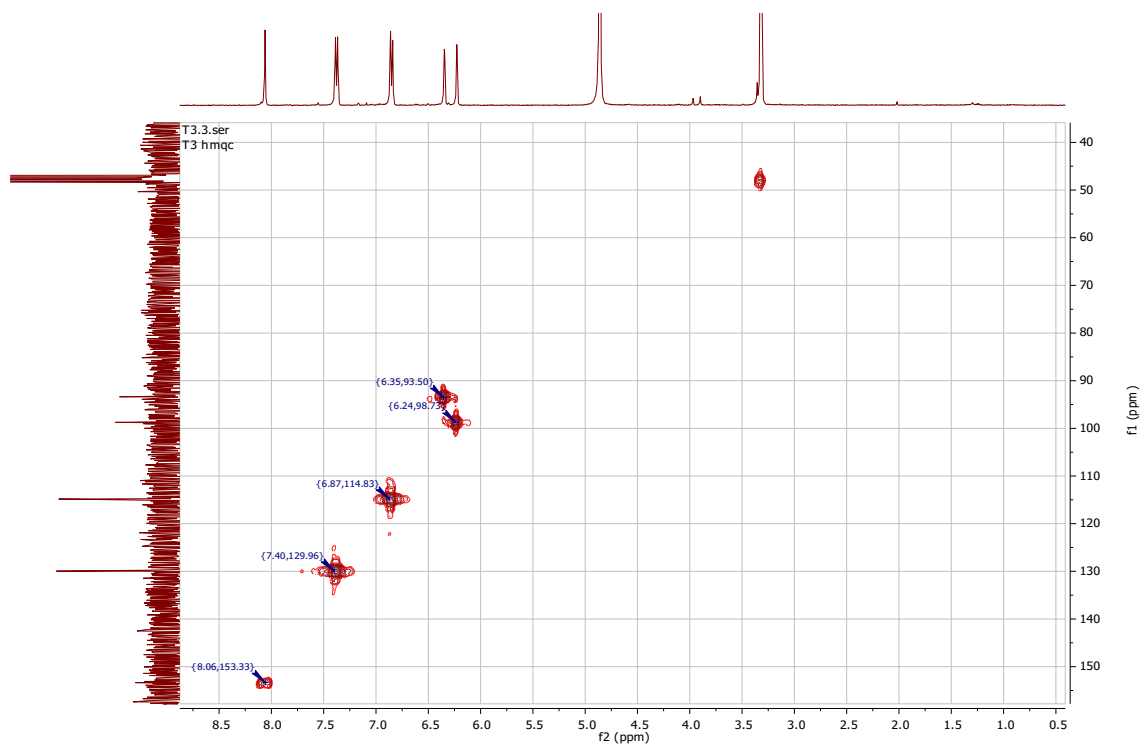


Figure II.1. 55. HMQC Spectrum of Compound CVS2



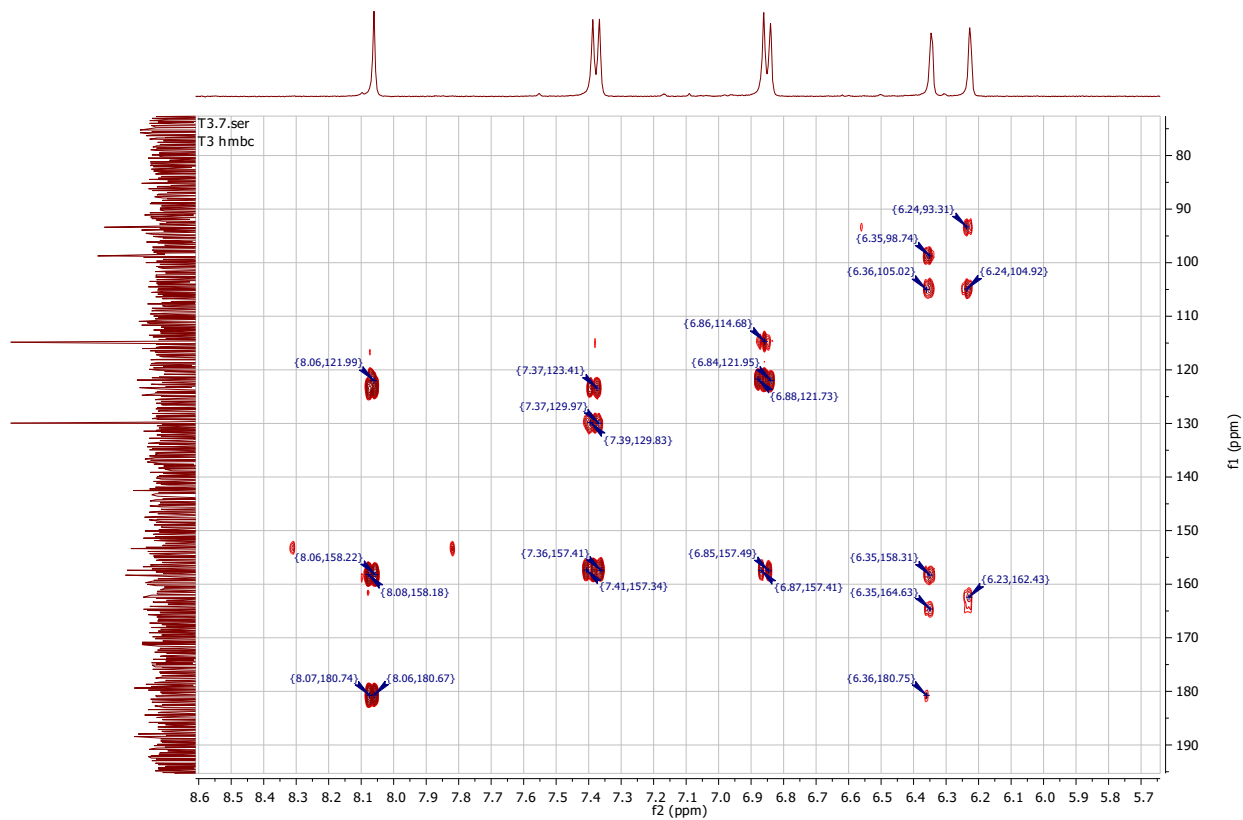


Figure II.1. 56. HMBC Spectrum of Compound CVS2

#### II.1.4.4. FLAVONOIDS

##### II.1.4.4.1. Compound CVF1

###### i. Physical properties

Compound CVF1 (4 mg) was obtained as a yellowish amorphous powder.

###### ii. Chromatographic characters:

Compound CVF1 appeared as a dark spot under UV  $\lambda_{\max}$  254 which attained a yellow color after spraying with 10% v/v vanillin/H<sub>2</sub>SO<sub>4</sub> and heating at 110 °C. It showed  $R_f$  value of 0.36 in system XXVII (Page 48).

###### iii. Spectroscopic data

A. UV (MeOH)  $\lambda_{\max}$ nm (log  $\epsilon$ ) : 270.9 (4.05), 320 (3.70)

B. HR-ESI-MS  $m/z$  : 253.037 [M-H]<sup>-</sup>,  $m/z$  : 255.035 [M+H]<sup>+</sup>

###### C. <sup>1</sup>H-, <sup>13</sup>C-NMR and HMBC spectral analysis:

The <sup>1</sup>H, <sup>13</sup>C-NMR and HMBC spectral data of compound CVF1 are listed in table II.1.7 and illustrated in figures thereafter.

**Table II.1. 7.** <sup>13</sup>C-NMR and HMBC spectral data of compound CVF1 (400 MHz, 100 MHz, DMSO-*d*<sub>6</sub>).

Position	$\delta_H$ (ppm), multiplicity, $J$ (Hz)	$\delta_C$ (ppm)	HMBC (H→C)
2	-	165.4	-
3	6.97, s, 1H	105.6	C2,4,10-
4	-	182.2	-
5	-	161.9	-
5-OH	12.82, s, 1H	161.9	-
6	6.21, d, $J = 2.1$ Hz, 1H	99.6	C-8, 10, 7
7	-	163.5	-
8	6.52, d, $J = 2.1$ Hz, 1H	94.6	C-6, 7, 10, 9
9	-	157.9	-
10	-	104.2	-
1'	-	131.2	-
2', 6'	8.07, br d, $J = 7.3$ Hz, 2H	126.8	C-3', 5', 1'
3',4',5'	7.55 – 7.64, m, 3H	129.6	C-2', 6'-

**iv. Discussion and conclusion:**

**CVF1** molecular formula was established as  $C_{15}H_{10}O_4$  from its Negative HREIMS spectral data which showed a molecular ion peak at  $m/z$  253.037 [ $M-H$ ]<sup>-</sup> (calcd. 253.047) and confirmed by its positive HREIMS spectrum which gave a molecular ion peak at  $m/z$ : 255.035 [ $M+H$ ]<sup>+</sup> (calcd. 255.067) (Figure II.1.58).

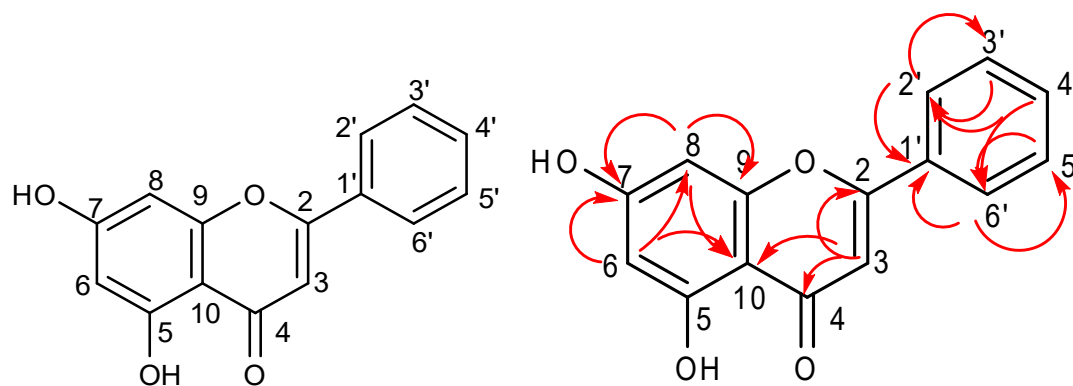
The UV spectrum exhibited absorption maxima at 270.9 nm (**Band II**) and 320 (**Band I**) that are characteristic absorption bands of a flavone skeleton (Mabry et al., 1970a).

The <sup>1</sup>H-NMR spectrum (Figure II.1.59) exhibited a flavonoid pattern and showed signals at 6.51 (1H, d, 2.1 Hz) and 6.21 ppm (1H, d, 2.1 Hz) typical of protons at C-8 and C-6 of a flavonoid skeleton. Chemical shifts of 8.08 (br d, H2', H6') and 7.55-7.64 (m, H3', H4', H5') suggested that there is no substitution in the B ring of the flavonoid. The signal at  $\delta_H$  = 12.82 ppm was assigned to the C-5 hydroxyl.

<sup>13</sup>C-NMR and DEPT spectra (Figures II.1.60-61) confirm precedent analysis. The <sup>1</sup>H- and <sup>13</sup>C- NMR values for all the carbons were assigned on the basis of HMQC and HMBC correlations (Figures II.1.62-64).

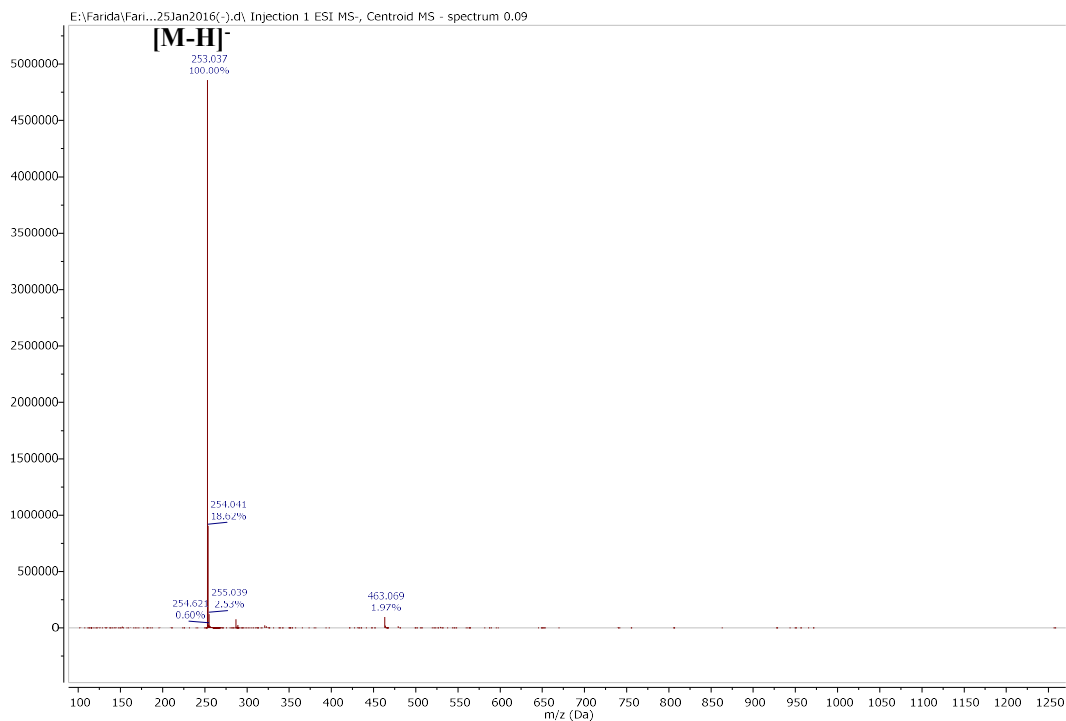
Based on the above evidence and comparison with the values in literature (Antri et al., 2004; Mouffok et al., 2012), the structure of **CVF1** was established as the known (5,7-di-OH-flavone) namely chrysin, previously reported in *Cytisus* genus (Pereira et al., 2012).

Chrysin is one of the important natural plant flavonoids, several studies have been reported its possess of multiple biological activities and pharmacological effects including antioxidant, anti-inflammatory, anti-aging and anticancer (Araújo et al., 2011; Souza et al., 2015).

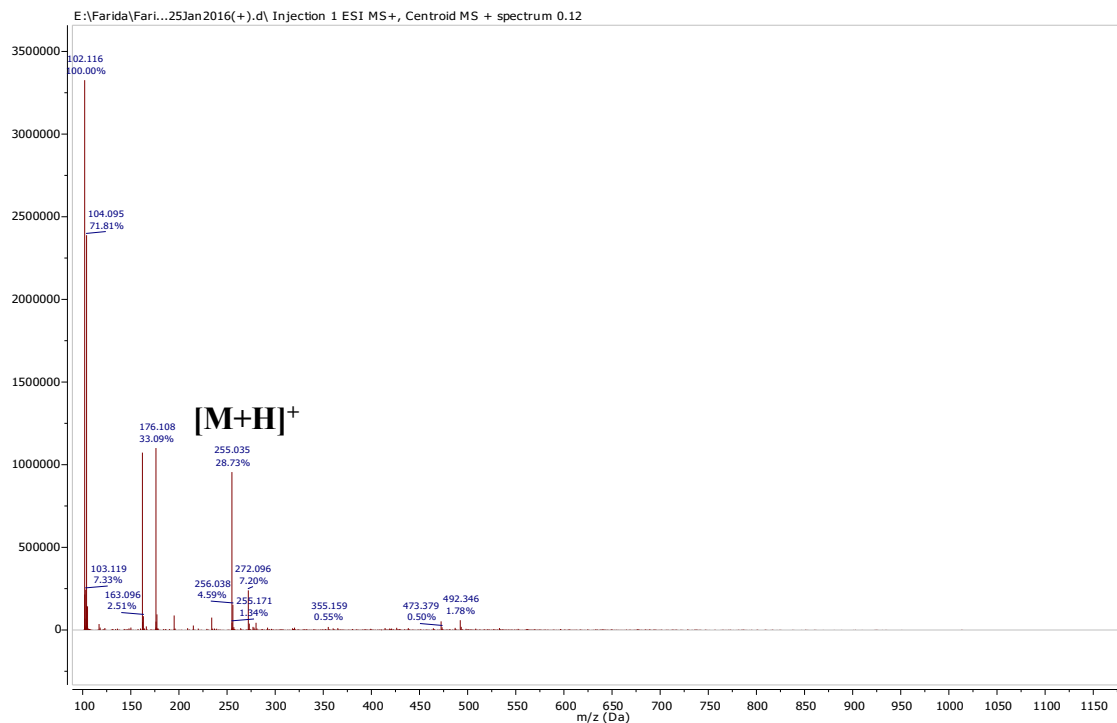


Structure of compound CVF1  
Chrysin

Figure II.1. 57. Important HMBC (H→C) correlations of the compound CVF1



A



B

**Figure II.1. 58.** Mass spectra of compound CVF1

A. Negative HR-ESI-MS, B. Positive HR-ESI-MS



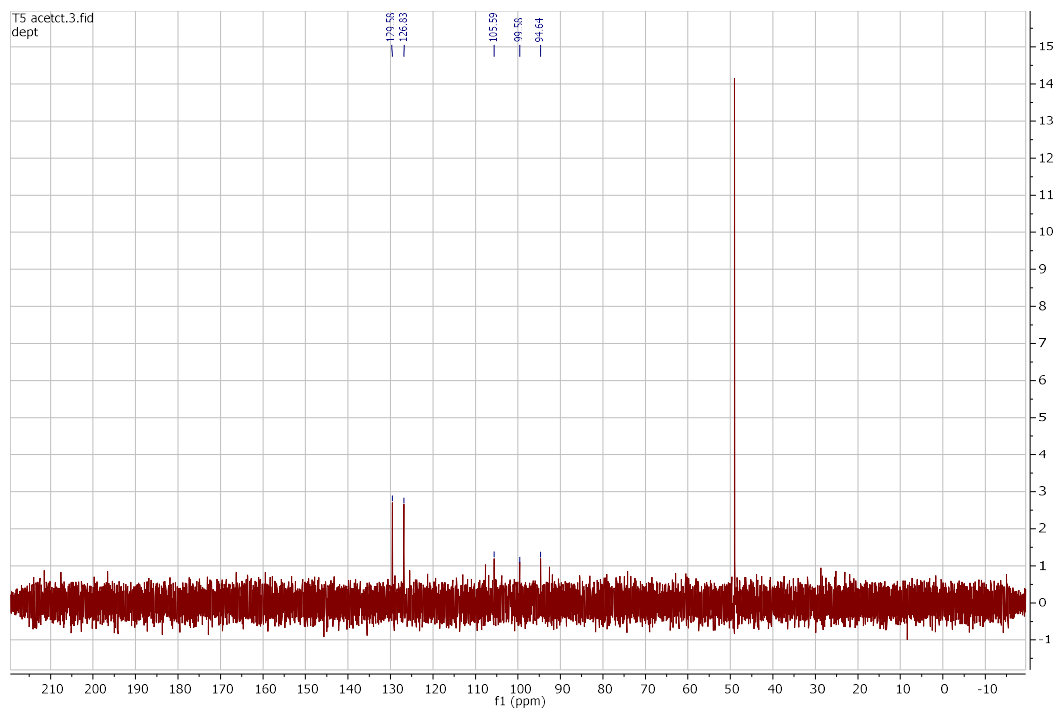


Figure II.1. 61.DEPT-135 Spectrum of compound CVF1

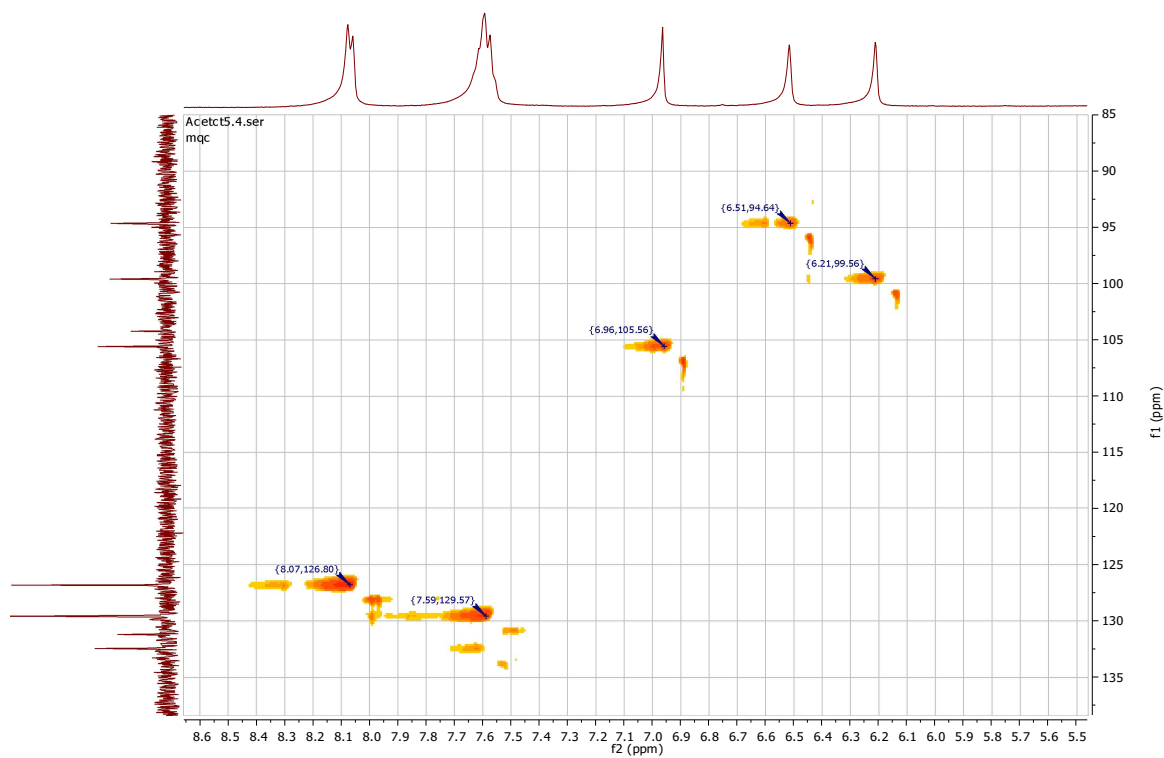
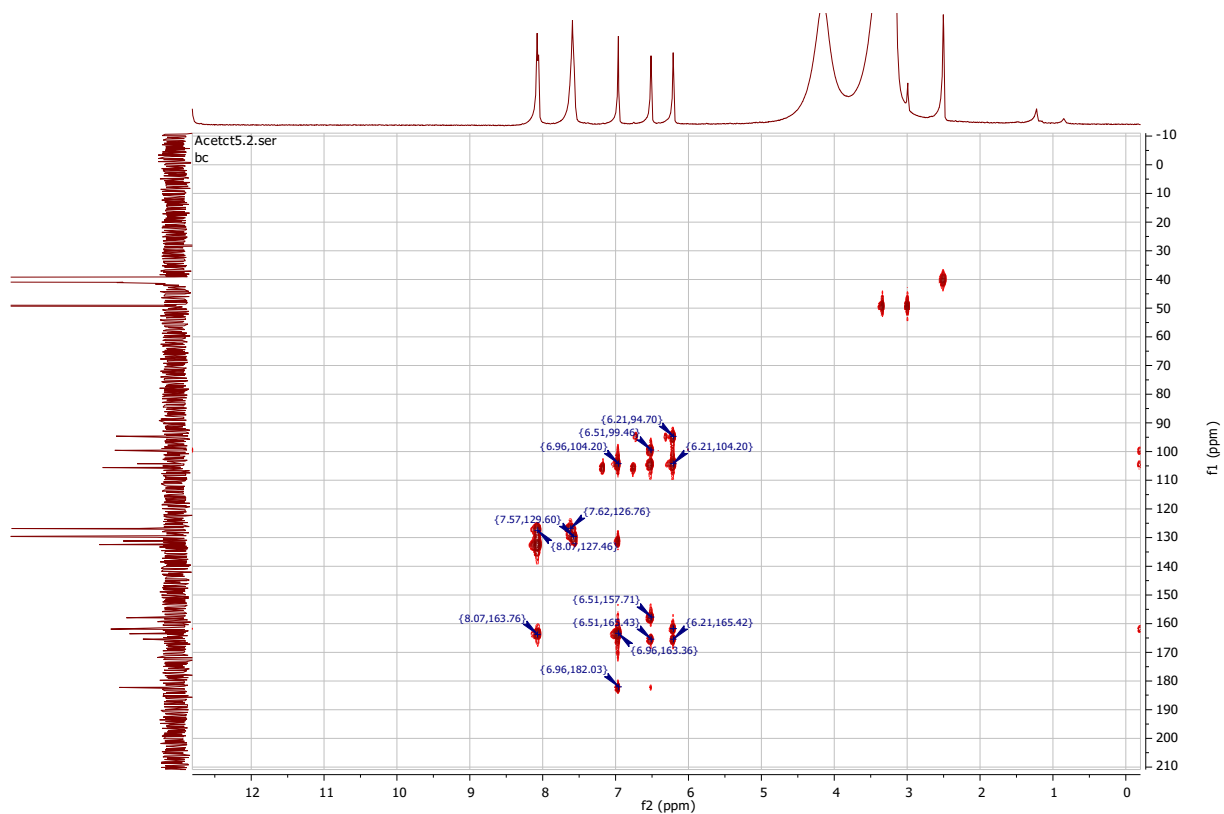
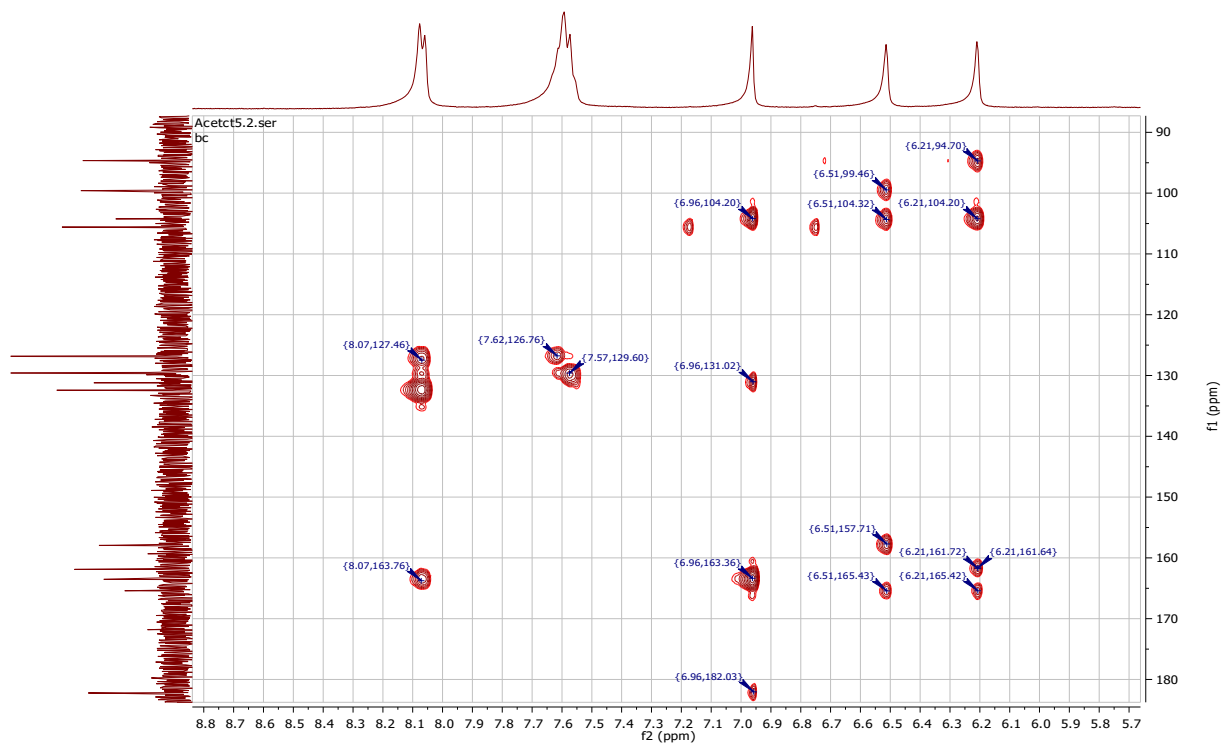


Figure II.1. 62.HMQC Spectrum of compound CVF1



**Figure II.1. 63.. HMBC Spectrum of compound CVF1**



**Figure II.1. 64.. Expanded HMBC Spectrum of compound CVF1**

#### II.1.4.4.2. Compound CVF2

##### i. Physical properties

Compound CVF2 (3 mg) was obtained as a white amorphous powder

##### ii. Chromatographic characters

Compound CVF2 appeared as a dark spot under UV  $\lambda_{\max}$  254 which attained a yellow colour after spraying with 10% v/v vanillin/H<sub>2</sub>SO<sub>4</sub> and heating at 110 °C. It showed  $R_f$  value of 0.32 in system IX (Page 48).

##### iii. Spectroscopic data

**A. UV (MeOH)  $\lambda_{\max}$  nm (log  $\epsilon$ ) :** 269.0 (4.52), 307 (4.35)

**B. HR-ESI-MS  $m/z$  :** 417.127 [M+H]<sup>+</sup>, 855.223[2M+Na]<sup>+</sup>

##### C. <sup>1</sup>H-, <sup>13</sup>C-NMR and HMBC spectral analysis:

The <sup>1</sup>H, <sup>13</sup>C-NMR and HMBC spectral data of compound CVF2 are listed in table II.1.8 and illustrated in figures thereafter.

**Table II.1. 8.** <sup>1</sup>H-, <sup>13</sup>C-NMR and HMBC spectral data of compound CVF2 (400 MHz, 100 MHz, DMSO-*d*<sub>6</sub>)

Position	$\delta_H$ (ppm), multiplicity, J(Hz)	$\delta_C$ (ppm)	HMBC (H→C)
2	-	164.1	-
3	7.04, s, 1H	105.9	C-2, 4
4	-	182.6	-
5	-	161.5	-
5-OH	12.80	161.5	
6	6.47, d, J=2.1, 1H	100.1	C-5, 8, 10
7	-	163.6	-
8	6.87, d, J= 2.1, 1H	95.4	C-7, 6, 10
9	-	157.6	-
10	-	106.0	-
1'	-	131.0	-
2', 6'	8.08, m, 2H	127.0	C-3', 5', 4', 2
3', 5'	7.56-7.65, m, 3H	129.6	C-2', 6'
4'	7.56-7.65, m, 3H	132.7	3', 5'
1''	5.08, d, J = 7.3, 1H	100.3	C-7
2''	3.28, m, 1H	73.5	C-1''
3''	3.30, m, 1H	76.9	C-2'', 4''



4"	3.18, m, 1H	70.0	C-3", 6"
5"	3.46, m, 1H	77.6	C-4"
6"	H-6a, 3.71, d, $J=10.2$ , 1H H-6b, 3.47, d, $J=3.1$ , 1H	61.0	C-4"

#### iv. Discussion and conclusion:

Compound **CVF2** was isolated as a white powder which had the molecular formula  $C_{21}H_{20}O_9$  as established from the positive HR-ESI-MS (Figure II.1.66) by providing a molecular ion peak at  $m/z$  417.127  $[M+H]^+$  (calcd. 417.121) and a molecular ion peak at  $m/z$  855.223  $[2M+Na]^+$  (calcd. 855.211). A fragment at  $m/z$  255.070 was observed, suggesting aglycone as chrysin. A loss of 162 mass units from the molecular ion and a signal at  $\delta_C = 61.05$  ppm, shown by DEPT (Figure II.1.69) to represent a  $CH_2$  group, suggested glucose or galactose.

The UV spectrum exhibited absorption maxima at 269 (MeOH) nm (**band II**) and 306 nm (**band I**) that are characteristic absorption bands of flavone skeleton (Mabry et al., 1970a). The  $^1H$  and  $^{13}C$ -NMR chemical shifts presented in table (II.1.8) were assigned according to the analysis of its  $^1H$ ,  $^{13}C$ -NMR, HSQC, and HMBC NMR spectra (Figures II.1.67, 68, 71-72).

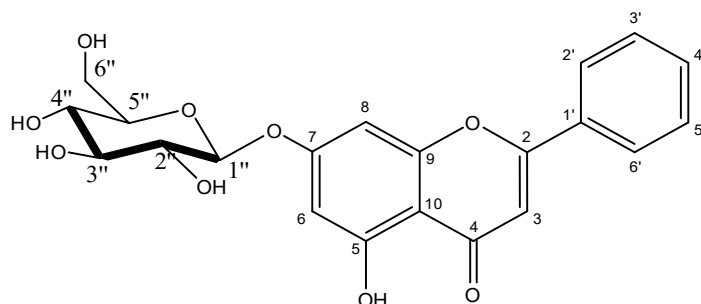
Besides the characteristic signals of the chrysin aglycone ( $\delta_H$  7.04,  $\delta_H$  6.87,  $\delta_H$  6.47,  $\delta_H$  8.08, and  $\delta_H$  7.56-7.65), the spectra showed typical  $^1H$  and  $^{13}C$ -NMR shifts for  $\beta$ -glucopyranoside ( $\delta_H = 5.08$  ppm, d,  $J = 7.3$  Hz;  $\delta_C = 100.3$  ppm) with a coupling constant ( $J = 7.3$  Hz) indicating a  $\beta$ -linkage of the sugar unit to the aglycone (Mabry et al., 1970c). Comparison of the  $^{13}C$ -NMR spectrum of compound **CVF2** with that of chrysin aglycone (**CVF1**) showed that the signal of C-7 was observed to shift downfield slightly (0.11 ppm), whereas the signals of C-3, C-4, C-6, C-8 and C-10 were displaced downfield by 0.32, 0.42, 0.56, 0.81 and 1.82 ppm respectively. However, the signals of C-5 and C-9 were observed to shift upfield by -0.34 and -0.38 ppm respectively.

DEPT experiment (Figure II.1.69-70) indicated the presence of one methylene carbon ( $\delta_C$  61.05 ppm) and seven quaternary carbons. The signal at  $\delta_C$  61.05 ppm, shown by DEPT to represent a  $CH_2$  group, suggested glucose or galactose.

$^1H$ -NMR resonances at  $\delta_H = 3.18$  to 3.70 ppm and signals in the  $^{13}C$ -NMR spectrum just below  $\delta_C = 77$  ppm indicated the presence of a glucose moiety (Markham et al., 1978).

Moreover, the correlation between the proton H-1'' ( $\delta_H = 5.08$  ppm) and C-7 ( $\delta_C 163.64$ ) in the HMBC spectrum (Figure II.1.72), allowed to confirm that the anomeric carbon of glucose was linked to C-7 of the flavone skeleton.

On the basis of the above evidence and by comparison with literature data for analogues compounds and further comparison to those of chrysin and its derivatives to the literature data (Antri et al., 2004), the structure of compound **CVF2** was established as the known flavonoid chrysin-7-*O*- $\beta$ -D-glucopyranoside. It was previously reported from *Cytisus* (Pereira et al., 2012).



**Structure of compound CVF2**  
**Chrysin-7-*O*- $\beta$ -D-glucopyranoside**

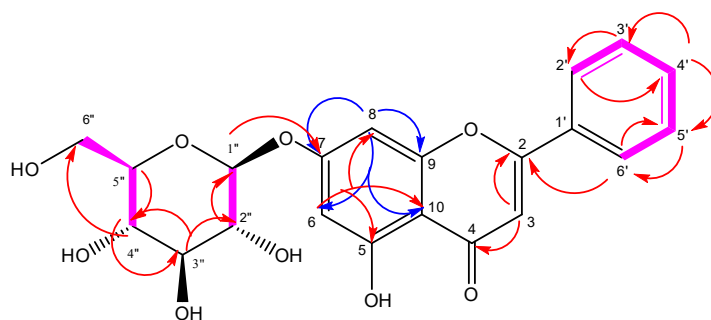


**Figure II.1. 65.** Important HMBC (H→C) and  $^1\text{H}$ - $^1\text{H}$  COSY (—) correlations of compound **CVF2**

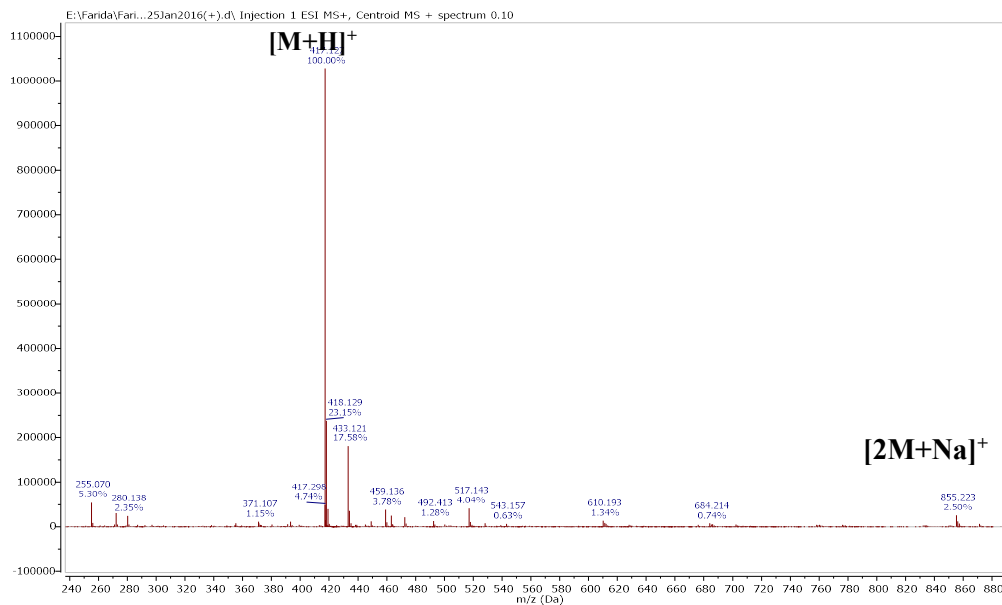


Figure II.1. 66. Positive HR-ESI-MS of compound CVF2

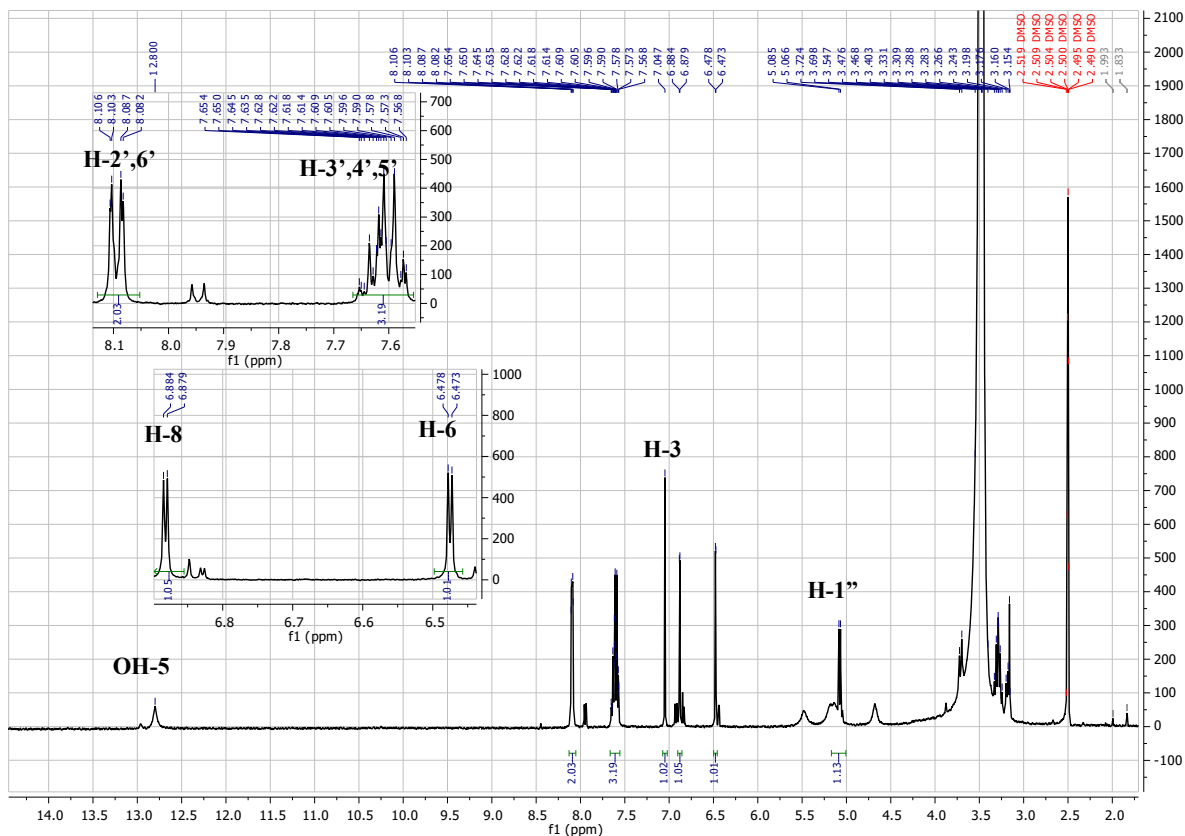


Figure II.1. 67. <sup>1</sup>H-NMR Spectrum of compound CVF2 (400 MHz, DMSO-*d*<sub>6</sub>)

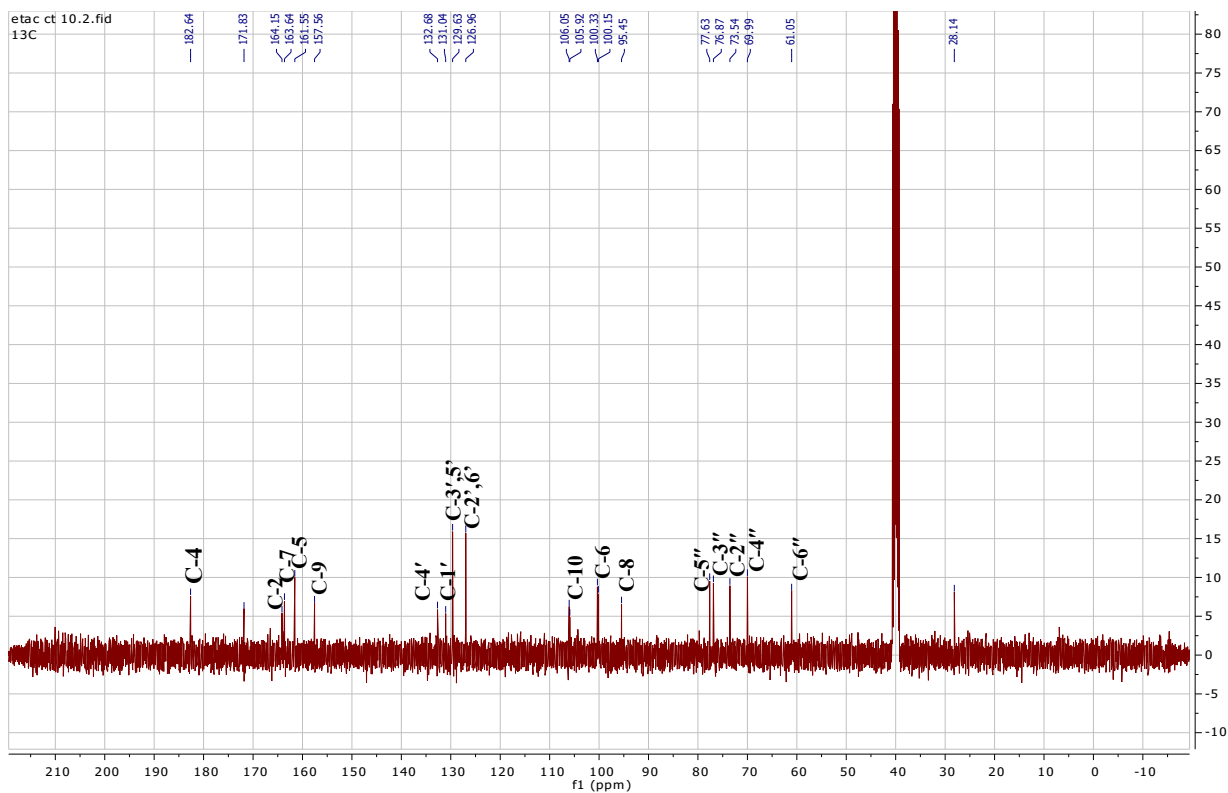


Figure II.1. 68.  $^{13}\text{C}$ -NMR Spectrum of compound CVF2 (100 MHz,  $\text{DMSO-}d_6$ )

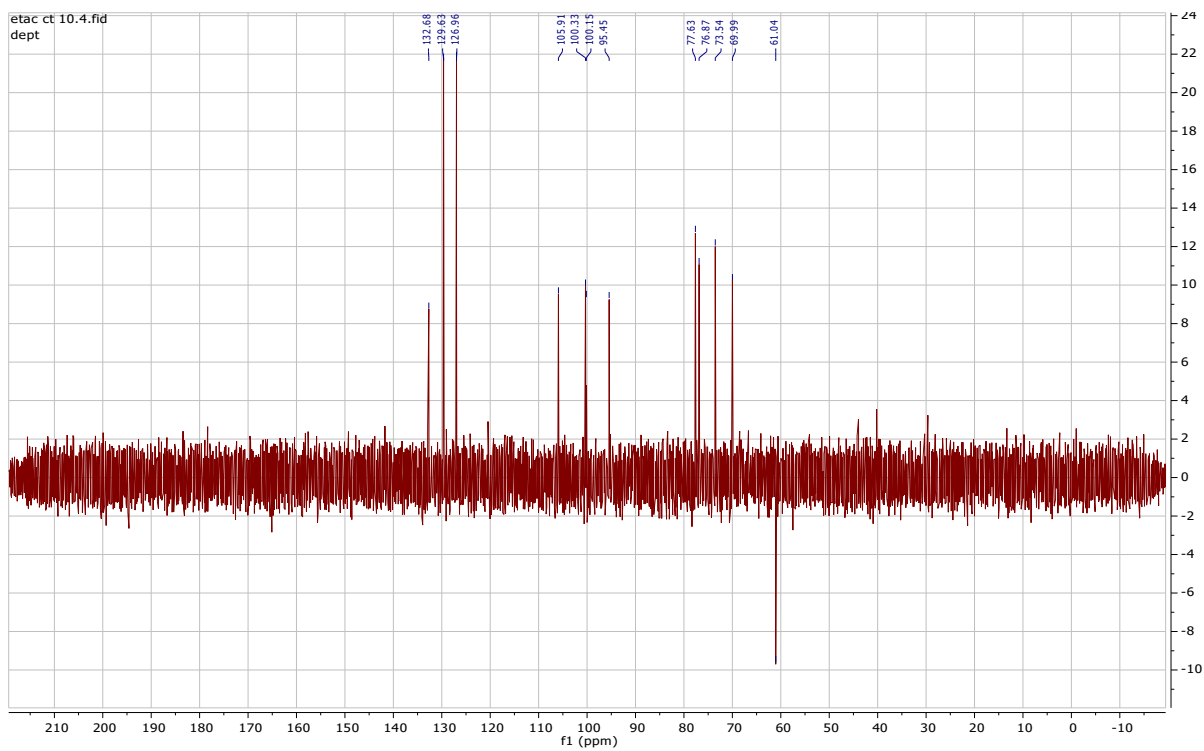


Figure II.1. 69. DEPT 135 Spectrum of compound CVF2



Figure II.1. 70. Comparison of  $^{13}\text{C}$ - and DEPT NMR spectra of compound CVF2

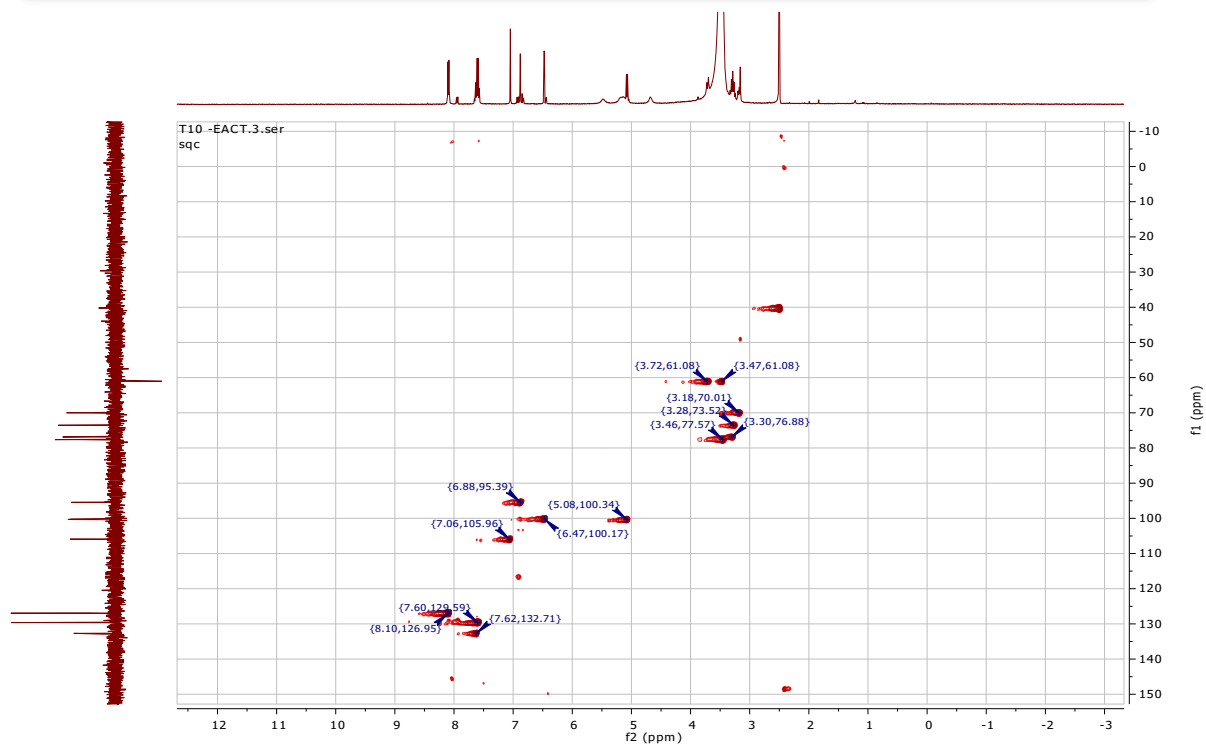


Figure II.1. 71. HSQC Spectrum of Compound CVF2

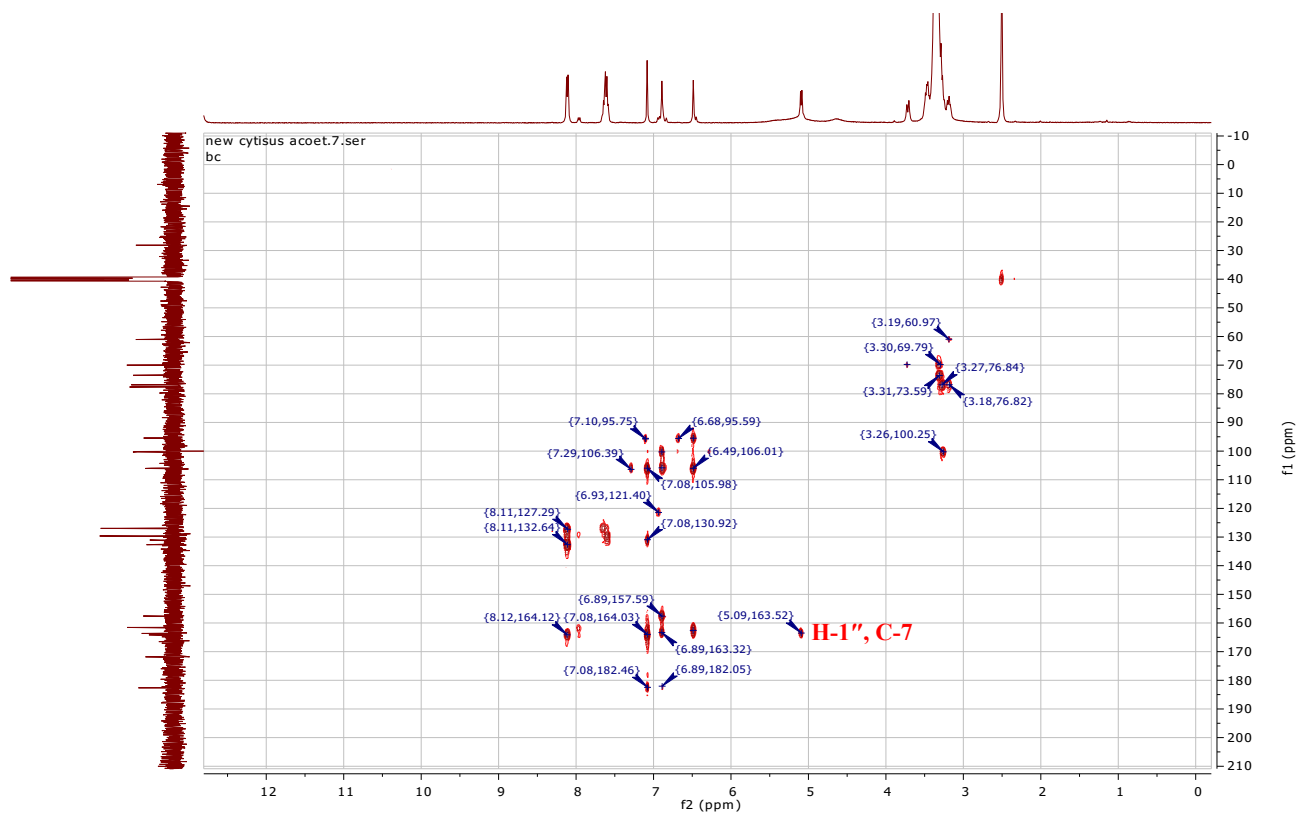


Figure II.1. 72.HMBC Spectrum of Compound CVF2

### II.1.4.4.3. Compound CVF3

#### i. Physical properties

Compound CVF3 (6 mg) was obtained as yellow needles.

#### ii. Chromatographic characters

Compound CVF3 appeared as a dark spot which attained a yellow colour after spraying with 10% v/v vanillin/H<sub>2</sub>SO<sub>4</sub> using precoated silica gel plates after heating at 110 °C for 10 minutes. It showed *R<sub>f</sub>* value of 0.67 in system I (Page48).

#### iii. Spectroscopic data

**A. UV (MeOH)  $\lambda_{\max}$  nm (log  $\epsilon$ ):** 348.0 (4.42) ; 256.0 (4.47).

**B. HRESIMS,** positive-ion mode *m/z* 595.200 [M+H]<sup>+</sup>, Negative-ion mode *m/z* 593.146 [M-H]<sup>-</sup>.

#### C. <sup>1</sup>H-, <sup>13</sup>C-NMR and HMBC spectral analysis

The <sup>1</sup>H- and <sup>13</sup>C-NMR spectral data of compound CVF3 are listed in table II.1.9 and illustrated in figures thereafter.

**Table II.1. 9.** <sup>1</sup>H-, and <sup>13</sup>C-NMR spectral data of compound CVF3 (500 MHz, 126 MHz, Methanol-*d*<sub>4</sub>).

Position	$\delta_H$ (ppm), multiplicity, <i>J</i> (Hz)	$\delta_C$ (ppm)	HMBC (H→C)	<sup>1</sup> H- <sup>1</sup> H COSY
2	-	165.4	-	-
3	6.56, s, 1H	102.3	C-2, 4, 10, 1'	-
4	-	182.8	-	-
5	-	161.3	-	-
6	6.29, s, 1H	98.5	C-5,8	-
7	-	162.9	-	-
8	-	104.5	-	-
9	-	156.5	-	-
10	-	104.2	-	-
1'	-	122.6	-	-
2'	7.57, d, <i>J</i> = 2.2 Hz, 1H	113.6	C-3', 4', 6'	-
3'	-	145.6	-	-
4'	-	149.5	-	-
5'	6.94, d, <i>J</i> = 8.3 Hz, 1H	115.4	C-1', 3'	H-6'
6'	7.53, dd, <i>J</i> = 8.5, 2.1 Hz, 1H	119.6	C-2', 4'	H-5'

Glc	1''	5.04, d, $J = 9.9$ Hz, 1H	72.3	C-8, 9, 2'', 5''	H-2''
	2''	4.27, t, 9.1 Hz, 1H	76.7	C-1'', 3'', 1''', 8	H-1'', 3'', 4'', 6'' <sup>a</sup>
	3''	3.66, m, 2H	80.2	C-2'', 4''	H-2'', 4''
	4''	3.70, m, 2H	71.0	C-3'', 6''	H-2''
	5''	3.49, m, 1H	81.5	C-3'', 4'', 6''	-
	6''	3.89 H-6a, d, 12.0 Hz, 1H 4.0 H-6b, dd, 12.6, 3.5 Hz, 1H	61.8	C-5'' C-4'', 5''	H-2''
Rhm	1'''	5.12, br s, 1H	101.1	C-2'', 2''', 5''',	-
	2'''	3.40-3.43, dd, 9.6, 3.2 Hz, 1H	70.5	C-1'', 2'', 5'''	4'''
	3'''	3.87, m, 1H	70.8	C-4'''	4'''
	4'''	3.14, t, 9.5 Hz, 1H	72.1	C-2''', 3''', 5''', 6'''	H-5''', 2'''
	5'''	2.44, dq, 9.5, 6.2 Hz, 1H	68.6	4'''	H-4''', 6'''
	6'''	0.67, d, 6.2 Hz, 3H	16.7	C-5''', 4'''	H-5'''

#### iv. Discussion and conclusion

Compound **CVF3** was obtained as yellow crystals. The molecular formula  $C_{27}H_{30}O_{15}$  was established from the positive **HR-ESI-MS** by providing molecular ion peaks at  $m/z$  595.200  $[M+H]^+$  (calcd. 595.170) and  $m/z$  617.123  $[M+Na]^+$  (calcd. 617.138) and confirmed by the negative **HR-ESI-MS** which showed molecular ion peaks at  $m/z$  593.146  $[M-H]^-$  (calcd. 593.148) and  $m/z$  1187.298  $[2M-H]^-$  (calcd. 1187.306) (Figure II.1.74).

The **UV** absorption pattern ( $\lambda_{max}$  256, 348 nm) together with **<sup>1</sup>H-NMR** spectrum that showed a signal at  $\delta_H$  6.56 (s, 1H) characteristic of C-3 proton, indicated that the structure belongs to a flavone.

Characteristic signals of protons at  $\delta_H$  7.57 (d,  $J = 2.2$  Hz, 1H),  $\delta_H$  7.53 (dd,  $J = 8.5, 2.1$  Hz, 1H), and  $\delta_H$  6.94 (d,  $J = 8.3$  Hz, 1H) appeared in the **<sup>1</sup>H-NMR** spectrum (Figure II.1.75-76) indicated the presence of an **ABX** spin system for ring B. These protons are attributed to protons H-2', H-6' and H-5'.

Two anomeric proton signals were detected in **<sup>1</sup>H-NMR** spectrum at 5.12 (s, 1H), and 5.04 (d,  $J = 9.9$  Hz, 1H).

From its **<sup>13</sup>C-NMR** spectrum (Figure II.1.77), two anomeric carbons were observed at  $\delta_C = 72.35$  and 101.1 ppm. **DEPT 135** (Figure II.1.78) experiment indicated the presence of one methylene carbon ( $\delta_C = 60.58$  ppm), suggesting glucose or galactose unit.

The **<sup>1</sup>H-NMR** spectrum of **CVF3** together with **<sup>13</sup>C-NMR**, **DEPT** and **HSQC** spectra



(Figures II.1.75-80) presented diagnostic proton signal at  $\delta_H$  (0.67, d,  $J = 6.2$  Hz, 3H) which directly connected to carbon signal at  $\delta_C = 16.25$  ppm characteristic of a rhamnosyl unit.

$^{13}\text{C-NMR}$  and **DEPT** spectra showed free carbon signal at ( $\delta_C$  98.51) attributed to C-6 and quaternary C-8 signal at ( $\delta_C$  104.5), these data with the observed lack of aromatic proton signal for H-8 in  $^1\text{H NMR}$  spectrum confirmed that the two sugar moieties were attached at C-8.

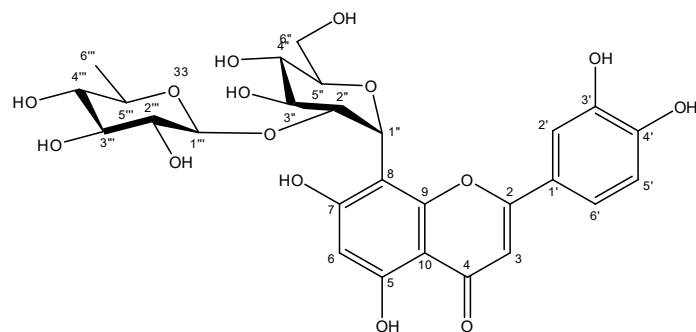
The nature of sugar unit deduced from  $^1\text{H-NMR}$  signals indicating characteristic of glucose unit. The  $\beta$ -D-glucosyl anomeric proton at  $\delta_H$  5.04 (d,  $J = 9.9$  Hz, 1H) was deduced to be attached to aglycone at C-8 from the HMBC correlation between it and C-8 at  $\delta_C = 104.55$ , and C-9 at  $\delta_C = 156.48$  ppm.

The established structure for compound **CVF3** confirmed by the **2D NMR** including **HSQC**, **HMBC** and **COSY** (Figures II.1.80-82).

From the **HMBC** spectrum (Figure II.1.81), the correlation between the anomeric proton of glucose at  $\delta_H = 5.04$  ppm and the deshielded carbon at  $\delta_C = 104.5$  ppm (C-8) supported the linkage of the glycosyl unit at C-8 in compound **CVF3**.

The anomeric proton at  $\delta_H = 5.12$  ppm (H-1'') of the terminal rhamnosyl moiety showed **HMBC** correlation with C-2'' ( $\delta_C$  76.72) of the glucosyl unit, which together with the deshielding effect on the C-2'' signal at  $\delta_C = 76.72$  ppm confirm the connection of two sugar moieties at C-2'' (Figure). In addition, the coupling constant of configuration  $\beta$ -glucopyranoside is affected ( $J = 9.9$  Hz) which indicate the coupling axial-axial between H-1'' and H-2'' of the glucose moiety.

Comparing the spectral data of compound **CVF3** with the reported ones (Kumamoto et al., 1985) confirmed its structure to be 8-((2S,3R,4S,5S,6R)-4,5-dihydroxy-6-(hydroxymethyl)-3-(((2S,3R,4R,5R,6S)-3,4,5-trihydroxy-6-methyltetrahydro-2H-pyran-2-yl)oxy)tetrahydro-2H-pyran-2-yl)-2-(3,4-dihydroxyphenyl)-5,7-dihydroxy-4H-chromen-4-one, known as **2''-O- $\alpha$ -L-rhamnosylorientin**. According to the available current literature, this is the first report for the isolation of 2''-O- $\alpha$ -L-rhamnosylorientin from the genus *Cytisus*.



**Structure of compound CVF3  
2''-O-α-L-rhamnosylorientin**

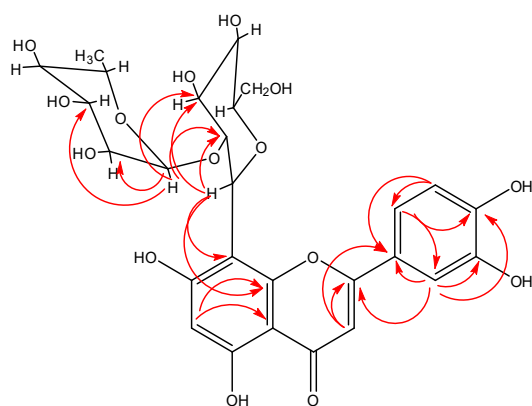
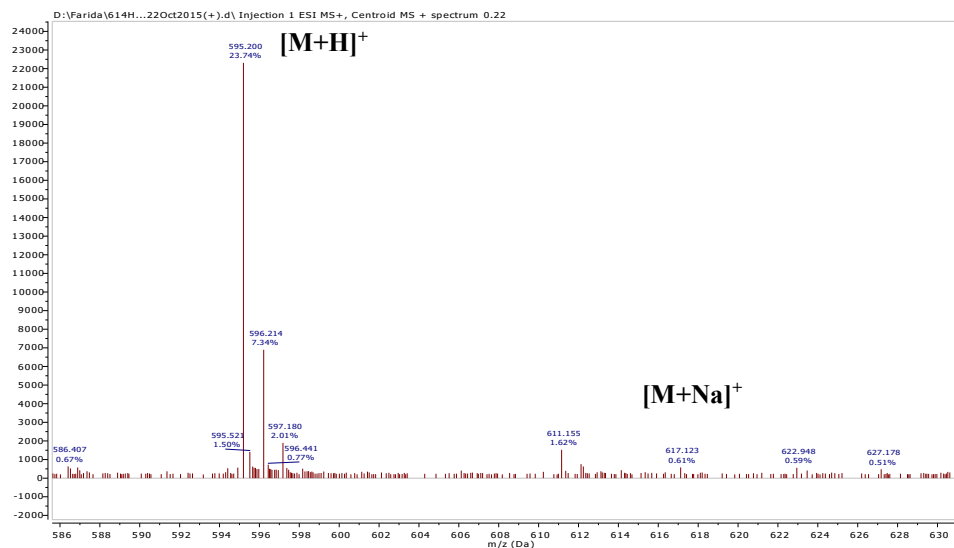
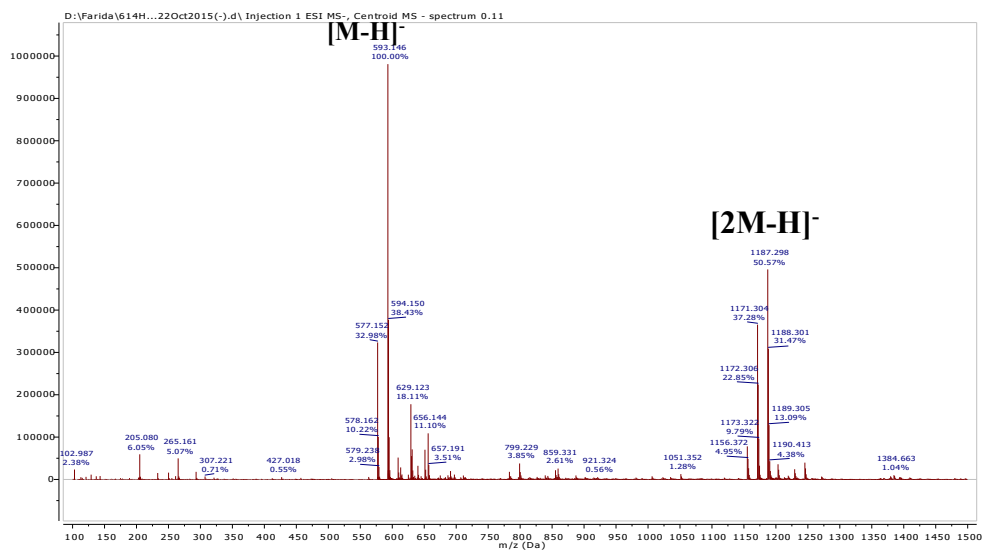


**Figure II.1. 73. Important HMBC correlation (H→C) of  
compound CVF3**



A.



B.

**Figure II.1. 74.** Mass spectra of compound CVF3  
 A. Positive HR- ESI-MS, B. Negative HR-ESI-MS

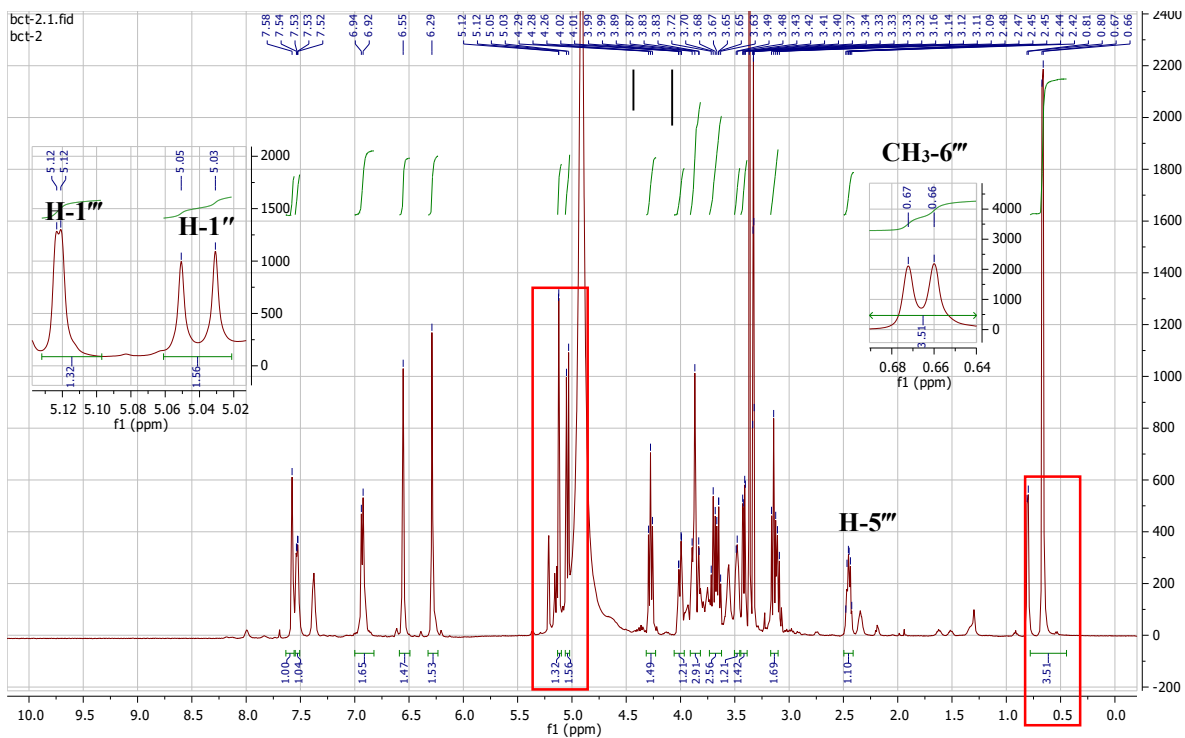


**Figure II.1. 75.**  $^1\text{H-NMR}$  Spectrum of compound CVF3 (Methanol- $d_4$ , 500 MHz)

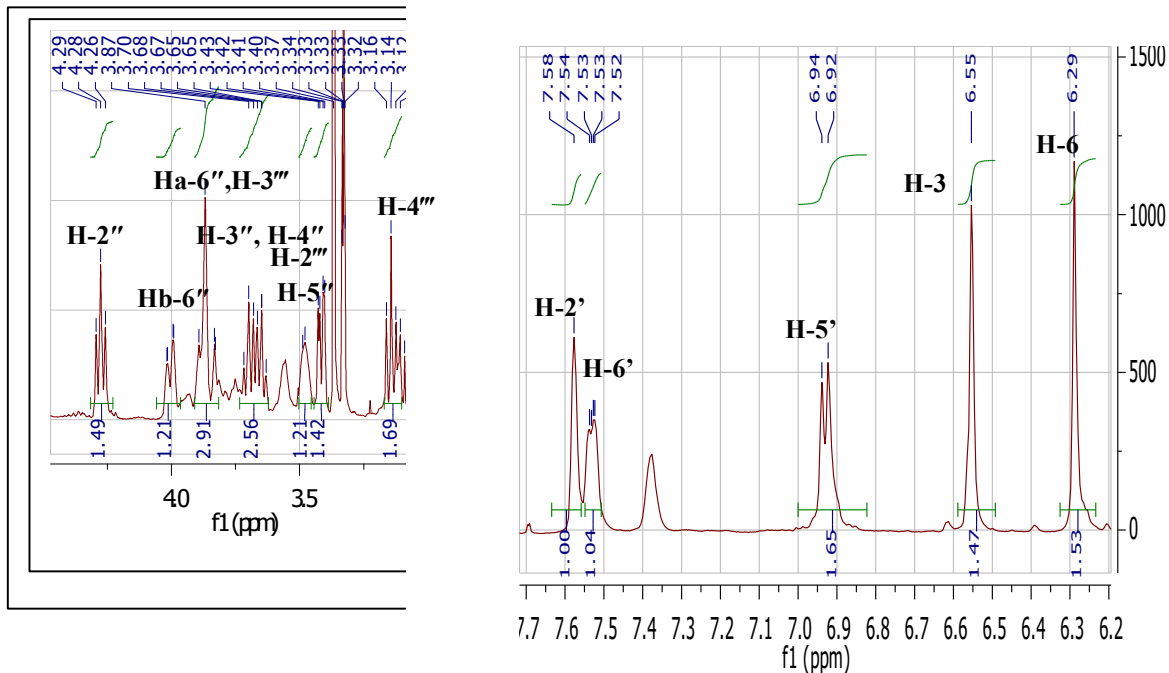


**Figure II.1. 76.** Expanded  $^1\text{H-NMR}$  Spectrum of compound CVF3 (Methanol- $d_4$ , 500 MHz)

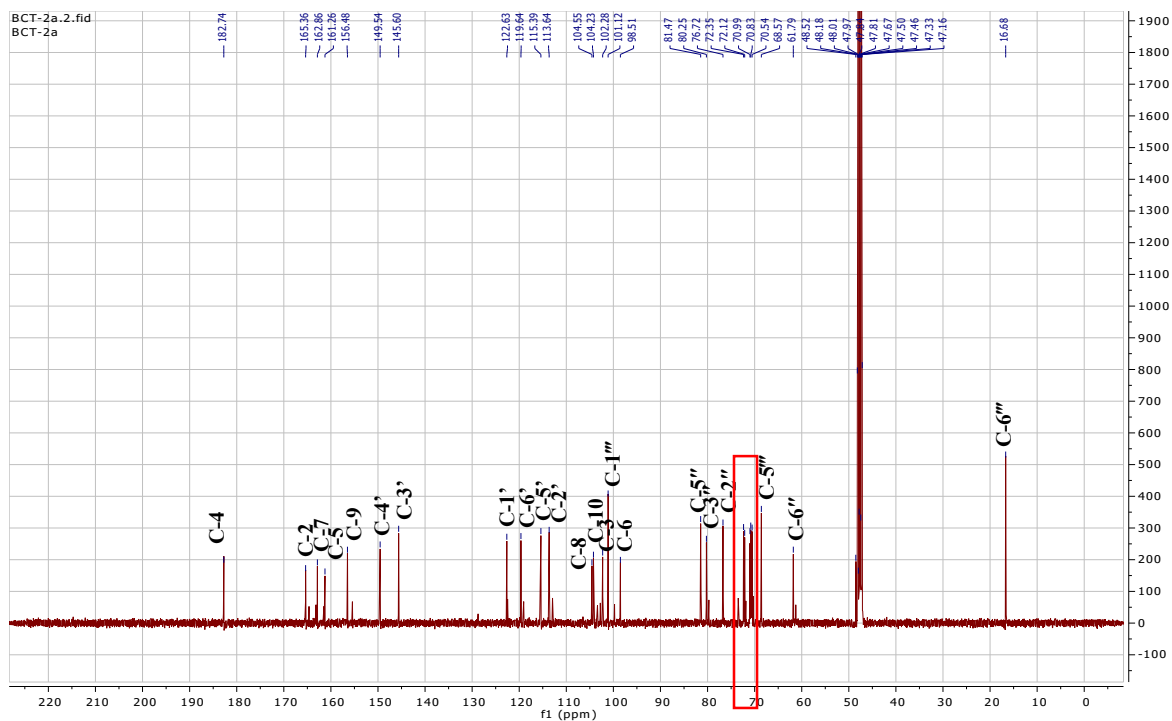


Figure II.1. 77.13C-NMR Spectrum of compound CVF3 (126 MHz, Methanol- $d_4$ )

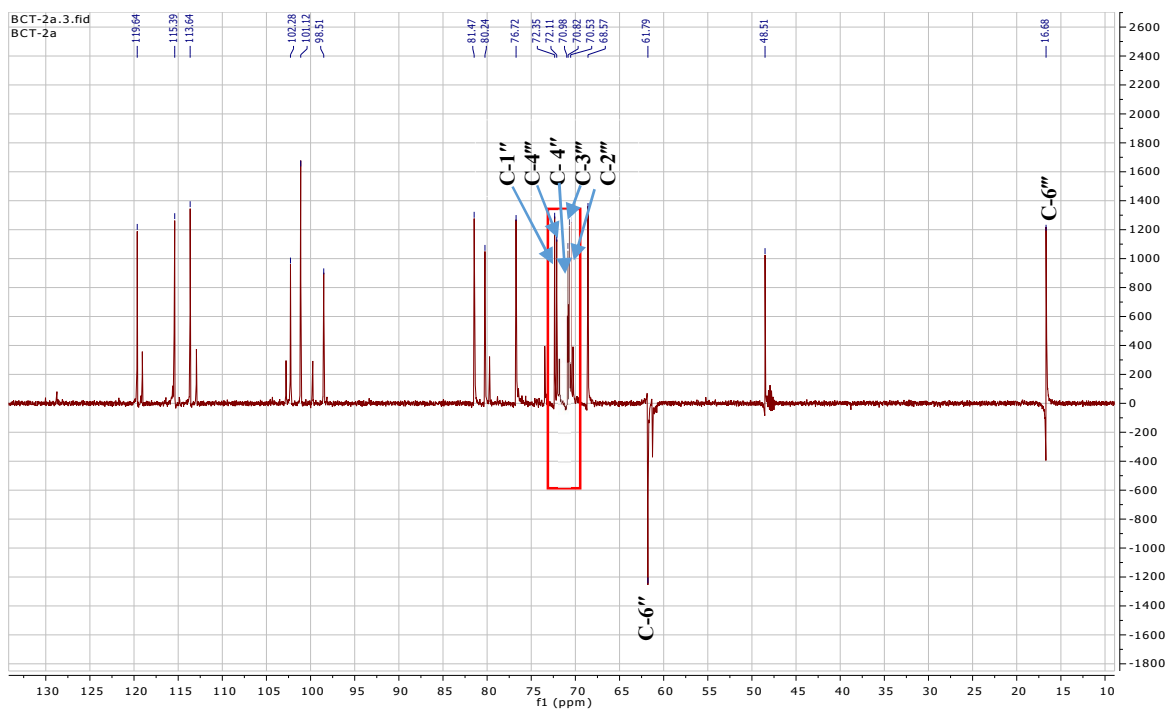
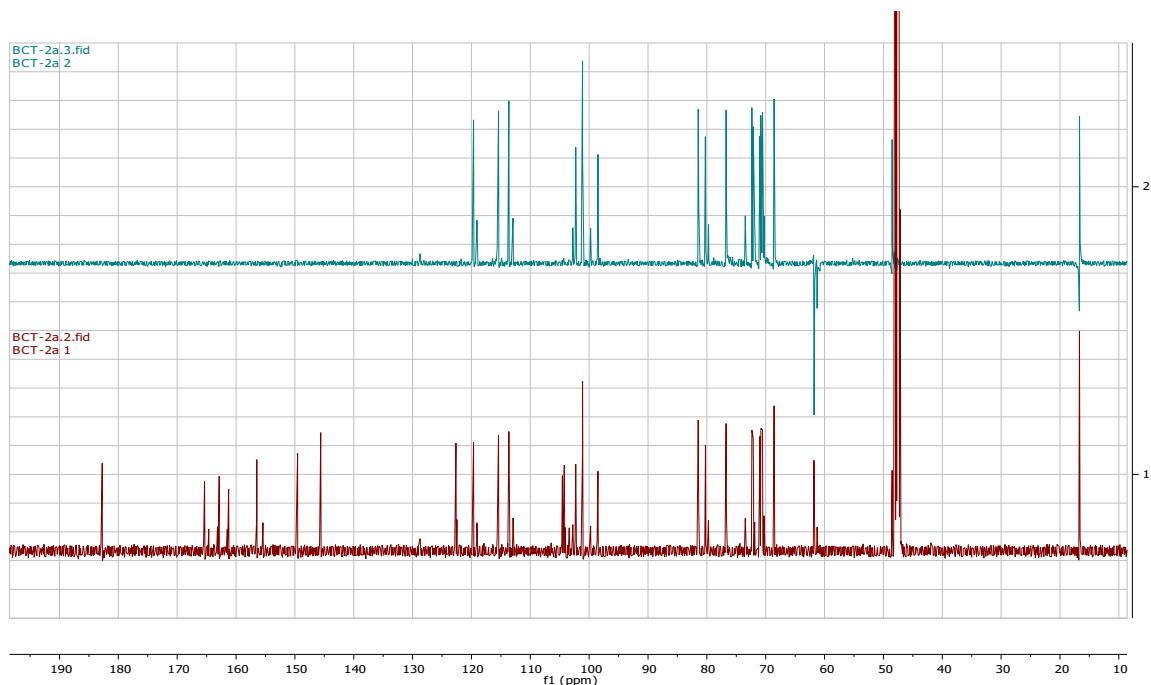
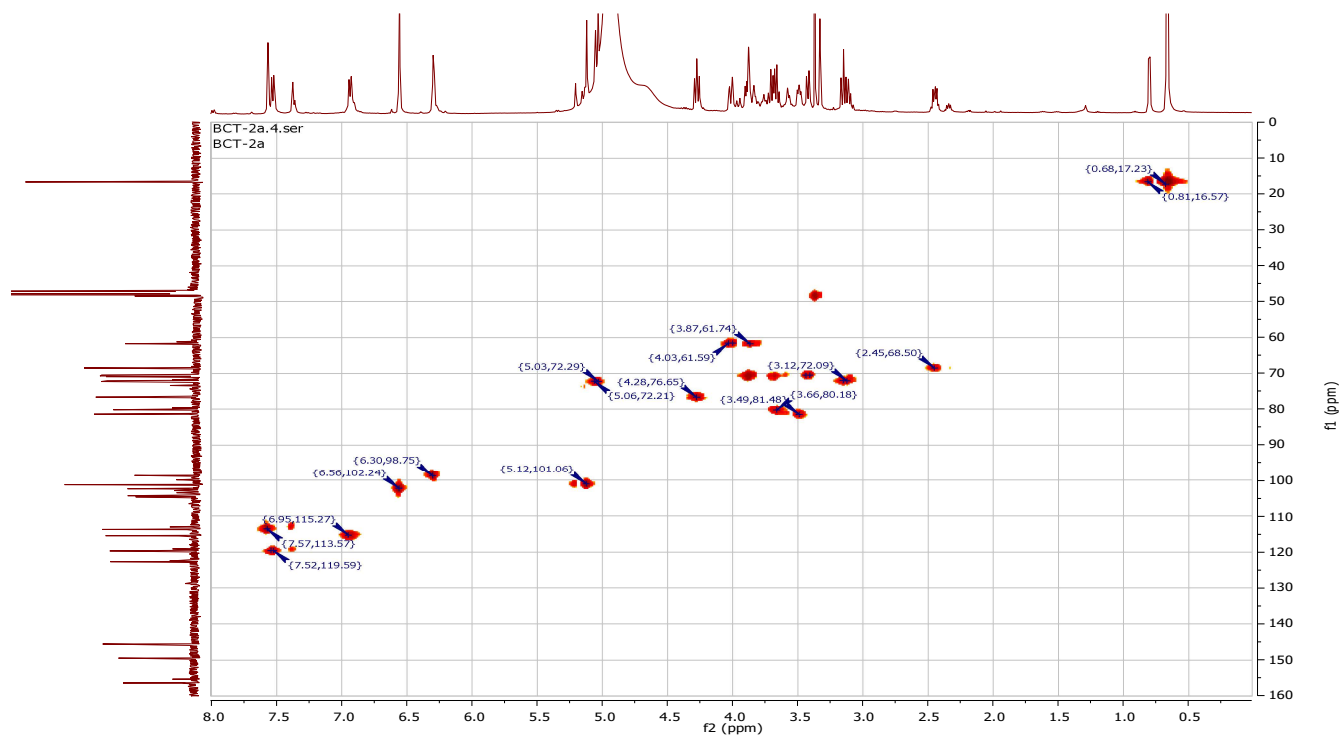


Figure II.1. 78. DEPT-135 Spectrum of compound CVF3



**Figure II.1. 79.** Comparison of <sup>13</sup>C-NMR and DEPT-135 spectra of compound CVF3



**Figure II.1. 80.** HSQC spectrum of compound CVF3

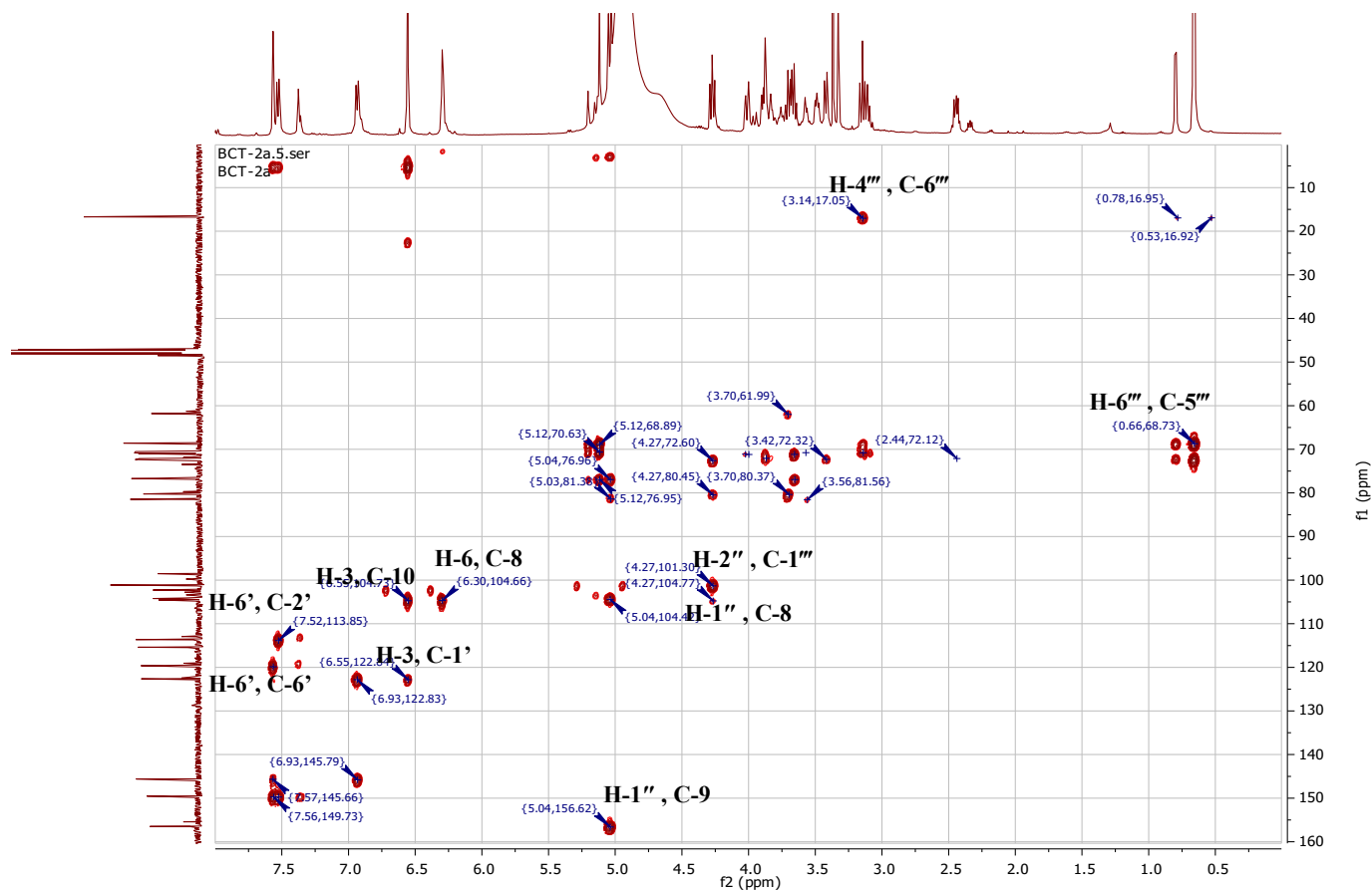


**Figure II.1. 81.HMBC spectrum of compound CVF3**

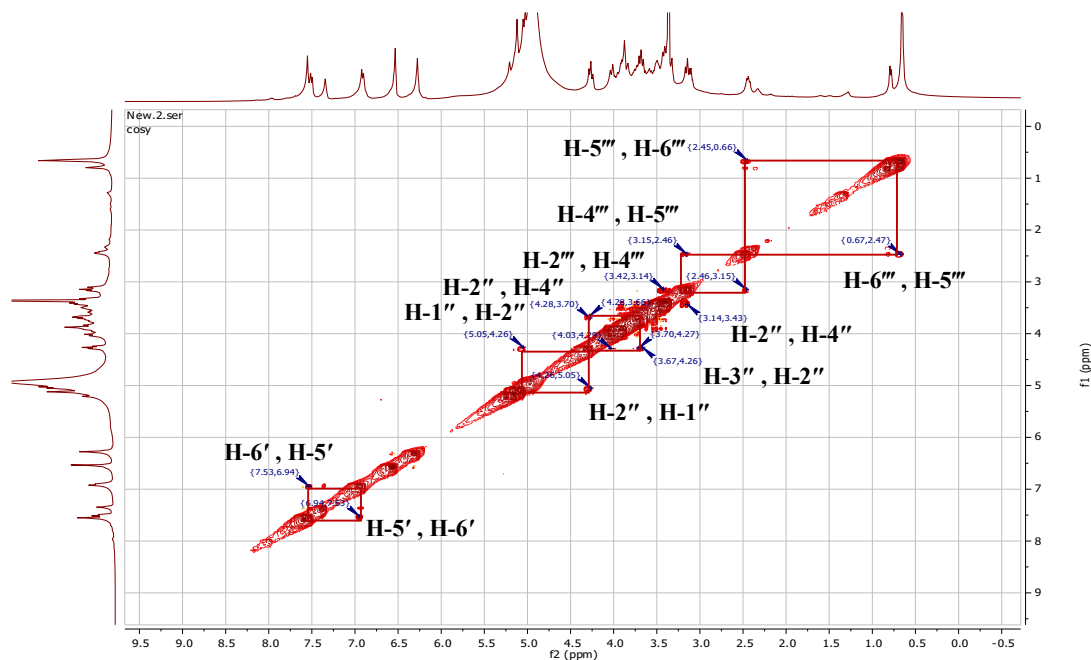


**Figure II.1. 82. <sup>1</sup>H-<sup>1</sup>H COSY spectrum of compound CVF3**

## REFERENCES

- Akiyama, T., Ishida, J., Nakagawa, S., Ogawara, H., Watanabe, S.-i., Itoh, N., Shibuya, M., Fukami, Y., 1987. Genistein, a specific inhibitor of tyrosine-specific protein kinases. *Journal of Biological Chemistry* 262, 5592-5595.
- Antri, A.E., Messouri, I., Tlemçani, R.C., Bouktaib, M., El Alami, R., El Bali, B., Lachkar, M., 2004. Flavone glycosides from *Calycotome Villosa* subsp. *intermedia*. *Molecules* 9, 568-573.
- Araújo, J.R., Gonçalves, P., Martel, F., 2011. Chemopreventive effect of dietary polyphenols in colorectal cancer cell lines. *Nutrition Research* 31, 77-87.
- Bojase, G., Wanjala, C.C., Majinda, R.R., 2001. Flavonoids from the stem bark of *Bolusanthus speciosus*. *Phytochemistry* 56, 837-841.
- Bornträger, H., 1880. Schneller Nachweis der Aloë in Elixiren, Liqueuren und im Bier. *Zeitschrift für Analytische Chemie* 19, 165-167.
- Brukwicki, T., Wysocka, W., 2003. NMR spectra and geometry of epi N-oxides of sparteine and some of its derivatives in solution. *Journal of Molecular Structure* 647, 275-286.
- Brukwicki, T., Wysocka, W., 2008. Effect of hydroxy groups on conformational equilibrium in bis-quinolizidine systems. *Tetrahedron* 64, 1440-1458.
- Bub, O., Raschack, M., 1974. Method of treating cardiac arrhythmia with 2-(2'-diethylaminoethyl)-3-phenyl-phthalimidine and its salts. Google Patents.
- Carter, B.B., 1947. Preliminary report on a substance which inhibits anti-Rh serum. *American journal of clinical pathology* 17, 646-649.
- Chandra, S., Khan, S., Avula, B., Lata, H., Yang, M.H., ElSohly, M.A., Khan, I.A., 2014. Assessment of total phenolic and flavonoid content, antioxidant properties, and yield of aeroponically and conventionally grown leafy vegetables and fruit crops: A comparative study. *Evidence-Based Complementary and Alternative Medicine* 2014.
- Chaturvedula, V.S.P., Prakash, I., 2013. Isolation and structure elucidation of daidzein and genistein from *Siraitia grosvenorii*. *Asian J. Pharm. Res. Dev* 1, 67-72.
- Cook, R., 1961. Reactions of steroids with acetic anhydride and sulphuric acid (the Liebermann-Burchard test). *Analyst* 86, 373-381.
- Coward, L., Barnes, N.C., Setchell, K.D., Barnes, S., 1993. Genistein, daidzein, and their beta-glycoside conjugates: antitumor isoflavones in soybean foods from American and Asian diets. *Journal of Agricultural and Food Chemistry* 41, 1961-1967.
- Dewick, P.M., 2002. *Medicinal natural products: a biosynthetic approach*. John Wiley & Sons.
- Divi, R.L., Chang, H.C., Doerge, D.R., 1997. Anti-thyroid isoflavones from soybean: isolation, characterization, and mechanisms of action. *Biochemical pharmacology* 54, 1087-1096.
- Duddeck, H., Skolik, J., Majchrzak-Kuczynska, U., 1995. Tetracyclic alkaloids of the sparteine group. <sup>1</sup>H and <sup>13</sup>C NMR spectroscopy and conformational analysis. *Chemistry of Heterocyclic Compounds* 31, 893-899.
- Ferris, J., Boyce, C., Briner, R., Weiss, U., Qureshi, I., Sharpless, N., 1971. Lythraceae alkaloids. X. Assignment of absolute stereochemistries on the basis of chiroptical effects. *Journal of the American Chemical Society* 93, 2963-2968.
- Geissman, T.A., 1962. *The chemistry of flavonoid compounds*. Oxford, London, New York, Paris.: Pergamon Press.
- Gołębiewski, W.M., 1986. Application of two-dimensional NMR spectroscopy to the analysis of the proton NMR spectrum of sparteine and its lactams. *Magnetic resonance in chemistry* 24, 105-112.



- Hanganu, D., Vlase, L., Olah, N., 2010. LC/MS analysis of isoflavones from Fabaceae species extracts. *Farmacia* 58, 177-183.
- Hardman, R., Sofowora, E.A., 1972. Antimony trichloride as a test reagent for steroids, especially diosgenin and yamogenin, in plant tissues. *Stain technology* 47, 205-208.
- Kamel, M.R., Nafady, A.M., Allam, A.E., Hassanein, A.M., Haggag, E.G., 2016. Phytochemical and Biological Study of the Aerial Parts of *Chrozophora oblongifolia* (Delile) Spreng. (Euphorbiaceae). *Journal of Pharmacognosy and Phytochemistry* 5, 17.
- Kolodziejski, J., Gill, S., LUCZKIEWICZ, I., 1964. Localization of sparteine in *Cytisus scoparius* link. (*Sarothamnus scoparius* L. Wimm.) during the vegetation stage. *Acta poloniae pharmaceutica* 21, 501.
- Kumamoto, H., Matsubara, Y., Iizuka, Y., Okamoto, K., Yokoi, K., 1985. Structure and hypotensive effect of flavonoid glycosides in kinkan (*Fortunella japonica*) peelings. *Agricultural and biological chemistry* 49, 2613-2618.
- Lamartiniere, C.A., Zhang, J.-X., Cotroneo, M.S., 1998. Genistein studies in rats: potential for breast cancer prevention and reproductive and developmental toxicity. *The American journal of clinical nutrition* 68, 1400S-1405S.
- Li, S., Wang, P., Deng, G., Yuan, W., Su, Z., 2013. Cytotoxic compounds from invasive giant salvinia (*Salvinia molesta*) against human tumor cells. *Bioorganic & medicinal chemistry letters* 23, 6682-6687.
- Li, X.-C., Ferreira, D., Ding, Y., 2010. Determination of absolute configuration of natural products: theoretical calculation of electronic circular dichroism as a tool. *Current organic chemistry* 14, 1678-1697.
- Mabry, T.J., Markham, K., Thomas, M., 1970a. The ultraviolet spectra of flavones and flavonols, *The systematic identification of flavonoids*. Springer, pp. 41-164.
- Mabry, T.J., Markham, K.R., Thomas, M.B., 1970b. Reagents and procedures for the ultraviolet spectral analysis of flavonoids, *The systematic identification of flavonoids*. Springer, pp. 35-40.
- Mabry, T.J., Markham, K.R., Thomas, M.B., 1970c. *The systematic identification of flavonoids*. Springer.
- Markham, K., Ternai, B., Stanley, R., Geiger, H., Mabry, T., 1978. Carbon-13 NMR studies of flavonoids—III: Naturally occurring flavonoid glycosides and their acylated derivatives. *Tetrahedron* 34, 1389-1397.
- Mouffok, S., Haba, H., Lavaud, C., Long, C., Benkhaled, M., 2012. Chemical constituents of *Centaurea omphalotricha* Coss. & Durieu ex Batt. & Trab. *Records of Natural Products* 6, 292.
- Pereira, O.R., Silva, A.M., Domingues, M.R., Cardoso, S.M., 2012. Identification of phenolic constituents of *Cytisus multiflorus*. *Food Chemistry* 131, 652-659.
- Robinson, T., 1980. *The organic constituents of higher plants: their chemistry and interrelationships*. North Amherst (Mass.: Cordus Press, 1980. iv, 352p.-. En *Chemotaxonomy* (KR, 198206450).
- Saito, K., Suzuki, H., Yamashita, Y., Murakoshi, I., 1994. Isolation and enzymatic synthesis of an ester alkaloid, (-)-3 $\beta$ -hydroxy-13 $\alpha$ -tigloyloxylupanine, from *Cytisus scoparius*. *Phytochemistry* 36, 309-311.
- Shellard, E.J., 1957. *Practical plant chemistry for pharmacy students*. Pitman Medical.
- Slade, D., Ferreira, D., Marais, J.P., 2005. Circular dichroism, a powerful tool for the assessment of absolute configuration of flavonoids. *Phytochemistry* 66, 2177-2215.
- Souza, L.C., Antunes, M.S., Borges Filho, C., Del Fabbro, L., de Gomes, M.G., Goes, A.T.R., Donato, F., Prigol, M., Boeira, S.P., Jesse, C.R., 2015. Flavonoid Chrysin prevents age-related

cognitive decline via attenuation of oxidative stress and modulation of BDNF levels in aged mouse brain. *Pharmacology Biochemistry and Behavior* 134, 22-30.

Wall, M.E., Krider, M.M., Krewson, C., Eddy, C.R., Willaman, J., Corell, D., Gentry, H., 1954. Steroidal sapogenins VII. Survey of plants for steroidal sapogenins and other constituents. *Journal of the American Pharmaceutical Association* 43, 1-7.

Walter, E., 1941. Genistin (an isoflavone glucoside) and its aglucone, genistein, from soybeans. *Journal of the American chemical Society* 63, 3273-3276.

Wiewiorowski, M., Edwards, O., Bratek-Wiewiórska, M., 1967. Conformation of the C15 lupine alkaloids. *Canadian Journal of Chemistry* 45, 1447-1457.

*CHAPTER 2*  
*PHYTOCHEMICAL SCREENING,*  
*EXTRACTION, FRACTIONATION AND*  
*ISOLATION OF CONSTITUENTS OF*  
*HYPERICUM AFRUM*

## II.2. Phytochemical screening, extraction, fractionation and isolation of constituents of *Hypericum afrum*

### II.2.1. Preliminary phytochemical screening

Air-dried powdered aerial parts were subjected to preliminary phytochemical screening for their constituents following the methods described in pages 55-57. The results are summarized in the following table:

**Table II.2. 1.** Results of the preliminary phytochemical screening of *H. afrum* aerial parts

No.	Test	Method/Reagent	Results
1	Alcaloïdes	Dragendorff (Robinson, 1980; Shellard, 1957)	+
2	Tanins	Ferric chloride Formaldehyde (Robinson, 1980; Shellard, 1957)	+
3	Flavonoïdes	Neu's reagent TLC test Sodium hydroxide Ferric chloride (Geissman, 1962)	+
4	Coumarins	UV test (365 nm) (Kamel et al., 2016)	+
5	Terpenes and Steroids	Antimony trichloride test (Hardman and Sofowora, 1972) Lieberman – Buchard's Salkowski's (Carter, 1947; Cook, 1961)	+
6	Saponins	Froth formation Test (Wall et al., 1954)	+
7	Anthraquinones	Borntrager reaction (Bornträger, 1880)	+
+ = present - = absent			

### II.2.2. Determination of Total phenolic and Total flavonoid contents

Total phenolic and Flavonoid contents were measured for the chloroform, ethyl acetate and *n*-butanol fractions of the ethanolic crud extract of *Hypericum afrum*. Lam species as described previously in pages (54-55). The butanol fraction showed the highest phenolic content with a value of 393 mg GAE/g dried extract, followed by ethyl acetate fraction with a value of 386 mg GAE/g dried extract, and chloroform fraction with a value of 260 mg GAE/g dried extract (Figure II.2.1). The results of Flavonoid content were expressed as mg of Quercetin per g dried extract. The ethyl acetate (AcOEt) fraction was found to exhibit the highest TFC values with values of 40.49 and mg Quercetin/ g dried extract. The results are shown in (Table II.2.2).

**Table II.2. 2.** Total phenolic and flavonoid contents of crud extract fractions of *H. afrum*  
 Values expressed are means  $\pm$ SD of three parallel measurements

Fraction	Total phenolic content (mg GA/g dried extract)	Total flavonoid content (mg QE/g dried extract)
Chloroform (CHCl <sub>3</sub> )	260.0 $\pm$ 0.10	23.08 $\pm$ 1.713
Ethyl acetate (EtOAc)	386.0 $\pm$ 21.46	40.49 $\pm$ 0.570
<i>n</i> -butanol ( <i>n</i> -but)	393.0 $\pm$ 15.94	38.08 $\pm$ 0.737

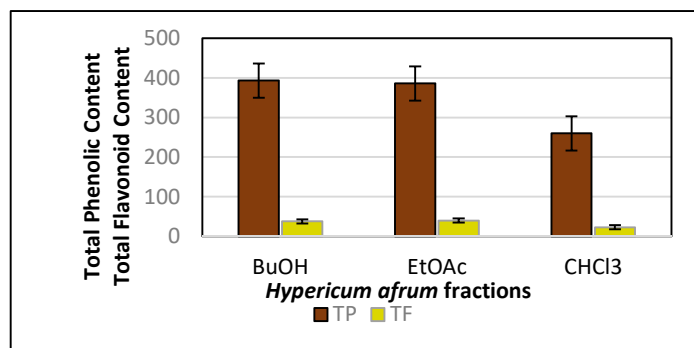


**Figure II.2. 1.** Evaluation of total phenolic and flavonoids in the *H. afrum* fractions

### II.2.3. Extraction and initial fractionation

#### II.2.3.1. Hydroalcoholic extraction

Dried powdered aerial parts (1000 g) of *H. afrum* were macerated at room temperature with EtOH–H<sub>2</sub>O (80:20, v/v) for 24 h, three times. The filtered solvents were combined and evaporated under vacuum at a temperature of 40 °C to give a residue (30 g). The obtained extract was suspended in water (800 mL) and successively partitioned with CHCl<sub>3</sub>, EtOAc and *n*-butanol, yielding 1g (CHCl<sub>3</sub>), 7g (EtOAc) and 12g (*n*-but) soluble fractions.

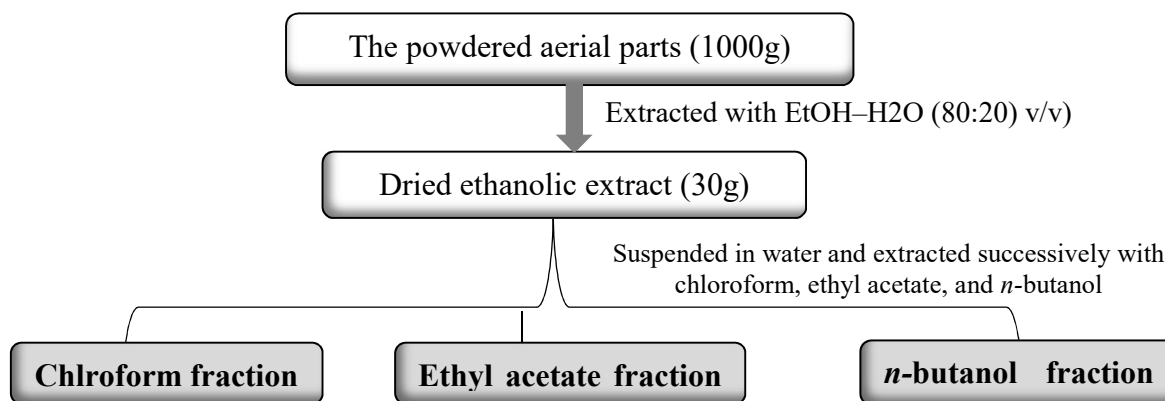


**Figure II.2. 2.** Extraction and fractionation of the powdered aerial parts of *Hypericum afrum*

### II.2.3.2. Isolation of the active constituents of the chloroform soluble fraction

The chloroformic extract (1 g) was subjected to silica gel column chromatography (230–400 mesh) using a step-gradient system hexane/CHCl<sub>3</sub> and then with increasing percentages of MeOH to afford ten fractions (HCF-1 to -10) obtained by combining the eluates on the basis of TLC analysis. Each fraction was monitored by TLC on silica gel using system AcOEt/MeOH (8:2)

- HCF-4 (50 mg, hexane/CHCl<sub>3</sub> 7:3) yielded compound **HAT1** (β-sitosterol) (14 mg) through crystallization with MeOH.
- HCF-6 (350 mg, CHCl<sub>3</sub> 100%) was subjected to SPE RP-18 column chromatography, using MeOH/H<sub>2</sub>O elution to give six subfractions S1 to S6. Each fraction was monitored by TLC on silica gel using system AcOEt/MeOH (8:2)
- The subfraction S1 (200mg) was subjected to Sorbadex 20-LH column chromatography using CH<sub>2</sub>Cl<sub>2</sub>/MeOH (1:1, v/v) elution and yielded compound **HAP1**(New compound) (50 mg)

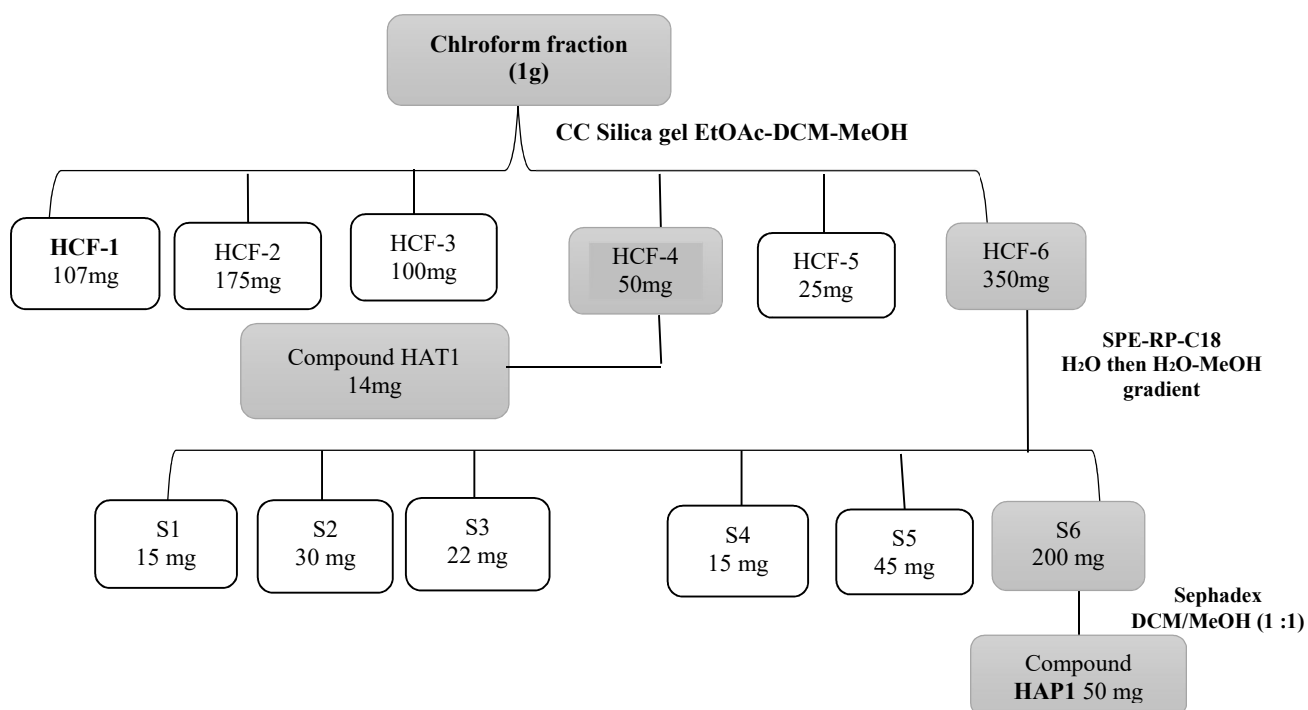


**Figure II.2. 3.** Fractionation of the Chloroform fraction and isolation of its compounds

### II.2.3.3. Isolation of the active constituents of the ethyl acetate soluble fraction

The ethyl acetate fraction (EtOAc) (7 g) was chromatographed on a silica gel column and eluted with CH<sub>2</sub>Cl<sub>2</sub>/MeOH solvent system of increasing polarity to yield 10 subfractions according to their TLC behavior. The subfractions HEF-1 to HEF-10. Each fraction was monitored by TLC on silica gel using system EtOAc/MeOH (8:2)

- The subfraction HEF-3 (115 mg) was subjected to a column of sephadex LH-20 with CH<sub>2</sub>Cl<sub>2</sub>/MeOH (1:1) as eluent yielding compound **HAF1** (16 mg) as a yellow precipitate, the liquid supernatant was further rechromatographed on column of sephadex LH-20 using CH<sub>2</sub>Cl<sub>2</sub>/MeOH (1:1) as eluent to afford compound **HAN1** (2mg) and compound **HAN2** (1mg).
- The subfraction HEF-4(10%MeOH) was rechromatographed on SephadexLH-20 eluted with methanol to furnish compound **HAB1** (10 mg).
- **HEF-5** (20%MeOH). (125 mg), was rechromatographed on Sephadex LH-20 column with Methanol to afford compound **HAN2**(1 mg) and compound **HAF2** (10mg).
- A yellow precipitate was obtained from the subfraction HEF-7 (40% MeOH in CH<sub>2</sub>Cl<sub>2</sub>). The solid was combined and subjected to a column of sephadex LH-20 eluted with methanol to furnish compound **HAF3** (7 mg).

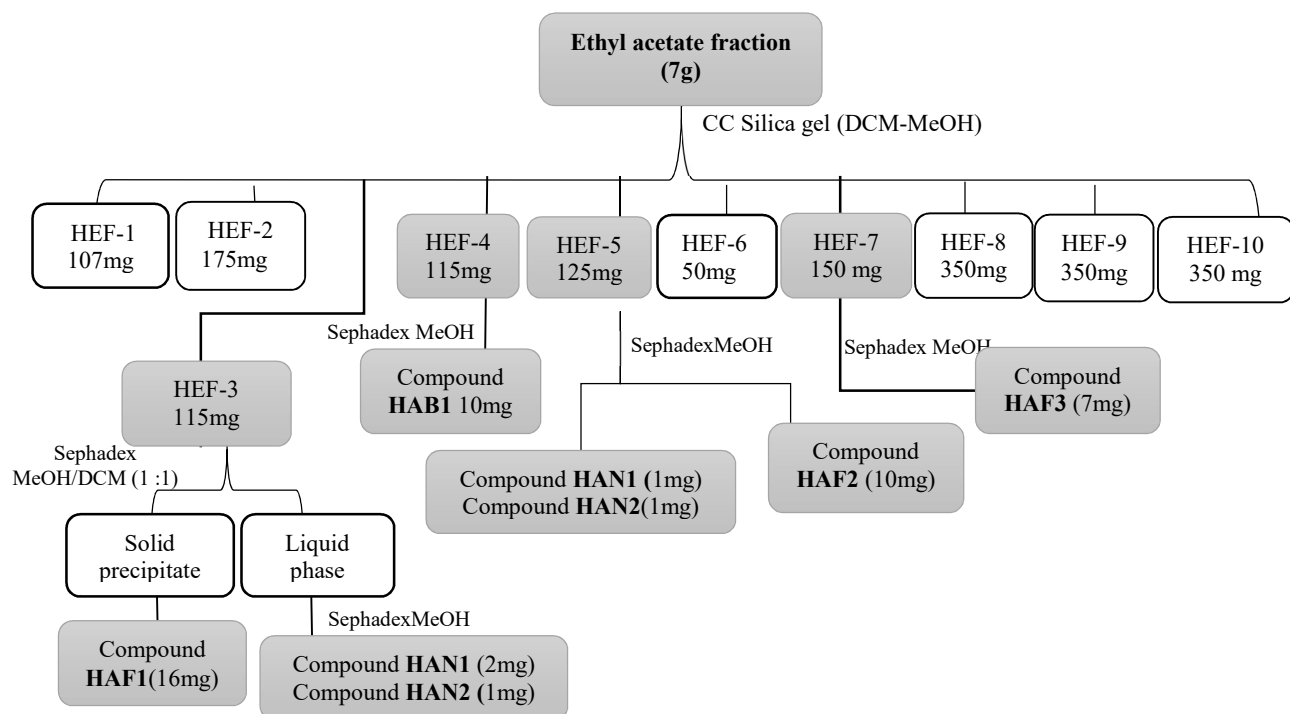


**Figure II.2. 4.** Fractionation of the Ethyl acetate fraction and isolation of its compounds

#### II.2.3.4. Isolation of the active constituents of the *n*-butanol soluble fraction

The *n*-butanol fraction (12g) was subjected to Diaion-HP20 (30 g) CC [5 (ID)× 30 (L) cm] which was eluted with distilled water then methanol to give two main fractions.

- Fraction HBF-2 (5 g) was subjected to MN-polyamide-SC-6 (225 g) CC [5 (ID)× 100 (L) cm] which was eluted initially with water then gradient decreased polarities with water-methanol systems 100% H<sub>2</sub>O, (90:10), (80:20), (70:30) and (60:40) (50:50) (30:70) and 100% MeOH to deliver 8 main fractions (HBF2-A to HBF2-H) Each fraction was monitored by TLC on silica gel using system AcOEt/MeOH (8:2)
- Subfraction HBF-2-C (250 mg) was subjected to Sephadex LH-20 (50 g) eluted with MeOH to afford compounds **HAC1** (10.0 mg) and **HAC2** (11.5mg).
- Subfraction HBF-2-D (H<sub>2</sub>O 6/4 MeOH). (50 mg) was further subjected to a column of Sephadex LH-20(20 g) eluted with MeOH/CH<sub>2</sub>Cl<sub>2</sub> (1:1) to afford compounds **HAF4**(4.0 mg).
- HBF-2-E (70 mg) was subjected to a column of Sephadex LH-20 (30 g) eluted with MeOH/CH<sub>2</sub>Cl<sub>2</sub> (1:1) to afford compounds **HAF5**(5 mg) and compound **HAF6** (10.6 mg).

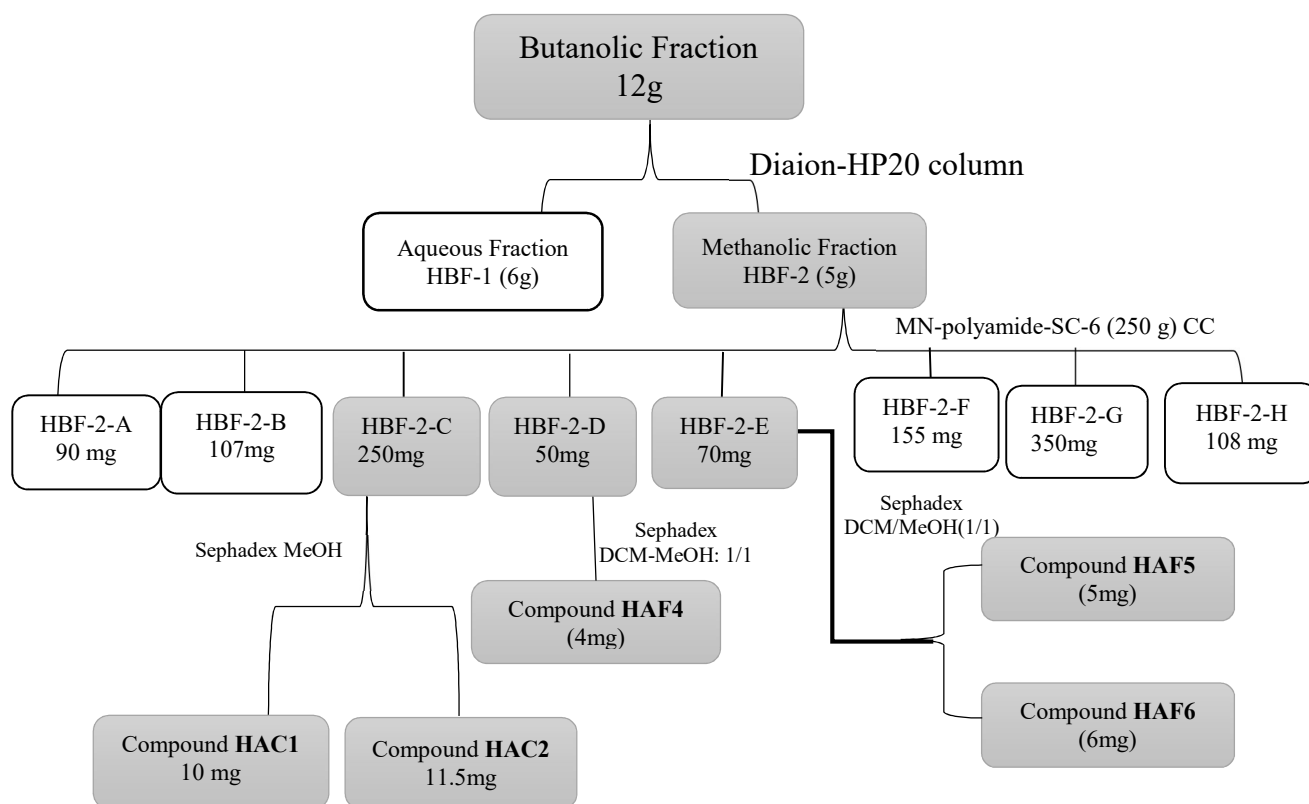


**Figure II.2. 5.** Fractionation of the *n*-butanol fraction and isolation of its compounds



## II.2.4. Identification and structure elucidation of the isolated compounds

### II.2.4.1. Sterols

#### II.2.4.1.1. Compound HAT1

##### i. Physical properties

Compound **HAT1** (10 mg) was obtained as a white amorphous powder.

##### ii. Chromatographic characters

Compound **HAT1** appeared as a single spot, which gave a violet color with pinkish tinge after spraying with 10% v/v vanillin/H<sub>2</sub>SO<sub>4</sub> using precoated silica gel plates after heating at 110 °C. It had *R<sub>f</sub>* value of 0.64 using system VII (page 48).

##### iii. Spectroscopic data

**A. UV (MeOH):**  $\lambda_{\max}$  (log  $\epsilon$ ): 292,1 (3.80).

##### **B. <sup>1</sup>H-, <sup>13</sup>C-NMR and HMBC spectral analysis**

The <sup>1</sup>H-, <sup>13</sup>C-NMR and HMBC spectral data of compound **HAT1** are listed in (Table II.2.3) and illustrated in figure thereafter.

**Table II.2. 3.** <sup>1</sup>H-, <sup>13</sup>C-NMR and HMBC spectral data of compound **HAT1** (600 MHz, 175 MHz, CDCl<sub>3</sub>)

Position	$\delta_H$ (ppm), multiplicity, <i>J</i> (Hz)	$\delta_C$ (ppm)
1	0.70-2.0 (m, 2H)	37.3
2	0.70-2.0 (m, 2H)	29.7
3	3.55 (m, 1H)	71.8
4	2.30 (m, 1H)	42.3
5	-	140.7
6	5.37 (d, <i>J</i> =5.3 Hz, 1H)	121.7
7	0.70-2.0 (m, 2H)	31.9
8	0.70-2.0 (m, 1H)	31.6
9	0.70-2.0 (m, 1H)	50.1
10	-	36.2
11	0.70-2.0 (m, 2H)	21.2
12	0.70-2.0 (m, 2H)	39.8
13	-	42.3
14	0.70-2.0 (m, 1H)	56.8

15	0.70-2.0 (m, 2H)	24.7
16	0.70-2.0 (m, 2H)	28.3
17	0.70-2.0 (m, 1H)	56.1
18	1.01(s, 3H)	11.9
19	0.70(s, 3H)	19.4
20	0.70-2.0 (m, 1H)	40.5
21	0.95(d, 3H)	24.3
22	0.70-2.0 (m, 2H)	33.9
23	0.70-2.0 (m, 2H)	26.1
24	0.70-2.0 (m, 1H)	51.2
25	0.70-2.0 (m, 1H)	29.2
26	0.90(t, 3H)	19.1
27	0.83(d, 6.0, 3H)	19.4
28	0.70-2.0 (m, 2H)	25.0
29	0.86 (d, 3H)	12.0

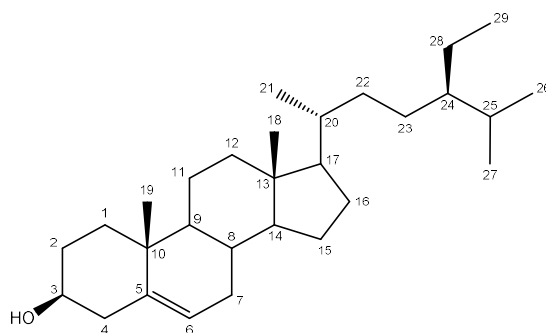
#### iv. Discussion and Conclusion

Compound **HAT1** was isolated as a white powder. The  $^1\text{H-NMR}$  spectrum (Figure II.2.6) of compound **HAT1** showed one olefinic proton at  $\delta_H = 5.37$  (d,  $J=5.3$  Hz, 1H), corresponding to the ethylenic proton connected to C-6, and a proton signal appeared at  $\delta_H = 3.55$  (m, 1H), corresponding to a proton connected to an oxygenated carbon, should be the proton connected to C-3 of sterol.

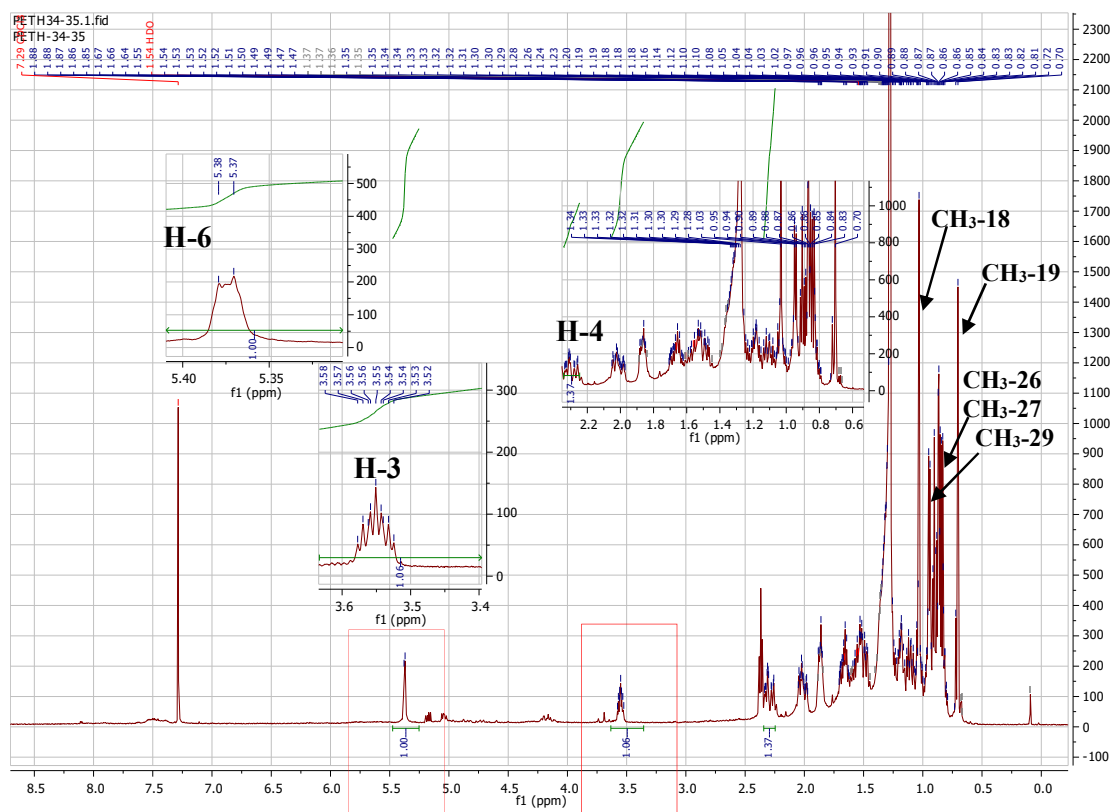
The  $^1\text{H-NMR}$  spectrum of **HAT1** showed also the presence of six methyl signals that appeared as two methyl singlets at  $\delta_H = 0.70$ , and  $\delta_H = 1.01$ ; three methyl doublets that appeared at  $\delta_H = 0.83$ ,  $0.86$ , and  $0.95$  ppm; and a methyl triplet at  $\delta_H = 0.90$ . Rest of protons appeared in the high field region in between  $\delta_H$  0.70-2.0 ppm (Sultana et al., 2011).

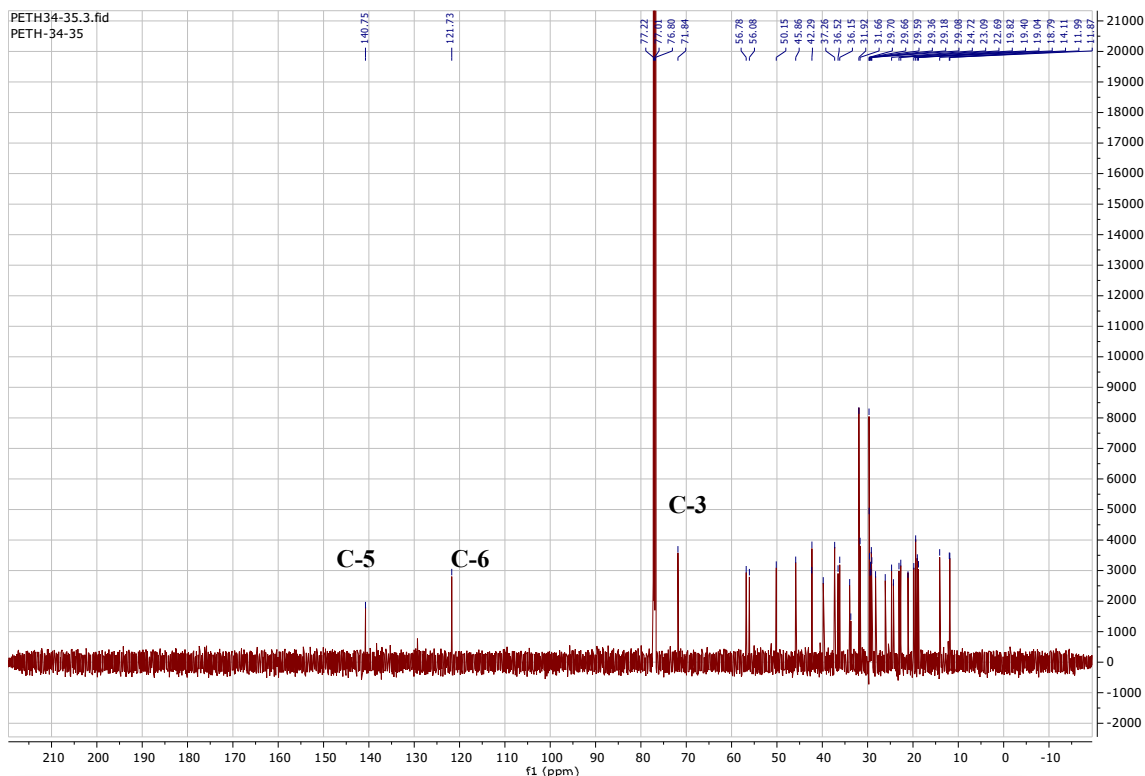
The  $^{13}\text{C-NMR}$  spectrum (Figure II.2.7) together with **DEPT** (Figure II.2.8) and **HSQC** (Figure II.2.10) showed twenty-nine carbon signal including six methyls, eleven methylenes, ten methane and three quaternary carbons, the alkene carbons appeared at  $\delta_C = 140.7$  and  $121.7$  ppm. Thus, the structure of **HAT1** was assigned as  **$\beta$ -sitosterol** that was consistent to the reported literature values (Habib et al., 2007; Zhang et al., 2005) and confirmed by co-chromatography with an authentic sample of  **$\beta$ -sitosterol**.

$\beta$ -sitosterol also known as phytosterol is the most common plant sterol. It has been proved to have many important bioactivities, such as anti-inflammatory, antibacterial, antifungal and antitumor properties (Ling and Jones, 1995; Loizou et al., 2010). It is usually used for heart disease, hypercholesterolemia, modulating the immune system, prevention of cancer, as well as for rheumatoid arthritis, tuberculosis, cervical cancer, hair loss and benign prostatic hyperplasia (Saeidnia et al., 2014).

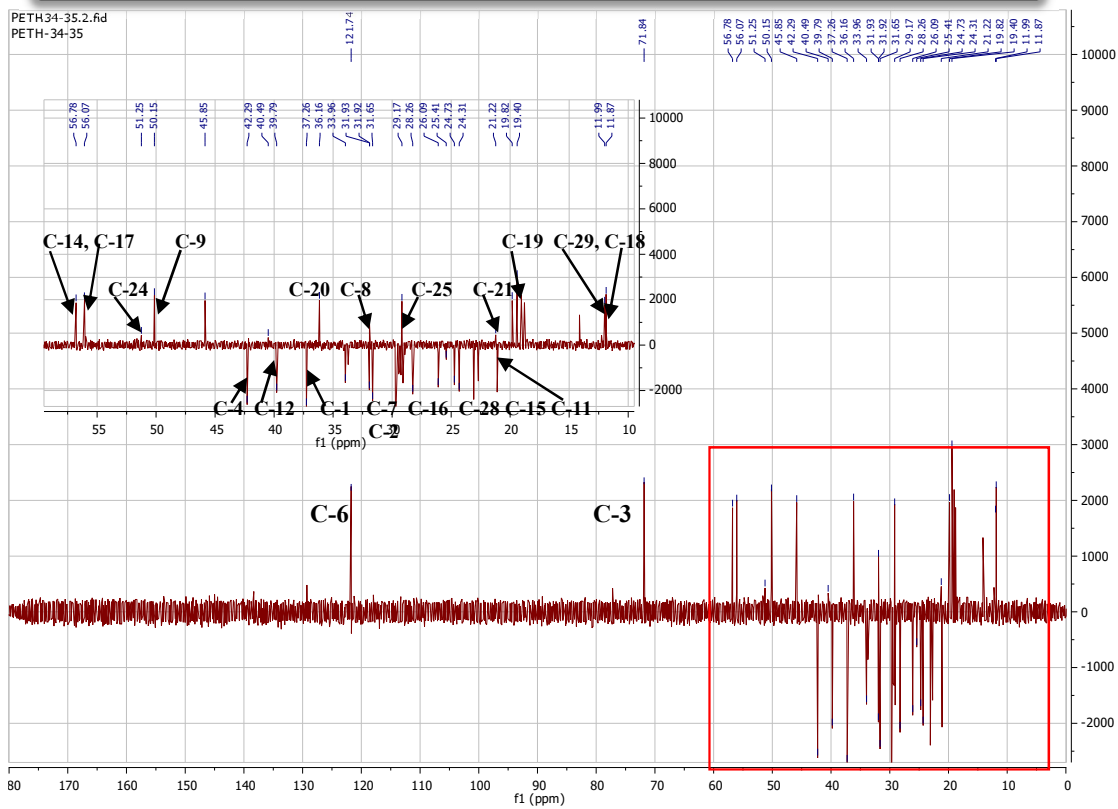


**$\beta$ -Sitosterol**





**FigureII.2. 7. <sup>13</sup>C-NMR Spectrum of compound HAT1(CDCl<sub>3</sub>, 175 MHz)**



**FigureII.2. 8. DEPT135 Spectrum of compound HAT1**

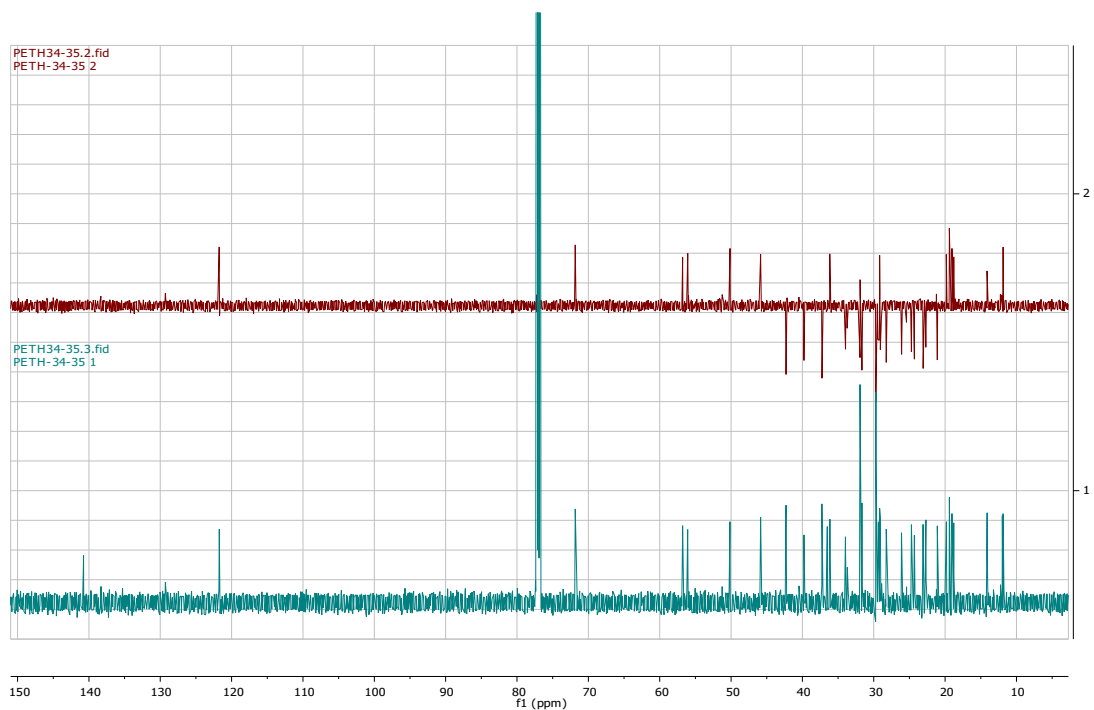


Figure II.2. 9. Comparison of  $^{13}\text{C}$ -NMR and DEPT135 Spectrum of compound HAT1

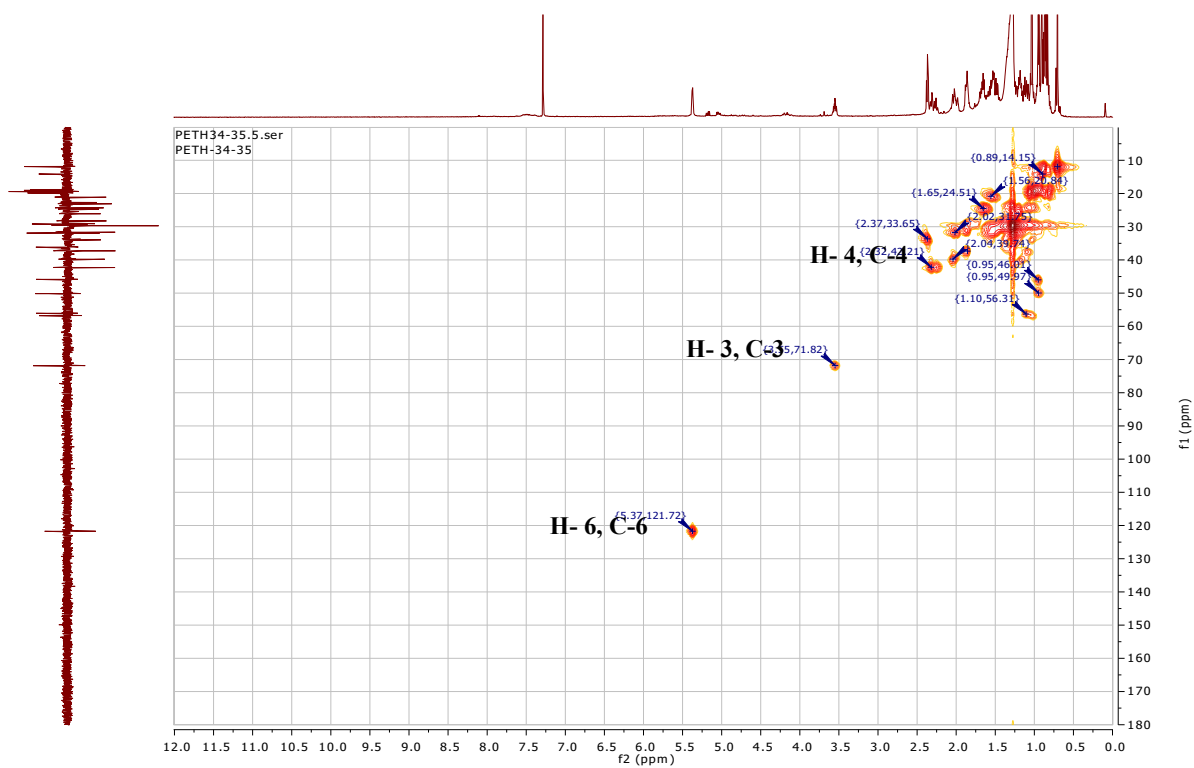


Figure II.2. 10. HSQC Spectrum of compound HAT1

### II.2.4.2. Phloroglucinols

#### II.2.4.2.1. Compound HAP1

##### i. Physical properties

Compound **HAP1** (50 mg) was obtained as a yellow amorphous solid;  $[\alpha]_D^{25} + 21$  (c 0.05, MeOH).

##### ii. Chromatographic characters

Compound **HAP1** appeared as a dark spot under UV  $\lambda_{\max}$  254 which attained a clear yellowish color after spraying with 10% v/v vanillin/H<sub>2</sub>SO<sub>4</sub> and heating at 110 °C (Figure II.2.11). It showed  $R_f$  value of 0.40 in system VII (Page 48).



**Figure II. 11.** Profiles of silica gel TLC of compound **HAP1**

##### iii. Spectroscopic data

**A. UV (MeOH)**  $\lambda_{\max}$  (log  $\epsilon$ ): 220 (5.05), 291.0 (4.88) 330.0 (4.83)

**B. IR (KBr)**  $\nu_{\max}$ : 3440, 1742, 1683, 1450, 1415, 1237, 765  $\text{cm}^{-1}$ .

**C. HR-ESI-MS:** A molecular ion peak at  $m/z$  313.1050  $[\text{M}-\text{H}]^-$  (calcd. 313.1054) for **C<sub>18</sub>H<sub>18</sub>O<sub>5</sub>**.

**D. <sup>1</sup>H-, <sup>13</sup>C-NMR and HMBC** spectral analysis

The <sup>1</sup>H-, <sup>13</sup>C-NMR, <sup>1</sup>H-<sup>1</sup>H-COSY and HMBC spectral data of compound **HAP1** are listed in table II.2.4 and illustrated in figures thereafter.

**Table II.2. 4.**  $^1\text{H}$ -,  $^{13}\text{C}$ -NMR and HMBC spectral data of compound **HAP1**  
(500 MHz, 125MHz  $\text{CDCl}_3$ )

Position	$\delta_H$ (ppm), multiplicity and $J$ in Hz	$\delta_C$ (ppm)	HMBC (H $\rightarrow$ C)	$^1\text{H}$ - $^1\text{H}$ -COSY
1	-	200.3	-	-
2	-	181.5	-	-
3	-	121.9	-	-
4	-	213.9	-	-
5	-	50.6	-	-
6	1.04, s, 3H	19.0	C-1', 5, 1, 4	-
1'	Ha -1' ; 2.30, dd, $J = 14.1, 8.1$ Hz, 1H Hb -1' ; 2.38, dd, $J = 14.1, 7.4$ Hz, 1H	34.2	C-1, 4, 3',2'	2'
2'	4.93, t, $J = 7,7$ Hz, 1H	118.6	C-4', 5', 1'	1', 4'
3'	-	135.2		-
4'	1.54, s, 3H	25.8	C-2', 3'	2'
5'	1.56, s, 3H	17.6	C-2', 3'	-
"1	-	139.0		-
2'',6''	7.55, d, $J = 7,5$ Hz,2H	129.0	C-7'', 3'', 4''	3'', 5''
3'', 5''	7.28, t, $J = 7,6$ Hz,2H	127.7	C-1'', 4''	2'',6'', 4''
"4	7.42, t, $J = 7,4$ Hz,1H	132.1	C-3'', 5''	3'', 5''
7''	-	194.7	-	-

#### iv. Discussion and conclusion

Compound **HAP1** was isolated as a yellow powder and its molecular formula was established as  $\text{C}_{18}\text{H}_{18}\text{O}_5$  on the basis of the negative HR-ESI-MS ( $[\text{M}-\text{H}]^-$ ) at  $m/z$  313.1050 (calcd. 313.1054) (FigureII.2.15).

The IR (FigureII.2.15) absorptions implied the presence of hydroxyl at ( $3430\text{ cm}^{-1}$ ), and carbonyl and phenyl groups at ( $1742\text{ cm}^{-1}$ ,  $1683$ ,  $1450\text{ cm}^{-1}$ ) functionalities.

In the UV spectrum of **HAP1**, absorption maxima were observed at 220, 291, 330 nm revealing the presence of the conjugated system (Yoshikawa et al., 2006).

The  $^1\text{H}$  NMR spectrum (FigureII.2.17) showed characteristic signals for three methyl groups at  $\delta_H = 1.56$  and  $1.54$  ppm (each, 3H, s), and  $\delta_H = 1.04$  ppm (3H, s) the first two methyl corresponding to a gem-dimethyl group attached to a double bond; along with

the signals at  $\delta_H$  2.30 and 2.38 ppm (dd,  $J = 14.1, 7.4$  Hz, and dd,  $J = 14.1, 8.1$  Hz, 1H) characteristic of aliphatic protons; and vinylic proton at  $\delta_H = 4.93$  ppm (1H, t,  $J = 7,7$  Hz) suggested the presence of an isoprenyl group in the molecule, which was confirmed by COSY and HMBC experiments (Figures II.2.21-22)

Also, in the  $^1H$  NMR spectrum we had three signals at  $\delta_H = 7.55$  ppm (2H, d,  $J = 7,5$  Hz), 7.42 ppm (1H, t,  $J = 7,4$  Hz) and 7.29 ppm (1H, t,  $J = 7,6$  Hz) indicated a monosubstituted phenyl group.

The  $^{13}C$  NMR together DEPT 135 spectra (Figures II.2.18-20) of HAP1 disclosed 18 carbons, which were indicative of four ketone carbonyl carbons at  $\delta_C = 213.9, 200.3, 194.7$  and  $181.5$  ppm; additional two  $sp^2$  quaternary carbons at  $\delta_C = 139.0$  and  $135.2$  ppm, one  $sp^3$  quaternary carbon at  $\delta_C = 50.6$  ppm and one oxygenated quaternary carbon at  $\delta_C = 121.9$  ppm, six methine, three methyl and one methylene carbons.

The full assignment of  $^1H$ - and  $^{13}C$ -NMR resonances was supported by  $^1H$ - $^1H$  COSY, DEPT, HSQC and HMBC spectral analyses.

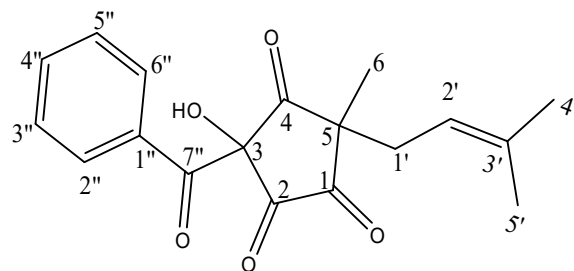
According to the HSQC spectrum (Figure II.2.21), the three methyl signals were found at  $\delta_C = 25.8, 19.0,$  and  $17.6$  ppm.

$^1H$ - $^1H$ -COSY (Figure II.2.22) cross peaks of H-2' to H-1'-b and H-1'-a, and of both H-1'-a and H-1'-b to H-2', together with HMBC (Figure II.2.23) correlations which showed cross peaks from CH<sub>3</sub>-4' to C-5', CH<sub>3</sub>-5' to C-2', H-2' to C-4', C-5' and C-2', H-1' to both C-2' and C-5, and CH<sub>3</sub>-6 to C-1', C-1, C-4 and C-5 indicated that HAP1 had a 3'-methylbut-2'-en-1'-yl group at C-5.

HMBC spectrum showed cross peaks from H<sub>3</sub>C-6 to C-1', C-1 and C-4, and from both H<sub>3</sub>C-6 and H-1' to C-5 permit joining to the remaining methyl (CH<sub>3</sub>-) and determining the connections among the rest of the structural fragments.

According to the above data, compound HAP1 is established as a new natural phloroglucinol (*Prenylated benzoyl nor-phloroglucinol*) with three ketocyclopentane moiety. Interestingly, the presences of compounds with two or three ketocyclopentane moiety like compound HAP1 only have been reported from *Humulus lupulus* as phloroglucinol derivatives (Van Cleemput et al., 2009). Therefore, compound HAP1 was identified as **3-benzoyl-3-hydroxy-5-methyl-5-(3-methylbut-2-en-1-yl) cyclopentane-1,2,4-trione**.





Structure of Compound HAP1

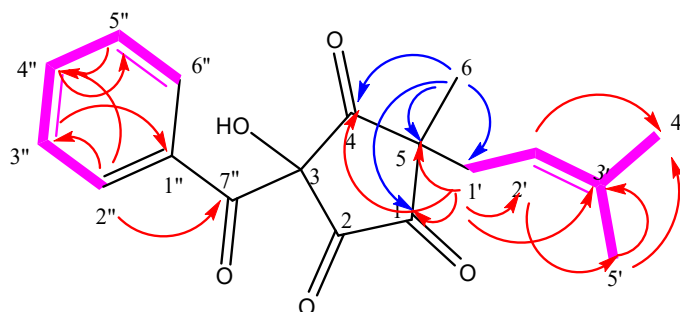
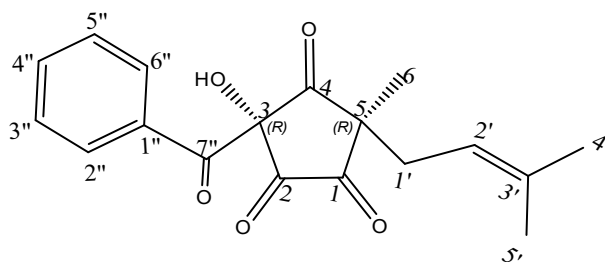


Figure II.2. 12. Important COSY (—) and HMBC (H→C) correlation of compound HAP1

#### - Determination of the absolute configuration

The new compound **HAP1** possess two stereogenic centers (C-3, C-5) and was optically active ( $[\alpha]_{D}^{25} = +21$ ). Circular dichroism spectra were taken to determine the absolute configuration at carbons **C-3** and **C-5** in the molecule.

The experimental **ECD** spectrum showed a high-amplitude negative cotton effect at **250 nm**. The ECD spectra of the possible stereoisomers of new compound **HAP1** were calculated to match with the experimental one, using both NMR and ECD to confirm the structure of compound **HAP1**. The dominant conformer of the assigned stereoisomer of compound **HAP1** is the one whose calculated ECD spectrum showed the best matching to the experimental ECD spectrum. The calculated ECD spectra of all possible isomers were compared with the experimental one (Figure II.2.13). The (**R, R**) isomer matched well the experimental results. Therefore, the compound **HAP1** was identified as (**3R,5R**)-3-benzoyl-3-hydroxy-5-methyl-5-(3-methylbut-2-en-1-yl) cyclopentane-1,2,4-trione. Among the conformers obtained for the (**R, R**) isomer, five of them contributed more than 98% in the Boltzmann distribution (Figure II.14).



**Stereochemistry of compound HAP1:**  
**(3*R*,5*R*)-3-benzoyl-3-hydroxy-5-methyl-5-(3-methylbut-2-en-1-yl)**  
**cyclopentane-1,2,4-trione.**

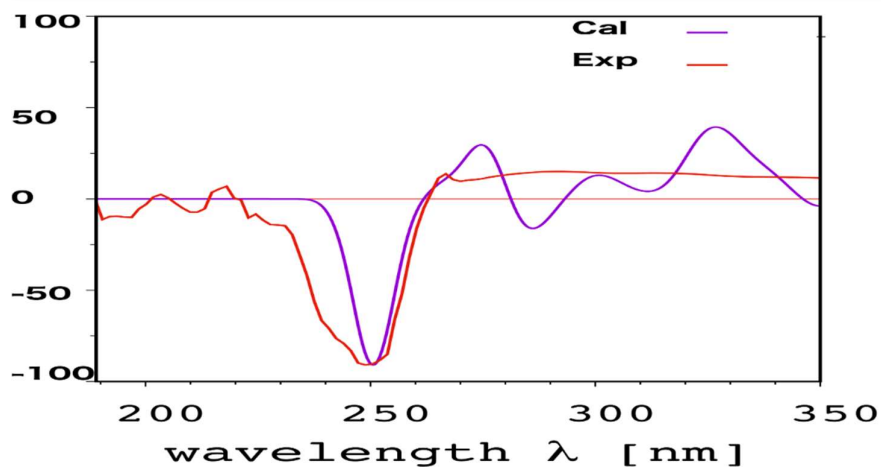


**Figure II.2. 13.** The experimental and calculated ECD spectra of compound HAP1  
 Both spectra showed a negative cotton effect at 250 nm.

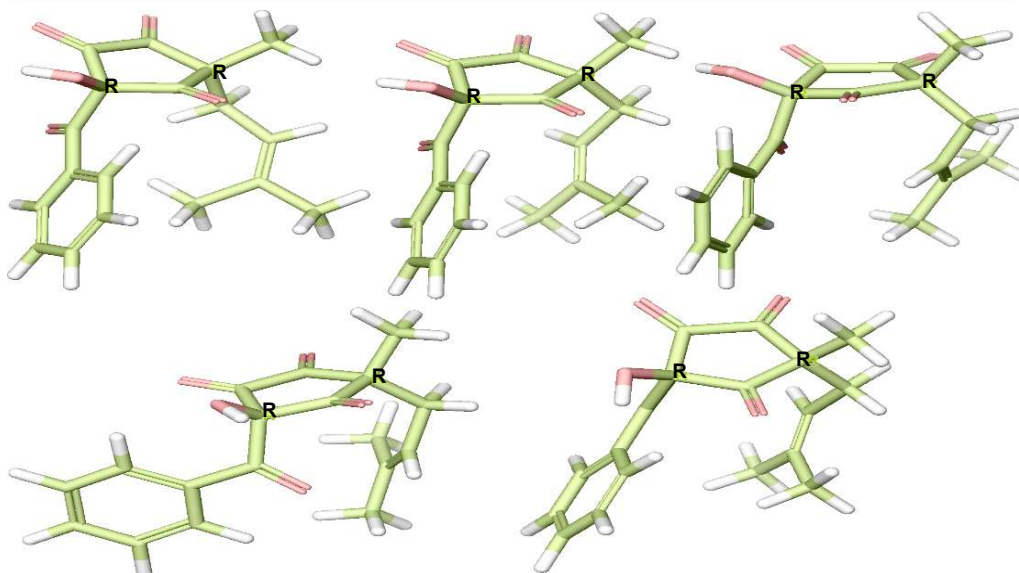


**Figure II.2. 14.** The most abundant conformers of isomer (*R*, *R*) of compound HAP1

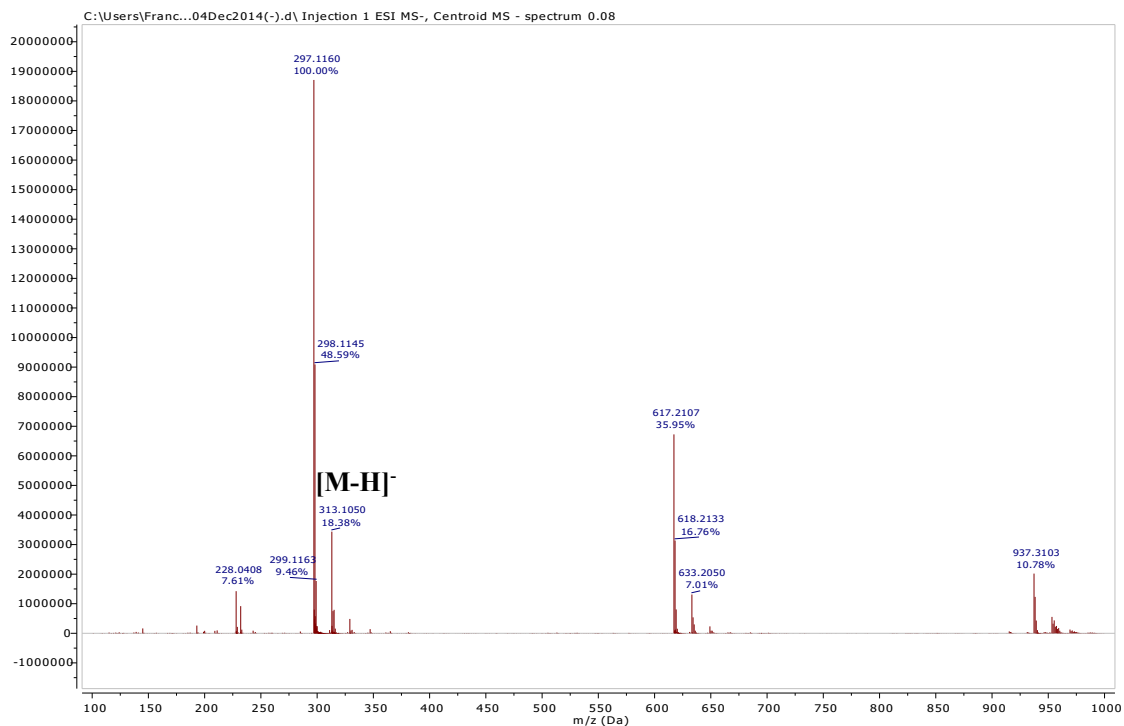


Figure II.2. 15. Negative HRESIMS of compound HAP1

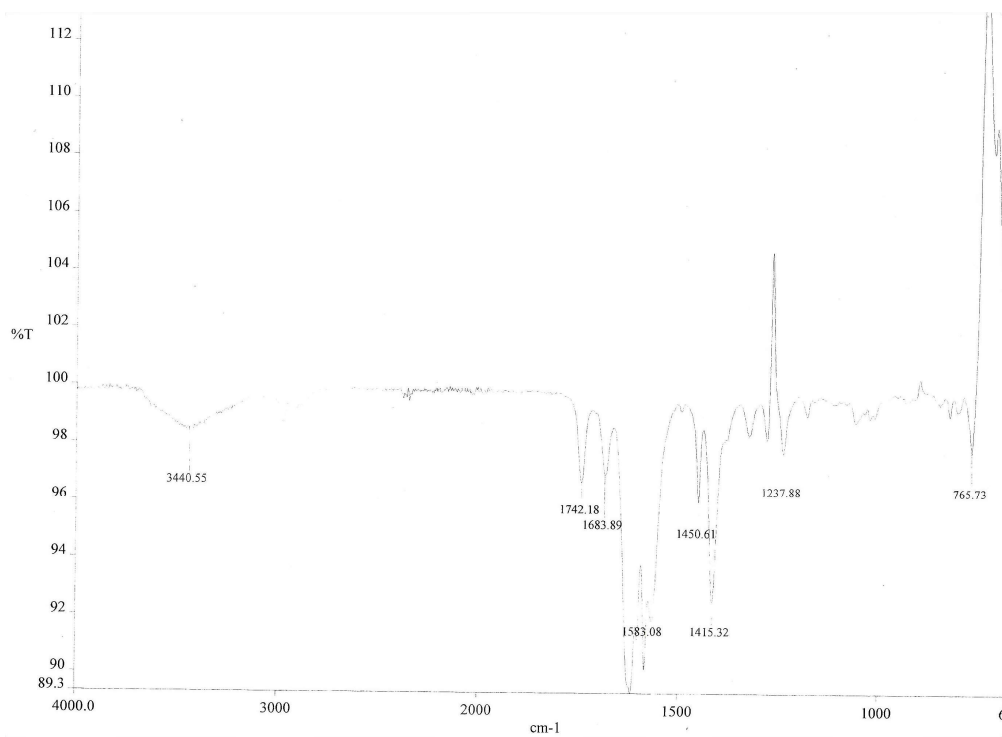


Figure II.2. 16. The IR spectrum of compound HAP1

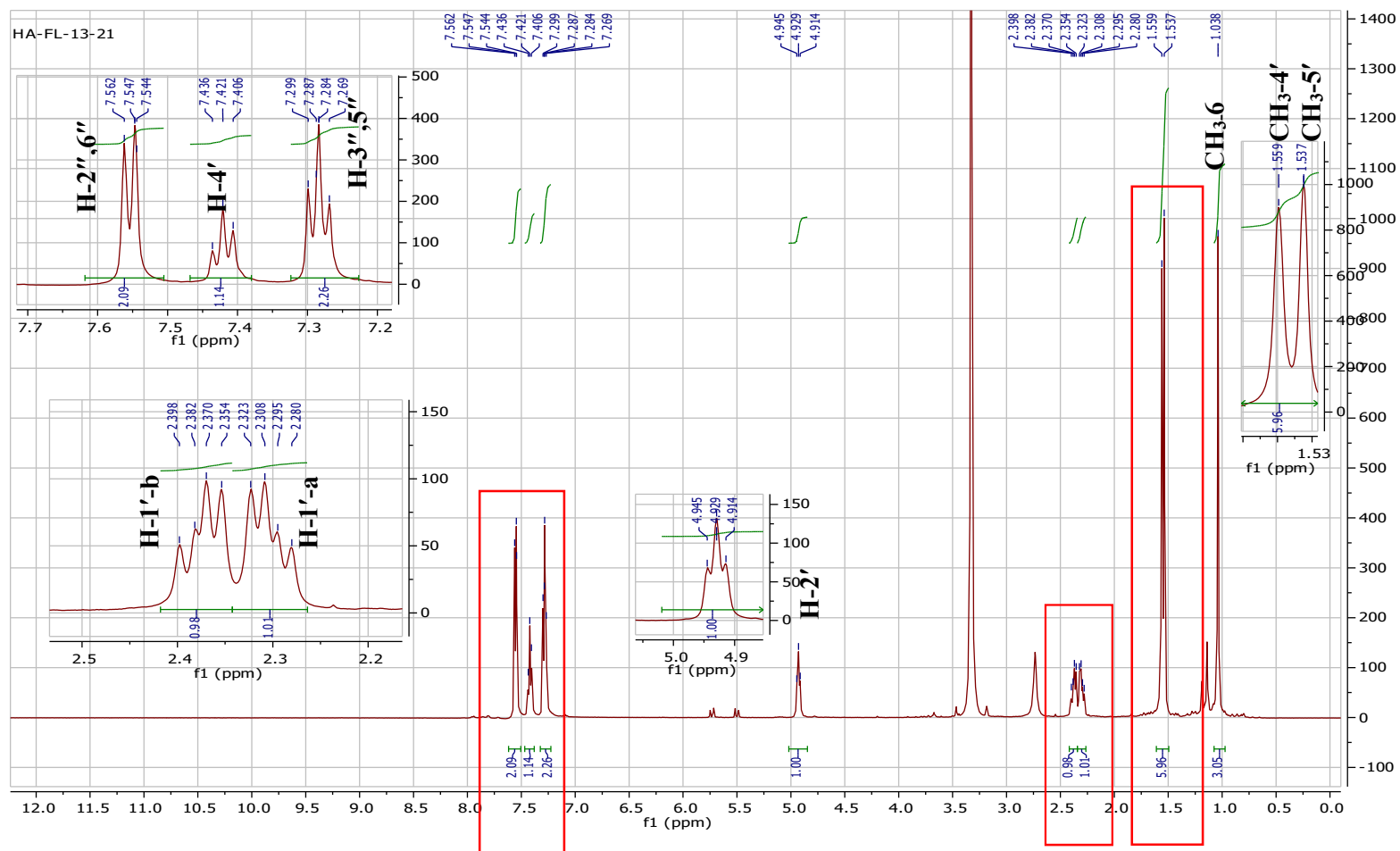


Figure II.2.  $^1\text{H-NMR}$  Spectrum of compound HAP1 ( $\text{CDCl}_3$ , 500 MHz)

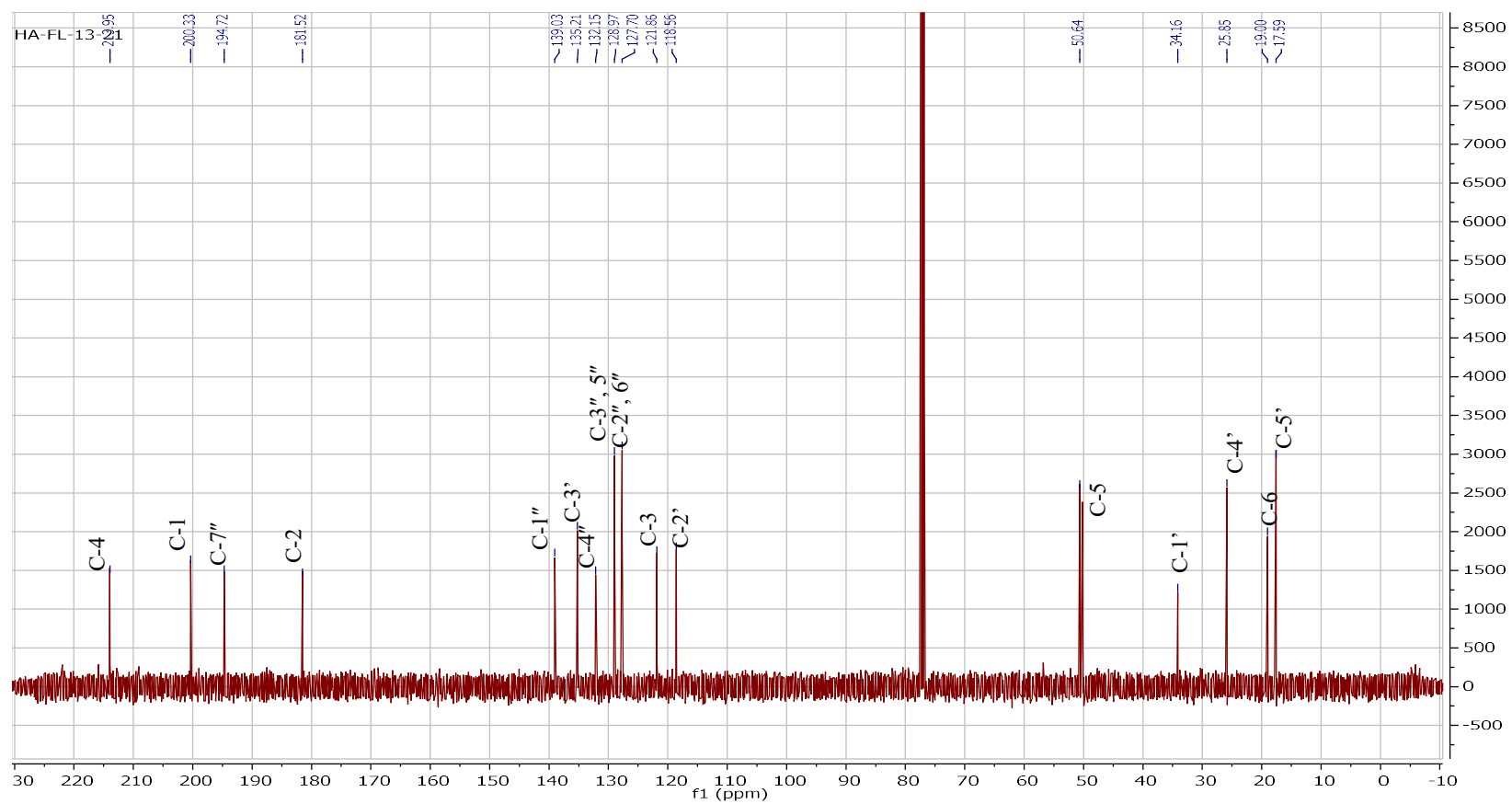


Figure II.2. 18. <sup>13</sup>C-NMR Spectrum of compound HAP1 (CDCl<sub>3</sub>, 125 MHz)

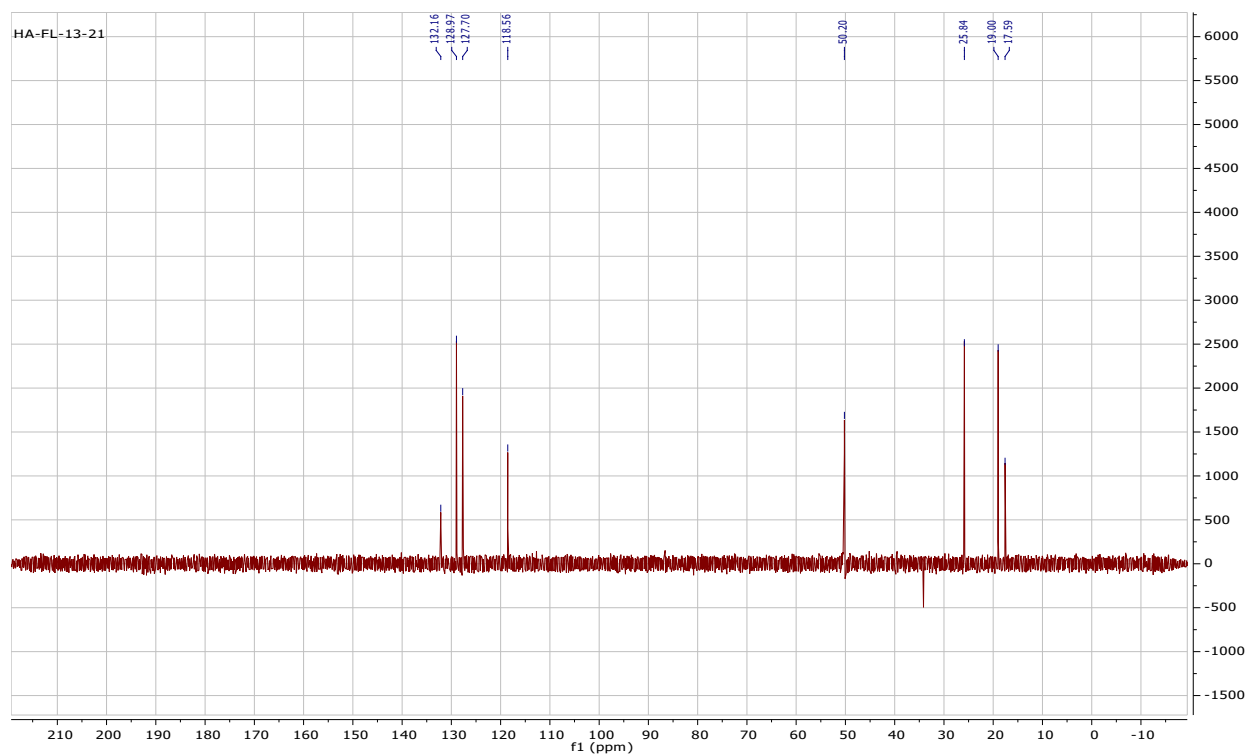


Figure II.2. 19. DEPT135 Spectrum of compound HAP1

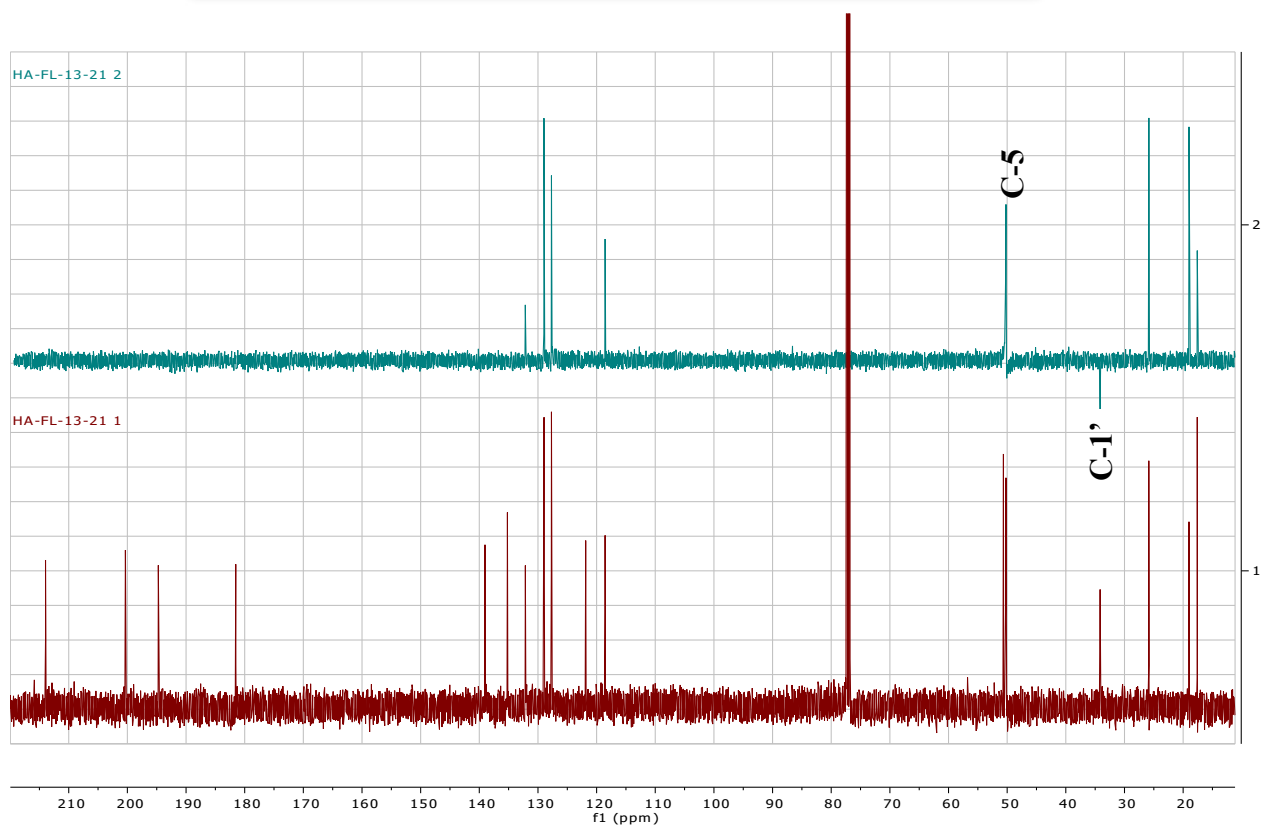


Figure II.2. 20. Comparison of  $^{13}\text{C}$ -NMR and DEPT135 Spectra of compound HAP1

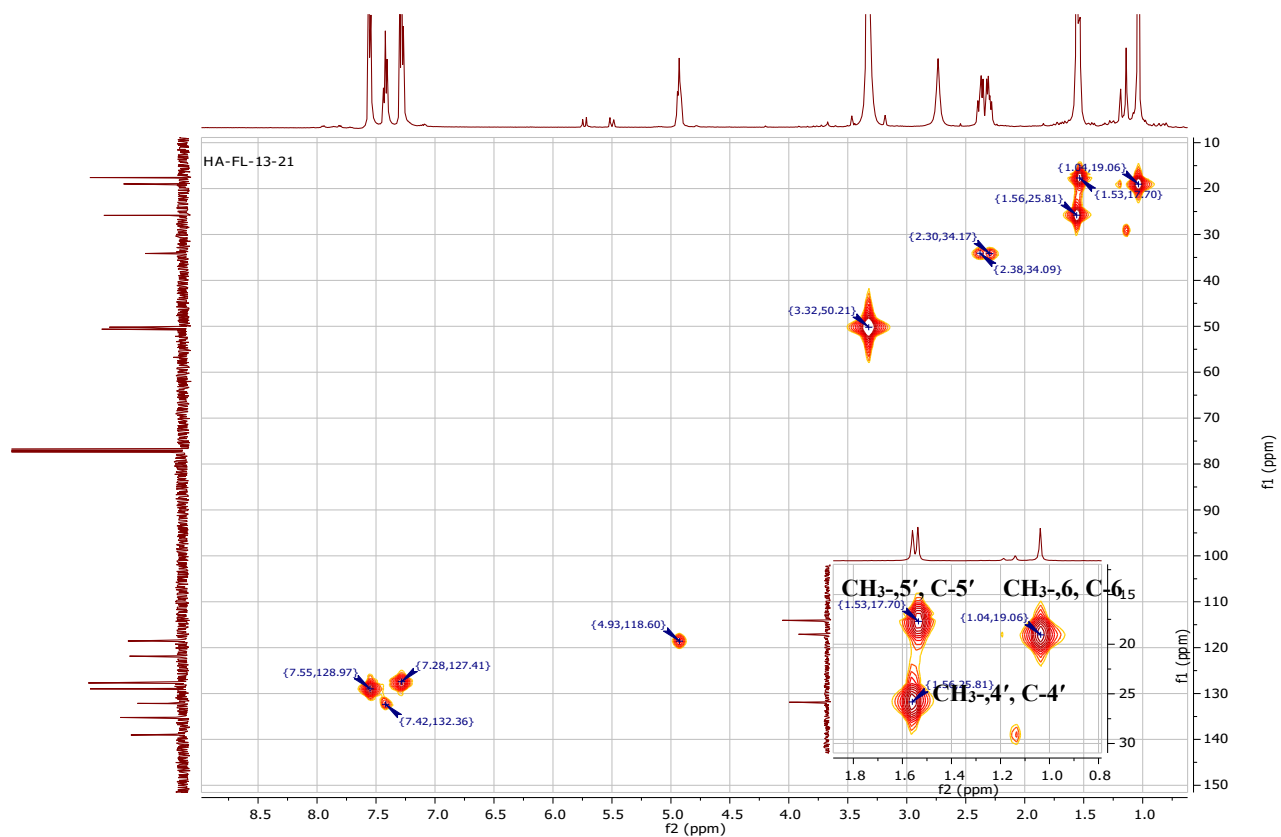


Figure II.2. 21. HSQC Spectrum of compound HAP1

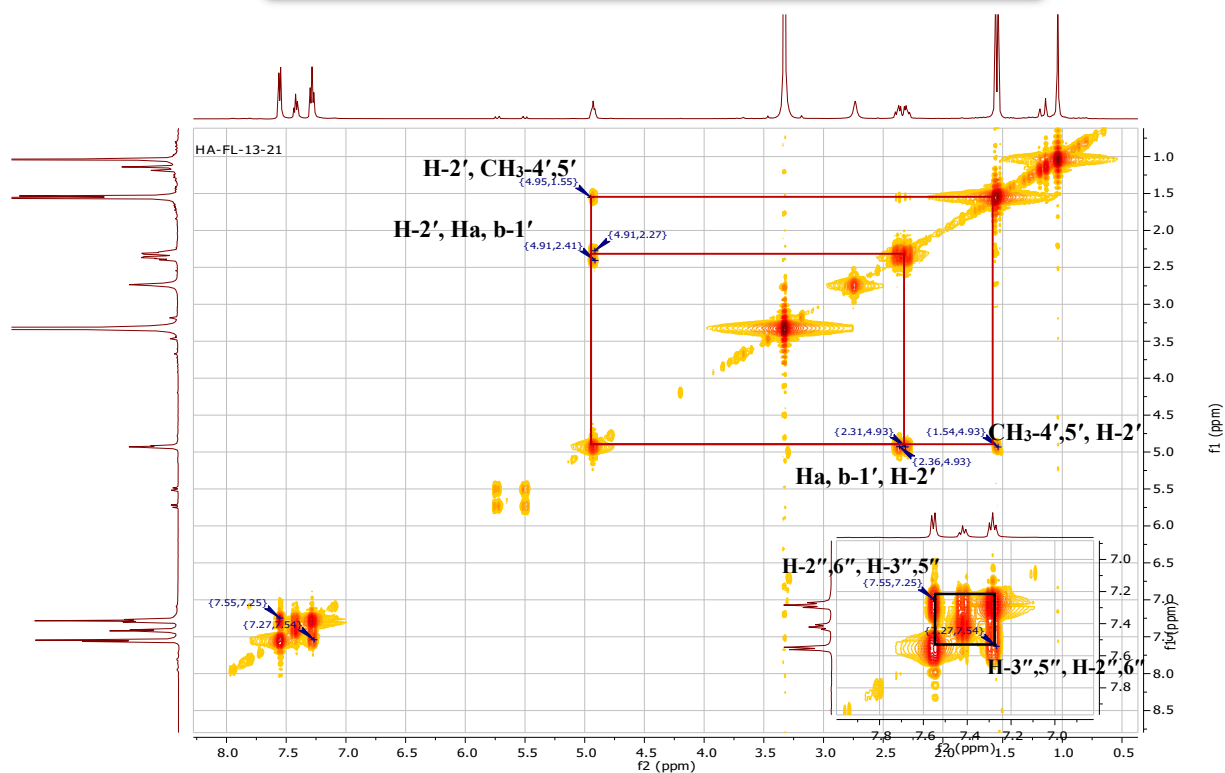


Figure II.2. 22.  $^1\text{H}$ - $^1\text{H}$  COSY Spectrum of compound HAP1

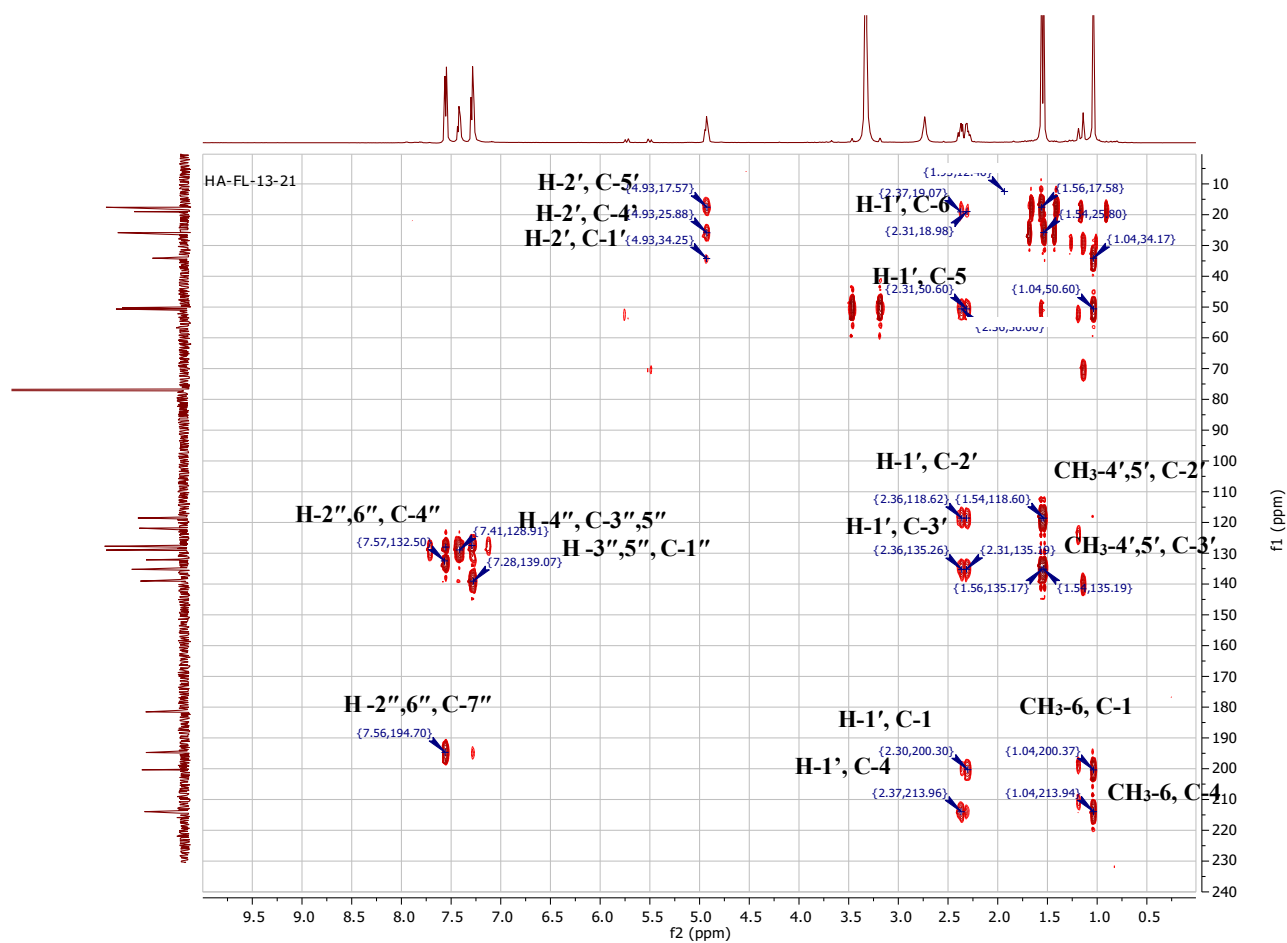


Figure II.2. 23. HMBC Spectrum of compound HAP1



### II.2.4.3. Naphtodianthrones

#### II.2.4.3.1 Compound HAN1

##### i. Physical properties

Compound **HAN1** (2 mg) was obtained as a reddish-black powder. It is soluble in methanol, ethanol, acetone and DMSO, yielding cherry-red solutions with red fluorescence. It is insoluble in chloroform and water.

##### ii. Chromatographic characters:

Compound **HAN1** appeared as a light orange zone under UV  $\lambda_{\max}$  366. It showed  $R_f$  value of 0.42 in system VII (page 48).

##### iii. Spectroscopic data:

**A. UV (MeOH)  $\lambda_{\max}$  nm (log  $\epsilon$ ):** 590.0 (4.40), 546 (4.07), 472(3.80), 509(3.56)

**B. HR-ESI-MS:** m/z 503.077 [M-H]<sup>-</sup> (calcd, 503.074) for formula C<sub>30</sub>H<sub>16</sub>O<sub>8</sub>.

##### C. <sup>1</sup>H-NMR spectral analysis:

The full assignment of proton chemical shifts of compound **HAN1** is presented in the following table:

**Table II.2. 5.** <sup>1</sup>H-NMR spectral data of compound **HAN1** (500 MHz , DMSO-*d*<sub>6</sub>)

Position	$\delta_H$ (ppm), multiplicity and <i>J</i> in Hz
OH-C-1, OH-C-6	14.74
H-2, 5	6.59
OH-C-8, OH-C-13	14.11
H-9, H-12	7.46
CH <sub>3</sub> -10, -11	2.75

##### iv. Conclusion

Compound **HAN1** was isolated as a reddish-black powder and its molecular formula was established as C<sub>30</sub>H<sub>16</sub>O<sub>8</sub> by negative HRESIMS (Figure II.2.24) at m/z 503.077[M-H]<sup>-</sup> (calcd, 503.074).

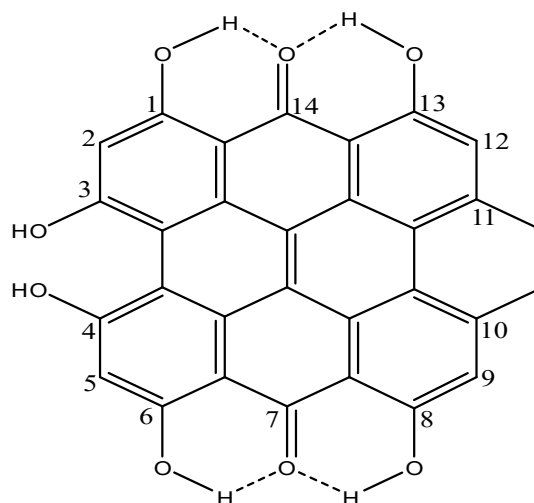
The UV-vis spectrum of compound **HAN1** in MeOH had absorbance maxima at 589 nm.

The <sup>1</sup>H-NMR spectrum of **HAN1** (Figure II.2.25) indicates significantly deshielded signals in the region of  $\delta_H$  =14-15 ppm. These resonances are attributed to the *peri*-hydroxyl protons OH (C-1), OH (C-6) and OH (C-8), OH (C-13) of hypericins, which participate in a strong six-membered ring

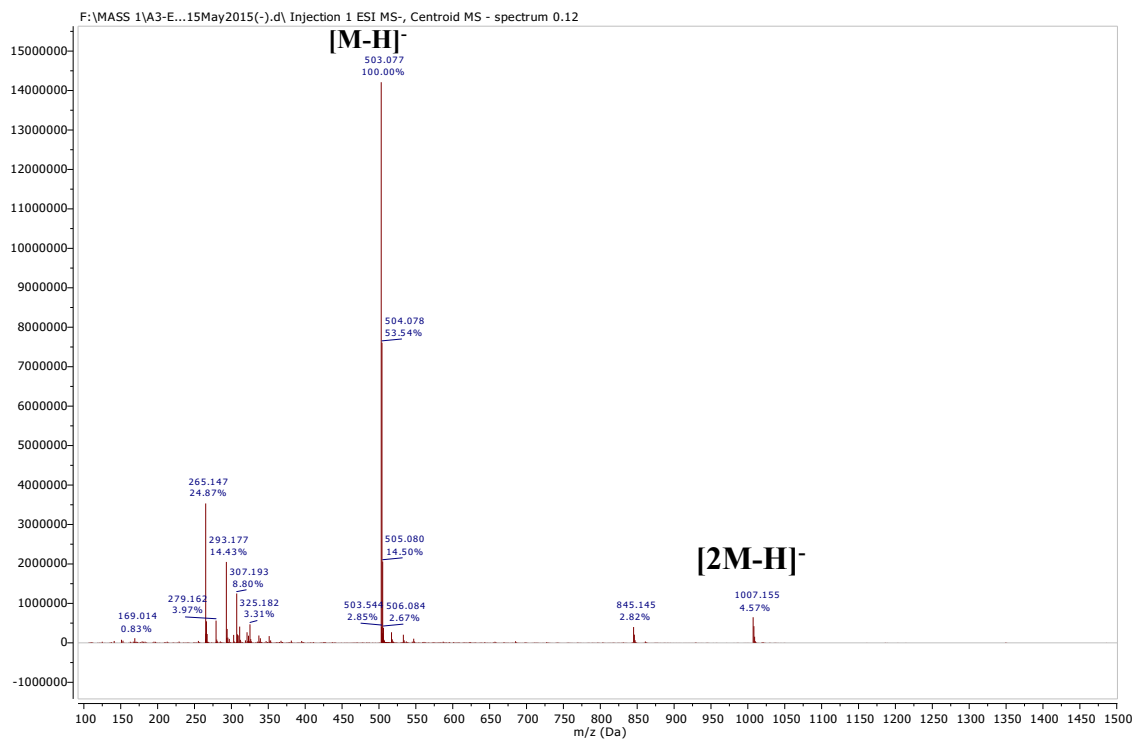
intramolecular hydrogen bond with C=O(7) and C=O(14), respectively, and therefore, they are strongly deshielded (Tatsis et al., 2008).

The aromatic signals at  $\delta_H=6.59$  and 7.46 ppm (Figure) are assigned to aromatic protons attached to carbons C-2, C-5 and C-9, C-12, respectively. The protons H-C (2) and H-C(5) are more shielded than those of H-C(9) and H-C (12), since they experience a double shielding effect due to presence of two hydroxyl groups (OH -1, OH-3 and OH-4, OH-6, respectively) in *ortho* position in the ring, instead of one hydroxyl group for H-9 and H-12 (OH-8 and OH-13, respectively).

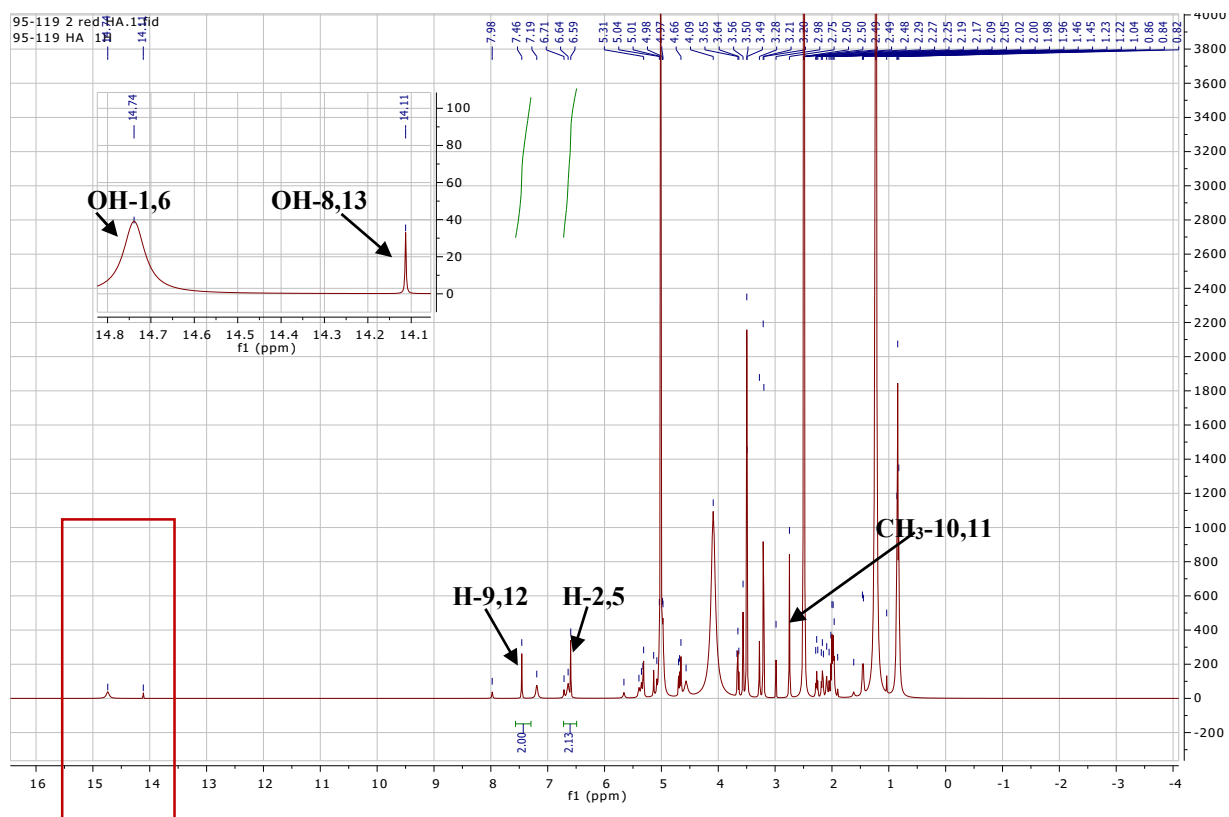
From the above mentioned spectroscopic data and physical and chromatographic characters, compound **HAN1** was identified as **hypericin**, a naphthodianthrone (red-colored anthraquinone derivative), which is one of the principal active constituents of *Hypericum* (Kusari et al., 2009; Moiseev, 2016). It has been of interest for its photoactivatable antiviral properties (CARPENTER and KRAUS, 1991; Hudson et al., 1991).



**Structure of compound HAN1:  
Hypericin**



FigureII.2. 24. Negative HR-ESI-MS of compound HAN1



FigureII.2. 25. <sup>1</sup>H-NMR Spectrum of compound HAN1(DMSO-*d*<sub>6</sub>, 500 MHz)

### II.2.4.3.2. Compound HAN2

#### i. Physical properties

Compound **HAN2** (1 mg) was obtained as a reddish-black powder. It is soluble in methanol, acetone, ethanol and DMSO.

#### ii. Chromatographic characters

Compound **HAN2** appeared as a light orange zone under UV  $\lambda_{\max}$  366. It showed  $R_f$  value of 0.57 in system VII (page 49).

#### iii. Spectroscopic data

A. UV (MeOH)  $\lambda_{\max}$  nm (log  $\epsilon$ ): 590.0 (3.82), 547.0 (3.52), 328.0 (3.43).

B. HR-ESI-MS: m/z 519.066 [M-H]<sup>-</sup> (calcd.519.069) for formula C<sub>30</sub>H<sub>16</sub>O<sub>9</sub>.

#### C. <sup>1</sup>H-NMR spectral analysis

The full assignment of proton chemical shifts of compound **HAN2** is presented in the following table:

**Table II.2. 6.** <sup>1</sup>H-NMR spectral data of compound **HAN2** (500 MHz , DMSO-*d*<sub>6</sub>)

Position	$\delta_H$ (ppm), multiplicity and <i>J</i> in Hz
OH-C-1, OH-C-6	14.78, 14.76
H -2	6.62, 1H
H-5	6.58, 1H
OH-C-8, OH-C-13	14.13, 14.12
H -9	7.72
(-CH <sub>2</sub> -OH)-C-10	H-a 4.69 (d, 12.5 Hz, 1H) H-b 5.14(d, 12.5 Hz, 1H)
CH <sub>3</sub> -11	2.69
H-12	7.48

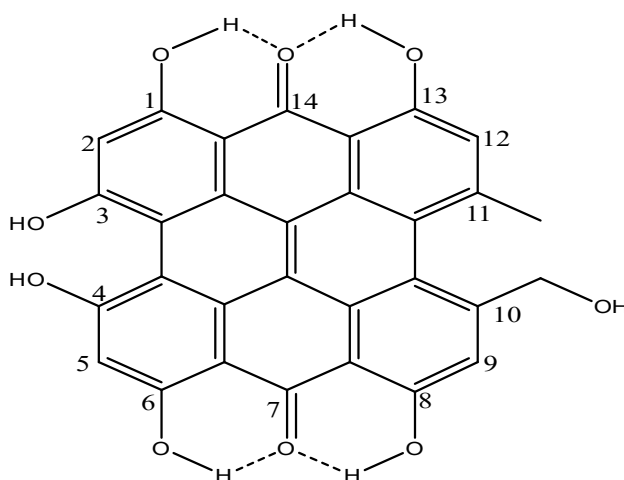
#### iv. Conclusion

Compound **HAN2** was isolated as a reddish-black powder. It showed similar physical and chromatographic characters as compound **HAN1**. Its molecular formula was established as C<sub>30</sub>H<sub>16</sub>O<sub>9</sub> by negative HRESIMS at m/z 519.066 [M-H]<sup>-</sup> (calcd. 519.069) (Figure II.2.26) implying one more oxygen atom than **HAN1**.

The UV-vis spectrum of HAN2 was compared to the one obtained of compound HAN1 and seem to be identical. Both compounds are assumed to have the same absorption coefficient at  $\lambda_{\max}$  590 nm. The  $^1\text{H-NMR}$  spectrum (Figure II.2.27) of compound HAN2 found to be also similar of compound HAN1, indicates significantly deshielded signals in the region of 14-15 ppm. In addition, it shows two signals at  $\delta_H$  5.14 (d,  $J$  12.5 Hz) and 4.69(d,  $J$  12.5 Hz) ppm indicating the presence of an AX system in  $-\text{CH}_2\text{OH}$  group (Tatsis et al., 2008). The substitution of one methyl by a  $\text{CH}_2\text{OH}$  group in the molecule of HAN2 results in the lack of the axis of symmetry, in contrast to hypericin. The resonance signals of ex-symmetrical protons, such as aromatic and *peri* hydroxyl protons, are not magnetically equivalent.

The most important differences are observed in the chemical shifts of the  $^1\text{H-NMR}$  aromatic protons H-9 ( $\delta_H$  7.72) and H-12 ( $\delta_H$  7.48), since H-12 has a methyl group in *ortho* position when H-9 has a hydroxymethyl group and therefore is deshielded.

From the above mentioned spectroscopic data and physical and chromatographic characters, compound HAN2 was identified as pseudohypericin an oxidized derivative of hypericin (HAN1), which both are characteristic bioactive components native from *Saint John's wort* (Kusari et al., 2009; Moiseev, 2016). These compounds are used as antidepressant, anticarcinogenic (photodynamic), antimicrobial and virostatic agents (Vacek et al., 2007).



**Structure of compound HAN2:  
Pseudohypericin**

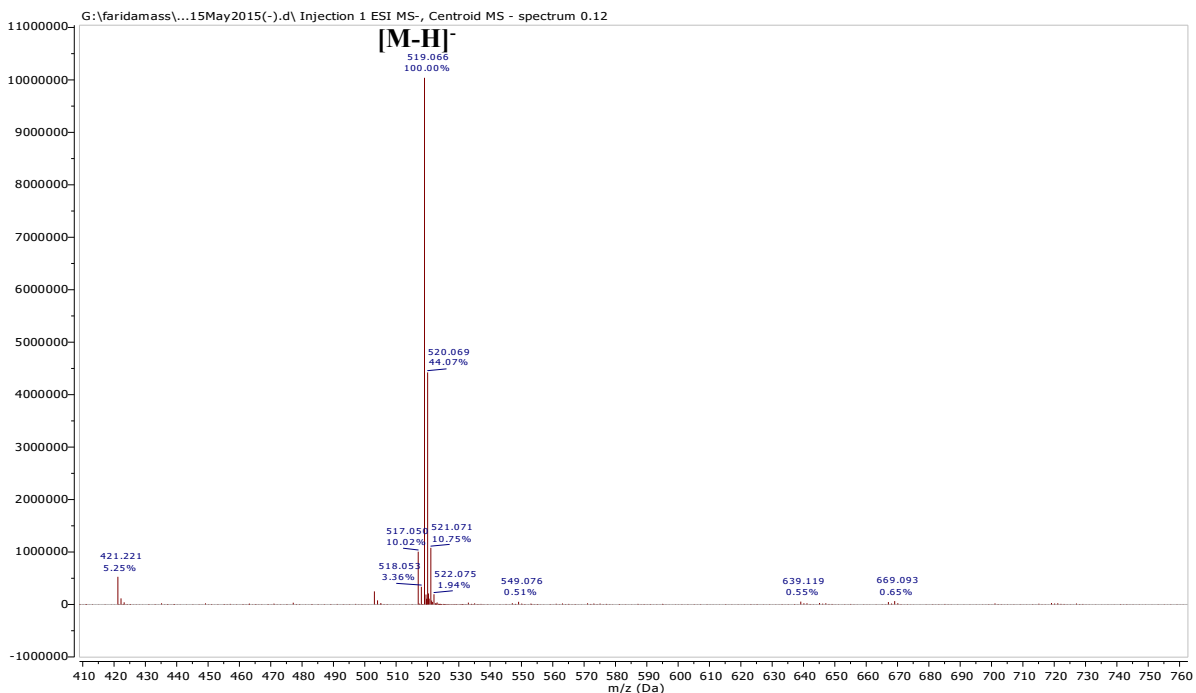


Figure II.2. 26. Negative HR-ESI-MS of compound HAN2

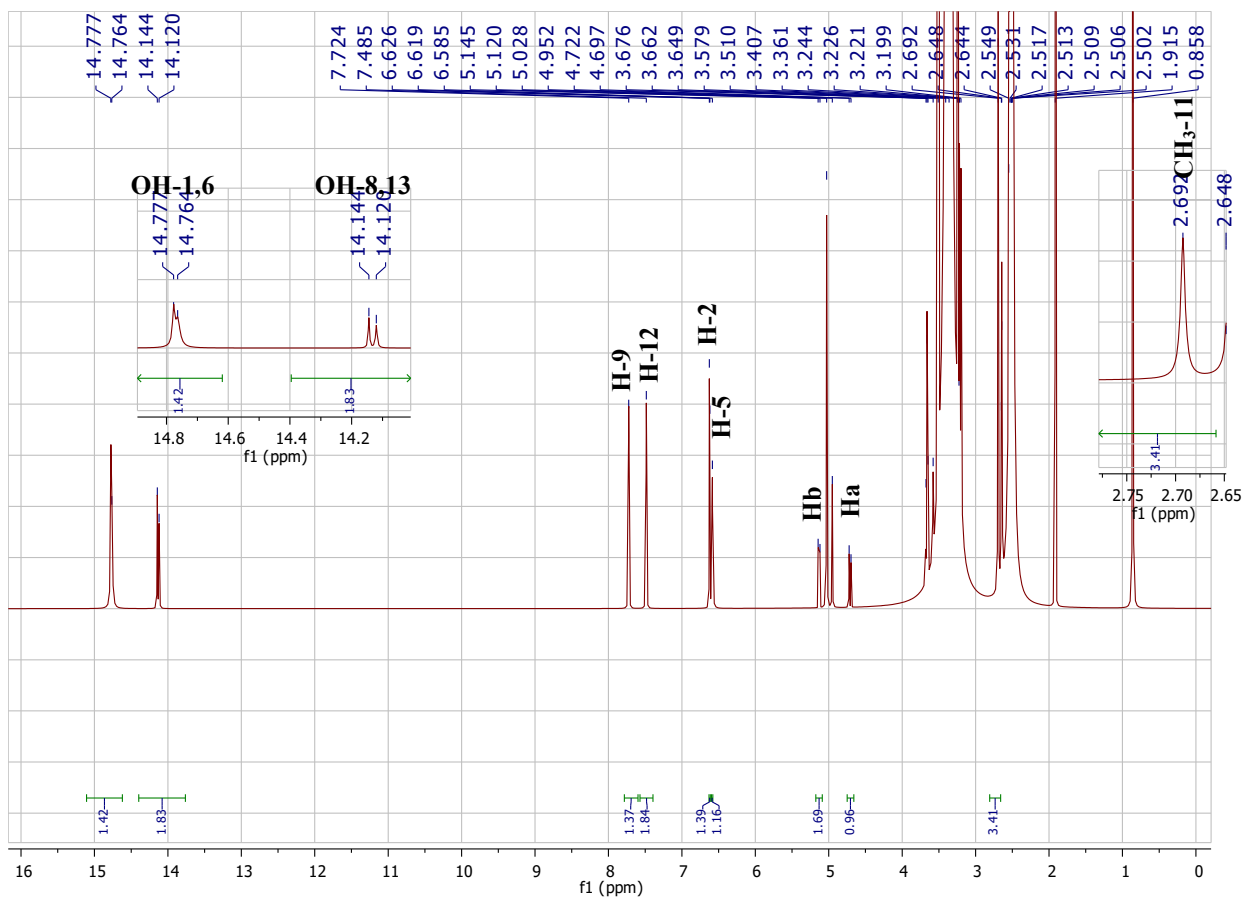


Figure II.2. 27. <sup>1</sup>H-NMR Spectrum of compound HAN2 (DMSO-*d*<sub>6</sub>, 500 MHz)

## II.2.4.4. Flavonoids

### II.2.4.4.1. Compound HAF1

#### i. Physical properties

Compound **HAF1** (16 mg) was obtained as a yellowish amorphous powder.

#### ii. Chromatographic characters

Compound **HAF1** appeared as a dark spot under UV  $\lambda_{\max}$  254 which attained a yellow color after spraying with 10% v/v vanillin/H<sub>2</sub>SO<sub>4</sub> and heating at 110 °C. It showed *R<sub>f</sub>* value of 0.50 in system VII (page 48).

#### iii. Spectroscopic data

**A. UV (MeOH)  $\lambda_{\max}$  nm (log  $\epsilon$ ):** 254.0 (4.80), 370.0 (4.76)

**B. HR-ESI-MS:** *m/z* 303.049 [M+H]<sup>+</sup> (calcd. 303.052) for formula C<sub>15</sub>H<sub>10</sub>O<sub>7</sub>

**C. <sup>1</sup>H-, <sup>13</sup>C-NMR and HMBC spectral analysis:** The <sup>1</sup>H-, <sup>13</sup>C-NMR and HMBC spectral data of compound **HAF1** are listed in table II.2.7 and illustrated in figures thereafter.

**Table II.2. 7.** <sup>1</sup>H-, <sup>13</sup>C-NMR and HMBC spectral data of compound **HAF1** (400 MHz, 100MHz, DMSO-*d*<sub>6</sub>)

Position	$\delta_H$ (ppm), multiplicity, <i>J</i> (Hz)	$\delta_C$ (ppm)	HMBC (H→C)
2	-	147.8	-
3	-	136.0	-
4	-	175.9	-
5	-	160.9	-
6	6.15, d, 2.0	98.7	C-8, 10, 7
7	-	164.0	-
8	6.40, d, 2.0	93.9	C-7, 6, 10, 9
9	-	156.6	-
10	-	103.3	-
1'	-	122.4	-
2'	7.59, d, 2.0	116.0	C-3', 6'
3'	-	145.3	-
4'	-	147.2	-
5'	6.86, d, 8.8	115.7	C-3', 1'
6'	7.50, dd, 2.0, 8.8	120.7	C-2', 2

#### iv. Discussion and conclusion

Compound **HAF1** had the molecular formula  $C_{15}H_{10}O_7$  as established from the positive HR-ESI-MS (Figure II.2.28) by providing a molecular ion peak at  $m/z$  303.049  $[M+H]^+$  (calcd. 303.052).

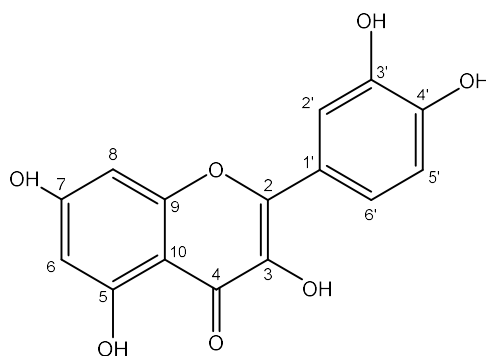
The UV spectrum of compound **HAF1** exhibited band I absorption at 370.0 nm revealed that it was a flavonol with free 3-OH group (Mabry et al., 1970a).

The structure of **HAF1** was elucidated by interpretation of its NMR spectra, including  $^1H$ ,  $^{13}C$ , HSQC, and HMBC.

Its  $^1H$ -NMR spectrum (Figure II.2.29) showed the characteristic signals pattern of quercetin, namely 2H with an AX coupling system at  $\delta_H$  6.15 (d, 2.0, 1H) and  $\delta_H$  6.40 (d, 2.0, 1H) are attributable to H-6 and H-8 of ring A.

3 proton signals at  $\delta_H = 7.59$  ppm (1H, d,  $J = 2.0$  Hz),  $\delta_H = 7.50$  ppm (1H, dd,  $J = 8.8, 2.0$  Hz) and  $\delta_H = 6.86$  ppm (1H, d,  $J = 8.8$  Hz) indicated the presence of an ABX coupling system characteristic for ring B of quercetin, these protons are attributable to H-2', H-6' and H-5'. The signal at  $\delta_H = 12.47$  ppm was assigned to the C-5 hydroxyl.

All data were consistent with that of quercetin (Chimenti et al., 2006; Eldahshan, 2011). Therefore, it was identified as quercetin previously isolated from the genus *Hypericum* (Chimenti et al., 2006).



Structure of compound **HAF1**:  
Quercetin



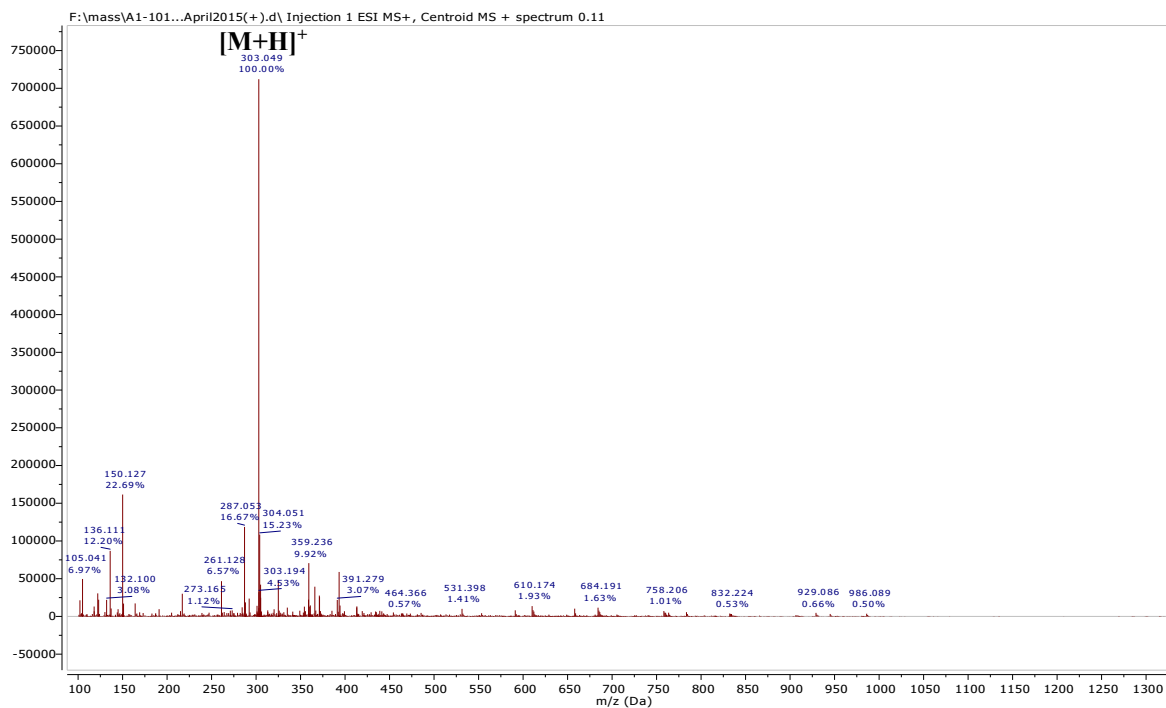


Figure II.2. 28. Positive HR-ESI-MS of compound HAF1

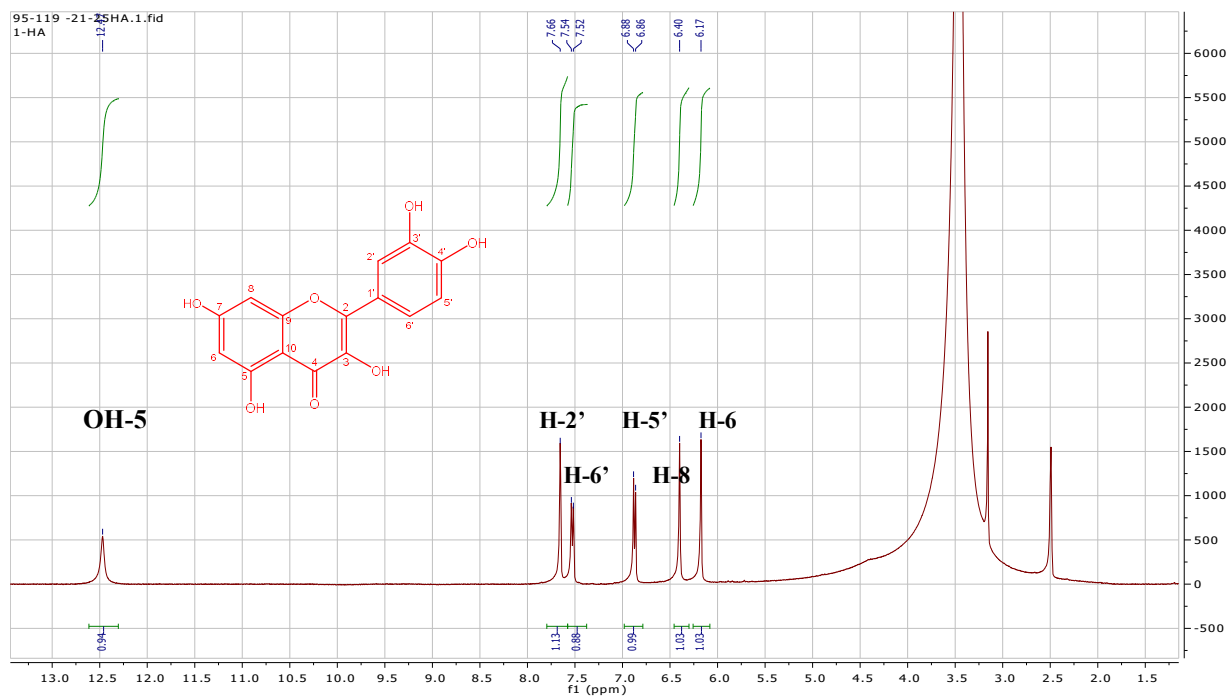


Figure II.2. 29. <sup>1</sup>H-NMR Spectrum of compound HAF1(DMSO-*d*<sub>6</sub>, 400 MHz)

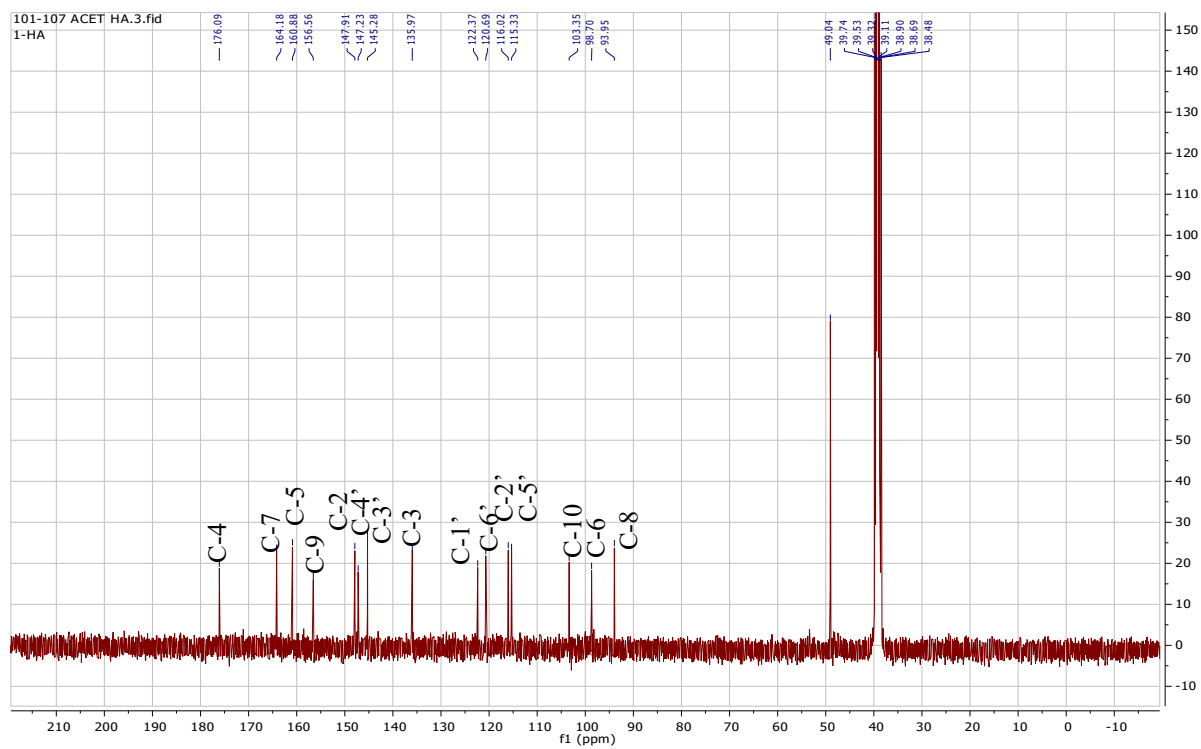


Figure II.2. 30.  $^{13}\text{C}$ -NMR Spectrum of compound HAF1(DMSO- $d_6$ , 100 MHz)

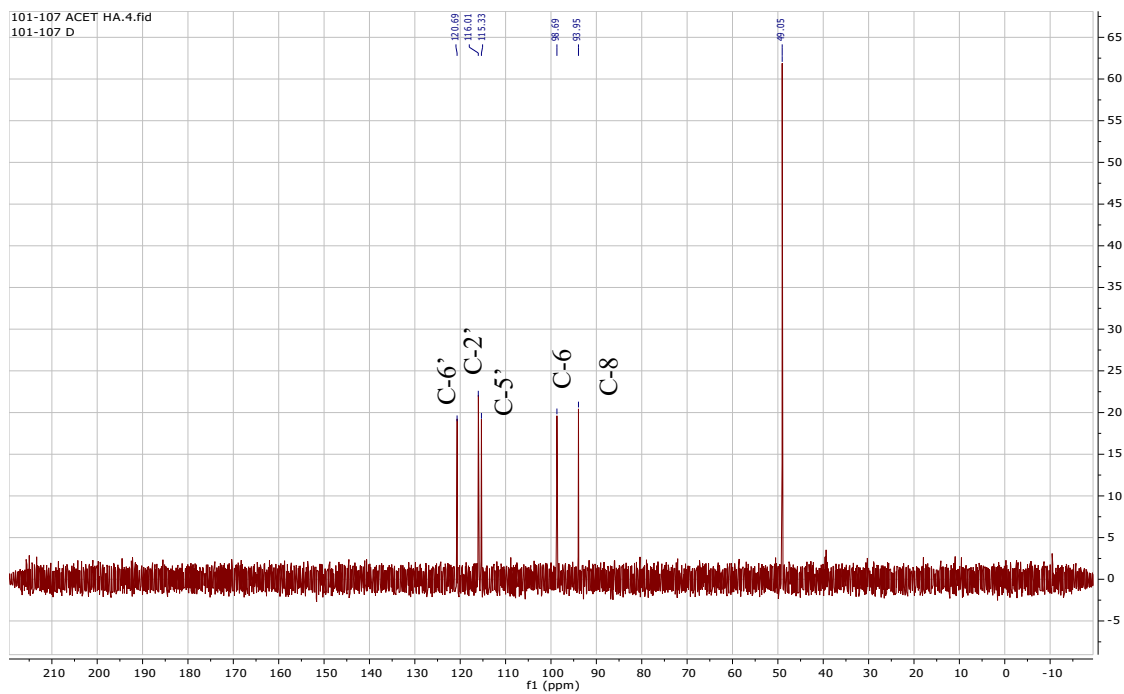


Figure II.2. 31. DEPT-135 Spectrum of compound HAF1

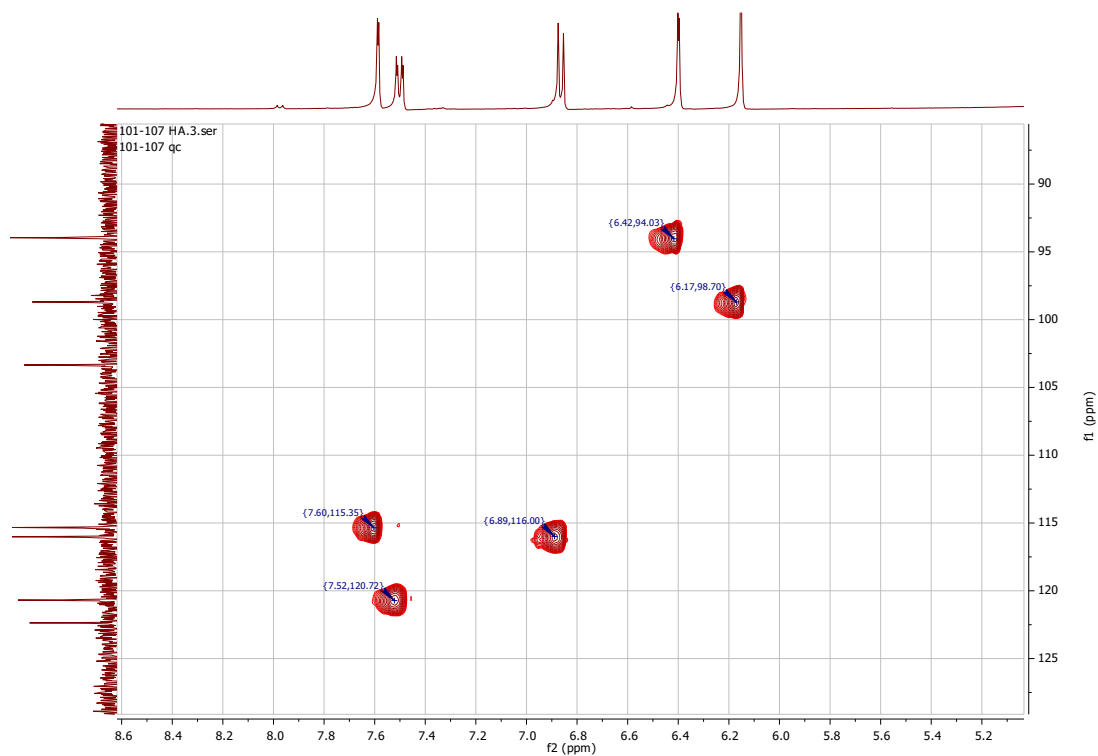


Figure II.2. 32. HSQC Spectrum of compound HAF1

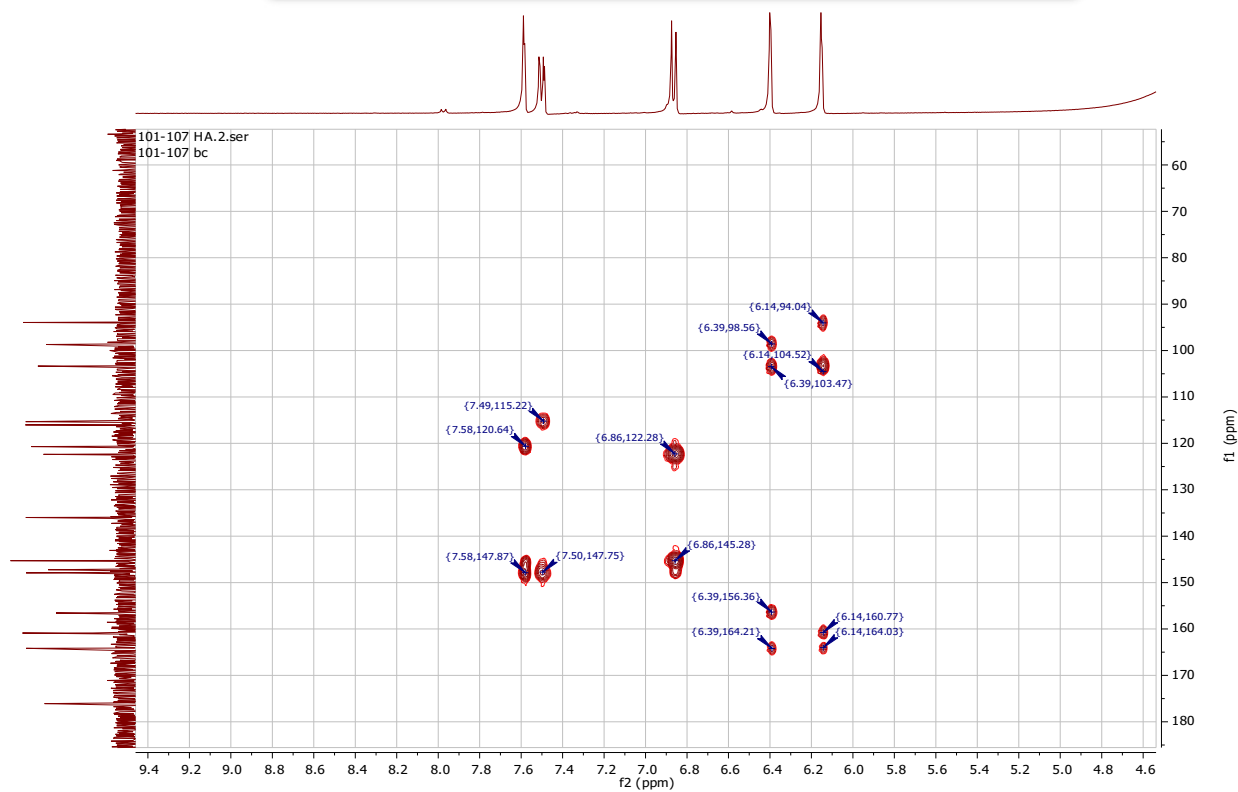


Figure II.2. 33. HMBC Spectrum of compound HAF1

**II.2.4.4.2. Compound HAF2****i. Physical properties**

Compound **HAF2** (10 mg) was obtained as a yellowish amorphous powder.

**ii. Chromatographic characters**

Compound **HAF2** appeared as a dark spot under UV  $\lambda_{\max}$  254 which attained an orange color after spraying with 10% v/v vanillin/H<sub>2</sub>SO<sub>4</sub> and heating at 110 °C. It showed *R<sub>f</sub>* value of 0.75 in system VII (Page 48).

**iii. Spectroscopic data**

**A- UV (MeOH)  $\lambda_{\max}$  nm (log  $\epsilon$ ):** 373.0 (4.76), 254.0 (4.80).

**B- HR-ESI-MS, m/z:** 319.070 [M-H]<sup>+</sup> (calcd. 319.050 ) for formula C<sub>15</sub>H<sub>10</sub>O<sub>8</sub>.

**C- <sup>1</sup>H-, <sup>13</sup>C-NMR and HMBC spectral analysis:** The <sup>1</sup>H-, <sup>13</sup>C-NMR and HMBC spectral data of compound **HAF2** are listed in table II.2.8 and illustrated in figures thereafter.

**Table II.2. 8.** <sup>1</sup>H-, <sup>13</sup>C-NMR and HMBC spectral data of compound **HAF2** (400 MHz, 100MHz, DMSO-*d*<sub>6</sub>)

Position	$\delta_H$ (ppm), multiplicity, J(Hz)	$\delta_C$ (ppm)	HMBC (H→C)
2	-	147.3	-
3	-	136.3	-
4	-	176.2	-
5	-	161.1	-
6	6.18, d, J = 2.3 Hz, 1H	98.6	C-8, 10, 7
7	-	164.3	-
8	6.37, d, J = 2.4 Hz, 1H	93.6	C-7, 6, 10, 9
9	-	156.5	-
10	-	103.4	-
1'	-	121.2	-
2', 6'	7.24, s, 2H	107.6	C-1', 2, 4'
3', 5'	-	146.1	-
4'	-	136.3	-

#### iv. Discussion and conclusion

Compound **HAF2** had the molecular formula  $C_{15}H_{10}O_8$  as established from the positive HR-ESI-MS (Figure II.2.34) by providing a molecular ion peak at  $m/z$  319.070  $[M+H]^+$  (calcd. 319.050).

Similarly to compound **HAF1**, The UV spectrum of compound **HAF2** exhibited band II absorption at 254 nm and band I absorption at 373.0 nm revealed that it was a flavonol with free 3-OH group (Mabry et al., 1970a).

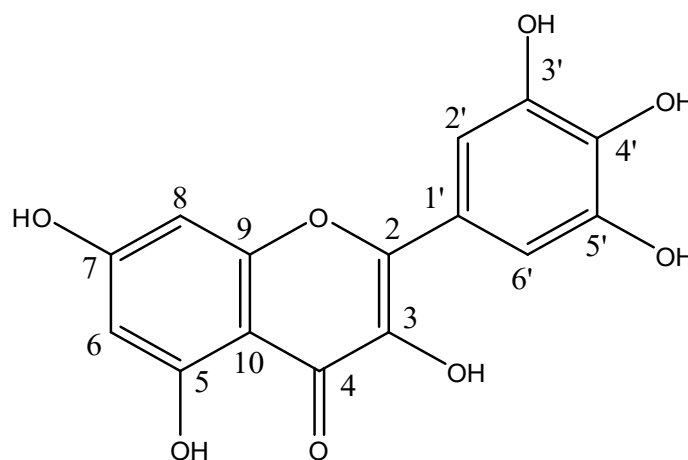
The  $^1H$ -NMR spectrum (Figure II.2.34) exhibited a characteristic meta-coupled proton signal at  $\delta_H$  6.18 (1H, d,  $J = 2.3$  Hz) and 6.37 (1H, d,  $J = 2.4$  Hz) corresponding to H-6 and H-8 of flavonoid A ring.

A proton signal at  $\delta_H = 7.24$  (2H, br s) was assigned to H-2' and H-6' of B ring. The signal at  $\delta_H$  12.49 ppm was assigned to the C-5 hydroxyl.

The  $^{13}C$ -NMR and DEPT spectra (Figures II.2. 36-37) showed 15 signals comprising one carbonyl carbon at  $\delta_C = 176.2$  ppm, 4 sp<sup>2</sup> methine and 10 sp<sup>2</sup> quaternary signals.

The established structure for compound **HAF2** confirmed by the 2D NMR including HSQC and HMBC (Figures II.2.38-39). The HSQC experiment revealed one overlapped  $^{13}C$  signal confirming four methine (CH) in the molecule and the molecular formula.

By comparing the NMR spectral data with those reported in literature, the structure of **HAF2** was determined as myricetin (Miean and Mohamed, 2001), previously isolated from the genus *Hypericum* (Erdelmeier, 1998; Nedialkov et al., 2007).



Structure of compound HAF2 :  
Myricetin

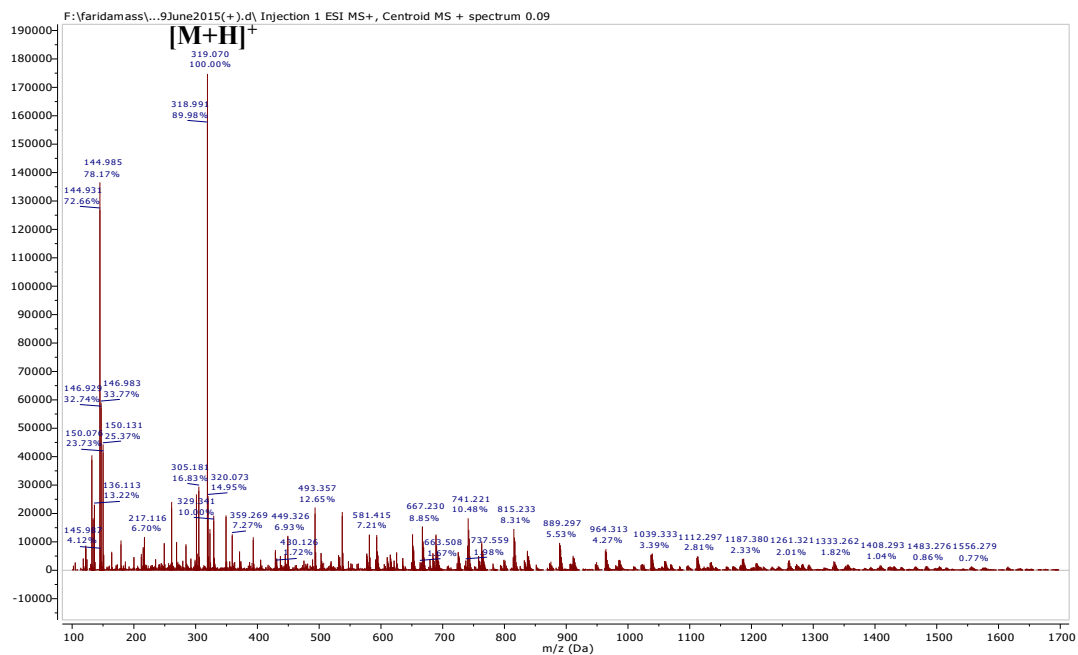


Figure II.2. 34. Positive HR-ESI-MS of compound HAF2

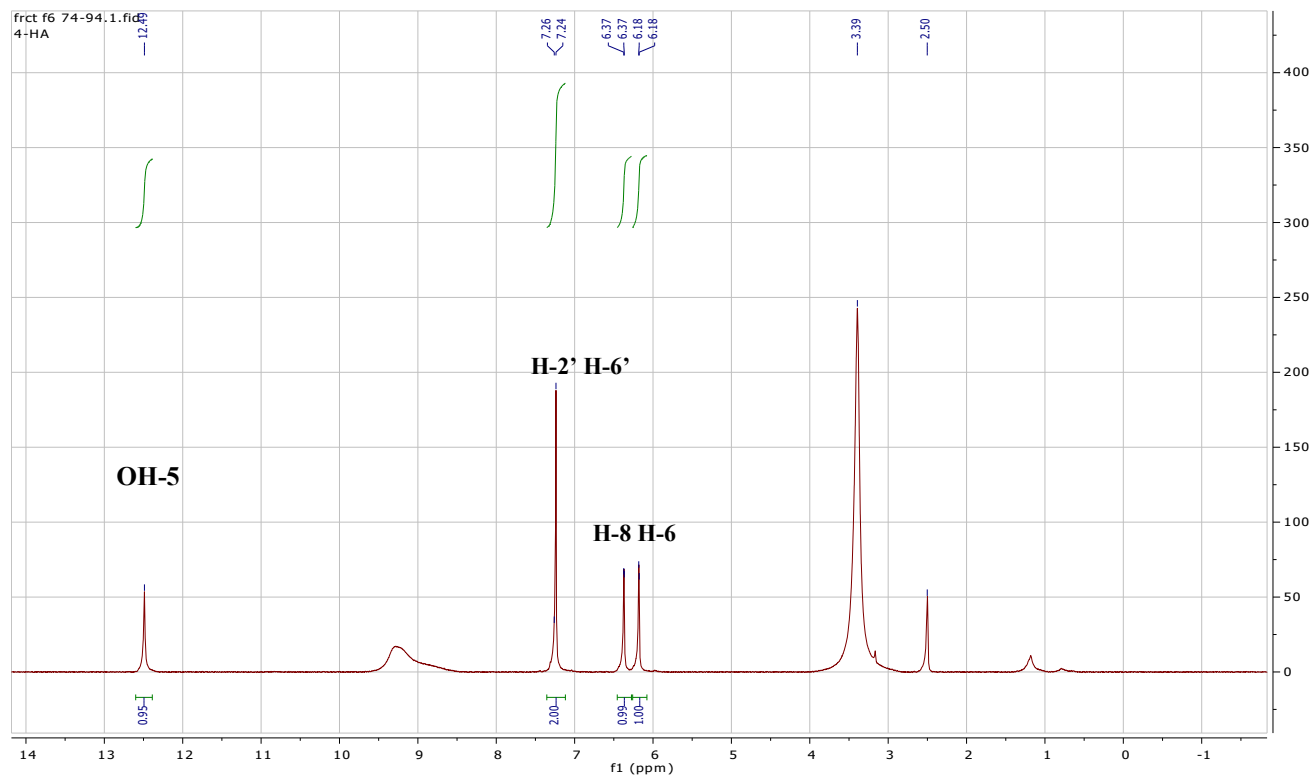


Figure II.2. 35. <sup>1</sup>H-NMR Spectrum of compound HAF2 (DMSO-*d*<sub>6</sub>, 400 MHz)

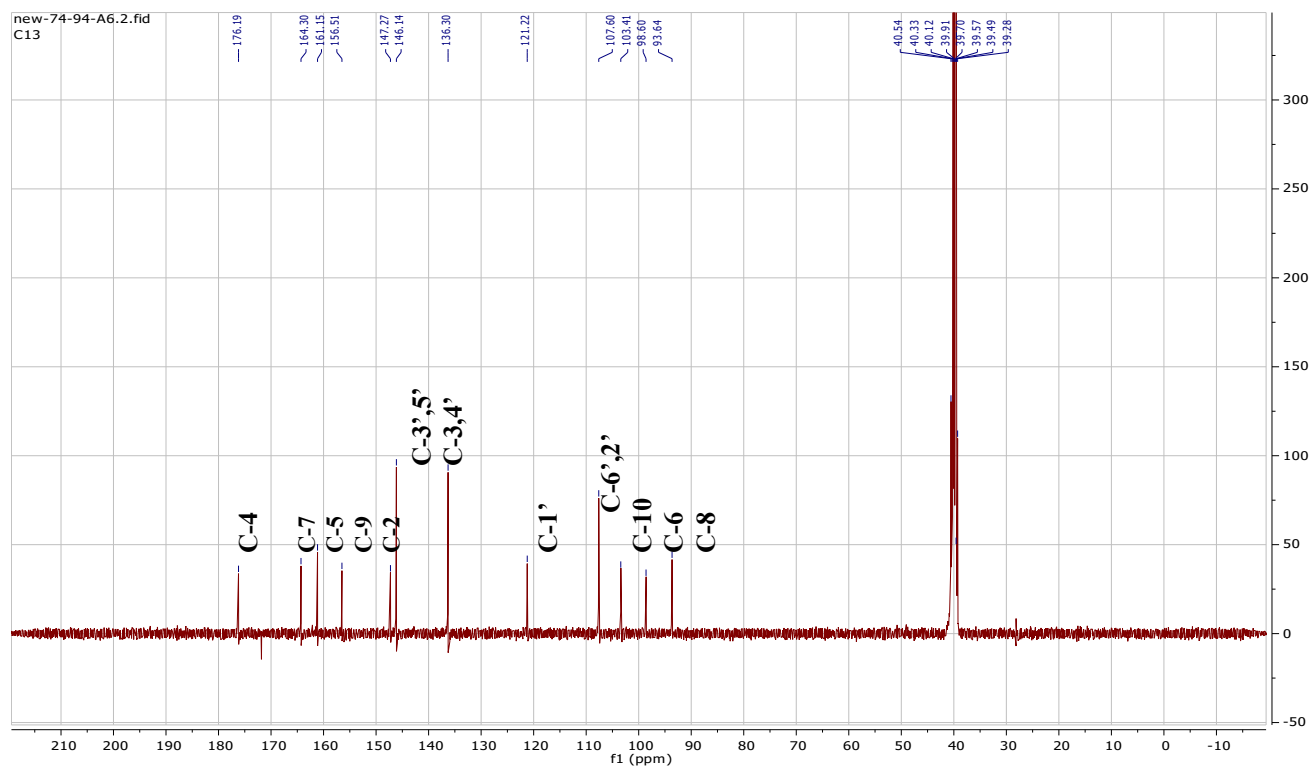


Figure II.2. 36.  $^{13}\text{C}$ -NMR Spectrum of compound HAF2 (DMSO- $d_6$ , 100 MHz)

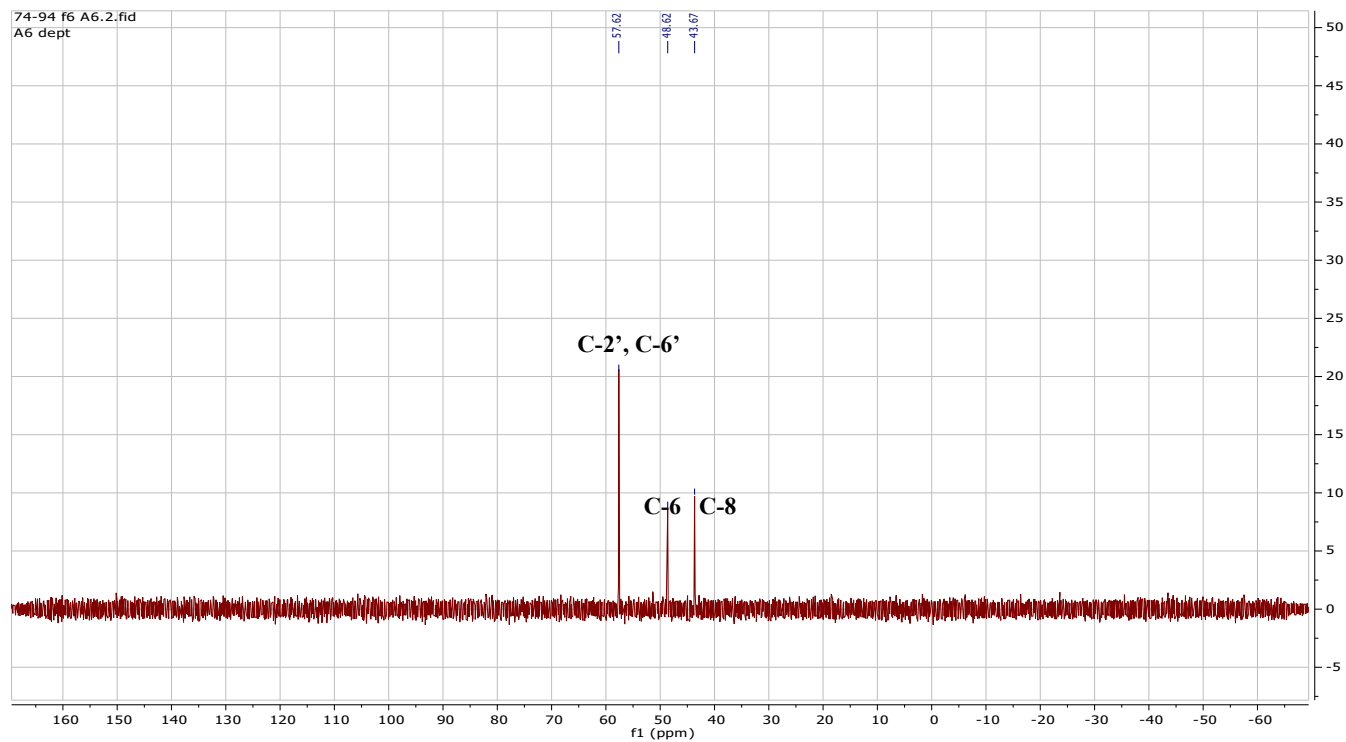


Figure II.2. 37. DEPT-135 Spectrum of compound HAF2

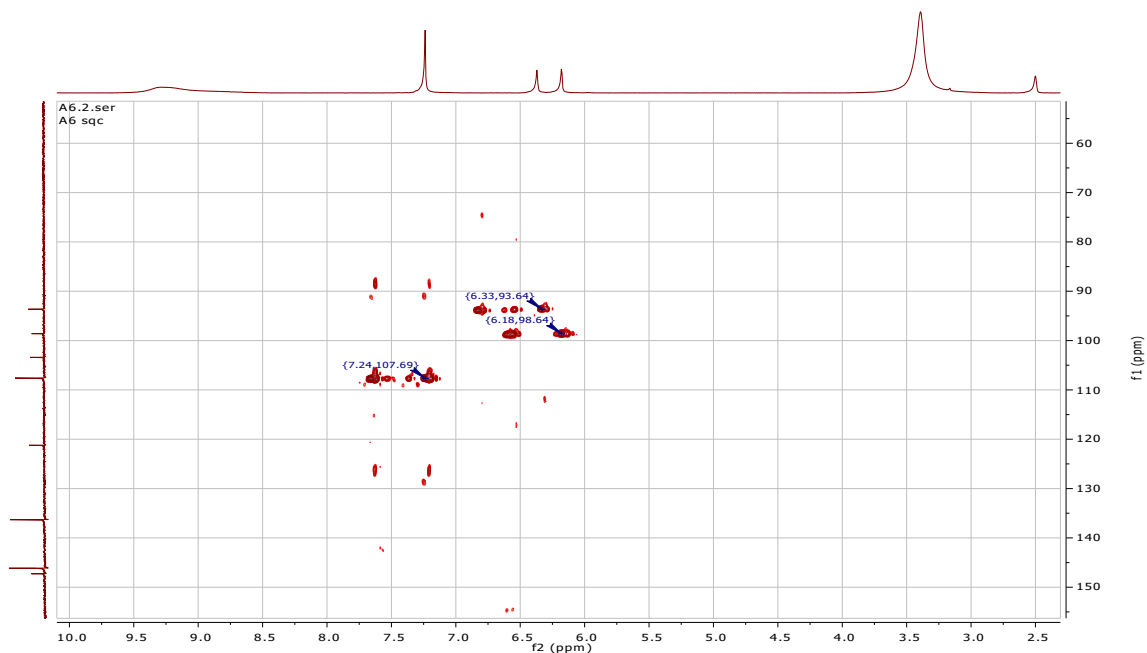


Figure II.2. 38. HSQC Spectrum of compound HAF2

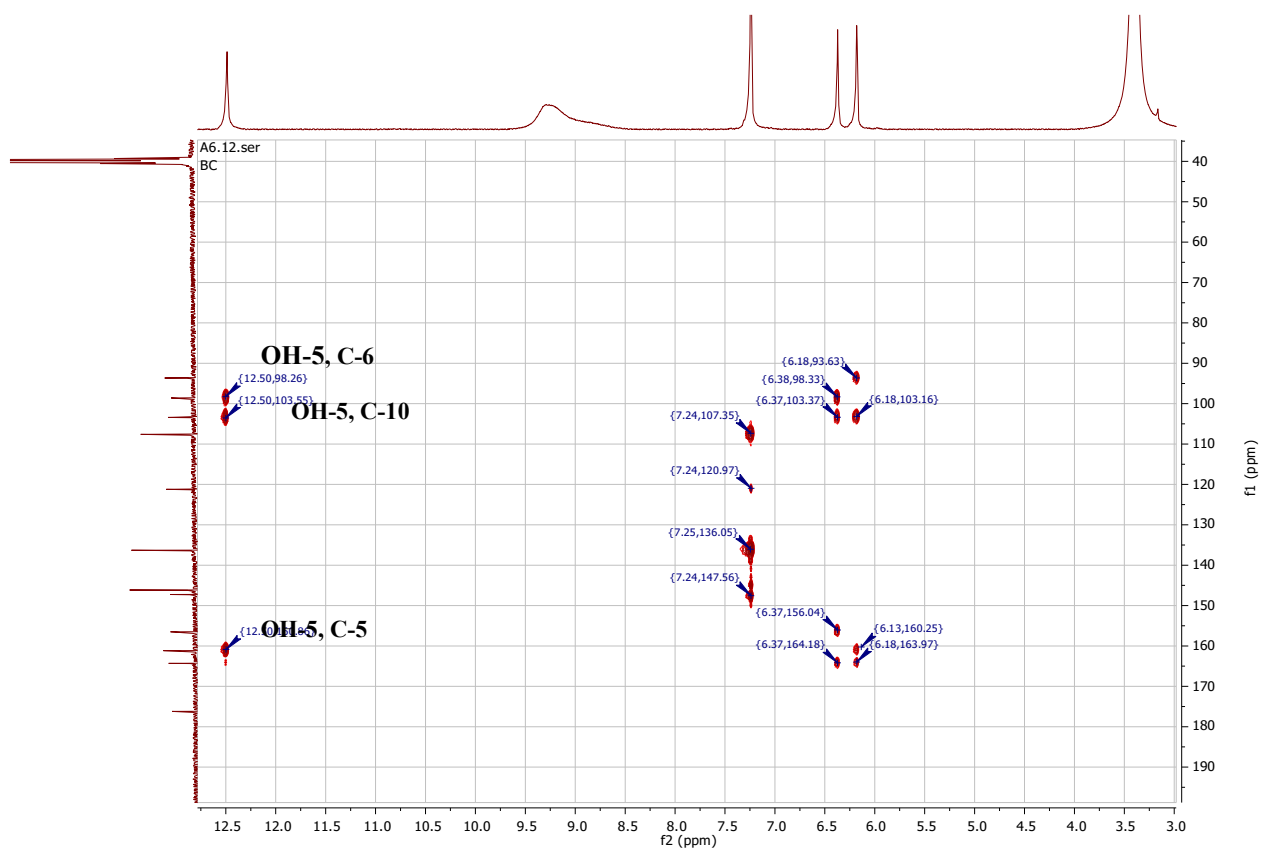


Figure II.2. 39. HMBC Spectrum of compound HAF2



### II.2.4.4.3. Compound HAF3

#### i. Physical properties

Compound **HAF3** (7 mg) was obtained as a yellowish amorphous powder.

#### ii. Chromatographic characters:

Compound **HAF3** appeared as a dark spot under UV  $\lambda_{\max}$  254 which attained an orange color after spraying with 10% v/v vanillin/H<sub>2</sub>SO<sub>4</sub> and heating at 110 °C. It showed *R<sub>f</sub>* value of 0.60 in system I (Page 48).

#### iii. Spectroscopic data

A. UV (MeOH)  $\lambda_{\max}$  nm (log  $\epsilon$ ): 357.0(4.28), 256.9(4.40)

B. HR-ESI-MS: m/z: 463.100 [M-H]<sup>-</sup>

#### C. <sup>1</sup>H-, <sup>13</sup>C-NMR and HMBC spectral analysis

The <sup>1</sup>H, <sup>13</sup>C-NMR and HMBC spectral data of compound **HAF3** are listed in table II.2.9 and illustrated in thereafter.

**Table II.2. 9.** <sup>1</sup>H-, <sup>13</sup>C-NMR and HMBC spectral data of compound **HAF3** (400 MHz, 100MHz, DMSO-*d*<sub>6</sub>)

Position	$\delta_H$ (ppm), multiplicity, <i>J</i> (Hz)	$\delta_C$ (ppm)	HMBC (H→C)	<sup>1</sup> H- <sup>1</sup> H COSY
2	-	157.1	-	-
3	-	134.9	-	-
4	-	178.2	-	-
5	-	161.8	-	-
6	6.22, d, <i>J</i> = 2.3 Hz, 1H	98.4	C-8,5, 7,10	-
7	-	164.4	-	-
8	6.38, d, <i>J</i> = 2.4 Hz, 1H	93.3	C-6, 7, 9,10	-
9	-	158.0	-	-
10	-	104.4	-	-
1'	-	120.5	-	-
2', 6'	6.97, br s, 2H	108.2	C-2, 1',3',4', 5'	-
3', 5'	-	145.4	-	-
4'	-	136.5	-	-
1''	5.33, d, <i>J</i> = 1.8 Hz, 1H	102.2	C-2'', C-3	2''
2''	4.24, dd, <i>J</i> = 3.3, 1.7 Hz, 1H	70.5	C-4''	1''
3''	3.81, dd, <i>J</i> = 9.5, 3.4 Hz, 1H	70.6	C-4''	4''
4''	3.39-3.35 m, 1H	71.9	C-6''	3''
5''	3.53, dq, 12.2, 6.1 Hz, 1H	70.7	C-1''	6''
6''	0.98, d, <i>J</i> = 6,2 Hz, 3H	16.2	C-5''	5''

#### iv. Discussion and conclusion

Compound **HAF3** had the molecular formula  $C_{21}H_{20}O_{12}$  as established from the negative HR-ESI-MS by providing a molecular ion peak at  $m/z$  463,100  $[M-H]^-$  (calcd. 463.085) (Figure II.2.41). A fragment ion obtained by the negative HR-ESI-MS at  $m/z$  317.038 characterized aglycone as myricetin (Saldanha et al., 2013).

The compound **HAF3** exhibited **band I** absorption at 357.0 nm and **band II** absorption at 256.9 nm characteristic of flavonol with hydroxyl 3-OH substituted (Mabry et al., 1970b).

Its  $^1H$ -NMR spectrum (Figure II.2.42) exhibited the characteristic pattern of myricetin derivatives. A characteristic meta-coupled proton signal at  $\delta_H$  6.22 (1H, d,  $J = 2.3$  Hz) and 6.38 (1H, d,  $J = 2.4$  Hz) corresponding to H-6 and H-8 of flavonoid A ring. A singlet proton signal at  $\delta_H = 6.97$  (2H, br s) was assigned to H-2' and H-6' of B ring.

Its  $^{13}C$ -NMR spectrum (Figure II.2.43) showed the upfield and downfield shifts of myricetin consistent with 3-*O*-glycosilation. Comparison of the  $^{13}C$ -NMR spectrum of compound (**HAF3**) with that of myricetin aglycone (**HAF2**) showed that the signal of C-3 was observed to shift upfield by (-1.41) ppm), whereas the signals of C-2 and C-4 were displaced downfield by (+9.81) and (+2.06) respectively, suggesting a 3-*O*-glycosilation.

$^{13}C$ -NMR with DEPT 135 experiments (Figures II.2.43-45) indicated the presence of one methyl group ( $CH_3$ ) at  $\delta_C = 16.3$  ppm, eight methine groups and eleven quaternary carbons.

The established structure for compound **HAF3** confirmed by the 2D NMR including  $^1H$ - $^1H$  COSY, HSQC and HMBC (Figures II.2.46-48)

The diagnostic proton signal at  $\delta_H$  (0.98, d,  $J = 6,2$  Hz, 3H) and carbon at  $\delta_C = 16.2$  ppm should belong to a rhamnosyl unit.

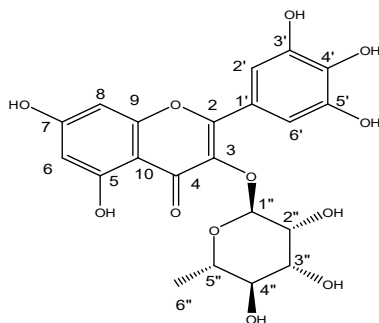
The anomeric proton of rhamnose H-1'' shows equatorial -equatorial coupling with H-2'' ( $J = 1.8$  Hz), indicating  $\alpha$  configuration of the sugar unit.

The sugar type was confirmed by an acid hydrolysis realized according to the method described in page (54) which allowed us to determine a sugar type L-rhamnosyl.

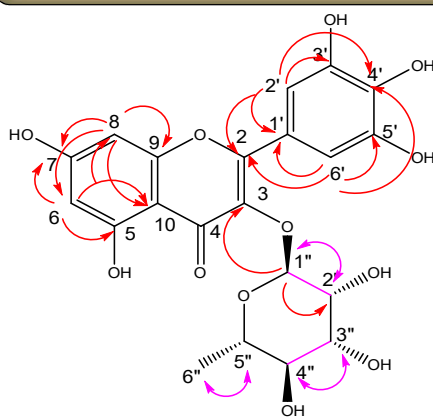
The position of  $\alpha$ - L-rhamnosyl unit was confirmed by HMBC correlation between the anomeric proton at  $\delta_H$  5.33 (H-1'', d,  $J = 1.8$  Hz, 1H) and carbon C-3 at  $\delta_C$  134.93.

All data were consistent with that of **myricetin -3-*O*- $\alpha$ -L-rhamnopyranoside** known as myricitrin (David et al., 1996). Therefore, it was identified as myricitrin previously isolated from the genus *Hypericum* (Demirkiran et al., 2013). Myricitrin is a common bioactive flavonoid, it was shown to possess antioxidant, anti-psychotic and anti-anxiolytic-like effects (Pereira et al., 2011), it

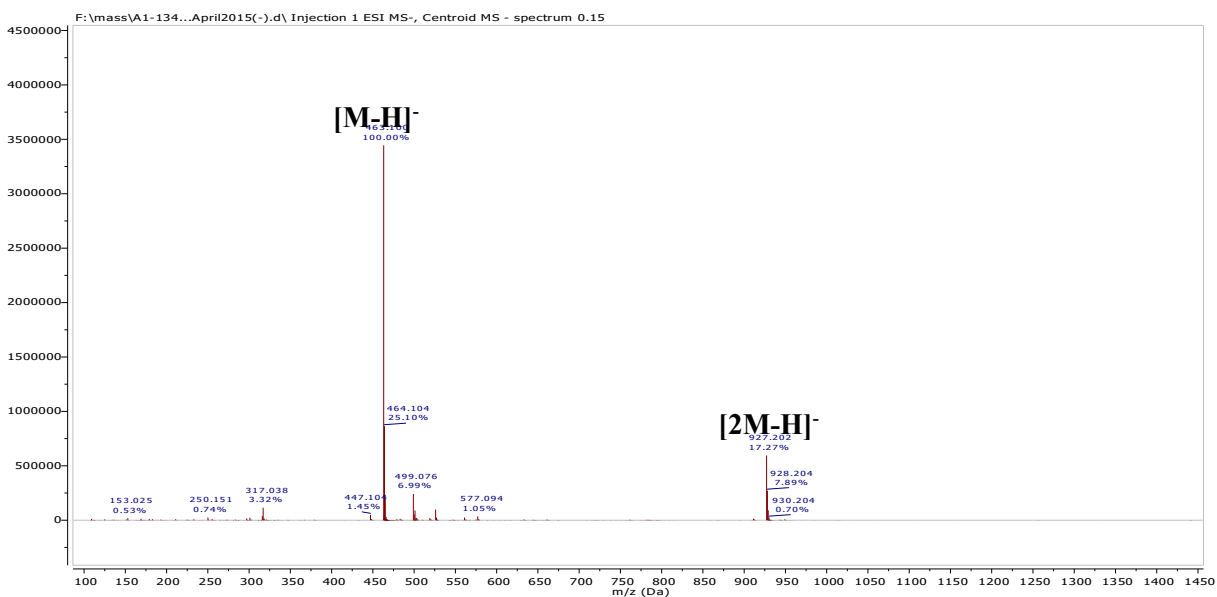
was also found to exert anti-mutagenic activity and potential to modulate the expression patterns of cellular genes involved in oxidative stress and in DNA damaging repair (Hayder et al., 2008).



**Structure of compound HAF3:  
Myricetin -3-O- $\alpha$ -L-rhamnopyranoside**



**FigureII.2. 40..Important HMBC (H→C) and COSY (H↔H) correlations of compound HAF3**



**FigureII.2. 41. Negative HR-ESI-MS of compound HAF3**



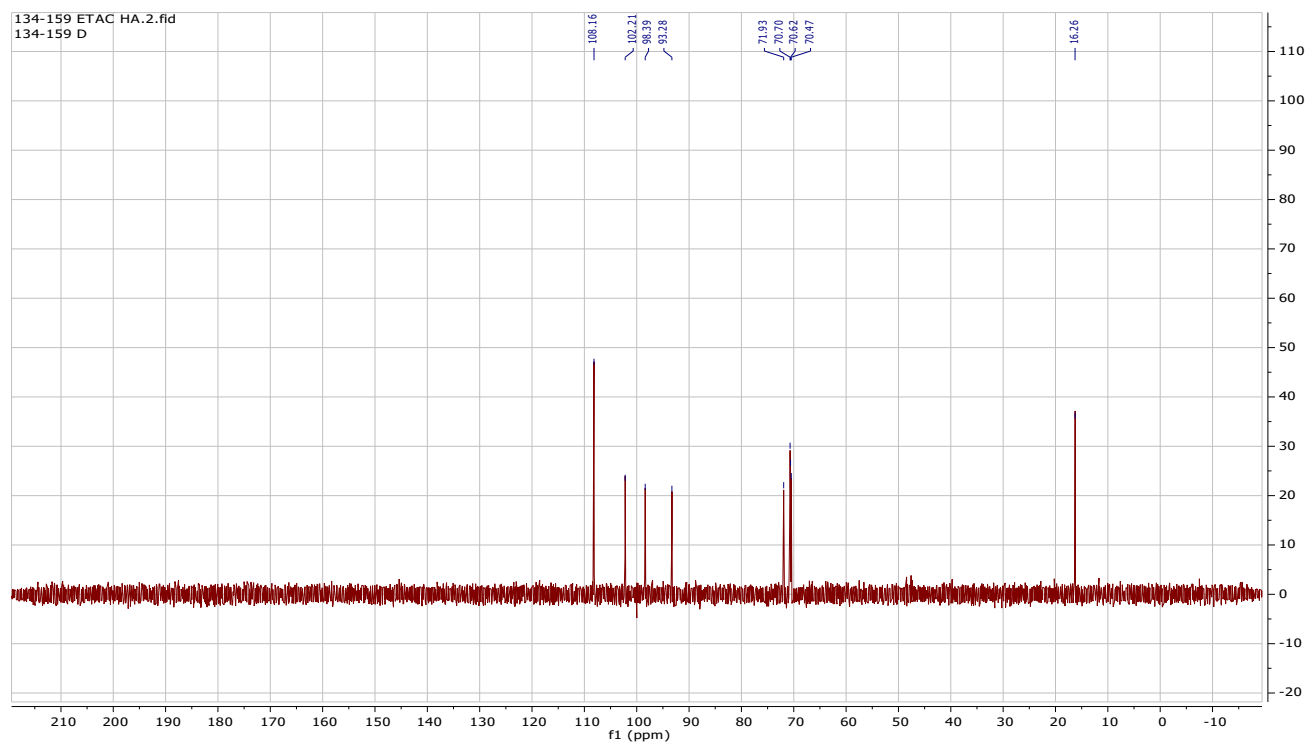


Figure II.2. 44. DEPT135 Spectrum of compound HAF3

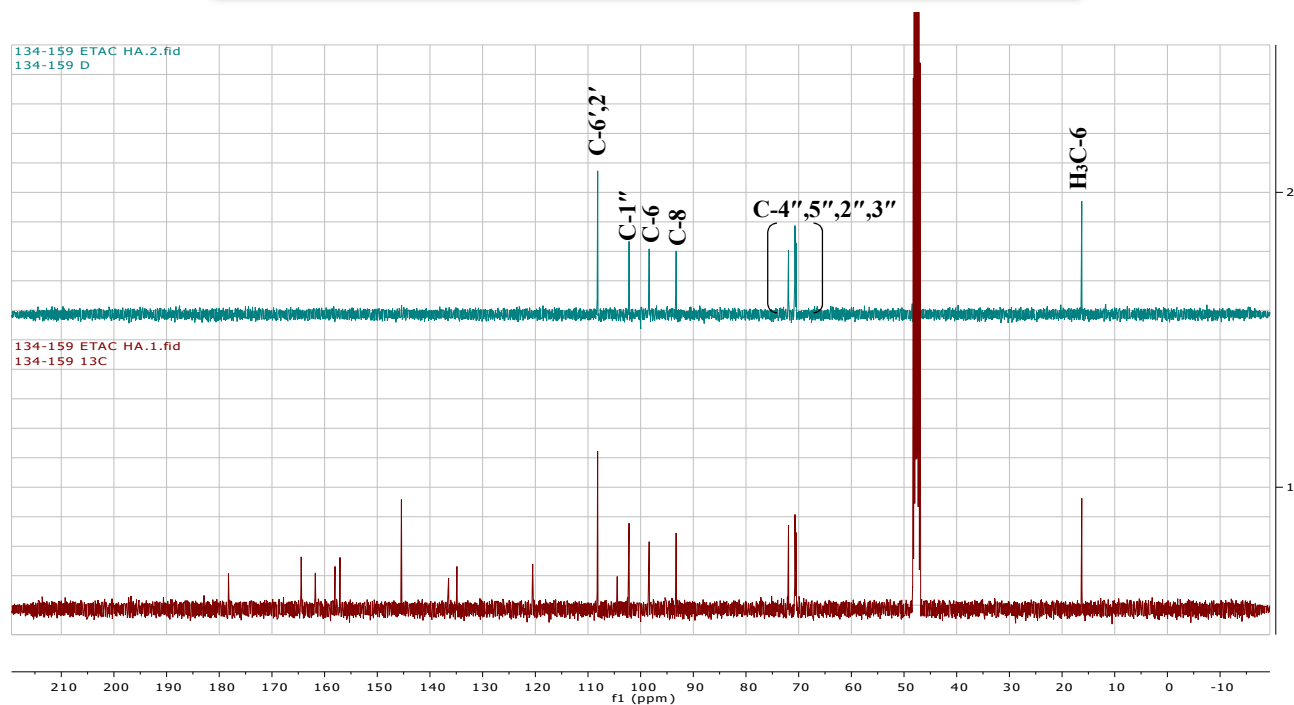


Figure II.2. 45. . Comparison of <sup>13</sup>C-NMR and DEPT135 Spectra of compound HAF3

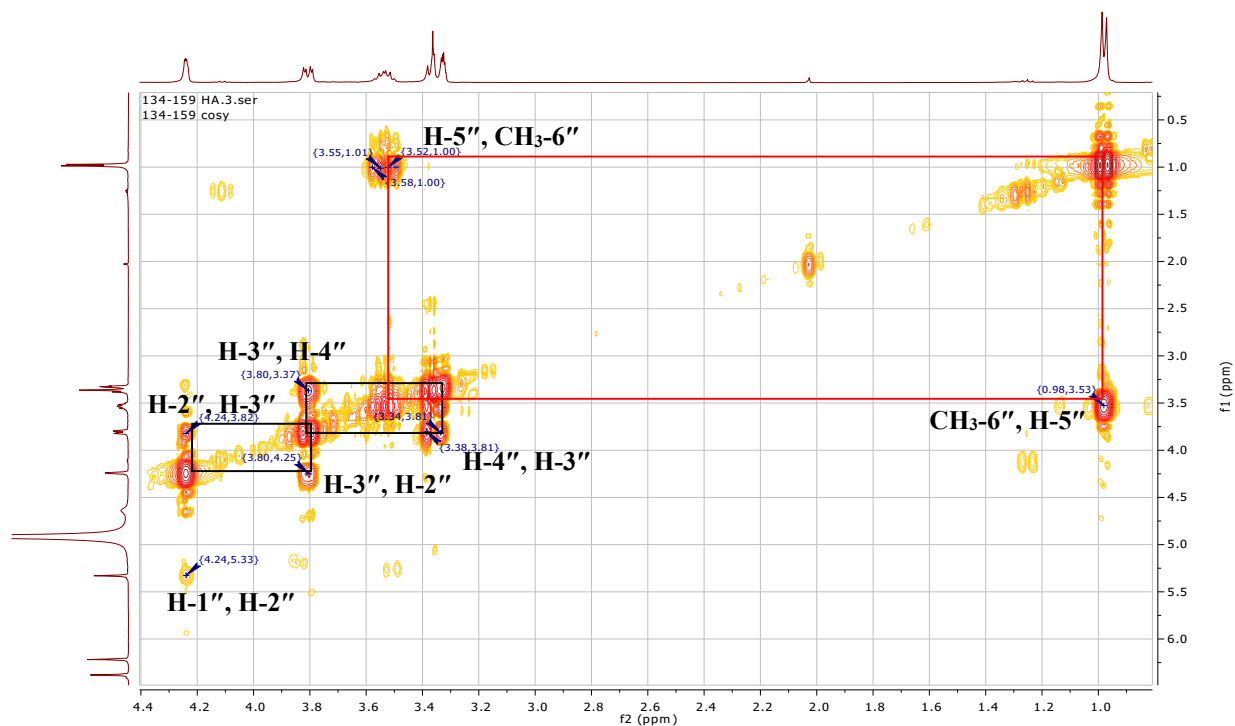


Figure II.2. 46.  $^1\text{H}$ - $^1\text{H}$  COSY Spectrum of compound HAF3

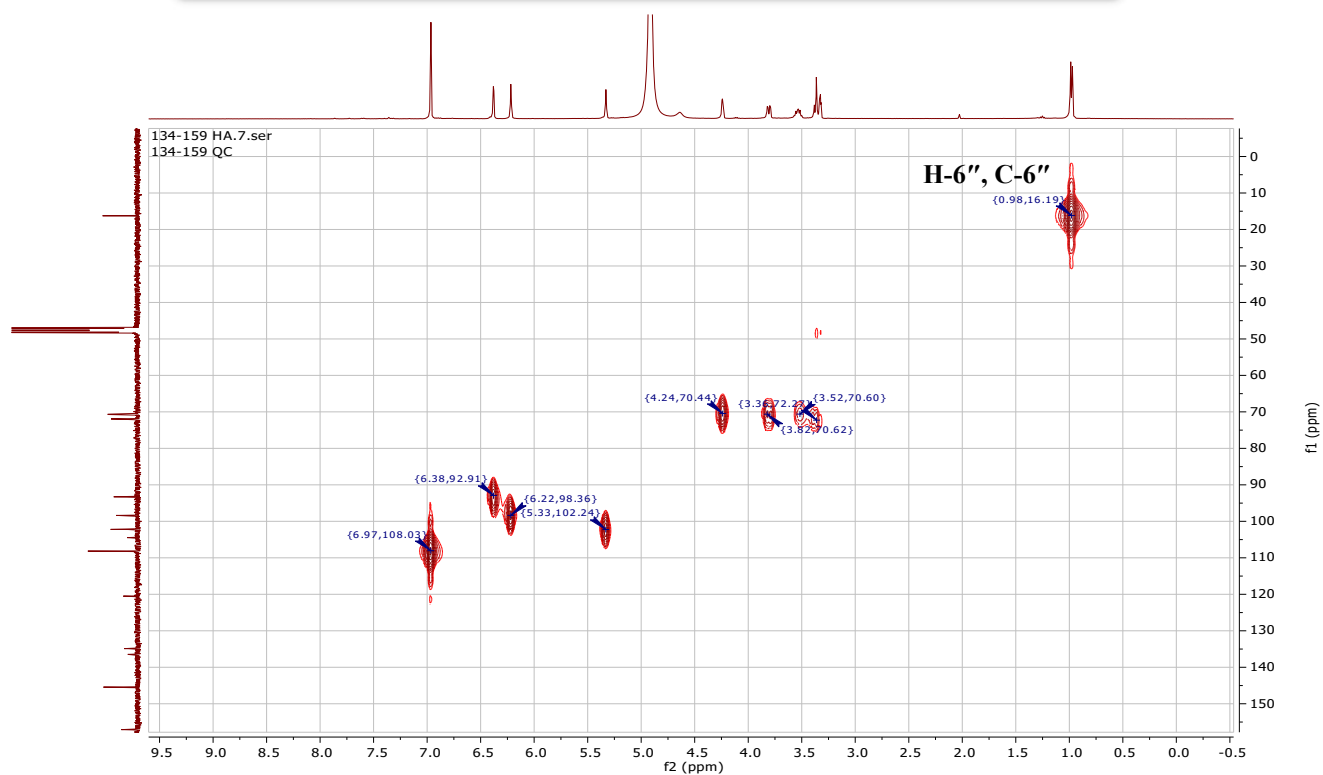


Figure II.2. 47. HSQC Spectrum of compound HAF3



Figure II. 48. HMBC Spectrum of compound HAF3

#### II.2.4.4.4. Compound HAF4

##### i. Physical properties

Compound **HAF4** (4 mg) was obtained as a light yellow amorphous powder.

##### ii. Chromatographic characters

Compound **HAF4** appeared as a dark spot under UV  $\lambda_{\max}$  254 which attained a yellow colour after spraying with 10% v/v vanillin/H<sub>2</sub>SO<sub>4</sub> and heating at 110 °C. It showed *R<sub>f</sub>* value of 0.66 in system I (Page 48).

##### iii. Spectroscopic data

**A. UV (MeOH)  $\lambda_{\max}$  nm (log  $\epsilon$ ):** 357.0 (4.28) , 256.9 (4.40)

**B. HR-ESI-MS :** *m/z* 463.066 [M-H]<sup>-</sup> .

##### C. <sup>1</sup>H-, <sup>13</sup>C-NMR and HMBC spectral analysis

The <sup>1</sup>H-, <sup>13</sup>C-NMR and HMBC spectral data of compound **HAF4** are listed in table II.2.10 and illustrated in figures thereafter.

**Table II.2.** <sup>1</sup>H-, <sup>13</sup>C-NMR and HMBC spectral data of compound **HAF4** (400 MHz, 100MHz , Methanol-*d*<sub>4</sub>, DMSO-*d*<sub>6</sub>).

Position	$\delta_H$ (ppm), multiplicity, <i>J</i> in Hz	$\delta_C$ (ppm)	HMBC (H→C)	<sup>1</sup> H- <sup>1</sup> H COSY
2		156.6	-	-
3		133.9	-	-
4		177.9	-	-
5		161.6	-	-
6	6.20, d, <i>J</i> = 2.0 Hz, 1H	99.2	C-5, 7, 8, 10	-
7	-	165.1	-	-
8	6.40, d, <i>J</i> = 2.0 Hz, 1H	94.0	C-6, 7, 9, 10	-
9	-	156.8	-	-
10	-	104.2	-	-
1'	-	121.6	-	-
2'	7.86, d, <i>J</i> = 2.2 Hz, 1H	116.4	C-2, 1', 3', 4'	-
3'	-	145.3	-	-
4'	-	148.9	-	-
5'	6.88, d, 8.5 Hz, 1H	115.6	C-3', 4', 6'	6'



6'	7.60, dd, 8.6, 2.2 Hz, 1H	122.4	C-2, 2', 4'	5'
1''	5.17, <i>d</i> , 7.9, 1H	102.3	C-3, 2''	2''
2''	3.83, <i>d</i> , 8.1, 1H	71.6	C-1'', 3''	1'', 3''
3''	3.58, dd, 6.4, 2.6 Hz, 1H	73.6	C-2'', 4'', 5''	2''
4''	3.87, <i>d</i> , 3.3 Hz, 1H	68.4	C-2'', 4''	
5''	3.50, <i>m</i> , , 1H	76.3	C-1'', 4'', 6''	
6''	H-6a 3.66 dd, 11.1, 6 Hz, 1H	60.6	C-4'', 5'',	
	H-6b 3.56, <i>d</i> , 5.9 Hz, 1H			

#### iv. Discussion and conclusion

Compound **HAF4** had the molecular formula  $C_{21}H_{20}O_{12}$  as established from the negative HR-ESI-MS by providing a molecular ion peak at  $m/z$  463,066  $[M-H]^-$  (calcd. 463,085) (Figure II.2.50)

The UV spectrum of compound **HAF4** exhibited **band I** absorption at 357.0 nm and **band II** absorption at 256.9 nm characteristic of flavonol with hydroxyl 3-OH substituted.

Its  $^1H$ -NMR spectrum (Figure II.2.51) showed the characteristic signals pattern of quercetin (**HAF1**). Two proton signals at 6.20, *d*,  $J = 2.0$  Hz, 1H) and 6.40, *d*,  $J = 2.0$  Hz, 1H) indicated the presence of a meta coupling system for H-6 and H-8 protons of ring A. Three proton signals at  $\delta_H$  6.87 (1H, *d*,  $J = 8.8$  Hz),  $\delta_H$  7.59 (1H, *dd*,  $J = 8.8, 2.0$  Hz) and  $\delta_H$  7.86 (1H, *d*,  $J = 2.0$  Hz) indicated the presence of an ABX coupling system characteristic for ring B of quercetin.

Its  $^{13}C$ -NMR spectrum (Figure II.2.52) showed 21 carbons. The upfield and downfield shifts of quercetin (**HAF1**) consistent with 3-*O*-glycosilation (Markham et al., 1978). Comparison of the  $^{13}C$ -NMR spectrum of compound (**HAF4**) with that of quercetin aglycone (**HAF1**) showed that the signal of C-3 was observed to shift upfield by (-2.07 ppm), whereas the signals of C-2 and C-4 were displaced downfield by (+8.82) and (+1.98) respectively.

**DEPT 135** (Figure II.2.53) experiment indicated the presence of one methylene carbon ( $\delta_C$  60.58 ppm), suggesting glucose or galactose unit.

The established structure for compound **HAF4** confirmed by the 2D NMR including HSQC,  $^1H$ - $^1H$ -COSY and HMBC (Figures II.2.54-56)

The nature of sugar unit deduced from  $^1H$ -NMR signal at  $\delta_H = 3.58$  ppm (*dd*,  $J = 6.4, 2.6$  Hz, 1H) of the proton H-3'', indicating axial-axial coupling of H-3''/H-2'' and axial-equatorial coupling of H-3''/H-4'' characteristic of galactose unit.

The acid hydrolysis was realized according to the method described in page (54) which allowed us

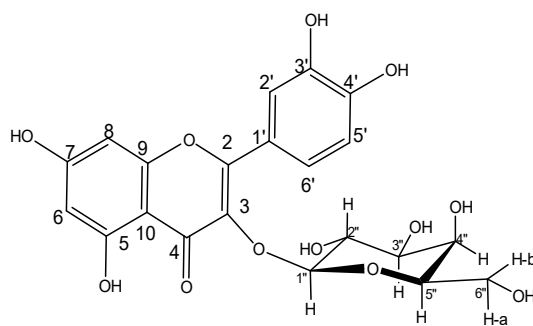
to identify a sugar type D-galactose.

The anomeric proton of galactose H-1'' shows axial -axial coupling with H-2'' ( $J = 7.9$  Hz), indicating  $\beta$  configuration of the sugar unit.

The position of  $\beta$ -D-galactopyranosyl unit was confirmed by HMBC correlation between the anomeric proton at  $\delta_H = 5.17$  ppm and carbon C-3 at  $\delta_C = 133.9$  ppm (Figure II.2.55).

All data were consistent with that of Quercetin -3-O- $\beta$ -D-galactopyranoside (Moon et al., 2001)

Therefore, it was identified as hyperoside or hyperin previously isolated from the genus *Hypericum* (Wu et al., 2002). Hyperoside has been reported as antioxidant agent, in previous studies it was shown to exert anti-inflammatory and anti-arthritic effects and to inhibit proliferation (Jin et al., 2016; Zhang et al., 2014).



**Structure of compound HAF4:  
Quercetin -3-O- $\beta$ -D-galactopyranoside**

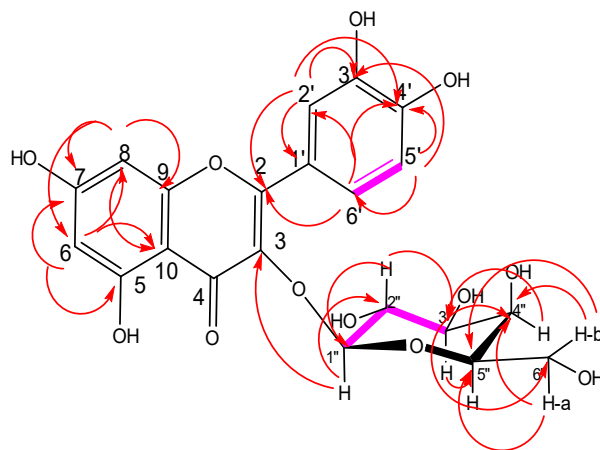


**Figure II.2. 49. Important HMBC (H→C) and COSY (→) correlation of compound HAF4**

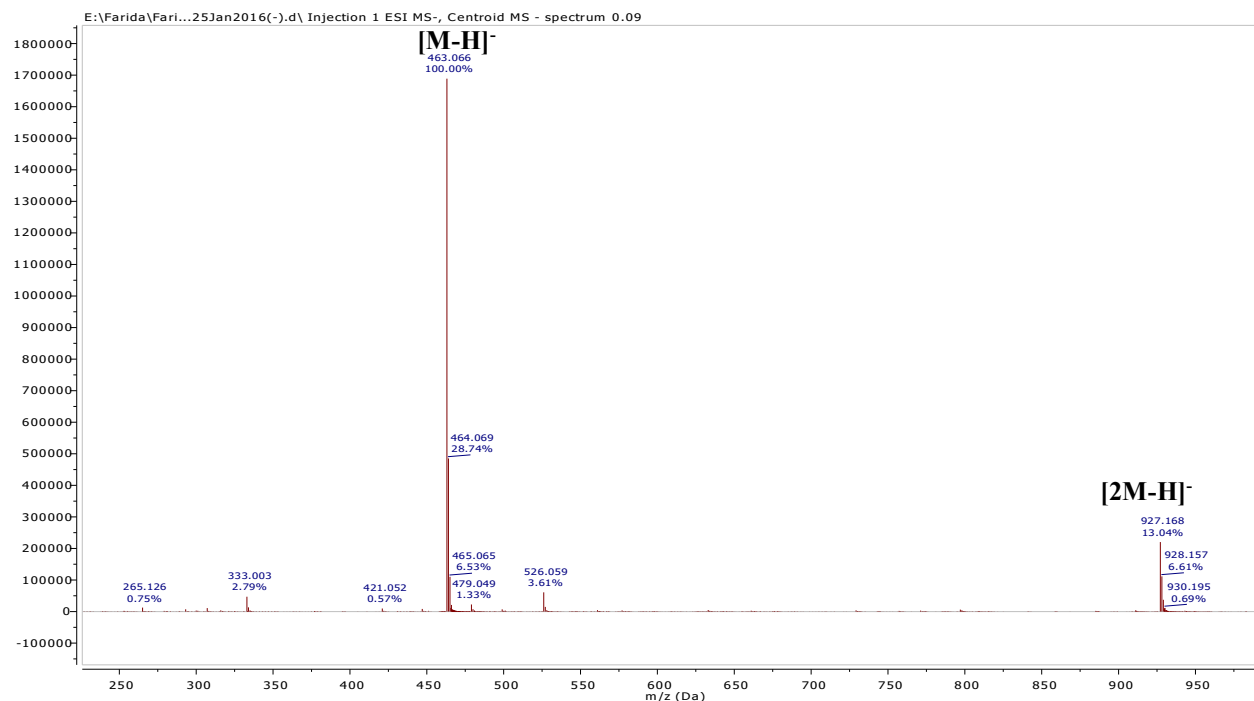


Figure II.2. 50. Negative HR-ESI-MS spectrum of compound HAF4

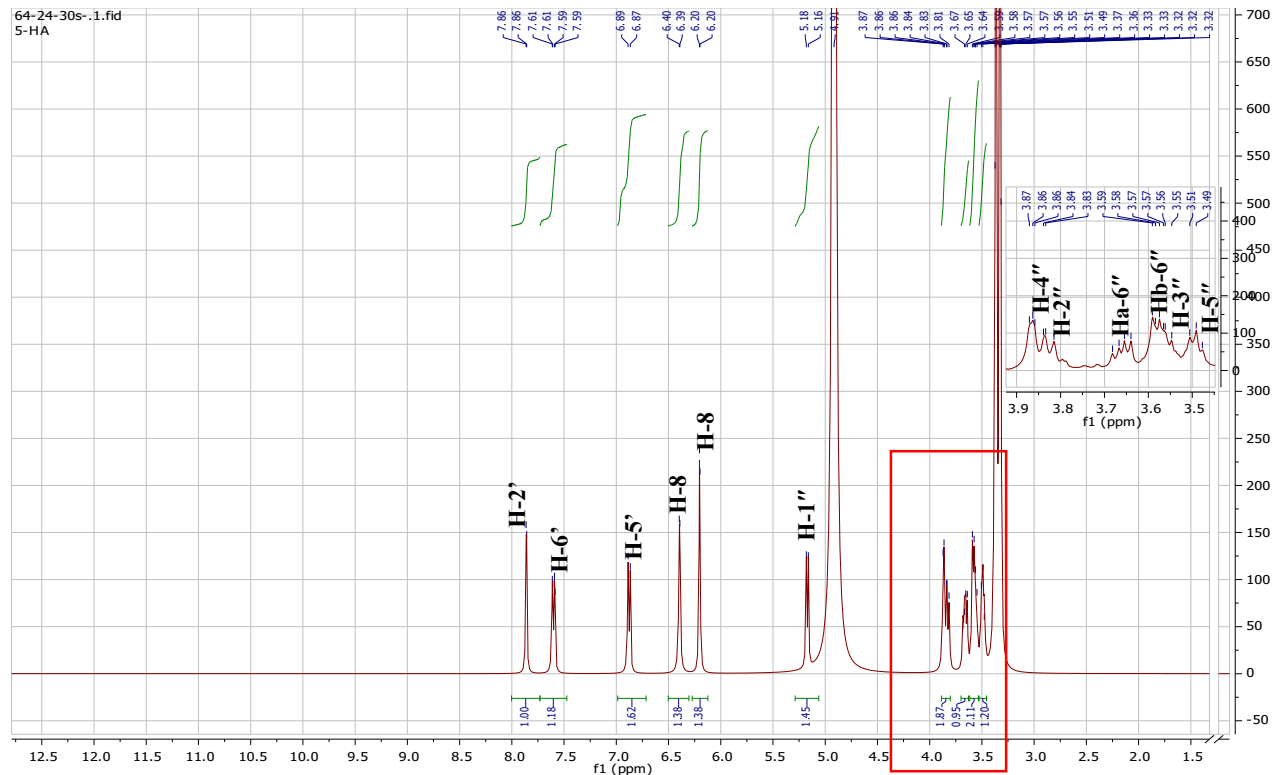


Figure II.2. 51. <sup>1</sup>H-NMR Spectrum of compound HAF4( Methanol-*d*<sub>4</sub>, 400 MHz)

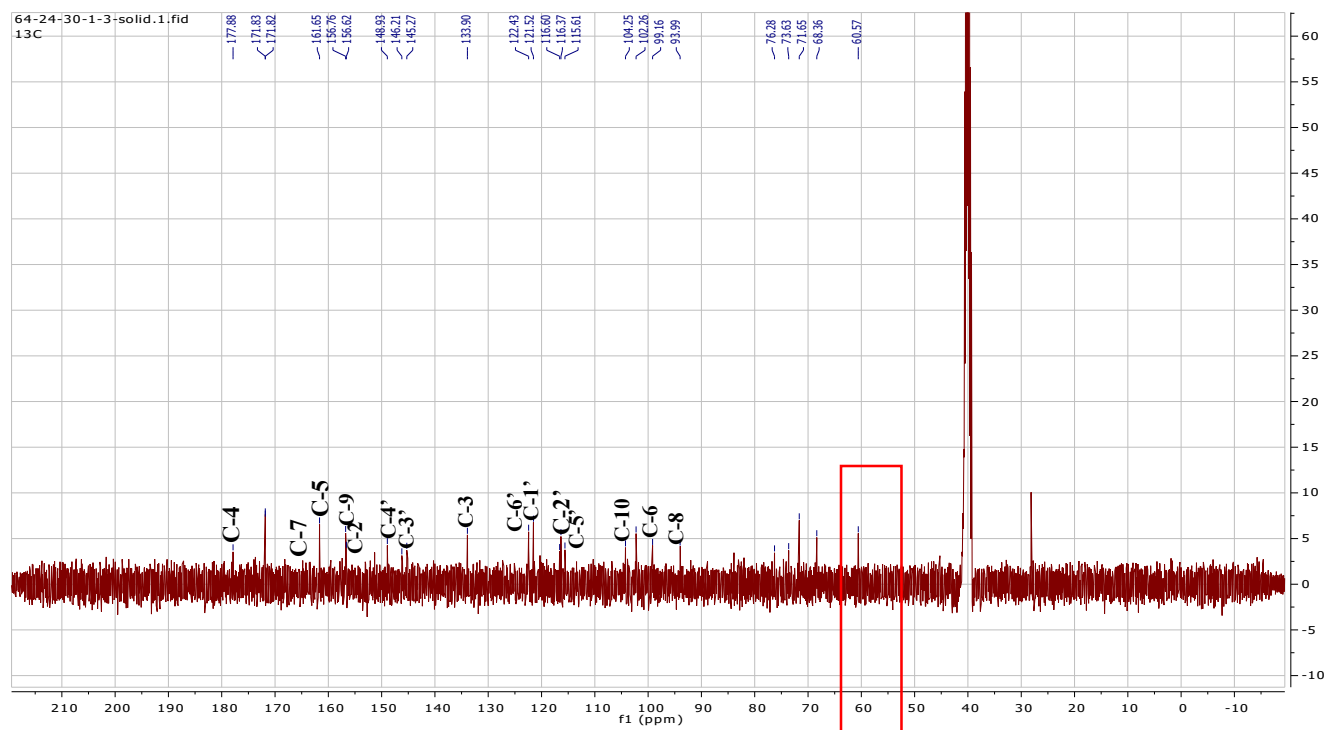


Figure II.2. 52.  $^{13}\text{C}$ -NMR Spectrum of compound HAF4 (Methanol- $d_4$ , 100 MHz)

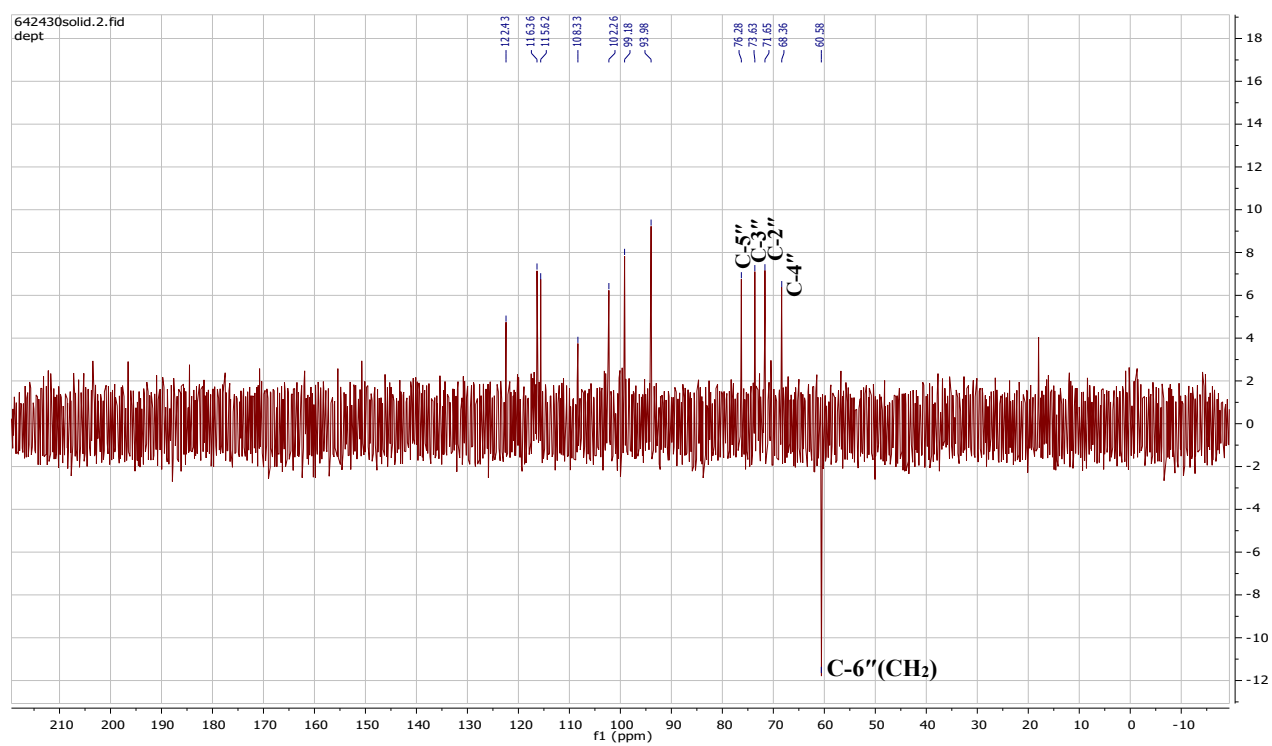


Figure II.2. 53. DEPT135 Spectrum of compound HAF4

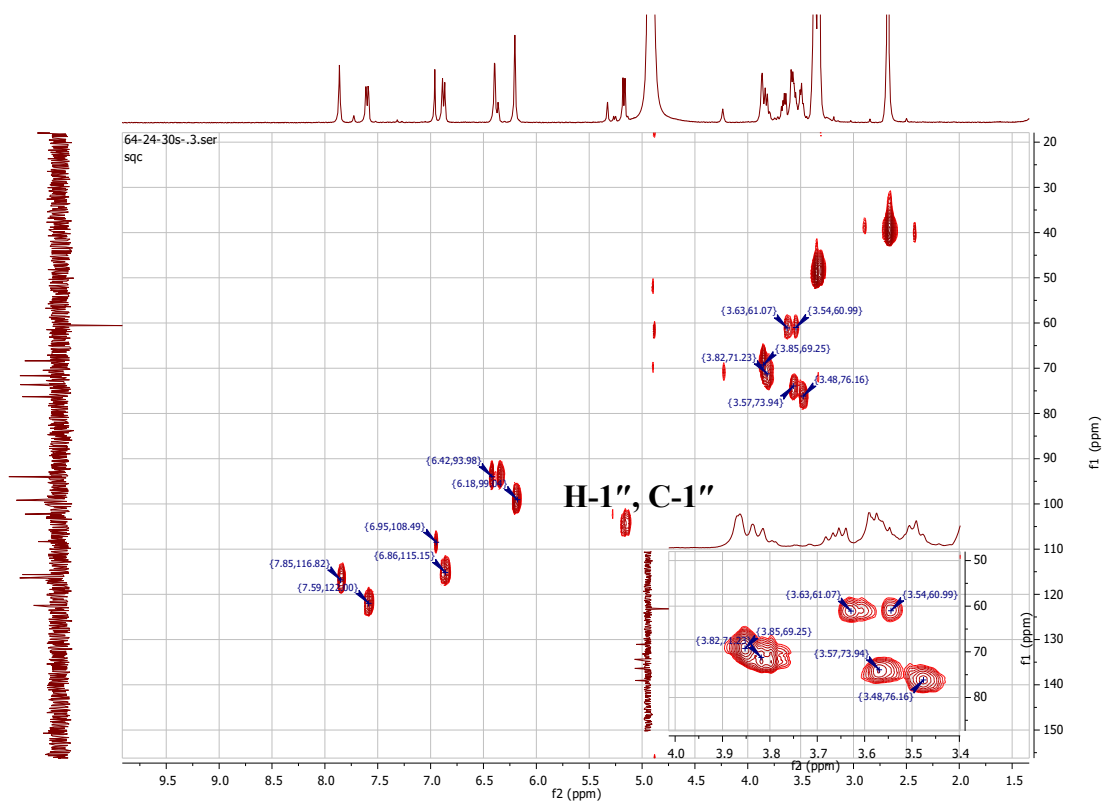


Figure II.2. 54. HSQC Spectrum of compound HAF4

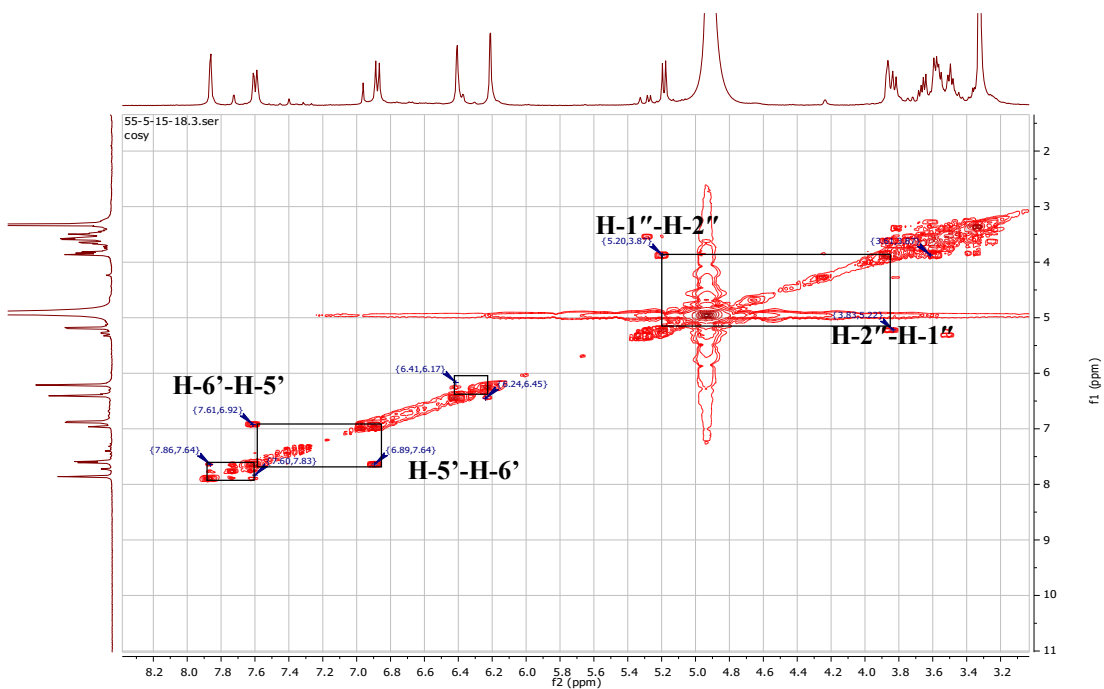
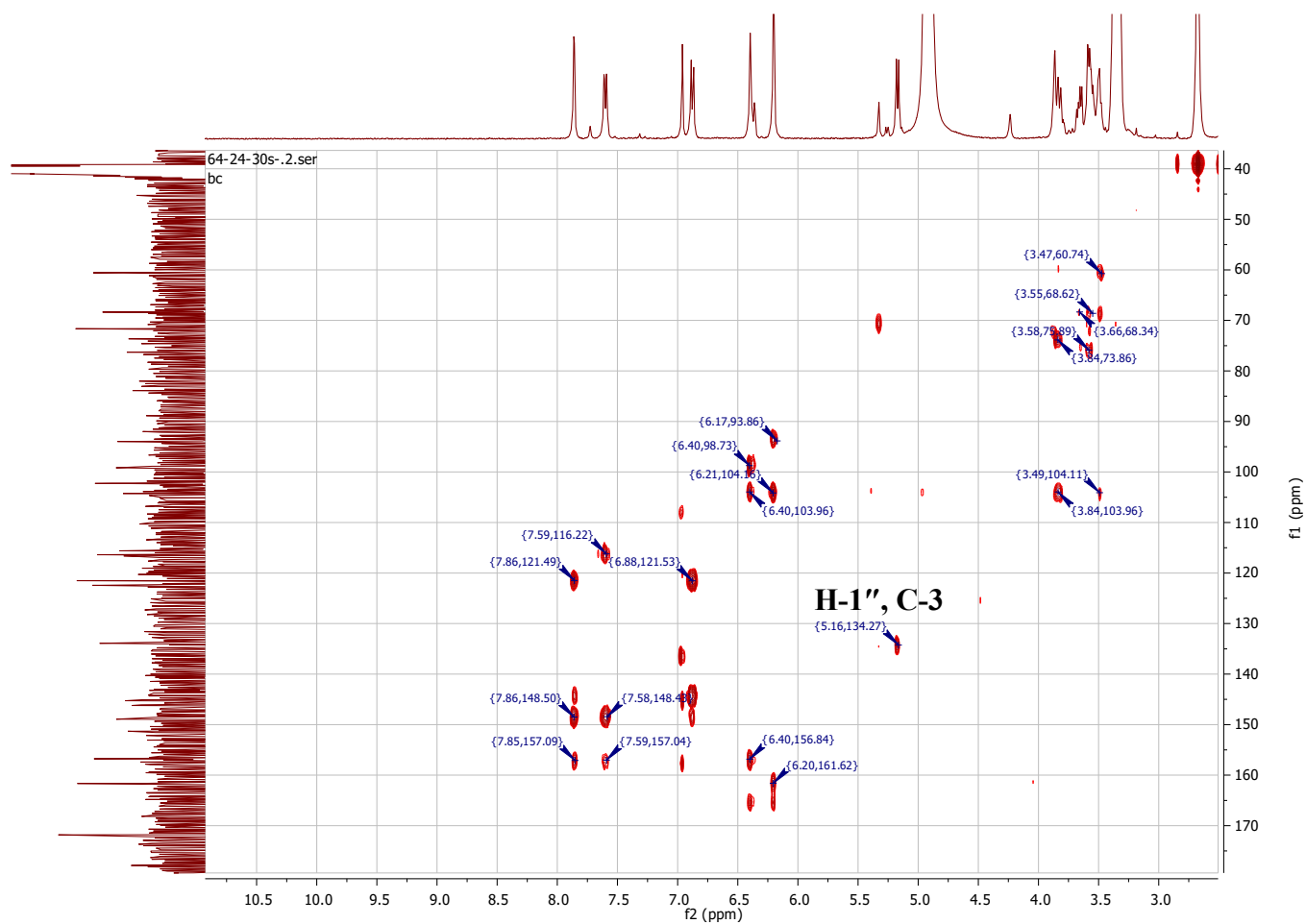


Figure II.2. 55. COSY spectrum of compound HAF4



FigureII. 56. HMBC Spectrum of compound HAF4

#### II.2.4.4.5. Compound HAF5

##### i. Physical properties

Compound **HAF5** (5 mg) was obtained as a yellow amorphous powder.

##### ii. Chromatographic characters

Compound **HAF5** appeared as a dark spot under UV  $\lambda_{\max}$  254 which attained a yellow color after spraying with 10% v/v vanillin/H<sub>2</sub>SO<sub>4</sub> and heating at 110 °C. It showed *R<sub>f</sub>* value of 0.62 in system I (Page 48).

##### iii. Spectroscopic data

A. **UV (MeOH)  $\lambda_{\max}$  nm (log  $\epsilon$ ):** 256.0 (4.60), 359.0 (4.50).

B. **HR-ESI-MS:** *m/z* 479.095 [M-H]<sup>-</sup>

C. **<sup>1</sup>H-, <sup>13</sup>C-NMR and HMBC spectral analysis**

The <sup>1</sup>H, <sup>13</sup>C-NMR and HMBC spectral data of compound **HAF5** are listed in table II.2.11 and illustrated in figures thereafter.

**Table II.2. 11.** <sup>1</sup>H-, <sup>13</sup>C-NMR and HMBC spectral data of compound **HAF5** (400 MHz, 100MHz Mthanol-*d*<sub>4</sub>.)

Position	$\delta_H$ (ppm), multiplicity, J(Hz)	$\delta_C$ (ppm)	HMBC (H→C)
2	-	156.0	-
3	-	133.8	-
4	-	177.0	-
5	-	160.5	-
6	6.19, d, J = 2.3 Hz, 1H	97.7	C-5, 7, 8, 10
7	-	163.7	-
8	6.37, d, J = 2.4 Hz, 1H	92.5	C-6, 7, 9, 10
9	-	156.4	-
10	-	107.8	-
1'	-	119.4	-
2', 6'	7.40, s, 2H	107.8	C-2, 1', 3', 4', 5'
3', 5'	-	144.0	-
4'	-	135.8	-
1''	5.21, d, J = 7.8 Hz, 1H	103.3	C-3,2''
2''	3.85, d, 8.0, 1H	71.1	C-3''

3"	3,60, dd, 6.9, 4.2 Hz, 1H	72.9	C-5"
4"	3.89, d, 5.0 Hz, 1H	67.8	C-3"
5"	3,55, m, 1H	74.9	C-4", 6"
6"	<b>H-6-a</b> 3.68, dd, 10.9, 6.0 Hz, <b>H-6-b</b> 3.63 d, 3.2 Hz, 1H	59.8	C-5"

#### iv. Discussion and conclusion

Compound **HAF5** had the molecular formula  $C_{21}H_{20}O_{13}$  as established from the negative HR-ESI-MS (Figure II.2.58) by providing a molecular ion peak at  $m/z$ : 479,095  $[M-H]^-$  (calcd. 479,080) A fragment ion obtained at  $m/z$  317.096 characterized aglycone as myricetin.

The UV spectrum of compound **HAF5** exhibited **band I** absorption at 359.0 nm and **band II** absorption at 256.0 nm characteristic of flavonol with hydroxyl 3-OH substituted (REF THESE RH). Its  $^1H$ -NMR spectrum (Figure II.2.59) showed the characteristic signals pattern of myricetin, The  $^1H$ -NMR spectrum exhibited a characteristic meta-coupled proton signal at  $\delta$  6.19 (1H, d,  $J = 2.3$  Hz) and 6.37 (1H, d,  $J = 2.4$  Hz) corresponding to H-6 and H-8 of flavonoid A ring.

The singlet signal at  $\delta$  7.39 (2H, br s) was assigned to H-2' and H-6' of B ring.

Its  $^{13}C$ -NMR spectrum (Figure II.2.60) showed the upfield and downfield shifts of myricetin consistent with 3-*O*-glycosilation.

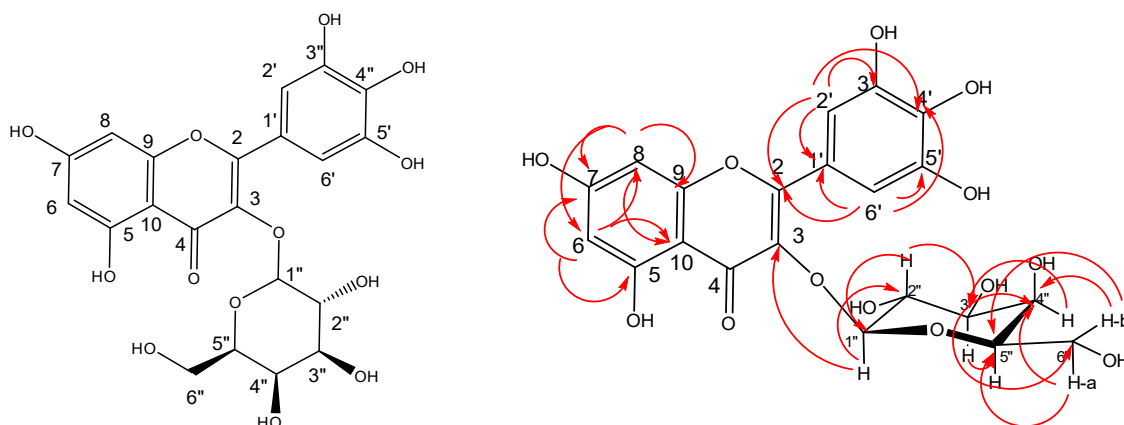
**DEPT** (Figure II.2.61) experiment indicated the presence of one methylene carbon ( $\delta_C$  59.8 ppm), suggesting glucose or galactose unit.

The nature of sugar unit deduced from  $^1H$ -NMR signal at  $\delta_H$  3,66 (*dd*,  $J = 9.5, 3.4$  Hz, 1H) of the proton H-3", indicating axial-axial coupling of H-3"/H-2" and axial-equatorial coupling of H-3"/H-4" characteristic of galactose unit.

The anomeric proton of galactose H-1" shows axial -axial coupling with H-2" ( $J = 7.8$  Hz), indicating  $\beta$  configuration of the sugar unit. The acid hydrolysis was realized according to the method described in page 54 which allowed us to identify a sugar type D-galactose.

The position of  $\beta$ -D-galactopyranosyl unit was confirmed by HMBC correlation between the anomeric proton at  $\delta_H$  5.17 (H-1", *d*, 7.8 Hz, 1H) and carbon C-3 at  $\delta_C = 133.8$  ppm (Figure II.2.64). All data were consistent with that of myricetin-3-*O*- $\beta$ -D-galactopyranoside (Paul et al., 1974). Therefore, it was identified as myricetin-3-*O*- $\beta$ -D-galactopyranoside previously isolated from the genus *Hypericum* (Zdunić et al., 2011).





**Structure of compound HAF5:  
Myricetin-3-*O*- $\beta$ -D-galactopyranoside**

**Figure II.2. 57 Important HMBC (H $\rightarrow$ C) correlation of compound HAF5.**

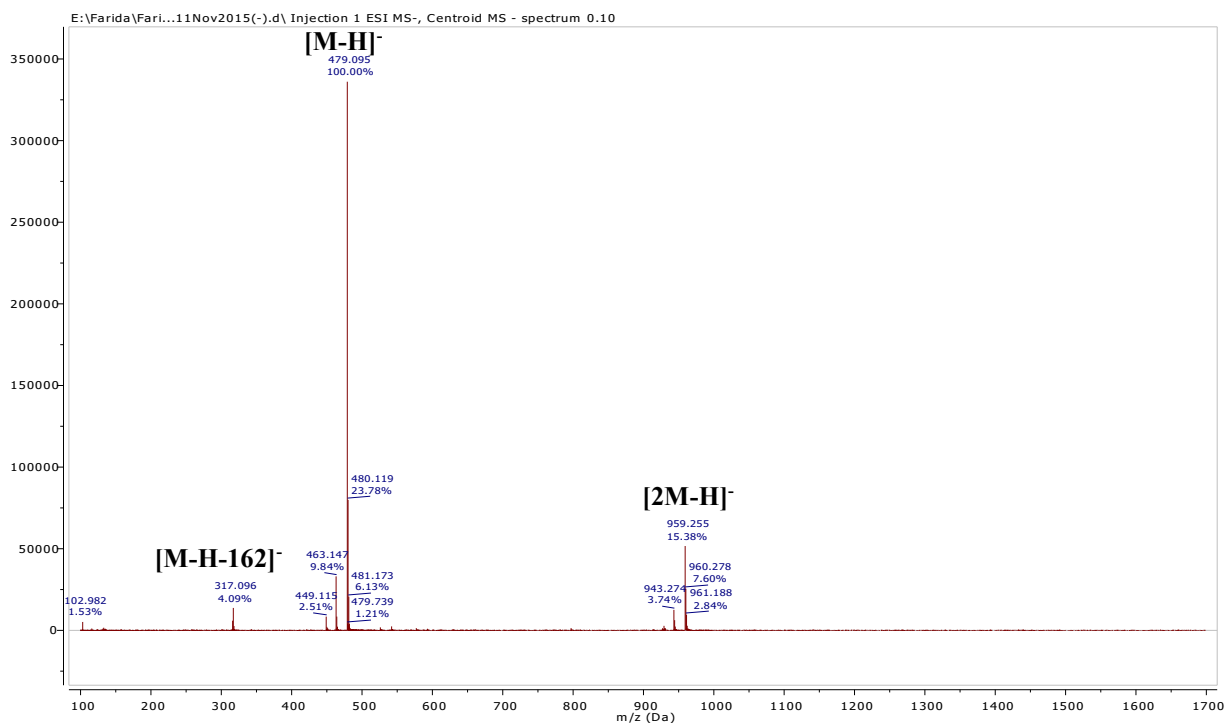


**Figure II.2. 58. Negative HR-ESI-MS of compound HAF5**

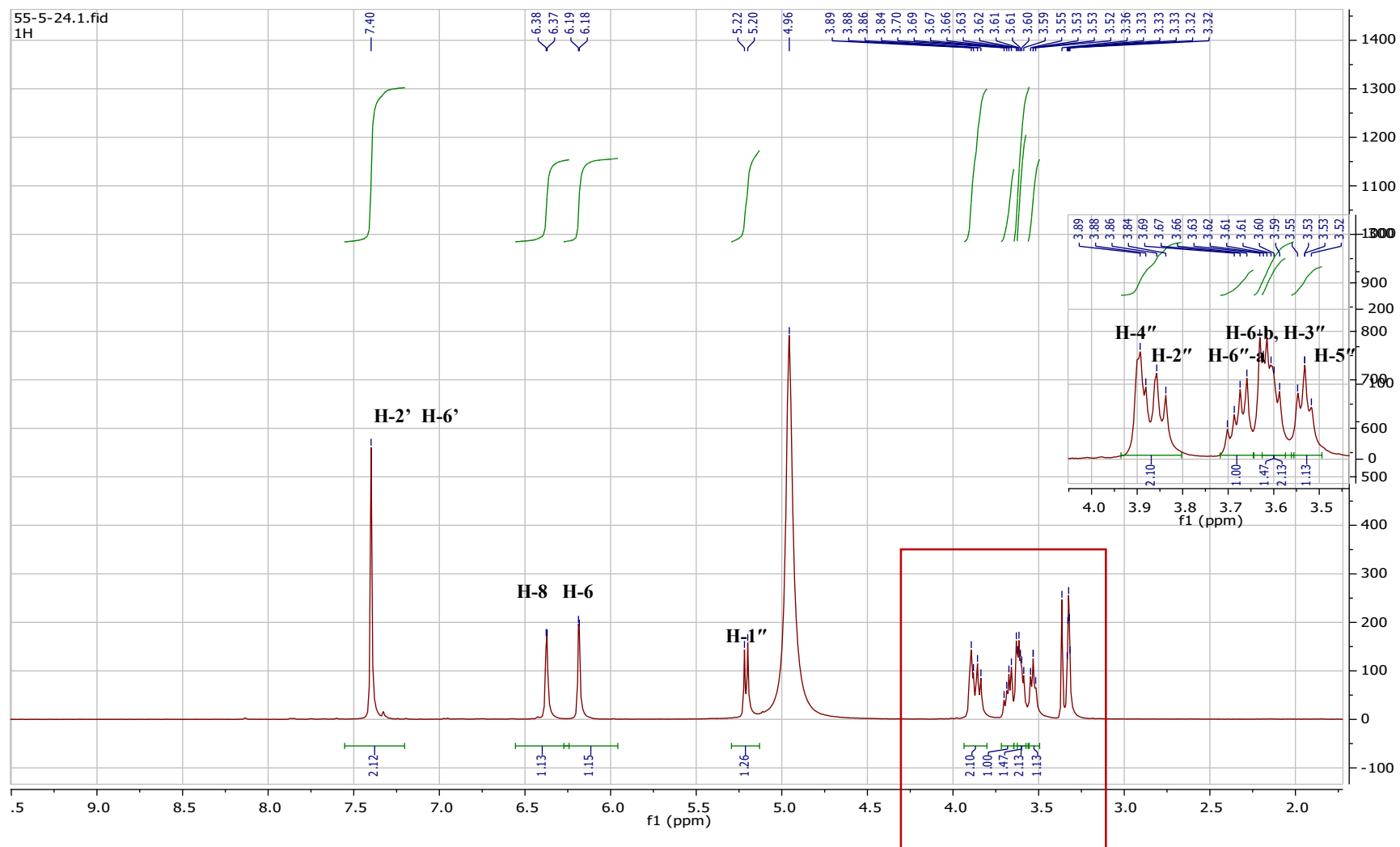


Figure II.2. 59.  $^1\text{H}$ -NMR Spectrum of compound HAF5 (Methanol- $d_4$ , 400 MHz)

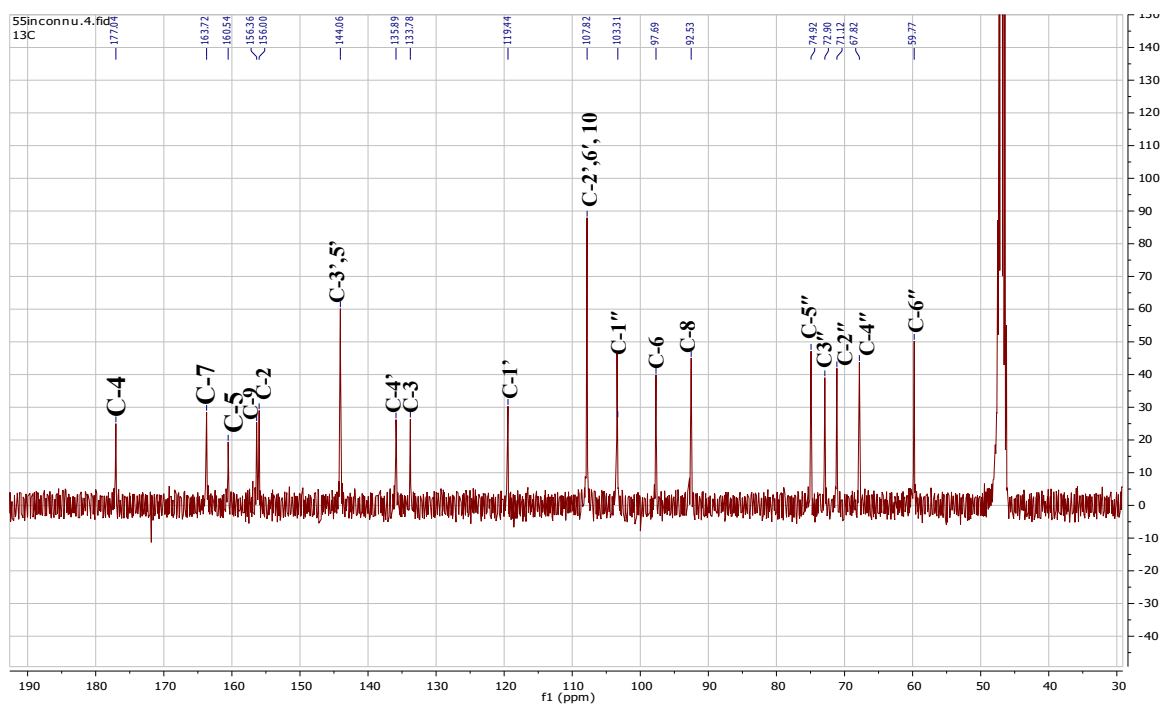


Figure II.2. 60.  $^{13}\text{C}$ -NMR Spectrum of compound HAF5 (Methanol- $d_4$ , 100 MHz)

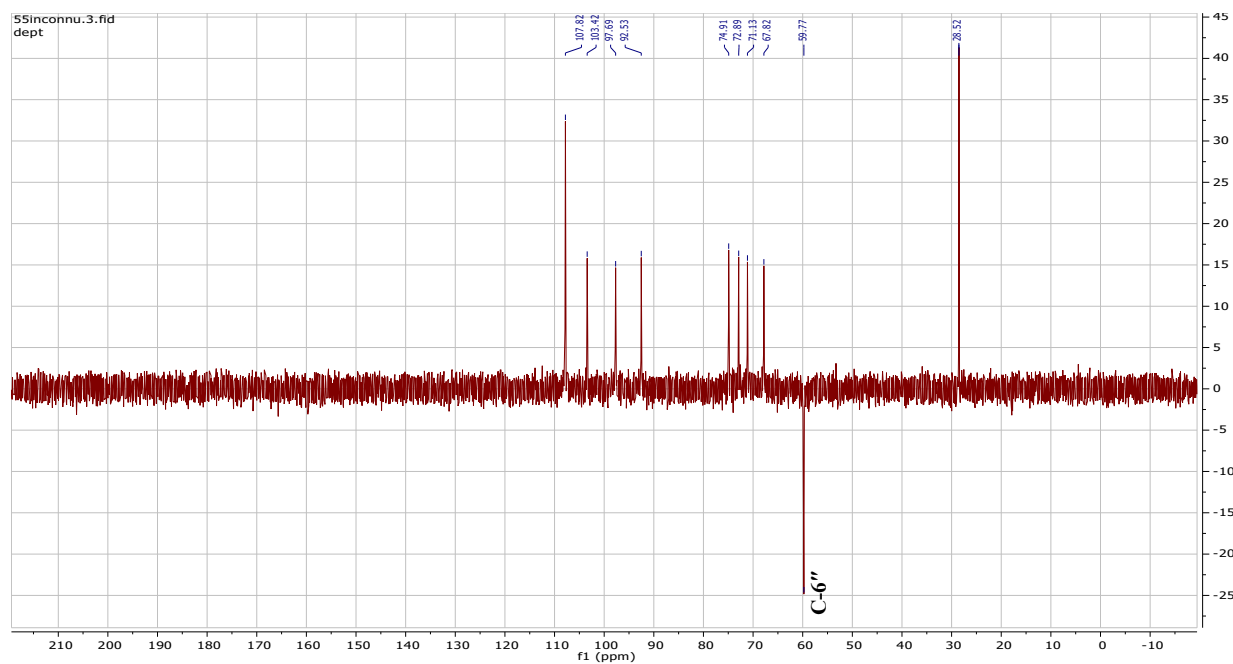


Figure II.2. 61. DEPT135 Spectrum of compound HAF5

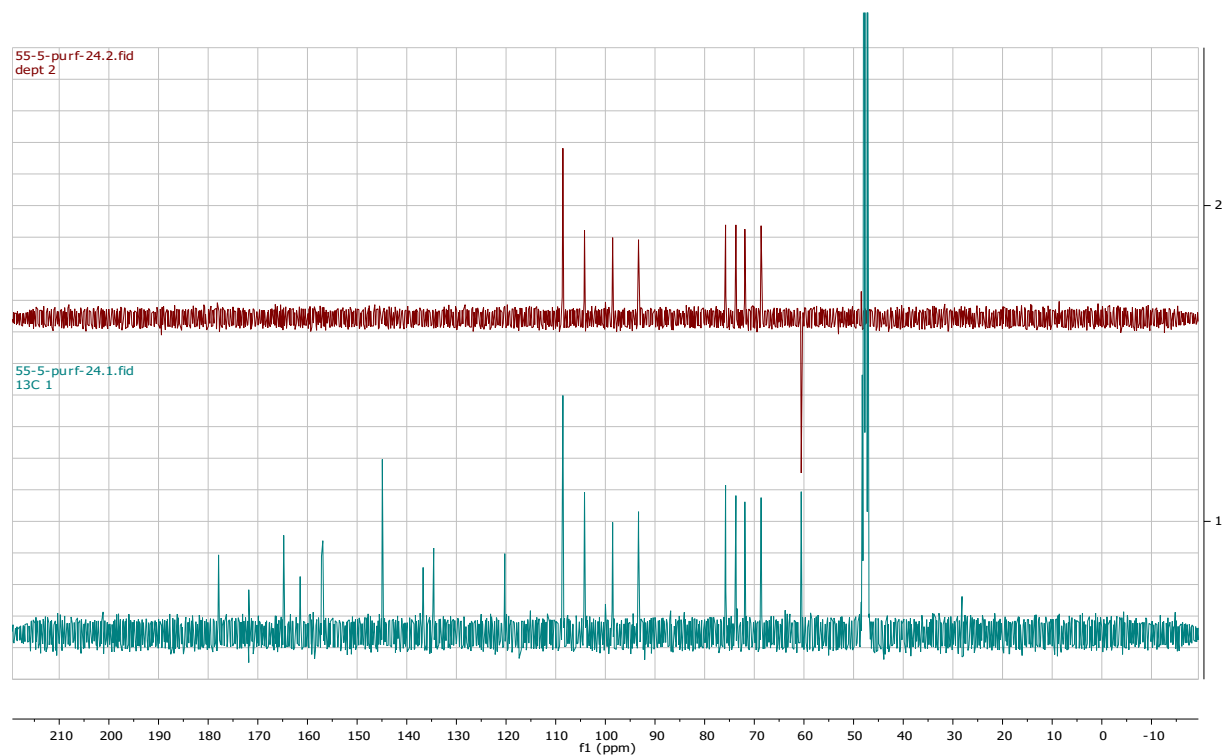


Figure II.2. 62. Comparison of  $^{13}\text{C}$ -NMR and DEPT 135 spectra of compound HAF5

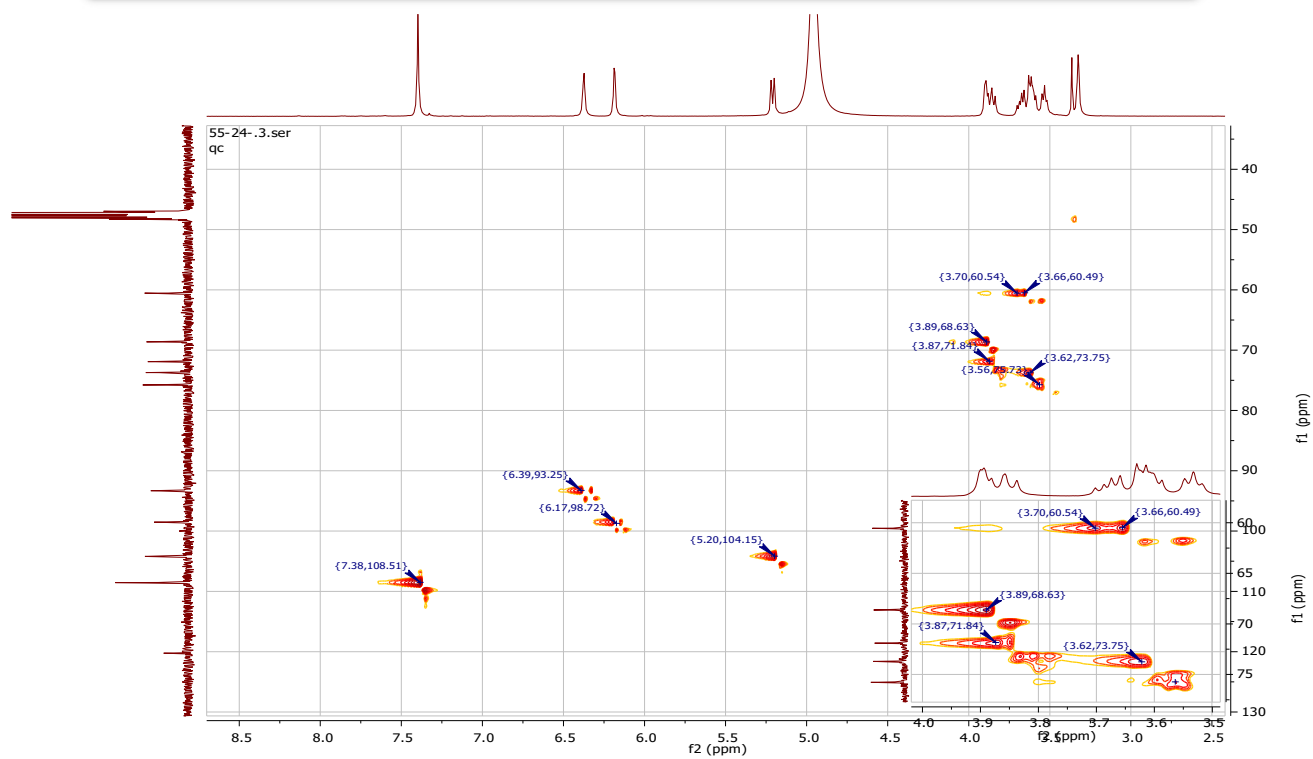


Figure II.2. 63. HSQC Spectrum of compound HAF5

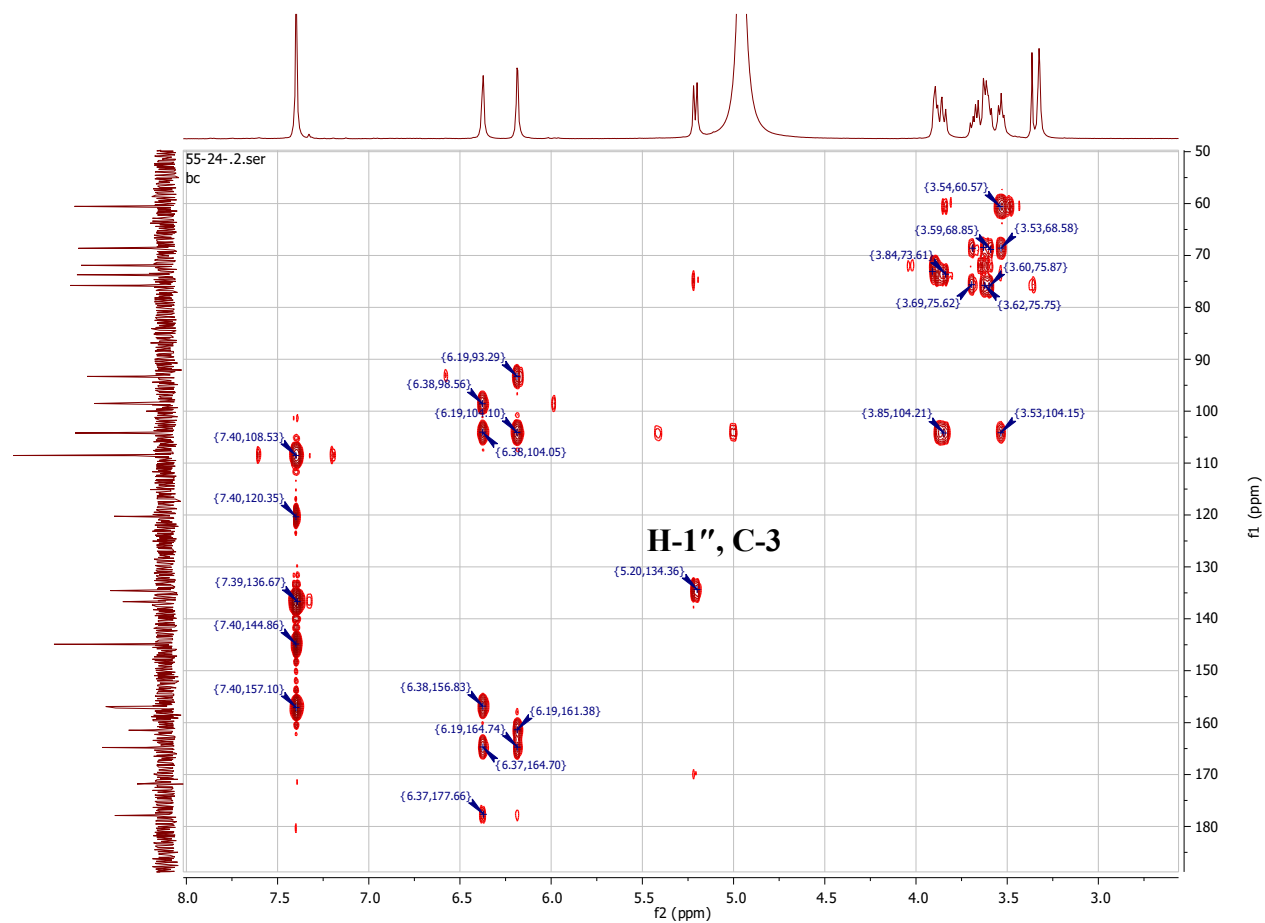


Figure II. 64. HMBC Spectrum of compound HAF5

#### II.2.4.4.6. Compound HAF6

##### i. Physical properties

Compound **HAF6** (10.6 mg) was obtained as a yellow amorphous powder.

##### ii. Chromatographic characters:

Compound **HAF6** appeared as a dark spot under UV  $\lambda_{\max}$  254 which attained a yellow color after spraying with 10% v/v vanillin/H<sub>2</sub>SO<sub>4</sub> and heating at 110 °C. It showed  $R_f$  value of 0.67 in system I (Page 48).

##### iii. Spectroscopic data

A. UV (MeOH)  $\lambda_{\max}$  nm (log  $\epsilon$ ): 369.9 (4.41), 253.0 (4.49)

B. HR-ESI-MS: m/z: 479,103 [M-H]<sup>-</sup>

##### C. <sup>1</sup>H-, <sup>13</sup>C-NMR and HMBC spectral analysis

The <sup>1</sup>H, <sup>13</sup>C-NMR and HMBC spectral data of compound **HAF6** are listed in table II.2.12 and illustrated in figures thereafter.

**Table II.2. 12.** <sup>1</sup>H-, <sup>13</sup>C-NMR and HMBC spectral data of compound **HAF6** (400 MHz, 100MHz, Methanol-*d*<sub>4</sub>)

Position	$\delta_H$ (ppm), multiplicity, $J$ (Hz)	$\delta_C$ (ppm)	HMBC (H→C)
2	-	145.9	-
3	-	136.1	-
4	-	175.8	-
5	-	160.9	-
6	6.13, d, $J = 2.0$ Hz, 1H	97.7	C-5, 8,10
7	-	164.2	-
8	6.36, d, $J = 2.0$ Hz, 1H	92.9	C-6, 9, 10
9	-	156.7	-
10	-	102.9	-
1'	-	121.9	-
2'	7.67 d, $J = 2.0$ Hz, 1H	108.4	C-6',4', 6'
3'	-	145.4	-
4'	-	137.2	-
5'	-	145.8	-
6'	7.51 d, $J = 2.0$ Hz, 1H	110.2	C-1', 2', 3', 4'

1"	4.89, d, $J = 7.9$ Hz, 1H	102.9	C-3', 2''
2"	3.59 – 3.55, m, 2H	73.4	C-3''
3"	3.59 – 3.55, m, 2H	76.2	C-4"
4"	3.52, m, 2H	69.8	C-3'', 5"
5"	3.52, m, 2H	76.9	C-1", 3''
6"	H-6-a 3.97, d, $J = 12.0$ Hz, 1H H-6-b 3.83, dd, $J = 12.3, 4.4$ Hz, 1H	61.0	C-5'', 4''

#### iv. Discussion and conclusion

Compound **HAF6** had the molecular formula  $C_{21}H_{20}O_{13}$  as established from the negative HR-ESI-MS (Figure II.2.66), by providing a molecular ion peak at  $m/z$ : 479.103  $[M-H]^-$  (calcd. 479,080). In addition, the negative HR-ESI-MS shows fragment ion at  $m/z$  317.059 characterized aglycone as myricetin, suggesting a molecule of myricetin glycoside derivative. A loss of 162 mass units from the molecular ion and a signal at  $\delta_C = 61.0$  ppm, shown by **DEPT** (Figure II.2.69) to represent a  $CH_2$  group, suggested glucose or galactose unit.

The  $^1H$  and  $^{13}C$ -NMR spectra (Figures II.2.67-68) of **HAF6** were very similar to those of **HAF5**, except for the appearance of two characteristic meta-coupled proton signals at  $\delta_H$  7.50 (d,  $J = 2.0$  Hz) and  $\delta_H$  7.67 (d,  $J = 2.0$  Hz) instead of a singlet of protons H-2' and H-6'.

Its  $^{13}C$ -NMR spectrum showed the upfield and downfield shifts of myricetin consistent with 3'-*O*-glycosilation.

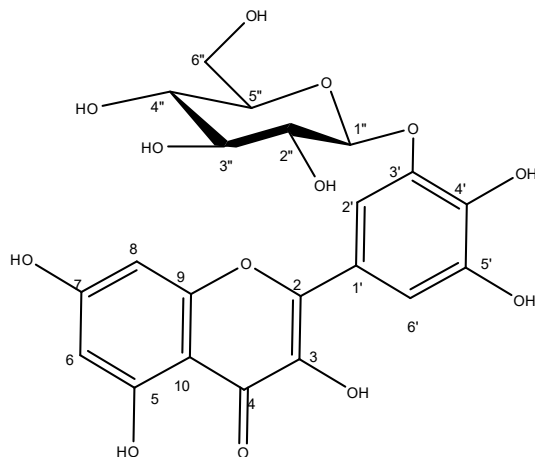
The acid hydrolysis was realized according to the method described in page 54 which allowed us to identify a sugar type D-glucose.

The anomeric proton of glucose H-1''' shows axial -axial coupling with H-2'' ( $J = 7.9$  Hz), indicating  $\beta$  configuration of the sugar unit.

The position of  $\beta$ -D-glucopyranosyl unit was confirmed by **HMBC** correlation between the anomeric proton at  $\delta_H = 4.89$  ppm (H-1'', d, 7.9 Hz, 1H) and carbon C-3' at  $\delta_C = 145.4$  ppm (Figure II.2.71).

From the above data the compound **HAF6** was identified as myricetin-3'-*O*- $\beta$ -D-glucopyranoside known as cannabiscitrin. This conclusion was also clarified by 2D-NMR spectra correlations (Figures II.2.70-71). The data was consistent with the previously reported data (Baoliang et al., 1993). Reviewing the available current literature, it is the first report for its isolation from the genus *Hypericum*.

Myricetin-3'-*O*- $\beta$ -D-glucopyranoside or Cannabiscitrin, is a very rare flavonoid, it was isolated for first time from *Abelmoschus manihot* (L.) (李春梅 et al., 2010).



**Structure of compound HAF6:  
Myricetin-3'-*O*- $\beta$ -D-glucopyranoside**

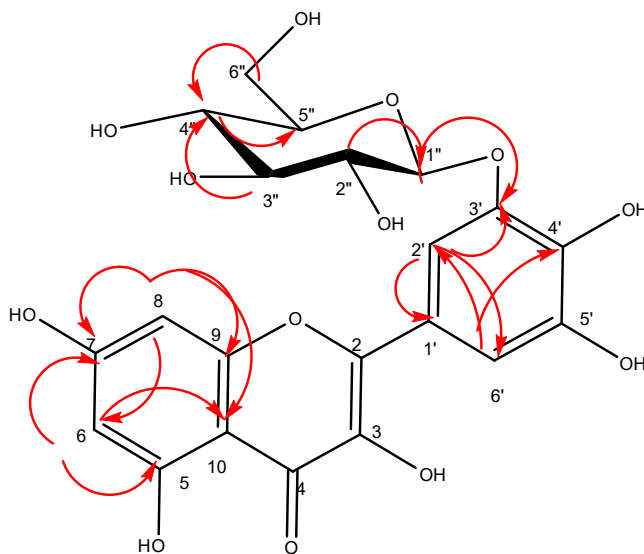


**Figure II.2. 65. Important HMBC (H $\rightarrow$ C) correlation of compound HAF6**



[M-H]<sup>-</sup>

[M-H-162]<sup>-</sup>

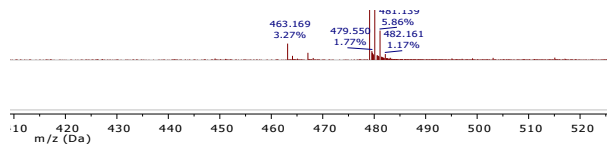


Figure II.2. 66. Negative HR-ESI-MS of compound HAF6

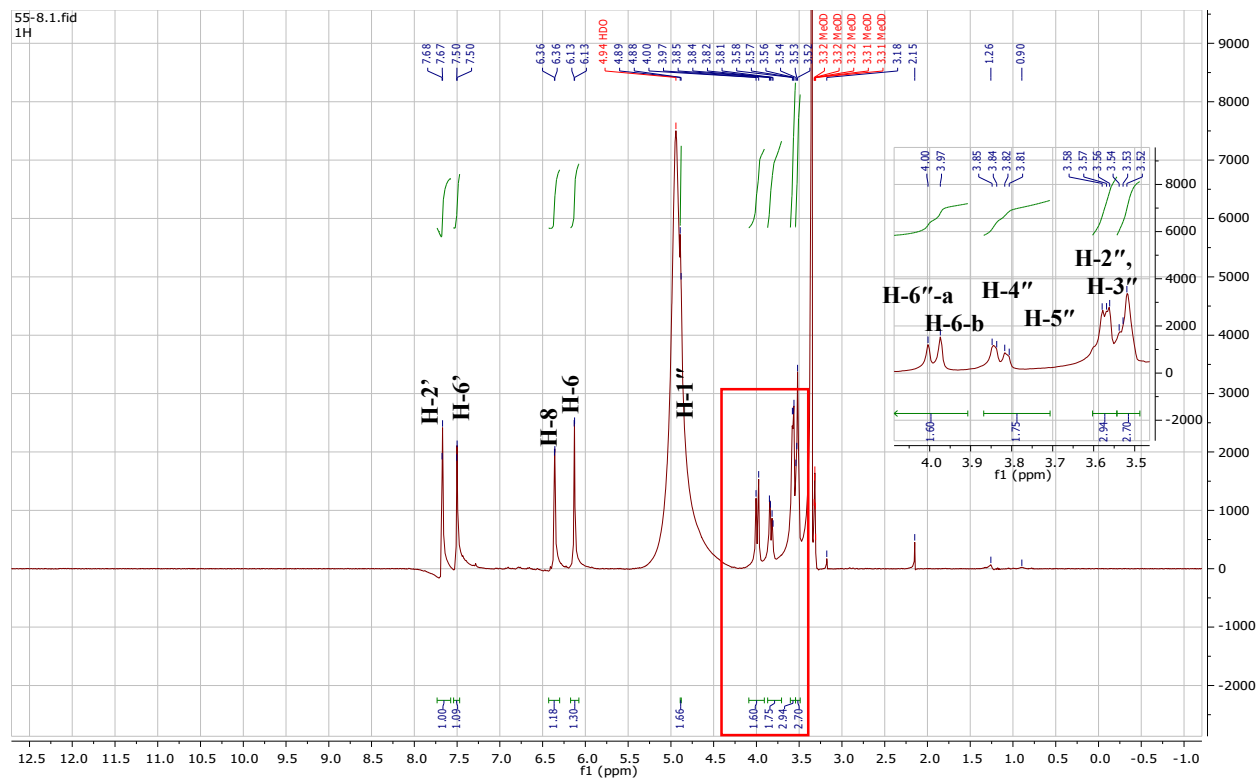
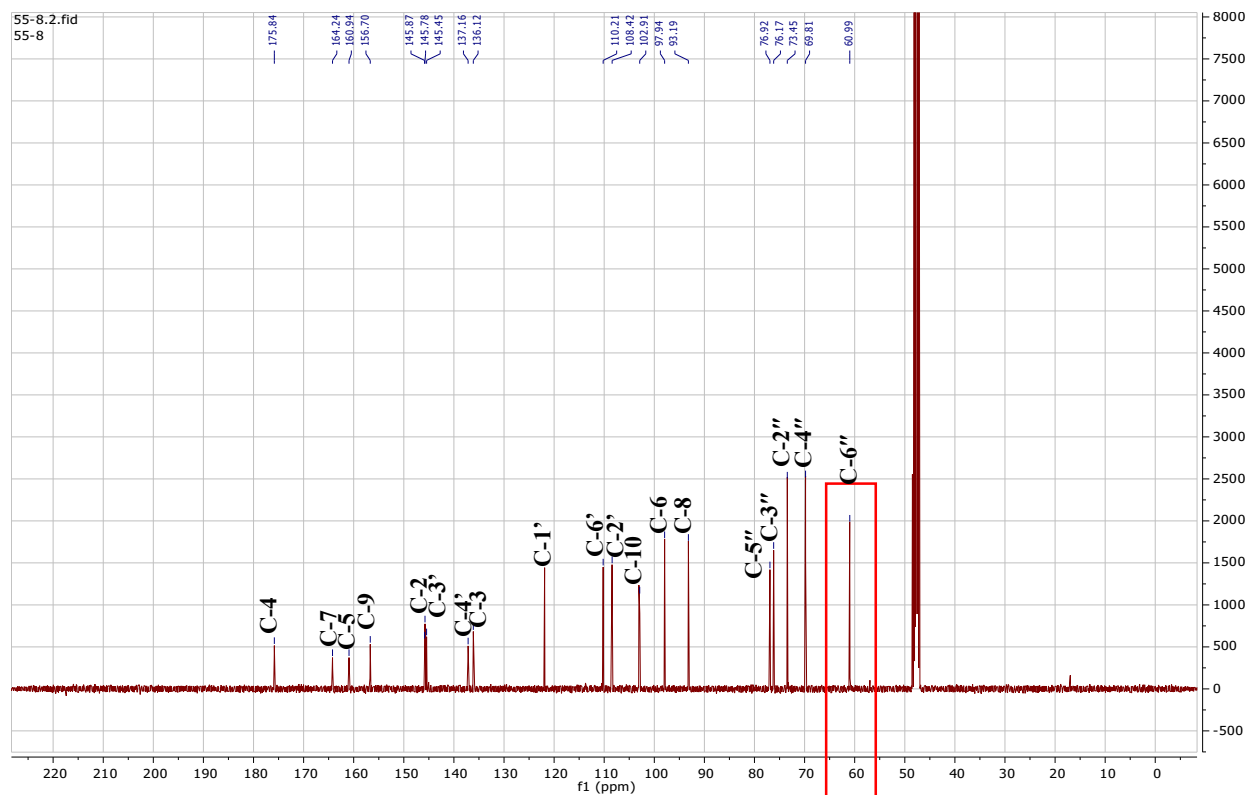
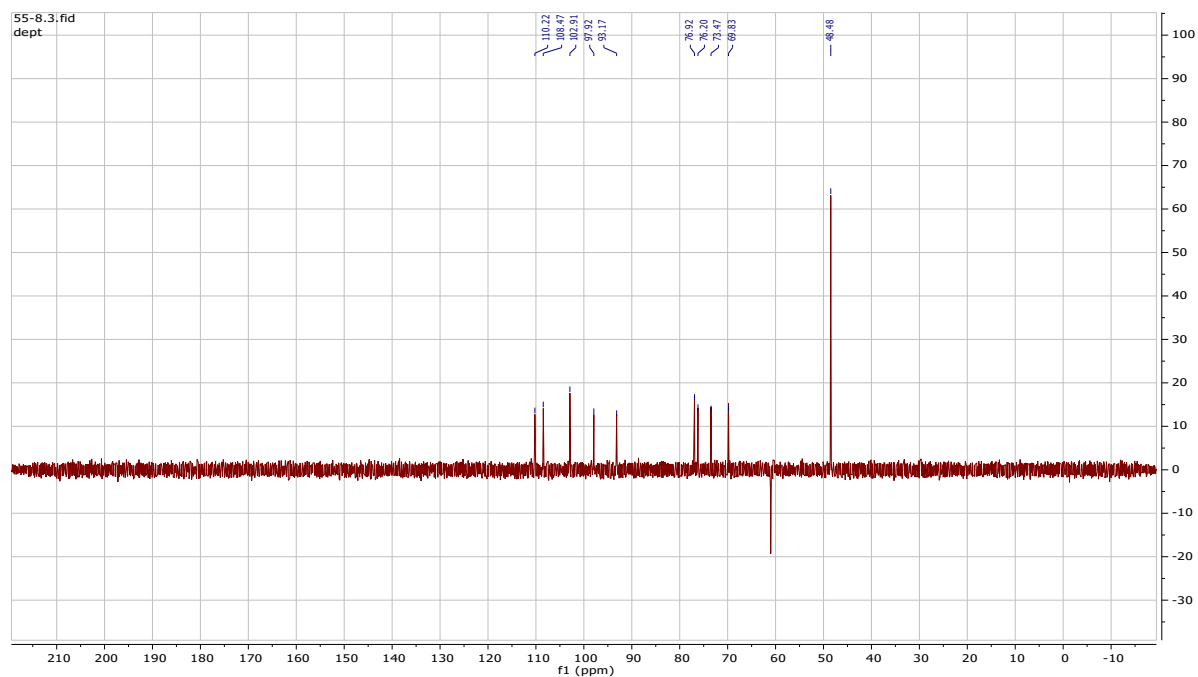


Figure II.2. 67. <sup>1</sup>H-NMR Spectrum of compound HAF6 (Methanol-*d*<sub>4</sub>, 400 MHz)



**Figure II.2. 68.**  $^{13}\text{C}$ -NMR Spectrum of compound **HAF6** (Methanol- $d_4$ , 100 MHz)



**Figure II.2. 69.** DEPT135 Spectrum of compound **HAF6**

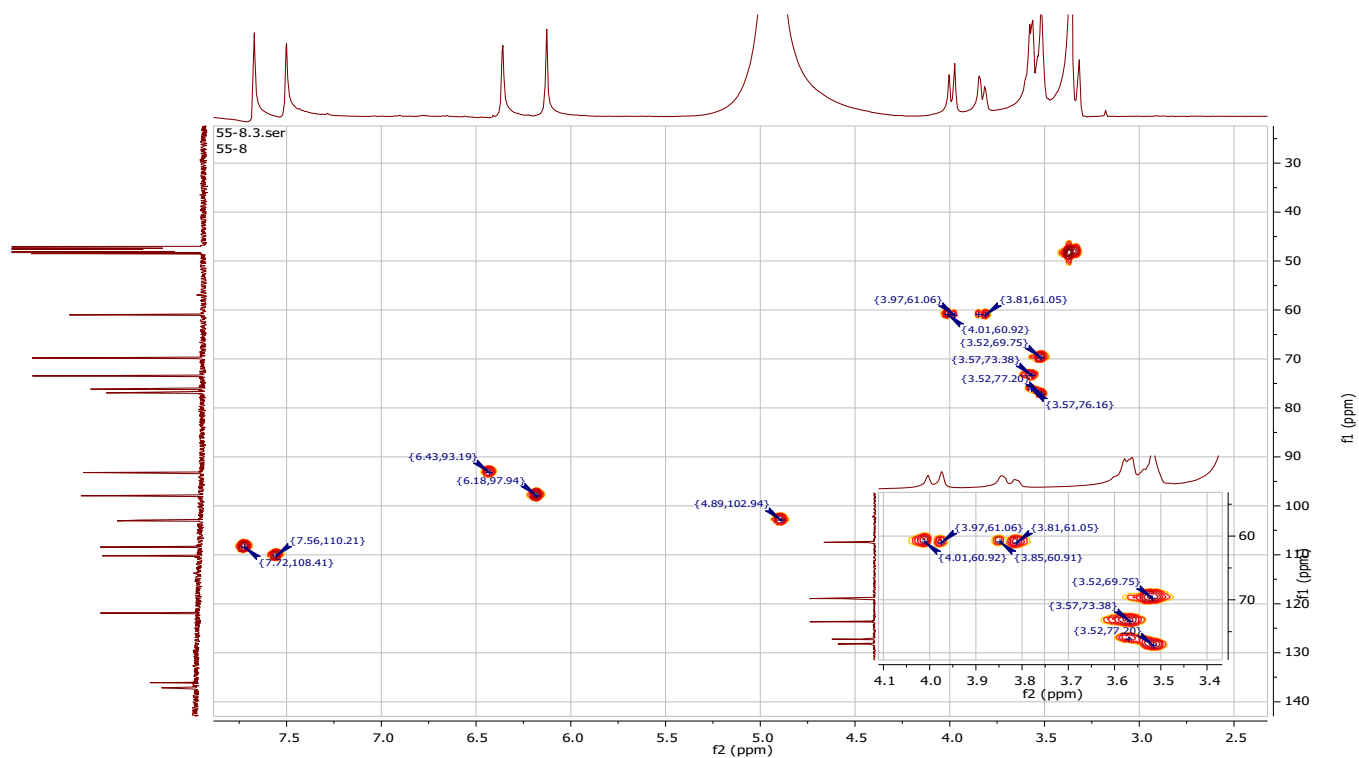


Figure II.2. 70. HSQC Spectrum of compound HAF6

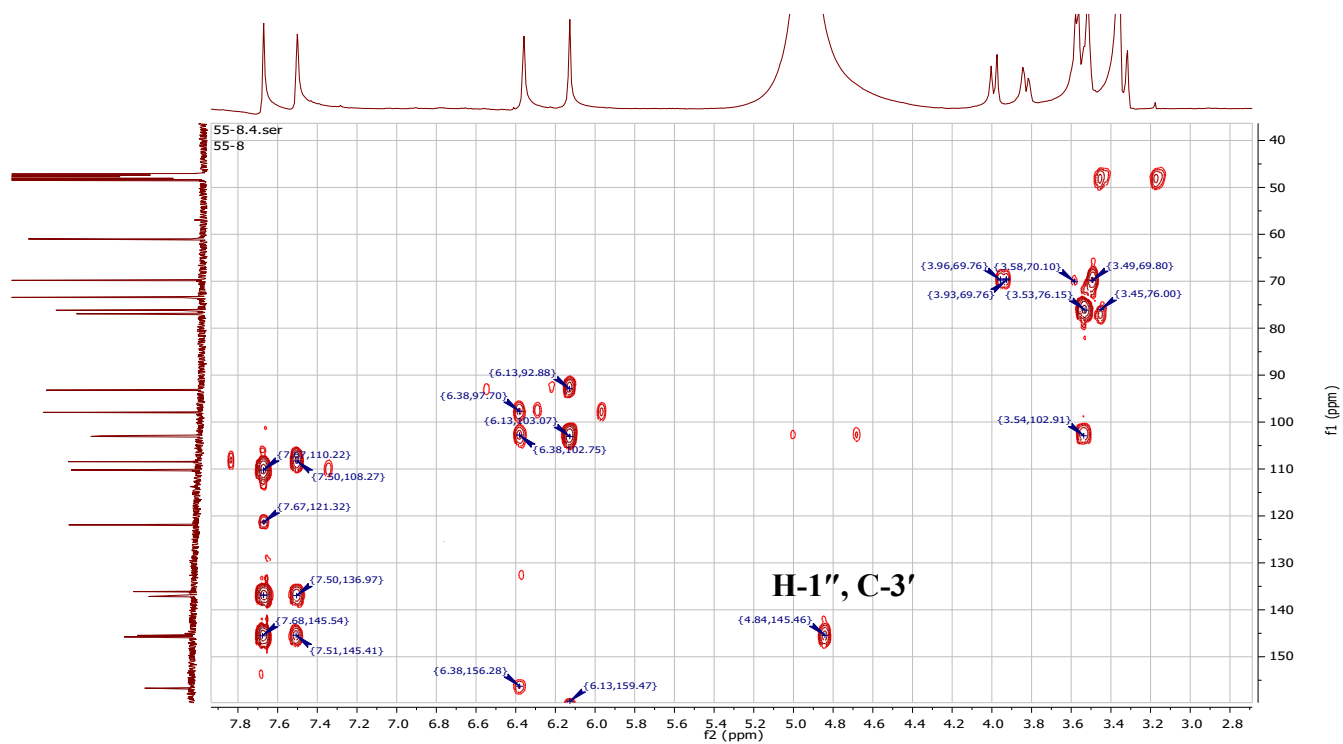


Figure II.2. 71. HMBC Spectrum of compound HAF6

## II.2.4.5. Biflavonoids

### II.2.4.5.1. Compound HAB1

#### i. Physical properties

Compound **HAB1** (10 mg) was obtained as brownish yellow amorphous powder.

#### ii. Chromatographic characters

Compound **HAB1** appeared as a dark spot under UV  $\lambda_{\max}$  254 which attained a yellowish color after spraying with 10% v/v vanillin/H<sub>2</sub>SO<sub>4</sub> and heating at 110 °C. It showed *R<sub>f</sub>* value of 0.25 in system **VII** (Page 48).

#### iii. Spectroscopic data

**A- UV (MeOH):**  $\lambda_{\max}$  (log  $\epsilon$ ): 204.9 (4.99), 207.0 (4.98), 269.0 (4.88).

**B- HR-ESI-MS:** *m/z* 539,143 [M+H]<sup>+</sup> (calcd. 539,100) for formula C<sub>30</sub>H<sub>18</sub>O<sub>10</sub>.

#### C- <sup>1</sup>H-NMR and HMBC spectral analysis

<sup>1</sup>H-, <sup>13</sup>C-NMR and HMBC spectral data of compound **HAB1** are listed in table II.2.13 and illustrated in figures thereafter.

**Table II.2. 13.** <sup>1</sup>H-, <sup>13</sup>C-NMR and HMBC spectral data of compound **HAB1** (400 MHz, 100MHz, DMSO-*d*<sub>6</sub>,)

Position	$\delta_H$ (ppm), multiplicity, <i>J</i> (Hz)	$\delta_C$ (ppm)	HMBC (H→C)
1	-	-	-
2	-	163.9	-
3	-	110.5	-
4	-	180.9	-
5	-	164.9	-
6	6.27,s, 2H	99.5	C-6
7	-	162.0	
8	6.53, d, <i>J</i> = 2.0 Hz, 1H	94.3	C-6, 10
9		157.8	
10	-	103.4	
1'	-	123.3	
2', 6'	7.35, d, <i>J</i> = 8.4 Hz, 2H	130.1	C-2, 1',2',6', 4'

3', 5'	6.68, d, $J = 8.5$ Hz, 2H	115.7	C-1'
4'	-	160.3	-
2''	-	162.8	-
3''	6.74, s, 1H	103.2	C-3'', 2'', 4'', 10''
4''	-	182.3	
5''	-	164.0	
6''	6.27, s, 2H	99.2	C-10''
7''	-	161.6	-
8''	-	99.7	-
9''	-	155.3	-
10''	-	104.1	-
1'''	-	121.6	-
2''', 6'''	7.56, d, $J = 8.5$ Hz, 2H)	128.4	C-2'', 2''', 6''', 4'''
3''', 5'''	6.78, d, $J = 8.5$ Hz, 2H	116.4	C-1'''
4'''	-	161.5	-
OH-5	12.85, s, 1H	-	C-6, 7, 10
OH-5''	13.03, s, 1H	-	C-6'', 7'', 10''

#### iv. Discussion and conclusion

Compound **HAB1** had the molecular formula  $C_{30}H_{18}O_{10}$  as established from the positive **HR-ESI-MS** (Figure II.2.73) by providing a molecular ion peak at  $m/z$  539,143  $[M+H]^+$  (calcd. 539.100).

The structure of **HAB1** was proposed by the analysis of  $^1H$ - and  $^{13}C$ - and DEPT NMR and HMBC spectra.

The  $^{13}C$ -NMR and **DEPT 135** spectra (Figures II.2.75-76) of compound **HAB1** shows 26 signals including, two signals at  $\delta_C = 130.1$  and 115.7 ppm, and two signals at  $\delta_C = 128.4$  and 116.4 ppm, each representing two carbon atoms, twelve  $sp^2$  CH, sixteen  $sp^2$  quaternary carbons (6x C and 10x C-O) and two carbonyl groups ( $\delta_C$  180.9 and 182.3 ppm).

The  $^1H$ -NMR spectrum (Figure II.2.74) shows two signals at  $\delta_H = 12.85$  and 13.03 ppm, indicating the presence of two chelated hydroxyls which attributed to OH-5 of flavone (GUILHON and RODRIGUES).

The  $^1\text{H-NMR}$  spectrum shows two doublets at  $\delta_H$  7.35 and 6.68 ( $J = 8.5$  Hz, 2H), and two doublets at  $\delta_H = 7.56$  and  $\delta_H = 6.78$  ppm ( $J = 8.5$  Hz, 2H) of two **AA'BB'** systems of two flavonoid moieties. These data are in agreement with a flavonoid dimeric structure.

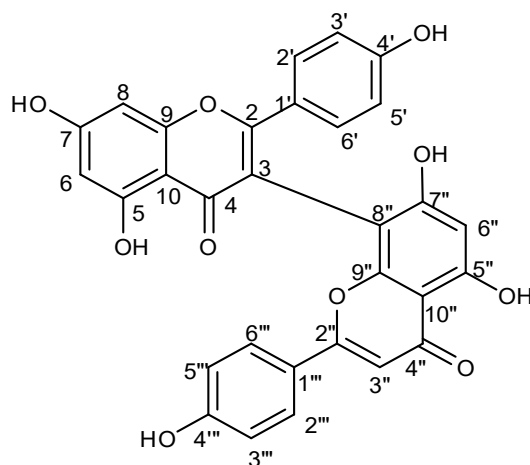
The HMBC spectrum (Figures II.2.78-79) of **HAB1** show heteronuclear long-range couplings of C-1' with H-5' and of C-1'' with H-3'', 5'' which confirm rings B of both flavones of dimer.

These observations and comparison of the UV absorption maxima (278 and 350 nm) and NMR data with those of biflavonoids.

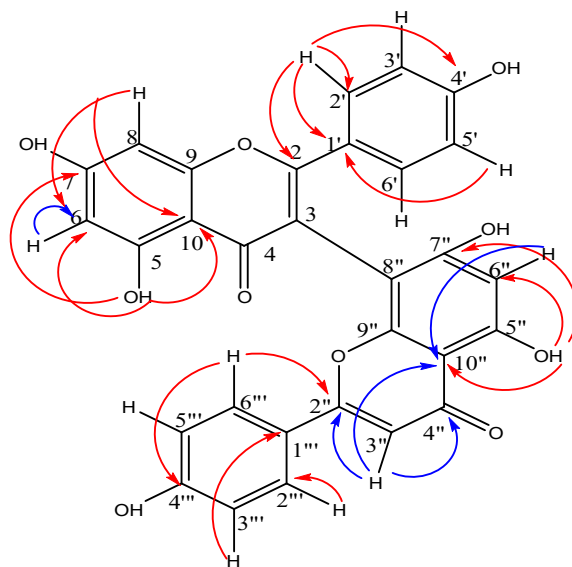
All data was compared with those of biflavonoids isolated from *Hypericum*. and were identical to I3, II8-Biapigenin (Berghöfer and Hölzl, 1987).

This compound has been reported as the major biflavone in *Hypericum perforatum* extracts (Berghöfer and Hölzl, 1987; Colovic and Caccia, 2008).

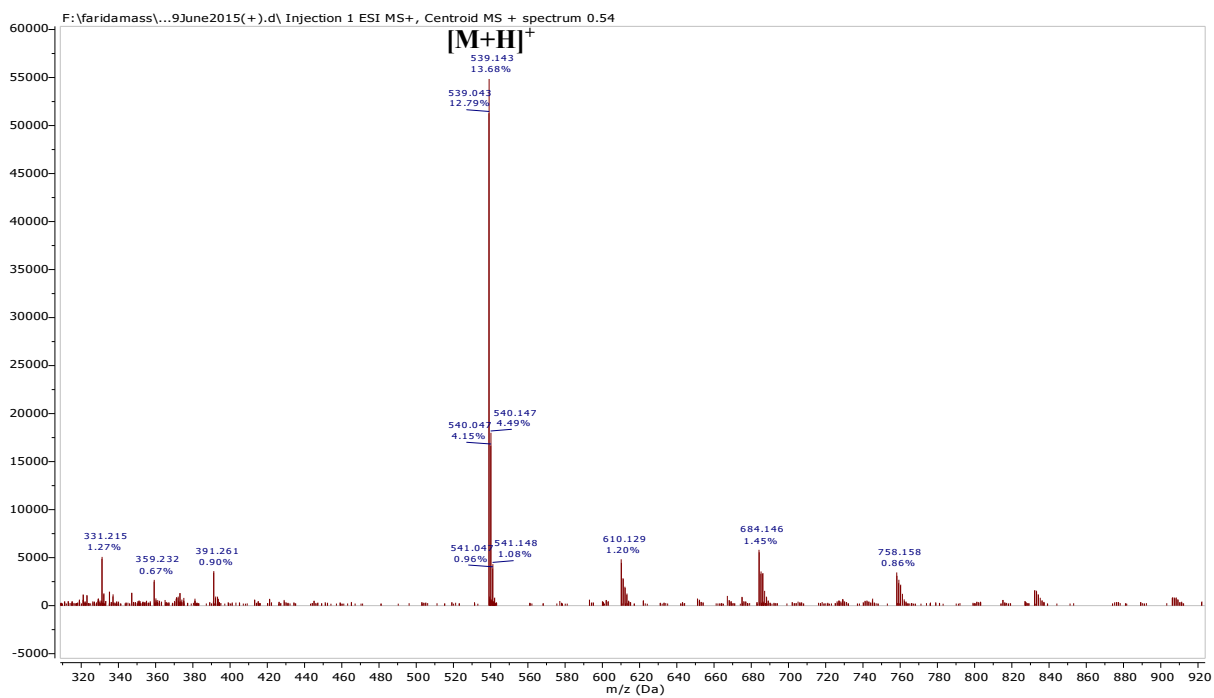
Several pharmacological activities such as antioxidant, cytotoxic and antitumoral activities of I3, II8-Biapigenin have been described (Cakir et al., 2003; Conforti et al., 2007).



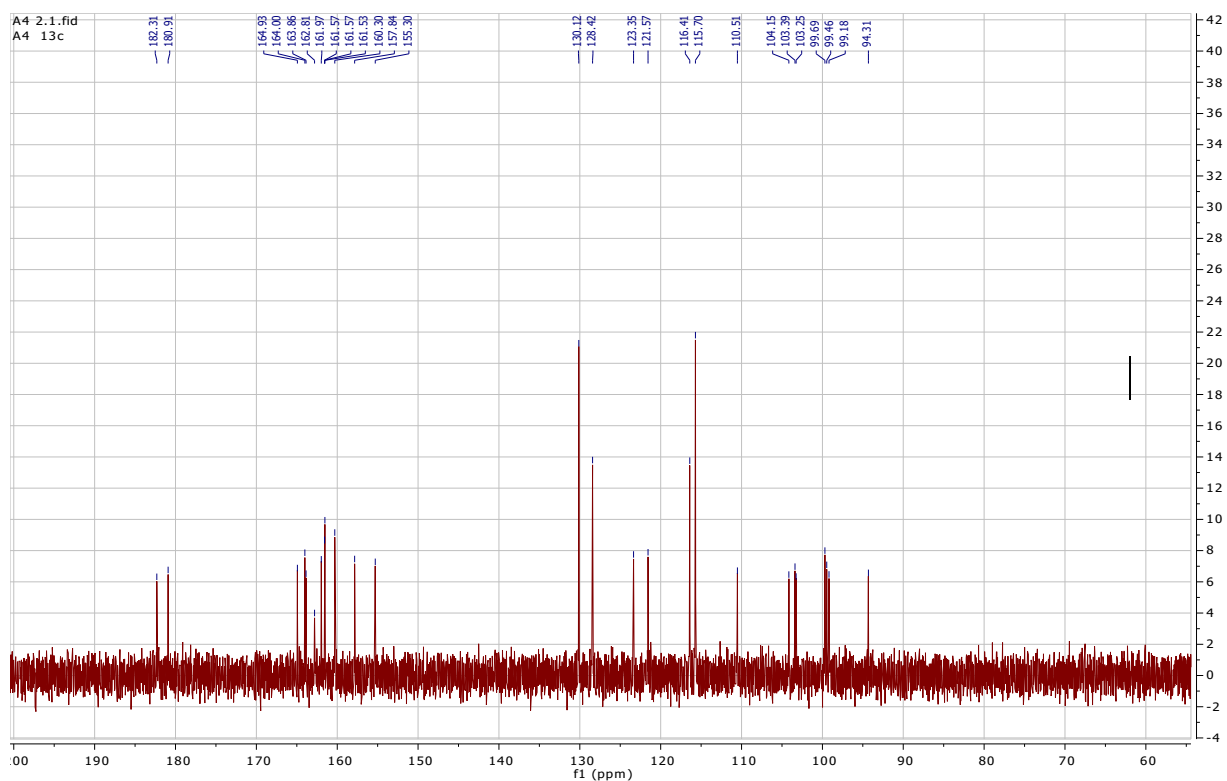
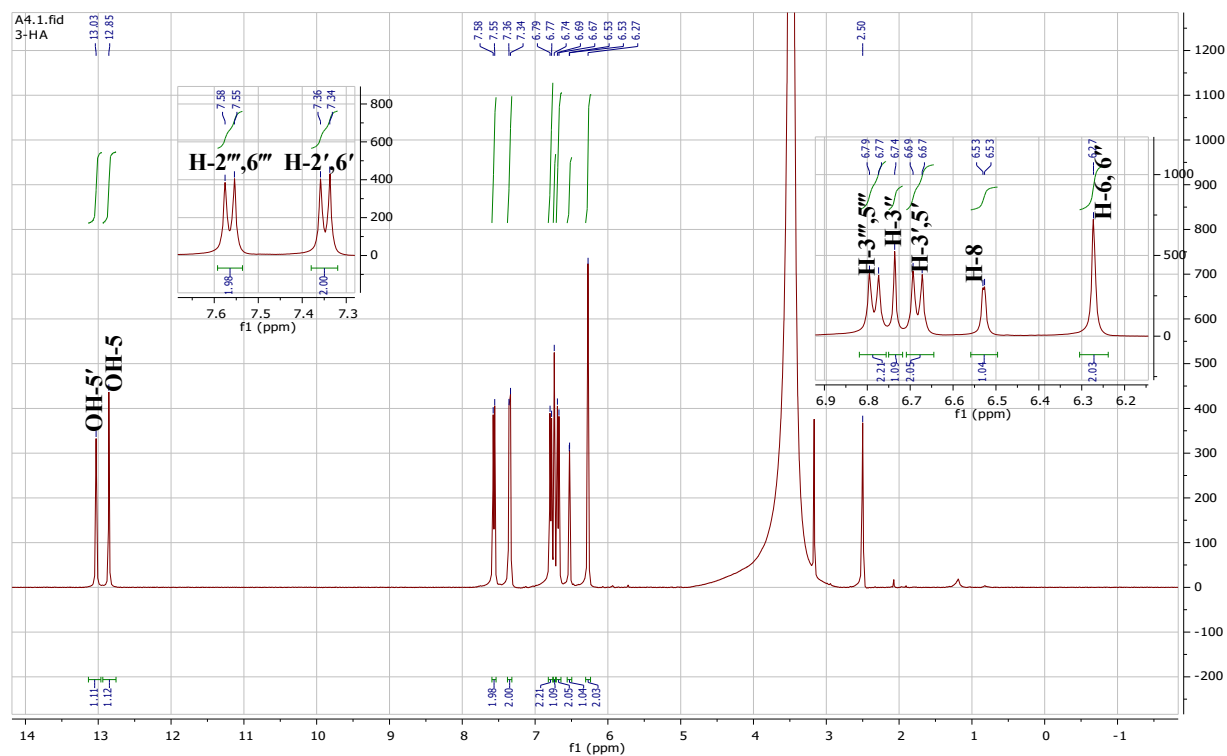
**Structure of compound HAB1:  
I3, II8-Biapigenin**



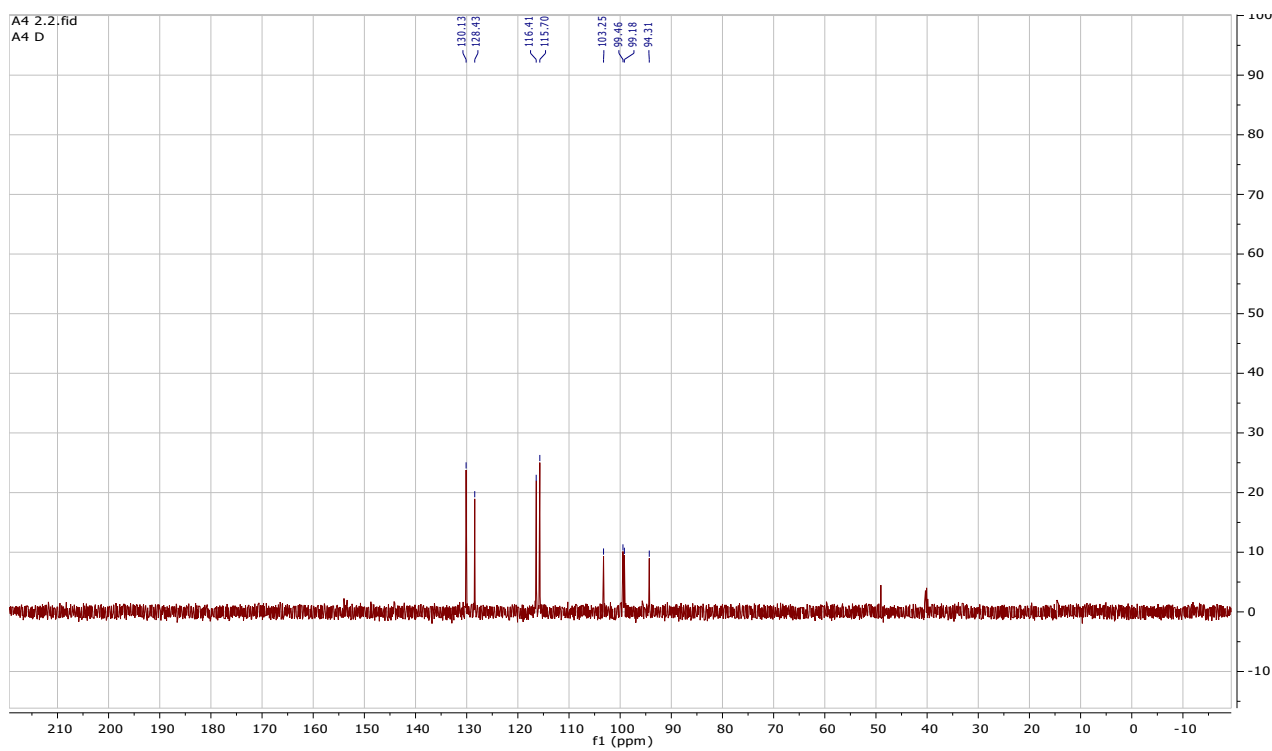
**Figure II.2. 72.** Important HMBC (H→C) correlation of compound **HAB1**



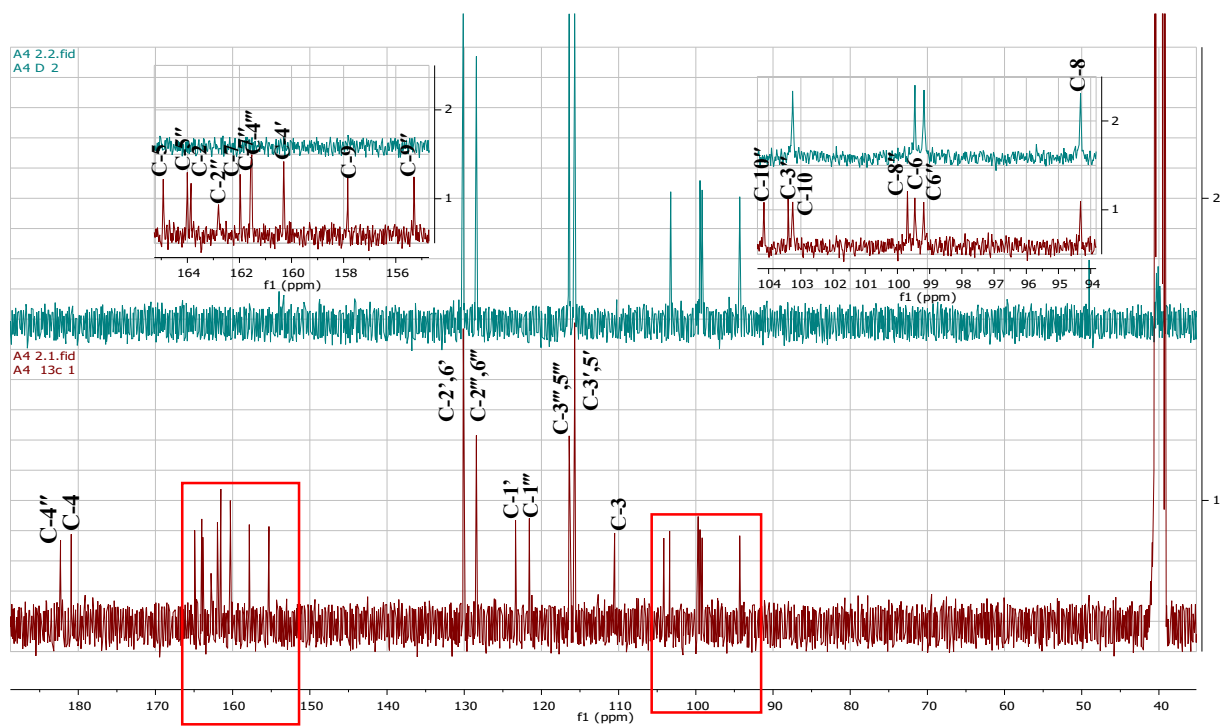
**Figure II.2. 73.** Positive HR-ESI-MS of compound **HAB1**



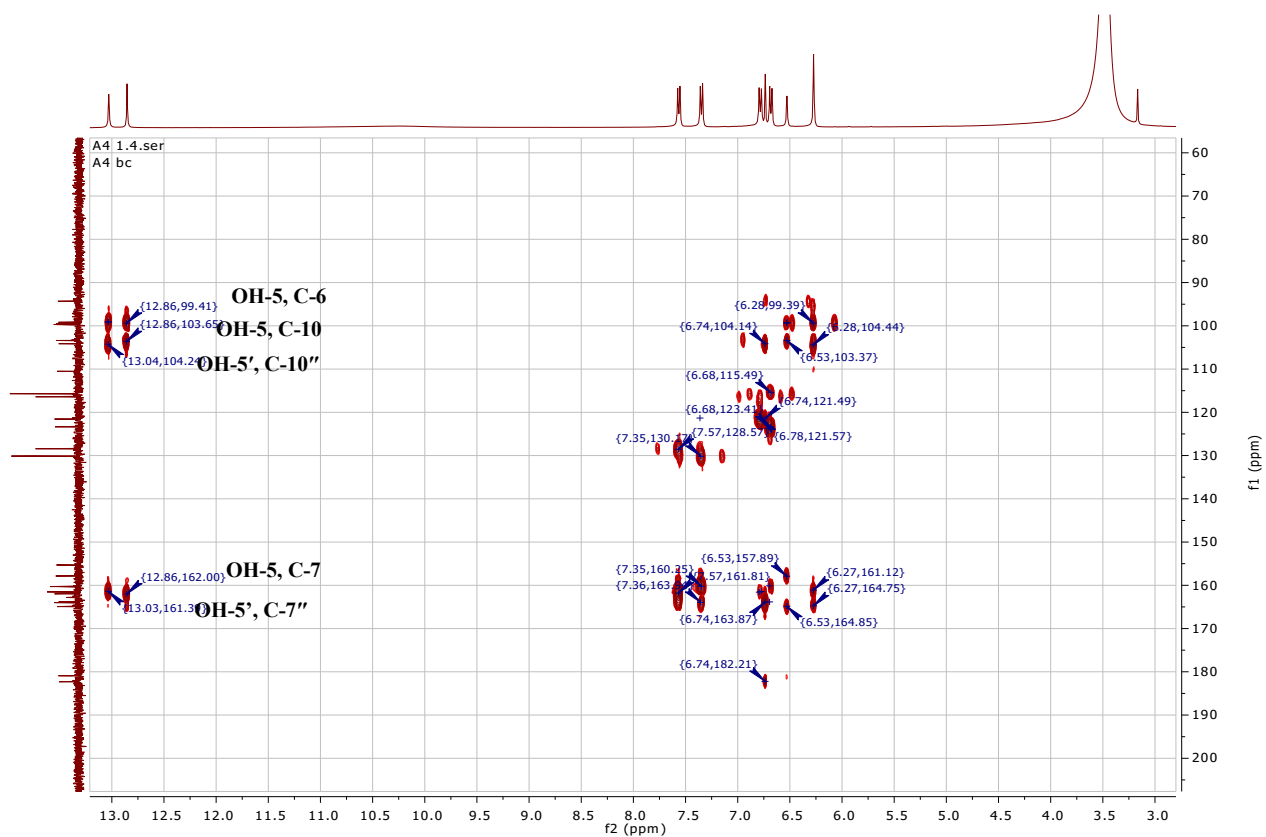




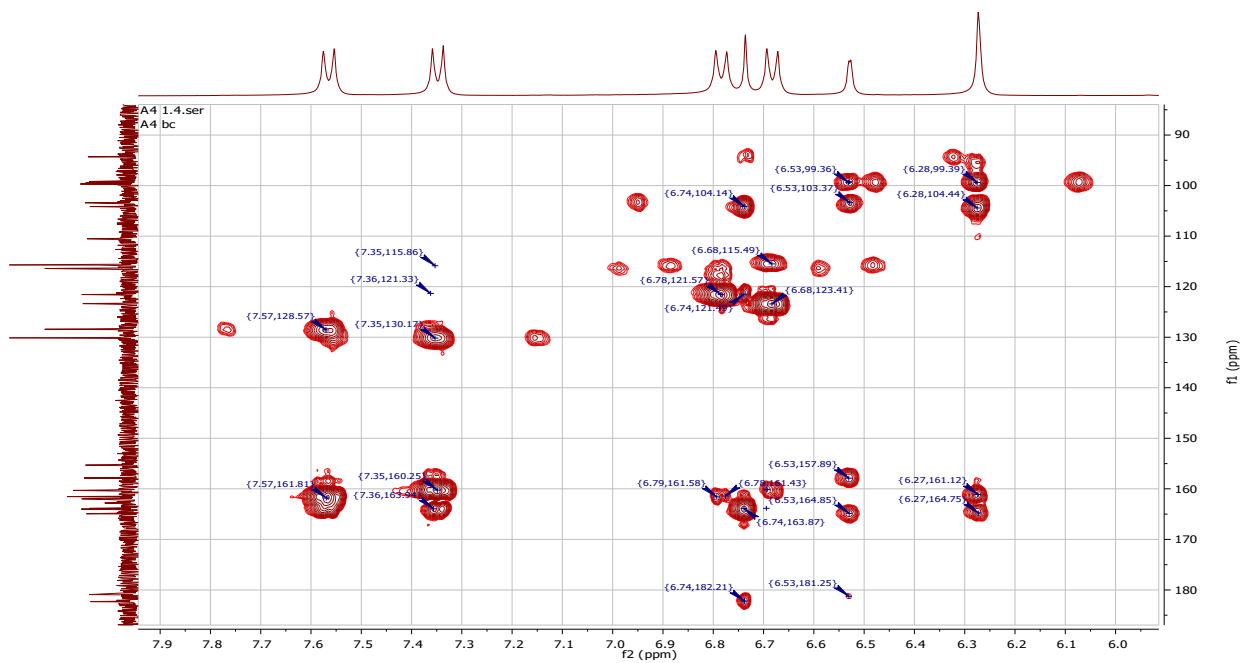
FigureII.2. 76. DEPT-135 Spectrum of compound HAB1



FigureII.2. 77. Comparison of  $^{13}\text{C}$ -NMR and DEPT 135 spectra of compound HAB1



FigureII.2. 78. HMBC Spectrum of compound HAB1



FigureII.2. 79. Expanded HMBC Spectrum of compound HAB1

## II.2.4.6. Cinnamic acid derivatives

### II.2.4.6.1. Compound HAC1

#### i. Physical properties

Compound HAC1 (30 mg) was obtained as a yellow crystalline solid. It was soluble in methanol.

#### ii. Chromatographic characters

Compound HAC1 appeared as a light blue fluorescent zone under UV  $\lambda_{\max}$  366 which attained a faint pink color after spraying with 10% v/v vanillin/H<sub>2</sub>SO<sub>4</sub> and heating at 110 °C. It showed  $R_f$  value of 0.64 in system I (Page 48).

#### iii. Spectroscopic data

**A. UV (MeOH)  $\lambda_{\max}$  nm (log  $\epsilon$ ):** 329.1 (4.6), 244.0 (4.3), 217.0 (4.5).

**B. HR-ESI-MS:**  $m/z$  353.085 (calcd. 353.085) [M-H]<sup>-</sup>  $m/z$  355.103 [M+H]<sup>+</sup> (calcd. 355.105) for formula C<sub>16</sub>H<sub>18</sub>O<sub>9</sub>.

#### C. <sup>1</sup>H-, <sup>13</sup>C-NMR and HMBC spectral analysis

The <sup>1</sup>H-, <sup>13</sup>C-NMR and HMBC spectral data of compound HAC1 are listed in table II.2.14 and illustrated in figures thereafter.

**Table II.2. 14.** <sup>1</sup>H-, <sup>13</sup>C-NMR and HMBC spectral data of compound HAC1 (400 MHz, 100MHz, DMSO-*d*<sub>6</sub>).

Position	$\delta_H$ (ppm), multiplicity, <i>J</i>	$\delta_C$ (ppm)	HMBC (H→C)	<sup>1</sup> H- <sup>1</sup> H-COSY
1	-	75.7	-	
2	2 $\alpha$ 1.63, d, 13.9, 1H	38.6	C-1, 3, 7	H $\beta$ -2, H-3
	2 $\beta$ 1.98, dd, 14.5,2.9, 1H			H $\alpha$ -2, H-3
3	3.91, d,3.2, 1H	71.9	-	H $\alpha$ -2, H $\beta$ -2,H-4
4	3.47, dd, 9.9, 3.1, 1H	73.8	C-5	H-3, H-5
5	5.17, m, 1H	72.0	C-1, 4, 9'	H-4,H-6
6	6 $\alpha$ 1.81, overlapped, 1H	40.0	C-1, 2, 5, 7	H-5
	6 $\beta$ 1.81, overlapped, 1H			
7	-	177.0	-	-
1'	-	126.0	-	-
2'	7.05, br s, 1H	115.1	C-4', 6', 7'	
3'	-	146.6	-	-
4'	-	149.4		-

5'	6.75, d, 8.1, 1H	116.2	C-1', 3'	H-6'
6'	6.96, d, 8.2, 1H	121.7	C-2', 7', 4'	H-5'
7'	7.45, d, $J = 15.8$ , 1H	145.1	C-2', 6'	H-8'
8'	6.23, d, $J = 15.9$ , 1H	115.0	C-1'	H-7'
9'	-	166.3	-	-

#### iv. Discussion and conclusion

Compound **HAC1** was isolated as a yellow solid. The molecular formula  $C_{16}H_{18}O_9$  was established from the positive HR-EIS-MS by providing molecular ion peaks at  $m/z$  377.086  $[M+Na]^+$  (calcd. 377.080),  $m/z$  355.103  $[M+H]^+$  (calcd. 355.105) and  $m/z$  731.183  $[2M+Na]^+$  (calcd. 731.180) and confirmed by the negative HR-EIS-MS by molecular ion peaks at  $m/z$  353.085  $[M-H]^-$  (calcd. 353.085). Characteristic fragment ions at  $m/z$  191.063, 179.040, 161.035 and 135.058. Ions at  $m/z$  191 indicated fragments of the quinic moiety, and ions at  $m/z$  179 or 161 indicated fragments of the caffeoyl moiety, and they were [quinic-H] $^-$ , [caffeic-H] $^-$ , [caffeic-H<sub>2</sub>O-H] $^-$ , respectively. Ions at  $m/z$  135 indicated another fragment of caffeic acid (Figure II.2.81).

The  $^1H$  NMR spectrum (Figure II.2.82) displayed two ortho-coupled doublet each for 1H, at  $\delta_H$  6.96 and  $\delta_H$  6.75, a broad singlet for 1H at  $\delta_H$  7.06, confirming the presence of a tri-substituted aromatic ring; and two doublets, each for 1H, at  $\delta_H$  7.45 (H-7', d,  $J = 15.8$  Hz) and at  $\delta_H$  6.23 (H-8', d,  $J = 15.9$  Hz), indicating the presence of trans-di-substituted ethylene moiety in the molecule.

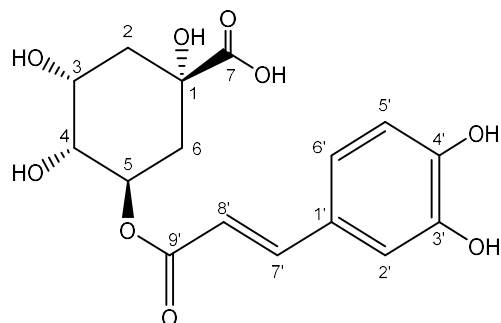
The  $^{13}C$  NMR and DEPT 135 spectra (Figure II.2. 83-85) showed the presence of sixteen carbon atoms, including two carbonyl groups at  $\delta_c = 177.0$  and  $\delta_c = 166.3$  ppm, corresponding to carbons 7 and 9', respectively; two aromatic carbons bonded to hydroxyl groups at  $\delta_c = 149.4$  and  $\delta_c = 145.15$  ppm, identified as C4' and C3'; two olefinic carbons at  $\delta_c = 146.22$  and  $\delta_c = 114.95$  ppm corresponding to C7' and C8'; four aromatic carbons assigned to C1', C2', C5', and C6' at  $\delta_c = 125.82$ , 114.95, 115.07, and 121.72 ppm, respectively; three carbons bonded to hydroxyl groups at  $\delta_c = 75.7$ ,  $\delta_c = 71.9$ , and  $\delta_c = 73.8$  ppm, identified as C1, C3, and C4; one carbon bonded to an ester group at  $\delta_c = 72.0$  ppm attributed to C5; and two methylene identified as C2 and C6 at  $\delta_c = 40.0$  and  $\delta_c = 38.5$  ppm, respectively.

The established structure for compound **HAC1** was confirmed by 2D NMR including HSQC, HMBC,  $^1H$ - $^1H$  COSY and NOESY (Figures II.2.86-89).

The  $^1H$  NMR signal of proton H-4 at  $\delta_H = 3.47$  ppm as doublet of doublet (dd,  $J = 9.9, 3.1$ , 1H) indicative of the proton axial orientation (Forino et al., 2015).

Results are consistent with the Chlorogenic acid data reported in the literature (Zhang et al., 2013).

Chlorogenic acids (CGA) are phenolic compounds formed by the esterification of cinnamic acids, such as caffeic, ferulic, and *p*-coumaric acids, with (-)-quinic acid. The chlorogenic acid is one of the most abundant polyphenols in the human diet with coffee, fruits and vegetables as its major source. Its antioxidant and anticarcinogenic anti-inflammatory, anti-HIV, hypoglycemic, hepatoprotective activities and inhibition of mutagenesis and carcinogenesis properties have been well established (Feng et al., 2005; Meng et al., 2013; Sato et al., 2011).



**Structure of compound HAC1 :  
Chlorogenic acid**

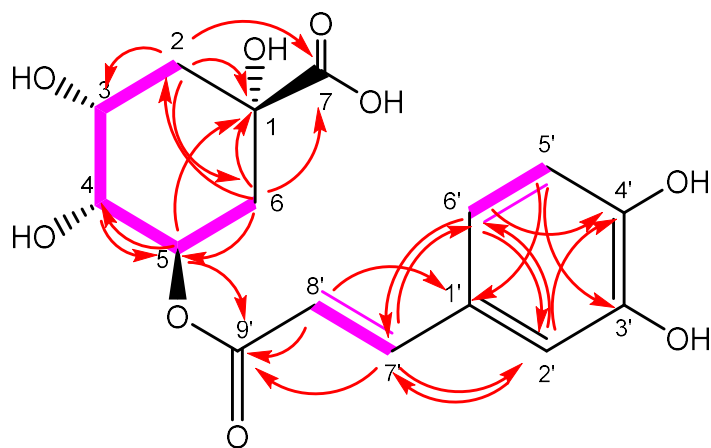
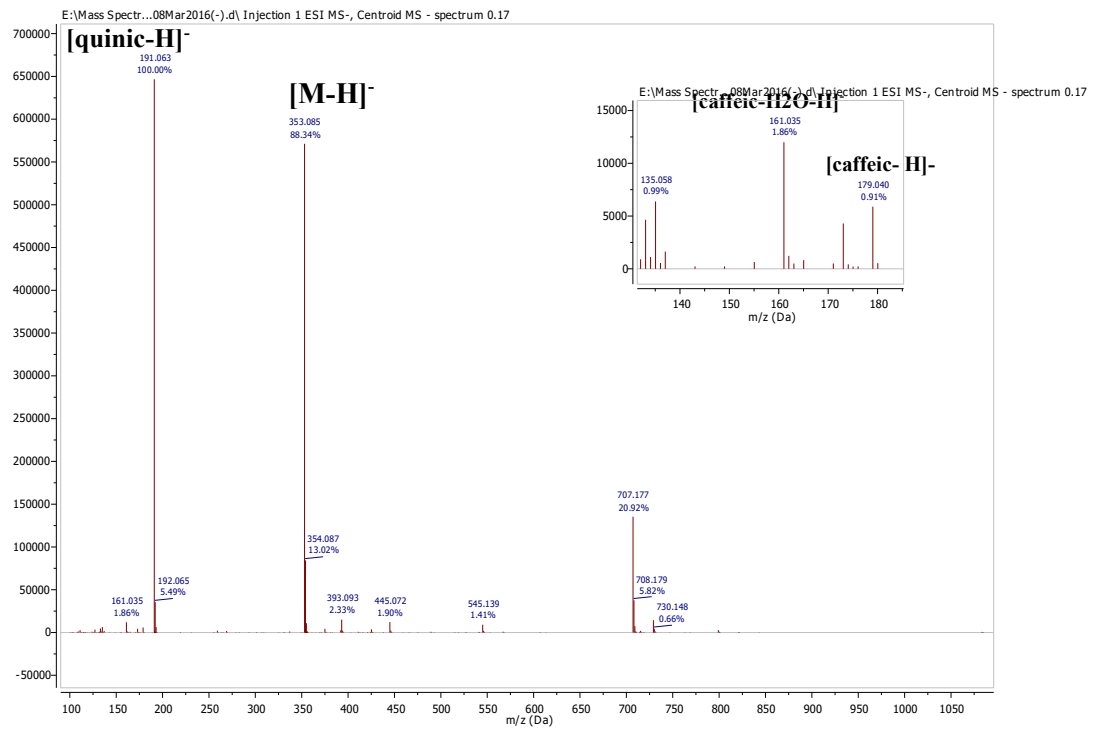
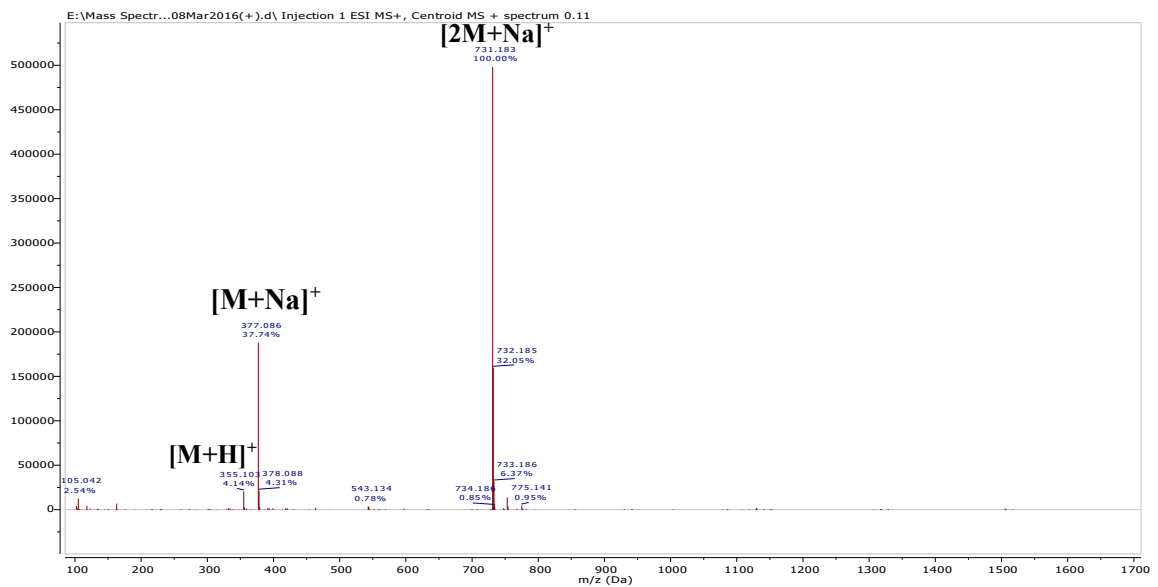


**Figure II.2. 80.** Key HMBC (H $\rightarrow$ C) and 1H-1H COSY (    ) correlations of compound **HAC1**



A.



B.

**Figure II.2. 81.** Mass spectra of compound HAC1. A. Negative HR-ESI-MS  
B. Positive HR-ESI-MS

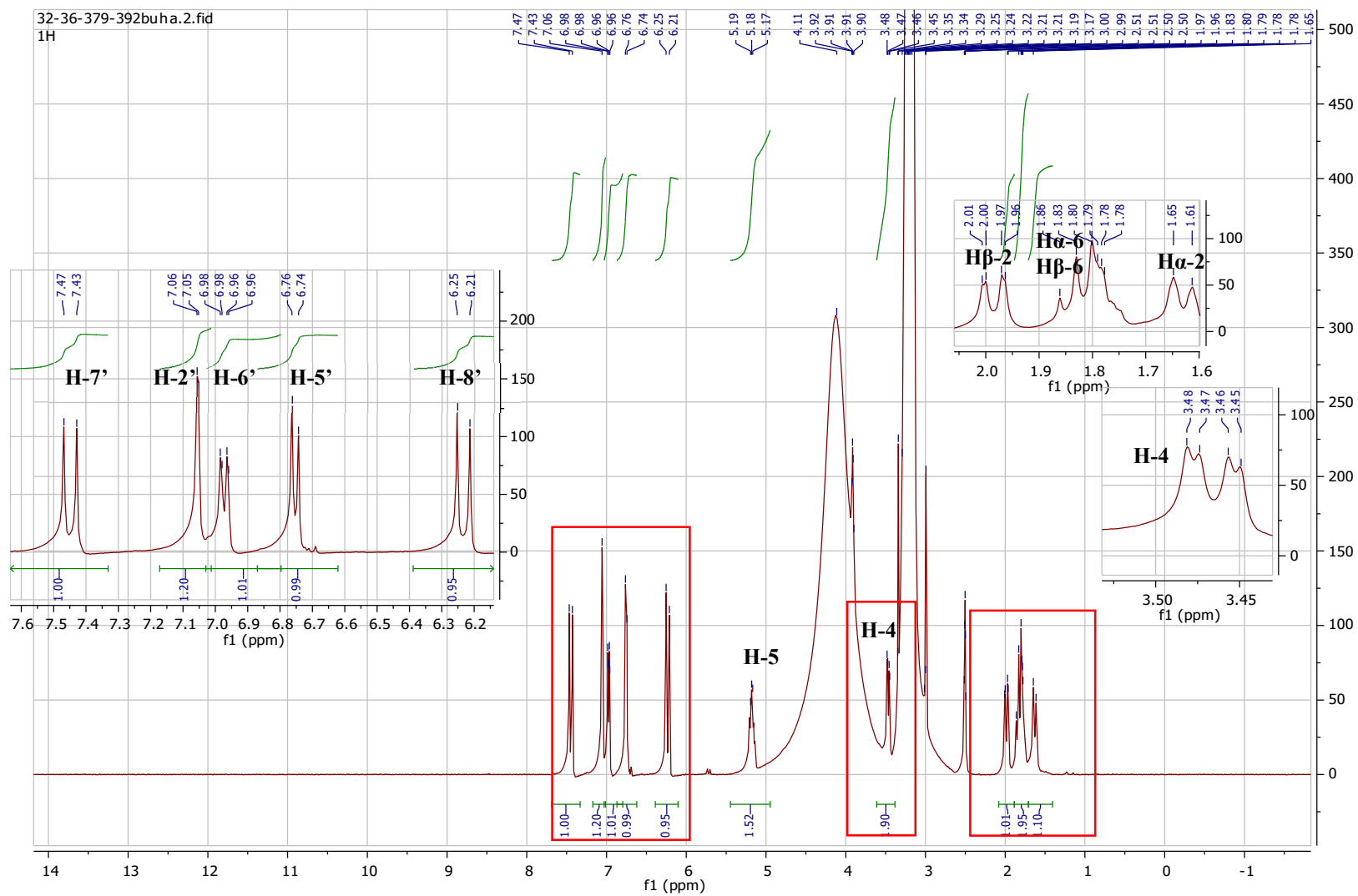


Figure II.2. 82.  $^1\text{H-NMR}$  Spectrum of compound HAC1 (DMSO- $d_6$ , 400 MHz)

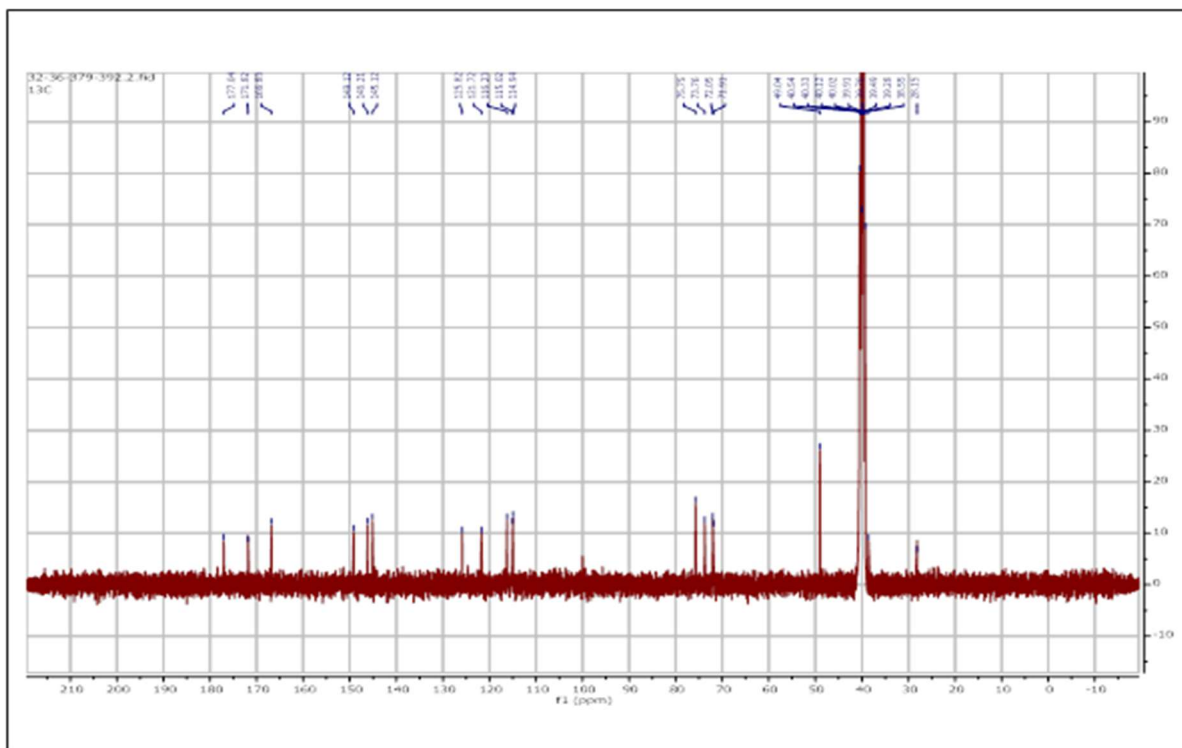


Figure II.2. 83.  $^{13}\text{C}$ -NMR Spectrum of compound HAC1(DMSO- $d_6$ ,100MHz)

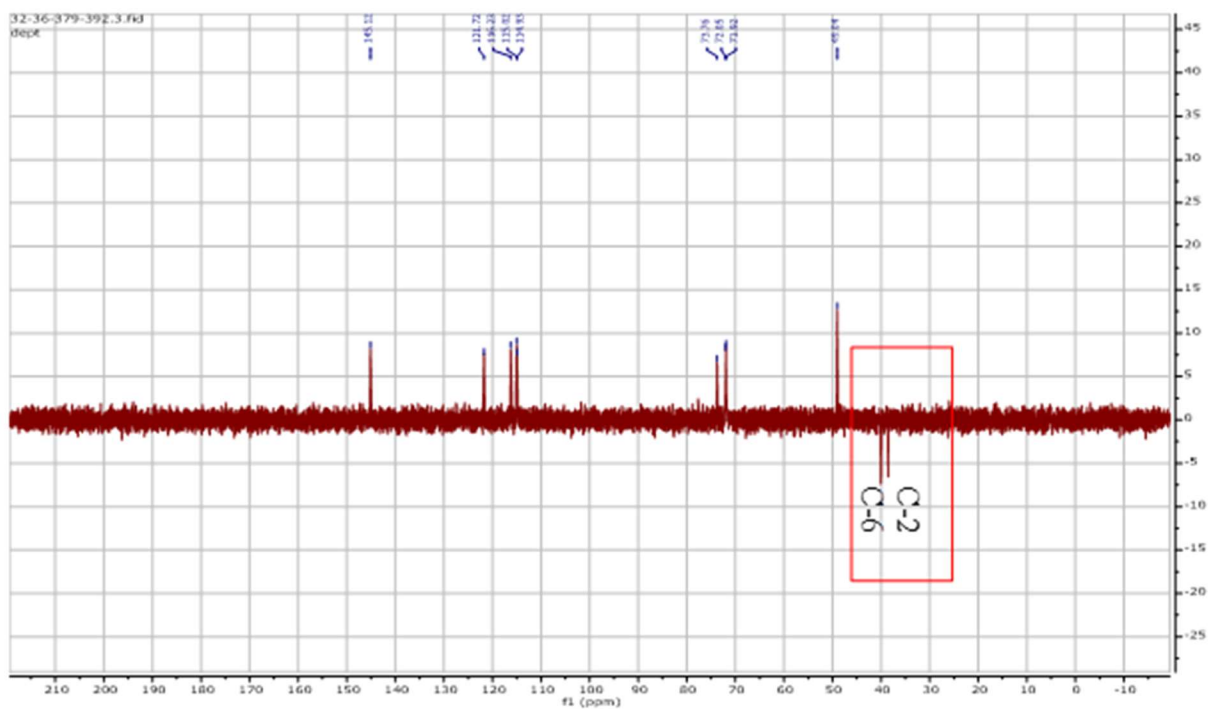
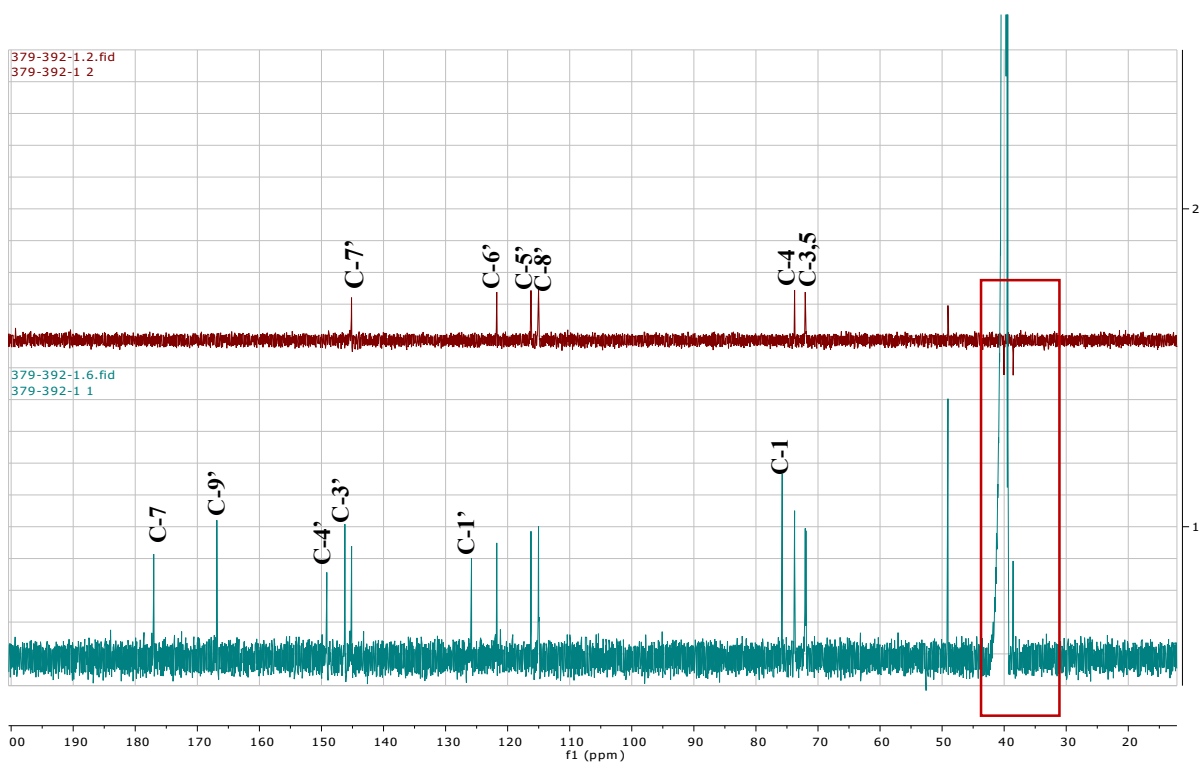
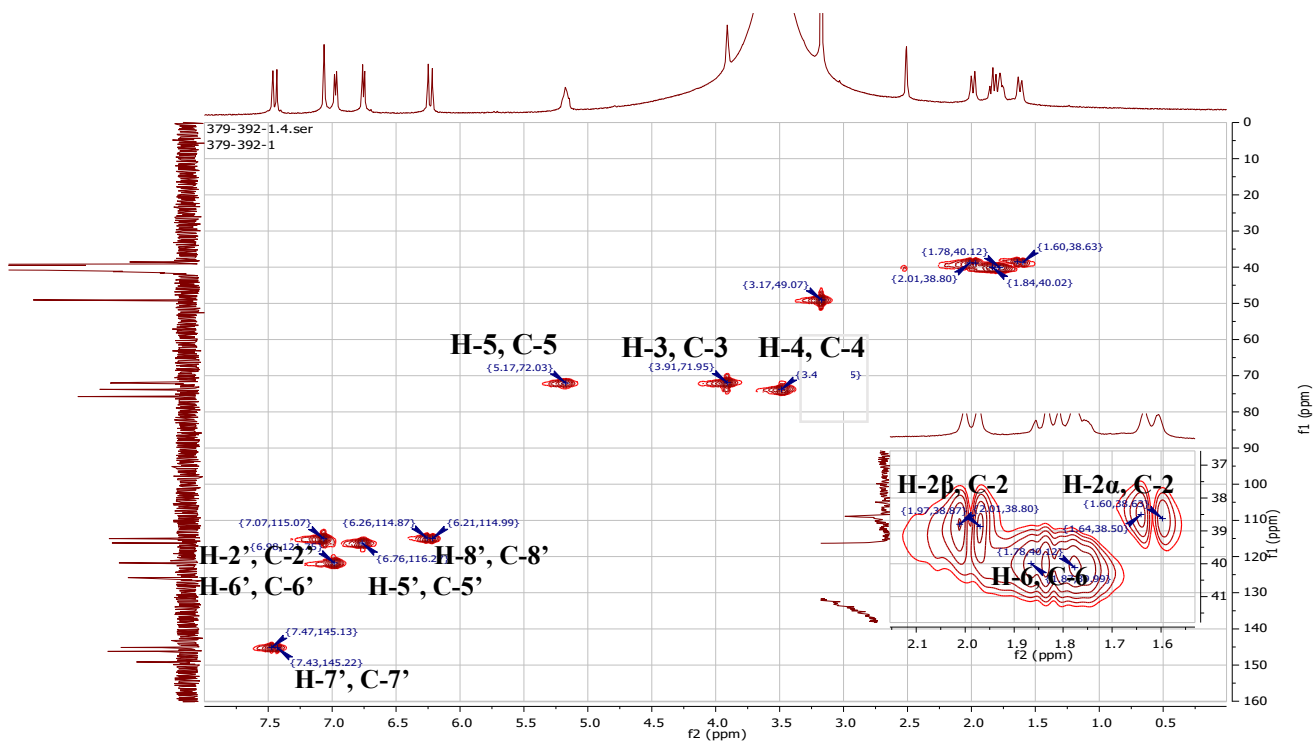


Figure II.2. 84. DEPT135 Spectrum of compound HAC1





**Figure II.2. 85.** Comparison of DEPT135 and  $^{13}\text{C}$ -NMR spectra of compound HAC1



**Figure II.2. 86.** HSQC Spectrum of compound HAC1

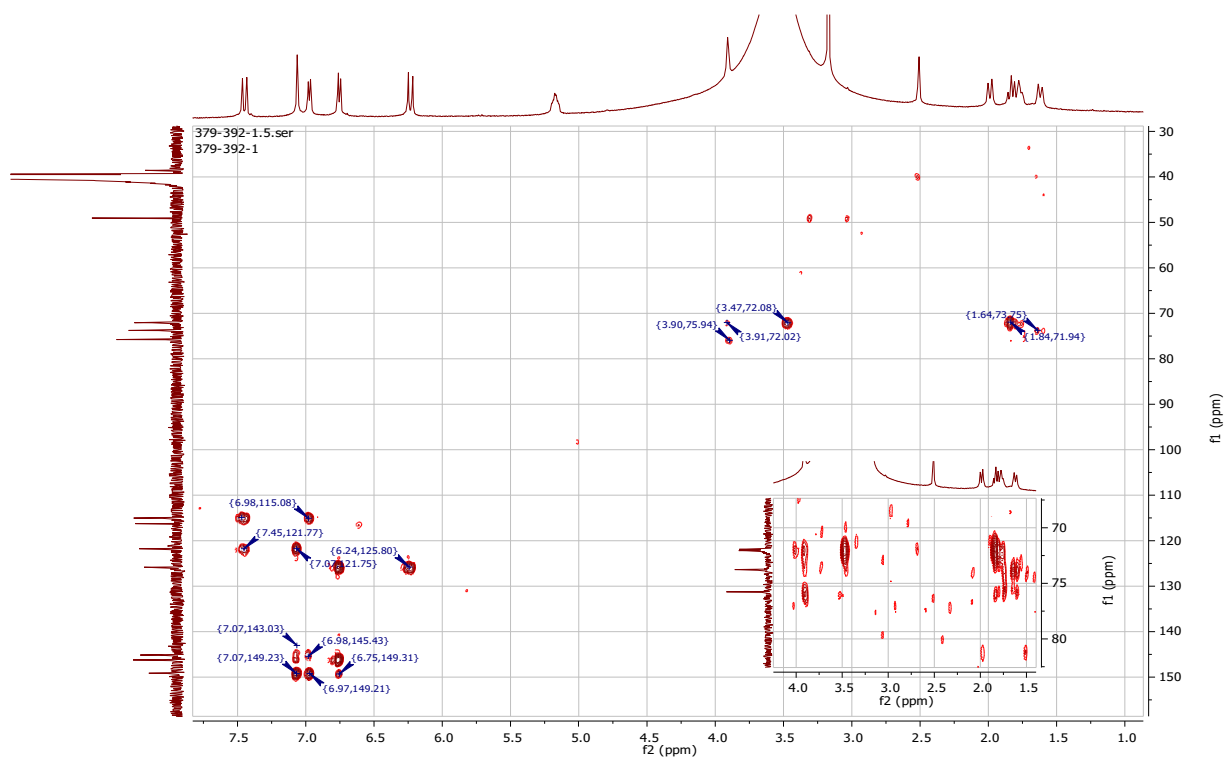


Figure II.2. 87. HMBC Spectrum of compound HAC1

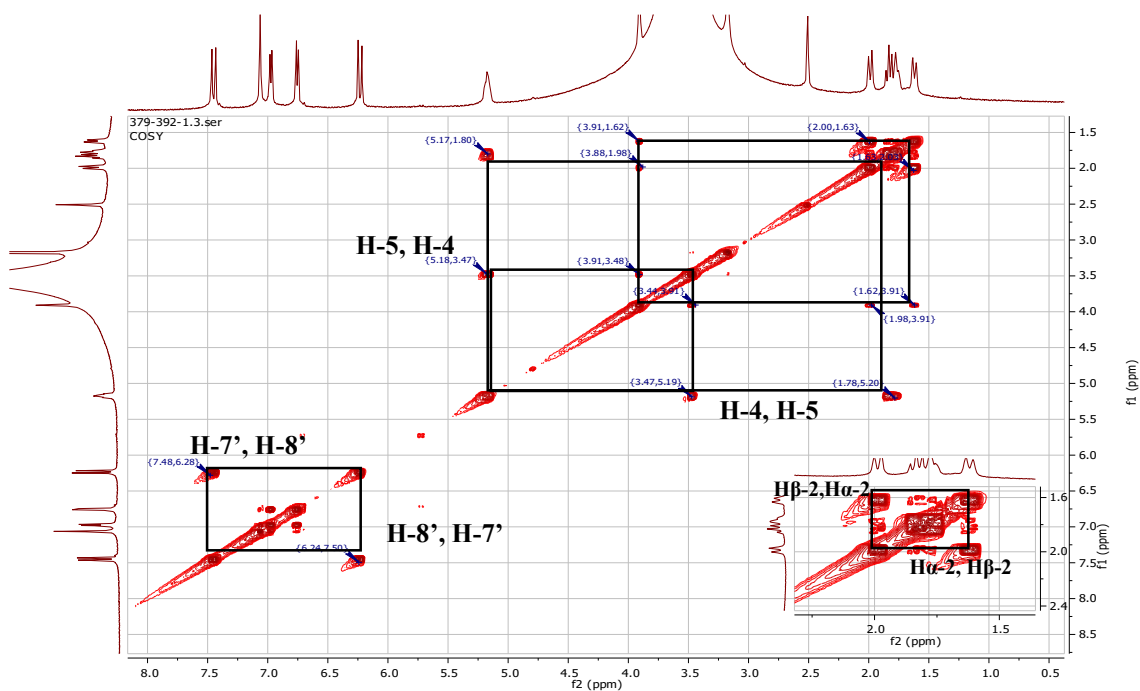


Figure II.2. 88.  $^1\text{H}$ - $^1\text{H}$  COSY Spectrum of compound HAC1

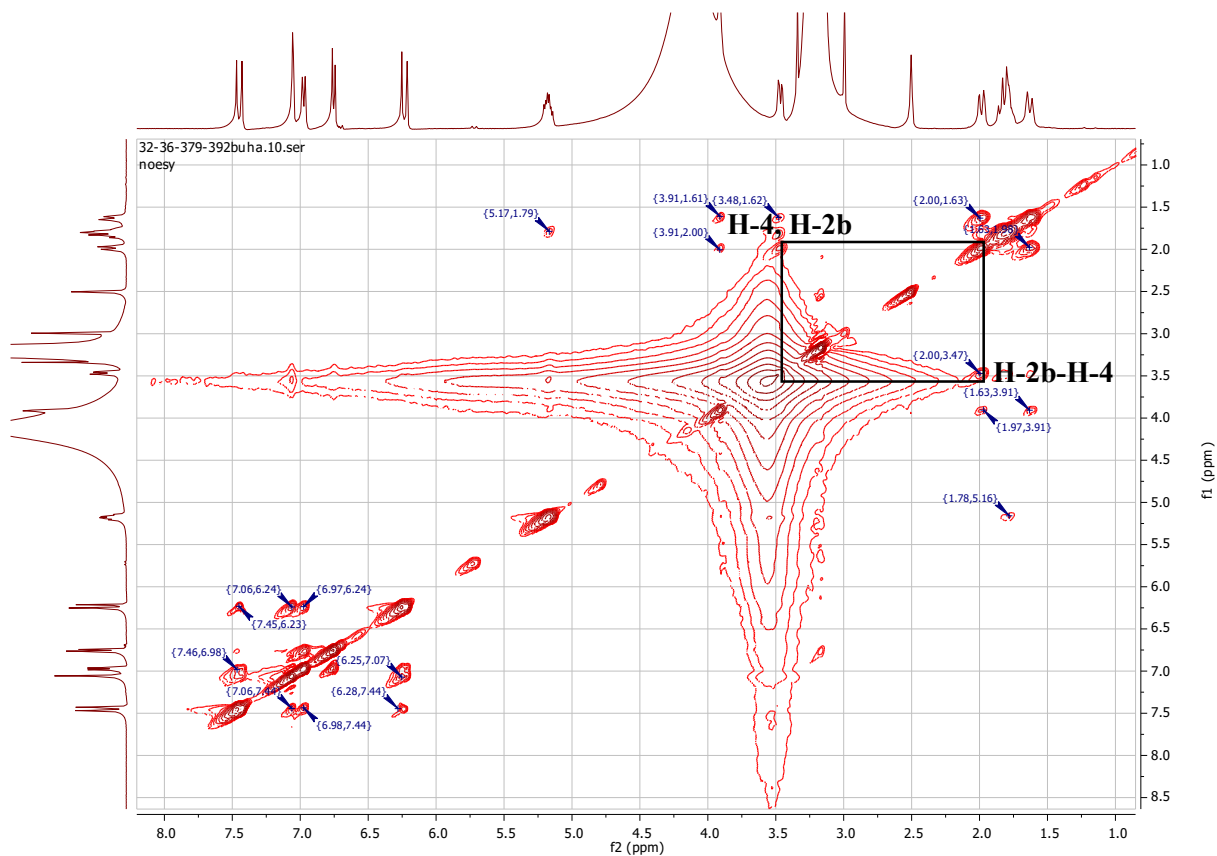


Figure II.2. 89. NOESY spectrum of compound HAC1

### II.2.4.6.2. Compound HAC2

#### i. Physical properties

Compound **HAC2** (25 mg) was obtained as yellow solid.

#### ii. Chromatographic characters

Compound **HAC2** appeared as a light blue zone under UV  $\lambda_{\max}$  366 which attained a yellow color after spraying with 10% v/v vanillin/H<sub>2</sub>SO<sub>4</sub> and heating at 110 °C. It showed *R<sub>f</sub>* value of 0.30 in system VI (Page 48).

#### iii. Spectroscopic data

**A. UV (MeOH)  $\lambda_{\max}$  nm (log  $\epsilon$ ):** 329.1 (4.6), 244.0 (4.3), 217.0 (4.5).

**B. HR-ESI-MS:** *m/z* 367.099 [M-H]<sup>-</sup> (calcd. 369.100), *m/z* 369.121 [M+H]<sup>+</sup> (calcd. 369.120) for formula C<sub>17</sub>H<sub>20</sub>O<sub>9</sub>.

#### C. <sup>1</sup>H-, <sup>13</sup>C-NMR and HMBC spectral analysis

The <sup>1</sup>H-, <sup>13</sup>C-NMR and HMBC spectral data of compound **HAC2** are listed in table II.2.15 and illustrated in figures thereafter.

**Table II.2. 15.** <sup>1</sup>H-, <sup>13</sup>C-NMR and HMBC spectral data of compound **HAC2** (400 MHz, 100MHz Methanol-*d*<sub>4</sub>).

Position	$\delta_H$ (ppm), multiplicity, <i>J</i> (Hz)	$\delta_C$ (ppm)	HMBC (H→C)	<sup>1</sup> H- <sup>1</sup> H COSY
1	-	74.4	-	-
2	H $\alpha$ -2, 2.02, dd, 13.9, 6.3, 1H H $\beta$ -2, 2.23, overlapped, 1H	36.6	C-1, 3, 6, 7	H-3
3	4.14, m, 1H	68.9	-	H $\alpha$ -2, H $\beta$ -2
4	3.75, dd, 7.6, 3.1, 1H	70.9	C-5	H-5, H $\alpha$ -2
5	5.29, m, 1H	70.7	C-9', 4, 1	H-4, H-6
6	H $\alpha$ -6, 2.20, overlapped, 1H H $\beta$ -6, 2.20, overlapped, 1H	36.4	C-2, 5, 1, 7	H-5
7	-	174.0	-	-
7-OCH <sub>3</sub>	3.70, s	51.6	C-7	-
1'	-	126.2	-	-
2'	7.05, d, 2.1, 1H	113.7	C-6', 7', 4'	
3'	-	145.4	-	-
4'	-	148.3	-	-
5'	6.79, d, 8.1, 1H	115.1	C-1', 3'	H-6'

6'	6.95, <i>dd</i> , 8.2, 2.1, 1H	121.6	C-2', 7', 4'	H-5'
7'	7.53, <i>d</i> , 15.9, 1H	145.8	C-2', 6', 9'	H-8'
8'	6.22, <i>d</i> , 15.9, 1H	113.6	C-1', 9'	H-7'
9'	-	166.9	-	-

#### iv. Discussion and conclusion

Compound **HAC2** was isolated as yellow solid. The molecular formula  $C_{17}H_{20}O_9$  was established from the positive HR-EIS-MS by providing molecular ion peaks at  $m/z$  369.121  $[M+H]^+$  (calc. 369.120) and  $m/z$  759.214  $[2M+Na]^+$  (calcd. 759.211) and confirmed by the negative HR-EIS-MS by molecular ion peaks at  $m/z$  367.099  $[M-H]^-$  (calcd. 367.100) (Figure II.2.91).

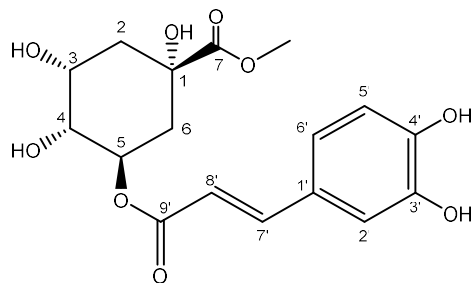
Similarly, to compound **HAC1**, the  $^1H$ -NMR (Figure II.2.92) of **HAC2** showed an E-caffeoyl acid moiety was assigned from the three aromatic protons with an ABX system at  $\delta_H = 7.05$  (*br s*), 6.95 (*dd*,  $J = 8.2, 2.1$ , Hz, 1H) and 6.79 (*d*,  $J = 8.1$  Hz); two trans olefinic protons with an AB system and large coupling constant at  $\delta_H$  7.53 (1H, *d*,  $J = 15.9$  Hz) and 6.22 (1H, *d*,  $J = 15.9$  Hz).

$^{13}C$ -NMR (Figure II.2.93) shows seventeen carbon signals. From its DEPT-135 spectrum (Figure II.2.94), we have assigned: one quaternary carbon at  $\delta_C = 74.4$ , three aromatic carbons (CH) at  $\delta_C = 113.7, 115.1$  and 121.6 ppm, two  $CH_2$  at  $\delta_C = 36.4$  and 36.6 ppm, and one  $CH_3$  at  $\delta_C$  51.57 ppm, two carbonyl group C-atoms at  $\delta_C$  166.86 and  $\delta_C$  174.01 ppm.

The presence of a quinic acid methyl ester moiety in the molecule was suggested by the presence of carbon signals at  $\delta_C = 74.4$  (C), 38.8 ( $CH_2$ ), 68.9 (CH), 70.9 (CH), 70.7 (CH), 174.0 (C) and 51.6 ppm ( $CH_3$ ), and confirmed by the presence of protons of quinic acid at  $\delta_H$  2.02 (1H, H $\alpha$ -2), 2.23 (1H, H $\beta$ -2), 4.14 (1H, H-3), 3.75 (1H, H-4), 5.29 (1H, H-5), 2.20 (2H, H2-6) and 3.70 (3H, 7-O $CH_3$ ) which were assigned according to multiplicity,  $^1H$ - $^1H$  COSY (Figure II.2.96) and HSQC (Figure II.2.97) spectral analysis.

The position of the caffeoyl substitution and the location of the methoxy group in the quinic acid were confirmed from HMBC (Figure II.2.98) which correlated H-5 at  $\delta_H$  (5.29, *m*) with carbonyl group at  $\delta_C = 166.7$  ppm. This carbonyl group correlated also with the two trans positioned olefinic protons while the methoxy group at  $\delta_H$  (3.70, *s*) showed correlation with another carbonyl group ( $\delta_C$  174.0) which correlated also with H-2 and H-6 of the quinic acid.

From the results above the compound is identified as chlorogenic acid methyl ester, a known quinic acid derivative, previously reported for *Hypericum* genus.



Structure of compound **HAC2**:  
Chlorogenic acid methyl ester

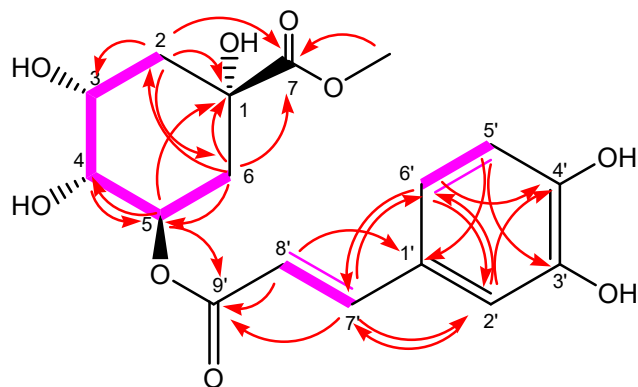
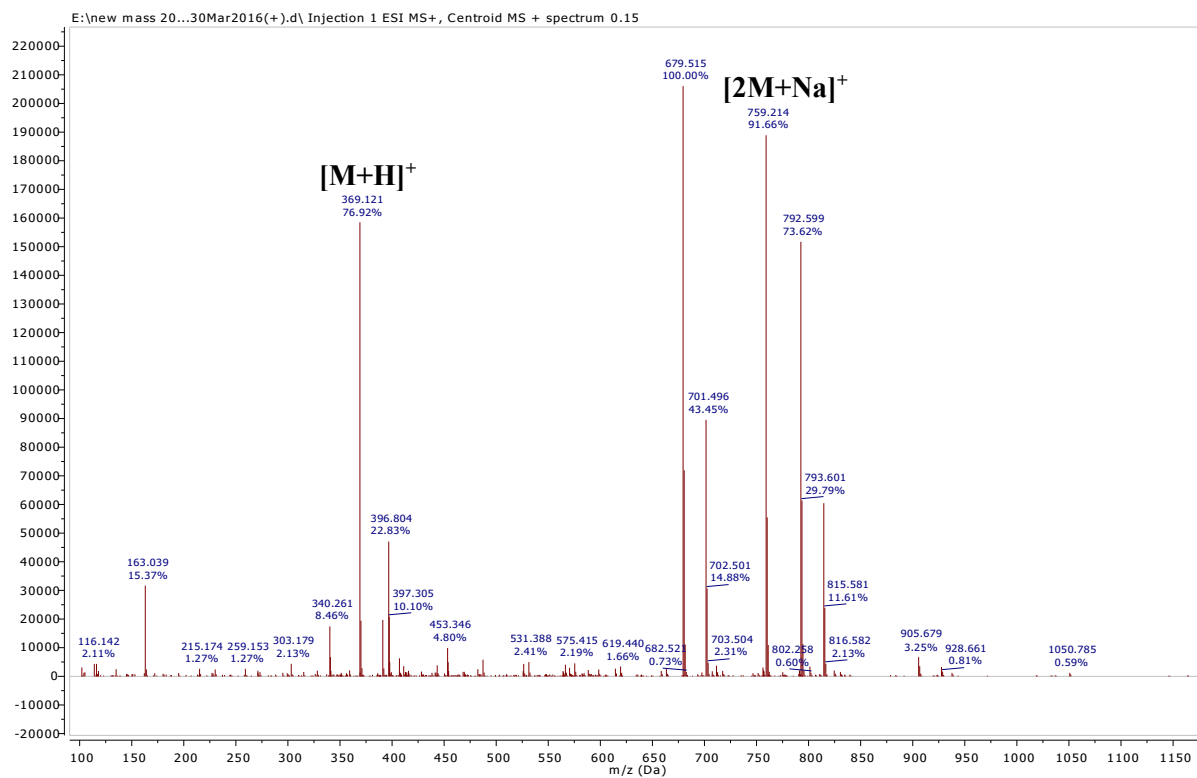
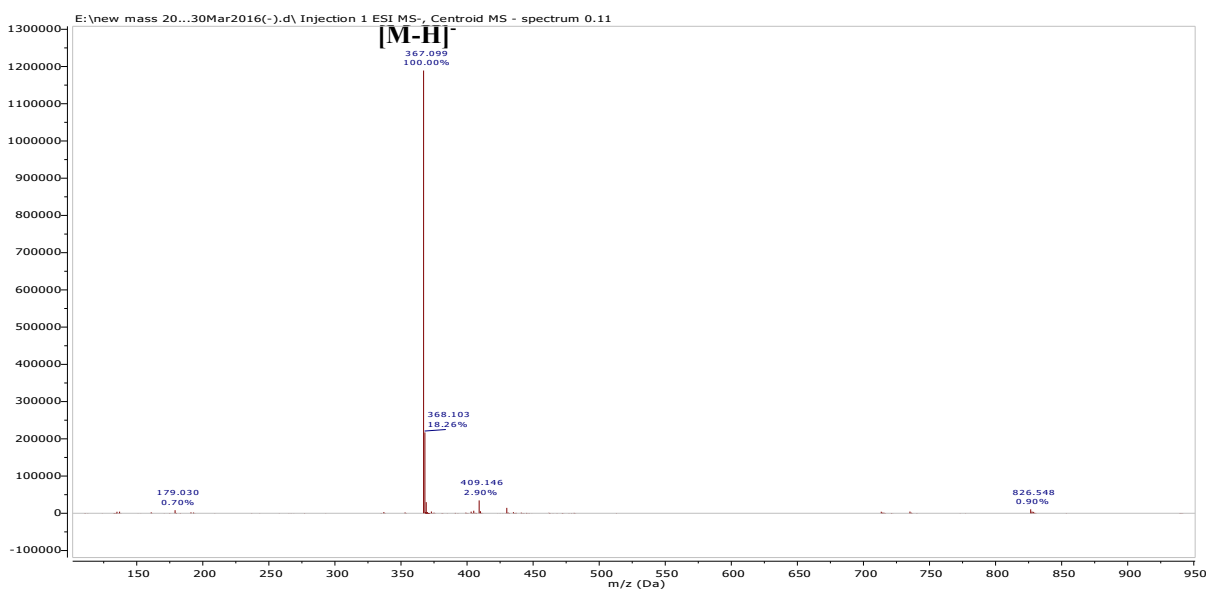


**Figure II.2. 90.** Key HMBC (H→C) and  $^1\text{H}$ - $^1\text{H}$  COSY (—) correlations of compound **HAC2**



A.



B.

**Figure II. 91.** Mass spectra of compound **HAC2**. A. Positive HR-ESI-MS B. Negative HR-ESI-MS

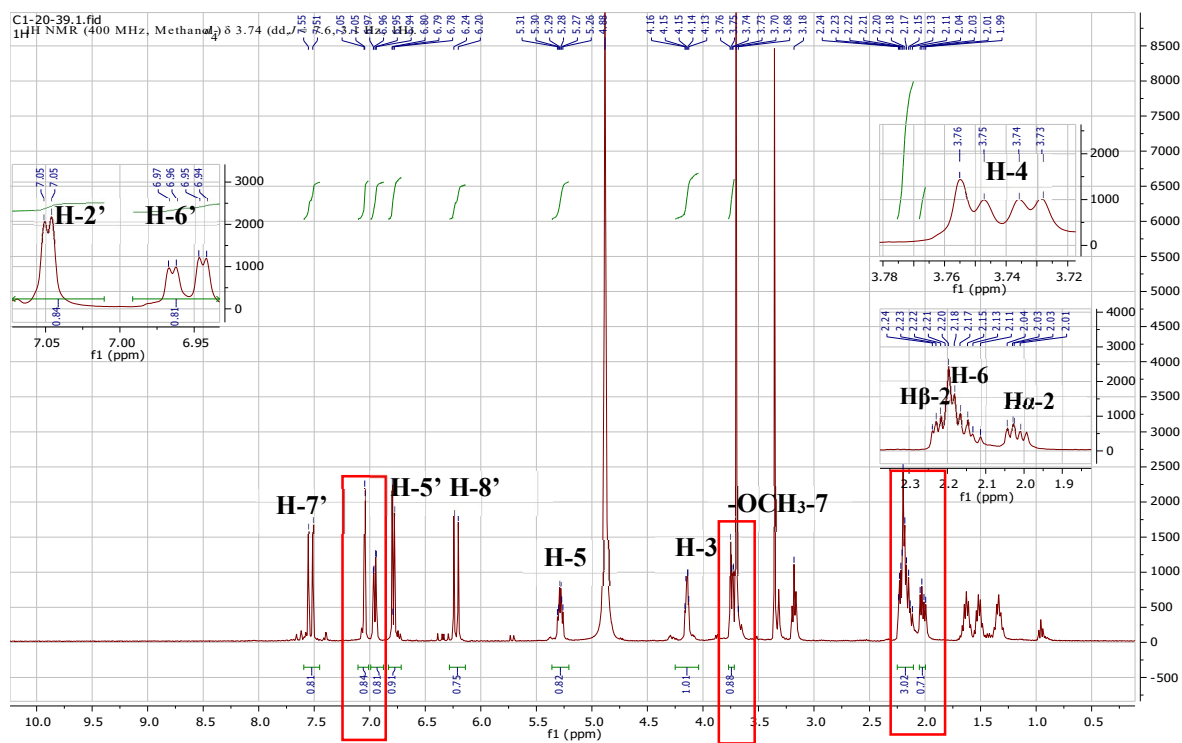


Figure II.2. 92. <sup>1</sup>H-NMR Spectrum of compound HAC2 (400 MHz)

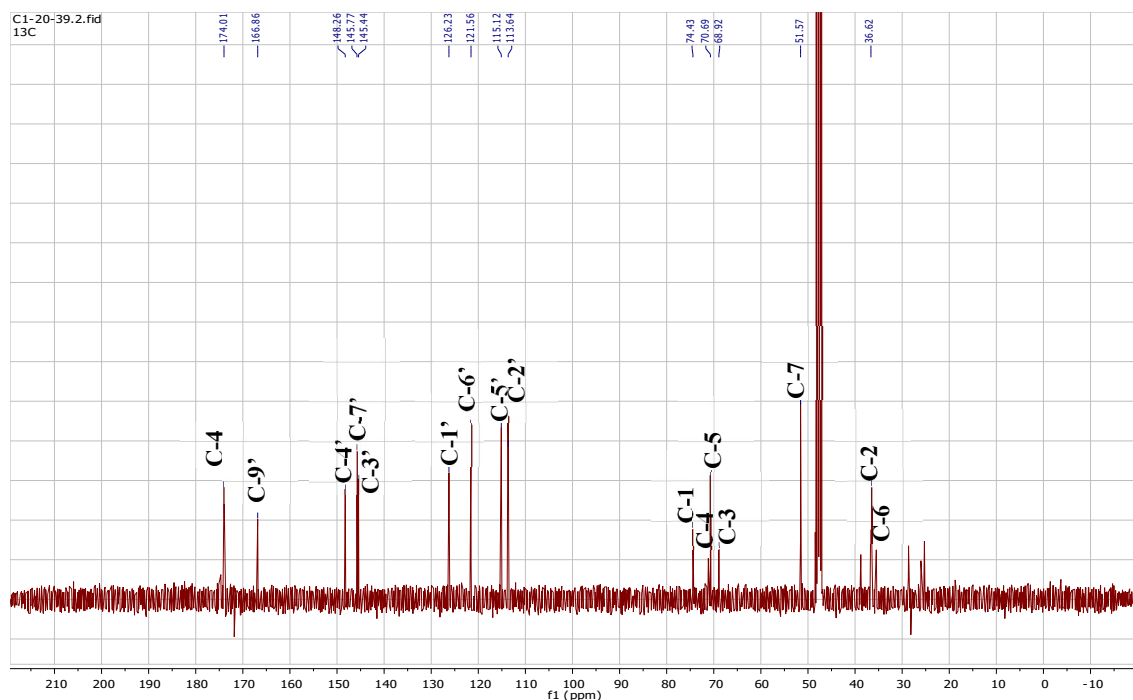


Figure II.2. 93. <sup>13</sup>C-NMR Spectrum of compound HAC2 (100 MHz)



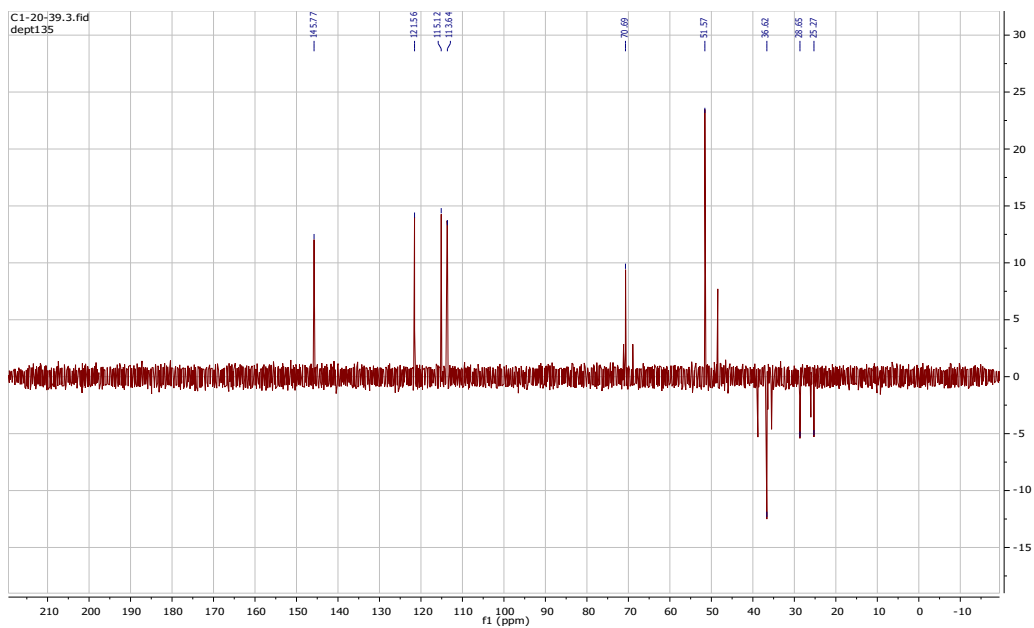


Figure II.2. 94. DEPT-135 Spectrum of compound HAC2

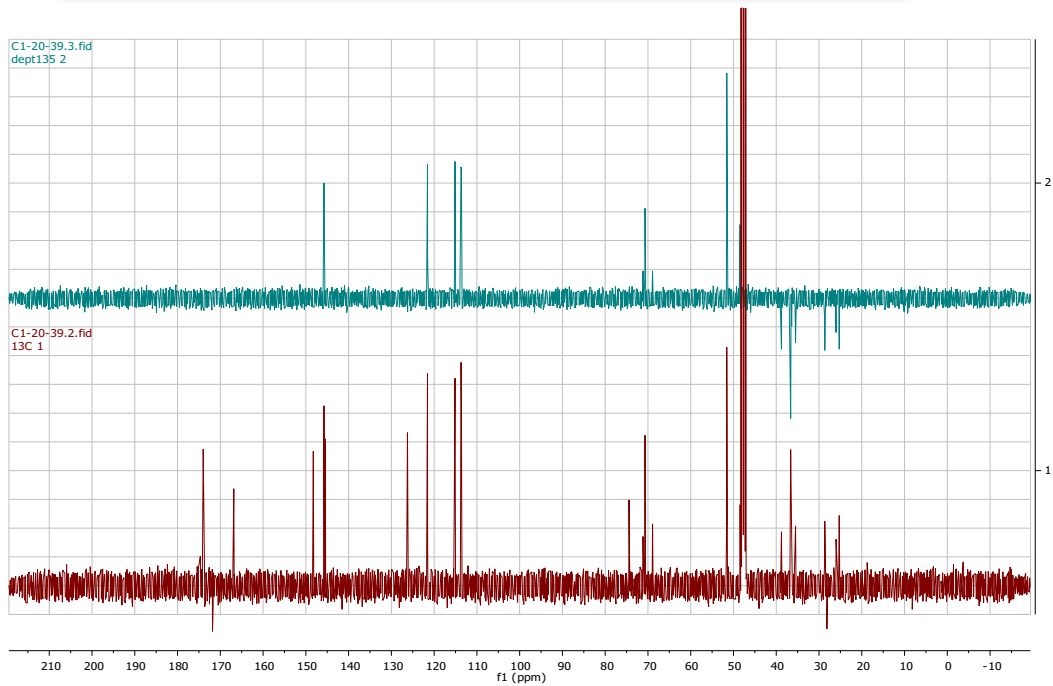
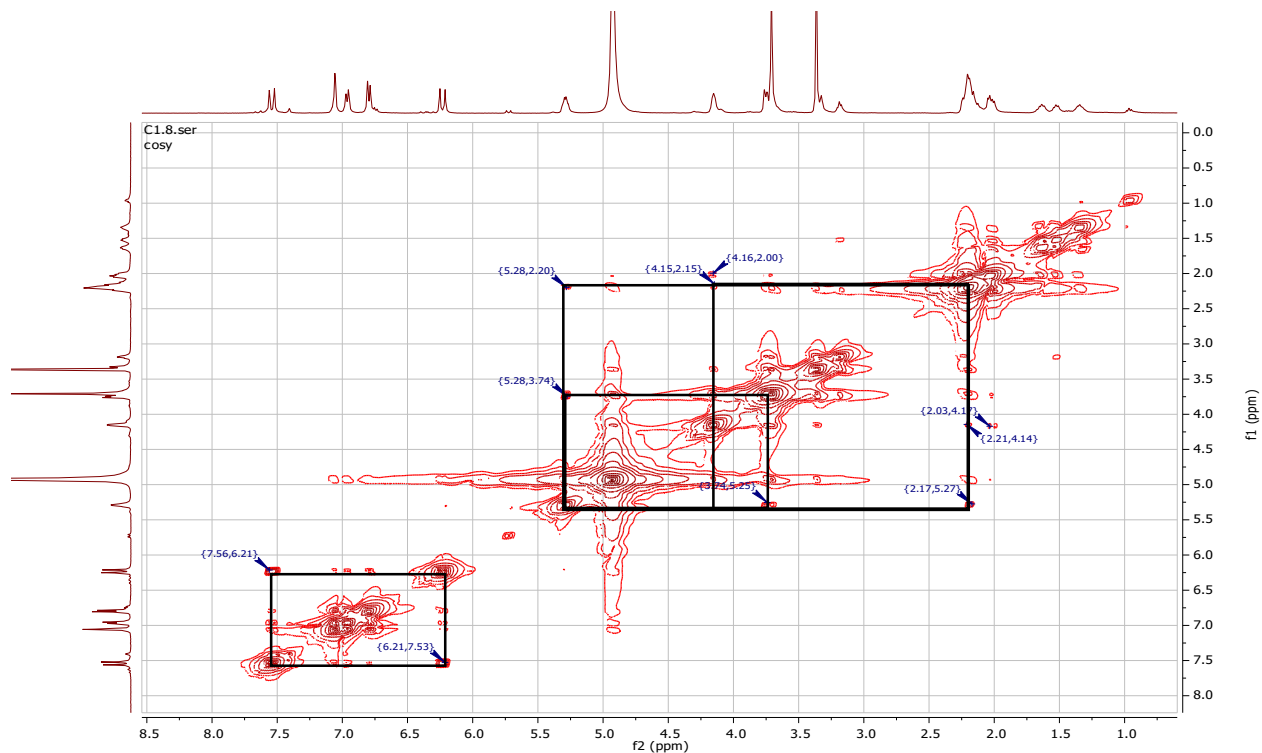
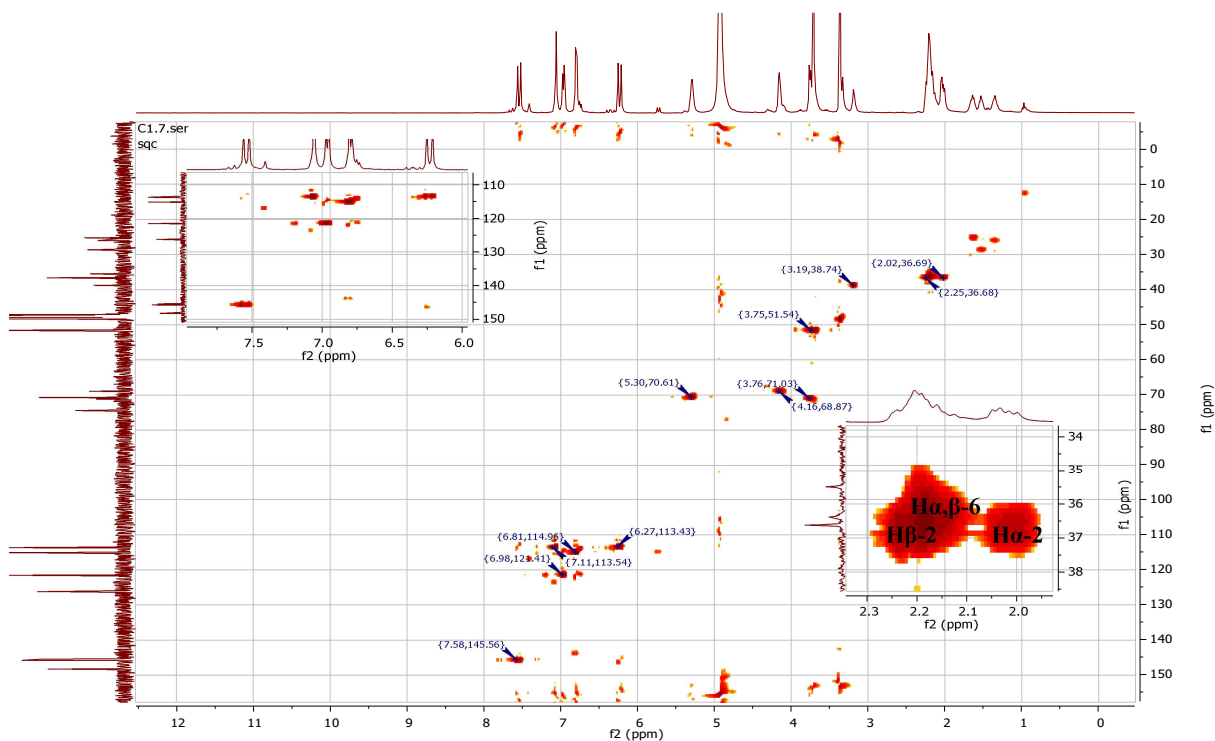


Figure II.2. 95. Comparison of  $^{13}\text{C}$ -NMR and DEPT-135 Spectra of compound HAC2



**Figure II.2. 96.  $^1\text{H}$ - $^1\text{H}$  COSY Spectrum of compound HAC2**



**Figure II.2. 97. HSQC Spectrum of Compound HAC2**

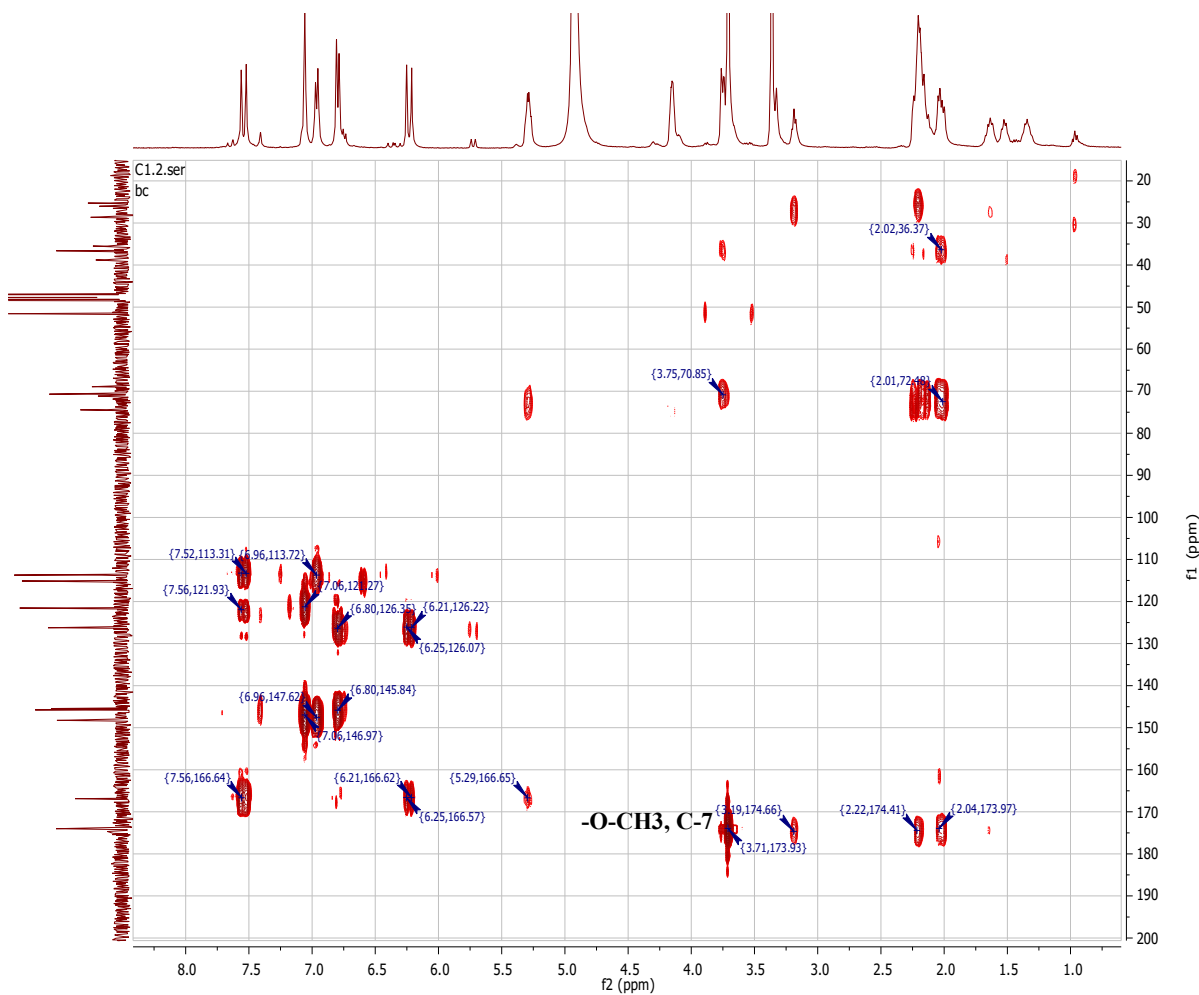


Figure II.2. 98. HMBC Spectrum of compound HAC2

## REFERENCES

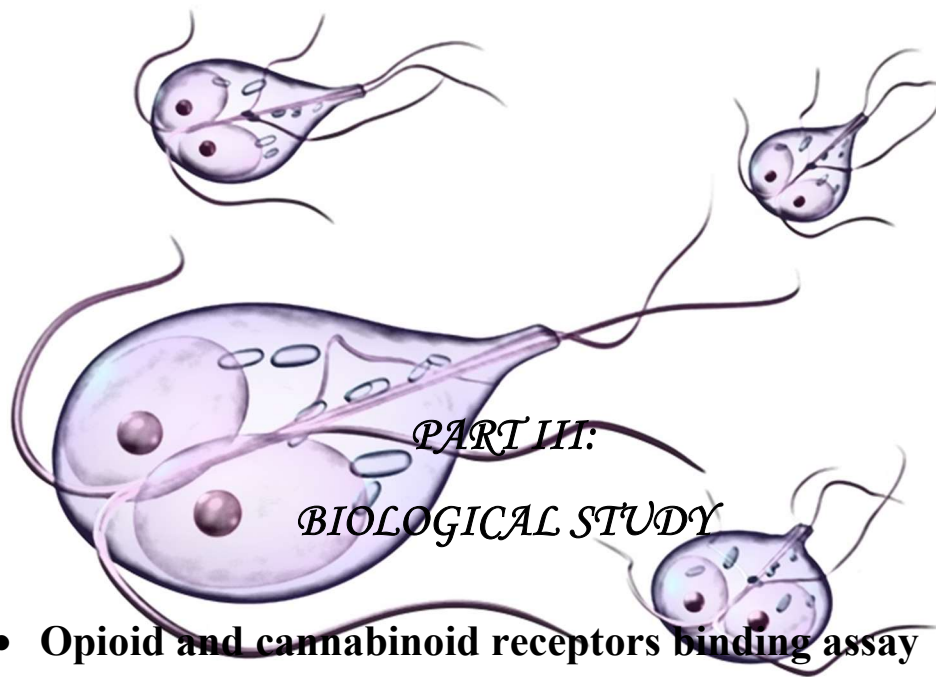
- Baoliang, C., Nakamura, M., Kinjo, J., NOHARA, T., 1993. Chemical constituents of Astragalus semen. Chemical and pharmaceutical bulletin 41, 178-182.
- Berghöfer, R., Hölzl, J., 1987. Biflavonoids in *Hypericum perforatum* L.; Part 1. Isolation of I3, II8-Biapiogenin. *Planta medica* 53, 216-217.
- Bornträger, H., 1880. Schneller Nachweis der Aloë in Elixiren, Liqueuren und im Bier. *Zeitschrift für Analytische Chemie* 19, 165-167.
- Cakir, A., Mavi, A., Yildirim, A., Duru, M.E., Harmandar, M., Kazaz, C., 2003. Isolation and characterization of antioxidant phenolic compounds from the aerial parts of *Hypericum hyssopifolium* L. by activity-guided fractionation. *Journal of Ethnopharmacology* 87, 73-83.
- CARPENTER, S., KRAUS, G.A., 1991. Photosensitization is required for inactivation of equine infectious anemia virus by hypericin. *Photochemistry and photobiology* 53, 169-174.
- Carter, B.B., 1947. Preliminary report on a substance which inhibits anti-Rh serum. *American journal of clinical pathology* 17, 646-649.
- Chimenti, F., Cottiglia, F., Bonsignore, L., Casu, L., Casu, M., Floris, C., Secci, D., Bolasco, A., Chimenti, P., Granese, A., 2006. Quercetin as the Active Principle of *Hypericum hircinum* Exerts a Selective Inhibitory Activity against MAO-A: Extraction, Biological Analysis, and Computational Study. *Journal of natural products* 69, 945-949.
- Colovic, M., Caccia, S., 2008. Liquid chromatography–tandem mass spectrometry of I3, II8-biapiogenin, the major biflavone in *Hypericum perforatum* extracts. *Journal of Chromatography B* 863, 74-79.
- Conforti, F., Loizzo, M., Statti, A., Menichini, F., 2007. Cytotoxic activity of antioxidant constituents from *Hypericum triquetrifolium* Turra. *Natural product research* 21, 42-46.
- Cook, R., 1961. Reactions of steroids with acetic anhydride and sulphuric acid (the Liebermann-Burchard test). *Analyst* 86, 373-381.
- David, J.M., Cruz, F.G., Guedes, M.L.S., Chávez, J.P., 1996. Flavonol glycosides from *Davilla flexuosa*. *J Braz Chem Soc* 7, 115-118.
- Demirkiran, O., Mesaik, M.A., Beynek, H., Abbaskhan, A., Choudhary, M.I., 2013. Immunosuppressive Phenolic Constituents from *Hypericum montbretii* Spach. *Records of Natural Products* 7, 210.
- Eldahshan, O., 2011. Isolation and structure elucidation of phenolic compounds of carob leaves grown in Egypt. *Curr Res J Biol Sci* 3, 52-55.
- Erdelmeier, C., 1998. Hyperforin, possibly the major non-nitrogenous secondary metabolite of *Hypericum perforatum* L. *Pharmacopsychiatry* 31, 2-6.
- Feng, R., Lu, Y., Bowman, L.L., Qian, Y., Castranova, V., Ding, M., 2005. Inhibition of activator protein-1, NF- $\kappa$ B, and MAPKs and induction of phase 2 detoxifying enzyme activity by chlorogenic acid. *Journal of Biological Chemistry* 280, 27888-27895.
- Forino, M., Tenore, G.C., Tartaglione, L., Novellino, E., Ciminiello, P., 2015. (1S, 3R, 4S, 5R) 5-O-Caffeoylquinic acid: Isolation, stereo-structure characterization and biological activity. *Food chemistry* 178, 306-310.
- Geissman, T.A., 1962. The chemistry of flavonoid compounds. Oxford, London, New York, Paris.: Pergamon Press.
- GUILHON, P., RODRIGUES, S.T., BIFLAVONOIDS AND TERPENOIDS ISOLATED FROM THE LEAVES.

- Habib, M., Nikkon, F., Rahman, M., Haque, Z., Karim, M., 2007. Isolation of stigmasterol and  $\beta$ -sitosterol from methanolic extract of root. *Pak. J. Biol. Sci* 10, 4174-4176.
- Hardman, R., Sofowora, E.A., 1972. Antimony trichloride as a test reagent for steroids, especially diosgenin and yamogenin, in plant tissues. *Stain technology* 47, 205-208.
- Hayder, N., Bouhlel, I., Skandrani, I., Kadri, M., Steiman, R., Guiraud, P., Mariotte, A.-M., Ghedira, K., Dijoux-Franca, M.-G., Chekir-Ghedira, L., 2008. In vitro antioxidant and antigenotoxic potentials of myricetin-3-o-galactoside and myricetin-3-o-rhamnoside from *Myrtus communis*: modulation of expression of genes involved in cell defence system using cDNA microarray. *Toxicology in vitro* 22, 567-581.
- Hudson, J., Lopez-Bazzocchi, I., Towers, G., 1991. Antiviral activities of hypericin. *Antiviral research* 15, 101-112.
- Jin, X.-n., Yan, E.-z., Wang, H.-m., Sui, H.-j., Liu, Z., Gao, W., Jin, Y., 2016. Hyperoside exerts anti-inflammatory and anti-arthritic effects in LPS-stimulated human fibroblast-like synoviocytes in vitro and in mice with collagen-induced arthritis. *Acta Pharmacologica Sinica*.
- Kamel, M.R., Nafady, A.M., Allam, A.E., Hassanein, A.M., Haggag, E.G., 2016. Phytochemical and Biological Study of the Aerial Parts of *Chrozophora oblongifolia* (Delile) Spreng. (Euphorbiaceae). *Journal of Pharmacognosy and Phytochemistry* 5, 17.
- Kusari, S., Zühlke, S., Borsch, T., Spittler, M., 2009. Positive correlations between hypericin and putative precursors detected in the quantitative secondary metabolite spectrum of *Hypericum*. *Phytochemistry* 70, 1222-1232.
- Ling, W., Jones, P., 1995. Dietary phytosterols: a review of metabolism, benefits and side effects. *Life sciences* 57, 195-206.
- Loizou, S., Lekakis, I., Chrousos, G.P., Moutsatsou, P., 2010.  $\beta$ -Sitosterol exhibits anti-inflammatory activity in human aortic endothelial cells. *Molecular nutrition & food research* 54, 551-558.
- Mabry, T.J., Markham, K., Thomas, M., 1970a. The ultraviolet spectra of flavones and flavonols, The systematic identification of flavonoids. Springer, pp. 41-164.
- Mabry, T.J., Markham, K.R., Thomas, M.B., 1970b. The systematic identification of flavonoids. Springer.
- Markham, K., Ternai, B., Stanley, R., Geiger, H., Mabry, T., 1978. Carbon-13 NMR studies of flavonoids—III: Naturally occurring flavonoid glycosides and their acylated derivatives. *Tetrahedron* 34, 1389-1397.
- Meng, S., Cao, J., Feng, Q., Peng, J., Hu, Y., 2013. Roles of chlorogenic acid on regulating glucose and lipids metabolism: a review. *Evidence-Based Complementary and Alternative Medicine* 2013.
- Miean, K.H., Mohamed, S., 2001. Flavonoid (myricetin, quercetin, kaempferol, luteolin, and apigenin) content of edible tropical plants. *Journal of agricultural and food chemistry* 49, 3106-3112.
- Moiseev, D., 2016. Determination of hypericin in *St. John's wort* by derivative spectrophotometry. *Journal of Pharmacognosy and Phytochemistry* 5, 249.
- Moon, J.-H., Tsushida, T., Nakahara, K., Terao, J., 2001. Identification of quercetin 3-O- $\beta$ -D-glucuronide as an antioxidative metabolite in rat plasma after oral administration of quercetin. *Free Radical Biology and Medicine* 30, 1274-1285.
- Nedialkov, P.T., Kitanov, G.M., Zheleva-Dimitrova, D.Z., Girreser, U., 2007. Flavonoids and a xanthone from *Hypericum umbellatum* (Guttiferae). *Biochemical systematics and ecology* 35, 118-120.

- Paul, B., Rao, G.S., Kapadia, G.J., 1974. Isolation of myricadiol, myricitrin, taraxerol, and taraxerone from *Myrica cerifera* L. root bark. *Journal of pharmaceutical sciences* 63, 958-959.
- Pereira, M., Siba, I., Chioca, L., Correia, D., Vital, M., Pizzolatti, M., Santos, A., Andreatini, R., 2011. Myricitrin, a nitric oxide and protein kinase C inhibitor, exerts antipsychotic-like effects in animal models. *Progress in Neuro-Psychopharmacology and Biological Psychiatry* 35, 1636-1644.
- Robinson, T., 1980. The organic constituents of higher plants: their chemistry and interrelationships. North Amherst (Mass.: Cordus Press, 1980. iv, 352p.-. En *Chemotaxonomy* (KR, 198206450).
- Saeidnia, S., Manayi, A., Gohari, A.R., Abdollahi, M., 2014. The Story of Beta-sitosterol-A Review.
- Saldanha, L.L., Vilegas, W., Dokkedal, A.L., 2013. Characterization of flavonoids and phenolic acids in *Myrcia bella* cambess. Using FIA-ESI-IT-MSn and HPLC-PAD-ESI-IT-MS combined with NMR. *Molecules* 18, 8402-8416.
- Sato, Y., Itagaki, S., Kurokawa, T., Ogura, J., Kobayashi, M., Hirano, T., Sugawara, M., Iseki, K., 2011. In vitro and in vivo antioxidant properties of chlorogenic acid and caffeic acid. *International Journal of Pharmaceutics* 403, 136-138.
- Shellard, E.J., 1957. Practical plant chemistry for pharmacy students. Pitman Medical.
- Sultana, N., Rahman, M., Ahmed, S., Akter, S., Haque, M., Parveen, S., Moeiz, S., 2011. Antimicrobial Compounds from the Rhizomes of *Sansevieria hyacinthoides*. *Bangladesh Journal of Scientific and Industrial Research* 46, 329-332.
- Tatsis, E.C., Exarchou, V., Troganis, A.N., Gerothanassis, I.P., 2008. 1 H NMR determination of hypericin and pseudohypericin in complex natural mixtures by the use of strongly deshielded OH groups. *analytica chimica acta* 607, 219-226.
- Vacek, J., Klejduš, B., Kuban, V., 2007. Hypericin and hyperforin: bioactive components of St. John's Wort (*Hypericum perforatum*). Their isolation, analysis and study of physiological effect. *Ceska a Slovenska farmacie: casopis Ceske farmaceuticke spolecnosti a Slovenske farmaceuticke spolecnosti* 56, 62-66.
- Van Cleemput, M., Cattoor, K., De Bosscher, K., Haegeman, G., De Keukeleire, D., Heyerick, A., 2009. Hop (*Humulus lupulus*)-derived bitter acids as multipotent bioactive compounds. *Journal of natural products* 72, 1220-1230.
- Wall, M.E., Krider, M.M., Krewson, C., Eddy, C.R., Willaman, J., Corell, D., Gentry, H., 1954. Steroidal saponin VII. Survey of plants for steroidal saponin and other constituents. *Journal of the American Pharmaceutical Association* 43, 1-7.
- Wu, Y., Zhou, S., Li, P., 2002. Determination of flavonoids in *Hypericum perforatum* by HPLC analysis. *Yao xue xue bao= Acta pharmaceutica Sinica* 37, 280-282.
- Yoshikawa, K., Suzuki, K., Umeyama, A., Arihara, S., 2006. Abietane Diterpenoids from the Barks of *Cryptomeria japonica*. *Chemical and pharmaceutical bulletin* 54, 574-578.
- Zdunić, G., Gođevac, D., Šavikin, K., Novaković, M., Milosavljević, S., Petrović, S., 2011. Isolation and identification of phenolic compounds from *Hypericum richeri* Vill. and their antioxidant capacity. *Natural product research* 25, 175-187.
- Zhang, M., Liu, W.-X., Zheng, M.-F., Xu, Q.-L., Wan, F.-H., Wang, J., Lei, T., Zhou, Z.-Y., Tan, J.-W., 2013. Bioactive quinic acid derivatives from *Ageratina adenophora*. *Molecules* 18, 14096-14104.
- Zhang, N., Ying, M.-D., Wu, Y.-P., Zhou, Z.-H., Ye, Z.-M., Li, H., Lin, D.-S., 2014. Hyperoside, a flavonoid compound, inhibits proliferation and stimulates osteogenic differentiation of human osteosarcoma cells. *PloS one* 9, e98973.

Zhang, X., Julien-David, D., Miesch, M., Geoffroy, P., Raul, F., Roussi, S., Aoudé-Werner, D., Marchioni, E., 2005. Identification and quantitative analysis of  $\beta$ -sitosterol oxides in vegetable oils by capillary gas chromatography–mass spectrometry. *Steroids* 70, 896-906.

李春梅, 王涛, 张祎, 高秀梅, 李天祥, 2010. 中药黄蜀葵花化学成分的分离与鉴定 (I). *瀋陽藥科大學學報* 27, 711-714.



- **Opioid and cannabinoid receptors binding assay**
- **Antimalarial assay.**
- **Antimicrobial assay**
- **Antiprotozoal assay**
- **Cytotoxicity**
- **Antioxidant assay**
- **Anti-inflammatory assay**
- **MAOs Inhibition**



### **III. Biological study of extracts and some isolated compounds from plants under investigation**

Extracts, fractions and isolated pure compounds of *C. villosus* and *H. afrum* species were submitted for biological activity testing. Bioassays were done at the National Center for Natural Products Research (University of Mississippi).

#### **III.1. Opioid & cannabinoid receptor binding affinity**

Opioid and cannabinoid receptors are G-protein coupled receptors, which are a group of signaling receptors that are involved in the recognition of and transduction of messages across cell membranes (Tarawneh et al., 2015). Various subtypes of each receptor system have been recognized; the opioid receptor system mainly includes  $\mu$ ,  $\kappa$ , and  $\delta$  receptors, while the cannabinoid receptor system includes CB1 and CB2 receptors. The opioid receptors are known to regulate various physiological functions including neurohormonal secretion of the adrenal and pituitary glands and also possess direct action on the adrenal glands. They play a major role in the central nervous system (CNS), as well as in cardiovascular, immune, reproductive, endocrine, and gastrointestinal systems (Felder et al., 1995; Reisine and Brownstein, 1994). Within the endocannabinoid systems, the CB1 receptor is mainly expressed in the CNS, while CB2 is primarily expressed in the peripheral nervous system, where it plays a crucial role in the stimulation of hematopoietic lineage growth.

The extracts, fractions and pure compounds isolated of species under investigation have been submitted for testing to determine their affinity for opioid receptors (subtype  $\delta$ ,  $\kappa$  and  $\mu$ ) and cannabinoid receptors (subtype CB1 and CB2) employing the protocol described previously in page (64), but demonstrated activities that were too low in the initial screen to submit for secondary assays. The results are shown in Table III.3.

**Table III. 1.** Results for cannabinoid and opioid receptor binding assay (percent of inhibition)

N0.	Cannabinoid receptors			Opioid receptors		
Compound code	Compound name	CB1 % inhibition	CB2 % inhibition	delta % inhibition	kappa % inhibition	mu % inhibition
HAP1	<i>3-Benzoyl-3-hydroxy-5-(3-methylbut-2-en-1-yl)cyclopentane-1,2,4-trione</i>	23.0	12.8	16.6	-	16.4
HAF1	Quercetin	-	-	8.2	-	1.6
HAF2	Myricetin	-	-	6.5	3.2	-
HAF3	Myricitrin	-	-	-	5.3	11.8
HAF4	Hyperoside	8.5	-	17.0	17.9	16.1
HAF6	myricetin-3'-O-β-D-glucopyranoside	10.0	5.0	11.4	23.9	13.8
HAB1	Biapigenin	-	1.9	24.0	40.5	25.2
CVF1	Chrysin	7.7	0.8	8.7	12.8	12.2

### - Conclusion

- Demonstrated activities were too low in the initial screen to submit for secondary assays. Similarly, the pure compounds tested were inactive.

### III.2. Antimalarial assay

Malaria, a major tropical infectious disease caused primarily by the protozoan parasite *Plasmodium falciparum*, is responsible for the death of more than 1.12 million individuals every year. Antimalarial drugs are the major focus in the prevention and treatment of malaria (Njokah et al., 2016). Antimalarial activities of *H. afrum* and *C. villosus* were evaluated following the method previously demonstrated in page (63).

Fractions of the ethanolic crud extract and certain pure compounds of *H. afrum* and *C. villosus* species were initially tested for its antimalarial activity, but demonstrated activities were too low in the initial screen to submit for secondary assays. The results are presented in Tables III.4 and III.5.

**Table III. 2.** Antimalarial screen results of extracts

Sample		%inhibition		Concentration ng/mL
Extract/Fraction	Genus species	P. falciparum D6	P. falciparum W2	
EtOAc	<i>H. afrum</i>	7	NT	158667
BuOH	<i>H. afrum</i>	3	NT	158667
CHCl <sub>3</sub>	<i>H. afrum</i>	33	NT	158667
BuOH	<i>C. villosus</i>	0	NT	158667
EtOAc	<i>C. villosus</i>	0	NT	158667
<b>CQ</b>		100	NT	79.3

CQ: Chloroquine (Positive Control)

**Table III. 3.** Antimalarial screen results of some isolated compounds

Sample	Compound name	P. falciparum D6		P. falciparum W2		VERO IC <sub>50</sub>	[C] ng/mL
		IC <sub>50</sub> (ng/mL)	SI	IC <sub>50</sub> (ng/mL)	SI		
<b>CQ</b>	Chloroquine	<26.0	>9	116	>2.1	>238	238-26.4
Compounds isolated from <i>Hypericum Afrum</i> aerial parts							
HAT1	β-sitosterol	>4760	1	>4760	1	>4760	4760-528.9
HAP1	3-Benzoyl-3-hydroxy-5-(3-methylbut-2-en-1-yl)cyclopentane-1,2,4-trione	>4760	1	>4760	1	>4760	4760-528.9
HAF1	quercetin	>4760	1	>4760	1	>4760	4760-528.9
HAB1	Biapigenin	>4760	1	>4760	1	>4760	4760-528.9
HAF2	Myricetin	>4760	1	>4760	1	>4760	4760-528.9
HAF3	Myricitrin	>4760	1	>4760	1	>4760	4760-528.9
HAF4	Hyperoside	>4760	1	>4760	1	>4760	4760-528.9
HAF6	myricetin-3'-O-β-D-glucopyranoside	4360.1	>1.1	3930.5	>1.2	>4760	4760-528.9
Compounds isolated from <i>Cytisus villosus</i> aerial parts							
CVF1	Chrysin	>4760	1	>4760	1	>4760	4760-528.9
CVF2	Chrysin-7-O-β-D-glucopyranoside	>4760	1	>4760	1	>4760	4760-528.9
CVK1	Sparteine	>4760	1	>4760	1	>4760	4760-528.9

**- Conclusion**

- Compound **HAF6**, myricetin-3'-O-β-D-glucopyranoside, showed weak antiplasmodial activity against the chloroquine-sensitive (D6) and resistant (W2) *Plasmodium falciparum* with IC<sub>50</sub>

values of 4.36 (SI >1.1) and 3.93 (SI >1.2) µg/mL, respectively.

### **III.3 . Antimicrobial activity**

The antibacterial and antifungal activities of *H. afrum* and *C. villosus* were evaluated employing the protocol described previously in page (58).

The antibacterial activities were tested against *Staphylococcus aureus*, methicillin-resistant *S. aureus* (MRS), *Escherichia coli*, *Pseudomonas aeruginosa*, and *Mycobacterium intracellulare*.

**Ciprofloxacin** was used as positive control for antibacterial activity.

The antifungal activities were evaluated against a panel of pathogenic fungi including *Candida albicans*, *C. glabrata*, *C. krusei*, *Aspergillus fumigatus* and *Cryptococcus neoformans* associated with opportunistic infections.

**Amphotericin B** was included as a standard antifungal drug for comparison.

The results are shown in Tables III.6 and III.7.

#### **- Conclusion**

- All fractions of the ethanolic crud extract and isolated pure compounds of both two plants tested were inactive.

**Table III. 4.** Antibacterial and antifungal results of plant extracts.

Sample	% Growth Inhibition <sup>1,2</sup>											
	Anti-Fungal Anti-Bacterial						Anti-Fungal Anti-Bacterial					
Extract/ Fraction	Genus Species	C.albicans inhibition	C.glabra ta inhibition	C.krusei inhibition	A.fumigatus inhibition	C.neformans inhibition	S.aureus inhibition	MRS inhibition	E.coli inhibition	P.aeruginosa inhibition	Kp Inhibition	VRE Inhibition
EtOAc	<i>H.afrum</i>	7	47	2	5	0	3	2	14	12	NT-	NT-
BuOH	<i>H.afrum</i>	10	31	5	0	0	7	0	22	11	NT-	NT-
CHCl <sub>3</sub>	<i>H.afrum</i>	14	5	7	2	18	0	5	13	10	NT-	NT-
BuOH	<i>C.villosus</i>	9	40	0	2	0	0	0	14	9	NT-	NT-
EtOAc	<i>C.villosus</i>	9	11	2	4	0	3	0	12	5	NT-	NT-
<b>FLU</b>	Control	<b>77</b>	<b>NT</b>	<b>NT</b>	<b>0</b>	<b>96</b>	<b>NT</b>	<b>14</b>	<b>0</b>	<b>0</b>	<b>3</b>	<b>2</b>
<b>AMB</b>	Control	100	NT	NT	93	100	NT	1	0	0	4	3
<b>CIPRO</b>	Control	0	NT	NT	8	0	NT	0	100	96	0	6

Concentration: 50µg/mL. <sup>1</sup> Samples showing % Growth Inhibition < 50 are considered inactive.; <sup>2</sup> Samples showing % Growth Inhibition > 50 in any organisms are confirmed in secondary assay

**Table III. 5.** Antibacterial and antifungal results of pure compounds isolated

Sample Code	Sample name	C. albicans IC <sub>50</sub> µg/mL	C. glabrata IC <sub>50</sub> µg/mL	C. krusei IC <sub>50</sub> µg/mL	A. fumigatus IC <sub>50</sub> µg/mL	C. neoformans IC <sub>50</sub> µg/mL	S. aureus IC <sub>50</sub> µg/mL	MRS IC <sub>50</sub> µg/mL	E. coli IC <sub>50</sub> µg/mL	P. aeruginosa IC <sub>50</sub> µg/mL	M. intracellulare IC <sub>50</sub> µg/mL	K. pneumoniae IC <sub>50</sub> µg/mL	VRE IC <sub>50</sub> µg/mL
<b>FLU</b>	<b>Fluconazole</b>	5.74	NT	NT	>100	10.91	>100	>100	>100	>100	NT	>100	>100
<b>AMB</b>	<b>Amphotericin B</b>	1.26	0.84	1.4	1.22	0.2	-	-	-	-	-	NT	NT
<b>CIPRO</b>	<b>Ciprofloxacin</b>	NT	NT	NT	NT	NT	0.124	0.103	0.006	0.085	0.399	NT	NT
<b>Compounds isolated from <i>Hypericum Afrum</i> aerial parts</b>													
HAT1	β-sitosterol	>20	>20	>20	>20	>20	>20	>20	>20	>20	>20	NT	NT
HAP1	<i>3-Benzoyl-3-hydroxy-5-(3-methylbut-2-en-1-yl) cyclopentane-1,2,4-trione</i>	>20	NT	NT	>20	>20	NT	>20	>20	>20	NT	>20	>20
HAF1	quercetin	>20	NT	NT	>20	>20	NT	>20	>20	>20	NT	>20	>20
HAB1	Biapigenin	>20	NT	NT	>20	>20	NT	>20	>20	>20	NT	>20	>20
HAF2	Myricetin	>20	NT	NT	>20	>20	NT	>20	>20	>20	NT	>20	>20
HAF3	Myricitrin	>20	NT	NT	>20	>20	NT	>20	>20	>20	NT	>20	>20
HAF4	Hyperoside	>20	NT	NT	>20	>20	NT	>20	>20	>20	NT	>20	>20
HAF6	myricetin-3'-O-β-D-glucopyranoside	>20	NT	NT	>20	>20	NT	>20	>20	>20	NT	>20	>20
<b>Compounds isolated from <i>Cytisus villosus</i> aerial parts</b>													
CVF1	Chrysin	>20	NT	NT	NT	>20	>20	NT	>20	>20	>20	>20	>20
CVK1	Sparteine	>20	NT	NT	NT	>20	>20	NT	>20	>20	>20	>20	>20

Concentration: 100-4 µg/mL Pure compounds that have an IC<sub>50</sub> of ≤ 7 µg/mL in the secondary assay proceed to the tertiary assay.

### III.4. Antiprotozoal assay

Leishmaniasis is a parasitic disease remaining a major public health problem. It causes illness and death especially in developing countries. Common chemotherapeutic agents currently used are often inadequate, requiring long courses of parenteral administration, having toxic side effects or becoming less effective due to the emergence of resistant strains.

There are twenty pathogenic *Leishmania* species for human. They can be transmitted by the bit of an infected female sandfly introducing parasites into the host. There are thirty sandfly species proven vectors. They can become infected when taking a blood meal from a reservoir host. Hosts are infected humans and wild and domestic animals. Leishmaniasis presents itself in three main clinical forms which have devastating consequences. In visceral Leishmaniasis (VL or “kala-azar”), the parasites reside in the liver, spleen, and bone marrow causing a severe systemic disease which is fatal if it is not treated. Mucocutaneous Leishmaniasis (MCL) is characterized by lesions in the mucous tissues of the nose and mouth and often progresses to massive tissue destruction and disfigurement. Cutaneous leishmaniasis (CL) involves the development of self-healing but chronic skin ulcers at the site of sandfly bites. According to World Health Organization (WHO) statistics, there are 12 million people currently affected by leishmaniasis in 88 countries on five continents- Africa, Asia, Europe, North America, and South America- with a total of 350 million people at risk. Two million new cases, 1.5 million for CL and 500,000 for VL, are considered to occur annually. 90% of VL cases reside in five countries: Bangladesh, India, Nepal, Sudan, and Brazil, while 90% of CL cases occur in seven countries: Afghanistan, Algeria, Brazil, Iran, Peru, Saudi Arabia, and Syria (Alvar et al., 2012).

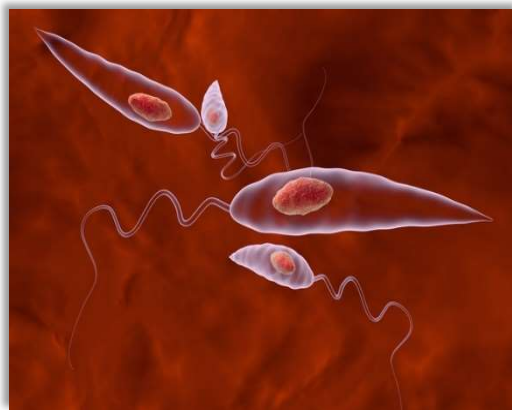


**Figure III. 1.** Leishmania parasite.

*Trypanosoma brucei* is the causative agent of several serious and neglected tropical diseases in Sub-Saharan Africa. These different diseases are inflicted by various sub-species of *T. brucei*, which are defined by their respective host reservoirs or their geographical location, but they are all transmitted by the tse-tse fly (*Glossina* sp.). *T. brucei brucei* mainly infects the blood of cattle and other domestic and wild animals, causing Nagana, which manifests as the following symptoms: fever, muscular wasting, anemia, swelling of tissues (edema) and eventual paralysis. While *T. brucei brucei* is restricted to non-human mammals, *T. brucei rhodosiense* and *T. brucei gambiense* infect humans in East Africa and West Africa, respectively, causing Human African Trypanosomiasis (HAT) also known as sleeping sickness (Franco et al., 2014).

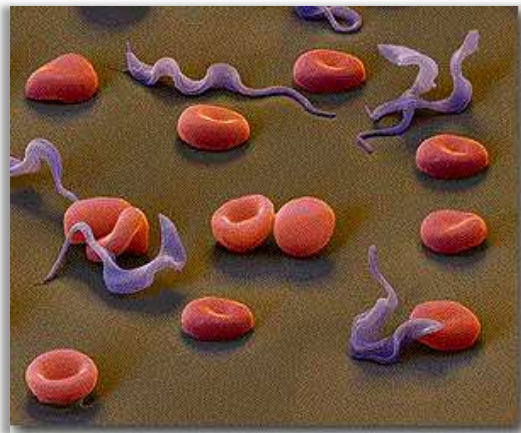


**Figure III. 2.** Parasite, *Trypanosoma brucei* surrounded by red blood cells in a smear of infected blood.

In the last few decades there has been a significant increase in the amount of research directed at developing treatments for African trypanosomiasis and although few new drugs have emerged, notable progress has been made. Several antitrypanosomal agents from plants have been characterized while considerable efforts are still being put into the search for more antiparasitic compounds that have been evolutionarily derived from nature, resulting from the co-existence of parasitic pathogens with other life forms.

- **Parasite Transmission and Life Cycle**

Leishmaniasis is a spectrum of disease caused by protozoan parasites belonging to the genus *Leishmania*. There are twenty pathogenic *Leishmania* species for human. They can be transmitted by the bite of an infected female sandfly introducing parasites into the host. There are thirty sandfly species proven vectors. They can become infected when taking a blood meal from a reservoir host. Hosts are infected humans and wild and domestic animals. Epidemiologically, the transmission cycle

can be zoonotic, meaning animal reservoir hosts are involved, or anthroponotic, where man is the sole source of infection for the insect vector. The life cycle of *Leishmania* (Figure III.3) involves two parasite forms, the flagellated motile promastigote stage inhabiting the gut of the sandfly, and the non-flagellated amastigote stage growing inside the phagolysosomes of mammalian macrophages.

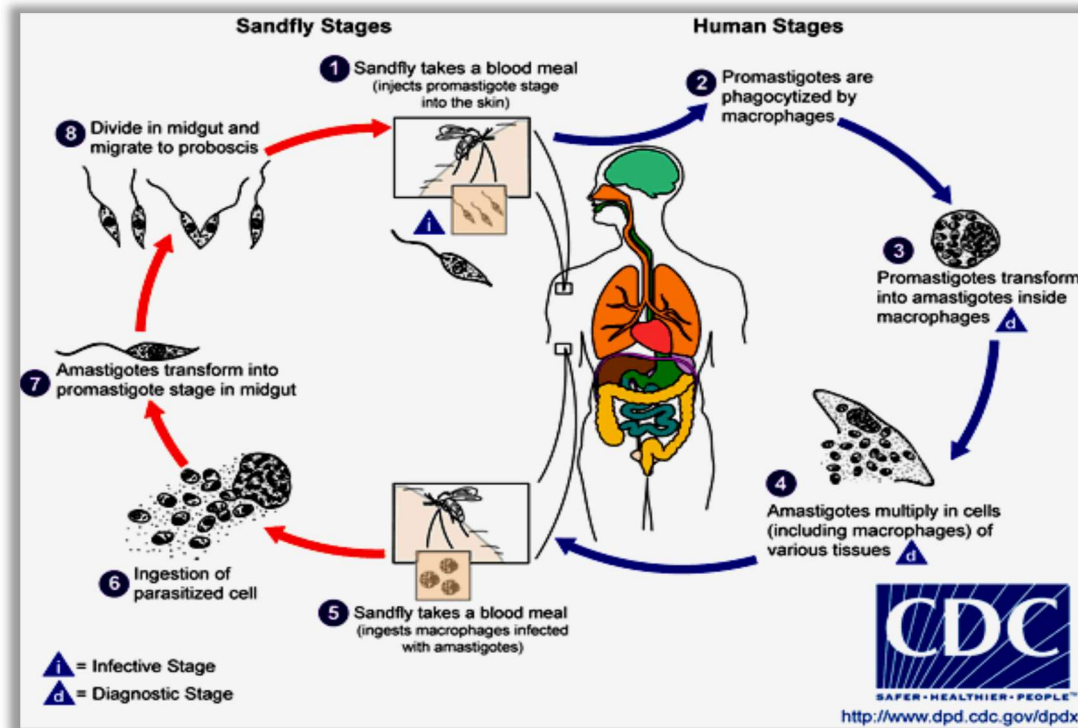


Figure III. 3. Life Cycle of *Leishmania* (Centers for Disease Control and Prevention).

- **Life cycle of African trypanosomiasis**

During a blood meal on the mammalian host, an infected tsetse fly (genus *Glossina*) injects metacyclic trypomastigotes into skin tissue. The parasites enter the lymphatic system and pass into the bloodstream ①. Inside the host, they transform into bloodstream trypomastigotes ②, are carried to other sites throughout the body, reach other blood fluids (e.g., lymph, spinal fluid), and continue the replication by binary fission ③. The entire life cycle of African Trypanosomes is represented by extracellular stages. The tsetse fly becomes infected with bloodstream trypomastigotes when taking a blood meal on an infected mammalian host (④, ⑤). In the fly's midgut, the parasites transform into procyclic trypomastigotes, multiply by binary fission ⑥, leave the midgut, and transform into epimastigotes ⑦. The epimastigotes reach the fly's salivary glands and continue multiplication by binary fission ⑧ (Figure III.4). The cycle in the fly takes approximately 3 weeks. Humans are the



main reservoir for *Trypanosoma brucei gambiense*, but this species can also be found in animals. Wild game animals are the main reservoir of *T. b. rhodesiense* (Steverding, 2008).

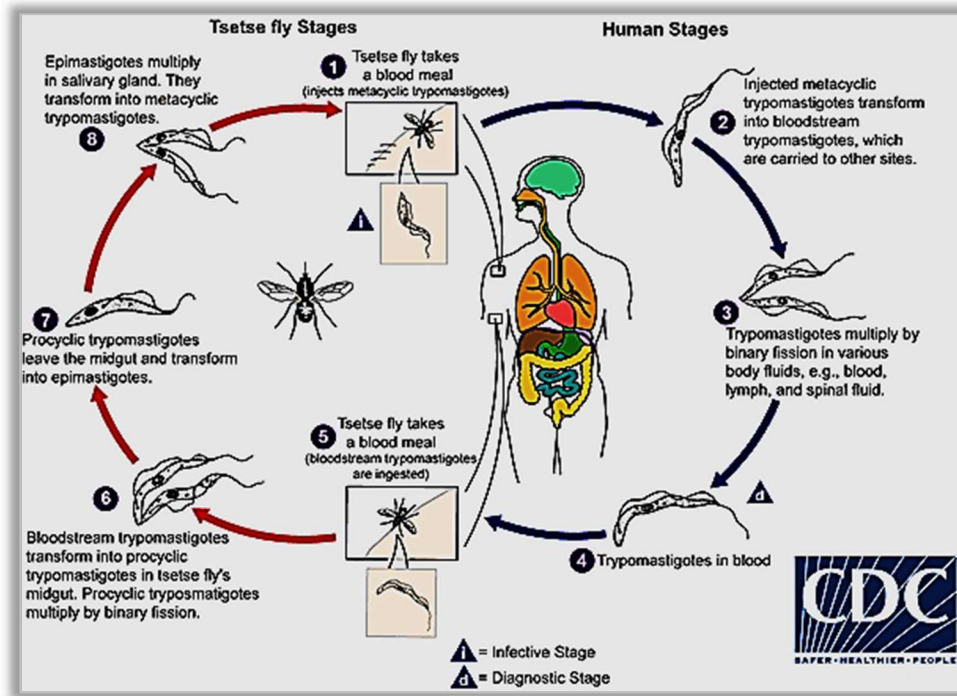


Figure III. 4. Life cycle of African trypanosomiasis (Centers for Disease Control and Prevention).

In the fight against leishmaniasis, natural products are important sources of novel therapeutic agents. Fractions of the ethanolic crud extract of *Hypericum afrum* and *Cytisus villosus* species have been screened for antiparasitic activity against *Leishmania donovani* and *Plasmodium falciparum* and *Trypanosoma brucei brucei* employing the protocols previously described in pages (63-64). The active samples were further evaluated regarding their toxicity versus mammalian cell lines.

The results are shown in tables III.8, III.9 and III.10.

Table III. 6. Antiprotozoal activities of the plants extracts

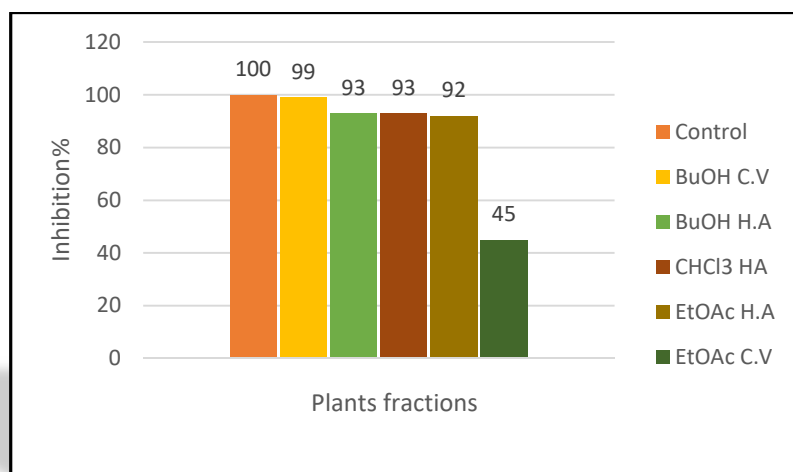
Tested organism	Plant	L. donovani promastigotes	L. donovani axenic amastigotes	L. donovani Macrophage amastigote	T. brucei	THP1 cytotoxicity	Test concentration (µg/mL)
Fraction	Species	% of inhibition					
EtOAc	<i>H. afrum</i>	9	0	1	92	1	20.0
BuOH	<i>H. afrum</i>	0	0	0	93	2	20.0
CHCl <sub>3</sub>	<i>H. afrum</i>	37	0	5	93	3	20.0
BuOH	<i>C.villosus</i>	10	0	0	99	5	20.0
EtOAc	<i>C.villosus</i>	1	0	0	45	7	20.0
AMB	Amphotericin	100	98	96	NT	4	0.4
PENT		NT	NT	NT	100	NT	0.02

Table III. 7. Results of secondary antiprotozoal screening of plants fractions

Fraction	Genus species	L. donovani Promastigote IC <sub>50</sub> µg/mL	L. donovani Promastigote IC <sub>90</sub> µg/mL	L. donovani Amastigote IC <sub>50</sub> µg/mL	L. donovani Amastigote IC <sub>90</sub> µg/mL	L. donovani Amastigote/THP IC <sub>50</sub> µg/mL	L. donovani Amastigote/THP IC <sub>90</sub> µg/mL	T. brucei IC <sub>50</sub> µg/mL	T. brucei IC <sub>90</sub> µg/mL	THP1 Cytotoxicity IC <sub>50</sub> µg/mL	THP1 Cytotoxicity IC <sub>90</sub> µg/mL	Test conc.(µg/mL)
CHCl <sub>3</sub>	<i>H.afrum</i>	>20	>20	>20	>20	>20	>20	12.35	14.94	>20	>20	20-0.8
EtOAc	<i>H. afrum</i>	>20	>20	>20	>20	>20	>20	13.53	19.31	>20	>20	20-0.8
BuOH	<i>H. afrum</i>	>20	>20	>20	>20	>20	>20	12.93	18.67	>20	>20	20-0.8
EtOAc	<i>C.villosus</i>	>20	>20	>20	>20	>20	>20	19.48	>20	>20	>20	20-0.8
BuOH	<i>C.villosus</i>	>20	>20	>20	>20	>20	>20	7.99	12.61	>20	>20	20-0.8
AMB	Amphotericin	0.138	0.188	0.304	0.362	0.187	0.264	NT	NT	>2	>2	2.0-0.08
PENT	Pentamidine	1.478	2.382	9.581	>10	1.157	5.587	0.001	0.002	>10	>10	0.02
DFMO	alpha-difluoromethylornithine	NT	NT	NT	NT	NT	NT	3.634	8.804	NT	NT	20-0.8

**Table III. 8.** Results of secondary antiprotozoal screening of pure compounds isolated from *H. afrum* and *C. villosus*

Compound Code	Compound name	L. donovani Promastigote IC <sub>50</sub> μM	L. donovani Promastigote IC <sub>90</sub> μM	L. donovani Amastigote IC <sub>50</sub> μM	L. donovani Amastigote IC <sub>90</sub> μM	L. donovani Amastigote/THP1 IC <sub>50</sub> μM	L. donovani Amastigote/THP1 IC <sub>90</sub> μM	T. brucei IC <sub>50</sub> μM	T. brucei IC <sub>90</sub> μM	THP1 Cytotoxicity IC <sub>50</sub> μM	THP1 Cytotoxicity C <sub>90</sub> μM
<b>AMB</b>	Amphotericin	0.136	0.215	0.211	0.374	0.188	0.421	NT	NT	>2	>2
<b>PENT</b>	Pentamidine	1.478	2.382	9.581	>10	1.157	5.587	0.001	0.002	>10	>10
<b>DFMO</b>	difluoromethylornithine	NT	NT	NT	NT	NT	NT	3.634	8.804	NT	NT
compounds isolated from <i>H. afrum</i>											
HAT1	β-sitosterol	>10	>10	>10	>10	>10	>10	0.98	1.34	>10	>10
HAP1	<i>3-Benzoyl-3-hydroxy-5-(3-methylbut-2-en-1-yl) cyclopentane-1,2,4-trione</i>	>10	>10	>10	>10	>10	>10	>10	>10	>10	>10
HAF1	Quercetin	>10	>10	>10	>10	>10	>10	7.52	9.76	>10	>10
HAF3	Miricitrin	>10	>10	>10	>10	>10	>10	>10	>10	>10	>10
HAB1	Biapigenin	>10	>10	>10	>10	>10	>10	>10	>10	>10	>10
HAF2	Myricetin	>10	>10	>10	>10	>10	>10	5.71	7.97	>10	>10
HAF4	Hyperoside	>10	>10	>10	>10	>10	>10	>10	>10	>10	>10
HAF5	Myricetin-3-O-β-D-glucopyranoside	>10	>10	>10	>10	>10	>10	>10	>10	>10	>10
HAF6	Cannabicitrin	>10	>10	>10	>10	>10	>10	>10	>10	>10	>10
compounds isolated from <i>C. villosus</i>											
CVF2	Chrysin-7-O-β-D-glucopyranoside	>10	>10	>10	>10	>10	>10	>10	>10	>10	>10
CVF3	2''-O-α-L-rhamnosylorientin	>10	>10	>10	>10	>10	>10	>10	>10	>10	>10
CVK1	Spartein	>10	>10	>10	>10	>10	>10	7.67	>10	>10	>10
NT, not tested; IC-50 and IC-90 values are expressed as μM and are mean ±S.D. of duplicate observations. Tested concentrations range (0.4–10 ug/mL ).											



**Figure III. 5.** In vitro primary screening of *C. villosus* (C.V) and *H. afrum* (H.A) aerial parts fractions for antitrypanosomal activity against *Trypanosoma brucei brucei*.

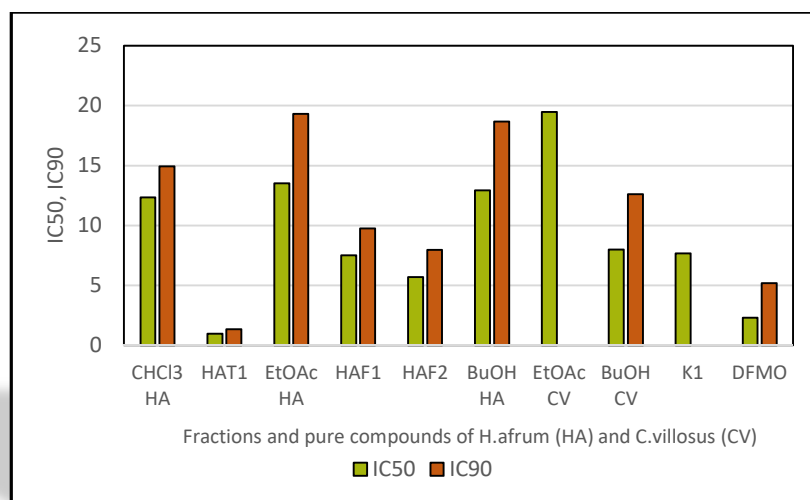


**Figure III. 6.** In vitro screen of compounds isolated from *C. villosus* and *H. afrum* aerial parts against *Trypanosoma brucei brucei*.

**Difluoromethylornithine**, the clinically used antitrypanosomal drug, was tested as a positive control.

IC<sub>50</sub> and IC<sub>90</sub> (μg/mL) values were computed with XLfit software.

#### - Conclusion

- The antiprotozoal activity of the fractions and certain pure isolated compounds of *C. villosus* and *H. afrum* were evaluated *in vitro* against *L. donovani* promastigotes, axenic amastigotes and intracellular amastigotes in THP1 cells.
- No one of the fractions or compounds tested showed antileishmanial activity.
- All fractions of ethanolic crud extracts of both plants and compounds tested were found to be

active against intracellular leishmania amastigotes in THP1 cells.

- The fractions and certain pure isolated compounds of plants under investigation were also evaluated against *T. brucei brucei* forms.
- All the samples were simultaneously tested against THP1 cell for determination of general cytotoxicity.
- Pentamidine was used as a positive control drug for antileishmanial assays.
- DMFO was used as a positive control drug for antitrypanosomal assay.
- Regarding antitrypanosomal activity, the chloroform, ethyl acetate and butanol fractions of *H. afrum* showed potent antitrypanosomal activity against *T. brucei .brucei* culture with IC<sub>50</sub> values of 12.35, 13.53, 12.93 and with IC<sub>90</sub> values of 14.94, 19.31, 18.67 µg/mL, respectively.
- The ethyl acetate fraction of *C. villosus* showed weakly antitrypanosomal activity against *T. brucei. brucei* culture with IC<sub>50</sub> values of 19.48 µg/mL.
- The butanol fraction of *C. villosus* showed highly potent antitrypanosomal activity against *T. brucei* with IC<sub>50</sub> values of 7.99 and IC<sub>90</sub> values of 12.61µg/mL.
- Compounds HAF1 (quercetin) and HAF2 (myricetin), isolated from *H. afrum* ethyl acetate fraction showed potent activity toward *T. brucei* with IC<sub>50</sub> values of 7.52 and 5.71 and with IC<sub>90</sub> values of 9.76 and 7.97µM, respectively.
- Compound HAT1 namely β-sitosterol isolated from *H. afrum* chloroform fraction showed high potent activity toward *T. brucei* with IC<sub>50</sub> values of 0.98 µM and with IC<sub>90</sub> values of 1.34 µM
- Compound CVK1 namely sparteine. isolated from *C. villosus* Alkaloid fraction showed potent activity toward *T. brucei* with IC<sub>50</sub> values of 7.67 µM.

### **III.5. Cytotoxic activity**

Fractions and certain isolated compounds of species under investigation were subjected to *in vitro* cytotoxicity screening against 6 human cancer cell lines; (SK-MEL, KB, BT-549, SKOV-3) and two non-cancerous kidney cell lines (LLC-PK11 and Vero) following the protocol described earlier in page (59). The results are shown in Table III.11.

**Table III. 9.** Cytotoxic activity of Fractions and certain pure compounds from *C. villosus* and *H. afrum*

Cytotoxicity activity (IC <sub>50</sub> µg/mL)							
Fractions							
Fraction	Plant	SK-MEL	KB	BT-549	SK-OV-3	LLC-PK1	Vero
EtAc	<i>C.villosus</i>	NA	NA	NA	NA	NC	NC
BuOH	<i>C.villosus</i>	NA	NA	NA	NA	NC	NC
EtAc	<i>H.afrum</i>	NA	NA	NA	NA	NC	NC
BuOH	<i>H.afrum</i>	NA	NA	NA	NA	NC	NC
Pure compounds							
Compound code	Compound name	SK-MEL	KB	BT-549	SK-OV-3	LLC-PK1	Vero
HAF1	quercetin	NA	NA	NA	NA	36	>50
HAF2	Myricitrin	NA	NA	NA	NA	NC	NC
HAF3	Biapigenin	30	33	38	48	NC	NC
HAF4	Hyperoside	NA	NA	NA	NA	NC	NC
HAF6	myricetin-3'-O-β-D-glucopyranoside	NA	NA	NA	NA	NC	NC
HAB1	Myricetin	NA	NA	NA	NA	NC	NC
CVF2	Chrysin-7-O-β-D-glucopyranoside	NA	NA	NA	NA	NC	NC
doxorubicin		0.8	1.3	0.9	2	1.2	NC
<i>a</i> IC <sub>50</sub> : the concentration that affords 50% inhibition of cell growth. <i>b</i> human cell lines of leukemia, <i>c</i> epidermal carcinoma, <i>d</i> breast carcinoma, <i>e</i> ovarian carcinoma, <i>f</i> skin melanoma, <i>g</i> cervical carcinoma, <i>h</i> pig kidney epithelial cells, <i>i</i> African green monkey kidney cell line. NA no activity, <i>j</i> no activity at 100 µg, NC: no cytotoxicity.							

**- Conclusion**

- All fractions tested were inactive against human solid tumor cells of epidermal(KB), breast (BT-459), skin melanoma (SK-MEL), SK-OV-3, and also inactive against noncancerous cell lines. LLC-PK1 (monkey kidney fibroblast; Vero).
- Compound HAF1, quercetin, was found to be weakly active against a noncancerous cell line LLC-PK1 (IC<sub>50</sub> values 36 µM).
- Compound HAB1, biapigenin, was found to be weakly active against the human cancer lines SK-MEL, KB, BT-549 and SK-OV-3 (IC<sub>50</sub> values of 30, 33, 38 and 48 µM, respectively).

### III.6. Transfection and luciferase assays

Modulation of the activity of cancer related signaling pathways was assessed using a battery of luciferase reporter gene vectors; where luciferase expression was driven by the binding of transcription factors to multiple copies of synthetic enhancers within each vector. The Luciferase activity was determined employing the protocol described previously in page (60).

The results are presented in the following table.

**Table III. 10.**Activity of New Compound **HAP1** (IC<sub>50</sub> values in  $\mu$ M) against Cancer-Related Signaling Pathways in HeLa Cells

SAMPLE DETAILS	Stat3 IL-6	Smad TGF-b	Ap-1 PMA	NF-kB PMA	E2F PMA	Myc PMA	Ets PMA	Notch (CSL-Luc) PMA	FoxO in 10% FBS	Wnt wnt 3a	Hdghog PMA	pTK (4h)	miR-21	k-Ras	AhR
HAP1 (30 $\mu$ M)	103	104	83	83	113	103	102	150	112	104	95	123	119	97	103
HAP1 (20 $\mu$ M)	120	92	90	89	113	91	105	147	128	138	95	120	110	82	102
HAP1 (10 $\mu$ M)	106	105	84	85	146	94	100	126	102	123	97	115	119	103	126
HAP1 (5 $\mu$ M)	114	98	90	84	123	116	108	136	112	93	98	124	132	99	119

<sup>a</sup>Values (from two independent experiments) are the IC<sub>50</sub> or lowest concentration (both in  $\mu$  mol/L) that maximally inhibited luciferase induction by 50–60%. A dash indicates that luciferase induction was not inhibited more than 40% at 100  $\mu$  M. Compounds (final concentrations of 40, 60, 80, or 100  $\mu$  M) were added to cells 30 min before the addition of the indicated inducer and were harvested for the luciferase assay 4 or 6 h (Notch, FoxO, Wnt, and Hedgehog) later. No inducer was added to cells transfected with FoxO vector or pTK control vector.

#### - Conclusion

- The new compound HAP1 did not show any activity since it did not inhibit any of the cancer-related signaling pathways.

### III.7. Antioxidant activity

Plants are potential sources of natural antioxidants. These natural protective effects have been attributed to various components such as carotenoids, vitamins C and E, and phenolic and thiol (SH) compounds.

The antioxidant capacity can be tested using a wide variety of methods (Chandra et al., 2014).

In the present study, the antioxidant activity of the fractions and isolated pure compounds of plants under investigation was evaluated in terms of their free radical scavenging capacity by DPPH assay. Their activity against intracellular oxidative stress was determined by CAA assay. These assays have

frequently been used by researchers to assess antioxidant capacity of different food products (Ak and Gülçin, 2008; Alam et al., 2013; Thaipong et al., 2006).

The cellular Antioxidant Activity Assay (CAA Assay) is a more biologically relevant method than a chemical assay because it represents the complexity of biological system and accounts for cellular uptake, bioavailability, and metabolism of the antioxidant agent (Chandra et al., 2014).

### **III.7.1. 2,2-Diphenyl-1-picrylhydrazyl (DPPH) Assay**

The capacity of *C. villosus* and *H. afrum* fractions to directly react with free radicals was evaluated as described earlier in pages (60-62).

The chloroform and EtOAc fractions of *C. villosus* showed modest radical scavenging activities toward DPPH (AAE values of 0,093 and 0,100 mg/mL respectively), while the *n*-butanol fraction showed higher antioxidant activity against DPPH (AAE=0,268).

The fractions CHCl<sub>3</sub>, EtOAc and *n*-BuOH of the ethanolic crud extract of *H. afrum*, showed good antiradical activities on DPPH radical, their (AAE) values ranged between 0,472 and 0,891.

The maximum antioxidant activity was observed in the fractions of *H. afrum* with IC<sub>50</sub> values range between 0,049 mg/mL and 0,090 mg/mL.

According to the IC<sub>50</sub>, ARP and AAE values, the extracts of the plants present an interesting antioxidant activity. The reducing power increased with the increasing of the extracts concentrations (Figures III.7 and 8). The importance of this activity for the extracts should be attributed by the richness in molecules with high antioxidant potentials. The total phenolic and flavonoid contents show correlation with the results of scavenging activity (IC<sub>50</sub>). These results and its comparison are demonstrated in Figure III.9.

The antioxidant activity of the studied fractions, expressed in (IC<sub>50</sub>), antiradical power (ARP) and in ascorbic acid equivalents (AAE) (mg AAE/g of extract) are shown in table III.13. The IC<sub>50</sub> values of Ascorbic acid was also calculated and reported for comparison.



**Table III. 11.** Antioxidant properties of fractions from *C. villosus* and *H. afrum* as determined by 2,2 diphenyl 1-picrylhydrazyl (DPPH) radical scavenging  
 Values expressed are means  $\pm$ SD of three parallel measurements

Fractions	Plant	Code	IC <sub>50</sub> (mg/mL )	ARP= 1/IC <sub>50</sub>	mg AAE/g extract=ARP extract/ARP Ascorbic acid
Chloroform	<i>C.villosus</i>	CHCV	0,459 $\pm$ 0,002	2,180 $\pm$ 0,01	0,093 $\pm$ 0,004
Ethyl acetate	<i>C.villosus</i>	EACV	0,425 $\pm$ 0,003	2,355 $\pm$ 0,018	0,100 $\pm$ 0,001
Butanolic	<i>C.villosus</i>	BUCV	0,164 $\pm$ 0,004	6,113 $\pm$ 0,157	0,268 $\pm$ 0,007
Chloroformic	<i>H.afrum</i>	CHHA	0,069 $\pm$ 0,004	14,456 $\pm$ 0,856	0,617 $\pm$ 0,037
Ethyl acetate	<i>H.afrum</i>	EAHA	0,049 $\pm$ 0,009	20,893 $\pm$ 4,112	0,891 $\pm$ 0,175
Butanolic	<i>H.afrum</i>	BUHA	0,090 $\pm$ 0,003	11,075 $\pm$ 0,363	0,472 $\pm$ 0,015
Acid ascorbic			0,043 $\pm$ 0,006	23,761 $\pm$ 3,257	

IC<sub>50</sub>: (mg/mL); ARP (Anti Radical Power) = 1/IC<sub>50</sub> ; Ascorbic Acid Equivalent (Antioxidant Capacity) = ARP extract/ARP Ascorbic acid

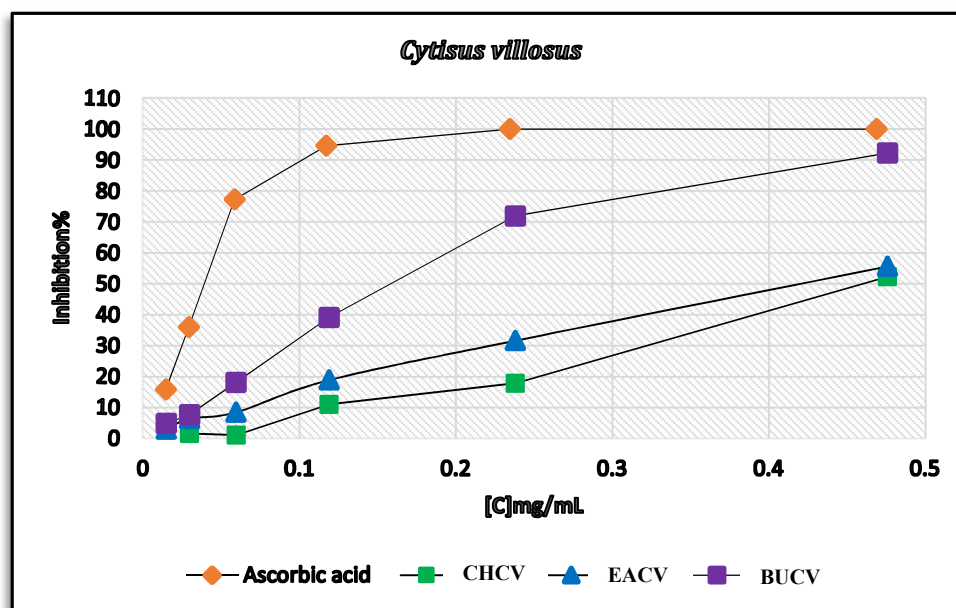


**Figure III. 7.** Radical scavenging effect of *Cytisus villosus* fractions on DPPH radical.  
 Each value is represented as mean  $\pm$ SD.

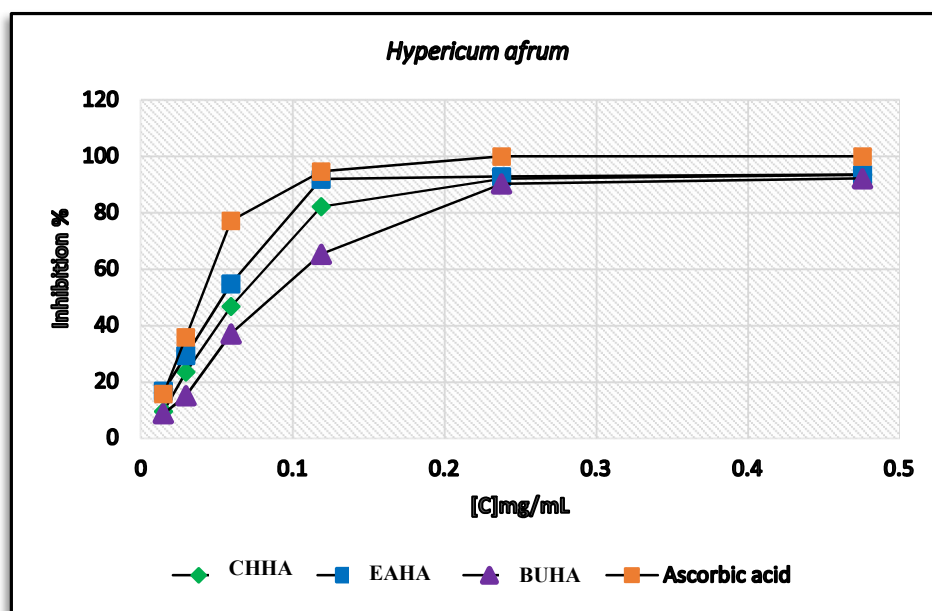


**Figure III. 8.** Radical scavenging effect of *Hypericum afrum* fractions on DPPH radical.

Each value is represented as mean  $\pm$  SD.

- **The relationship between total phenolic and flavonoid contents and radical scavenging**

Phenolics and flavonoids, in general, constitute a major group of compounds, which act as primary antioxidants (Balasundram et al., 2006; Robards et al., 1999), and are known to react with hydroxyl radicals (Husain et al., 1987) and superoxide anion radicals (Yasuhisa et al., 1993). They are also known to protect DNA from oxidative damage, inhibit growth of tumor cells and possess anti-inflammatory and antimicrobial properties. Similarly, a significant positive correlation between the antioxidant activity and the contents of total flavonoids and total phenolic have been reported (Wojdyło et al., 2007; Zheng and Wang, 2001).

Total phenolic and flavonoid contents were evaluated following the protocol demonstrated in pages (60-62).

Following DPPH assay, regression analysis shows that phenolic compounds contribute to about 74% ( $r^2 = 0.744$ ,  $P < 0.05$ ) of radical scavenging properties in the two plants fractions (Figure III.10). Similarly, flavonoid compounds contribute to about 74% ( $r^2 = 0.736$ ,  $P < 0.05$ ) of antioxidant activity in the two plants fractions (Figure III.11).

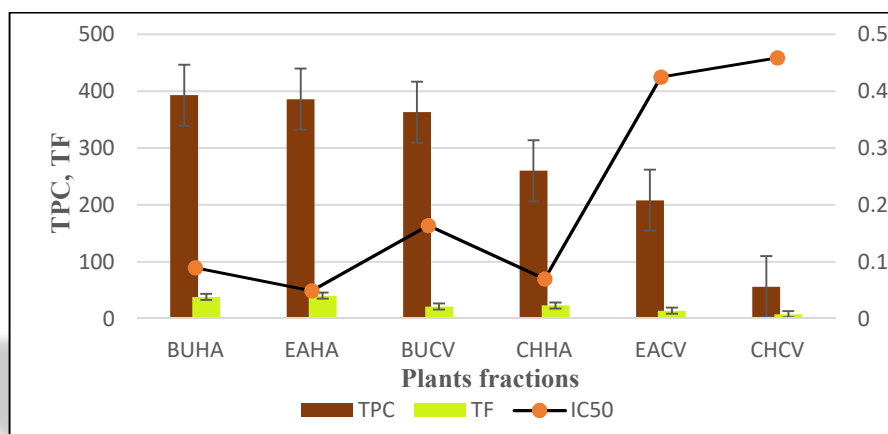


Figure III. 9. Comparison between total phenolic and flavonoid contents (TPC, TF) and DPPH (IC<sub>50</sub>) data in different fractions of plants under investigation.

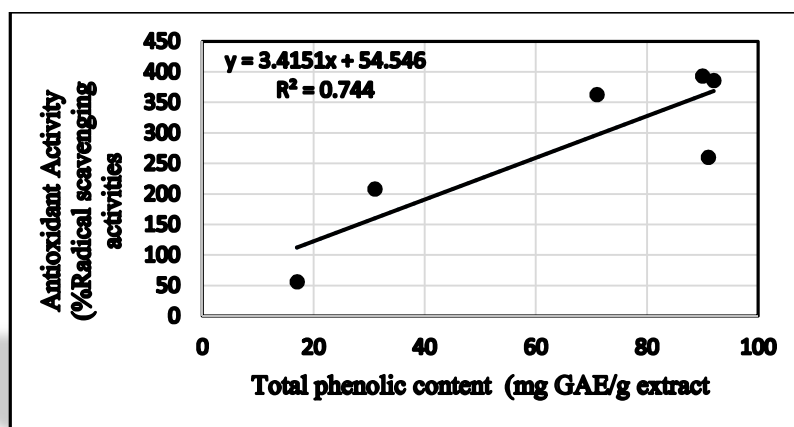


Figure III. 10. Relationship between total phenolic content and antioxidant activity of *C. villosus* and *H. afrum*. fractions by DPPH assay.

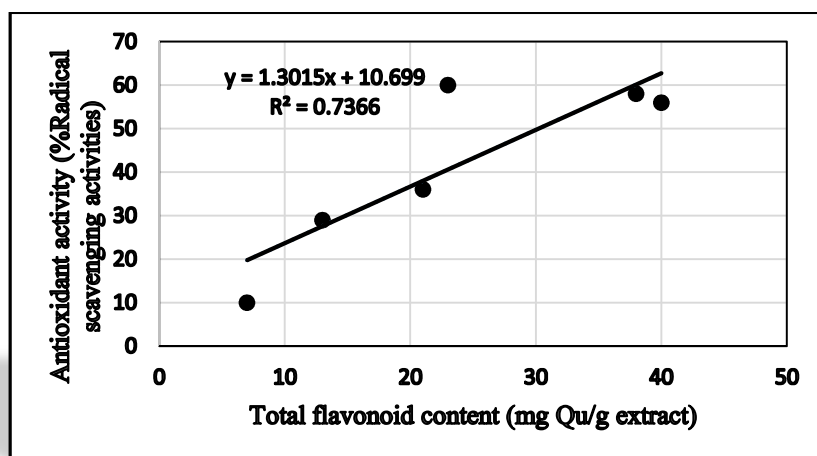


Figure III. 11. Relationship between total flavonoid content and antioxidant activity of *C. villosus* and *H. afrum* fractions by cellular antioxidant assay.

### **III.7.2. Assay for the Inhibition of Cellular Oxidative Stress and anti-inflammatory activity**

Oxidative stress is an imbalance between cellular production of reactive oxygen species and the counteracting antioxidant mechanisms. It may initiate and promote the progression of a number of mental disorders, including depression, anxiety disorders, schizophrenia and bipolar disorder (Salim, 2014). According to the World Health Organization (WHO), the year 2020, depressive disorder will be the illness with the highest burden of disease (Maria Michel et al., 2012). Inflammation is considered as a risk factor for several types of cancer, as well as a contributing factor in obesity and metabolic disorders. The activation of NF- $\kappa$ B in response to pro-inflammatory signals is associated with many diseases caused by unregulated inflammation. Since NF- $\kappa$ B is highly activated at the sites of inflammation in diverse diseases, the compounds that can suppress NF- $\kappa$ B activation have potential as anti-inflammatory agents. Excessive generation of nitric oxide (NO) and reactive oxygen species (ROS) also contributes significantly to the progress of inflammation and subsequent development of metabolic syndrome, characterized by obesity, diabetes, and cardiovascular disease. Inhibition of inducible nitric oxide synthase (iNOS) can reduce the intracellular NO production. NF- $\kappa$ B, iNOS, and ROS have been considered as important targets for inflammation. Although peroxisome proliferator-activated receptors (PPAR $\alpha$  and PPAR $\gamma$ ) and liver X receptor (LXR) play important roles in carbohydrate and lipid metabolism and have been considered as significant targets in treating metabolic diseases, they have also been linked with the inflammatory process by regulating the production of inflammatory cytokines. A growing body of evidence has suggested that the activation of PPARs results in suppressing the inflammatory process. In the present study, the anti-inflammatory activity of the fractions and constituents isolated from plants under investigation was evaluated in terms of their effects against oxidative stress and their interaction with cellular targets related to inflammation and metabolic disorders such as NAG-1, NF- $\kappa$ B, iNOS, ROS, PPAR $\alpha$ , PPAR $\gamma$ , and LXR, through the use of a battery of cellular assays (Zhao et al., 2014).

The antioxidant and anti-inflammatory activities were evaluated following the protocol described in pages (62-63).

The results are shown in tables III.14, -15 and -16.

**Table III. 12.** Potential antioxidant activity of fractions and certain isolated pure compounds

		% decrease in Oxidative stress			
		Plant	Concentration		
Fraction			1000 µg/mL	500 µg/mL	250 µg/mL
EtOAc	<i>H. afrum</i>		75	66	58
BuOH	<i>H. afrum</i>		63	60	60
EtOAc	<i>C. villosus</i>		47	37	29
BuOH	<i>C. villosus</i>		49	39	36
Pure compounds of <i>Hypericum afrum</i>					
Compound code	Compound name		1000 µg/mL	500 µg/mL	250 µg/mL
HAF1	quercetin		93	86	83
HAF2	Myricetin		78	71	65
HAF3	Myricitrin		65	59	53
HAF4	Hyperoside		74	67	64
HAF5	myricetin-3-O-β-D-glucopyranoside		56	50	42
HAF6	myricetin-3'-O-β-D-glucopyranoside		71	64	58
HAB1	Biapigenin		NA	NA	NA
Pure compounds <i>Cytisus villosus</i>					
CVS2	Genistein		NA	NA	NA
CVF1	Chrysin		NA	NA	NA
CVF2	Chrysin-7-O-β-D-glucopyranoside		NA	NA	NA
CVF3	2''-O-α-L-rhamnosylorientin		36	29	28
Positive control	Quercetin 25 µM		77		

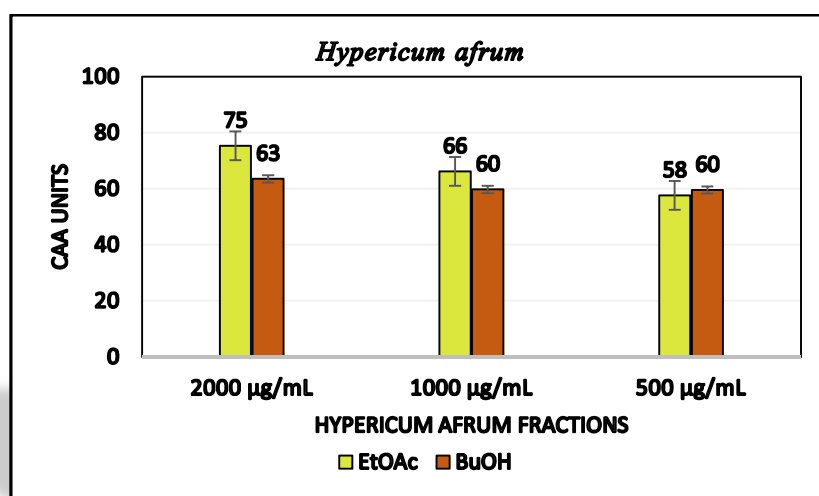


**Figure III. 12.** Antioxidant activity of *Hypericum afrum* fractions at different concentrations by cellular antioxidant assay(CAA); data represent mean ± SD; n=3 level of significance: \*P < 0.05.

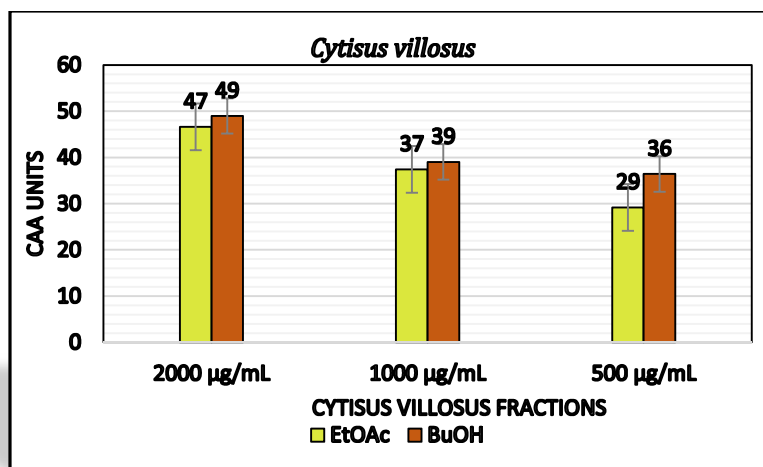


**Figure III. 13.** Antioxidant activity of *Cytisus villosus* fractions at different by cellular antioxidant assay(CAA).

data represent mean ± SD,  $n = 3$ ; level of significance:  $*P < 0.05$ .

- **Assay for the Inhibition of iNOS Activity**

**Table III. 13.** Potential Anti-inflammatory Activity of fractions and certain pure compounds

Sample	IC <sub>50</sub> (µg/mL)
<b>Fractions</b>	
EtOAc ( <i>H. afrum</i> )	>100
BuOH ( <i>H. afrum</i> )	NA
EtOAc ( <i>C. villosus</i> )	48
BuOH ( <i>C. villosus</i> )	90
<b>Pure compounds IC<sub>50</sub> (µg/mL)</b>	
HAF1	12
HAF2	>50
HAF3	NA
HAF4	NA
HAF5	NA
HAF6	NA
HAB1	22
CVS2	9
CVF1	>25
CVF2	20
CVF3	NA
Parthenolide (Positive control)	0.2
NA = no activity at 25 or 100 µg/mL for pure compounds and extract	

• **Reporter Gene Assay for the Inhibition of NF-κB Activity**

**Table III. 14.** Potential Anti-inflammatory Activity of fractions and certain pure compounds

Sample	IC <sub>50</sub> µg/ml NF-κB	IC <sub>50</sub> SP-1
CVS2	28	NA
CVF1	38	NA
CVF3	NA	NA
HAF4	NA	NA
HAF5	NA	NA
Parthenolide (Positive control)	1.63	
NA no activity at 50 or 200 µg/mL		

- **Conclusion**

- Our results showed that the antioxidant activities of the chloroform and ethyl acetate fractions of *H. afrum* in term of radical scavenging activity, using DPPH assay, were higher comparable to those of the *n*-butanol fraction of the same plant.
- The chloroform, ethyl acetate and butanol fractions of *C. villosus* showed all moderate antioxidant activities in term of radical scavenging activity, using DPPH assay.
- All tested fractions of *H. afrum* were shown to decrease cellular oxidative stress by inhibiting ROS generation (Table III.14).
- Compounds HAF1, HAF2 from ethyl acetate fraction of *H. afrum* showed potent effect against oxidative stress (inhibition values of 83 and 65%, respectively)
- Compounds HAF3, HAF4 and HAF6 from the *n*-butanol fraction showed considerable effect against oxidative stress (inhibition values of 53, 64 and 58 %, respectively), however, these compounds were lower potent than HAF1 and HAF2 as shown in Table III.14.
- *C. villosus* tested fractions showed weak effect against oxidative stress (inhibition values ranged between 29 and 36%).
- Compounds CVF1, CVF2 and CVS2 from *C. villosus* tested for their effect against oxidative stress were not effective. While compound CVF3 showed weak antioxidant activity (inhibition values of 36% at 1000 µg/mL).

- Regarding the results of the evaluation of anti-inflammatory activity, *H. afrum* fractions did not show any inhibition of iNOS and therefore did not affect cellular nitric oxide levels in lipopolysaccharide (LPS)-treated macrophages.
- Compounds HAF1 and HAB1 isolated from *H. afrum* ethyl acetate fraction showed moderate inhibition of iNOS (with IC<sub>50</sub> values of 12 and 22 µg/mL, respectively).
- The ethyl acetate and *n*-butanol fractions of *C. villosus* showed moderate inhibition of iNOS (IC<sub>50</sub> values of 48 and 90 µg/mL, respectively).
- Compounds CVF2 and CVS2 isolated from *C. villosus* ethyl acetate fraction showed mild inhibition of iNOS with IC<sub>50</sub> values of 20 and 9 µg/mL, respectively.
- The increase in transcriptional activity of NF-κB in PMA-treated cells was also not suppressed by the plant's fractions and isolated compounds (with the exception of compounds CVS2 and CVF1, which showed moderate inhibition of NF-κB with IC<sub>50</sub> values of 28 and 38 µg/mL, respectively).

### **III.8. Monoamine oxidase inhibition (MAOI) assay**

Monoamine oxidases (MAOs) are outer mitochondrial membrane. Their role is to catalyze the oxidative deamination of a variety of neurotransmitters. Inside the human brain, there are two isoforms of MAO, named MAO-A and MAO-B based by their sensitivity to selective inhibitors and specific substrates. MAO-A preferentially deaminates serotonin and norepinephrine, whereas MAO-B deaminates phenylethylamine and benzylamine. The two enzymes are selectively inhibited by clorgyline for the MAO-A, and by L-deprenil for MAO-B. MAO-A and MAO-B have been considered as targets in the research of inhibitors could be used clinically as antidepressants and anxiolytics, for the treatment neurodegenerative diseases and depression and in the management of symptoms associated with Parkinson's and Alzheimer's diseases. In particular, MAOs appear to form the first line of defense against monoamines absorbed from foods, such as tyramine and 3-phenylethanolamine, which would otherwise produce an indirect sympathomimetic response resulting in the precipitous rise in blood pressure known as the "cheese effect" (Pickar et al., 1981). The prevention of tyramine metabolism in the small intestine, liver and endothelium by irreversible monoamine oxidase A and B (MAOA/B) or MAOA inhibitors can lead to its presence in the circulation (Carradori et al., 2014). The uptake of tyramine by adrenergic neurons in the ventrolateral medulla, in which MAOA is also inhibited, initiates the release of noradrenaline, a substrate for inhibited MAOA, into the synaptic cleft, with consequent



stimulation of cardiovascular sympathetic nervous system activity This activity led to hypertensive crises, and, in some cases, death, resulting in the withdrawal of many MAO inhibitors from clinical use(Henry and Martin, 1987; Mann et al., 1989; Yamada and Yasuhara, 2004). Following reuptake of noradrenaline into the presynaptic terminal, this neurotransmitter can be degraded in the absence of MAOA activity, via an alternative pathway involving Catechol-*O*-methyl transferase (COMT). Because MAOB is not present in adrenergic neurons, the cheese reaction is not seen with irreversible MAOB inhibitors, except at higher doses, which cause the selectivity of these inhibitors to be lost. The use of reversible MAOA inhibitors avoids this problem, as dietary tyramine is able to displace the inhibitor from peripheral MAOA, allowing its metabolism.

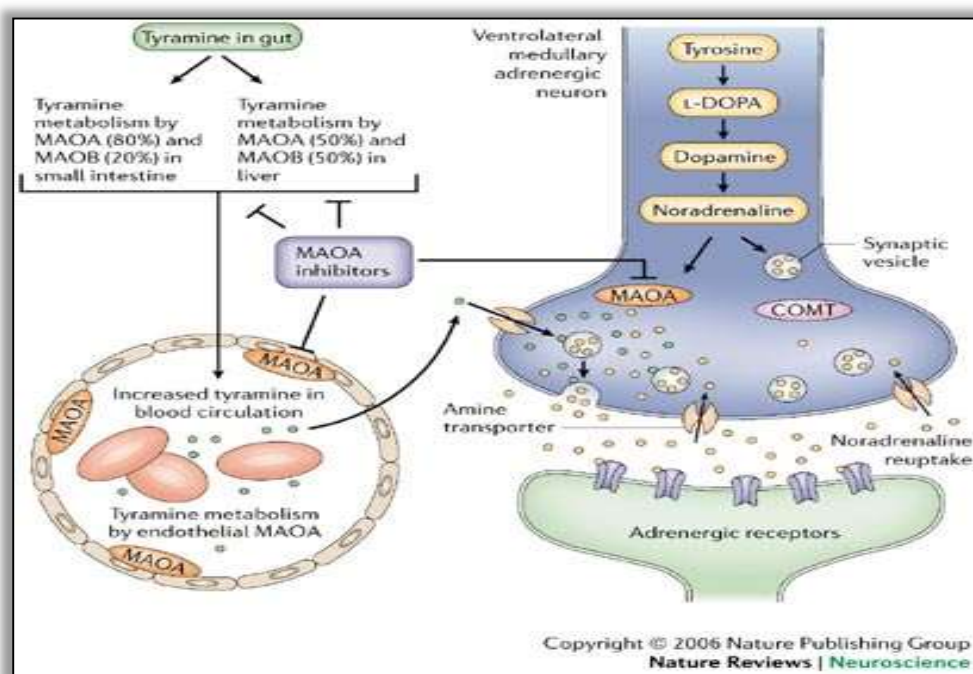


**Figure III. 14.** The mechanism of potentiation of cardiovascular effects of tyramine: the 'cheese reaction' (Youdim et al., 2006).

Identification of MAO inhibitors is of great interest in drug discovery (Kalgutkar et al., 1994). Recent efforts toward the development of MAO inhibitors are focused on selective MAO-A or MAO-B inhibitors. Selective MAO-A inhibitors are effective in the treatment of depression (Youdim and Bakhle, 2006; Youdim et al., 2006), whereas MAO-B inhibitors are useful for the treatment of depression, Alzheimer's disease and Parkinson's disease (Rabey et al., 2000; Thomas, 2000). Evaluation of natural products resources, botanicals and other dietary supplements for

MAO inhibitory constituents is of great interests, due to possible use of dietary supplements in improving neurological disorders as well as their possible interactions with drugs and the food rich in dietary-monoamines (Chaurasiya et al., 2014; Fugh-Berman and Cott, 1999). Herbal natural products have been suggested as important source for inhibitors of MAOs and also support traditional use of these herbal products as alternative for treatment of depression, Parkinson's disease and other neuropsychiatric as well as neurological disorders (Fugh-Berman and Cott, 1999).

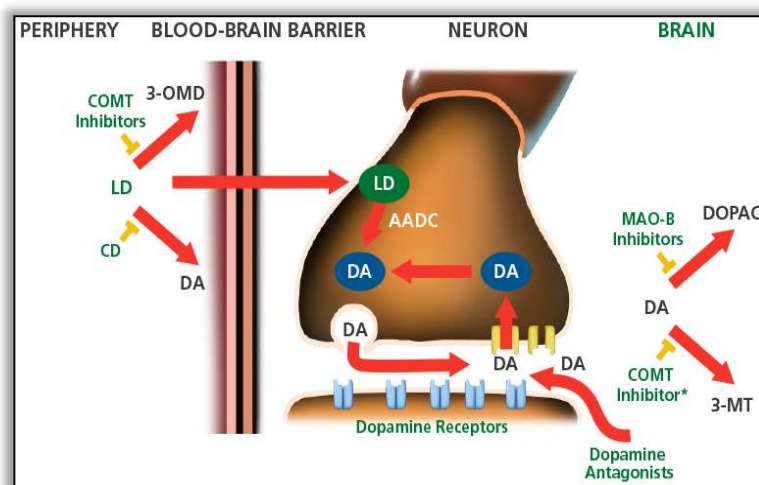


**Figure III. 15.** Sites of action of Parkinson's Disease Drugs role of Monoamine Oxidase in Dopamine Metabolism (Youdim et al., 2006).

The ethyl acetate (EtOAc) and butanol (*n*-but) fractions, subfractions and isolated pure compounds of *C. villosus* and *H. afrum*, in addition of fractions of the alkaloid extract of *C. villosus* were submitted for *in vitro* MAO inhibition using recombinant human monoamine oxidase (MAO-A and MAO-B) following the protocol described in pages (64-65) The results are shown in Table III.17.

**- Inhibition of MAO by *Cytisus villosus***

The EtOAc fraction demonstrated potent MAO-A and B inhibitory activities. The inhibition of MAO-A by EtOAc fraction was 3-fold more potent ( $IC_{50}$  1.875.  $\mu$ M) compared to the inhibition of MAO-B ( $IC_{50}$  value of 5.625  $\mu$ M). While the *n*-but fraction of the same plant showed moderate MAO-A and B inhibitory activities (Table III.17).

Among all alkaloid extract fractions, the fractions KORG1 and KORG3 were the most active with  $IC_{50}$  values of 1.55, 11.36 and 0.59, 1.76  $\mu\text{g}/\text{mL}$  for MAO-A and -B, respectively (Table III.17). Subfractions CEF-1, CEF-2 showed potent selective inhibition of MAO-B, while CEF-3 showed selective potent inhibition of MAO-A. Subfraction CEF-7 showed potent MAO-B inhibition indicating a high selectivity of MAO-B over MAO-A ( $IC_{50}$  values of 5.52  $\mu\text{g}/\text{mL}$  for MAO-B and  $IC_{50} > 100$  for MAO-A). Bioassay Guided fractionation of the EtOAc fraction resulted in the isolation and identification of two components indicated to be the major MAO inhibitors. Pure genistein (CVS2) and chrysin (CVF1) proved to be potent MAOIs. Genistein was shown to be more potent towards MAO-B than MAO-A with  $IC_{50}$  value of 0,65  $\mu\text{M}$  against MAO-B and  $IC_{50}$  value of 2,74  $\mu\text{M}$  for MAO-A, while chrysin was found to produce more pronounced inhibition of MAO-A than MAO-B with  $IC_{50}$  value of 0,25  $\mu\text{M}$  towards MAO-A and  $IC_{50}$  value of 1,04  $\mu\text{M}$  for MAO-B.

- **Inhibition of MAO by *Hypericum afrum***

The ethyl acetate soluble fraction of *H. afrum* demonstrated selective MAO inhibition activity towards MAO-A with  $IC_{50}$  value of 3.375  $\mu\text{g}/\text{mL}$  for MAO-A and  $IC_{50}$  value of 13.50  $\mu\text{g}/\text{mL}$  for MAO-B. The inhibition of MAO-A by the ethyl acetate fraction was about 4-fold more potent than MAO-B.

The *n*-butanol fraction showed lower selective inhibitory activity towards MAO-A comparing to the ethyl acetate fraction, the  $IC_{50}$  values of the *n*-but fraction were 16.50  $\mu\text{g}/\text{mL}$  for MAO-A and 22.50  $\mu\text{g}/\text{mL}$  for MAO-B.

Subfraction HEF-1 showed selective potent inhibition of MAO-B while subfraction HEF-3 showed selective potent inhibition of MAO-A. The pure compounds obtained from the bio-guided fractionation were further tested to determine the activity inhibition towards MAO-A and MAO-B. Quercetin (HAF1) and myricetin (HAF2) identified in the AcOEt fraction as the only compounds with MAO inhibitory activities. Quercetin showed a selective inhibitory activity with 18-fold selectivity towards MAO-A as compared with the value obtained for MAO-B. The values of  $IC_{50}$  were 1.52  $\mu\text{M}$  for MAO-A and  $IC_{50}$  value of 28.3  $\mu\text{M}$  against MAO-B, in addition, myricetin showed a selective inhibitory activity with 6-fold selectivity towards MAO-A, the  $IC_{50}$  values were 9.93  $\mu\text{M}$  for MAO-A and 59.34  $\mu\text{M}$  for MAO-B.

From the ethyl acetate fraction, the additional flavonoid glycoside namely myricitrin (HAF3) showed low selective activity towards MAO-B with  $IC_{50}$  value of 41.24  $\mu\text{M}$  for MAO-B and  $IC_{50}$

value of 96.77 $\mu$ M for MAO-A. The biflavone namely biapigenin (HAB1) showed moderate inhibitory activity towards MAOs. The flavonoids identified in the *n*-but fraction namely hyperoside (HAF4), myricetin-3-*O*- $\beta$ -D-galactopyranoside (HAF5) and myricetin-3'-*O*- $\beta$ -D-glucopyranoside (HAF6) all showed weak activities towards MAO isoforms (Table III.18).

**Table III. 15.** Inhibition of recombinant human Monoamine Amine Oxidase-A and B by *H. afrum* and *C. villosus* fractions and pure constituents

Genus/ species	Sample code	Sample Type	Unit	MAO-A IC50	SD	MAO-B IC50	SD
<i>Hypericum afrum</i> fractions							
<i>H.afrum</i>	BuOH	Fraction	$\mu$ g/ml	16.5	0.707	22.5	2.1213
<i>H.afrum</i>	EtOAc	Fraction	$\mu$ g/ml	3.375	0.035	13.5	0.7071
<i>H.afrum</i>	HEF-1	Subfraction	$\mu$ g/ml	16.56	0.85	<b>1.93</b>	0.21
<i>H.afrum</i>	HEF-3	Subfraction	$\mu$ g/ml	2.17	0.01	<b>4.12</b>	0.59
<i>H.afrum</i>	HEF-4	Subfraction	$\mu$ g/ml	<b>5.11</b>	0.38	9.05	1.92
<i>H. afrum</i>	HEF-5	Subfraction	$\mu$ g/ml	9.49	0.15	18.41	0.33
<i>Cystisus villosus</i> : fractions of the hydroalcoholic extraction							
<i>C.villosus</i>	BuOH	Fraction	$\mu$ g/ml	36	1.414	26	1.4142
<i>C. villosus</i>	EtOAc	Fraction	$\mu$ g/ml	5.625	0.106	1.875	0.0354
<i>C. villosus</i>	CEF-1	Subfraction	$\mu$ g/ml	0.800	0.055	<b>0.154</b>	0.014
<i>C. villosus</i>	CEF-2	Subfraction	$\mu$ g/ml	2.471	0.261	1.188	0.027
<i>C. villosus</i>	CEF-3	Subfraction	$\mu$ g/ml	7.223	1.438	11.535	1.955
<i>C. villosus</i>	CEF-7	Subfraction	$\mu$ g/ml	>100	-	<b>5.527</b>	0.566
<i>Cystisus villosus</i> : fractions of the alkaloids extraction							
<i>C. villosus</i>	KORG1	Fraction	$\mu$ g/ml	<b>1.55</b>	0.189	<b>0.59</b>	0.177
<i>C. villosus</i>	KORG3	Fraction	$\mu$ g/ml	11.36	0.899	<b>1.76</b>	0.261
<i>C. villosus</i>	KORG2	Fraction	$\mu$ g/ml	>100	NA	37.66	11.145
<i>C. villosus</i>	CKF-1	subFraction	$\mu$ g/ml	>100	NA	75.04	13.612
<i>C. villosus</i>	CKF-2	subFraction	$\mu$ g/ml	>100	NA	39.52	5.562
<i>C. villosus</i>	CKF-3	subFraction	$\mu$ g/ml	>100	NA	>100	NA
<i>C. villosus</i>	CKF-4	subFraction	$\mu$ g/ml	>100	NA	45.55	0.067
<i>C. villosus</i>	CKF-5	subFraction	$\mu$ g/ml	>100	NA	87.66	10.136
Phenelzine <sup>a</sup>	-	-	$\mu$ M	0.213	0.06	0.15	0.015
Clorgyline <sup>b</sup>	-	-	$\mu$ M	0.004	0.0005	-	-
Deprenyl <sup>c</sup>	-	-	$\mu$ M	-	-	0.049.	0.0036
<sup>a</sup> Positive control for both MAO enzyme; <sup>b</sup> Positive control selective for MAO-A; <sup>c</sup> selective for MAO-B							

**Table III. 16.** Inhibition of recombinant human Monoamine Amine Oxidase-A and B by *H. afrum* and *C. villosus* pure constituents

Compound name	Compound code	Unit	MAO-A IC50	SD	MAO-B IC50	SD
Pure compounds isolated from <i>H. afrum</i>						
<i>3-Benzoyl-3-hydroxy-5-(3-methylbut-2-en-1-yl)cyclopentane-1,2,4-trione</i>	HAP1	μM	>100	-	71.12	4.23
Quercetin	HAF1	μM	1.52	0.09	28.39	5.41
Myricetin	HAF2	μM	9.93	0.63	59.34	1.78
Myricitrin	HAF3	μM	96.77	1.98	41.24	1.98
Hyperoside	HAF4	μM	45.31	1.8	58.96	2.76
Myricetin 3-glucoside	HAF5	μM	61.6	1.61	35.66	7.17
Myricetin 3'-glucoside	HAF6	μM	36.32	1.16	36.12	3.01
Biapigenin	HAB1	μM	15.53	2.96	17.77	0.24
Hypericin	HAN1	μM	>100	NA	35.21	13.044
Pure compounds isolated from <i>C. villosus</i>						
chrysin	CVF1	μM	0.25	0.04	1.04	0.17
Chrysin 7-O-β-D-glucoside	CVF2	μM	>100	NA	>100	NA
2"-O-α-L-rhamnosylorientin,	CVF3	μM	>100	NA	>100	0.79
Genistein	CVS1	μM	2.74	0.01	0.65	0.11
Sparteine	CVK1	μM	>100	NA	>100	NA
Phenelzine <sup>a</sup>	-	μM	0.213	0.06	0.15	0.015
Clorgyline <sup>b</sup>	-	μM	0.004	0.0005	-	-
Deprenyl <sup>c</sup>	-	μM		-	0.049.	0.0036
<sup>a</sup> Positive control for both MAO enzyme; <sup>b</sup> Positive control selective for MAO-A; <sup>c</sup> selective for MAO-B						

**- Conclusion**

- The ethyl acetate fractions (EtOAc) of the two plants showed potent MAO-A and B inhibitory activities with IC<sub>50</sub> values of 3.375 μg/ml and 5.625 μg/ml for MAO-A and IC<sub>50</sub> values of 13.50 μg/mL and 1.875 μg/mL for MAO-B, respectively.
- The inhibition of MAO-A by EtOAc fraction of *H. afrum* was 4-fold more potent (IC<sub>50</sub>: 3.375 μg/ml) as compared to the inhibition of MAO-B (IC<sub>50</sub> value of 13.50 μg/ml), while the inhibition of MAO-B (IC<sub>50</sub> 1.875 μM) by EtOAc fraction of *C. villosus* was 3-fold more potent as compared to the inhibition of MAO-A (IC<sub>50</sub> value of 5.625 μM).

- Bioassay-guided fractionation resulted in the isolation and identification of quercetin (**HAF1**), myricetin (**HAF2**), genistein (**CVS2**) and chrysin (**CVF1**) as the active constituents.
- The results of our study revealed that both studied plants have properties indicative of potential neuroprotective ability. They may serve as new candidates for selective MAO-A and B inhibitors. The MAO-inhibiting activity of *H. afrum* and *C. villosus* fractions was primarily due to the presence of flavonoids such as quercetin, myricetin, genistein and chrysin.
- The above observations inspired us to use docking simulation to investigate the binding modes of quercetin, myricetin, chrysin and genistein in the structurally similar ligand binding pockets of MAO-A and MAO-B (**PART IV**).

## REFERENCES

- Ak, T., Gülçin, İ., 2008. Antioxidant and radical scavenging properties of curcumin. *Chemico-biological interactions* 174, 27-37.
- Alam, M.N., Bristi, N.J., Rafiquzzaman, M., 2013. Review on in vivo and in vitro methods evaluation of antioxidant activity. *Saudi Pharmaceutical Journal* 21, 143-152.
- Alvar, J., Vélez, I.D., Bern, C., Herrero, M., Desjeux, P., Cano, J., Jannin, J., den Boer, M., Team, W.L.C., 2012. Leishmaniasis worldwide and global estimates of its incidence. *PloS one* 7, e35671.
- Balasundram, N., Sundram, K., Samman, S., 2006. Phenolic compounds in plants and agri-industrial by-products: Antioxidant activity, occurrence, and potential uses. *Food chemistry* 99, 191-203.
- Carradori, S., D'Ascenzio, M., Chimenti, P., Secci, D., Bolasco, A., 2014. Selective MAO-B inhibitors: a lesson from natural products. *Molecular diversity* 18, 219-243.
- Chandra, S., Khan, S., Avula, B., Lata, H., Yang, M.H., ElSohly, M.A., Khan, I.A., 2014. Assessment of total phenolic and flavonoid content, antioxidant properties, and yield of aeroponically and conventionally grown leafy vegetables and fruit crops: A comparative study. *Evidence-Based Complementary and Alternative Medicine* 2014.
- Chaurasiya, N.D., Ibrahim, M.A., Muhammad, I., Walker, L.A., Tekwani, B.L., 2014. Monoamine oxidase inhibitory constituents of propolis: kinetics and mechanism of inhibition of recombinant human MAO-A and MAO-B. *Molecules* 19, 18936-18952.
- Felder, C.C., Joyce, K.E., Briley, E.M., Mansouri, J., Mackie, K., Blond, O., Lai, Y., Ma, A.L., Mitchell, R.L., 1995. Comparison of the pharmacology and signal transduction of the human cannabinoid CB1 and CB2 receptors. *Molecular pharmacology* 48, 443-450.
- Franco, J.R., Simarro, P.P., Diarra, A., Jannin, J.G., 2014. Epidemiology of human African trypanosomiasis. *Clinical epidemiology* 6, 257.
- Fugh-Berman, A., Cott, J.M., 1999. Dietary supplements and natural products as psychotherapeutic agents. *Psychosomatic Medicine* 61, 712-728.
- Henry, J., Martin, A., 1987. The risk-benefit assessment of antidepressant drugs. *Medical toxicology and adverse drug experience* 2, 445-462.
- Husain, S.R., Cillard, J., Cillard, P., 1987. Hydroxyl radical scavenging activity of flavonoids. *Phytochemistry* 26, 2489-2491.
- Kalgutkar, A.S., Castagnoli, K., Hall, A., Castagnoli Jr, N., 1994. Novel 4-(aryloxy) tetrahydropyridine analogs of MPTP as monoamine oxidase A and B substrates. *Journal of medicinal chemistry* 37, 944-949.
- Mann, J.J., Aarons, S.F., Wilner, P.J., Keilp, J.G., Sweeney, J.A., Pearlstein, T., Frances, A.J., Kocsis, J.H., Brown, R.P., 1989. A controlled study of the antidepressant efficacy and side effects of (—)-deprenyl: a selective monoamine oxidase inhibitor. *Archives of general psychiatry* 46, 45-50.
- Maria Michel, T., Pulschen, D., Thome, J., 2012. The role of oxidative stress in depressive disorders. *Current pharmaceutical design* 18, 5890-5899.
- Njokah, M.J., Kang'ethe, J.N., Kinyua, J., Kariuki, D., Kimani, F.T., 2016. In vitro selection of *Plasmodium falciparum* Pfert and Pfmdr1 variants by artemisinin. *Malaria Journal* 15, 381.
- Pickar, D., Cohen, R.M., Jimerson, D.C., Murphy, D.L., 1981. Tyramine infusions and selective monoamine oxidase inhibitor treatment. *Psychopharmacology* 74, 4-7.

- Rabey, J., Sagi, I., Huberman, M., Melamed, E., Korczyn, A., Giladi, N., Inzelberg, R., Djaldetti, R., Klein, C., Berecz, G., 2000. Rasagiline mesylate, a new MAO-B inhibitor for the treatment of Parkinson's disease: a double-blind study as adjunctive therapy to levodopa. *Clinical neuropharmacology* 23, 324-330.
- Reisine, T., Brownstein, M.J., 1994. Opioid and cannabinoid receptors. *Current opinion in neurobiology* 4, 406-412.
- Robards, K., Prenzler, P.D., Tucker, G., Swatsitang, P., Glover, W., 1999. Phenolic compounds and their role in oxidative processes in fruits. *Food chemistry* 66, 401-436.
- Salim, S., 2014. Oxidative stress and psychological disorders. *Current neuropharmacology* 12, 140-147.
- Steverding, D., 2008. The history of African trypanosomiasis. *Parasites & vectors* 1, 1.
- Tarawneh, A., Leon, F., Eakes, T., Petaway, S., Lambert, J., Mansoor, A., Cutler, S., 2015. Flavones with in vitro radioligand binding affinity for human opioid receptors isolated from *Perovskia atriplicifolia*. *Planta Medica* 81, PB5.
- Thaipong, K., Boonprakob, U., Crosby, K., Cisneros-Zevallos, L., Byrne, D.H., 2006. Comparison of ABTS, DPPH, FRAP, and ORAC assays for estimating antioxidant activity from guava fruit extracts. *Journal of food composition and analysis* 19, 669-675.
- Thomas, T., 2000. Monoamine oxidase-B inhibitors in the treatment of Alzheimer's disease. *Neurobiology of aging* 21, 343-348.
- Wojdyło, A., Oszmiański, J., Czemerys, R., 2007. Antioxidant activity and phenolic compounds in 32 selected herbs. *Food chemistry* 105, 940-949.
- Yamada, M., Yasuhara, H., 2004. Clinical pharmacology of MAO inhibitors: safety and future. *Neurotoxicology* 25, 215-221.
- Yasuhisa, T., Hideki, H., Muneyoshi, Y., 1993. Superoxide radical scavenging activity of phenolic compounds. *International journal of biochemistry* 25, 491-494.
- Youdim, M.B., Bakhle, Y., 2006. Monoamine oxidase: isoforms and inhibitors in Parkinson's disease and depressive illness. *British journal of pharmacology* 147, S287-S296.
- Youdim, M.B., Edmondson, D., Tipton, K.F., 2006. The therapeutic potential of monoamine oxidase inhibitors. *Nature Reviews Neuroscience* 7, 295-309.
- Zhao, J., Khan, S.I., Wang, M., Vasquez, Y., Yang, M.H., Avula, B., Wang, Y.-H., Avonto, C., Smillie, T.J., Khan, I.A., 2014. Octulosonic acid derivatives from Roman chamomile (*Chamaemelum nobile*) with activities against inflammation and metabolic disorder. *Journal of natural products* 77, 509-515.
- Zheng, W., Wang, S.Y., 2001. Antioxidant activity and phenolic compounds in selected herbs. *Journal of Agricultural and Food chemistry* 49, 5165-5170.



*PART IV:*  
*MOLECULAR MODELING AND*  
*MD SIMULATION STUDIES*

## **IV. Molecular Modeling and MD Simulation Studies**

### **IV.1 Introduction**

MAO-A and MAO-B have been considered as biological targets for treatment of depression, anxiety, neurodegenerative diseases and in the management of symptoms associated with Parkinson's and Alzheimer's diseases (Thomas, 2000; Yamada and Yasuhara, 2004). The inhibitory effects of natural products, especially the phenolic compounds on monoamine oxidases (MAO-A and MAO-B) have attracted more interests in the last years. Several herbs used in the folk medicine have been suggested as important source for treatment of depression, Parkinson's disease and other neuropsychiatric as well as neurological disorders (Adams et al., 2007; Schrader, 2000; Song et al., 2012). Flavonoids have attracted attention for preventing neurological disorders, and their consumption in the normal diet has been correlated with improvement in memory and learning processes (Spencer, 2009; Vauzour et al., 2010). Additionally, the benefits of flavonoids have been used to treat several neuronal pathological conditions and decrease the levels of dementia (Williams and Spencer, 2012). Evaluation of natural products resources, for MAO inhibitory constituents is of great interests, due to their significant role in the development of new therapeutic leads. Moreover, flavonoids such as myricetin have been not listed as a pan assay interference or PAINS compound.

Pure compounds isolated from *C. villosus* and *H. afrum* species have been evaluated for their *in vitro* MAO inhibitory activity against MAO-A and MAO-B, including genistein (**CVS2**), chrysin (**CVF1**), quercetin (**HAF1**) and myricetin (**HAF2**) (Figure IV.1) that proved to be potent MAO inhibitors.

The studies were extended further to evaluate the comparative binding and interaction of **CVS2**, **CVF1**, **HAF1** and **HAF2** with human MAO-A and -B employing enzyme-kinetics, enzyme-inhibitor complex formation with equilibrium dialysis dissociation analysis, and investigation of the docking poses of the compounds for interactions at the active site of the MAO-A and -B isoenzymes.

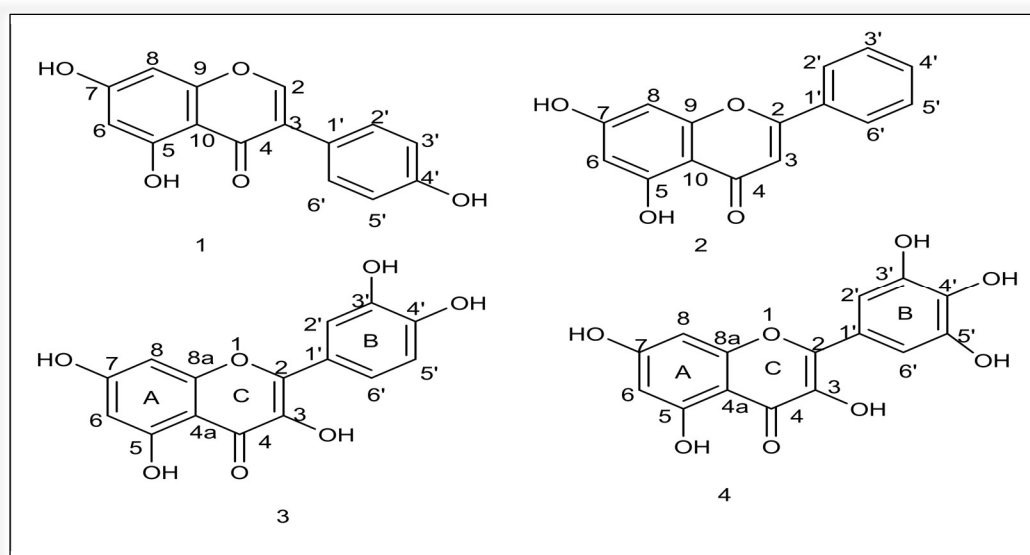


**Figure IV. 1.** Chemical Structures of compounds 1 (CVS2), 2 (CVF1), 3 (HAF1) and 4 (HAF2).

#### IV.2. Medicinal Chemistry and Drug discovery

A multiple discipline, chemistry-centered science primarily involved in the application of both chemical and biological principles to a study of chemical substances capable of exerting specific effects on a biological system. In practice, the medicinal chemist is involved in the design, synthesis and characterization of medicinal agents intended for the management and/or therapy of disease states. The multidiscipline approach to a study of the chemistry of biologically active agents requires a basic knowledge of both the chemical and biological sciences. The design of medicinal agents requires an understanding of biochemical and physiological principles in order to facilitate a rational approach to the discovery of novel therapeutic agents. A thorough understanding of organic, inorganic and physical chemistry is required in order to carry out the synthesis of the desired medicinal agent. Knowledge of the science and practice of analytical chemistry is essential to characterize fully the chemical and physical properties of a medicinal agent as a pure chemical substance, as a constituent of a pharmaceutical dosage form and as a part of the physiological system to which it is applied.

#### IV.3. Docking Methodologies: Background

Molecular modeling is described as a tool for understanding fundamental concepts of drug structure activity relationships in a medicinal chemistry context (Barreca et al., 2002; Guenard et al., 1993; Koga et al., 1980). The relevant molecular features of antimetabolite drugs were investigated by three-dimensional (3D) visualization, their physical properties measured, and the molecular

interaction pattern on target macromolecules illustrated by antineoplastic drugs (Nandi and Bagchi, 2010). This approach provides a computing and graphic tool to explore important aspects of biological molecules and drugs and the correlation of their structures and pharmacological actions. Drug discovery is a multidisciplinary field, which includes molecular biology, biophysics, biochemistry, and pharmacology. It usually deals with the identification of a biological target that is known to play a critical role in a particular disease. In drug discovery, computational methods are increasingly used for the structure-based drug design from target identification and validation to the design of new molecules. To identify molecules that inhibit a certain activity, hundreds of thousands of candidates generated with docking protocols are virtually screened to filter out top-scoring hits, the latter molecules are tested in appropriate biological assays, and many cycles of optimization are performed to obtain the candidates for further clinical trials.

### **IV.4. Molecular Mechanics**

#### **IV.4.1. Background**

The mechanical molecular model was developed out of a need to describe molecular structures and properties in as practical a manner as possible. Molecular Mechanics (MM) force fields are the methods of choice for protein simulations, which are essential in the study of conformational flexibility. Given the importance of protein flexibility in drug binding, MM is involved in most if not all Computational Structure-Based Drug Discovery (CSBDD) projects. We aim in this section to introduce the fundamentals of MM, with a special emphasis on how the target data used in the parametrization of force fields determine their strengths and weaknesses.

#### **IV.4.2. Molecular mechanics principles**

Molecular mechanics methods are based on the following principles:

- Nuclei and electrons lumped into atom-like particles.
- Atom-like particles are spherical (radii obtained from measurements or theory) and have a net charge (obtained from theory).
- Interactions based on springs and other classical potentials.
- Interactions pre-assigned to specific sets of atoms.
- Interactions determine spatial distribution of atom-like particles and their energies.

#### IV.4.3. Quantum mechanics (QM) compared to Molecular mechanics (MM)

Quantum mechanics is a set of equations that tell us how to compute the energy and “position” of a wave with a mass and a charge. What follows next is a motivation (as opposed to a derivation) of the key equation in quantum chemistry, the Schrödinger equation. The simplest wave is one that is moving in one dimension ( $x$ ) and does not interact with anything (Jensen, 2010)

$$\Psi(\lambda) = \sin\left(\frac{2\pi}{\lambda}x\right)$$

where  $\lambda$  is the wavelength, as before, and  $\Psi(x)$  is known as the wave function. The energy of this wave function can be obtained from its second derivative with respect to  $x$ , and the De Broglie equation:

$$\lambda = \frac{h}{mv}$$

where  $m$ , and  $v$  are the mass, and speed of the particle, respectively, and  $h$  is **Planck’s constant** (a fundamental constant).

$\hat{H}\Psi(x) = E\Psi(x)$ , which is the **Schrödinger equation** for an isolated electron, where  $\hat{H}$  is called the **Hamiltonian operator** or just the Hamiltonian.

Actually, the Schrodinger equation is used “in reverse.” First you define the Hamiltonian for your system of interest, and then you look for the wave function that satisfies the Schrodinger equation. So for an isolated electron moving in the  $x$  direction, we define the Hamiltonian operator [in this case just the kinetic energy operator, and then solve the Schrodinger equation by finding the wave function that “satisfies it.” That means we find a function for which the second derivative is the function multiplied by a constant ( $E$ ), which happens to be a  $\sin(x)$  function. So the Hamiltonian tells us both the wave function and the energy. Notice that  $\sin(2x)$ ,  $\sin(3x)$ , etc. also work, i.e., the Schrodinger equation has many solutions:

$$\Psi_n(x) = E(n)\Psi_n(x) \quad n=1,2,\dots \text{ etc.}$$

with different energies and wave functions.

$$\hat{H}\Psi_n(x) = \sin\left[2\pi/\lambda (nx)\right]$$

$n$  is an integer and is called the **quantum number**. The energy increases with increasing quantum number, and the energy with the lowest quantum number is called the **ground state** energy.

By contrast, quantum mechanics methods are based on the following principles:

- Nuclei and electrons are distinguished from each other.
- Electron-electron (usually averaged) and electron-nuclear interactions are explicit.
- Interactions are governed by nuclear and electron charges (i.e. potential energy) and electron

motions.

- Interactions determine the spatial distribution of nuclei and electrons and their energies.

#### **IV.4.4. Applicability of Molecular Mechanics**

The mechanical molecular model was developed out of a need to describe molecular structures and properties in as practical a manner as possible. The range of applicability of molecular mechanics (MM) includes:

- Macromolecules containing thousands of atoms.
- Organics, oligonucleotides, peptides, and saccharides (metallo-organics and inorganics in some cases).
- Vacuum, implicit, or explicit solvent environments.
- Ground state only.
- Cannot treat chemical reactions.
- Thermodynamic and kinetic (via molecular dynamics) properties.

The Great Computational Speed of Molecular Mechanics allows for its use in procedures such as molecular dynamics (MD), conformational energy searching, and docking, that require large numbers of energy evaluations.

#### **IV.4.5. Types of terms in molecular mechanics**

##### **IV.4.5.1. Bonded Interactions**

The class I potential energy function comprises 4 types of bonded interactions:

- - bond stretching terms
- - angle bending terms
- - dihedral or torsional terms
- - improper dihedrals

Bond and angle terms dominate the local covalent structure around each atom and, in theory, when angle bending terms are present for all angles in a molecule, planar centers are kept planar by the sum of the reference angles  $\theta_0$  being  $360^\circ$  or higher so that any deviation from planar geometry would imply an increase in energy. Therefore, most if not all class I potential energy functions include an additional out-of-plane term, usually in the form of an improper dihedral, where the potential energy is harmonic as a function of the out-of-plane angle  $\varphi$ .

#### IV.4.5.2. Anharmonicity and cross-terms

While the internal terms in Class I force fields are primarily harmonic or sinusoidal in nature, class II and III force fields contain cubic and/or quartic terms in the potential energy for bond and angles of the form  $E_{bond} = K_b(b - b_0)^2 + K_b'(b - b_0)^3 + K_b''(b - b_0)^4 + \dots$ . While these higher-order terms allow for a more accurate reproduction of QM Potential Energy Surfaces (PES) and experimental properties such as vibrational spectra, they also introduce more parameters in the force field ( $K_b'$ ,  $K_b''$ , ...), making optimization of the model more difficult. Moreover, Molecular Dynamics (MD) simulations associated with CSBDD are generally performed at room temperature, and the energy in bond and angle vibrations typically does not become high enough for anharmonicity to have a qualitatively important influence on the dynamics and energetics. Apart from anharmonic terms, class II and III force fields contain cross terms that reflect the coupling between adjacent bonds, angles and dihedrals.

#### IV.4.5.3. Non-bonded interactions

Non-bonded atoms interact through:

- van der Waals attraction
- steric repulsion
- electrostatic attraction/repulsion

These properties are easiest to describe mathematically when atoms are considered as spheres of characteristic radii.

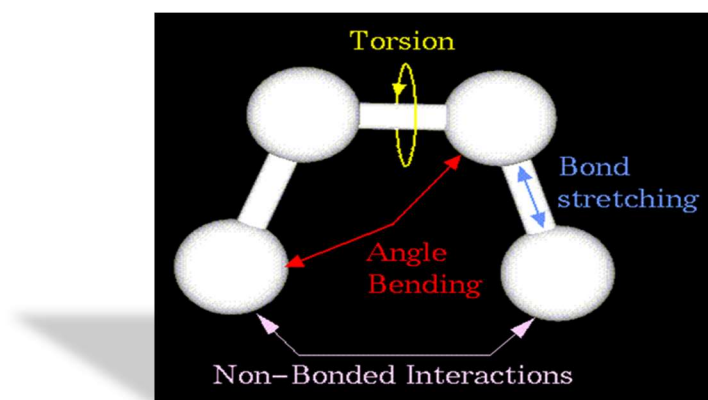


Figure IV. 2. Molecular Mechanics.

#### IV.4.6. Molecular Mechanics Energy

The object of molecular mechanics is to predict the energy associated with a given conformation of a molecule. A simple molecular mechanics energy equation is given by:

$$\text{Energy} = \text{Stretching Energy} + \text{Bending Energy} + \text{Torsion Energy} + \text{Non-Bonded Energy}$$

- MM energies have no meaning as absolute quantities
- Only differences in energy between two or more conformations have meaning
- The lowest energy structure is most probable
- The Stretching Energy is Based on Hooke's law
- Parameters are: the force constant  $k_b$  which controls the stiffness of the bond spring and  $r_o$  to define the equilibrium length
- Unique  $k_b$  and  $r_o$  parameters are assigned to each pair of bonded atoms based on their types (e.g. C-C, C-H, O-C)

This equation estimates the energy associated with vibration about the equilibrium bond length. This is the equation of a parabola, as can be seen in the plot:

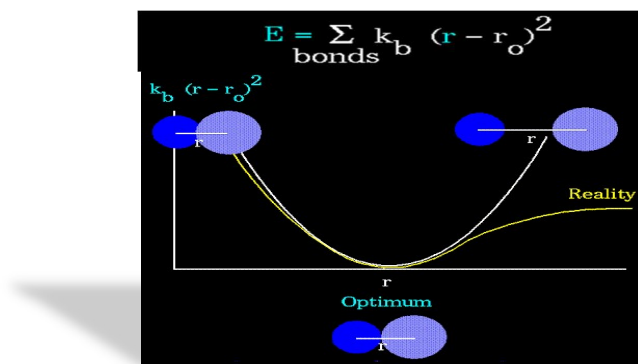


Figure IV. 3. Molecular Mechanics Energy.

**A. Bending Energy:** is Also based on Hooke's law

- **Parameters:**
  - $k_\theta$  controls the stiffness of the angle spring
  - $\theta^\circ$  defines the equilibrium angle
  - Unique  $k_\theta$  and  $\theta^\circ$  parameters are assigned to each triplet of bonded atoms based on their types (e.g. C-C-C, C-C-H, C-O-C).



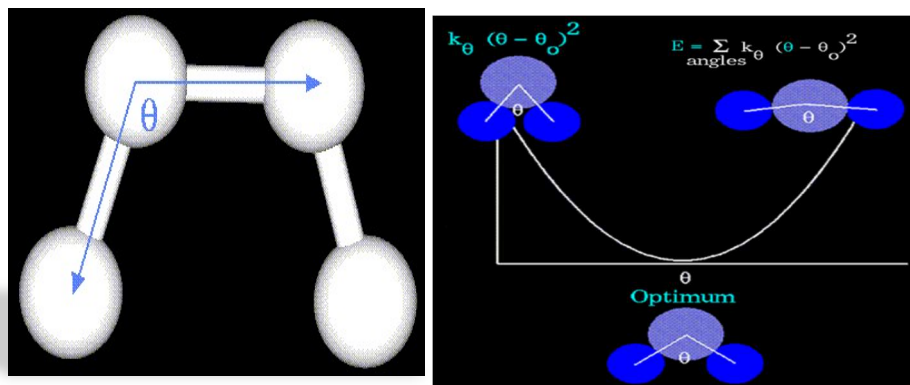


Figure IV. 4. Bending Energy.

### B. Torsional Energy

The torsion energy in molecular mechanics is primarily used to correct the remaining energy terms rather than to represent a physical process. It fits with the idea of what is the lowest energy conformation and how easy it is to rotate around a bond. It is Based on a simple periodic function.

#### - Parameters:

- A controls the Amplitude of the oscillation
- n defines the period of oscillation
- $\Phi$  phase factor

Unique A and n parameters are assigned to each set of 4 bonded atoms based on their types (e.g. C-C-C-C, C-C-C-H, C-C-O-C).

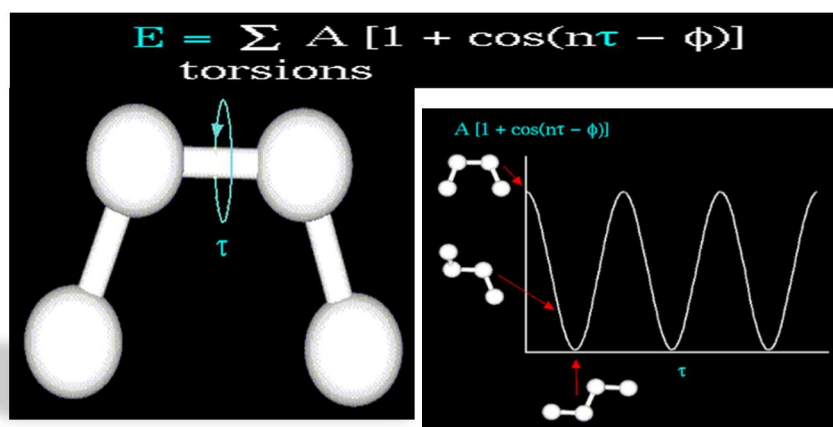
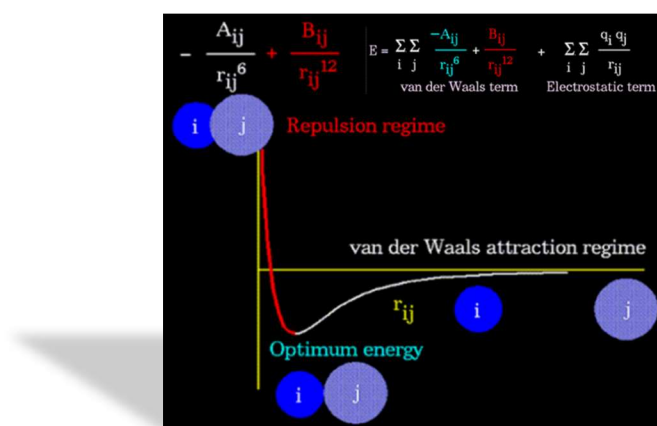


Figure IV. 5. Torsional energy.

### A. Non-Bonded Energy

The non-bonded energy accounts for repulsion, van der Waals attraction, and electrostatic interactions. van der Waals attraction occurs at short range, and rapidly dies off as the interacting atoms move apart by a few Angstroms. Repulsion occurs when the distance between interacting atoms becomes even slightly less than the sum of their contact radii. It is modeled by an equation that is designed to rapidly blow up at close distances ( $r^{-12}$  dependency).

These effects are often modeled using a “12-6” equation, as shown in the following plot:



**Figure IV. 6.** Non-bonded energy.

### IV.5. Force-field definition

A force-field consists of The energy equation and Data (parameters) to describe the behavior of different kinds of atoms and bonds.

The mathematical form of the energy terms varies from force-field to force-field.

Some force-fields include additional energy terms that describe other kinds of deformations and coupling between bending and stretching in adjacent bonds in order to improve the accuracy of the mechanical model

### IV.5.1. AMBER force field

$$\begin{aligned}
 E_{\text{total}} = & \sum_{\text{bonds}} K_r (r - r_{eq})^2 + \sum_{\text{angles}} K_\theta (\theta - \theta_{eq})^2 \\
 & + \sum_{\text{dihedrals}} \frac{V_n}{2} [1 + \cos(n\phi - \gamma)] \\
 & + \sum_{i < j} \left[ \frac{A_{ij}}{R_{ij}^{12}} - \frac{B_{ij}}{R_{ij}^6} + \frac{q_i q_j}{\epsilon R_{ij}} \right] \\
 & + \sum_{\text{H-bonds}} \left[ \frac{C_{ij}}{R_{ij}^{12}} - \frac{D_{ij}}{R_{ij}^{10}} \right]
 \end{aligned}$$

### IV.5.2. AMBER force field details

Original charges were obtained from a fit to the STO-3G wavefunction with little or no modification. More recently, a modified point charge fitting method called RESP (Restrained ElectroStatic Potential fit) has been used. Also, a better basis set (6-31G\*) is used.

OPLS vdW parameters are used, although it is possible to specify that the OPLS charges are to be used too. Bond and angle parameters were chosen to reproduce experimental normal modes for simple model compounds. Lone pair sites for sulfur atoms.

### IV.5.3. CHARMM/CHARMM force field

$$E = E_b + E_\theta + E_\phi + E_\omega + E_{vdW} + E_{el} + E_{hb} + E_c + E_{c\phi},$$

With bond, angle, dihedral energy terms, intermolecular electrostatic and van der Waals terms, hydrogen-bond terms, and distance and dihedral angle constraints.

$$\begin{aligned}
 E = & \sum_{\text{bonds}} k_b (r - r_0)^2 + \sum_{\text{angles}} k_\theta (\theta - \theta_0)^2 + \\
 & \sum_{\text{proper dihedrals}} |k_\phi| - k_\phi \cos(n\phi) + \sum_{\text{improper dihedrals}} k_\omega (\omega - \omega_0)^2 + \\
 & \sum_{\text{pairs}, i \neq j} \left[ \frac{A_{ij}}{r_{ij}^{12}} - \frac{B_{ij}}{r_{ij}^6} + \frac{q_i q_j}{\epsilon r_{ij}} \right] + \\
 & \sum \left[ \frac{A'}{r_{AD}^i} - \frac{B'}{r_{AD}^i} \right] \cos^m(\theta_{A-H-D}) x \cos^n(\theta_{AA-A-H}) + \\
 & \sum K_i (r_i - r_{i0})^2 + \sum K_i (\phi_i - \phi_{i0})^2
 \end{aligned}$$

#### IV.5.4. CVFF force field

Great efforts were taken so that vibrational features of biochemical molecules could be reproduced. Note the cross terms (bond-bond, bond-angle, angle-angle, angle-dihedral, dihedral-dihedral) are normally not present in other force fields and are included here so that vibrational features of molecular can be reproduced. For most of what people do with proteins, these are not necessary.

$$\begin{aligned}
 E_{pot} = & \sum_b D_b [1 - e^{-\alpha(b-b_0)}] + \\
 & \sum_{\theta} H_{\theta}(\theta - \theta_0)^2 + \\
 & \sum_{\phi} H_{\phi}[1 + s\cos(n\phi)] + \\
 & \sum_x H_x \chi^2 + \\
 & \sum_b \sum_{b'} F_{bb'}(b - b_0)(b' - b'_0) + \\
 & \sum_{\theta} \sum_{\theta'} F_{\theta\theta'}(\theta - \theta_0)(\theta' - \theta'_0) + \\
 & \sum_b \sum_{\theta} F_{b\theta}(b - b_0)(\theta - \theta_0) + \\
 & \sum_{\phi} F_{\phi\theta\theta'} \cos\phi(\theta - \theta_0)(\theta' - \theta'_0) + \\
 & \sum_x \sum_{x'} F_{xx'} \chi\chi' + \\
 & \sum \epsilon [(r^*/r)^{12} - 2(r^*/r)^6] + \\
 & \sum q_i q_j / \epsilon r_{ij}
 \end{aligned}$$

#### IV.5.5. OPLS force field

$$\begin{aligned}
 E = & \sum_{i < j} \left[ \frac{A_{ij}}{r_{ij}^{12}} - \frac{C_{ij}}{r_{ij}^6} + \frac{q_i q_j}{r_{ij}} \right] + \\
 & \sum_{\text{torsions}} (V_1/2)(1 - \cos\phi) + (V_2/2)(1 - \cos 2\phi)
 \end{aligned}$$

Note that bond and angle stretching/bending energy functions are not in the true OPLS potential. The reason for this is that the OPLS parameters are primarily developed to be used in a Monte Carlo program that doesn't permit the changing of bonds and angles. If they are needed, AMBER parameters are used (Jorgensen, 1998).

### IV.6 Molecular Dynamics (MD) and related methods

#### IV.6.1. Background

Computer simulation is a powerful and modern tool for solving scientific problems as numerical experiments can be performed for new materials without synthesizing them. One of the aims of computer simulation is to reproduce experiment to elucidate the invisible microscopic details and further explain experiments. On the other hand, simulation can also be used as a useful predictive

tool. The most widely used simulation methods for molecular systems are Monte Carlo, Brownian dynamics and molecular dynamics.

Molecular dynamics is the most detailed molecular simulation method (Allen and Tildesley, 1989) which computes the motions of individual molecules. (MD) and related methods are Computational tools for drug discovery. They are widely used technique for computer simulation of complex systems. Their main advantage is in explicitly treating structural flexibility and entropic effects. This allows a more accurate estimate of the thermodynamics and kinetics associated with drug–target recognition and binding, as better algorithms and hardware architectures increase their use.

Molecular dynamics is a method to simulate the motion of a group of molecules, using a force-field to represent the molecules and give them an initial velocity. Newton's law used to calculate how they move : $F = ma$

### IV.6.2. Molecular Dynamics: aspects

- Can study a large system—100,000 atoms
- Can follow the time progress—up to 1  $\mu$ s
- Can represent different lab conditions:
  - Constant Number of atoms, Volume, Energy
  - Constant N, V, Temperature

### - Molecular Dynamics of Enzyme Action

-

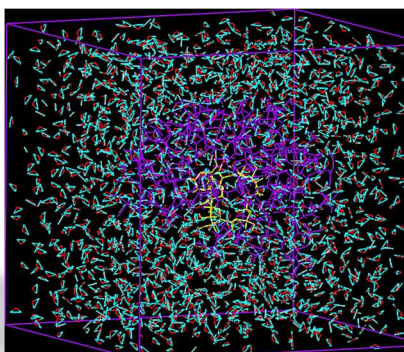


**Figure IV. 7.** Biliverdin reductase with NADPH cofactor, in water (Fu et al., 2012).

### IV.6.3. Molecular Dynamics Simulation : Applicability

Molecular dynamics has evolved from a niche method mainly applicable to model systems into a cornerstone in molecular biology (Karplus and Petsko, 1990). It is applicable for equilibrium and transport properties of a classical many-body system and for classical means that the nuclei obey the laws of classical mechanics (Frenkel and Smit, 2002) . Molecular Dynamics (MD) Simulations

provide a time dependent microscopic properties of biomolecules, which could not be explained by experimental methods like X-ray crystallography.

These specifications enable MD simulations as most widely used computational techniques for the study of dynamical properties of proteins, DNAs and other bio-macromolecules (Ebbinghaus et al., 2007; Karplus and McCammon, 2002; Tarek and Tobias, 2002).

### IV.7. Monoamine Oxidases Properties

Monoamine oxidases (MAOs) are outer mitochondrial membrane. Their role is to catalyze the oxidative deamination of a variety of neurotransmitters. Inside the human brain, there are two isoforms of MAO, named MAO-A and MAO-B based by their sensitivity to selective inhibitors and specific substrates. MAO-A preferentially deaminates serotonin and norepinephrine, whereas MAO-B deaminates phenylethylamine and benzylamine. The two enzymes are selectively inhibited by clorgyline for the MAO-A, and by L-deprenil for MAO-B.

MAO-A consist of 527 and MAO-B consist of 520 amino acids respectively. MAO isoenzymes have 70% similarity based on amino acid sequences (Figure-IV.8, IV.9). The active sites of both of these isoenzymes include cysteine, which is bonded covalently with coenzyme FAD (flavin adenine dinucleotide) (Ser-Gly-Gly-Cys-koenzyme-Tyr). Cys406 of MAO-A and Cys497 of MAO-B are making covalent bonds with 8- $\alpha$ -methyl group of FAD via thioether linkage(Edmondson et al., 2004). FAD' s molecular structure can be seen in Figures IV.8 and IV.9.

#### IV.7.1. Crystallographic and Structural Properties of MAO Isoenzymes

Previous crystallographic studies and computational molecular simulations show us some important information about these molecules. According to these studies both MAOs are composed of an FAD-binding domain, conserved among a number of other flavoprotein oxidases, a substrate-binding domain, and a membrane-binding domain. While NMR studies have demonstrated that both forms of rat and human MAOs exist as dimers in solution(De Colibus et al., 2005), human MAO A crystallizes as a monomer(Edmondson et al., 2007) Both MAOs bind the outer mitochondrial membrane through a C-terminal  $\alpha$ -helical region, with additional membrane interactions occurring with other hydrophobic residues(Edmondson et al., 2009; Gaweska and Fitzpatrick, 2011). MAO-A crystallizes as monomers but MAO-B crystallizes as dimer. MAO-A includes only one cavity, which is named as *substrate binding cavity*, but MAO-B has an additional cavity named as entrance cavity (Edmondson et al., 2009; Pekcan et al.; VARNALI, 2012).

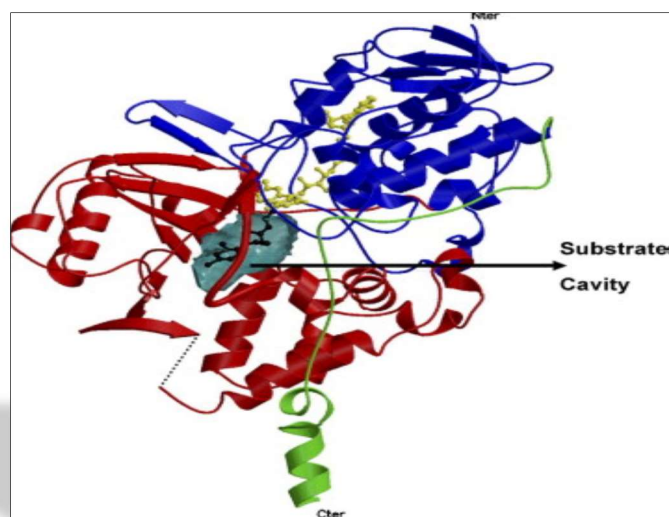


**Figure IV. 8.** MAO-A structure is shown in illustration. The FAD-binding domain illustrated with blue, the substrate-binding domain red, and the C-terminal membrane region green.

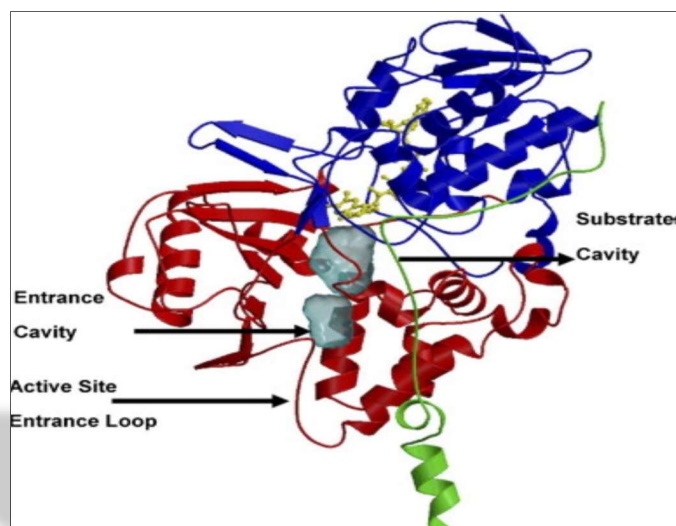


**Figure IV. 9.** MAO-B structure is shown in illustration. The FAD-binding domain illustrated with blue, the substrate-binding domain red, and the C-terminal membrane region green.

#### IV.7.2. Biosynthesis and Biodegradation of Neurotransmitters

MAO catalyzes the oxidative deamination of neurotransmitters and some other biologic amines. Some of these neurotransmitters and amines are dopamine, epinephrine (adrenaline), norepinephrine (noradrenalin, NA), serotonin (5-HT), tyramine, tryptamine, PEA (2-phenylethylamine) and MPTP (1-methyl-4-phenyl-1, 2,3,6-tetrahydropyridine). Furthermore, MAO also serves as a cytoprotective role by degrading exogenous amines, which exert their toxicity by

affecting cardiovascular and endocrine homeostasis (Bortolato et al., 2010). Norepinephrine and serotonin are inhibited by MAO-A and phenylethylamine and benzylamine are inhibited by MAO-B. Both of the two enzymes inhibit dopamine, and tyramine, but dopamine by MAO-A, and tyramine by MAO-B are inhibited much more effectively (Figure-IV.10). MAO-A inhibition regulates depressive and anxiolytic influences caused by increasing of 5-HT and NA levels at the brain. MAO-B inhibition (e.g. with *l*-deprenyl) helps the treatment of neurodegenerative diseases caused by increasing of PEA, benzylamine, and MPTP levels.

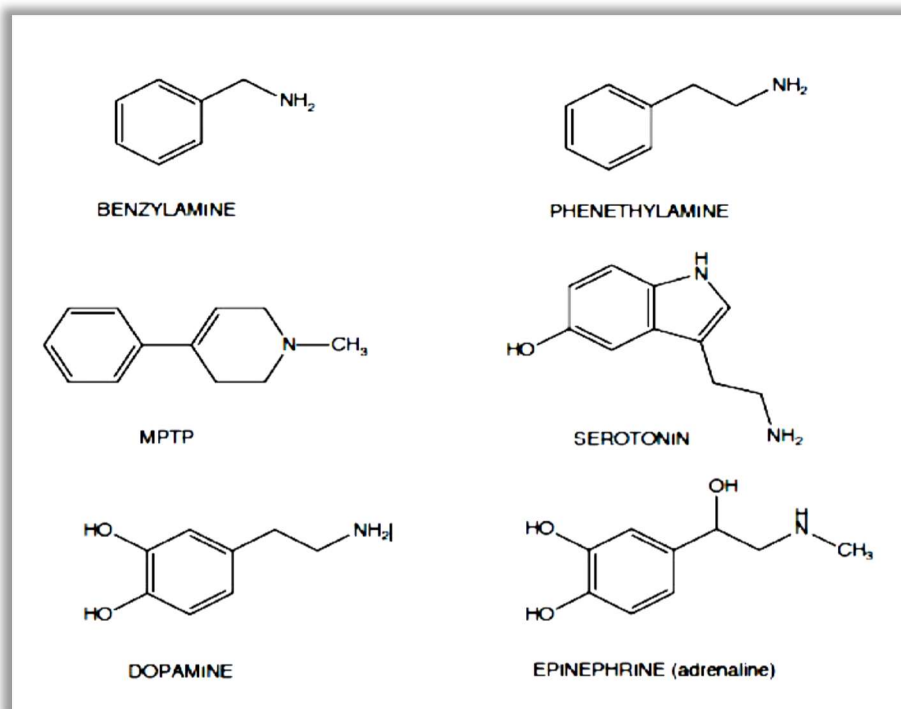


**Figure IV. 10.** Chemical structures of some amines which are related with MAO isoenzymes (VARNALI, 2012).

L-DOPA (3,4-dihydroxy phenylalanine) is synthesized from tyrosine by tyrosine hydroxylase enzyme. L-DOPA is decarboxylated into dopamine by dopa decarboxylase enzyme. After crossing blood-brain barrier, L-DOPA is converted to dopamine. (Figure-IV.11).

For serotonin biosynthesis, 5-hydroxy tryptophan is produced from tryptophan amino acid by *tryptophan hydroxylase* enzyme. After that 5-hydroxy tryptamine (serotonin) is produced by using L-amino acid decarboxylase enzyme (Figure IV.11).



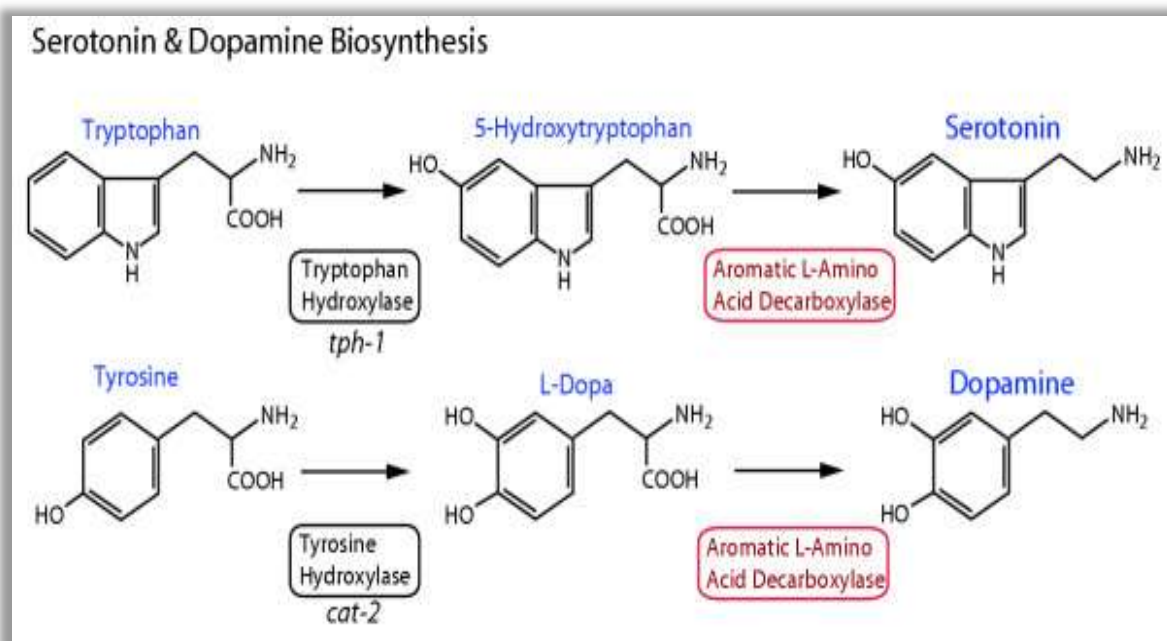


Figure IV. 11. Biosynthesis of neurotransmitters Serotonin and Dopamine (Hare and Loer, 2004).

Catecholamines are released into synaptic cleft, and then they bind into effectors cell receptors and perform their specific activity. After that catecholamines biodegrade in intercellular or extracellular environment by MAO isoenzymes, and catechol-O-methyl-transferase (COMT) reuptake from synaptic (Figure IV.12).

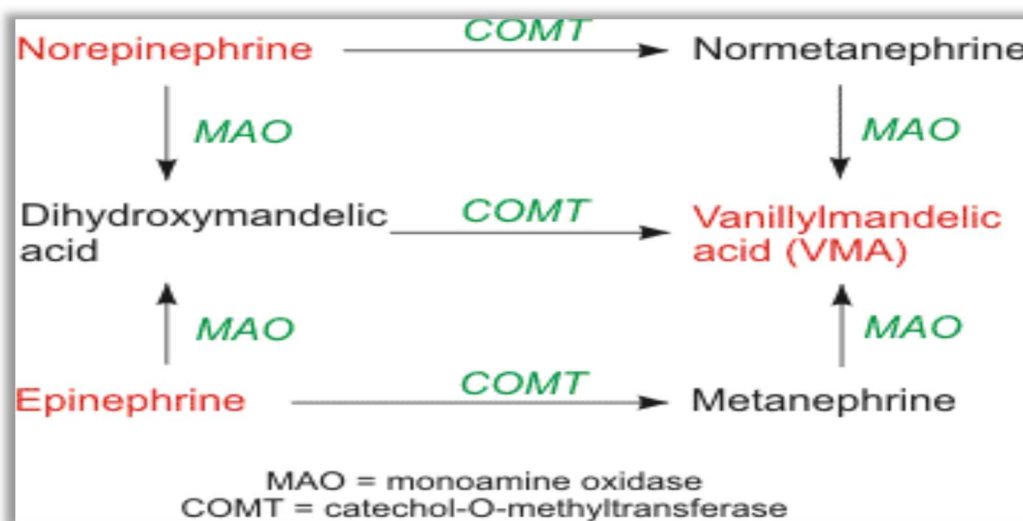


Figure IV. 12. Biodegradation of catecholamines via COMT and MAO enzymes (Klabunde, 2009).

### **IV.7.3. Classifications of Monoamine Oxidase Inhibitors**

Monoamine Oxidase inhibitors (MAOIs) are classified as, reversible (competitive or slow tight-binding), and irreversible (affinity labelling agents or mechanism-based inactivators) MAOIs. First produced MAOIs were performing a mechanism-based inhibition by covalently binding to proteins to yield reactive products. At the same time most of these compounds caused some hepatotoxic side effects by inactivating the P450 (Kamel and Harriman, 2013). Reversible inhibitors of monoamine oxidase A (MAO A) are used as antidepressants. The influence of inhibitors such as pirlindole (pyrazinocarbazole) on the redox co-factor (flavin adenine dinucleotide, FAD) is a key factor in the inhibition (Hynson et al., 2003). One of the major side effects is called “*cheese effect*”. Application of nonselective MAOI and consumption of tyramine contained foods causes the inactivation of both MAO isoenzymes resulting an increased blood tyramine level. Thus the increased tyramine level effects blood pressure and this causes fatal hypertensive crisis. These hypertensive and hepatotoxic side effects caused by the unknown selectivity of MAOIs has substantially limited the application of these drugs, until reversible and selective MAOIs came out. The increasing research on structural and functional information about MAO and their selective inactivation mechanism has created a substantial attention on reversible and selective MAOIs. Research based on new generation of MAO-A selective inhibitors tends to yield promising results for the treatment of depression and MAO-B inhibitors seem to be promising for the treatment of Parkinson and Alzheimer diseases (Youdim and Weinstock, 2004).

### **IV.8. Aim of the Molecular Modeling study**

In this study, Monoamine Oxidase isozymes, which play an essential role in the oxidative deamination of the biogenic amines were studied using techniques described in pages 65-66. Compounds that inhibit these isozymes were shown to have promising therapeutic value in several psychiatric and neurological as well as neurodegenerative diseases. Several flavonoids like quercetin and quercetin glycosides, kaempferol, luteolin, apigenin, naringenin and galangin isolated from different natural resources have been suggested to induce MAO inhibition (Bandaruk et al., 2012; Lee et al., 2000; Olsen et al., 2008; Sloley et al., 2000), their IC<sub>50</sub> values obtained from different studies cannot be compared as the assays have been evaluated in different experimental conditions.

Quercetin (HAF1) is a common flavonol, this compound and its related flavonoids were reported to exhibit several biological and pharmacological activities, including anti-inflammatory, anti-oxidant effects and cytotoxic potentials (Choiprasert et al., 2010; Maciel et al., 2013), the molecule of quercetin has been described to exhibit neuroprotection properties (Zhang et al., 2011). In previous

studies, it has been identified as a selective MAO-A inhibitor (Bandaruk et al., 2014; Chimenti et al., 2006).

Myricetin (HAF2) which is one of such flavonoids very common in various plants, fruits and vegetables, also in several foods and beverages, this flavonol and its derivatives have been indicated to display a range of biological activities, such as anti-oxidant, anti-cancer and anti-inflammatory activities (Dimas et al., 2000; Pan et al., 2016; Sun et al., 2012). Recently, myricetin was investigated for its protective effects on brain injury and neurological deficits (Wu et al., 2016).

Genistein(CVS2), an isoflavone, is found in several used medicinal plants, this molecule largely studied, exerts inhibitory effects on the proliferation of various cancer cells and plays an important role in cancer prevention (Lamartiniere et al., 1998; Sarkar et al., 2006) . Previous studies were reported its potential neuroprotective effects (Baluchnejadmojarad et al., 2009). Chrysin (CVF1) is one of the important natural plant flavonoids, several researches have been reported its possess of multiple biological potentials, including antioxidative and anti-inflammatory properties (Pushpavalli et al., 2010), chrysin was also suggested to exert neuroprotective effect against brain damage (He et al., 2012; Kandhare et al., 2014). Recently, the molecule of chrysin was investigated to elucidate the roles of inflammation and the iNOS pathway in mediated neuroprotection against traumatic SCI in rats (Jiang et al., 2014).

The binding modes of compounds HAF1, HAF2, CVS2 and CVF1 at the enzymatic site of MAO-A and -B were predicted through molecular modeling algorithms, illustrating the high importance of ligand interaction with negative and positive free energy regions of the enzyme active site.

### IV.9. Results and discussion

#### IV.9.1. Docking

MAO models. Statistical thermodynamics and distance analysis allowed the estimation of state functions of the complexation process and identification of the important residues involved in the selective recognition of genistein, chrysin, quercetin and myricetin in the MAO enzymatic clefts.

- **Genistein (CVS2) and chrysin (CVF1)**

The best docking pose of genistein in MAO-A exhibited a score of -10.4 kcal/mol (Figure IV.13). Several strong hydrogen bonds and  $\pi$ - $\pi$  interactions are contributing to ligand binding. Genistein interacts with Phe208, Gln215 and Thr336.

Chrysin showed a docking score of -13.34 kcal/mol in MAO-A (Figure IV.14). There is only one hydroxyl group different between chrysin and genistein which lead a considerable difference in their binding affinity towards MAO A.

The 4'-hydroxyphenyl of genistein could form hydrogen bonds with water molecules inside the binding pocket or with the surrounding amino acid residues. This increased polarity seems not to be favorable for tight binding.

In case of chrysin, there is no 4'-hydroxyl group and the ligand oriented itself inside the binding pocket to have strong interactions with FAD, Ile180 and Asn181.

Chrysin and genistein displayed docking scores of -12.22 and -11.51 kcal/mol in MAO-B (Figures IV.15 and IV.16).

The binding pocket of MAO B exhibited different thermodynamics to allow for higher polarity on the phenyl group compared to that of MAO A. Both compounds showed favorable interactions with the amino acid residues, water molecules and co-factor in the binding pocket.

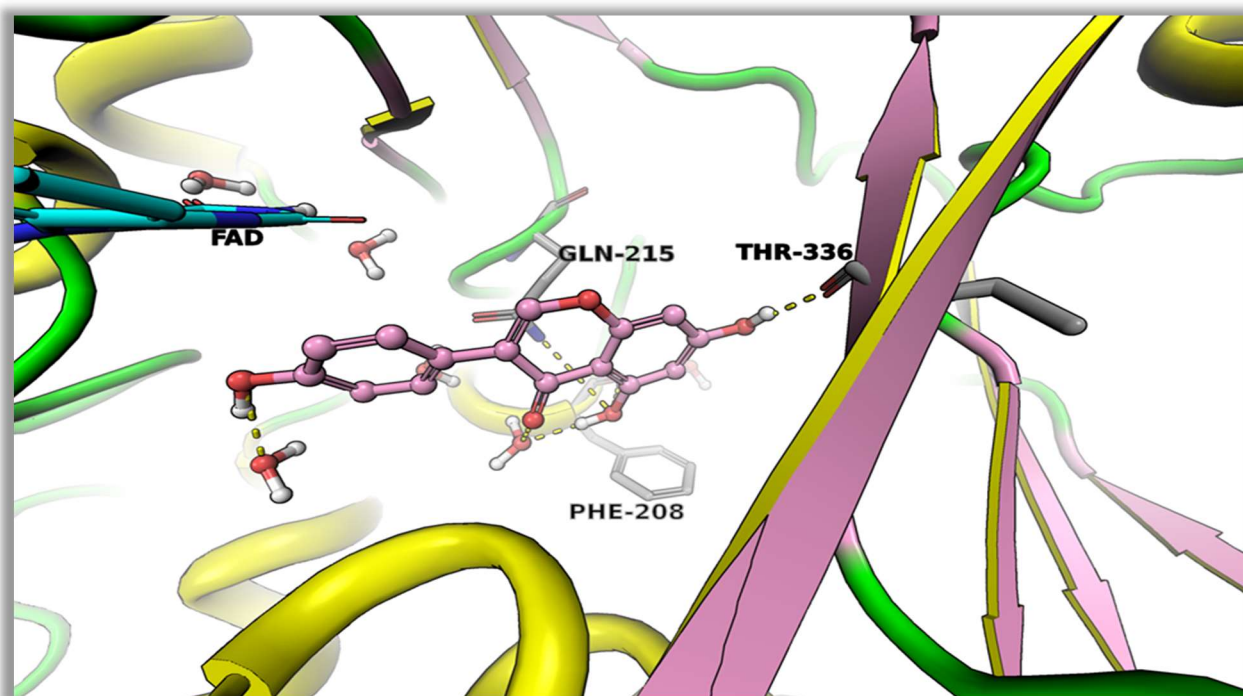


**Figure IV. 13.** The binding mode of genistein in MAO A. Genistein is shown as pink balls and sticks. The interacting amino acids are shown as grey sticks. Protein is shown as cartoon with yellow helices, pink strands and green loops. All possible hydrogen bonds in the range of 3.5 Å are shown as yellow dots.

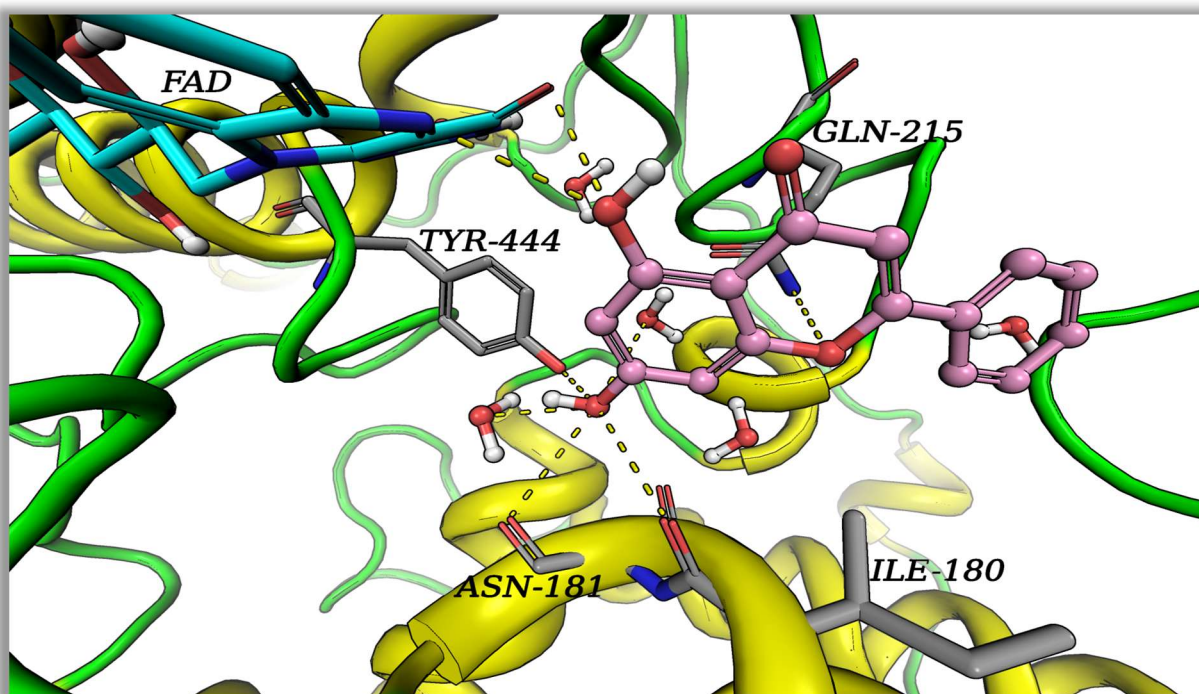


**Figure IV. 14.** The binding mode of chrysin in MAO A. Chrysin is shown as pink balls and sticks. The interacting amino acids are shown as grey sticks. Protein is shown as cartoon with yellow helices, pink strands and green loops. All possible hydrogen bonds in the range of 3.5 Å are shown as yellow dots.

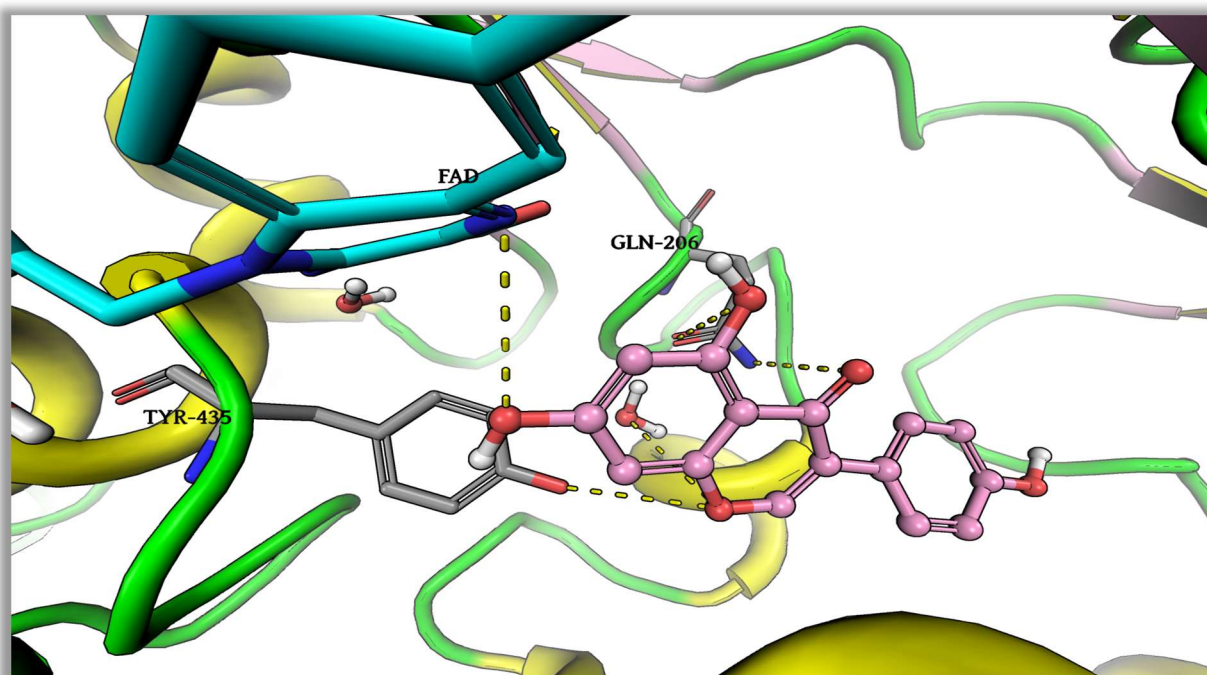


**Figure IV. 15.** The binding mode of genistein in MAO B. Genistein is shown as pink balls and sticks. The interacting amino acids are shown as grey sticks. Protein is shown as cartoon with yellow helices, pink strands and green loops. All possible hydrogen bonds in the range of 3.5 Å are shown as yellow dots.

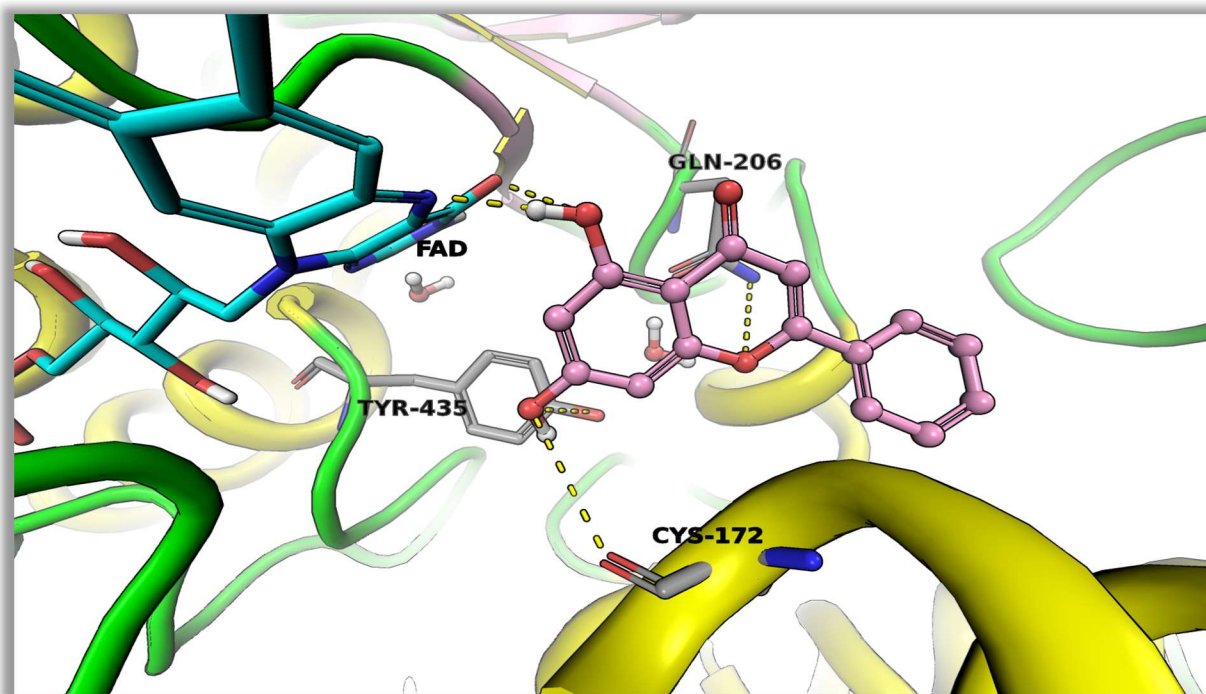


**Figure IV. 16.** The binding mode of chrysin in MAO B. Chrysin is shown as pink balls and sticks. The interacting amino acids are shown as grey sticks. Protein is shown as cartoon with yellow helices, pink strands and green loops. All possible hydrogen bonds in the range of 3.5 Å are shown as yellow dots.

- **Quercetin (HAF1) and myricetin (HAF2)**

Quercetin showed a favorable docking pose in MAO A with a docking score of -11.3 kcal/mol. Quercetin interacts with the amino acid residues (Ala111, Ile180, Asn181, Phe208, Gln215, Thr336, and Tyr444) and water molecules inside the ligand binding pocket (Figure IV.17). It forms  $\pi$ - $\pi$  stacking with FAD.

The polar groups of quercetin are in appropriate locations to create hydrogen bonds with several residues in the binding site.

Myricetin has a docking score of -9.8 in MAO A (Figure IV.18). Myricetin forms strong hydrogen bonds with Ala111, Ile180, Asn181, and Thr336.

Solvent molecules in the binding pocket play an important role in ligand stabilization as demonstrated by the strong hydrogen bonds with ligand atoms. The ligand showed hydrogen bonds and  $\pi$ - $\pi$  stacking with FAD.

Energetically, the binding pose of quercetin is more favorable than that of myricetin, however, both compounds are fitting well inside the ligand binding pocket of MAO A.

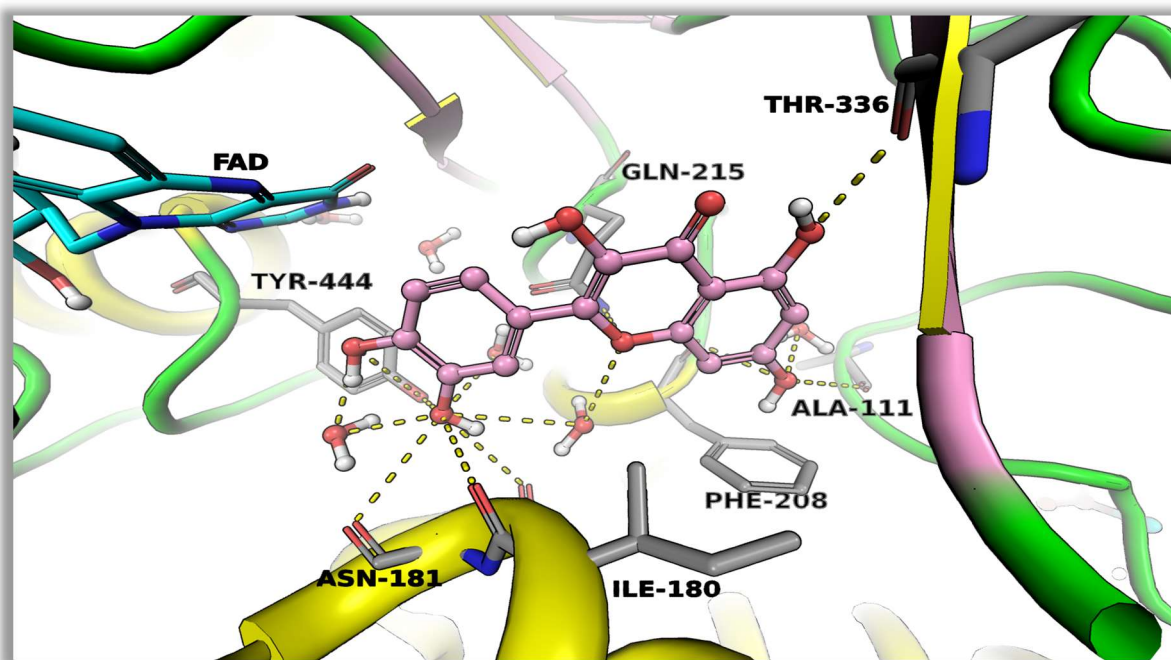


**Figure IV. 17.** The binding mode of quercetin in MAO A. Quercetin is shown as pink balls and sticks. The interacting amino acids are shown as grey sticks. Protein is shown as cartoon with yellow helices, pink strands and green loops. All possible hydrogen bonds in the range of 3.5 Å are shown as yellow dots.

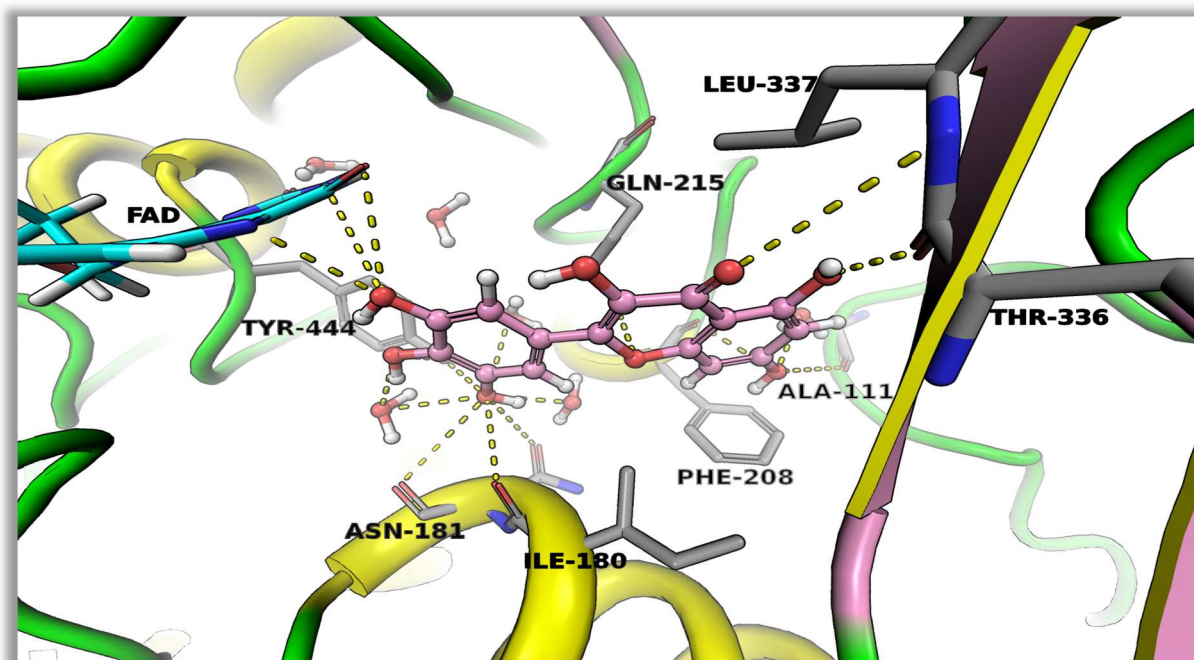


**Figure IV. 18.** The binding mode of myricetin in MAO A. Myricetin is shown as pink balls and sticks. The interacting amino acids are shown as grey sticks. Protein is shown as cartoon with yellow helices, pink strands and green loops. All possible hydrogen bonds in the range of 3.5 Å are shown as yellow dots.

### IV.9.2. MD Simulation

The binding modes and interaction profiles of compounds **HAF1** (Quercetin) and **HAF2** (Myricetin) were further investigated by performing MD simulations for 40 ns. The binding pose of compound **HAF1** was stable during the course of MD as demonstrated by root mean square deviation (RMSD) fluctuations of less than 1 Å. Several hydrogen bonds, hydrophobic contacts and interactions bridged by hydrogen bonded water molecules were found to be preserved during the MD simulation time (Figures IV.19 IV.20, 22, 23, 24 and 26). An intramolecular hydrogen bond was traced for 87% of the simulation time. Three stable hydrogen bonds were observed with Ala111, Asn181 and Gly443. We also observed that Phe208 formed a  $\pi$ - $\pi$  interaction with compound **HAF1** for 29% of the simulation time. In case of compound **HAF2** the fluctuations of RMSD through the simulation time was less 1 Å indicating stability of the docking pose. Similar to compound **HAF1**, a long-lived intramolecular hydrogen bond was monitored. Some interactions were found to be well-kept such as hydrogen bonds with Asn181, Tyr197, Phe208 and Gly443. In addition, Phe352 and Tyr407 showed stable  $\pi$ - $\pi$  contacts with compound **HAF2** (Figures IV. 21 and IV. 25).

#### - **HAF1** (Quercetin)

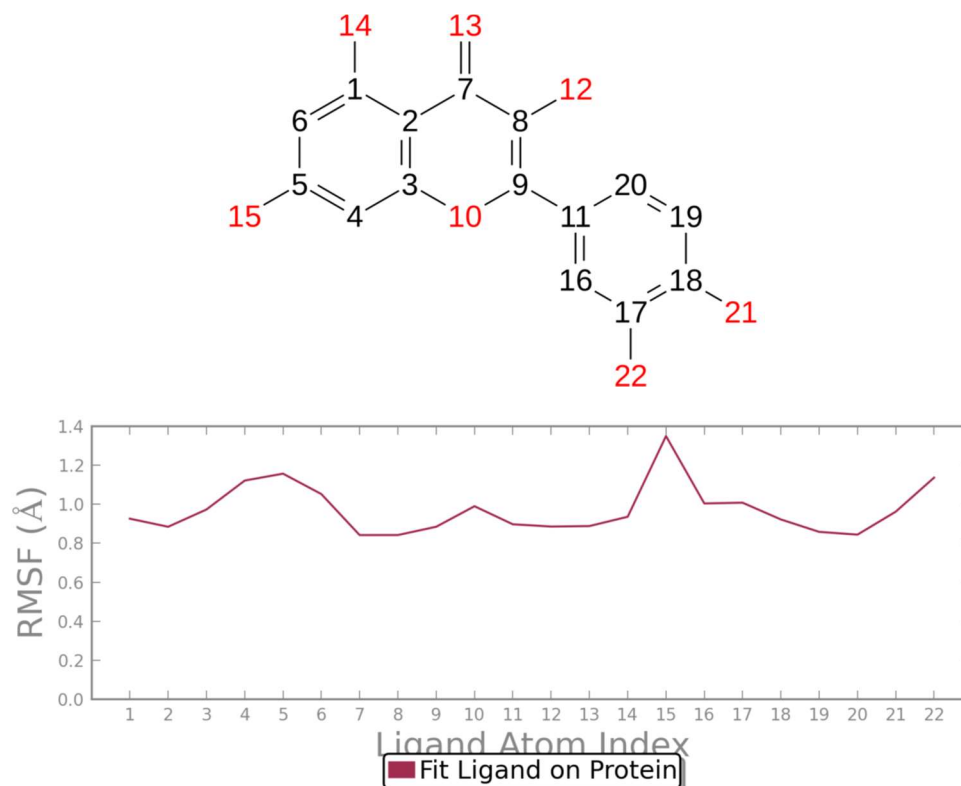


Figure IV. 19. Ligand RMSF (HAF1).



The Ligand Root Mean Square Fluctuation (L-RMSF) is useful for characterizing changes in the ligand atom positions. The RMSF for atom  $i$  is:

where  $T$  is the trajectory time over which the RMSF is calculated,  $T_{ref}$  is the reference time (usually for the first frame, and is regarded as the *zero* of time);  $r$  is the position of atom  $i$  in the reference at time  $T_{ref}$ , and  $r'$  is the position of atom  $i$  at time  $t$  after superposition on the reference frame.

Ligand RMSF shows the ligand's fluctuations broken down by atom, corresponding to the 2D structure in the top panel. The ligand RMSF may give you insights on how ligand fragments interact with the protein and their entropic role in the binding event. In the bottom panel, the 'Fit Ligand on Protein' line shows the ligand fluctuations, with respect to the protein. The protein-ligand complex is first aligned on the protein backbone and then the ligand RMSF is measured on the ligand heavy atoms.

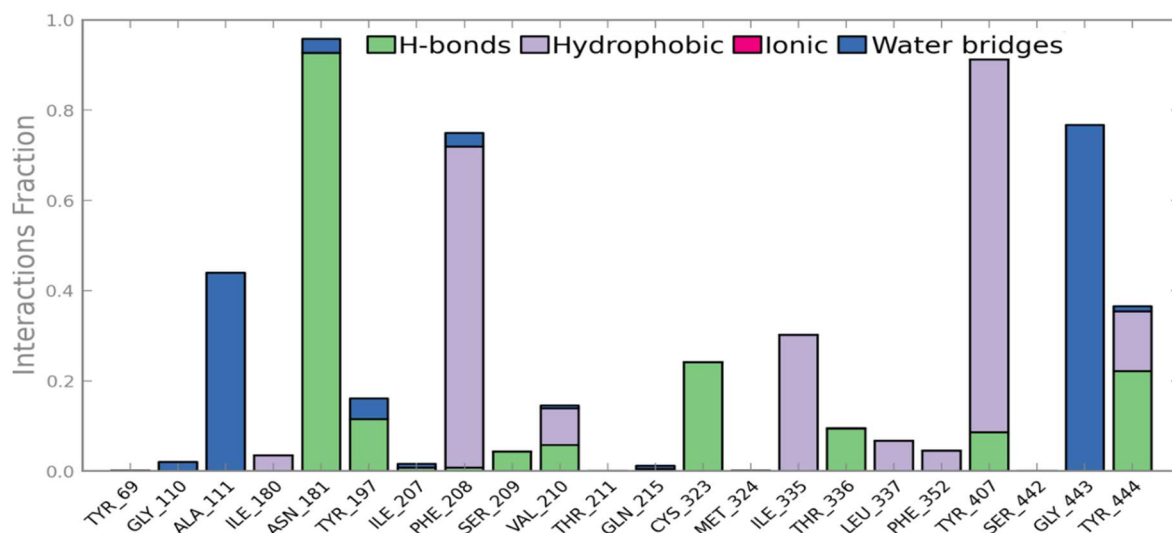


**Figure IV. 20.** Protein-ligand contacts of compound HAF1. Four types protein-ligand interactions were monitored throughout the simulation: hydrogen bond, hydrophobic, ionic and water bridges.

Protein interactions with the ligand can be monitored throughout the simulation. These interactions can be categorized by type and summarized, as shown in the plot above. Protein-ligand interactions (or 'contacts') are categorized into four types: Hydrogen Bonds, Hydrophobic, Ionic and Water Bridges. Each interaction type contains more specific subtypes, which can be explored through the 'Simulation Interactions Diagram' panel. The stacked bar charts are normalized over the course of the trajectory: for example, a value of 0.7 suggests that 70% of the simulation time the specific interaction is maintained. Values over 1.0 are possible as some protein residue may make multiple contacts of same subtype with the ligand.

**Hydrogen Bonds:** (H-bonds) play a significant role in ligand binding. Consideration of hydrogen-bonding properties in drug design is important because of their strong influence on drug specificity, metabolism and adsorption. Hydrogen bonds between a protein and a ligand can be further broken down into four subtypes: backbone acceptor; backbone donor; side-chain acceptor; side-chain donor. The current geometric criteria for protein-ligand H-bond is: distance of 2.5 Å between the donor and acceptor atoms (D—H···A); a donor angle of  $\geq 120^\circ$  between the donor-hydrogen-acceptor atoms (D—H···A); and an acceptor angle of  $\geq 90^\circ$  between the hydrogen-acceptor-bonded atom atoms (H···A—X).

**Hydrophobic contacts:** fall into three subtypes:  $\pi$ -Cation;  $\pi$ - $\pi$ ; and Other, non-specific interactions. Generally, these type of interactions involve a hydrophobic amino acid and an aromatic or aliphatic group on the ligand, but we have extended this category to also include  $\pi$ -Cation interactions. The current geometric criteria for hydrophobic interactions is as follows:  $\pi$ -Cation — Aromatic and charged groups within 4.5 Å;  $\pi$ - $\pi$  — Two aromatic groups stacked face-to-face or face-to-edge; Other — A non-specific hydrophobic sidechain within 3.6 Å of a ligand's aromatic or aliphatic carbons.

**Ionic interactions:** or polar interactions, are between two oppositely charged atoms that are within 3.7 Å of each other and do not involve a hydrogen bond. We also monitor Protein-Metal-Ligand interactions, which are defined by a metal ion coordinated within 3.4 Å of protein's and ligand's heavy atoms (except carbon). All ionic interactions are broken down into two subtypes: those mediated by a protein backbone or side chains.

**Water Bridges:** are hydrogen-bonded protein-ligand interactions mediated by a water molecule. The hydrogen-bond geometry is slightly relaxed from the standard H-bond definition.

The current geometric criteria for a protein-water or water-ligand H-bond are: a distance of 2.7 Å between the donor and acceptor atoms (D—H···A); a donor angle of  $\geq 110^\circ$  between the donor-hydrogen-acceptor atoms (D—H···A); and an acceptor angle of  $\geq 80^\circ$  between the hydrogen-acceptor-bonded atom atoms (H···A—X).

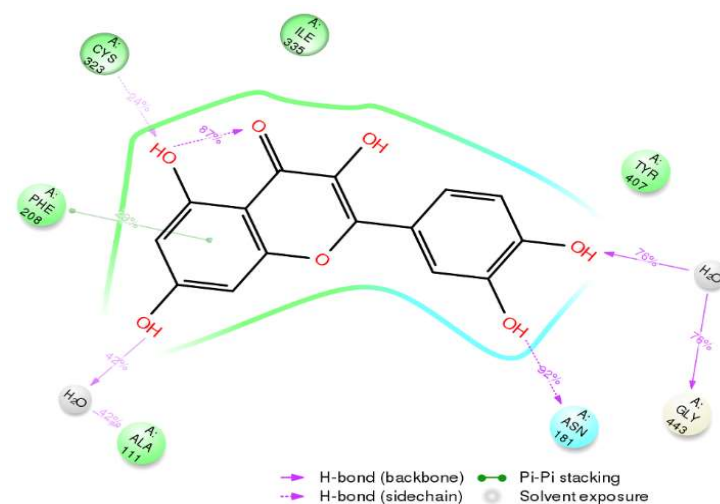


**Figure IV. 21.** 2D interaction diagram of the detailed ligand atom interactions of compound **HAF1** with the surrounding amino acid residues of MAO-A.

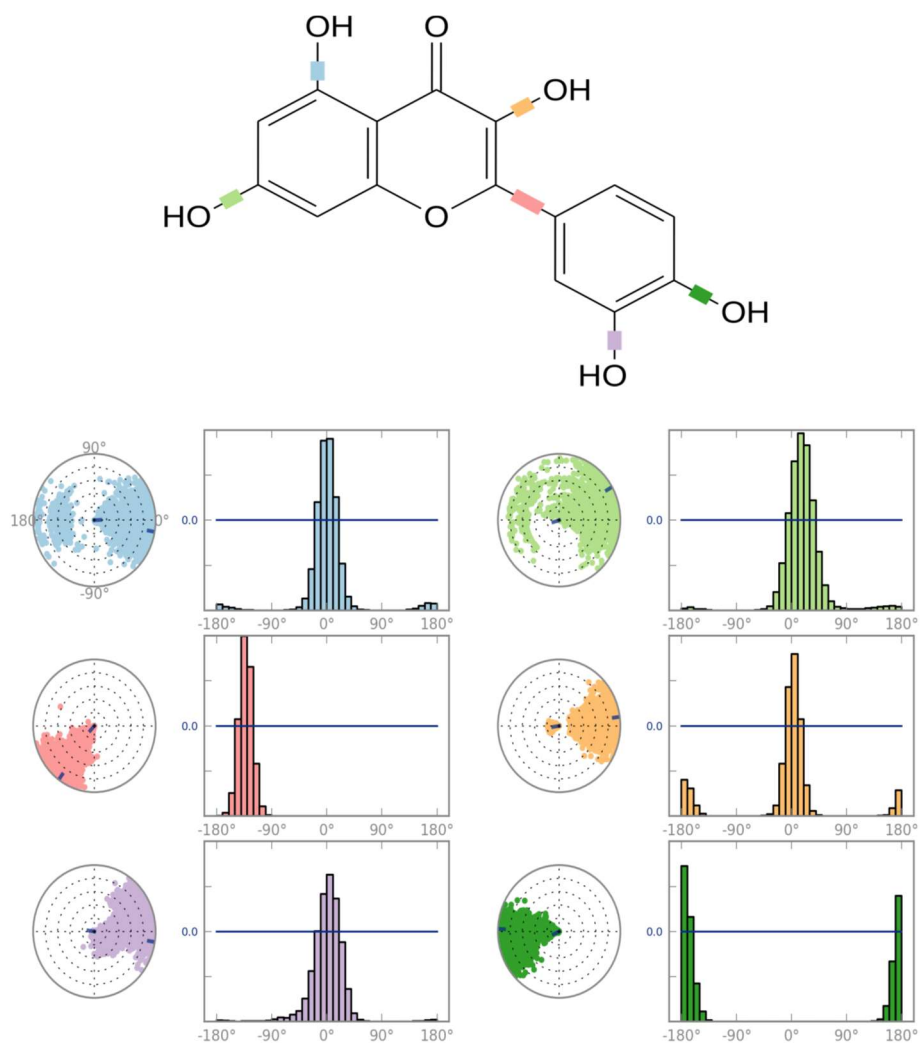


**Figure IV. 22.** Ligand Torsion Profile (**HAF1**).

The ligand torsions plot summarizes the conformational evolution of every rotatable bond (RB) in the ligand throughout the simulation trajectory (0.00 through 40.00 nsec). The top panel shows the 2d schematic of a ligand with color-coded rotatable bonds. Each rotatable bond torsion is accompanied by a dial plot and bar plots of the same color. Dial (or radial) plots describe the conformation of the torsion throughout the course of the simulation. The beginning of the simulation is in the center of the radial plot and the time evolution is plotted radially outwards. The bar plots summarize the data on the dial plots, by showing the probability density of the torsion. If torsional potential information is available, the plot also shows the potential of the rotatable bond (by summing the potential of the related torsions). The values of the potential are on the left Y-axis of the chart, and are expressed in *kcal/mol*. Looking at the histogram and torsion potential relationships may give insights into the conformational strain the ligand undergoes to maintain a protein-bound conformation.

- **HAF2** (Myricetin)

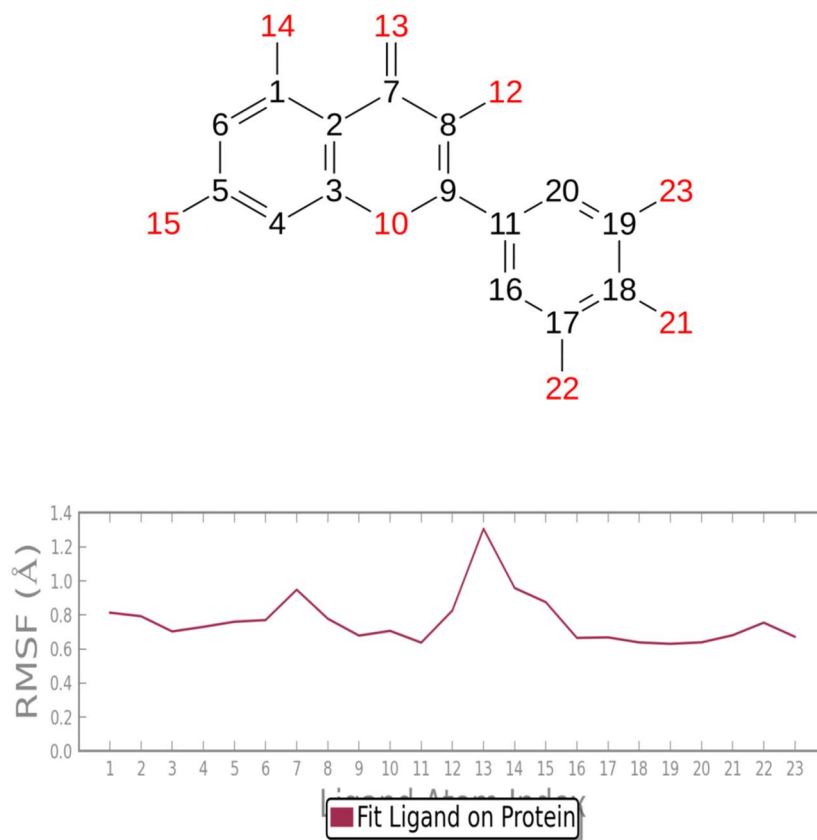


**Figure IV. 23.** Ligand RMSF (HAF2).

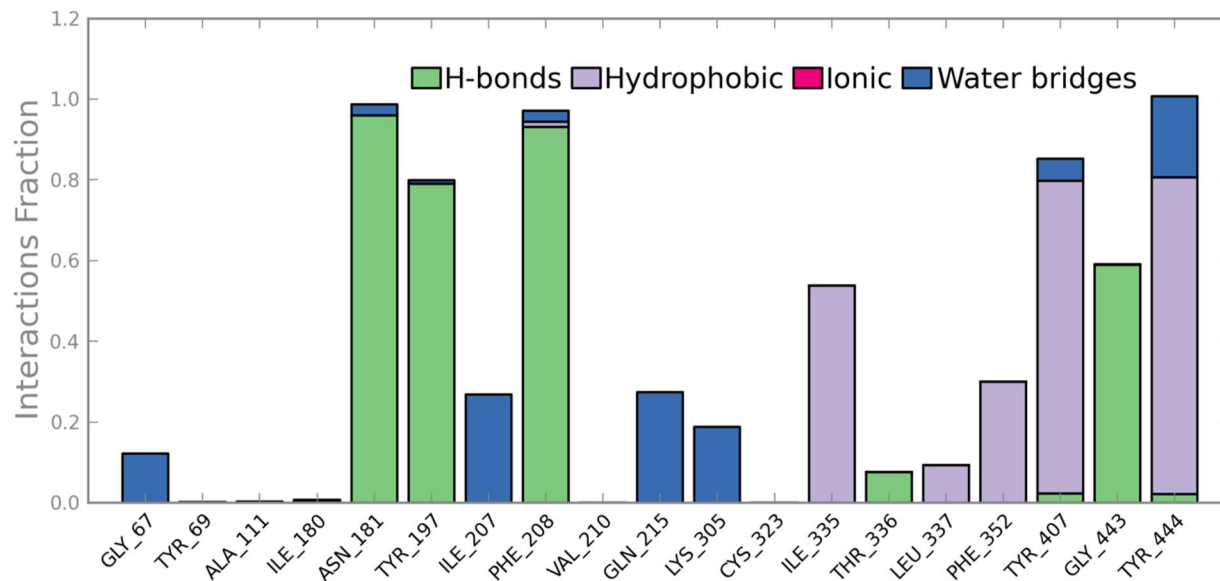


**Figure IV. 24.** Protein-ligand contacts of compound **HAF2**. Hydrogen bonds, hydrophobic, ionic and water bridges were monitored throughout the simulation.

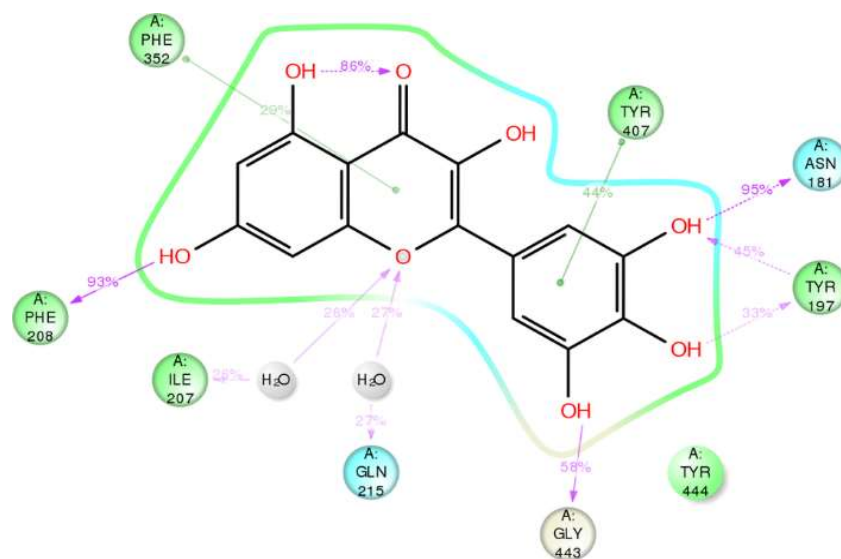


**Figure IV. 25.** 2D interaction diagram of compound **HAF2** with the amino acid residues of binding site of MAO-A.

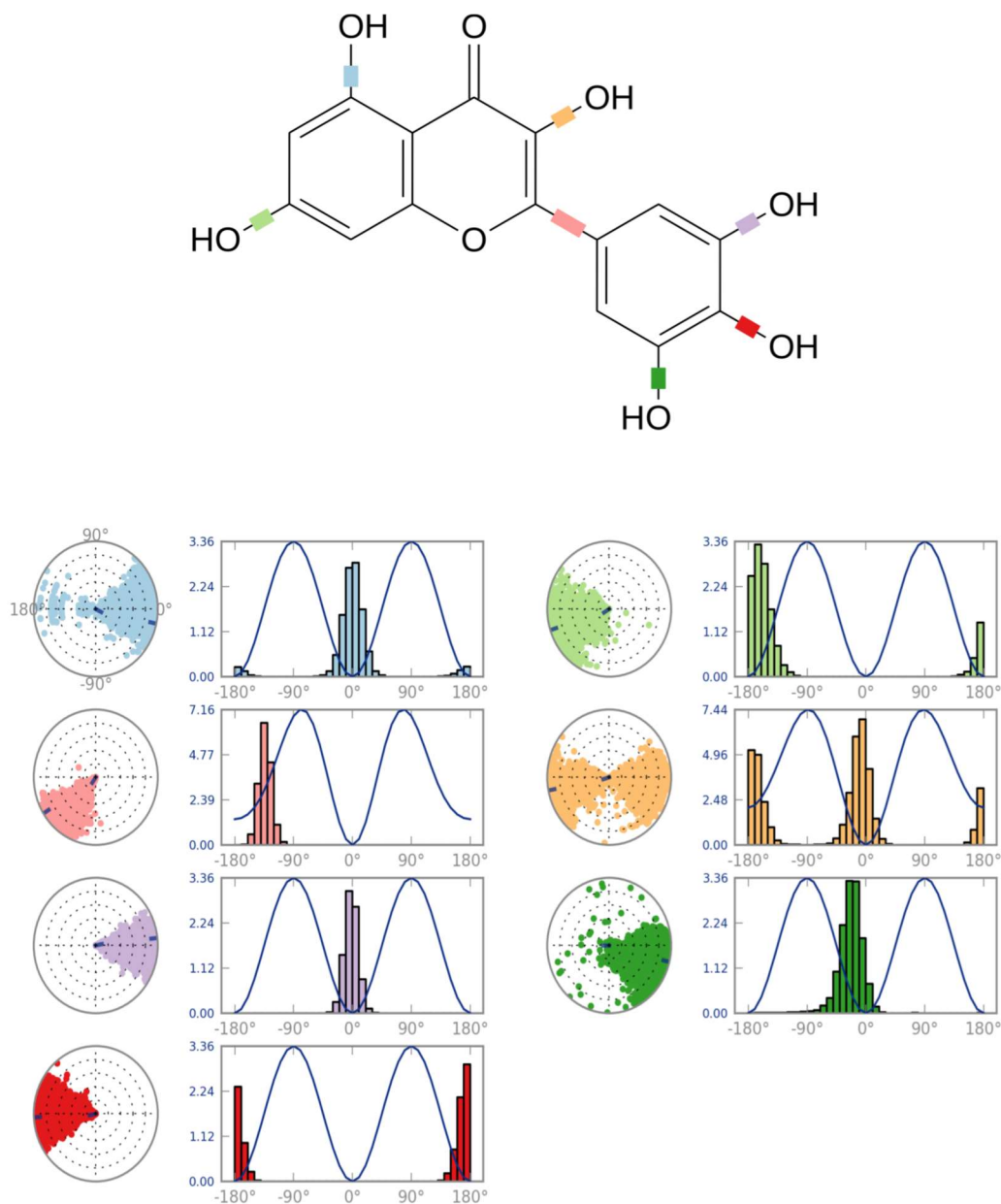


Figure IV. 26. Ligand Torsion Profile (HAF2).

### **IV.9.3. Conclusion**

- The docking and thermodynamic studies of chrysin, genistein, quercetin and myricetin with MAO-A and -B were considered, and these results are consistent with the experimental data.
- Genistein and chrysin displayed docking scores of -10.4 kcal/mol. -13.34 kcal/mol in MAO-A respectively.
- In case of chrysin, there is no 4'-hydroxyl group and the ligand oriented itself inside the binding pocket to have strong interactions with FAD, Ile180 and Asn181.
- Chrysin and genistein displayed docking scores of -12.22 and -11.51 kcal/mol in MAO B respectively.
- The binding pocket of MAO-B exhibited different thermodynamics to allow for higher polarity on the phenyl group compared to that of MAO A.
- Both compounds showed favorable interactions with the amino acid residues, water molecules and co-factor in the binding pocket.
- Quercetin showed a favorable docking pose in MAO A with a docking score of -11.3 kcal/mol.
- Myricetin forms strong hydrogen bonds with Ala111, Ile180, Asn181, and Thr336.
- Solvent molecules in the binding pocket play an important role in ligand stabilization as demonstrated by the strong hydrogen bonds with ligand atoms. The ligand showed hydrogen bonds and  $\pi$ - $\pi$  stacking with FAD.
- Energetically, the binding pose of quercetin is more favorable than that of myricetin, however, both compounds are fitting well inside the ligand binding pocket

## REFERENCES

- Adams, M., Gmünder, F., Hamburger, M., 2007. Plants traditionally used in age related brain disorders—A survey of ethnobotanical literature. *Journal of Ethnopharmacology* 113, 363-381.
- Allen, M.P., Tildesley, D.J., 1989. *Computer simulation of liquids*. Oxford university press.
- Baluchnejadmojarad, T., Roghani, M., Nadoushan, M.R.J., Bagheri, M., 2009. Neuroprotective effect of genistein in 6-hydroxydopamine Hemi-parkinsonian rat model. *Phytotherapy Research* 23, 132-135.
- Bandaruk, Y., Mukai, R., Kawamura, T., Nemoto, H., Terao, J., 2012. Evaluation of the inhibitory effects of quercetin-related flavonoids and tea catechins on the monoamine oxidase-A reaction in mouse brain mitochondria. *Journal of agricultural and food chemistry* 60, 10270-10277.
- Bandaruk, Y., Mukai, R., Terao, J., 2014. Cellular uptake of quercetin and luteolin and their effects on monoamine oxidase-A in human neuroblastoma SH-SY5Y cells. *Toxicology Reports* 1, 639-649.
- Barreca, M.L., Balzarini, J., Chimirri, A., Clercq, E.D., Luca, L.D., Höltje, H.D., Höltje, M., Monforte, A.M., Monforte, P., Pannecouque, C., 2002. Design, synthesis, structure-activity relationships, and molecular modeling studies of 2, 3-diaryl-1, 3-thiazolidin-4-ones as potent anti-HIV agents. *Journal of medicinal chemistry* 45, 5410-5413.
- Bortolato, M., Chen, K., Shih, J.C., 2010. 4-The Degradation of Serotonin: Role of MAO. *Handbook of Behavioral Neuroscience* 21, 203-218.
- Chimenti, F., Cottiglia, F., Bonsignore, L., Casu, L., Casu, M., Floris, C., Secci, D., Bolasco, A., Chimenti, P., Granese, A., 2006. Quercetin as the Active Principle of *Hypericum hircinum* Exerts a Selective Inhibitory Activity against MAO-A: Extraction, Biological Analysis, and Computational Study. *Journal of natural products* 69, 945-949.
- Choiprasert, W., Dechsupa, N., Kothan, S., Garrigos, M., Mankhetkorn, S., 2010. Quercetin, quercetrin except rutin potentially increased pirarubicin cytotoxicity by non-competitively inhibiting the P-glycoprotein-and MRP1 function in living K562/adr and GLC4/adr cells. *American Journal of Pharmacology and Toxicology* 5, 24-33.
- De Colibus, L., Li, M., Binda, C., Lustig, A., Edmondson, D.E., Mattevi, A., 2005. Three-dimensional structure of human monoamine oxidase A (MAO A): relation to the structures of rat MAO A and human MAO B. *Proceedings of the National Academy of Sciences of the United States of America* 102, 12684-12689.



- Dimas, K., Demetzos, C., Angelopoulou, D., Kolokouris, A., Mavromoustakos, T., 2000. Biological activity of myricetin and its derivatives against human leukemic cell lines in vitro. *Pharmacological Research* 42, 475-478.
- Ebbinghaus, S., Kim, S.J., Heyden, M., Yu, X., Heugen, U., Gruebele, M., Leitner, D.M., Havenith, M., 2007. An extended dynamical hydration shell around proteins. *Proceedings of the National Academy of Sciences* 104, 20749-20752.
- Edmondson, D., DeColibus, L., Binda, C., Li, M., Mattevi, A., 2007. New insights into the structures and functions of human monoamine oxidases A and B. *Journal of neural transmission* 114, 703-705.
- Edmondson, D.E., Binda, C., Mattevi, A., 2004. The FAD binding sites of human monoamine oxidases A and B. *Neurotoxicology* 25, 63-72.
- Edmondson, D.E., Binda, C., Wang, J., Upadhyay, A.K., Mattevi, A., 2009. Molecular and mechanistic properties of the membrane-bound mitochondrial monoamine oxidases. *Biochemistry* 48, 4220-4230.
- Frenkel, D., Smit, B., 2002. Understanding molecular simulation: from algorithms to applications. *Computational sciences series* 1, 1-638.
- Fu, G., Liu, H., Doerksen, R.J., 2012. Molecular modeling to provide insight into the substrate binding and catalytic mechanism of human biliverdin-IX $\alpha$  reductase. *The Journal of Physical Chemistry B* 116, 9580-9594.
- Gaweska, H., Fitzpatrick, P.F., 2011. Structures and mechanism of the monoamine oxidase family. *Biomolecular concepts* 2, 365-377.
- Guenard, D., Gueritte-Voegelein, F., Potier, P., 1993. Taxol and taxotere: discovery, chemistry, and structure-activity relationships. *Accounts of chemical research* 26, 160-167.
- Hare, E.E., Loer, C.M., 2004. Function and evolution of the serotonin-synthetic bas-1 gene and other aromatic amino acid decarboxylase genes in *Caenorhabditis*. *BMC evolutionary biology* 4, 1.
- He, X.-L., Wang, Y.-H., Bi, M.-G., Du, G.-H., 2012. Chrysin improves cognitive deficits and brain damage induced by chronic cerebral hypoperfusion in rats. *European journal of pharmacology* 680, 41-48.

- Hynson, R.M., Wouters, J., Ramsay, R.R., 2003. Monoamine oxidase A inhibitory potency and flavin perturbation are influenced by different aspects of pirlindole inhibitor structure. *Biochemical pharmacology* 65, 1867-1874.
- Jensen, J.H., 2010. *Molecular modeling basics*. CRC Press.
- Jiang, Y., Gong, F.-L., Zhao, G.-B., Li, J., 2014. Chrysin suppressed inflammatory responses and the inducible nitric oxide synthase pathway after spinal cord injury in rats. *International journal of molecular sciences* 15, 12270-12279.
- Jorgensen, W.L., 1998. OPLS force fields. *Encyclopedia of computational chemistry*.
- Kamel, A., Harriman, S., 2013. Inhibition of cytochrome P450 enzymes and biochemical aspects of mechanism-based inactivation (MBI). *Drug Discovery Today: Technologies* 10, e177-e189.
- Kandhare, A.D., Shivakumar, V., Rajmane, A., Ghosh, P., Bodhankar, S.L., 2014. Evaluation of the neuroprotective effect of chrysin via modulation of endogenous biomarkers in a rat model of spinal cord injury. *Journal of natural medicines* 68, 586-603.
- Karplus, M., McCammon, J.A., 2002. Molecular dynamics simulations of biomolecules. *Nature Structural & Molecular Biology* 9, 646-652.
- Karplus, M., Petsko, G.A., 1990. Molecular dynamics simulations in biology. *Nature* 347, 631-639.
- Klabunde, R.E., 2009. *Cardiovascular pharmacology concepts*. Retrieved, Indianapolis, Indiana.
- Koga, H., Itoh, A., Murayama, S., Suzue, S., Irikura, T., 1980. Structure-activity relationships of antibacterial 6, 7-and 7, 8-disubstituted 1-alkyl-1, 4-dihydro-4-oxoquinoline-3-carboxylic acids. *Journal of medicinal chemistry* 23, 1358-1363.
- Lamartiniere, C.A., Zhang, J.-X., Cotroneo, M.S., 1998. Genistein studies in rats: potential for breast cancer prevention and reproductive and developmental toxicity. *The American journal of clinical nutrition* 68, 1400S-1405S.
- Lee, S.-J., Chung, H.-Y., Lee, I.-K., Oh, S.-U., Yoo, I.-D., 2000. Phenolics with inhibitory activity on mouse brain monoamine oxidase (MAO) from whole parts of *Artemisia vulgaris* L (Mugwort). *Food Science and Biotechnology* 9, 179-182.
- Maciel, R., Costa, M., Martins, D., Franca, R., Schmatz, R., Graca, D., Duarte, M., Danesi, C., Mazzanti, C., Schetinger, M., 2013. Antioxidant and anti-inflammatory effects of quercetin in functional and morphological alterations in streptozotocin-induced diabetic rats. *Research in veterinary science* 95, 389-397.

- Nandi, S., Bagchi, M.C., 2010. 3D-QSAR and molecular docking studies of 4-anilinoquinazoline derivatives: a rational approach to anticancer drug design. *Molecular diversity* 14, 27-38.
- Olsen, H.T., Stafford, G.I., van Staden, J., Christensen, S.B., Jäger, A.K., 2008. Isolation of the MAO-inhibitor naringenin from *Mentha aquatica* L. *Journal of Ethnopharmacology* 117, 500-502.
- Pan, H., Hu, Q., Wang, J., Liu, Z., Wu, D., Lu, W., Huang, J., 2016. Myricetin is a novel inhibitor of human inosine 5'-monophosphate dehydrogenase with anti-leukemia activity. *Biochemical and Biophysical Research Communications* 477, 915-922.
- Pekcan, Ö., Evingür, G.A., Uğur, Ş., Yelekçi, K., Uçar, G., Yargı, Ö., Erim, B.F., Gökhan-Kelekçi, N., Kaygusuz, H., Doğruyol, S.K., Monoamin oksidaz (MAO) inhibitör etkili yeni prazolin türevlerinin moleküler modelleme yöntemiyle tasarlanması, sentezi ve inhibisyon kinetiklerinin hesapsal ve deneysel olarak tayini.
- Pushpavalli, G., Kalaiarasi, P., Veeramani, C., Pugalendi, K.V., 2010. Effect of chrysin on hepatoprotective and antioxidant status in D-galactosamine-induced hepatitis in rats. *European journal of pharmacology* 631, 36-41.
- Sarkar, F.H., Adsule, S., Padhye, S., Kulkarni, S., Li, Y., 2006. The role of genistein and synthetic derivatives of isoflavone in cancer prevention and therapy. *Mini reviews in medicinal chemistry* 6, 401-407.
- Schrader, E., 2000. Equivalence of St John's wort extract (Ze 117) and fluoxetine: a randomized, controlled study in mild/moderate depression. *International clinical psychopharmacology* 15, 61-68.
- Sloley, B., Urchuk, L., Morley, P., Durkin, J., Shan, J., Pang, P., Coutts, R., 2000. Identification of kaempferol as a monoamine oxidase inhibitor and potential neuroprotectant in extracts of *Ginkgo biloba* leaves. *Journal of pharmacy and pharmacology* 52, 451-459.
- Song, J.-X., Sze, S.C.-W., Ng, T.-B., Lee, C.K.-F., Leung, G.P., Shaw, P.-C., Tong, Y., Zhang, Y.-B., 2012. Anti-Parkinsonian drug discovery from herbal medicines: what have we got from neurotoxic models? *Journal of ethnopharmacology* 139, 698-711.
- Spencer, J.P., 2009. Flavonoids and brain health: multiple effects underpinned by common mechanisms. *Genes & nutrition* 4, 243-250.
- Sun, F., Zheng, X.Y., Ye, J., Wu, T.T., Wang, J.L., Chen, W., 2012. Potential anticancer activity of myricetin in human T24 bladder cancer cells both in vitro and in vivo. *Nutrition and cancer* 64, 599-606.

- Tarek, M., Tobias, D., 2002. Role of protein-water hydrogen bond dynamics in the protein dynamical transition. *Physical Review Letters* 88, 138101.
- Thomas, T., 2000. Monoamine oxidase-B inhibitors in the treatment of Alzheimers disease. *Neurobiology of aging* 21, 343-348.
- VARNALI, F., 2012. DESIGNING INHIBITORS VIA MOLECULAR MODELLING METHODS FOR MONOAMINE OXIDASE ISOZYMES A AND B. Kadir Has University.
- Vauzour, D., Rodriguez-Mateos, A., Corona, G., Oruna-Concha, M.J., Spencer, J.P., 2010. Polyphenols and human health: prevention of disease and mechanisms of action. *Nutrients* 2, 1106-1131.
- Williams, R.J., Spencer, J.P., 2012. Flavonoids, cognition, and dementia: actions, mechanisms, and potential therapeutic utility for Alzheimer disease. *Free Radical Biology and Medicine* 52, 35-45.
- Wu, S., Yue, Y., Peng, A., Zhang, L., Xiang, J., Cao, X., Ding, H., Yin, S., 2016. Myricetin ameliorates brain injury and neurological deficits via Nrf2 activation after experimental stroke in middle-aged rats. *Food & function*.
- Yamada, M., Yasuhara, H., 2004. Clinical pharmacology of MAO inhibitors: safety and future. *Neurotoxicology* 25, 215-221.
- Youdim, M.B., Weinstock, M., 2004. Therapeutic applications of selective and non-selective inhibitors of monoamine oxidase A and B that do not cause significant tyramine potentiation. *Neurotoxicology* 25, 243-250.
- Zhang, Z.J., Cheang, L.C.V., Wang, M.W., Lee, S.M.-Y., 2011. Quercetin exerts a neuroprotective effect through inhibition of the iNOS/NO system and pro-inflammation gene expression in PC12 cells and in zebrafish. *International journal of molecular medicine* 27, 195.

*GENERAL SUMMARY*

## General Summary, Conclusion and Perspectives

### Phytochemical and Biological Studies of Two Algerian Medicinal Plants: *Cytisus villosus* Pourr. (Fabaceae) and *Hypericum afrum* Lam. (Hypericaceae)

*Cytisus villosus* Pourr. is a plant belonging to the Fabaceae family (Papilionaceae). This species frequently growing in France, Italy, Spain, Portugal, Algeria and Tunisia. In Algeria, it is common in the region of the Tell Algéro-constantinois.. Numerous works reported that *Cytisus* showed antioxidant and cytoprotective activities, diuretic, hypnotic, anxiolytic, antiparasitic and antidiabetic effects. According to previous studies, *Cytisus* genus contain a high composition of polyphenol compounds, including flavonoids, that can explain their bioactivities. *Hypericum afrum lam.*, is an endemic species from Northeastern Algeria, belonging to the Hypericaceae (Guttiferae) family. Due to their many therapeutic properties, a number of studies have been previously reported on *Hypericum* genus, showing the diversity of the species plant in secondary metabolite which their pharmacology importance has been reported. *Hypericum* genus has a high reputation as a wound-healing and an anti-inflammatory drug. However, the current use of the plant is mainly consistent with an antidepressant. The high biological value of *Hypericum* has worldwide led to an increased interest for the study of the chemical and pharmacological properties of other related species. However, this is the first phytochemical and biological investigation on *Hypericum afrum* species.

The aim of this study was to investigate the secondary metabolite and the biological activity of the two species *C. villosus* and *H. afrum*. The present study includes the following topics:

- ❖ **A review** of the background information about the two plants as sources of natural products (**Part I: Chapter 1**)
- ❖ **Phytochemical study of *Cytisus villosus*** (**Part II: Chapter 1**)  
Including the phytochemical screening, extraction, fractionation, isolation and identification of the constituents of the plant aerial parts.
- ❖ **Phytochemical study of *Hypericum afrum*** (**Part II: Chapter 2**)  
Including the phytochemical screening, extraction, fractionation, isolation and identification of the different constituents of the flowers and leaves of the plant.
- ❖ **Biological Study of the plant under investigation (Part III)** including:

1. Opioid and cannabinoid receptors binding assay.
2. Antimalarial assay.
3. Antimicrobial assay
4. Cytotoxicity
5. Antioxidant & Anti-inflammatory assays
6. Antiprotozoal assay
7. MAOIs assay

❖ **Molecular modeling (Part IV)** including:

- Ligand Preparation
- Protein Preparation
- Receptor grid preparation
- Docking simulations
- Molecular dynamics simulations

## Part II: Chapter 1

### Phytochemical screening, extraction, fractionation and isolation of constituents of *Cytisus villosus*

- **Total phenolic and flavonoid content**

*C. villosus* fractions of ethanolic crud extract were analyzed for their phenolics and flavonoids content. The highest phenolic content was found in the butanilic fraction (363 mgGAE/g dried extract) followed by ethyl acetate fraction (208 mgGAE/g dried extract), and chloroform fraction (56 mgGAE/g dried extract). The results of Flavonoid content were expressed as mg of Quercetin per g dried extract. The value of TFC. Of fractions from *C. villosus* ranged between (7.7 and 21.16 mg Quercetin/ g dried extract, respectively). The results are shown in table 1.

- **Extraction and fractionation**

Dried powdered aerial parts of *Cytisus villosus* Pourr. (1000 g) were macerated with ETOH-H<sub>2</sub>O (80:20, v/v) to give 25 g residue. Initial fractionation of the ethanolic extract gave three main fractions after partitionation of the resulted residue with CHCl<sub>3</sub>, EtOAc and *n*-butanol.

- **Alkaloid extraction**

Dried powdered aerial parts of of *Cytisus villosus* Pourr. were extracted with with EtOH–H<sub>2</sub>O (80:20, v/v) for 24 h. The combined extracts were concentrated, acidified with hydrochloric acid

(0.1 M) and then, extracted with chloroform. The aqueous layer was made alkaline with ammonium hydroxide to pH (10-12). The chloroform extracts were combined and dried over anhydrous sodium sulfate and evaporated to give crude alkaloid mixture.

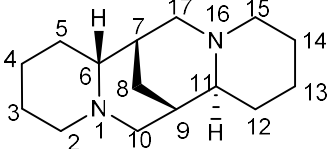
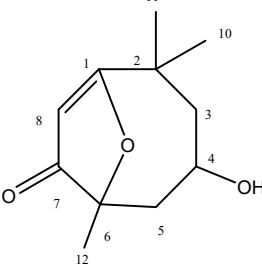
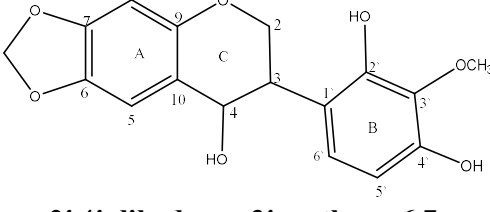
• **Isolation of the active constituents**

Nine compounds had been isolated from aerial parts of *Cytisus villosus* using different chromatographic techniques including column chromatographic fractionation on Diaion-HP-20, MN-polyamide- SC-6, SPE C-18, Silica gel, and Sephadex LH-20.

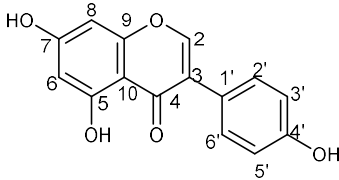
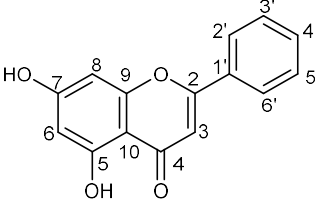
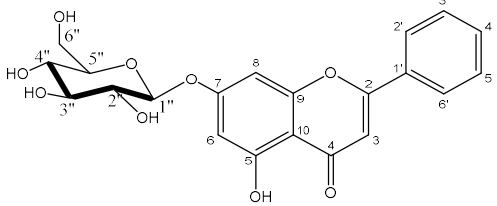
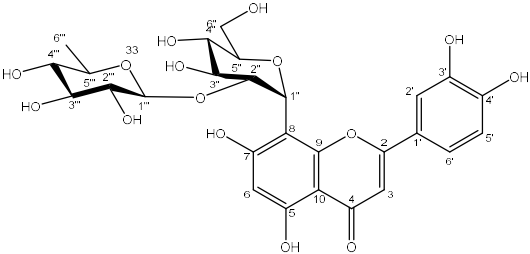
• **Identification and structure elucidation of the isolated compounds**

The structure elucidation of isolated compounds was deduced on the basis of spectroscopic methods: (UV, IR, <sup>1</sup>H-NMR, <sup>13</sup>C-NMR, <sup>1</sup>H-<sup>1</sup>H COSY, HMQC, HMBC, NOESY, ROESY, HR-ESI-MS and ESI-MS), in addition to ECD analysis. A list of the identified compounds was recorded in table 1.

**Table 1.** A list of the isolated compounds from *Cytisus villosus* aerial parts

No.	Code	Type	Structure & Name	Comment
1	CVK1	Alkaloid	 <p><b>Sparteine</b></p>	Previously isolated from the genus <i>Cytisus</i>
2	CVT1	Terpenoid	 <p><b>4-hydroxy-2,2,6-trimethyl-9-oxabicyclo[4.2.1]non-1(8)-en-7-one</b></p>	New compound
3	CVS1	4-hydroxyisoflavan	 <p><b>2',4'-dihydroxy-3'-methoxy-6,7-methylenedioxyisoflavan-4-ol</b></p>	New compound



4	CVS2	Isoflavone	 <p style="text-align: center;"><b>Genistein</b></p>	Previously isolated from the genus <i>Cytisus</i>
5	CVF1	Flavone	 <p style="text-align: center;"><b>Chrysin</b></p>	Previously isolated From the genus <i>Cytisus</i>
6	CVF2	Flavonoid glycoside	 <p style="text-align: center;"><b>Chrysin-7-O-β-D-glucopyranoside</b></p>	Previously isolated from the genus <i>Cytisus</i>
7	CVF3	Flavonoid glycoside	 <p style="text-align: center;"><b>2''-O-α-L-rhamnosylorientin</b></p>	Isolated for first time from the genus <i>Cytisus</i>

## Part II: Chapter 2

### Phytochemical screening, extraction, fractionation and isolation of constituents of

#### *Hypericum afrum*

- **Total phenolic and flavonoid content**

*Hypericum afrum* fractions of ethanolic crud extract were analyzed for their phenolics and flavonoids content.

The highest phenolic content was found in the butanilc fraction (393 mg GAE/g dried extract) followed by ethyl acetate fraction (386 mg GAE/g dried extract), and chloroform fraction (260mgGAE/g dried extract)

The results of Flavonoid content were expressed as mg of Quercetin per g dried extract. The highest value of TFC. Both CHCl<sub>3</sub> and EtOAc fractions exhibited high TFC values for *H. afrum* (40,49 and 38,081 mg Quercetin/ g dried extract, respectively).

- **Extraction and fractionation**

Dried powdered aerial parts of *Hypericum afrum*. (1000 g) were macerated with ETOH-H<sub>2</sub>O (80:20, v/v) to give 30 g residue. Initial fractionation of the ethanolic extract gave three main fractions after partitionation of the resulted residue with CHCl<sub>3</sub>, EtOAc and *n*-butanol.

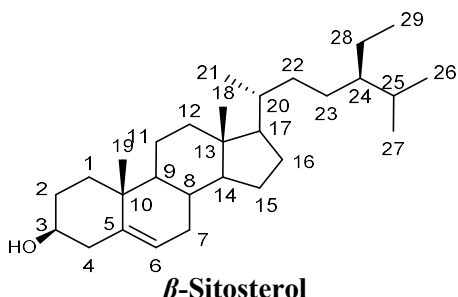
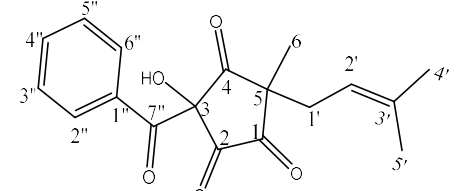
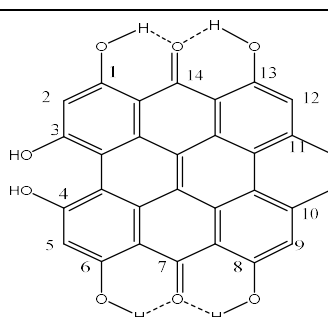
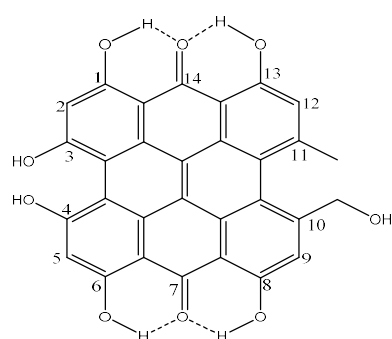
- **Isolation of the active constituents**

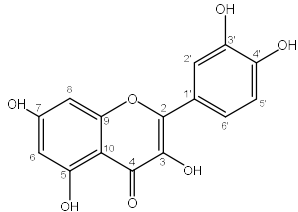
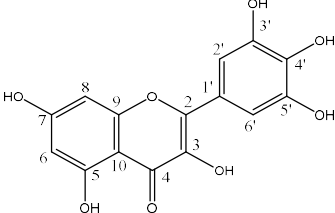
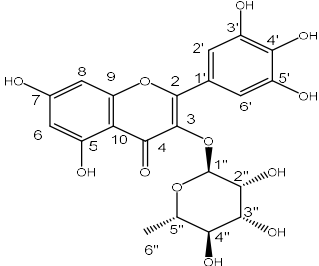
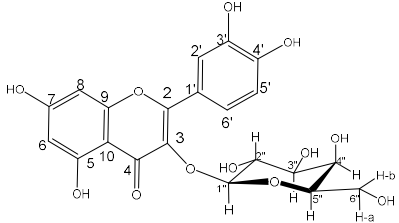
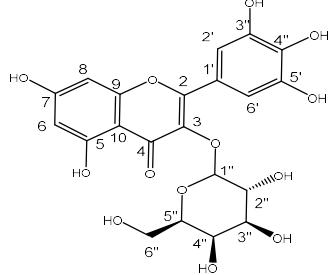
Thirteen compounds had been isolated from aerial parts of *Mussaenda luteola* using different chromatographic techniques including semi preparative HPLC, column chromatographic fractionation on Diaion-HP-20, MN-polyamide- SC-6, Silica gel, and Sephadex LH-20.

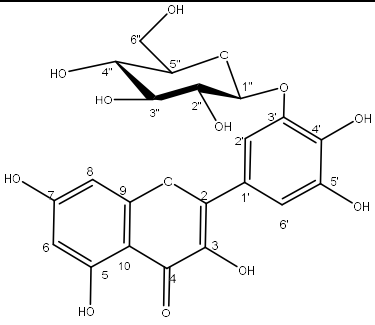
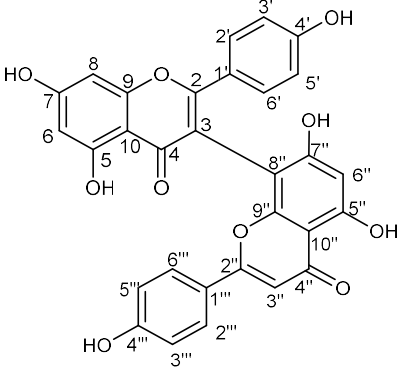
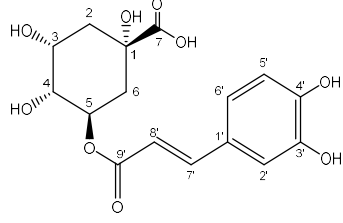
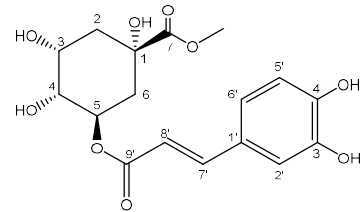
- **Identification and structure elucidation of the isolated compounds**

The structure elucidation of isolated compounds was deduced on the basis of spectroscopic methods: (UV, IR, <sup>1</sup>H-NMR, <sup>13</sup>C-NMR, <sup>1</sup>H-<sup>1</sup>H COSY, HMQC, HMBC, NOESY, ROESY and HR-ESI-MS). A list of the identified compounds was recorded in the following table:

**Table 2.** A list of the isolated compounds from *Hypericum afrum* aerial parts

No.	Code	Type	Structure & Name	Comment
1	HAT1	Phytosterol	 <p><b><math>\beta</math>-Sitosterol</b></p>	Previously isolated from the genus <i>Hypericum</i>
2	HAP1	Phloroglucinol	 <p><b>3-Benzoyl-3-hydroxy-5-(3-methylbut-2-en-1-yl) cyclopentane-1,2,4-trione</b></p>	New compound
3	HAN1	Naphthodianthrone	 <p><b>Hypericin</b></p>	Previously isolated from the genus <i>Hypericum</i>
4	HAN2	Naphthodianthrone	 <p><b>Pseudohypericin</b></p>	Previously isolated from the genus <i>Hypericum</i>

5	HAF1	Flavonol	 <p style="text-align: center;"><b>Quercetin</b></p>	Previously isolated from the genus <i>Hypericum</i>
6	HAF2	Flavonol	 <p style="text-align: center;"><b>Myricetin</b></p>	Previously isolated from the genus <i>Hypericum</i>
7	HAF3	Flavonoid glycoside	 <p style="text-align: center;"><b>Myricetin-3-O-<math>\alpha</math>-L-rhamnopyranoside</b></p>	Previously isolated from the genus <i>Hypericum</i>
8	HAF4	Flavonoid glycoside	 <p style="text-align: center;"><b>Quercetin-3-O-<math>\beta</math>-D-galactopyranoside</b></p>	Previously isolated from the genus <i>Hypericum</i>
9	HAF5	Flavonoid glycoside	 <p style="text-align: center;"><b>Myricetin-3-O-<math>\beta</math>-D-galactopyranoside</b></p>	Previously isolated from the genus <i>Hypericum</i>

10	<b>HAF6</b>	Flavonoid glycoside	 <p><b>Myricetin-3'-O-β-D-glucopyranoside</b></p>	Isolated for the first time from the genus <i>Hypericum</i>
11	<b>HAB1</b>	Biflavone	 <p><b>Biapigenin</b></p>	Previously isolated from the genus <i>Hypericum</i>
12	<b>HAC1</b>	Cinnamic acid	 <p><b>Chlorogenic acid</b></p>	Previously isolated from the genus <i>Hypericum</i>
13	<b>HAC2</b>	Cinnamic acid	 <p><b>Chlorogenic acid methyl ester</b></p>	Previously isolated from the genus <i>Hypericum</i>

### Part III: Biological Study

#### 1. Opioid and cannabinoid receptors binding assay

- All fractions and isolated pure compounds tested were inactive.

#### 2. Antimalarial assay

- Compound HAF6, myricetin-3'-O- $\beta$ -D-glucopyranoside, showed weak antiplasmodial activity against the chloroquine-sensitive (D6) and resistant (W2) *Plasmodium falciparum* with IC<sub>50</sub> values of 4.53 (SI, >1.1) and 3.93 (SI, >1.2)  $\mu$ g/mL, respectively.

#### 3. Antimicrobial assay

- All fractions and isolated pure compounds tested didn't show activity.

#### 4. Antiprotozoal assay

- The antiprotozoal activity of the plants fractions and certain pure isolated compounds were evaluated in vitro against *L. donovani* promastigotes, axenic amastigotes and intracellular amastigotes in THP1 cells, they were also evaluated against *T. brucei* trypomastigote forms.
- All the samples were simultaneously tested against THP1 cell for determination of general cytotoxicity.
- Regarding antitrypanosomal activity, the chloroform, ethyl acetate and butanol fractions of *H. afrum* species showed potent antitrypanosomal activity against *T. brucei* trypomastigotes culture with IC<sub>50</sub> values of 12.35, 13.53, 12.93 and with IC<sub>90</sub> values of 14.94, 19.31, 18.67  $\mu$ g/mL, respectively.
- The ethyl acetate fraction of *C. villosus* showed weakly antitrypanosomal activity against *T. brucei* trypomastigotes culture with IC<sub>50</sub> values of 19.48  $\mu$ g/mL.
- The *n*-butanol fraction of *C. villosus* showed highly potent antitrypanosomal activity against *T. brucei* with IC<sub>50</sub> values of 7.99 and IC<sub>90</sub> values of 12.61  $\mu$ g/mL.
- Compounds HAF1 (quercetin) and HAF2 (myricetin), isolated from *H. afrum* ethyl acetate fraction showed potent activity toward *T. brucei* with IC<sub>50</sub> values of 7.52 and 5.71 and with IC<sub>90</sub> values of 9.76 and 7.97  $\mu$ M, respectively.
- Compound HAT1 namely  $\beta$ -sitosterol isolated from *H. afrum* chloroform fraction showed highly potent antitrypanosomal activity with IC<sub>50</sub> values of 0.98  $\mu$ M and with IC<sub>90</sub> values of 1.34  $\mu$ M, which are more efficient than the DFMO, the antitrypanosomal drug employed as positive control (IC<sub>50</sub> and IC<sub>90</sub> values 3.634 and 8.804  $\mu$ M).

- Compound CVK1 namely sparteine. isolated from *C. villosus* Alkaloid fraction showed potent activity toward *T. brucei* with IC<sub>50</sub> values of 7.67 μM.
- No one of the fractions or compounds tested showed antileishmanial activity
- All fractions of the ethanolic crud extracts of both plants and all the compounds tested were found to be active against intracellular leishmania amastigotes in THP1 cells.

## 5. Cytotoxicity

- All fractions tested were inactive.
- Compound HAF1 showed moderate activity against LLC-PK1 (IC<sub>50</sub> value of 36 μM).
- Compound HAB1 was weakly active against SK-MEL, KB, BT-549 and SK-OV-3 with IC<sub>50</sub> values of 30, 33, 38 and 48 μM, respectively.

## 6. Antioxidant & Anti-inflammatory assays

- Our results showed that the antioxidant activities of the chloroform and ethyl acetate fractions of *H. afrum* in term of radical scavenging activity, using DPPH assay, were higher comparable to those of the *n*-butanol fraction of the same plant.
- The chloroform, ethyl acetate and butanol fractions of *C. villosus* showed all moderate antioxidant activities in term of radical scavenging activity, using DPPH assay.
- All tested fractions of *H. afrum* were shown to decrease cellular oxidative stress by inhibiting ROS generation (Table III.14).
- Compounds HAF1, HAF2 from ethyl acetate fraction of *H. afrum* showed potent effect against oxidative stress (inhibition values of 83 and 65%, respectively)
- Compounds HAF3, HAF4 and HAF6 from the *n*-butanol fraction showed considerable effect against oxidative stress (inhibition values of 53, 64 and 58 %, respectively), however, these compounds were lower potent than HAF1 and HAF2 as shown in Table III.14.
- *C. villosus* tested fractions showed weak effect against oxidative stress (inhibition values ranged between 29 and 36%).
- Compounds CVF1, CVF2 and CVS2 from *C. villosus* tested for their effect against oxidative stress were not effective. While compound CVF3 showed weak antioxidant activity (inhibition values of 36% at 1000 μg/mL).

- Regarding the results of the evaluation of anti-inflammatory activity, *H. afrum* fractions did not show any inhibition of iNOS and therefore did not affect cellular nitric oxide levels in lipopolysaccharide (LPS)-treated macrophages.
- Compounds HAF1 and HAB1 isolated from *H. afrum* ethyl acetate fraction showed moderate inhibition of iNOS (with IC<sub>50</sub> values of 12 and 22 µg/mL, respectively).
- The ethyl acetate and *n*-butanol fractions of *C. villosus* showed moderate inhibition of iNOS (IC<sub>50</sub> values of 48 and 90 µg/mL, respectively).
- Compounds CVF2 and CVS2 isolated from *C. villosus* ethyl acetate fraction showed mild inhibition of iNOS with IC<sub>50</sub> values of 20 and 9 µg/mL, respectively.
- The increase in transcriptional activity of NF-κB in PMA-treated cells was also not suppressed by the plant's fractions and isolated compounds (with the exception of compounds CVS2 and CVF1, which showed moderate inhibition of NF-κB with IC<sub>50</sub> values of 28 and 38 µg/mL, respectively).

### 7. MAOIs assay

- The ethyl acetate fractions (EtOAc) of the two plants showed potent MAO-A and B inhibitory activities with IC<sub>50</sub> values of 3.375 µg/ml and 5.625 µg/ml for MAO-A and IC<sub>50</sub> values of 13.50 µg/mL and 1.875 µg/mL for MAO-B, respectively.
- The inhibition of MAO-A by EtOAc fraction of *H. afrum* was 4-fold more potent (IC<sub>50</sub>: 3.375 µg/ml) as compared to the inhibition of MAO-B (IC<sub>50</sub> value of 13.50 µg/ml), while the inhibition of MAO-B (IC<sub>50</sub> 1.875 µM) by EtOAc fraction of *C. villosus* was 3-fold more potent as compared to the inhibition of MAO-A (IC<sub>50</sub> value of 5.625 µM).
- Bioassay-guided fractionation resulted in the isolation and identification of quercetin (**HAF1**), myricetin (**HAF2**), genistein (**CVS2**) and chrysin (**CVF1**) as the active constituents.
- The results of our study revealed that both studied plants have properties indicative of potential neuroprotective ability. They may serve as new candidates for selective MAO-A and B inhibitors. The MAO-inhibiting activity of *H. afrum* and *C. villosus* fractions was primarily due to the presence of flavonoids such as quercetin, myricetin, genistein and chrysin.
- Comparison of the IC<sub>50</sub> values of related flavonoids quercetin, myricetin, mericitrin, myricetin 3-glucoside, myricetin 3'-glucoside, hyperoside, Chrysin 7-O-β-D-glucosidechrysin, and 2"-O-α-L-rhamnosylorientin gave us an idea about its structural



requirements.

- The above observations inspired us to use docking simulation to investigate the binding modes of quercetin, myricetin, chrysin and genistein in the structurally similar ligand binding pockets of MAO-A and MAO-B (**PART IV**).

#### **Part IV: Molecular Modeling and MD Simulation Studies**

- The best docking pose of genistein (**CVS2**) in MAO-A exhibited a score of -10.4 kcal/mol.
- . Chrysin (**CVF1**) showed a docking score of -13.34 kcal/mol in MAO-A
- In case of chrysin, there is no 4'-hydroxyl group and the ligand oriented itself inside the binding pocket to have strong interactions with FAD, Ile180 and Asn181.
- Chrysin (**CVF1**) and genistein (**CVS2**) displayed docking scores of -12.22 and -11.51 kcal/mol in MAO-B.
- The binding pocket of MAO-B exhibited different thermodynamics to allow for higher polarity on the phenyl group compared to that of MAO-A.
- Both compounds showed favorable interactions with the amino acid residues, water molecules and co-factor in the binding pocket.
- Quercetin (**HAF1**) showed a favorable docking pose in MAO-A with a docking score of -11.3 kcal/mol.
- Myricetin (**HAF2**) forms strong hydrogen bonds with Ala111, Ile180, Asn181, and Thr336. Solvent molecules in the binding pocket play an important role in ligand stabilization as demonstrated by the strong hydrogen bonds with ligand atoms. The ligand showed hydrogen bonds and  $\pi$ - $\pi$  stacking with FAD.
- Energetically, the binding pose of quercetin (**HAF1**) is more favorable than that of myricetin (**HAF2**), however, both compounds are fitting well inside the ligand binding pocket of MAO- A.

### Future Directions

This dissertation work has generated fundamental information about the two species *Hypericum afrum* and *Cytisus villosus*. Due to the interdisciplinary nature of this work, future research could proceed in several directions.

In terms of phytochemistry, both species remain largely uncharacterized and require further investigation into their metabolites, especially non-phenolic metabolites. It would be highly desirable to carry out further fractionation and isolation work using bioassay-guided fractionation on the remaining fractions of both species. Both species should also undergo further phytochemical studies in an attempt to isolate and characterize more novel bioactive compounds. With respect to the pharmacological activity of the species included in this work, there is clearly much more to be done. It would be desirable to screen the remaining samples for cytotoxic activity, Antioxidant activity, inhibition of nitric oxide and modulation of natural killer cell activity, modulation of the activity of cancer related signaling pathways. Several other bioassays relevant to potential anti-inflammatory activity could be applied. These include inhibition of phospholipase A2 (PLA2), 5-lipoxygenase (5-LOX) and TNF- $\alpha$ , and effects on COX-1 and COX-2 expression and on the key transcription factor nuclear factor kappa B (NF $\kappa$ B). The most promising samples in these assays could be targeted for bioassay-guided fractionation provided the active compounds were not already identified.

In terms of the two species that were found to possess good MAO inhibitory activity, further pharmacological investigations would be highly desirable to determine the structures of the compounds that are responsible for the MAOs inhibitory activity.

Certain fractions of the ethyl acetate of *H. afrum* and *C. villosus*, and alkaloid fractions of *C. villosus* aerial parts showed potent selective MAO-B inhibition. Therefore, further studies are needed to elucidate the structure of the bioactive compounds or components in the ethyl acetate of *H. afrum* and *C. villosus* and alkaloid *C. villosus* aerial parts extracts and evaluate their efficacies *in vitro* and *in vivo*. However, pure compounds isolated from the extracts may not have greater bioactivity and efficacy than extracts due to the synergistic effect of several components in the crude mixture, but at present remains unknown for both species.

Finally, a number of *in vivo* experiments remain to be completed, including the pharmacodynamics, pharmacokinetics and tissue-specific bioavailabilities of active phytochemicals or metabolites and the assessment of efficacy.

## RÉSUMÉ

*Étude Phytochimique et Biologique de deux Plantes Médicinales  
Algériennes Cytisus villosus Pourr. (Fabaceae) et Hypericum afrum Lam.  
(Hypericaceae)*

Ce travail est consacré à l'étude phytochimique et biologique de deux espèces végétales Algériennes. La sélection des plantes a été faite sur la base d'une recherche bibliographique indiquant l'absence de toute étude phytochimique et biologique de l'espèce endémique *Hypericum afrum Lam.* (Guttiferae). La deuxième espèce étudiée est une Fabaceae (*Cytisus villosus Pourr.*). La recherche bibliographique effectuée a montré le peu de travaux reportés sur cette espèce.

*Cytisus villosus Pourr.* (Syn. : *Cytisus triflorus* : *Cytise à trois fleurs*) est une espèce appartenant à la famille des Légumineuses (Fabaceae), sous famille de Papilionaceae (Faboideae). Cette espèce est répartie dans la région méditerranéenne. En Algérie, elle est très répandue dans le Tell algéro-constantinois. La floraison jaune se déroule au printemps. D'après la bibliographie, le genre *Cytisus* montre une richesse en composés phénoliques, notamment les flavonoïdes et les isoflavonoïdes, ainsi que les alcaloïdes, connus pour leurs activités biologiques diverses.

*Hypericum afrum Lam.* (*Millepertuis de Numidie*) endémique de la Numidie, est une espèce appartenant à la famille des Hypericaceae (Guttiferae). Assez commune dans les régions du Nord-est Algérien. La floraison a lieu du mois de juin jusqu'à la fin du mois de juillet au sein des lieux de la récolte de l'échantillon dans la région d'El TARF : (Tourbière du Cap Rosa où ce millepertuis a la forme d'un arbrisseau) et aulnaie d'Aïn Khiar où cette même espèce est une herbacée.

Cette thèse s'organise en quatre Parties :

- ❖ **Partie I** : La première partie sera divisée en deux chapitres :
  - Le premier chapitre est consacré à la description botanique et l'étude bibliographique de la famille, des genres et des espèces étudiées.
  - Le deuxième chapitre est consacré à La description des techniques de séparation et les différentes méthodes physico-chimiques d'analyse ainsi que les différentes méthodes

d'évaluation biologique et de modélisation.

### ❖ **Partie II** : Cette partie se divise en deux Chapitres

Les deux chapitres seront consacrés à l'étude phytochimique, extraction, fractionnement, séparation et détermination structurale des composés séparés des deux espèces *Cytisus villosus* et *Hypericum afrum*. Nous présenterons les étapes d'extraction, de fractionnement, d'isolement, de la détermination des structures et les tests de la teneur en composés phénoliques effectués sur les extraits.

### ❖ **Partie III** : Représentant l'évaluation biologique des différents extraits, Fractions et des produits purs isolés issus des deux plantes.

Dans ce chapitre nous exposerons les différents résultats des activités étudiées de tous les extraits, fractions et de certaines molécules isolées :

1. Affinité pour les récepteurs aux Opioides et cannabinoïdes
2. Activité Antipaludique
3. Activité Antimicrobienne
4. Cytotoxicité
5. Activité Antioxydante & Anti-inflammatoire
6. Activité Antiparasitaire
7. Activité inhibitrice des Monoamine Oxydases (MAO-A et MAO-B).

### ❖ **Partie IV** : **Modélisation Moléculaire**

Dans cette partie on fait appel aux méthodes de modélisation moléculaire par docking et simulation. Nous présenterons les différentes techniques appliquées telles que :

- ❖ La Préparation du Ligand
- ❖ La Préparation de la Protéine
- ❖ La Préparation du Récepteur
- ❖ Le Docking
- ❖ La Simulation Dynamique Moléculaire

## PARTIE II : Chapitre 1

### Extraction, fractionnement et séparation des composés de l'espèce *Cytisus villosus*

#### II.1.1. Extraction et fractionnement

##### ➤ Extraction Hydro-alcoolique

Après le séchage dans un endroit sec et à l'abri des rayons solaires, les parties aériennes broyée de la *Cytisus villosus* Pourr. (1000 g) ont subi une première macération à température ambiante dans un mélange hydroalcoolique dans un mélange (ETOH-H<sub>2</sub>O : 80 :20, v/v)

Cette macération est répétée 3 fois (3×24 h) Après filtration et puis concentration, on ajoute de l'eau distillée. La solution obtenue a subi des extractions successives de type liquide-liquide en utilisant des solvants de polarité croissante en commençant par le chloroforme, puis l'acétate d'éthyle et en termine avec le *n*-butanol.

##### ➤ Extraction des alcaloïdes

La matière végétale subit une macération dans l'éthanol à température ambiante, sous agitation mécanique. Après filtration, le solvant alcoolique est évaporé à l'aide d'un évaporateur rotatif à une température maximale de 40°C et pression réduite.

Le résidu est repris dans une solution d'acide chlorhydrique 0.1 M, ce qui permet d'entraîner les alcaloïdes dans l'eau sous forme de sels, puis de les extraire avec du chloroforme (CHCl<sub>3</sub>). Par la suite, la phase aqueuse est basifiée avec de l'ammoniaque (28%) et extraite au CHCl<sub>3</sub>. Ensuite, la phase organique obtenue est filtrée et le solvant évaporé jusqu'à obtention d'un résidu sirupeux.

La présence des alcaloïdes a d'abord été détectée dans les différents extraits par la chromatographie sur couches minces (CCM) en utilisant le réactif de Dragendorff qui a été pulvérisée sur les plaques. Il s'agit d'iodobismuthate de potassium qui donne en présence d'alcaloïdes des taches jaune-orange.

#### II.1.2. Détermination de la Teneur totale en Composés Phénolique et flavonoïdes

Des déterminations quantitatives des principaux groupes de métabolites secondaires ont été effectuées sur les fractions chloroforme, acétate d'éthyle et *n*-butanol.

##### ➤ La teneur totale en composés phénolique

A été déterminée en utilisant le réactif de Folin-Ciocalteu, elle est de 363mgGAE/g. Ps dans l'extrait butanolique, 208 mg GAE/g. Ps dans l'extrait d'acétate d'éthyle et 56 mg GAE/g Ps dans l'extrait de chloroforme.

➤ **La teneur totale en flavonoïdes :**

Les flavonoïdes ont été évalués en utilisant la méthode  $AlCl_3$ , leur teneur est de 7,7, 13,95 et 21,16 mg EQ/g Ps dans les extraits de chloroforme, d'acétate d'éthyle et de butanol respectivement.

**Tableau 1.** La teneur totale en composés phénoliques et flavonoïdes de l'espèce *C. villosus*

Fractions	Plante	Teneur totale en composés phénolique ( mgGAE/g .Ps )	La teneur totale en flavonoïdes ( mg EQ/g Ps )
Chloroforme ( $CHCl_3$ )	<i>C.villosus</i>	56,00±2.50	7,7±0.547
Acétate d'éthyle (EtOAc)	<i>C.villosus</i>	208,00±8.49	13,95±1.058
<i>n</i> -butanol (BuOH)	<i>C.villosus</i>	363,00±8.32	21,16±1.022

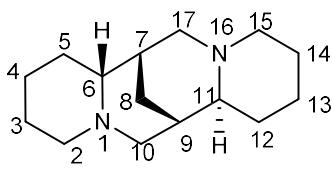
**II.1.3. Séparation des principes actifs**

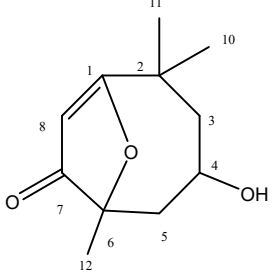
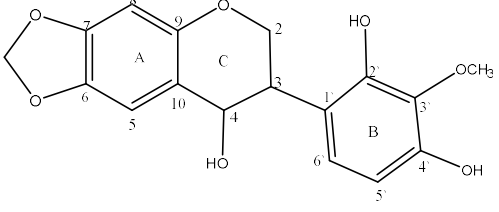
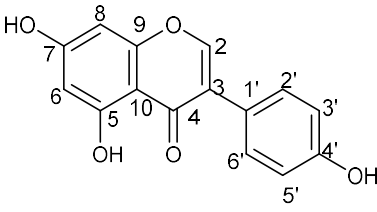
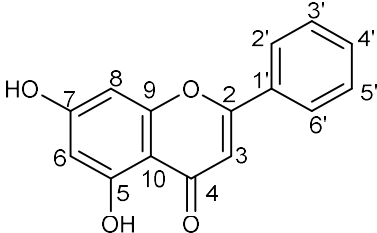
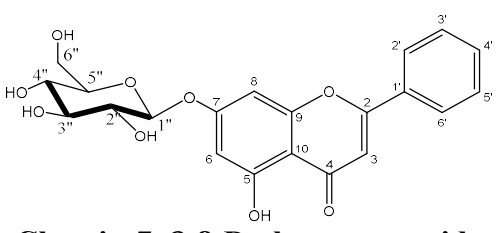
Huit produits purs ont été isolés des parties aériennes de l'espèce *Cytisus villosus*, utilisant les différentes techniques chromatographiques ; Diaion-HP-20, MN-polyamide- SC-6, SPE C-18, Silica gel, Sephadex LH-20 et chromatographie sur couche mince, préparatives et analytique.

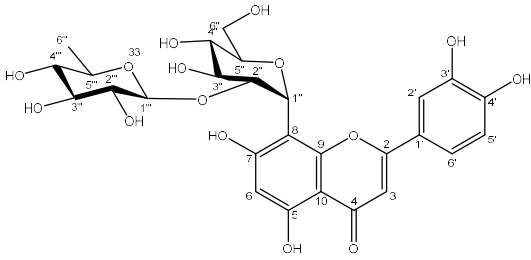
**II.1.4. Identification et élucidation structurale des composés isolés**

Les structures des composés isolés de l'espèce *Cytisus villosus* ont été déterminées utilisant les différentes techniques spectroscopiques : UV, IR,  $^1H$ -NMR,  $^{13}C$ -NMR,  $^1H$ - $^1H$  COSY, HMQC, HMBC, NOESY, ROESY et la spectroscopie de masse (HR-ESI-MS). La liste des composés identifiés sont représentés dans le tableau suivant :

**Tableau 2.** Liste des molécules séparées à partir de l'espèce *Cytisus villosus*

No.	Code	Famille	Structure & Nomenclature	Commentaire
1	CVK1	Alcaloïde	 <p>Spartéine</p>	Rapportée dans le genre <i>Cytisus</i>

2	CVT1	Terpenoïde	 <p><b>4-hydroxy-2,2,6-trimethyl-9-oxabicyclo[4.2.1]non-1(8)-en-7-one</b></p>	Inédit
3	CVS1	isoflavonoïde	 <p><b>4-(8-hydroxy-7,8-dihydro-6H-[1,3]dioxolo[4,5-g]chromen-7-yl)-2-methoxybenzene-1,3-diol</b></p>	Inédit
4	CVS2	Isoflavonoïde	 <p><b>Génistéine</b></p>	Rapportée dans le genre <i>Cytisus</i>
5	CVF1	Flavonoïde	 <p><b>Chryisine</b></p>	Rapportée dans le genre <i>Cytisus</i>
6	CVF2	Flavonoïde	 <p><b>Chrysin-7-O-β-D-glucopyranoside</b></p>	Rapportée dans le genre <i>Cytisus</i>

7	CVF3	Flavonoïde	 <p data-bbox="672 520 1081 558"><b>2''-O-α-L-rhamnosylorientine</b></p>	Rapportée pour la première fois du genre <i>Cytisus</i>
---	------	------------	--	---

- L'originalité de cette étude phytochimique de *Cytisus villosus* Pourr. réside dans le fait que tous les composés identifiés (alcaloïdes, terpenoïdes, isoflavonoïdes, flavonoïdes) n'ont jamais été reportés dans l'espèce. Parmi lesquels deux possèdent des structures nouvelles.

## Chapitre 2

### Extraction, fractionnement et séparation des composés purs de l'espèce

#### *Hypericum afrum*

##### II.2.1. Extraction et fractionnement

Après le séchage dans un endroit sec et à l'abri des rayons solaires, les parties aériennes broyée de la *Hypericum afrum*. (1000 g) ont subi une première macération à température ambiante dans un mélange hydroalcoolique dans un mélange (ETOH-H<sub>2</sub>O : 80 :20, v/v) Cette macération est répétée 3 fois (3×24 h) Après filtration et puis concentration, on ajoute de l'eau distillée. La solution obtenue a subi des extractions successives de type liquide-liquide en utilisant des solvants de polarité croissante en commençant par le chloroforme, puis l'acétate d'éthyle et en termine avec le *n*-butanol.

##### II.2.2. Détermination de la teneur totale en composés phénolique et flavonoïdes

Des déterminations quantitatives des principaux groupes de métabolites secondaires ont été effectuées sur les extraits

- **La teneur totale en composés phénolique** a été déterminée en utilisant le réactif de Folin-Ciocalteu, elle est de 393 mgGAE/g. Ps dans l'extrait butanolique,



386mgGAE/g.Ps dans l'extrait d'acétate d'éthyle et 260mgGAE/g .Ps dans l'extrait de chloroforme.

- **La teneur totale en flavonoïdes :** Les flavonoïdes ont été évalués en utilisant la méthode AlCl<sub>3</sub>, leur teneur est de 40.49 – 38.081 et 23.08 mg EQ/g Ps dans les extraits de chloroforme, d'acétate d'éthyle et butanol respectivement.

**Tableau 3.** La teneur totale en composés phénoliques et flavonoïdes des fractions de l'espèce *H. afrum*

Fraction	Teneur totale en composés phénolique (mg GAE/g .Ps )	La teneur totale en flavonoïdes ( mg EQ/g Ps )
Chloroform	260 ±0,10	23,08±1,713
Ethyl acetate	386±21,46	40,49 ±0,570
<i>n</i> -butanol	393±15,94	38.08±0,737

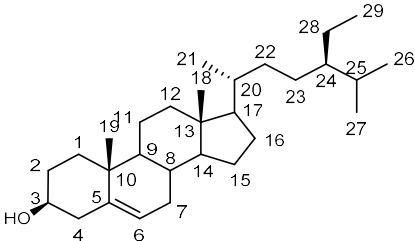
### II.2.3. Séparation des principes actifs :

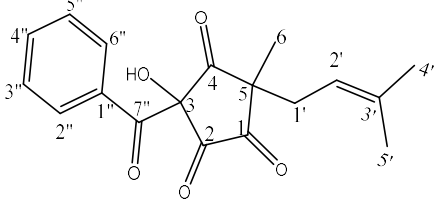
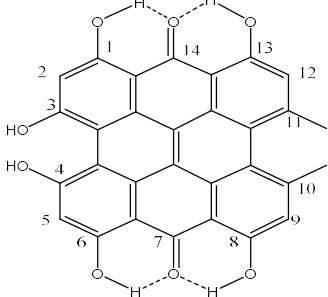
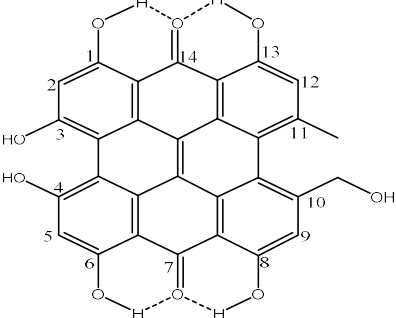
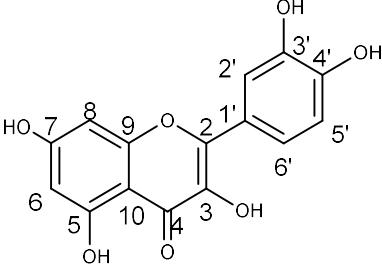
Treize produits purs ont été isolés de l'espèce *Hypericum afrum.*, utilisant les différentes techniques chromatographiques ; Diaion-HP-20, MN-polyamide- SC-6, SPE C-18, Silica gel, Sephadex LH-20 et chromatographie sur couche mince, préparatives et analytique.

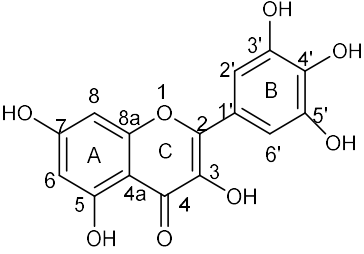
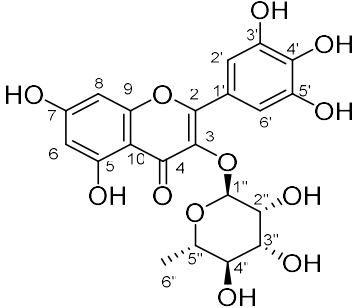
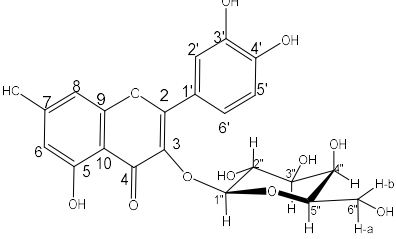
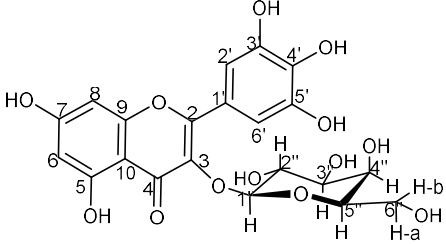
### II.2.4. Identification et élucidation structurale des produits isolés :

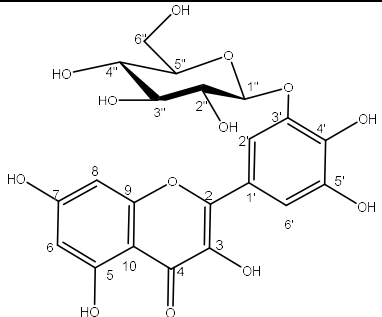
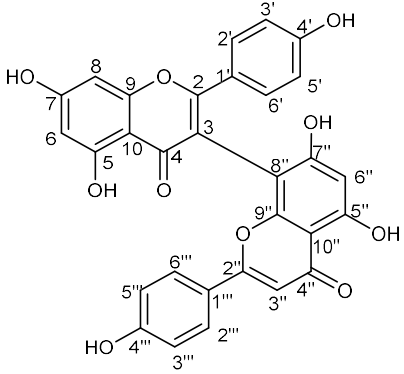
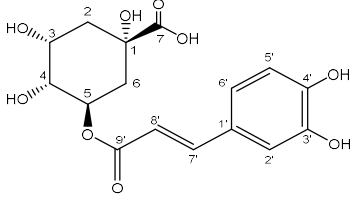
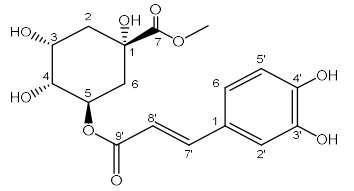
Les structures des molécules isolées de l'espèce *Hypericum afrum* ont été déterminées utilisant les différentes techniques spectroscopiques : UV, IR, 1H-NMR, 13C-NMR, 1H-1H COSY, HMQC, HMBC, NOESY, ROESY et la spectroscopie de masse (HR-ESI-MS). La liste des composés identifiés sont représentés dans le tableau suivant :

**Tableau 4.** Liste des molécules isolées à partir de l'espèce *Hypericum afrum*

No.	Code	Famille	Structure & nomenclature	Commentaire
1	HAT1	Phytostérol	 <p style="text-align: center;"><b>β-Sitostérol</b></p>	Rapportée dans le genre <i>Hypericum</i>

2	HAP1	Phloroglucinol	 <p><b>3-Benzoyl-3-hydroxy-5-(3-methylbut-2-en-1-yl) cyclopentane-1,2,4-trione</b></p>	Inédit
3	HAN1	Naphthodianthrone	 <p><b>l'hypericine</b></p>	Rapportée dans le genre <i>Hypericum</i>
4	HAN2	Naphthodianthrone	 <p><b>Pseudohypericine</b></p>	Rapportée dans le genre <i>Hypericum</i>
5	HAF1	Flavonoïde	 <p><b>Quercétine</b></p>	Rapportée dans le genre <i>Hypericum</i>

6	HAF2	Flavonoïde	 <p style="text-align: center;"><b>Myricétine</b></p>	Rapportée dans le genre <i>Hypericum</i>
7	HAF3	Flavonoïde	 <p style="text-align: center;"><b>Myricétine-3-O-<math>\alpha</math>-L-rhamnopyranoside</b></p>	Rapportée dans le genre <i>Hypericum</i>
8	HAF4	Flavonoïde	 <p style="text-align: center;"><b>Quercétine-3-O-<math>\beta</math>-D-galactopyranoside (hypéroside)</b></p>	Rapportée dans le genre <i>Hypericum</i>
9	HAF5	Flavonoïde	 <p style="text-align: center;"><b>Myricétine-3-O-<math>\beta</math>-D-galactopyranoside</b></p>	Rapportée dans le genre <i>Hypericum</i>

10	HAF6	Flavonoïde	 <p><b>Myricétine-3'-O-β-D-glucopyranoside</b></p>	Rapportée pour la première fois du genre <i>Hypericum</i>
11	HAB1	Biflavonoïde	 <p><b>Biapigénine</b></p>	Rapportée dans le genre <i>Hypericum</i>
12	HAC1	Acide-phénol	 <p><b>Acide chlorogénique</b></p>	Rapportée dans le genre <i>Hypericum</i>
13	HAC2	Acide Phénol	 <p><b>Ester méthylique de l'acide chlorogénique</b></p>	Rapportée dans le genre <i>Hypericum</i>

- Cette étude phytochimique a révélé l'espèce endémique *Hypericum afrum* Lam., comme étant une source d'une grande richesse en composés de types terpéniques, flavoniques, phloroglucinols, naphthodianthrones et acides caféoylquiniques. Tous ces composés sont

reportés pour la première fois pour cette plante endémique dont un est de structure nouvelle.

### **PARTIE III : Évaluation biologique des extraits, fractions et produits purs des deux plantes étudiées**

#### **1. Affinité pour les récepteurs aux Opiïde & cannabinoïdes récepteurs**

Les fractions et certaines molécules isolées des deux espèces étudiées ont fait l'objet d'une évaluation afin de déterminer leurs affinités pour les récepteurs aux opioïdes (subtype  $\delta$ ,  $\kappa$  and  $\mu$ ) et cannabinoïdes (subtype CB1 and CB2), nous avons constaté que les résultats préliminaires ne sont pas suffisants pour réaliser d'autres tests.

#### **2. Activité antipaludique**

Un criblage antiplasmodial *in vitro* des différentes fractions et certains composés isolés a été réalisé. Aucune des fractions ni des molécules testées n'a donné un effet antipaludique. Ils n'ont pas montré également d'effet cytotoxique.

- La molécule de myricetin-3'-O- $\beta$ -D-glucopyranoside (HAF6) a montré une activité antiplasmodique très faible contre *Plasmodium falciparum* (D6) ( $IC_{50}$  4.53  $\mu$ g/ml) avec un indice de selectivité  $SI > 1.1$  et *Plasmodium falciparum* (W2) ( $IC_{50}$  3.93,  $SI > 1.2$ )  $\mu$ g/ml).

#### **3. Activité antimicrobienne**

L'activité antimicrobienne des fractions de *C. villosus* et *H. afrum* et certains composés purs isolés des deux espèces a été évaluée sur des souches : *C.albicans*, *C.glabrata*, *C.krusei*, *A.fumigatus*, *C.neformans*, *S.aureus*, *MRS*, *E.coli*, *P.aeruginosa*, *Kp*, *VRE*. Aucune des fractions ni des molécules testées n'a montré une activité antibactérienne. Ils n'ont également pas montré d'activité antifongique.

#### **4. Activité Cytotoxique**

Les différentes fractions et certaines molécules isolées des deux plantes étudiées sont testés pour évaluer leur activité cytotoxique contre les cellules : SK-MEL, KB, BT-549, SK-OV-3 et LLC-PK1.

- Aucune des fractions testées ni les molécules, n'a montré d'activité cytotoxique.

- Le composé HAF1 (Quercétine) a montré une activité modérée contre les cellules LLC-PK1 (IC<sub>50</sub> 36 µM)
- Le composé HAB1 (Biapigénine) a montré une activité modérée contre les cellules SK-MEL, KB, BT-549 et SK-OV-3 (IC<sub>50</sub> 30, 33, 38 et 48 µM) respectivement.

### 5. L'Activité Antioxydante

L'activité antioxydante des fractions et molécules isolées a été évaluée *in vitro* en utilisant deux différentes méthodes :

#### A. Evaluation de l'Activité antiradicalaire par le test de DPPH

Le test au DPPH a été utilisé pour une évaluation préliminaire de l'efficacité des antioxydants contenus dans les extraits des deux espèces étudiées. Après un test au DPPH effectués sur les fractions de l'extrait brut et les composés purs isolés des deux plantes, nos résultats révèlent un grand pouvoir antioxydant pour l'espèce *H. afrum*.

- L'IC<sub>50</sub> a été estimée à 0.459, 0.425 et 0.164 µg/ml pour les fractions de chloroforme, acétate d'éthyle et butanol respectivement de l'espèce *Cytisus villosus* :
- L'IC<sub>50</sub> a été estimée à 0.069, 0.049 et 0.090 µg/ml pour les fractions de chloroforme, acétate d'éthyle et butanol respectivement pour l'espèce *H. afrum*.
- Les analyses montrent que les composés phénoliques contribuent à 74% ( $r^2 = 0.744$ ,  $P < 0.05$ ) de l'activité antiradicalaire.

#### B. Test du Potentiel antioxydant sur cellules /effet protecteur contre le Stress Oxydatif & Activité anti-inflammatoire

- L'effet préventif des fractions et des molécules isolées des espèces *C. villosus* et *H. afrum* contre le stress oxydatif a été évalué *in vitro*.
- Il a été montré *in vitro* que les deux espèces avaient des effets protecteurs sur des modèles de stress oxydatif.
- Les fractions et certaines molécules testées ont montré une activité antioxydante prometteuse exprimée par l'inhibition du stress oxydatif cellulaire.
- Les fractions acétate d'éthyle et *n*-butanol de l'espèce *C. villosus* ont montré une activité anti-inflammatoire modérée exprimée par l'inhibition de la production d'oxyde nitrique (IC<sub>50</sub> 48 et 90 µg/mL) respectivement.

### 6. Activité antiparasitaire

- Les fractions et certaines molécules isolées des espèces *C. villosus* et *H. afrum* sont testées *in vitro* pour leur activité antiparasitaire (antileishmanienne et trypanocide).
- Les évaluations biologiques ont été réalisées *in vitro* sur les amastigotes de la souche : *L. donovani* et les promastigotes de la souche *L. donovani*.
- Les fractions et certaines molécules isolées sont testées sur les trypomastigotes de la souche *T. brucei*.
- Les fractions et les molécules isolées sont testées pour leur cytotoxicité contre une lignée cellulaire humaine (Cellule THP-1).
- La fraction de butanol et d'acétate d'éthyle des deux espèces exhibent des activités assez intéressantes envers *T. brucei*.
- Le Composé HAF1, Quercétine, a montré une bonne activité trypanocide ( $IC_{50} = 7.52 \mu M$ ).
- Le composé HAF2, Myricétine, a aussi montré une bonne activité trypanocide ( $IC_{50} = 5.71 \mu M$ ) et ( $IC_{90} = 7.97 \mu M$ ).

### 7. Activité inhibitrice de la Monoamine Oxydase (MAO-A et MAO-B)

Monoamine oxydase (MAO), est une enzyme responsable du métabolisme des neurotransmetteurs monoamines, a un rôle important dans le développement et le fonctionnement du cerveau. Les inhibiteurs de la MAO furent parmi les premiers antidépresseurs développés. Il existe deux forme de MAO ; la MAO-A et MAO-B. En général, les inhibiteurs sélectifs de la MAO-A semblent être efficaces dans le traitement des cas de dépression et d'autres troubles de l'anxiété, alors que les inhibiteurs sélectifs de la MAO-B sont utilisés dans le traitement de diverses maladies neurodégénératives ; comme les maladies d'Alzheimer et de Parkinson.

L'activité inhibitrice de la MAO-A et la MAO-B des fractions, sous-fractions et molécules isolées des deux espèces étudiées a été évaluée.

- Les Fractions acétate d'éthyle des deux espèces *C. villosus*, *H. afrum* ont montré une très bonne activité inhibitrice sélective contre MAO-A et B.
- Les extraits alcaloïdes ont montré également, une très bonne activité inhibitrice MAO.
- Par conséquent ces fractions ont été sélectionnée pour poursuivre la purification bio-guidée et

l'isolement.

- Les composés HAF1 (quercétine), et HAF2 (myricétine) isolés de la plante *H. afrum* ont montré une activité inhibitrice sélective contre MAO-A ( $IC_{50}$  1.52 $\mu$ M et 9.93 $\mu$ M), respectivement
- Le composé CVS2 (génistéine), isolé de l'espèce *C. villosus* a montré une activité inhibitrice sélective contre MAO-B ( $IC_{50}$  0,65  $\mu$ M)
- Le composé CVF1 (chryisine) isolé de l'espèce *C. villosus* a montré une activité inhibitrice sélective contre MAO-A ( $IC_{50}$  0.25  $\mu$ M).
- Pour justifier ces résultats, nous envisageons d'approfondir l'étude de l'activité inhibitrice sélective des molécules actives sur les MAO-A et B en faisant appel à des programmes d'étude de docking et de simulation de dynamique moléculaire.

### **PARTIE IV : Modélisation Moléculaire et Simulation MD**

Nous nous sommes intéressés aux interactions moléculaires entre MAO-A et MAO-B et les meilleurs inhibiteurs du MAO isolés à partir des deux espèces *C.villosus* et *H.afrum* à l'aide des méthodes de modélisation moléculaire. Les outils informatiques retenus pour mener à bien cette étude sont la mécanique moléculaire, la dynamique moléculaire et le Docking moléculaire en utilisant les structures cristallographiques les plus récentes de MAO-A et B. La modélisation par docking moléculaire nous a permis d'évaluer l'affinité des inhibiteurs de MAO les plus puissants parmi les molécules étudiées.

- Les résultats du docking indiquent que les molécules isolées : myricétine, quercétine, génistéine et chryisine montrent des interactions favorables avec les résidus des acides aminés, les molécules d'eau et co-facteur dans le site actif.
  - La molécule de genisteine exhibe un score de -10.4 kcal/mol pour la meilleure pose dans la MAO-A
  - . La molécule de chrysin a montré un score de -13.34 kcal/mol dans la MAO A.
  - Les deux molécules de chryisine et génistéine ont montré des scores de -12.22 et -11.51 kcal/mol respectivement dans la MAO-B.
  - Les molécules de quercétine et myricétine ont montré une pose favorable dans le MAO-A avec un score de -11.3 kcal/mol et de -9.8 kcal/mol, respectivement.



- Les molécules du solvant dans le site actif jouent un rôle important dans la stabilisation du ligand.

## Perspectives

Les résultats obtenus au cours de cette étude, nous encouragent à :

- Terminer l'identification structurale des composés originaux obtenus au cours de cette étude.
- Terminer les fractionnements bio-guidés afin d'isoler les principes actifs.
- Terminer les tests *in vitro* de l'activité biologique des constituants purs originaux obtenus.
- Réaliser des tests *in vivo* par la suite afin de confirmer les activités constatées lors de ce travail.

## PAPERS

Farida Larit , Francisco León, Narayan D. Chaurasiya, Babu L. Tekwani, Samira Benyahia, Samir Benayache and Stephen J. Cutler. A new phloroglucinol derivative isolated from *Hypericum afrum*, a plant endemic to Algeria. Rec. Nat. Prod. 2017, Vol. 11 Issue 1, p77-81.

## A New Phloroglucinol Derivative Isolated from *Hypericum afrum*, a Plant Endemic to Algeria

Farida Larit<sup>1,2</sup>, Francisco León<sup>1</sup>, Narayan D. Chaurasiya<sup>3</sup>, Babu L. Tekwani<sup>3</sup>,  
Samira Benyahia<sup>4</sup>, Samir Benayache<sup>5</sup>, and Stephen J. Cutler<sup>1,\*</sup>

<sup>1</sup>Department of BioMolecular Sciences, Division of Medicinal Chemistry, The University of Mississippi, University, MS 38677, United States

<sup>2</sup>Faculté des Sciences Exactes, Département de Chimie, Université Constantine 1, 25000 Constantine, Algeria

<sup>3</sup>National Center for Natural Products Research, School of Pharmacy, University of Mississippi, University, MS 38677, United States

<sup>4</sup>Laboratoire de Synthèse Organique, Modélisation et Optimisation des Procèdes (LOMOP), Université Badji Mokhtar, Faculté des Sciences, Département de Chimie, 23000 Annaba, Algeria

<sup>5</sup>Unité de Recherche Valorisation des Ressources Naturelles, Molécules Bioactives et Analyse Physico-Chimique et Biologique (VARENBIOMOL), Université des Frères Mentouri, Constantine, Algeria

(Received October 16, 2015; Revised March 21, 2016; Accepted March 27, 2016)

**Abstract:** A new phloroglucinol derivative, identified as 3-benzoyl-3-hydroxy-5-(3-methylbut-2-en-1-yl)cyclopentane-1,2,4-trione (**1**), together with eight previously reported compounds, quercetin, myricitrin, hypericin, biapeginin, pseudohypericin, myricetin, 1,3,5,6-tetrahydroxyxanthone, and  $\beta$ -sitosterol were isolated from the chloroform, ethyl acetate and butanol extracts of the aerial part of *Hypericum afrum* (Lam.). Their structures were elucidated by spectroscopic analyses, including 1D-, 2D-NMR and HRESIMS. The EtOAc extract showed moderate MAO-A inhibition with an IC<sub>50</sub> value of 3.35  $\mu$ g/mL. Bioassay-guided fractionation of the EtOAc extract resulted in the isolation of quercetin as the active component exhibiting MAO-A inhibitory activity with an IC<sub>50</sub> value of 1.25  $\mu$ M.

**Keywords:** *Hypericum*; phloroglucinol derivatives; MAO-A and MAO-B; spectroscopic analyses. © 2016 ACG publications. All rights reserved.

### 1. Plant Source

\* Corresponding author: E Mail: [cutler@olemiss.edu](mailto:cutler@olemiss.edu)

The genus *Hypericum* (Hypericaceae) comprises more than 480 species with worldwide distribution except in the Antarctica. It is found in different habitats including a variety of temperate, subtropical and tropical (high altitudes) regions, and isn't observed in places with extreme aridity and salinity [1]. The popular interest in *Hypericum* species have been based on their pharmacological properties and their use in traditional medicines around the world. In fact, *H. perforatum*, commonly known as St. John's wort, is used as poultice, decoction or infusion for sedative and tonic functions and more commonly to treat mild to moderate depression [1, 2]. The extracts of *H. perforatum* are available as dietary supplements in the United States and as a botanical medicine in Europe. It is one of the top best-selling botanicals for more than a decade in the US, with \$ 5.6 million in 2013 sales [3] and € 70 million in 2004 sales in Germany (latest data available) [1]. Pharmacological use of the *H. perforatum* and its economic impact prompted the phytochemical study of different plants belonging to the same genus. The predominant secondary metabolites isolated from this genus are phenolic compounds including hypericin, pseudohypericin, hyperfirin, hyperforin, quercetin and derivatives, chlorogenic acid and other flavonoids and phenolic acid, as well as, phloroglucinol and its derivatives [4].

The plant *Hypericum afrum* (Lam.) was collected in the El Kala region (El Tarf, Northeastern Algeria) in July of 2011 and identified by Belouahem-Abed Djamila from Institut National de recherche forestière. Station de recherche d'El Kala (El Tarf). Algeria. A voucher specimen (UM-10012014) has been deposited in the culture collection of the Department of BioMolecular Sciences, University of Mississippi. *H. afrum* is an endemic species growing in the wetlands in north-eastern Algeria. This plant grows in different forms existing as a shrub or herbaceous plant depending on its biological adaptation to the dampness of the environment [5]. The phytochemical study of *H. afrum* yielded a new phloroglucinol derivative **1**. Additionally, the bioassay-guided fractionation of the EtOAc extract resulted in the isolation and identification of the flavonoid quercetin, possessing selective inhibition of the human MAO-A enzyme.

## 2. Previous Studies

No phytochemical study has been reported

## 3. Present Study

Air-dried aerial parts (1000 g) of *H. afrum* were macerated at room temperature with EtOH–H<sub>2</sub>O (80:20, v/v) for 24 h, three times. After filtration, the filtrate was concentrated and dissolved in H<sub>2</sub>O (800 mL). The resulting solution was extracted successively with CHCl<sub>3</sub>, EtOAc and n-butanol. The organic phases were dried with Na<sub>2</sub>SO<sub>4</sub>, filtered and concentrated in vacuum at room temperature to obtain the following extracts: chloroform (1 g), EtOAc (7.9 g), and n-butanol (15.92 g).

The chloroform extract was subjected to silica gel column chromatography (230–400 mesh) using a step-gradient system hexane/CHCl<sub>3</sub> and then with increasing percentages of MeOH to afford ten fractions (FC1–FC10) obtained by combining the eluates on the basis of TLC analysis. FC4 (50 mg, hexane/CHCl<sub>3</sub> 7:3) yielded β-sitosterol (14 mg) through crystallization with MeOH. FC6 (350 mg, CHCl<sub>3</sub> 100%) was subjected to SPE RP-18 column chromatography (CC), using MeOH/H<sub>2</sub>O elution to give six subfractions SFC4-1 to SFC4-6. Fraction SFC4-1 (200mg) was subjected to Sorbadex 20-LH column chromatography using CH<sub>2</sub>Cl<sub>2</sub>/MeOH (1:1, v/v) elution and yielded compound **1** (50 mg). The EtOAc extract was chromatographed on a silica gel column (CH<sub>2</sub>Cl<sub>2</sub>/MeOH, gradient elution in a high polarity) to yield 10 fractions FE1 to FE10 according to their TLC behavior. From fraction FE3 (423 mg, CH<sub>2</sub>Cl<sub>2</sub>/MeOH 3%) quercetin (10 mg) was obtained as a yellow precipitate, the liquid supernatant was chromatographed on Sorbadex 20-LH eluted with CH<sub>2</sub>Cl<sub>2</sub>/MeOH (1:1), yielding six subfractions, subfraction four was subsequently purified by Sorbadex 20-LH eluted with CH<sub>2</sub>Cl<sub>2</sub>/MeOH (1:1) to yield hypericin (2 mg). The fraction FE4 (115 mg, CH<sub>2</sub>Cl<sub>2</sub>/MeOH 2%) was rechromatographed on Sorbadex 20-LH eluted with CH<sub>2</sub>Cl<sub>2</sub>/MeOH (1:1) to furnish biapigenin (15.6 mg). Fraction FE6 (125

mg, CH<sub>2</sub>Cl<sub>2</sub>/MeOH 5%) was chromatographed by Sorbadex 20-LH eluted with CH<sub>2</sub>Cl<sub>2</sub>/MeOH (1:1) and finally purified by preparative TLC developed with CHCl<sub>3</sub>/MeOH (10:1) to afford pseudohypericin (2 mg) and myricetin (7.3 mg) and 1,3,5,6-tetrahydroxyxanthone (5 mg). The fraction FE7 (1 g, CH<sub>2</sub>Cl<sub>2</sub>/MeOH 10%) yield myricitrin (15 mg) as a brownish powder precipitate.

*3-Benzoyl-3-hydroxy-5-(3-methylbut-2-en-1-yl)cyclopentane-1,2,4-trione (1)*: Yellow amorphous powder; mp 120-121 °C;  $[\alpha]_D^{25} + 21^\circ$  (c 0.5, MeOH); UV (MeOH)  $\lambda_{\max}$  (log  $\epsilon$ ): 339 (4,82); IR (KBr)  $\nu_{\max}$ : 3430, 1741, 1625, 1448, 1416, 1221, 770 cm<sup>-1</sup>; <sup>1</sup>H NMR (500 MHz, CDCl<sub>3</sub>):  $\delta$  (ppm) 1.04 ppm (3H, s, CH<sub>3</sub>-6), 1.54 ppm (3H, s, CH<sub>3</sub>-4'), 1.56 ppm (3H, s, CH<sub>3</sub>-5'), 2.28-2.40 (2H, m, CH<sub>2</sub>-1'), 4.93 (1H, t,  $J = 7,7$  Hz, CH-2'), 7.29 (2H, t,  $J = 7,6$  Hz, CH-3'' and CH-5''), 7.42 (1H, t,  $J = 7,4$  Hz, CH-4''), 7.55 (2H, d,  $J = 7,5$  Hz, CH-2'' and CH-6''); <sup>13</sup>C NMR (125 MHz, CDCl<sub>3</sub>):  $\delta$  (ppm) 213.9 (C, C-4), 200.3 (C, C-1), 194.7 (C, C- $\alpha$ ), 181.5 (C, C-2), 139.0 (C, C-1''), 135.2 (C, C-3'), 132.1 (C, C-4''), 129.0 (CH, C-2'' and C-6''), 127.7 (CH, C-3'' and C-5''), 121.9 (C, C-3), 118.6 (CH, C-2'), 50.6 (C, C-5), 34.2 (CH<sub>2</sub>, C-1'), 25.8 (CH<sub>3</sub>, C-4'), 19.0 (CH<sub>3</sub>, C-6), 17.6 (CH<sub>3</sub>, C-5'); negative HRESIMS:  $m/z$  313.1077 [M-H]<sup>-</sup> (calcd for C<sub>18</sub>H<sub>17</sub>O<sub>5</sub>, 313.1070).

Compound **1** was isolated as a yellow powder and its molecular formula was established as C<sub>18</sub>H<sub>18</sub>O<sub>5</sub> by negative HRESIMS ( $m/z$  313.1077 [M-H]<sup>-</sup>). The IR spectra showed the absorptions for OH (3430cm<sup>-1</sup>), and carbonyl (1747 cm<sup>-1</sup> and 1625 cm<sup>-1</sup>) groups. The <sup>1</sup>H NMR spectrum showed characteristic signals for three methyl groups at  $\delta_H$  1.56 ppm (3H, s), 1.54 ppm (3H, s), and 1.04 ppm (3H, s) the first two methyl corresponding to a gem dimethyl group attached to a double bond; along with the signals at  $\delta_H$  2.40-2.28 ppm (2H, m) characteristic of aliphatic protons; and vinylic proton at  $\delta_H$  4.93 ppm (1H, t,  $J = 7,7$  Hz) suggested the presence of a prenyl group in the molecule, which was confirmed by COSY and HMBC (Figure 1) experiments. Also in the <sup>1</sup>H NMR spectrum three signals at  $\delta_H$  7.55 ppm (2H, d,  $J = 7,5$  Hz), 7.42 ppm (1H, t,  $J = 7,4$  Hz) and 7.29 ppm (1H, t,  $J = 7,6$  Hz) indicated a monosubstituted phenyl group. The <sup>13</sup>C NMR and DEPT spectra of **1** disclosed 18 carbons, which were indicative of four ketone carbonyl carbons at  $\delta_C$  213.9, 200.3, 194.7 and 181.5 ppm; additional four quaternary carbons, six methine, three methyl and one methylene carbon. HMBC correlations (Figure 1) permit joining to the remaining methyl and determining the connections among the rest of the structural fragments. Thus, the structure for **1** has been established and proposed to be 3-benzoyl-3-hydroxy-5-(3-methylbut-2-en-1-yl)cyclopentane-1,2,4-trione. The stereochemistry of the two stereogenic centers have not been successfully determined. The known compounds were identified by comparison of their spectra and physical data with the available literature [6-8].

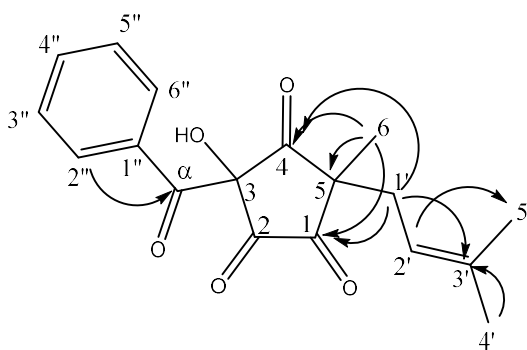


**Figure 1.** Selected <sup>1</sup>H -<sup>13</sup>C HMBC correlations of compound **1**.

Interestingly, the presences of compounds with two or three keto cyclopentane moiety like compound **1** only have been reported from *Humulus lupulus* as phloroglucinol derivatives [9]. In the same case, the high content of benzoylphloroglucinols in *Hypericum* genus [4, 10], suggested a benzoylphloroglucinol as precursor for compound **1**.

*Human MAO-A and MAO-B inhibition assay:* The extracts, fractions and constituents of *H. afrum*, were evaluated using MAO-A and-B enzymatic assays as previously reported [11]. The ethyl acetate extract showed moderate inhibition for MAO-A and B, following a bioassay-guided fractionation strategy. The compound responsible for that activity was identified as quercetin (Table 1). Quercetin has previously been identified as MAO-A inhibitor with comparable values in this report [12].

**Table 1.** Inhibition of recombinant human Monoamine Amine Oxidase-A and B by crude extract, fractions, and pure constituents of *Hypericum afrum*.

Samples	MAO-A IC <sub>50</sub> (µg/mL)	SD	MAO-B IC <sub>50</sub> (µg/mL)	SD
EtOAc extract <sup>#</sup>	3.35	0.035	13.500	0.7071
Fraction FE3 <sup>#</sup>	2.17	0.01	4.12	0.59
Compound* <b>1</b>	>100	--	71.12	4.24
Quercetin*	1.25	0.050	16.50	0.50
Phenelzine <sup>*a</sup>	0.268	0.0257	0.1430	0.025
Clorgyline <sup>*b</sup>	0.0076	0.0005	----	----
Deprenyl <sup>*c</sup>	----	----	0.050	0.0122

<sup>a</sup> Positive control for both MAO enzyme; <sup>b</sup> Positive control selective for MAO-A; <sup>c</sup> selective for MAO-B. \*Shows inhibition = µM and # shows inhibition = (µg/mL)

## Acknowledgments

The project described was supported by grant number P20GM104932 from the National Institute of General Medical Sciences (NIGMS) a component of the National Institutes of Health (NIH). The content is solely the responsibility of the authors and does not necessarily represent the official views of the NIGMS or the NIH. Furthermore, this investigation was conducted in a facility constructed with support from research facilities improvement program C06RR14503 from the NIH National Center for Research Resources (NCRR). Farida Larit was supported by a scholarship from the Algerian Ministry of Higher Education and Scientific Research.

## Supporting Information

Supporting Information accompanies this paper on <http://www.acgpubs.org/RNP>

## References

- [1] S. L. Crockett and N. K. B. Robson (2011). Taxonomy and chemotaxonomy of the genus *Hypericum*, *Med. Aromat. Plant Sci. Biotechnol.* **5**, 1-13.
- [2] R. Crupi, Y. A. K. Abusamra, E. Spina and G. Calapai (2013). Preclinical data supporting/refuting the use of *Hypericum perforatum* in the treatment of depression, *CNS Neurol. Disord.: Drug Targets* **12**, 474-486.
- [3] A. Lindstrom, C. Ooyen, M. E. Lynch, M. Blumenthal and K. Kawa (2014). Sales of herbal dietary supplements increase by 7.95 in 2013, marking a decade of rising sales: turmeric supplements climb to top ranking in natural channel, *HerbalGram* **103**, 52-56.
- [4] N. Camas, J. Radusiene, L. Ivanauskas, V. Jakstas, S. Kayikci and C. Cirak (2014). Chemical composition of *Hypericum* species from the *Taeniocarpium* and *Drosanthe* sections, *Plant Syst. Evol.* **300**, 953-960; J. Zhao, W. Liu and J.C. Wang, (2015). Recent advances regarding constituents and bioactivities of plants from the genus *Hypericum*, *Chem. Biodiv.* **12**, 309-349.
- [5] P. Quezel and S. Santa (1962). Nouvelle flore de l'Algerie et des regions desertiques meridionales, Centre National de la Recherche Scientifique, Paris, Vol I, p. 681.
- [6] X. W. Wang, Y. Mao, N-L. W and X. S. Yao (2008). A new phloroglucinol diglycoside derivative from *Hypericum japonicum* Thunb, *Molecules* **13**, 2796-2803.

- [7] B. Schmidt, J. W. Jaroszewski, R. Bro, M. Witt and D. Stärk (2008). Combining PARAFAC analysis of HPLC-PDA profiles and structural characterization using HPLC-PDA-SPE-NMR-MS experiments: commercial preparations of St. John's Wort, *Anal. Chem.* **80**, 1978-1987.
- [8] H. K. Wabo, T. K. Kowa, A. H. N. Lonfouo, A. T. Tchinda, P. Tane, H. Kikuchi, M. Frédérick and Y. Oshima (2012). Phenolic compounds and terpenoids from *Hypericum lanceolatum*, *Rec. Nat. Prod.* **6**, 94-100.
- [9] M. V. Cleemput, K. Cattoor, K. DeBosscher, G. Haegeman, D. DeKeukeleire and A. Heyerick (2009). Hop (*Humulus lupulus*) derived bitter acids as multipotent bioactive compounds, *J. Nat. Prod.* **72**, 1220-1230.
- [10] I. P. Singh and S. B. Bharate (2006). Phloroglucinol compounds of natural origin, *Nat. Prod. Rep.* **23**, 558-591.
- [11] V. Samoylenko, Md. M. Rahman, B. L. Tekwani, L. M. Tripathi, Y-H. Wang, S. I. Khan, L. S. Miller, V. C. Joshi and I. Muhammad (2010). *Banisteriopsis caapi*, a unique combination of MAO inhibitory and antioxidante constituents for the activities relevant to neurodegenerative disorders and Parkinson's disease, *J. Ethnopharmacol.* **127**, 357-367.
- [12] L. Saaby, H. B. Rasmussen and A. K. Jäger (2009). MAO-A inhibitory activity of quercetin from *Calluna vulgaris* (L.) Hull, *J. Ethnopharmacol.* **121**, 178-181.

**ACG**  
publications

© 2016 ACG publications

## ملخص

يرتكز بحثنا على الدراسة الفينوكيميائية و البيولوجية للأجزاء الهوائية لنبات *Hypericum afrum* Lam. وهي نبتة أصلية ونبات *Cytisus villosus*. Pourr.

تم تقييم النشاط البيولوجي للمستخلصات كمرحلة أولية لتحديد المركبات الفعالة ثم دراسة نشاطها البيولوجي بعد عزلها.

تم إجراء بعض التحاليل البيولوجية المضادة للأكسدة ، القدرة على الإخذاب لمستقبلات المواد الأيونية و مستقبلات شبيهات القنب ، دراسة التأثير على بعض أنواع من الطفيليات الأولية كمضادات للشمانيا والتريبانوسوما و فاعلية المستخلصات كمضادات لبلازموديوم الملاريا و دراسة تأثيرها على بعض أنواع من البكتيريا و الفطريات و أيضا دراسة قدرة المستخلصات على تثبيط انزيم

يسمى (Monoamine oxidase A and B) كما تمت دراسة فاعلية بعض المركبات المفصولة من النباتين

الدراسة الفينوكيميائية للنباتين تشمل المسح الكيميائي الأولي، الإستخلاص، التجزئة ثم الفصل و التعرف على المواد الفعالة المفصولة باستعمال الطرق الفيزيوكيميائية: مطيافية الأشعة فوق البنفسجية. (UV) و مطيافية الرنين النووي المغناطيسي، ( $^{13}\text{C}$ -RMN) و للكربون ( $^1\text{H}$ -RMN) و مطيافية الرنين النووي ثنائية البعد المغناطيسي للبروتون (COSY, TOCSY, HMQC, HMBC, NOESY) و مطيافية الكتلة (HR-ESI-MS, ESIMS) و مقارنة البيانات المختلفة مع المراجع البيولوجية.

تم فصل و تحديد بنيتي سبعة مركبات من نبات *Cytisus villosus* منها من كين فصلا لأول مرة من نوع Isoflavan و Terpenoid.

كما تم فصل و تحديد بنيتي ثلاثة عشر من المركبات من نبات *Hypericum afrum* باستخدام تقنيات الكروماتوجرافيا المختلفة منها مركب جديد فصل لأول مرة من نوع Phloroglucinol

لمعالجة النتائج المحصلت من خلال الأبحاث البيولوجية قمنا بدراسة حساسية استعمال أدوات الكمبيوتر بواسطة تقنيات النمذجة الجزيئية والمعروف عليها بالمصطلح "الانحمار" و أيضا باستعمال تقنيات ديناميكية المحاكاة الجزيئية.

الكلمات المفتاحية: *Hypericum* : *Cytisus* ; MAO-A. MAO-B: تقنيات النمذجة الجزيئية، مضاد للأكسدة، مضاد للشمانيا، مضاد الملاريا ، مضاد الترپانوسوما.



*ABSTRACT*

Natural products are important sources of novel therapeutic agents. Bioactive secondary metabolites isolated from natural sources, can act as drugs or as lead compounds for synthetic drugs. In our work, two plants have been studied; the endemic species of *Hypericum afrum* Lam.(Hypericaceae) and *Cytisus villosus* Pourr. (Fabaceae). Fractions of the aerial parts of these two plants have been screened *in vitro* for several biological assays including cannabinoid and opioid receptors agonist assays, antifungal, antibacterial, antimalarial, antileishmanial, antiproliferative, antioxidant, anti-inflammatory and MAO inhibition.

The chloroform, ethyl acetate and *n*-butanol fractions of *H. afrum* showed significant antioxidant activity and potent antitrypanosomal activity against *T. brucei*. The *n*-butanol fraction of *C. villosus* showed highly potent antitrypanosomal activity against *T. brucei*. In addition, the ethyl acetate fractions of both plants showed potent inhibition of recombinant human monoamine oxidases (MAO-A and -B).

A bioassay-guided fractionation paradigm has been used for the isolation of bioactive compounds of these plants and hence the subfractions that showed significant activity were further purified.

This study led to the isolation and identification of 20 compounds, three of which belonging to phloroglucinols, terpenoids and isoflavonoids are new. The structures of the isolated compounds were elucidated through various spectroscopic methods, including high- resolution mass spectrometry, one and two-dimensional nuclear magnetic resonance spectroscopy.

Computational study was carried out by conformational search and docking techniques to provide insight into the binding mode of molecules on the active site of MAO's isoenzymes.

**Key Words:** *Hypericum*, *Cytisus*, Secondary metabolites, Total phenolics; Antioxidant, Cytotoxicity, Antifungal, Antibacterial, Antimalarial, Antileishmanial, Activity, MAO-A and MAO-B, Docking, Simulation.

## RÉSUMÉ

Dans ce travail nous nous sommes concentrés sur l'étude phytochimique et biologique de deux plantes algériennes, l'espèce endémique *Hypericum afrum* Lam. (Hypericaceae) et l'espèces *Cytisus villosus* Pourr. (Fabaceae). Les extraits et fractions de ces deux espèces ont été évalués *in vitro* pour leurs activités biologiques y compris : l'affinités pour les récepteurs aux opioïdes ( $\delta$ ,  $\kappa$  and  $\mu$ ) et cannabinoïdes (CB1 and CB2), cytotoxicité, l'activité antifongique, antibactérienne, antipaludique, anti leishmanienne, antioxydante, anti-inflammatoire et l'activité inhibitrice de la MAO-A et -B.

Sept composés (alcaloïdes, terpenoïdes, isoflavonoïdes, flavonoïdes) ont été isolés et identifiés de l'espèce *C. villosus* dont deux de type terpenoïde et isoflavane correspondent à de nouvelles structures. Treize composés (stéroïdes, phloroglucinols, flavonoïdes, biflavones, naphthodianthrones, acides caféoylquiniques) ont été isolés et identifiés de l'espèce *H. afrum* dont un de type phloroglucinol correspond à une nouvelle structure.

Les structures moléculaires des composés isolés ont été élucidées par l'utilisation de la spectroscopie RMN-1D et 2D, par la spectrométrie de masse en *electrospray* et la masse haute résolution (ESIMS et HRESIMS), par la mesure des pouvoirs rotatoires et par la comparaison avec les données de la littérature, en plus de la spectroscopie UV et IR. La méthode de calcul du spectre de dichroïsme circulaire (ECD) a été utilisée pour la détermination des configurations absolues des molécules.

Nous nous sommes intéressés aux interactions moléculaires entre MAO-A et MAO-B et les meilleurs inhibiteurs de la MAO isolés à partir des deux espèces *C. villosus* et *H. afrum*. On a fait appel aux méthodes de modélisation moléculaire par docking et simulation en utilisant les structures cristallographiques de MAO-A et B. La modélisation par docking moléculaire nous a permis d'évaluer l'affinité des inhibiteurs MAO les plus puissants parmi les molécules étudiées.

**Mots clés :** *Hypericum*, *Cytisus*, Métabolites secondaires, Total phénoliques, Antioxydant, Cytotoxicité, Antifongique, Antibactérienne, Antipaludique, Antileishmanienne, MAO-A et MAO-B, Docking, Simulation.

## ABSTRACT

Natural products are important sources of novel therapeutic agents. Bioactive secondary metabolites isolated from natural sources, can act as drugs or as lead compounds for synthetic drugs. In our work, two plants have been studied; the endemic species of *Hypericum afrum* Lam.(Hypericaceae) and *Cytisus villosus* Pourr. (Fabaceae). Fractions of the aerial parts of these two plants have been screened *in vitro* for several biological assays including cannabinoid and opioid receptors agonist assays, antifungal, antibacterial, antimalarial, antileishmanial, antiproliferative, antioxidant, anti-inflammatory and MAO inhibition.

The chloroform, ethyl acetate and *n*-butanol fractions of *H. afrum* showed significant antioxidant activity and potent antitrypanosomal activity against *T. brucei*. The *n*-butanol fraction of *C. villosus* showed highly potent antitrypanosomal activity against *T. brucei*. In addition, the ethyl acetate fractions of both plants showed potent inhibition of recombinant human monoamine oxidases (MAO-A and -B).

A bioassay-guided fractionation paradigm has been used for the isolation of bioactive compounds of these plants and hence the subfractions that showed significant activity were further purified.

This study led to the isolation and identification of 20 compounds, three of which belonging to phloroglucinols, terpenoids and isoflavonoids are new. The structures of the isolated compounds were elucidated through various spectroscopic methods, including high- resolution mass spectrometry, one and two-dimensional nuclear magnetic resonance spectroscopy.

Computational study was carried out by conformational search and docking techniques to provide insight into the binding mode of molecules on the active site of MAO's isoenzymes.

**Key Words:** *Hypericum*, *Cytisus*, Secondary metabolites, Total phenolics; Antioxidant, Cytotoxicity, Antifungal, Antibacterial, Antimalarial, Antileishmanial, Activity, MAO-A and MAO-B, Docking, Simulation.

## RÉSUMÉ

Dans ce travail nous nous sommes concentrés sur l'étude phytochimique et biologique de deux plantes algériennes, l'espèce endémique *Hypericum afrum* Lam. (Hypericaceae) et l'espèce *Cytisus villosus* Pourr. (Fabaceae). Les extraits et fractions de ces deux espèces ont été évalués *in vitro* pour leurs activités biologiques y compris : l'affinités pour les récepteurs aux opioïdes ( $\delta$ ,  $\kappa$  and  $\mu$ ) et cannabinoïdes (CB1 and CB2), cytotoxicité, l'activité antifongique, antibactérienne, antipaludique, anti leishmanienne, antioxydante, anti-inflammatoire et l'activité inhibitrice de la MAO-A et -B.

Sept composés (alcaloïdes, terpenoïdes, isoflavonoïdes, flavonoïdes) ont été isolés et identifiés de l'espèce *C. villosus* dont deux de type terpenoïde et isoflavane correspondent à de nouvelles structures. Treize composés (stéroïdes, phloroglucinols, flavonoïdes, biflavones, naphthodianthrones, acides caféoylquiniques) ont été isolés et identifiés de l'espèce *H. afrum* dont un de type phloroglucinol correspond à une nouvelle structure.

Les structures moléculaires des composés isolés ont été élucidées par l'utilisation de la spectroscopie RMN-1D et 2D, par la spectrométrie de masse en *electrospray* et la masse haute résolution (ESIMS et HRESIMS), par la mesure des pouvoirs rotatoires et par la comparaison avec les données de la littérature, en plus de la spectroscopie UV et IR. La méthode de calcul du spectre de dichroïsme circulaire (ECD) a été utilisée pour la détermination des configurations absolues des molécules.

Nous nous sommes intéressés aux interactions moléculaires entre MAO-A et MAO-B et les meilleurs inhibiteurs de la MAO isolés à partir des deux espèces *C. villosus* et *H. afrum*. On a fait appel aux méthodes de modélisation moléculaire par docking et simulation en utilisant les structures cristallographiques de MAO-A et B. La modélisation par docking moléculaire nous a permis d'évaluer l'affinité des inhibiteurs MAO les plus puissants parmi les molécules étudiées.

**Mots clés :** *Hypericum*, *Cytisus*, Métabolites secondaires, Total phénoliques, Antioxydant, Cytotoxicité, Antifongique, Antibactérienne, Antipaludique, Antileishmanienne, MAO-A et MAO-B, Docking, Simulation.